



ANP-10311NP
Revision 0

COBRA-FLX: A Core Thermal-Hydraulic Analysis Code
Topical Report

March 2010

AREVA NP Inc.

(c) 2010 AREVA NP Inc.

Nature of Changes

| Item | Section(s) or Page(s) | Description and Justification |
|------|--------------------------|-------------------------------|
|------|--------------------------|-------------------------------|

Contents

| | <u>Page</u> |
|--|-------------|
| List of Tables | iv |
| List of Figures | v |
| Nomenclature | xxi |
| 1.0 Introduction | 1-1 |
| 1.1 Code Applications | 1-5 |
| 1.2 Requested Code Review and Approval..... | 1-6 |
| 1.3 References | 1-9 |
| 2.0 Problem Formulation and Solution..... | 2-1 |
| 2.1 Mixture Balance Equations..... | 2-1 |
| 2.1.1 Two-Phase Flow Definitions | 2-1 |
| 2.1.2 Local-Instantaneous Navier-Stokes Equations..... | 2-7 |
| 2.1.3 Averaging Operators..... | 2-12 |
| 2.2 Subchannel Formulation of the Basic Equations..... | 2-15 |
| 2.2.1 Fuel Rod Array Geometry..... | 2-17 |
| 2.2.1.1 Lateral scaling of crossflow resistance factor | 2-22 |
| 2.2.1.2 Lateral scaling of turbulent mixing | 2-22 |
| 2.2.1.3 Lateral scaling of the lateral momentum parameter..... | 2-23 |
| 2.2.2 Subchannel Mass Conservation Equation..... | 2-24 |
| 2.2.2.1 Diversion Crossflow | 2-26 |
| 2.2.2.2 Turbulent Interchange..... | 2-26 |
| 2.2.3 Subchannel Momentum Balance Equations..... | 2-27 |
| 2.2.3.1 Axial Momentum Equation | 2-27 |
| 2.2.3.2 Lateral Momentum Balance | 2-30 |
| 2.2.4 Subchannel Energy Conservation Equation | 2-32 |
| 2.2.5 COBRA-FLX Basic Equations | 2-35 |
| 2.2.5.1 Mass Conservation | 2-35 |
| 2.2.5.2 Momentum Balance Equations | 2-35 |
| 2.2.5.3 Energy Conservation | 2-37 |
| 2.2.5.4 Equation of State | 2-39 |
| 2.3 COBRA-FLX Numerical Solution Methodology | 2-40 |
| 2.3.1 SCHEME Solution Methods..... | 2-43 |
| 2.3.1.1 COBRA-FLX Finite-Difference Equations | 2-43 |
| 2.3.1.2 General Computational Procedure | 2-54 |
| 2.3.1.3 Crossflow SCHEME Solution Logic | 2-59 |
| 2.3.1.4 Pressure SCHEME Solution Logic..... | 2-61 |
| 2.3.2 Pressure-Velocity (PV) Solution Method | 2-66 |
| 2.3.2.1 Thermal-Hydraulic Model Equations..... | 2-67 |
| 2.3.2.2 Control Volume Equations | 2-72 |
| 2.3.2.3 Closure Relationships..... | 2-90 |

| | | |
|-----|---|-------|
| | 2.3.2.4 PV Numerics | 2-92 |
| 2.4 | Boundary Conditions | 2-119 |
| | 2.4.1 Inlet Enthalpy / Inlet Temperature..... | 2-119 |
| | 2.4.2 Power | 2-119 |
| | 2.4.3 System Pressure | 2-121 |
| | 2.4.4 Exit Pressure Distribution | 2-121 |
| | 2.4.5 Inlet Flow | 2-122 |
| | 2.4.6 Transient Forcing Functions | 2-122 |
| 2.5 | References | 2-123 |
| 3.0 | Code Structure And Flow Logic Description | 3-1 |
| 4.0 | Subroutine Description | 4-1 |
| 5.0 | Verification and Validation..... | 5-1 |
| | 5.1 Conservation of Mass and Energy | 5-2 |
| | 5.2 Experimental Validation of the Fluid Flow Solution | 5-4 |
| | 5.2.1 Inter-Bundle Diversion Cross-Flow Tests | 5-4 |
| | 5.2.2 MARIGNAN Crossflow Tests..... | 5-12 |
| | 5.3 Experimental Validation of Empirical Correlations..... | 5-18 |
| | 5.3.1 Critical Heat Flux Correlations | 5-19 |
| | 5.3.2 Validity of Steady-State Critical Heat Flux (CHF) Correlations in Transient Applications | 5-19 |
| | 5.4 Comparisons of Solution Algorithms (Solution Schemes)..... | 5-21 |
| | 5.5 Modeling Size | 5-27 |
| | 5.6 Heat Transfer Package | 5-28 |
| | 5.7 Comparison of Fluid Flow Solution to Other Subchannel codes | 5-32 |
| | 5.7.1 Steady-State Comparisons to Other Codes | 5-32 |
| | 5.7.1.1 2-Channel Calculations with No Crossflow | 5-32 |
| | 5.7.1.2 38-Channel Calculations With Crossflow | 5-35 |
| | 5.7.1.3 Examination of Void Model Impacts Between Codes | 5-39 |
| | 5.7.2 Transient Comparisons with Other Codes..... | 5-41 |
| | 5.7.2.1 4 Pump Coastdown Transient..... | 5-42 |
| | 5.7.2.2 Locked Rotor Transient..... | 5-48 |
| | 5.7.2.3 Main Steam Line Break Transient..... | 5-49 |
| | 5.8 Verification and Validation Conclusions | 5-50 |
| | 5.9 References | 5-52 |

List of Tables

| | <u>Page</u> |
|--|-------------|
| Table 1-1: The Extent of the COBRA-FLX Review and Approval Requests..... | 1-7 |
| Table 1-2: Empirical Correlation Application for Requested Review and Approval | 1-8 |
| Table 5-1: Example of COBRA-FLX Heat and Exit Mass Balance Errors | 5-3 |
| Table 5-2: Summary of COBRA-FLX Predictions Using the SCHEME-Pressure (P) and Pressure-Velocity (PV) Solution Methods versus Test Values for IBDCF Tests | 5-7 |
| Table 5-3: Summary of COBRA-FLX Predictions Using the Pressure-Velocity (PV) Solution Methods versus Test Values for the Severe Inlet Flow Asymmetry IBDCF DCF Tests | 5-8 |
| Table 5-4: DNBR Comparison During a 4 Pump Coastdown Using the P and PV Solution Methods | 5-23 |
| Table 5-5: Statistics for the P and PV Based Predictions for Subchannel Enthalpies | 5-26 |
| Table 5-6: Minimum DNBR Predictions for Various Core Model Sizes for a 4 Pump Coastdown | 5-28 |
| Table 5-7: COBRA-FLX Heat Transfer Modes | 5-29 |
| Table 5-8: Summary of DNBR Comparison for the 12-Channel Model for the 4 Pump Coastdown | 5-43 |
| Table 5-9: COBRA-FLX and LYNXT Minimum DNBR Sensitivity to Modeling Parameters for the 4 Pump Coastdown..... | 5-45 |
| Table 5-10: Summary of DNBR Comparison for the 12-Channel Model for the Locked Rotor | 5-48 |
| Table 5-11: COBRA-FLX and LYNXT Minimum DNBR Sensitivity to Modeling Parameters for the Locked Rotor..... | 5-49 |
| Table 5-12: Summary of DNBR Comparison for the 17-Channel Model for the Main Steam Line Break..... | 5-50 |

| | |
|--|------|
| Figure 5-8: Axial and Crossflow Velocity for Channel 4 of IBDCF Test 147 Using PV Solution Method | 5-11 |
| Figure 5-9: MARGIGNAN Test Configuration with Two Adjacent Fuel Assemblies with Defined Subchannels (lateral view)..... | 5-13 |
| Figure 5-10: Location of the Velocity Measurements in the MARGIGNAN Test Configuration (Full View)..... | 5-14 |
| Figure 5-11: Location of the Velocity Measurements in the MARGIGNAN Test Configuration (Exploded View)..... | 5-15 |
| Figure 5-12: Axial Velocity Comparisons by Subchannel Row at the Relative Axial Location of Y= - 200.0 mm in the MARGIGNAN Test..... | 5-16 |
| Figure 5-13: Axial Velocity Comparisons by Subchannel Row at the Relative Axial Location of Y= - 7.5 mm in the MARGIGNAN Test..... | 5-17 |
| Figure 5-14: Axial Velocity Comparisons by Subchannel Row at the Relative Axial Location of Y= +7.0 mm in the MARGIGNAN Test..... | 5-17 |
| Figure 5-15: Axial Velocity Comparisons by Subchannel Row at the Relative Axial Location of Y= +200.0 mm in the MARGIGNAN Test..... | 5-18 |
| Figure 5-16: DNBR Response During a 4 Pump Coastdown Using the P and PV Solution Methods..... | 5-22 |
| Figure 5-17: DNBR Response During a 4 Pump Coastdown Using the P and PV Solution Methods for the Axial Range of 200 to 350 cm | 5-23 |
| Figure 5-18: DNBR-Limiting Subchannel Mass Flux versus Axial Location at Three Times during a 4 Pump Coastdown for the P and PV Solution Methods | 5-24 |
| Figure 5-19: DNBR-Limiting Subchannel Enthalpy versus Axial Location at 0.0 Seconds During a 4 Pump Coastdown for the P and PV Solution Methods | 5-25 |
| Figure 5-20: DNBR-Limiting Subchannel Enthalpy versus Axial Location at 3.4 Seconds during a 4 Pump Coastdown for the P and PV Solution Methods..... | 5-25 |
| Figure 5-21: DNBR-Limiting Subchannel Enthalpy versus Axial Location at 4.8 Seconds during a 4 Pump Coastdown for the P and PV Solution Methods..... | 5-26 |
| Figure 5-22: Transient “A” Progression through Heat Transfer Modes..... | 5-30 |
| Figure 5-23: Transient “A” Clad Wall Temperature Response..... | 5-30 |
| Figure 5-24: Transient “B” Progression through Heat Transfer Modes..... | 5-31 |
| Figure 5-25: Transient “B” Clad Wall Temperature Response..... | 5-31 |
| Figure 5-26: 2-Channel Model with No Crossflow for Code Comparisons..... | 5-32 |
| Figure 5-27: Normalized Axial Pressure Drop Comparison for the 2-Channel Model with No Crossflow | 5-33 |
| Figure 5-28: Axial Void Fraction Comparison for the 2-Channel Model with No Crossflow | 5-34 |
| Figure 5-29: Coolant Density Comparison for the 2-Channel Model with No Crossflow..... | 5-34 |
| Figure 5-30: Coolant Enthalpy Comparison for the 2-Channel Model with No Crossflow..... | 5-35 |
| Figure 5-31: Radial Node Scheme for the 38 Channel Model (1/8 th Core Symmetry) With Crossflow for Code Comparisons..... | 5-36 |
| Figure 5-32: Mass Velocity Comparison for the 38-Channel Model With Crossflow..... | 5-37 |
| Figure 5-33: Void Fraction Comparison for the 38-Channel Model with Crossflow | 5-38 |
| Figure 5-34: Coolant Enthalpy Comparison for the 38-Channel Model with Crossflow | 5-39 |

| | |
|---|------|
| Figure 5-35: Mass Velocity Comparison for the 38-Channel Model Using the Homogenous Void Model | 5-40 |
| Figure 5-36: Void Fraction Comparison for the 38-Channel Model Using the Homogenous Void Model | 5-40 |
| Figure 5-37: Void Fraction Comparison for the 2-Channel Model Using the Homogenous Void Model | 5-41 |
| Figure 5-38: Radial Node Scheme for a 17-Channel Model (1/8 th Core Symmetry) for the Main Steam Line Break Event..... | 5-42 |
| Figure 5-39: DNBR Comparison for the 12-Channel Model for the 4 Pump Coastdown | 5-43 |
| Figure 5-40: Mass Velocity Comparison for the 12-Channel Model for the 4 Pump Coastdown | 5-44 |
| Figure 5-41: Thermodynamic Quality for the 12-Channel Model for the 4 Pump Coastdown | 5-44 |
| Figure 5-42: DNBR Comparison for the Combined Effect of All Modeling Parameters in Table 5-9 for the 4 Pump Coastdown..... | 5-46 |
| Figure 5-43: Mass Velocity Comparison for the Combined Effect of All Modeling Parameters in Table 5-9 for the 4 Pump Coastdown at the Time of Minimum DNBR..... | 5-47 |
| Figure 5-44: Thermodynamic Quality Comparison for the Combined Effect of All Modeling Parameters in Table 5-9 for the 4 Pump Coastdown at the Time of Minimum DNBR..... | 5-47 |
| Figure 5-45: DNBR Comparison for the 12 Channel Model for the Locked Rotor | 5-48 |
| Figure 5-46: DNBR Comparison for the 17-Channel Model for the Main Steam Line Break in the Limiting Subchannel..... | 5-50 |

Table of Contents

| | <u>Page</u> |
|---|--------------------|
| Appendix A : Empirical Correlations | A-1 |
| A.1 Introduction..... | A-1 |
| A.2 Water Properties | A-1 |
| A.3 Friction Factor | A-1 |
| A.3.1 Single-phase Flow | A-2 |
| A.3.2 Two-phase Flow | A-5 |
| A.4 Void Fraction Correlation..... | A-7 |
| A.4.1 Bulk Void..... | A-7 |
| A.4.2 Subcooled Void..... | A-18 |
| A.5 Heat Transfer Coefficients..... | A-23 |
| A.6 DNBR Iteration Scheme | A-38 |
| A.7 References | A-39 |
| Appendix B : COBRA-FLX Development History..... | B-1 |
| B.1 History | B-1 |
| B.2 History of COBRA Development | B-1 |
| B.2.1 COBRA Versions Leading to COBRA 3-CP | B-2 |
| B.2.2 Creation and Further Development of COBRA 3-CP | B-5 |
| B.3 References | B-8 |
| Appendix C : Critical Heat Flux Correlation Validation..... | C-1 |
| C.1.1 Validation Process | C-1 |
| C.2 The ACH-2 CHF Correlation | C-4 |
| C.2.1 Measured to Predicted CHF Performance..... | C-5 |
| C.2.2 Design Limit DNBR..... | C-8 |
| C.2.3 Ranges and Limitations | C-9 |
| C.3 The BHTP CHF Correlation..... | C-10 |
| C.3.1 Predicted to Measured CHF Performance..... | C-10 |
| C.3.2 Statistical Design Limit..... | C-12 |
| C.3.3 Ranges and Limitations | C-13 |
| C.4 The BWU-Z CHF Correlation for Mark-BW17 Fuel with MSMGs | C-14 |
| C.4.1 Measured to Predicted CHF Performance..... | C-15 |
| C.4.2 Statistical Design Limit..... | C-16 |
| C.4.3 Ranges and Limitations | C-18 |
| C.5 The BWU-Z CHF Correlation for Mark-BW17 Fuel | C-18 |
| C.5.1 Measured to Predicted CHF Performance..... | C-19 |
| C.5.2 Statistical Design Limit..... | C-21 |
| C.5.3 Ranges and Limitations | C-23 |

COBRA-FLX: A Core Thermal-Hydraulic Analysis Code

Topical Report

Appendix

Page ix

| | | |
|---|--|-------|
| C.6 | The BWCMV-A CHF Correlation | C-23 |
| C.6.1 | Measured to Predicted CHF Performance..... | C-24 |
| C.6.2 | Statistical Design Limit..... | C-26 |
| C.6.3 | Ranges and Limitations | C-27 |
| C.7 | The BWCMV CHF Correlation..... | C-28 |
| C.7.1 | Measured to Predicted CHF Performance..... | C-28 |
| C.7.2 | Statistical Design Limit..... | C-30 |
| C.7.3 | Ranges and Limitations | C-31 |
| C.8 | The BWU-N CHF Correlation | C-32 |
| C.8.1 | Measured to Predicted CHF Performance..... | C-32 |
| C.8.2 | Statistical Design Limit..... | C-34 |
| C.8.3 | Ranges and Limitations | C-37 |
| C.9 | The BWC CHF Correlation for 15x15 Geometry | C-38 |
| C.9.1 | Measured to Predicted CHF Performance..... | C-38 |
| C.9.2 | Statistical Design Limit..... | C-40 |
| C.9.3 | Ranges and Limitations | C-42 |
| C.9.4 | Local Conditions and Design Limits Summary | C-42 |
| C.10 | References | C-44 |
| Appendix D : Input Description of Keyword Based FORMAT (KBF)..... | | D-1 |
| D.1 | Input Description of Keyword Based Format (KBF)..... | D-1 |
| D.1.1 | Input block group_0_solver : Solution method of conservation equations | D-5 |
| D.1.2 | Input block group_0_general : Case control data | D-7 |
| D.1.3 | Input block group_1_coolant : Physical properties | D-8 |
| D.1.4 | Input block group_2_flow_correlations : Flow correlations | D-13 |
| D.1.5 | Input block group_3_power_distribution : Power distribution data ... | D-18 |
| D.1.6 | Input block group_3.2_hot_channel_factors : Axial heat flux data ... | D-22 |
| D.1.7 | Input block group_4_channels : Subchannel data and local coupling parameters | D-23 |
| D.1.8 | Input block group_5_channel_area_variation : Channel area variation | D-30 |
| D.1.9 | Input block group_5.1_channel_area_variation_data :Channel area variation data | D-31 |
| D.1.10 | Input block group_6_gap_variation : Gap spacing variation | D-33 |
| D.1.11 | Input block group_6.1_gap_variation_data :Gap spacing variation data | D-35 |
| D.1.12 | Input block group_7_spacer : Spacer data | D-37 |
| D.1.13 | Input block group_8_rod_data : Rod data | D-43 |
| D.1.14 | Input block group_9_calculation_variables : Calculation variables | D-95 |
| D.1.15 | Input block group_10_mixing : Turbulent mixing correlations..... | D-106 |
| D.1.16 | Input block group_11_operating_conditions : Operating conditions..... | D-109 |

COBRA-FLX: A Core Thermal-Hydraulic Analysis Code

Topical Report

Appendix

Page x

| | | |
|---|--|-------|
| D.2 | COBRA-FLX Restart Capability | D-122 |
| D.3 | Thermal-Hydraulics (COBRA-FLX) Stand-Alone Calculation..... | D-122 |
| Appendix E : Input Description Of Conventional Format | | E-1 |
| E.1 | Introductory Cards | E-5 |
| E.1.1 | I1: Problem array size..... | E-5 |
| E.1.2 | I2: Solution method of conservation equations..... | E-6 |
| E.1.3 | I2-1: Additional solution method parameters | E-6 |
| E.1.4 | I3: Case control card..... | E-7 |
| E.2 | Card Group 1..... | E-8 |
| E.2.1 | GCC1: Group control card for card group 1..... | E-8 |
| E.2.2 | G1-1: Physical properties | E-9 |
| E.2.3 | G1-2: Physical properties | E-9 |
| E.3 | Card Group 2..... | E-10 |
| E.3.1 | GCC2: Group control card for card group 2..... | E-10 |
| E.3.2 | G2-1: Friction factor correlation constants..... | E-11 |
| E.3.3 | G2-2: Void fraction polynomial coefficients or slip ratio specification | E-11 |
| E.3.4 | G2-3: Two-phase friction multiplier, polynomial in quality..... | E-12 |
| E.4 | Card Group 3..... | E-12 |
| E.4.1 | GCC3: Group control card for card group 3..... | E-12 |
| E.4.2 | G3-1: Axial heat flux data | E-13 |
| E.4.3 | G3-2: Hot channel factors..... | E-13 |
| E.4.4 | G3-3: DNB Limit Value For Heat Transfer | E-14 |
| E.5 | Card Group 4..... | E-14 |
| E.5.1 | GCC4a: Group control card for card group 4a (if IPILE=0 on card I3)..... | E-15 |
| E.5.2 | G4a-1: Subchannel data..... | E-15 |
| E.5.3 | G4a-2: Local coupling parameters..... | E-16 |
| E.5.4 | GCC4b: Group control card for card group 4b (if IPILE=1 or 2 on card I3)..... | E-16 |
| E.5.5 | G4b-1: Problem specification data..... | E-17 |
| E.5.6 | G4b-2: Alphanumeric data for problem identification..... | E-18 |
| E.5.7 | G4b-3: Hydraulic data | E-18 |
| E.5.8 | G4b-4: Spacer data | E-19 |
| E.5.9 | G4b-5: Radial power factors | E-20 |
| E.5.10 | G4b-6: Grid data | E-20 |
| E.5.11 | G4b-7: Channel lists by type..... | E-20 |
| E.5.12 | G4b-8: Array size specifications | E-21 |
| E.5.13 | G4b-9: Row declarations | E-21 |
| E.5.14 | G4b-10: Channel numbers by row..... | E-22 |
| E.5.15 | G4b-11: Boundary definitions | E-22 |
| E.5.16 | G4b-12: Half boundary identification | E-22 |
| E.5.17 | G4b-13: Fuel rod thermal specifications | E-23 |

COBRA-FLX: A Core Thermal-Hydraulic Analysis Code

Topical Report

Appendix

Page xi

| | | |
|--------|---|------|
| E.5.18 | G4b-14: CHF correlation input: selection of CHF correlation | E-23 |
| E.5.19 | G4b-15: CHF correlation input: non-linear profile, spacer grid and cold-wall factor..... | E-24 |
| E.5.20 | G4b-16: CHF correlation input: hot channel data | E-25 |
| E.5.21 | G4b-17: CHF correlation input: selection of characteristic diameter..... | E-26 |
| E.5.22 | G4b-18: CHF correlation input: input of characteristic diameter..... | E-26 |
| E.5.23 | G4b-19: CHF correlation input: grid factor for []-correlation | E-27 |
| E.5.24 | G4b-20: CHF correlation input: input for Tong's spacer correction..... | E-27 |
| E.6 | Card Group 5..... | E-28 |
| E.6.1 | GCC5: Group control card for card group 5..... | E-28 |
| E.6.2 | G5-1: Axial positions of area variations | E-28 |
| E.6.3 | G5-2: Subchannel number..... | E-29 |
| E.6.4 | G5-3: Area variation factors..... | E-29 |
| E.7 | Card Group 6..... | E-29 |
| E.7.1 | GCC6: Group control card for card group 6..... | E-29 |
| E.7.2 | G6-1: Axial positions of gap spacing variations | E-30 |
| E.7.3 | G6-2: Gap number..... | E-30 |
| E.7.4 | G6-3: Gap spacing variation factors | E-30 |
| E.8 | Card Group 7..... | E-31 |
| E.8.1 | GCC7: Group control card for card group 7..... | E-31 |
| E.8.2 | G7-1: Wire wrap geometry..... | E-32 |
| E.8.3 | G7-2: Gap specification | E-32 |
| E.8.4 | G7-3: Wire wrap inventory..... | E-32 |
| E.8.5 | G7-4: Spacer location and type | E-33 |
| E.8.6 | G7-5: Spacer data sets..... | E-33 |
| E.9 | Card Group 8..... | E-34 |
| E.9.1 | GCC8: Group control card for card group 8..... | E-35 |
| E.9.2 | GCC8-cont: Group control continuation card for card group 8 | E-37 |
| E.9.3 | G8-1: Rod layout data..... | E-38 |
| E.9.4 | G8-1-1: Performance factors for CHF correlations | E-38 |
| E.9.5 | G8-1-2: Rod-wise CHF correlations..... | E-39 |
| E.9.6 | G8-1-3: Definition of rod-types containing axial regions with different CHF correlations | E-39 |
| E.9.7 | G8-1-4: Axial node-wise regions for CHF correlations | E-40 |
| E.9.8 | G8-1-5: Assignment of axial CHF rod-types to individual rods | E-40 |
| E.9.9 | G8-1aa: Control of multiple CHF correlation input..... | E-41 |
| E.9.10 | G8-1a: CHF correlation input..... | E-41 |
| E.9.11 | G8-1b: CHF correlation input..... | E-42 |
| E.9.12 | G8-1c: CHF correlation input: selection of CHF correlation..... | E-42 |
| E.9.13 | G8-1c-1: CHF correlation input: non-linear profile, spacer grid and cold-wall factor..... | E-43 |
| E.9.14 | G8-1c-2: CHF correlation input: hot channel data | E-44 |

| | | |
|--------|--|------|
| E.9.15 | G8-1d: CHF correlation input: selection of characteristic diameter..... | E-45 |
| E.9.16 | G8-1d-1: CHF correlation input:input of characteristic diameter..... | E-45 |
| E.9.17 | G8-1e-1: CHF correlation input: grid factor for []-correlation.... | E-46 |
| E.9.18 | G8-1e-2: CHF correlation input: input for []..... | E-46 |
| E.9.19 | G8-1g: [] Correlation Geometry Parameters | E-46 |
| E.9.20 | G8-1h: Grid Heights..... | E-47 |
| E.9.21 | G8-1i: Mixing Grid Specification | E-47 |
| E.9.22 | G8-1j: [] Correlation Input..... | E-47 |
| E.9.23 | G8-1k: []..... | E-48 |
| E.9.24 | G8-1l: []..... | E-50 |
| E.9.25 | G8-1m: CHF correlation limits and debug options..... | E-50 |
| E.9.26 | G8-1n: CHF correlation limits and debug options..... | E-51 |
| E.9.27 | G8-1o: CHF correlation limits and debug options..... | E-51 |
| E.9.28 | G8-1p: CHF correlation grid spacing input | E-52 |
| E.9.29 | G8-1q: CHF correlation grid spacing input | E-52 |
| E.9.30 | G8-1r: CHF correlation channels for debug printout..... | E-52 |
| E.9.31 | G8-2: Fuel thermal properties..... | E-53 |
| E.9.32 | G8-2a: Nonuniform radial heating in fuel (number of data pairs)..... | E-53 |
| E.9.33 | G8-2a-1: Options for definition of radial power profile | E-53 |
| E.9.34 | G8-2a-2: Input parameters for calculation of radial power profile | E-54 |
| E.9.35 | G8-2b: Nonuniform radial heating in fuel (pellet data)..... | E-55 |
| E.9.36 | G8-2b-1: Nonuniform radial heating in fuel (pellet radii)..... | E-55 |
| E.9.37 | G8-2c: Number of transient gap conductance data pairs | E-55 |
| E.9.38 | G8-2d: Transient forcing function data pairs for gap conductance versus time | E-56 |
| E.9.39 | G8-2e: Fuel thermal properties..... | E-56 |
| E.9.40 | G8-2e-1: Iteration of Heat Transfer Coefficient..... | E-57 |
| E.9.41 | G8-2f: Fuel rod model (geometry) | E-57 |
| E.9.42 | G8-2g: Fuel rod model (model and data selection) | E-57 |
| E.9.43 | G8-2h: Fuel rod model (geometry) | E-58 |
| E.9.44 | G8-2i: Fuel rod model (fuel material data)..... | E-59 |
| E.9.45 | G8-2k: Fuel rod model (fuel material data)..... | E-59 |
| E.9.46 | G8-2l: Fuel rod model (fuel material data)..... | E-60 |
| E.9.47 | G8-2m: Fuel rod model (gap gas data)..... | E-60 |
| E.9.48 | G8-2n: Fuel rod model (gap gas data)..... | E-61 |
| E.9.49 | G8-2n-1: Fuel rod model (heat transfer coefficient)..... | E-62 |
| E.9.50 | G8-2o: Fuel rod model (heat transfer coefficient)..... | E-62 |
| E.9.51 | CAR_INP: Fuel rod data from file CAR_INP{.KASE}..... | E-62 |
| E.10 | Card Group 9..... | E-64 |
| E.10.1 | GCC9: Group control card for card group 9..... | E-64 |
| E.10.2 | G9-1: Calculation variables..... | E-65 |
| E.10.3 | G9-1a: Reference distance..... | E-67 |

| | | |
|---------|---|------|
| E.10.4 | G9-2: Axial node input | E-67 |
| E.10.5 | G9-3: Axial node input | E-67 |
| E.10.6 | G9-4: Axial node input | E-68 |
| E.10.7 | G9-5: PV-Solution Variables | E-68 |
| E.10.8 | G9-6: PV-Solution Variables | E-68 |
| E.10.9 | G9-7: PV-Solution Variables | E-69 |
| E.10.10 | G9-8: PV-Solution Variables | E-69 |
| E.10.11 | G9-9: PV-Solution Variables | E-70 |
| E.11 | Card Group 10 | E-70 |
| E.11.1 | GCC10: Group control card for card group 10 | E-71 |
| E.11.2 | G10-1: Mixing correlation constants | E-72 |
| E.11.3 | G10-1a: Mixing data input | E-72 |
| E.11.4 | G10-1b: Mixing data input | E-72 |
| E.11.5 | G10-1c: Mixing data input | E-73 |
| E.11.6 | G10-1d: Mixing data input | E-73 |
| E.11.7 | G10-2: Two-phase mixing data | E-73 |
| E.11.8 | G10-3: Thermal conduction geometry factor | E-73 |
| E.11.9 | G10-4: Reference distance | E-74 |
| E.12 | Card Group 11 | E-74 |
| E.12.1 | GCC11: Group control card for card group 11 | E-74 |
| E.12.2 | NLOOP: Transient data from file NLOOP (unit 96) | E-75 |
| E.12.3 | G11-1.0: Transient parameters with transient data read from file NLOOP | E-76 |
| E.12.4 | G11-1: Operating conditions | E-77 |
| E.12.5 | G11-1a: Setpoint iteration | E-77 |
| E.12.6 | G11-1b: Sensitivity calculation | E-78 |
| E.12.7 | G11-1c: Number of channels with given pressure difference at the outlet | E-80 |
| E.12.8 | G11-1d: Channels with given pressure difference at the outlet | E-80 |
| E.12.9 | G11-2: Inlet temperature or enthalpy | E-80 |
| E.12.10 | G11-3: Channel mass velocity factors | E-81 |
| E.12.11 | G11-4.a: Automatic time step control | E-81 |
| E.12.12 | G11-4: Transient forcing function data pairs for pressure versus time | E-81 |
| E.12.13 | G11-5.a: Automatic time step control | E-81 |
| E.12.14 | G11-5: Transient forcing function data pairs for inlet enthalpy or inlet temperature versus time | E-82 |
| E.12.15 | G11-6.a: Automatic time step control | E-82 |
| E.12.16 | G11-6: Transient forcing function data pairs for inlet flow versus time | E-82 |
| E.12.17 | G11-7.a: Automatic time step control | E-82 |
| E.12.18 | G11-7: Transient forcing function data pairs for heat flux versus time | E-83 |
| E.12.19 | G11-8: Write local coolant conditions to files COOLANT (tape77) and DNBDATA (tape9) | E-83 |

| | | |
|---------|---|-------|
| E.13 | Card Group 12..... | E-85 |
| E.13.1 | GCC12: Group control card for card group 12..... | E-85 |
| E.13.2 | G12-1: Subchannel numbers..... | E-86 |
| E.13.3 | G12-2: Fuel rod numbers..... | E-87 |
| E.13.4 | G12-3: Node numbers..... | E-87 |
| E.14 | Card Group 20..... | E-87 |
| E.14.1 | GCC20: Group control card for card group 20..... | E-89 |
| E.14.2 | 1-CNS: Channel map parameter..... | E-90 |
| E.14.3 | 2-CNS: Channel map..... | E-91 |
| E.14.4 | 3-CNS: Channel map..... | E-92 |
| E.14.5 | 4-HF: Heat flux specification..... | E-94 |
| E.14.6 | 5-HF: Heat flux profile..... | E-95 |
| E.14.7 | 6-HF: Rod power factors..... | E-96 |
| E.14.8 | 7-MD: Miscellaneous data..... | E-97 |
| E.14.9 | 8-CD: Channel Indicators..... | E-97 |
| E.14.10 | 9-CD: Fuel rod temperature convergence..... | E-98 |
| E.14.11 | 9-CD-1: Iteration of Heat Transfer Coefficient..... | E-99 |
| E.14.12 | 10-CD: Channel data for type I..... | E-99 |
| E.14.13 | 11-CD: Grid data for channel type I..... | E-100 |
| E.14.14 | 12-CD: Channels making up type I..... | E-101 |
| E.14.15 | 13-CD: Grid positions..... | E-101 |
| E.14.16 | 14-RD: Indicators..... | E-101 |
| E.14.17 | 15-RD: Rod layout information..... | E-102 |
| E.14.18 | 16-FD: Fuel temperature data..... | E-103 |
| E.14.19 | 17-FD: Fuel thermal properties..... | E-103 |
| E.14.20 | 17a-FD: Fuel rod model (geometry)..... | E-104 |
| E.14.21 | 17b-FD: Fuel rod model (geometry)..... | E-104 |
| E.14.22 | 17c-FD: Fuel rod model (model and data selection)..... | E-104 |
| E.14.23 | 17d-FD: Fuel rod model (geometry)..... | E-105 |
| E.14.24 | 18-FD: Fuel rod model (fuel material data)..... | E-105 |
| E.14.25 | 18a-FD: Fuel rod model (fuel material data)..... | E-106 |
| E.14.26 | 18b-FD: Fuel rod model (Fuel material data)..... | E-106 |
| E.14.27 | 19-FD: Fuel rod model (gap gas data)..... | E-107 |
| E.14.28 | 19a-FD: Fuel rod model (gap gas data)..... | E-107 |
| E.14.29 | 19b-FD: Fuel rod model (heat transfer coefficient)..... | E-108 |
| E.14.30 | 20-GB: Effective rod gap..... | E-108 |
| E.14.31 | 21-GB: Transverse momentum coupling parameters..... | E-109 |
| E.14.32 | 22-GB: PWR half-boundaries..... | E-110 |
| E.14.33 | 23-HM: Hydraulic model Indicators..... | E-110 |
| E.14.34 | 24-HM: Mixing model..... | E-111 |
| E.14.35 | 24-HM-1: Mixing model..... | E-112 |
| E.14.36 | 24-HM-2: Mixing model..... | E-112 |
| E.14.37 | 24-HM-3: Mixing model..... | E-112 |
| E.14.38 | 25-HM: Single phase friction model..... | E-113 |
| E.14.39 | 26-HM: Two-phase friction model..... | E-113 |

| | | |
|--------------------------------------|---|-------|
| E.14.81 | 45-OO: Channels to be printed..... | E-132 |
| E.14.82 | 46-OO: Rods to be printed..... | E-132 |
| E.14.83 | 47-OO: Fuel nodes to be printed..... | E-132 |
| E.14.84 | 48-NP: This card is obsolete..... | E-132 |
| E.14.85 | 49-NP: Fuel nodal powers..... | E-133 |
| E.14.86 | 50-NP: Coolant nodal powers..... | E-133 |
| E.14.87 | GCC: End input data and start calculation..... | E-133 |
| E.15 | Card Group HOSCAM..... | E-133 |
| E.15.1 | HOS1: HOSCAM Dimensions..... | E-134 |
| E.15.2 | HOS2: Spacer Grid Definitions..... | E-134 |
| E.15.3 | HOS3: Fuel Rod Types..... | E-134 |
| E.15.4 | HOS4: Fuel Rod Geometries and Pressure Loss Coefficients..... | E-134 |
| E.16 | References..... | E-151 |
| Appendix F : Output Description..... | | F-1 |
| F.1 | COBRA-FLX ASCII Output Description..... | F-3 |
| F.2 | COBRA-FLX HDF Output Description..... | F-7 |
| F.2.1 | Group thermal_hydraulics..... | F-7 |

List of Tables

| | <u>Page</u> |
|--|-------------|
| Table A-1: The Szablewski Function RXD as a Function of Relative Entrance Length | A-4 |
| Table A-2: Definition of Variables Used in Figure A-1 | A-27 |
| Table A-3: Definition of Variables Used in Heat Transfer Coefficient Definitions | A-29 |
| Table A-4: Summary of Heat Transfer Coefficient/Flux Correlations | A-38 |
| Table C-1: CHF Correlation Identifications Throughout the COBRA-FLX Topical Report | C-4 |
| Table C-2: Comparison of COBRA-FLX based and LYNXT based DNBRL Values for the ACH-2 CHF Correlation | C-9 |
| Table C-3: Comparison of COBRA-FLX Based and LYNXT Based DNBRL Values for the BHTP CHF Correlation | C-13 |
| Table C-4: Description of CHF Correlation Bases Using the BWU Correlation Form within the BAW-10199 Topical Report Revisions | C-14 |
| Table C-5: Comparison of COBRA-FLX based and LYNXT based DNBRL Values for the BWU-Z CHF Correlation for the Mark-BW17 Fuel with Mid-Span Mixing Grids | C-18 |
| Table C-6: Individual DNBRL Calculated for Each Pressure Group with the BWU-Z CHF Correlation for the Mark-BW17 Fuel Using COBRA-FLX | C-22 |
| Table C-7: Pressure Range Dependent Design Limits for the BWU-Z CHF Correlation for the Mark-BW17 Fuel Using COBRA-FLX and LYNXT | C-22 |
| Table C-8: Mark-BW17 Test Program Supporting the BWCMV-A Correlation and the Optimal Effective Grid Spacing | C-24 |
| Table C-9: Comparison of COBRA-FLX based and LYNXT based DNBRL Values for the BWCMV-A CHF Correlation | C-27 |
| Table C-10: Comparison of COBRA-FLX based and LYNX2 based DNBRL Values for the BWCMV CHF Correlation | C-31 |
| Table C-11: Individual DNBRL Calculated for Each Pressure Group with the BWU-N CHF Correlation for Non-Mixing Grids Using COBRA-FLX | C-35 |
| Table C-12: Individual DNBRL Calculated for Each Pressure Group with the BWU-N CHF Correlation for Non-Mixing Grids Using LYNX2 | C-35 |
| Table C-13: Pressure Range Dependent Design Limits for the BWU-N CHF Correlation for Non-Mixing Grids Using COBRA-FLX and LYNX2 | C-36 |
| Table C-14: Influence of the Grid Intersection CHF Test on the BWU-N Data Base | C-37 |
| Table C-15: Comparison of COBRA-FLX based and LYNX2 based DNBRL Values for the BWC CHF Correlation | C-41 |
| Table C-16: Proportion of the 15x15 BWC Data Base for Each Bundle Test Type | C-42 |
| Table C-17: Local Conditions and Design Limits for Various Correlations Using COBRA- FLX | C-43 |
| Table D-1: Input keywords for COBRA-FLX group_0_solver | D-5 |

| | |
|---|-------|
| Table D-2: Input keywords for COBRA-FLX group_0_general | D-7 |
| Table D-3: Input keywords for COBRA-FLX group_1_coolant | D-9 |
| Table D-4: Input keywords for COBRA-FLX coolant_properties..... | D-11 |
| Table D-5: Input keywords for COBRA-FLX group_2_flow_correlations | D-14 |
| Table D-6: Input keywords for COBRA-FLX group_3_power_distribution..... | D-20 |
| Table D-7: Input keywords for COBRA-FLX group_3.2_hot_channel_factors..... | D-22 |
| Table D-8: Input keywords for COBRA-FLX group_4_channels..... | D-25 |
| Table D-9: Input keywords for COBRA-FLX channels..... | D-26 |
| Table D-10: Input keywords for COBRA-FLX gaps_with_local_coupling_parameters | D-28 |
| Table D-11: Input keywords for COBRA-FLX group_5_channel_area_variation..... | D-30 |
| Table D-12: Input keywords for COBRA-FLX group_5.1_channel_area_variation_data..... | D-31 |
| Table D-13: Input keywords for COBRA-FLX group_6_gap_variation | D-34 |
| Table D-14: Input keywords for COBRA-FLX group_6.1_gap_variation_data | D-35 |
| Table D-15: Input keywords for COBRA-FLX group_7_spacer | D-39 |
| Table D-16: Input keywords for COBRA-FLX group_8_rod_data | D-44 |
| Table D-17: Input keywords for COBRA-FLX chf_data | D-55 |
| Table D-18: Input keywords for COBRA-FLX fuel_thermal_properties..... | D-77 |
| Table D-19: Input keywords for COBRA-FLX fuel_rod_models..... | D-80 |
| Table D-20: Input keywords for COBRA-FLX group_9_calculation_variables..... | D-96 |
| Table D-21: Input keywords for COBRA-FLX pv_solution_variables..... | D-101 |
| Table D-22: Input keywords for COBRA-FLX group_10_mixing..... | D-106 |
| Table D-23: Input keywords for COBRA-FLX group_11_operating_conditions..... | D-110 |
| Table D-24: Input keywords for COBRA-FLX set_point_parameters I..... | D-117 |
| Table D-25: Input keywords for COBRA-FLX sensitivity_parameters..... | D-118 |
| Table D-26: Input keywords for COBRA-FLX group_12_output_options | D-119 |
| Table E-1: Roadmap of the Key Inputs for AREVA U.S. Licensing Analyses..... | E-1 |
| Table F-1: Overview of COBRA-FLX Output File Content..... | F-2 |
| Table F-2: COBRA-FLX Data Types and Abbreviations for HDF Output..... | F-7 |
| Table F-3: Sub-groups in Group <i>thermal_hydraulics</i> | F-9 |
| Table F-4: Description of Stored Data in Group <i>thm_input</i> | F-11 |
| Table F-5: Description of Stored Data in Group <i>summary_results</i> | F-43 |
| Table F-6: Description of Stored Data in Group <i>bundle_averaged_results</i> | F-45 |
| Table F-7: Description of Stored Data in Group <i>crossflow_results</i> | F-46 |
| Table F-8: Description of Stored Data in Group <i>channel_results</i> | F-47 |

| | |
|---|------|
| Table F-9: Description of Stored Data in Group <i>chf_channel_results</i> | F-48 |
| Table F-10: Description of Stored Data in Group <i>chf_axial_results</i> | F-49 |
| Table F-11: Description of Stored Data in Group <i>rod_results</i> | F-50 |

List of Figures

| | <u>Page</u> |
|--|-------------|
| Figure A-1: COBRA-FLX's Heat Transfer Selection Logic Flowchart | A-24 |
| Figure B-1: Lineage of the AREVA Subchannel Codes | B-7 |
| Figure C-1: Timeline of CHF Correlation Approval and Spacer Grid Applicability | C-2 |
| Figure C-2: Measured CHF versus Predicted CHF for the ACH-2 CHF Correlation Using COBRA-FLX | C-6 |
| Figure C-3: Histogram of Measured to Predicted Values for the ACH-2 CHF Correlation Using COBRA-FLX | C-7 |
| Figure C-4: Predicted CHF versus Measured CHF for the BHTP CHF Correlation Using COBRA-FLX | C-11 |
| Figure C-5: Histogram of Predicted to Measured Values for the BHTP CHF Correlation Using COBRA-FLX | C-12 |
| Figure C-6: Measured CHF versus Predicted CHF for the BWU-Z CHF Correlation for Mark-BW17 Fuel with Mid-Span Mixing Grids Using COBRA-FLX | C-15 |
| Figure C-7: Histogram of Measured to Predicted Values for the BWU-Z CHF Correlation for Mark-BW17 Fuel with Mid-Span Mixing Grids Using COBRA-FLX | C-16 |
| Figure C-8: Measured CHF versus Predicted CHF for the BWU-Z CHF Correlation for Mark-BW17 Fuel Using COBRA-FLX | C-20 |
| Figure C-9: Histogram of Measured to Predicted Values for the BWU-Z CHF Correlation for Mark-BW17 Fuel Using COBRA-FLX | C-21 |
| Figure C-10: Measured CHF versus Predicted CHF for the BWCMV-A CHF Correlation Using COBRA-FLX | C-25 |
| Figure C-11: Histogram of Measured to Predicted Values for the BWCMV-A CHF Correlation Using COBRA-FLX | C-26 |
| Figure C-12: Measured CHF versus Predicted CHF for the BWCMV CHF Correlation Using COBRA-FLX | C-29 |
| Figure C-13: Histogram of Measured to Predicted Values for the BWCMV CHF Correlation Using COBRA-FLX | C-30 |
| Figure C-14: Predicted CHF versus Measured CHF for the BWU-N CHF Correlation for Non-Mixing Grid Fuel Using COBRA-FLX | C-33 |
| Figure C-15: Histogram of Measure to Predicted Values for the BWU-N CHF Correlation for Non-Mixing Vaned Fuel Using COBRA-FLX | C-34 |
| Figure C-16: Predicted CHF versus Measured CHF for the BWC CHF Correlation for 15x15 Geometry Fuel Using COBRA-FLX | C-39 |
| Figure C-17: Histogram of Measure to Predicted Values for the BWC CHF Correlation for 15x15 Geometry Fuel Using COBRA-FLX | C-40 |
| Figure E-1: Example Input Using Free Format | E-136 |
| Figure F-1: Example of ASCII Output File | F-51 |

Nomenclature

| Acronym | Definition |
|----------------|---|
| AO | Axial Offset |
| BWR | Boiling Water Reactor |
| CHF | Critical Heat Flux |
| CPU | Central Processing Unit |
| DNB | Departure from Nucleate Boiling |
| DNBR | Departure from Nucleate Boiling Ratio |
| DNBRL | Departure from Nucleate Boiling Ratio Limit |
| IAPWS | International Association for the Properties of Water and Steam |
| IBDCF | Inter-bundle Diversion Crossflow |
| ICE | Implicit Continuous Fluid Eulerian |
| KBF | Key Based Format |
| KWU | Kraftwerk Union |
| LOCA | Loss of Coolant Accident |
| LWR | Light Water Reactor |
| MDNBR | Minimum Departure from Nucleate Boiling Ratio |
| M/P | Measured to Predicted |
| MSMG | Mid-Span Mixing Grid |
| N | Number of axial locations |
| NC | Number of Subchannels |
| NG | Number of Gaps |
| P | Pressure |
| PV | Pressure-Velocity |
| PWR | Pressurized Water Reactor |
| RAI | Request for Additional Information |
| SER | Safety Evaluation Report |
| SLB | Steam Line Break |
| SOR | Successive Over-Relaxation |
| T-H | Thermal-Hydraulic |
| THM | Thermal-Hydraulic Module |
| U.S. NRC | United States Nuclear Regulatory Commission |
| V | Axial Velocity |

| Acronym | Definition |
|--------------------|--|
| SUBSCRIPTS | |
| <i>COBRA-FLX</i> | Calculated with COBRA-FLX |
| <i>I</i> | Index of the axial location in the hottest subchannel |
| <i>LYNXT</i> | Calculated with LYNXT |
| <i>Test</i> | Calculated with the experimental pressure measurements |
| <i>XCOBRA-IIIC</i> | Calculated with XCOBRA-IIIC |

Equation Nomenclature

| Acronym | Definition |
|-----------------|---|
| A | Assembly bare rod flow area |
| $A_{i,j}$ | Subchannel flow area at ends of mass cell |
| A_+, A_- | Axial flow area at boundary of momentum cell |
| $\bar{A}_{i,j}$ | Average flow area for momentum cell |
| $\bar{A}_{k,j}$ | Average lateral flow area at subchannel boundary |
| A_t | Transverse direction flow area |
| A_w | Wall surface area |
| C_k | Crossflow resistance for gap k |
| C_p | Specific heat |
| C_{pl} | Specific heat of liquid phase |
| C_Q | Fraction of rod power generated directly in coolant |
| C_T | Parameter for modeling fluid stresses between subchannels |
| $C_{U_{i,j}}$ | Axial pressure coefficient |
| $C_{V_{i,j}}$ | Lateral pressure coefficient |
| D | Mixture mass equation residual |
| D_e | Equivalent hydraulic diameter |
| D_r | Rod diameter |
| D_{hy}, d_h | Hydraulic diameter = $\frac{4A}{P_w}$ |
| D_H | Heated diameter = $\frac{4A}{P_H}$ |
| E | Mixture energy equation residual |
| e_{ik} | Switch function |
| F | Mass flow |
| F_g | Mass flow rate of vapor |
| $F_{i,j}$ | Axial mass flow rate |
| F_l | Liquid axial mass flow rate |
| F_t | Momentum turbulent shear factor crossflow mixing |
| F_v | Vapor axial mass flow rate |
| F_w | Momentum wall friction term |
| f | Darcy friction factor |

| Acronym | Definition |
|-------------------------------|---|
| f' | Friction factor |
| f_{lam} | Laminar flow friction factor |
| f_{urb} | Turbulent flow friction factor |
| G | Mass flux or mass velocity |
| G_g, G_v | Mass flux of vapor |
| G_{in} | Inlet mass flux |
| G_l | Mass flux of liquid |
| g, \bar{g} | Acceleration of gravity |
| H_{SAT} | Enthalpy of saturated fluid |
| h | Enthalpy |
| \hat{h} | Static enthalpy |
| h_c | Heat transfer coefficient |
| h_{fg} | Enthalpy of vaporization |
| h_f, h_g | Liquid and vapor saturation phase enthalpy |
| $h_{i,j}$ | Mixture enthalpy (flowing) |
| $h_{l,i,j}, h_{v,i,j}$ | Phase enthalpy |
| k | Thermal conductivity |
| K_G | Lateral friction coefficient |
| K_{ll} | Local loss coefficient |
| K_{ij}, K_{IJ} | Crossflow resistance for a gap with reference centroid distance |
| l_k | Centroid distance for gap k |
| $l_{ref_beta}, l_{ref_KIJ}$ | Reference centroid distance |
| M | Mass |
| M_l | Mass of liquid |
| M_v | Mass of vapor |
| M_x | Axial momentum residual |
| M_y | Lateral momentum residual |
| NC | number of subchannels |
| NG | number of gaps |
| P | Pressure |
| P_H | Heated perimeter |
| $P_{i,j}$ | Pressure relative to reference pressure |
| P_w | Wetted perimeter |

| Acronym | Definition |
|---------------------|---|
| ΔP | Pressure drop |
| q | Power |
| q' | Linear heat generation rate |
| q'' , \bar{q}'' | Heat transfer per unit area |
| q_{mix} | Heat transfer due to inter-channel turbulent mixing |
| q_w'' | Wall heat flux |
| q''' | Power per unit volume |
| r | Radial distance |
| Re | Reynolds number = $\frac{4F}{\mu P_w}$ |
| s | Rod-to-rod spacing (gap size) |
| $[S]$ | matrix with switch elements (e_{ik}) |
| S_A | Control volume surface area |
| S_f | Fluid-to-fluid surface area |
| $s_{k,j}$ | Actual rod gap spacing |
| $\bar{s}_{k,j}$ | Effective rod gap spacing for lateral momentum cell |
| T | Temperature |
| T_b | Bulk temperature |
| T_f | Fluid temperature |
| T_w | Wall temperature |
| ΔT | Bulk fluid temperature difference across cladding |
| Δt | Time increment |
| u | Internal energy |
| U | Axial velocity |
| U_g | Vapor velocity |
| $\hat{U}_{i,j}$ | Axial momentum velocity |
| U_l | Liquid axial velocity |
| U_v | Vapor axial velocity |
| V | Transverse velocity |
| V_{LM} | Volume of the lateral-momentum control volume |
| Vol, V | Mixture volume |
| Vol_f | Volume of the fluid control volume |
| Vol_l, V_l | Liquid volume |
| Vol_v, V_v | Vapor volume |

| Acronym | Definition |
|--------------------|---|
| \vec{v} | Velocity vector |
| $\hat{V}_{k,j}$ | Lateral momentum velocity |
| $v'_{i,j}, v'$ | Specific volume for momentum |
| $v'^*_{i,j}$ | Specific volume for momentum assigned to axial mass cell boundary |
| $v'^*_{k,j}$ | Specific volume for momentum assigned to lateral mass cell boundary |
| w | Lateral mass flow rate per unit length |
| $W_{k,j}$ | Lateral crossflow rate, $w_{k,j}\Delta x_j$ |
| $w_{k,j}$ | Lateral crossflow rate per unit length |
| $W'_{k,j}$ | Turbulent crossflow rate, $w'_{k,j}\Delta x_j$ |
| $w'_{k,j}, w'$ | Turbulent crossflow rate per unit length |
| x | Flowing quality |
| x_e | Thermodynamic quality |
| x_j | Axial distance |
| α | Void fraction |
| α_l | Liquid volume fraction |
| α_v | Vapor volume fraction (equivalent to α) |
| β_m | Turbulent mixing parameter |
| Δx | Axial space increment |
| ε_i | Eddy diffusivity |
| θ | Angle from horizontal |
| ϕ_{im} | Perimeter fraction associated with subchannel |
| $\varphi_{i,n}$ | Power fraction from rod n to subchannel i |
| μ | Viscosity |
| μ_f, μ_g | Phase viscosities |
| μ_{lw} | Liquid viscosity at wall temperature |
| μ_l | Liquid viscosity |
| μ_v | Vapor viscosity |
| v_f | Specific volume of saturated water |
| v_g | Specific volume of saturated steam |
| v_l | Specific volume of liquid |
| ρ_f, ρ_g | Saturation phase density |
| $\rho_{i,j}, \rho$ | Mixture density |
| ρ_l | Liquid density |

| Acronym | Definition |
|--------------------------------------|---|
| ρ_v | Vapor density |
| $\bar{\rho}$ | Two-phase density = $\alpha\rho_g + (1-\alpha)\rho_f$ |
| σ | Surface tension |
| τ_w | Shear stress at wall |
| $\bar{\tau}$ | Viscous shear stress in fluid |
| Φ_{lp}^2 | Two-phase local multiplier for components |
| l | Subchannel-to-subchannel centroid distance |
| Operators: | |
| $D_{k,i}$ | Rod to subchannel power fraction |
| \Leftarrow | Replacement — same function as '=' in FORTRAN |
| $\bar{\nabla}$ | Vector gradient operator |
| Subscripts: | |
| f | Saturated liquid |
| g | Saturated vapor |
| i | Subchannel i |
| ii | Subchannel ii |
| $ii(k), i(k)$ | Channel pair for gap k |
| $jj(k), j(k)$ | |
| i, j | Subchannel i , axial location j |
| j | Axial location j |
| jj | Subchannel jj |
| k | Gap k |
| k, j | Gap k , axial location j |
| l | Liquid |
| v | Vapor |
| w | Wall |
| Superscripts and Overstrikes: | |
| n | Time level n (old time) |
| $-$ | Average |
| \sim | Tentative assignment |
| $*$ | Donor assignment |
| \rightarrow | Vector |

1.0 INTRODUCTION

The COBRA-FLX core thermal-hydraulic code is the latest development by AREVA for performing nuclear core thermal-hydraulic simulations. The code reflects the availability of a core thermal-hydraulic tool that can meet the needs for not just U.S. pressurized water reactor (PWR) applications, but also for AREVA global PWR simulation needs. COBRA-FLX is the thermal-hydraulic code module for the core simulator ARTEMIS within the ARCADIA[®] code package in Reference 1-1, shown in Figure 1-1 that was developed for worldwide application of a converged code system within AREVA for neutronic and thermal-hydraulic core design and safety evaluation.

The COBRA-FLX code is being supported by a separate topical report for the U.S. Nuclear Regulatory Commission's (USNRC) review and approval primarily for logistical reasons and for potential future revisions, if needed. The code has been developed not only for stand-alone applications, where all inputs can be manually defined by the user, but also for coupled neutronic/thermal-hydraulic applications such as those defined and described in Section 4 of Reference 1-1 for the ARCADIA code package. The COBRA-FLX topical report supports the stand-alone application with descriptive information regarding the code's problem formulation, structure, verification, and validation, and technical information for validating the critical heat flux correlation applications.

AREVA selected the COBRA 3-CP code as the foundation for COBRA-FLX because COBRA 3-CP was previously selected as the thermal-hydraulic code basis for developing a coupled code system in Europe. In addition, COBRA 3-CP is a well-established thermal-hydraulic code in support of reload applications.

The COBRA 3-CP code, developed by Siemens/KWU, was originally built upon the COBRA-IIIC/MIT-2 code release. In order to serve the worldwide applications for AREVA PWR customers, COBRA-FLX has been developed to include versatile computational capabilities that can meet the full range of thermal-hydraulic evaluations needed to support safety-related analyses. These capabilities range from the simple

modeling of a core for general hydraulic calculations, where each fuel assembly is represented by a single channel, to an extensively detailed full core subchannel-by-subchannel modeling for calculating local conditions on a fuel rod/subchannel basis. COBRA-FLX possesses a collection of empirical correlations for fluid models and flow properties that allow the computation of pertinent fluid and heat transfer characteristics that are necessary to accurately simulate local fluid conditions for operational and safety-related analyses.

Three basic numerical solution methods are identified within the topical report, however, only two of them are technically supported within the topical report. They are the SCHEME-Pressure (P) solution, formulated to arrive at a system of equations which can be solved for the axial pressure differences, and the Pressure-Velocity (PV) solution to aid in simulating low flow, including flow recirculation, situations such as the steam line break (SLB) transient with no forced pump flow. In addition, the SCHEME-Pressure (P) solution method can be further improved to handle full-core subchannel-by-subchannel models through the utilization of a successive over-relaxation method and a more effective linear system solver.

In order to support thermal-hydraulic reload analyses, numerous critical heat flux (CHF) correlation are incorporated into COBRA-FLX for application with various fuel assembly designs. The validation of these CHF correlations using COBRA-FLX local conditions is provided in Appendix C of the report.

This topical report is structured with four additional sections and six appendices.

| | |
|------------|---|
| Section 2 | Problem Formulation |
| Section 3 | Code Structure and Flow Logic Description |
| Section 4 | Subroutine Description |
| Section 5 | Verification and Validation |
| Appendix A | Empirical Correlations |
| Appendix B | COBRA-FLX Development History |
| Appendix C | Critical Heat Flux Correlation Validation |
| Appendix D | Input Description of Keyword Based Format |

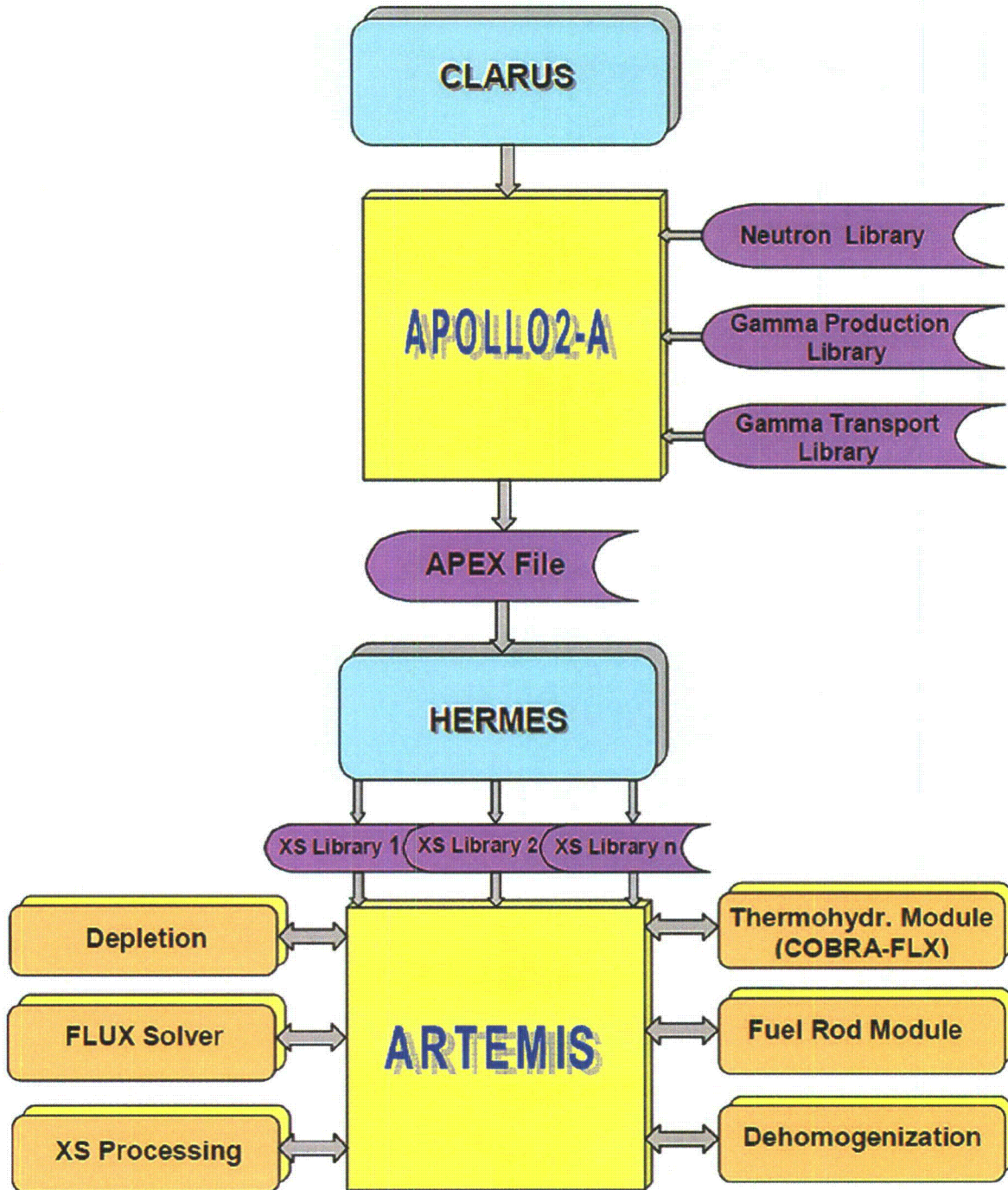
Appendix E

Input Description of Conventional Format

Appendix F

Output Description

Figure 1-1: ARCADIA® Code System



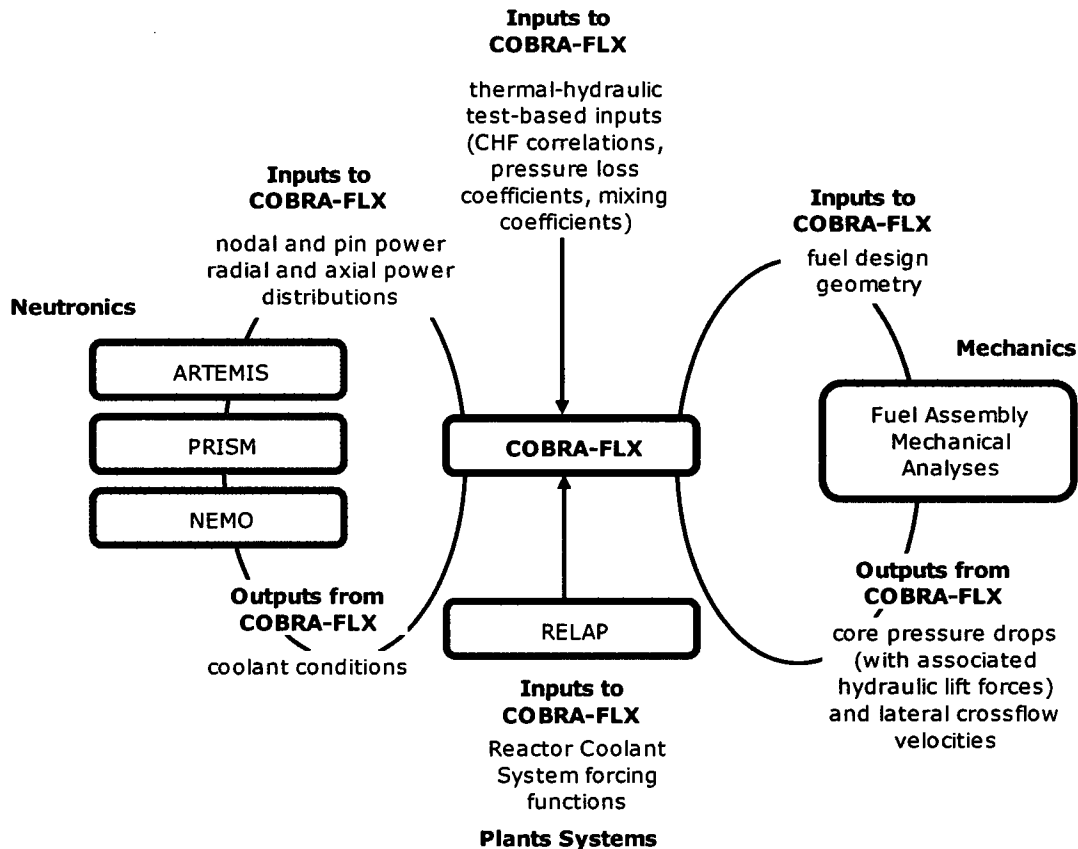
1.1 Code Applications

The COBRA-FLX code is intended to replace the current subchannel codes XCOBRA-IIIIC, Reference 1-2, and LYNXT, Reference 1-3, within the methodology applications where they are now applied. The general application of the COBRA-FLX code for safety-related analyses would include the determination of:

- core flow redistributions
- core and fuel assembly pressure drops
- lateral crossflow velocities
- core coolant conditions, e.g., for neutronic feedback
- minimum Departure from Nucleate Boiling Ratio (DNBR)
- steady-state thermal-hydraulic core conditions
- transient event thermal-hydraulic core conditions

An example of the typical COBRA-FLX input and output interfaces for U. S. application is shown in Figure 1-2. Inputs for safety-related analyses from neutronic and reactor coolant system codes will be provided from NRC approved codes.

Figure 1-2: Typical COBRA-FLX U.S. Application Input/Output Interfaces



1.2 Requested Code Review and Approval

Since COBRA-FLX is based primarily on the COBRA 3-CP code developed by Siemens/KWU, it possesses numerous parameter options that go beyond those necessary to perform PWR safety analyses in the U.S. An example of these extended options is the inclusion of various CHF correlations that are available for investigative purposes but are not being validated within this topical report for review by the NRC. The inclusion of such capabilities in this topical report is intentional for completeness and maintenance as an AREVA global code. Therefore, it is necessary to define the extent of the requested NRC review and approval of COBRA-FLX. Table 1-1 defines the extent of the requested code review and approval for several code characteristics.

Further details associated with the specific empirical correlations to be used within COBRA-FLX are shown in Table 1-2. These two tables are complimented by a “roadmap” for code user input in Table E-1 that defines the key input parameters for requested U.S. reload licensing.

Table 1-1: The Extent of the COBRA-FLX Review and Approval Requests

| Characteristic | Description |
|--------------------------------|---|
| Plant Type Application | Pressurized Water Reactors |
| AREVA CHF Correlations | Eight (8) AREVA-specific correlations validated in Appendix C |
| Two Numerical Solution Methods | SCHEME-Pressure (P) solution method (Section 2.3.1.4) and the Pressure-Velocity (PV) solution method (Section 2.3.2) |
| Steady-State Applications | For safety-related hydraulic and thermal-hydraulic calculations |
| Transient Applications | For safety-related transient analyses where a core surface heat flux transient forcing function is provided by an NRC approved code since the fuel rod model within COBRA-FLX will not be used for safety-related analyses (see below). |
| Fuel Rod Model | COBRA-FLX possesses a fuel rod model which can be observed in the code Input Description (Appendices D and E) and Output Description (Appendix F). This fuel rod model will not be used for safety-related analyses, therefore, AREVA is not requesting its review or approval. |
| No Re-wet | COBRA-FLX possesses a rewetting model, however, this model will not be used for safety-related analyses, therefore, AREVA is not requesting its review or approval. |

Table 1-2: Empirical Correlation Application for Requested Review and Approval

| Empirical Correlation Used for Safety-Related Analyses |
|--|
| Water Properties <ul style="list-style-type: none"> • IAPWS 97 |
| Friction Factor Correlation Constants <ul style="list-style-type: none"> • Lehman friction factor (with or without Szablewski correction) • Wall viscosity correlation option for the wall friction factor |
| Two-Phase Friction Multiplier <ul style="list-style-type: none"> • Homogeneous model |
| Bulk Void Correlation <ul style="list-style-type: none"> • Chexal-Lellouche void correlation using the full curve fit routine or tables with interpolation |
| Subcooled Void Option <ul style="list-style-type: none"> • Saha-Zuber subcooled void correlation |
| Subcooled Boiling Profile Fit <ul style="list-style-type: none"> • Zuber-Staub profile fit |

1.3 *References*

- 1-1 ANP-10297P, The ARCADIA™ Reactor Analysis System for PWRs Methodology Description and Benchmarking Results, AREVA, March 2010.
- 1-2 XN-75-21(P)(A), Rev. 2, XCOBRA-IIIC: A Computer Code to Determine the Distribution of Coolant During Steady-State and Transient Core Operation, Exxon Nuclear Company, Inc., March 1985.
- 1-3 BAW-10156-A, Rev. 1, LYNXT Core Transient Thermal-Hydraulic Program, B&W Fuel Company, August 1993.

2.0 PROBLEM FORMULATION AND SOLUTION

Section 2 describes the derivation of the flow field solution from the basic conservation principles of mass, energy, and momentum. Section 2.1 presents the mixture balance equations and the major assumptions used in their derivation. The subchannel formulation of the basic equations is discussed in Section 2.2. The numerical solution methodology is described in Section 2.3. The steady-state and transient boundary conditions are discussed in Section 2.4.

2.1 *Mixture Balance Equations*

In this section, the general transient balance laws for mass, energy and axial momentum for a single-component two-phase mixture are considered. The governing equations for subchannel geometry will be derived from integral balance on an arbitrary fixed (Eulerian) volume. The basic balance laws are presented, assumptions about the relative importance of various terms that are applied, and the set of integral equations is cast in terms of the geometry to be considered.

2.1.1 *Two-Phase Flow Definitions*

The integral balances are formed on an arbitrary Eulerian control volume, V , that is bounded by a fixed surface, A . The surface A may consist of both a solid boundary and a fluid boundary, but all solid material is outside V . The solid material thus excluded from the volume V is considered by the conduction model. The fluid in volume V is assumed to be a single-component two-phase mixture of liquid and vapor in thermodynamic equilibrium. The control volume is illustrated in Figure 2-1. A picture of the flow of a two-phase mixture is given in Figure 2-2. As shown in Figure 2-2, the mixture is flowing past fuel rods with diameter D_r , wetted perimeter P_W , heated perimeter P_H , and associated cross-sectional flow area A . In a fuel rod array the wetted perimeter includes all the solid surfaces within the bundle plus the bundle wall if present. The heated perimeter includes all the fuel rod surfaces. The vapor occupies the volume V_v and the liquid occupies the volume V_l . The vapor and liquid are

assumed to be uniformly distributed throughout the flow field and variations of the properties of the fluid across the flow channel, normal to the primary flow direction, are neglected. The primary flow is upward in the direction x parallel to the channel walls.

The local composition of the mixture is described by the space-averaged vapor volume fraction. The volume fraction occupied by the vapor per unit volume of the mixture in the control volume, the void fraction, is denoted by α_v :

$$\alpha_v = \frac{V_v}{V}. \quad 2-1$$

The volume fraction occupied by the liquid is then

$$\alpha_l = 1 - \alpha_v. \quad 2-2$$

Figure 2-1: Arbitrary Eulerian Control Volume

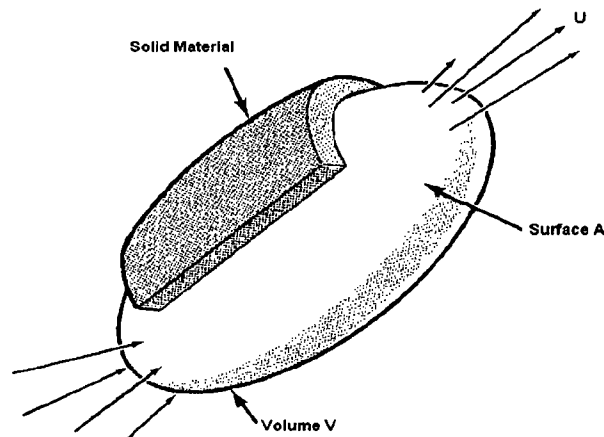
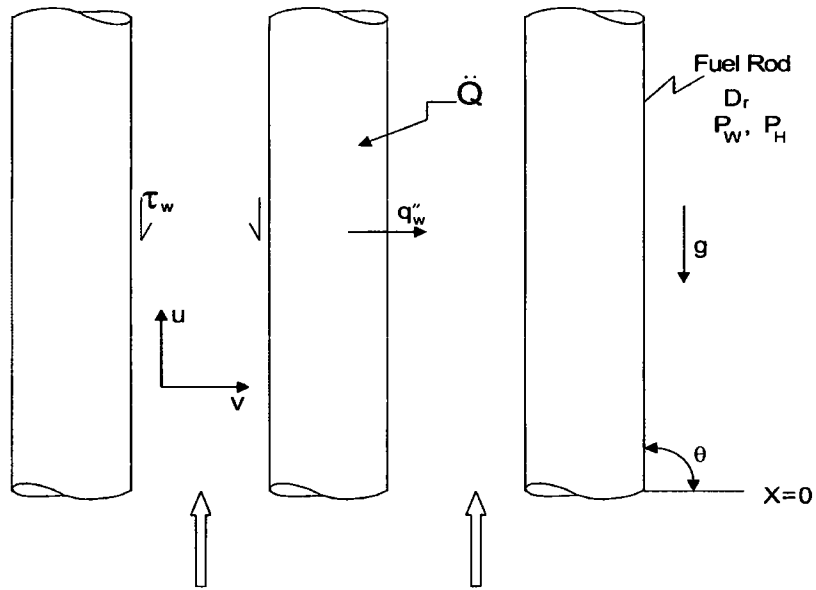


Figure 2-2: Vertical Flow Past Fuel Rods



The mass flow rate of the vapor in the primary flow direction is denoted by F_v , and of the liquid F_l . These flow rates are

$$F_v = \alpha_v \rho_v U_v A \tag{2-3}$$

for the vapor, and

$$F_l = (1 - \alpha_v) \rho_l U_l A \tag{2-4}$$

for the liquid. The mass flow rate of the mixture of liquid plus vapor in the primary flow direction is

$$F = F_v + F_l \tag{2-5}$$

Two components of the velocity vector are used in the COBRA-FLX code - the component parallel to the rod array, U , and the component transverse to the primary direction, V . The definitions given above will be further explained as the need arises in the description of the COBRA-FLX models.

The flowing quality, the ratio of the vapor mass flow rate to the mixture mass flow rate in the primary flow direction, is

$$\chi = \frac{F_v}{F} = \frac{F_v}{F_v + F_l} \quad 2-6$$

The basic-equation models in COBRA-FLX require that the flowing quality in the primary and transverse directions be equal.

The mass of the mixture of liquid plus vapor, $M = \rho V$, in the control volume is

$$M = M_v + M_l, \quad 2-7$$

where the mass of the vapor is

$$M_v = \alpha_v \rho_v V \quad 2-8$$

and the mass of liquid is

$$M_l = (1 - \alpha_v) \rho_l V. \quad 2-9$$

Putting Equations 2-8 and 2-9 into Equation 2-7 gives the density of the mixture

$$\rho = \alpha_v \rho_v + (1 - \alpha_v) \rho_l. \quad 2-10$$

The density of each phase in Equation 2-10 is a function of two independent thermodynamic properties, the pressure and temperature, for example. The equation of state and the transport properties used in COBRA-FLX are discussed later in this report.

Using Equations 2-3 and 2-4 the flowing quality of Equation 2-6 can be written as

$$\chi = \frac{\alpha_v \rho_v U_v}{\alpha_v \rho_v U_v + (1 - \alpha_v) \rho_l U_l}, \quad 2-11$$

which gives the void fraction in terms of the flow quality to be

$$\alpha_v = \frac{1}{1 + \left(\frac{1 - \chi}{\chi} \right) \frac{\rho_v U_v}{\rho_l U_l}}, \quad 2-12$$

where the ratio of the vapor velocity to the liquid velocity, U_v/U_l , is the slip ratio. (This corresponds to the slip void fraction model. Other void fraction models are also available.) The basic equation development used for the code requires that the slip ratio in the axial and lateral directions be the same value.

The equations and definitions given above can also be written in terms of the mass flux. The mass flux of each constitute of the mixture is

$$G_v = \chi G = \alpha_v \rho_v U_v \quad 2-13$$

for the vapor, and

$$G_l = (1 - \chi)G = (1 - \alpha_v) \rho_l U_l \quad 2-14$$

for the liquid. The mass flux of the mixture of liquid plus vapor is

$$G = \frac{F}{A}. \quad 2-15$$

The mass flux is convenient for describing flows in constant area channels.

Useful relationships between the mass flux, the flow quality, and the void fraction are as follows. From Equation 2-13, the velocity component of the vapor in the primary flow direction is

$$U_v = \frac{\chi G}{\alpha_v \rho_v} \quad 2-16$$

and Equation 2-14 gives the liquid velocity

$$U_l = \frac{(1-\chi)G}{(1-\alpha_v)\rho_l} \quad 2-17$$

The velocity component of the mixture in the primary flow direction can be determined by substitution using Equations 2-5, 2-10, 2-15, and $F = \rho UA$

$$U = \frac{\alpha_v \rho_v}{\rho} U_v + \frac{(1-\alpha_v)\rho_l}{\rho} U_l \quad 2-18$$

Equations 2-16 and 2-17 give quantities of interest for the momentum balance

$$\alpha_v \rho_v U_v^2 = \frac{\chi^2 G^2}{\alpha_v \rho_v} \quad 2-19$$

for the vapor phase, and

$$(1-\alpha_v)\rho_l U_l^2 = \frac{(1-\chi)^2 G^2}{(1-\alpha_v)\rho_l} \quad 2-20$$

for the liquid phase. Equations 2-19 and 2-20 can be written in terms of the mass flow rate, F , by use of Equation 2-15.

The sum of Equations 2-19 and 2-20 provides the momentum flux for the mixture of liquid plus vapor

$$\alpha_v \rho_v U_v^2 + (1-\alpha_v)\rho_l U_l^2 = G^2 \left[\frac{\chi^2}{\alpha_v \rho_v} + \frac{(1-\chi)^2}{(1-\alpha_v)\rho_l} \right] \quad 2-21$$

The quantity in square brackets on the right-hand side of Equation 2-21 is the effective specific volume for momentum

$$v' = \left[\frac{\chi^2}{\alpha_v \rho_v} + \frac{(1-\chi)^2}{(1-\alpha_v) \rho_l} \right]. \quad 2-22$$

The quantities developed in this section will be used in the two-phase flow model for COBRA-FLX.

2.1.2 *Local-Instantaneous Navier-Stokes Equations*

The subchannel-flow model equations used in the COBRA-FLX code are derived from the local-instantaneous formulation of the three-dimensional Navier-Stokes equations. These latter equations are given here without derivation. Derivation of the subchannel form from the local three-dimensional form is given following the local equations.

The mass conservation equation, or the continuity equation, for the fluid is

$$\frac{\partial}{\partial t} \rho + \vec{\nabla} \cdot \rho \vec{V} = 0 \quad 2-23$$

where the vector gradient operator is

$$\vec{\nabla} = \vec{i} \frac{\partial}{\partial x} + \vec{j} \frac{\partial}{\partial y} + \vec{k} \frac{\partial}{\partial z} \quad 2-24$$

and the velocity vector is

$$\vec{V} = \vec{i} V_x + \vec{j} V_y + \vec{k} V_z, \quad 2-25$$

where i , j , and k are unit vectors in the x , y , and z directions, respectively. In this report the x -direction is the primary flow direction and the velocity component $V_x = U$.

The y -direction is transverse to the primary flow direction and $V_y = V$.

The dot product of the $\vec{\nabla}$ operator and the velocity vector is

$$\vec{\nabla} \cdot \rho \vec{V} = \frac{\partial}{\partial x} \rho V_x + \frac{\partial}{\partial y} \rho V_y + \frac{\partial}{\partial z} \rho V_z. \quad 2-26$$

Putting Equation 2-26 into 2-23 gives

$$\frac{\partial}{\partial t} \rho + \frac{\partial}{\partial x} \rho V_x + \frac{\partial}{\partial y} \rho V_y + \frac{\partial}{\partial z} \rho V_z = 0. \quad 2-27$$

Two forms of the basic fluid flow equations are used in the COBRA-FLX code - the conservative and transportive forms. The conservative form of the mass conservation equation is the form used above. The transportive form is obtained by expanding the spatial derivative in Equation 2-23 to get

$$\frac{\partial}{\partial t} \rho + \rho \vec{\nabla} \cdot \vec{V} + \vec{V} \cdot \vec{\nabla} \rho = 0 \quad 2-28$$

or

$$\frac{D}{Dt} \rho + \rho \vec{\nabla} \cdot \vec{V} = 0, \quad 2-29$$

where

$$\frac{D}{Dt} \rho = \frac{\partial}{\partial t} \rho + V_x \frac{\partial}{\partial x} \rho + V_y \frac{\partial}{\partial y} \rho + V_z \frac{\partial}{\partial z} \rho \quad 2-30$$

and can also be obtained from Equation 2-27. The transportive form of the mass conservation equation is used to get the transportive forms of the momentum and energy equations.

The momentum balance for the fluid is

$$\frac{\partial}{\partial t} \rho \vec{V} + \vec{\nabla} \cdot \rho \vec{V} \vec{V} = -\vec{\nabla} P + \vec{\nabla} \cdot \vec{\tau} + \rho \vec{g} \quad 2-31$$

where P is the pressure and $\vec{\tau}$ is the viscous shear stress in the fluid. Equation 2-31 represents the three components of the momentum balance equations. The individual components will be used as required in development of the basic-equation model used

in COBRA-FLX. Neglecting the effects of compressibility on the viscous shear stresses, Equation 2-31 can be written as

$$\frac{\partial}{\partial t} \rho \vec{V} + \vec{\nabla} \cdot \rho \vec{V} \vec{V} = -\vec{\nabla} P + \mu \vec{\nabla}^2 \cdot \vec{V} + \rho \vec{g} \quad 2-32$$

where

$$\vec{\nabla}^2 = \frac{\partial^2}{\partial x^2} + \frac{\partial^2}{\partial y^2} + \frac{\partial^2}{\partial z^2} \quad 2-33$$

and the vector product of Equation 2-33 with the velocity vector \vec{V} gives the three components of the fluid shear stress needed for the components of the momentum equations.

The transportive form of the momentum balance is obtained by expanding the derivatives on the left-hand side of Equation 2-32 and subtracting the transportive form of the mass conservation equation, multiplied by the velocity vector, from the expanded momentum balance. This process gives

$$\rho \frac{D}{Dt} \vec{V} = -\vec{\nabla} P + \mu \vec{\nabla}^2 \cdot \vec{V} + \rho \vec{g} \quad 2-34$$

The x - and y -direction components of the left-hand side of Equation 2-34 are

$$\rho \frac{D}{Dt} V_x = \rho \frac{\partial}{\partial t} V_x + \rho V_x \frac{\partial}{\partial x} V_x + \rho V_y \frac{\partial}{\partial y} V_x + \rho V_z \frac{\partial}{\partial z} V_x$$

and

2-35

$$\rho \frac{D}{Dt} V_y = \rho \frac{\partial}{\partial t} V_y + \rho V_x \frac{\partial}{\partial x} V_y + \rho V_y \frac{\partial}{\partial y} V_y + \rho V_z \frac{\partial}{\partial z} V_y,$$

respectively.

The internal energy equation for the fluid is

$$\frac{\partial}{\partial t} \rho u + \vec{\nabla} \cdot \rho u \vec{V} = -\vec{\nabla} \cdot \vec{q}'' + q''' + P \vec{\nabla} \cdot \vec{V} + \Phi_{\mu} \quad 2-36$$

where \vec{q}'' is the conduction of heat in the fluid, q''' is the volumetric energy deposition directly into the fluid due to neutrons escaping from the fuel rods, and Φ_{μ} is the dissipation due to viscous stresses in the fluid. The heat conduction vector in the fluid is

$$\vec{q}'' = -k \left(\vec{i} \frac{\partial T_f}{\partial x} + \vec{j} \frac{\partial T_f}{\partial y} + \vec{k} \frac{\partial T_f}{\partial z} \right) \quad 2-37$$

where T_f is the fluid temperature, and its dot product with the $\vec{\nabla}$ operator gives

$$\vec{\nabla} \cdot \vec{q}'' = -k \left(\frac{\partial^2 T}{\partial x^2} + \frac{\partial^2 T}{\partial y^2} + \frac{\partial^2 T}{\partial z^2} \right) \quad 2-38$$

for constant thermal conductivity. Equation 2-36 is written in terms of the fluid enthalpy as

$$\frac{\partial}{\partial t} \rho h + \vec{\nabla} \cdot \rho h \vec{V} = -\vec{\nabla} \cdot \vec{q}'' + q''' + \frac{\partial P}{\partial t} + \vec{V} \cdot \vec{\nabla} P, \quad 2-39$$

where the viscous dissipation has been dropped as it is neglected in the COBRA-FLX model. The last two terms on the right-hand side of Equation 2-39 represent the pressure-volume work done by the fluid and this contribution to the energy equation is also neglected in the COBRA-FLX model.

The transportive form of the energy equation is obtained by expanding the derivatives on the left-hand side, multiplying the mass conservation equation by the fluid enthalpy, and subtracting the results of the latter operation from the expanded energy equation. Applying this process to the energy equation gives

$$\rho \frac{D}{Dt} h = -\vec{\nabla} \cdot \vec{q}'' + q'''$$

or

2-40

$$\rho \frac{\partial}{\partial t} h + \rho V_x \frac{\partial}{\partial x} h + \rho V_y \frac{\partial}{\partial y} h + \rho V_z \frac{\partial}{\partial z} h = -\vec{\nabla} \cdot \vec{q}'' + q''' .$$

The basic fluid flow equations are supplemented with the equation of state for the fluid that gives the density and temperature as functions of two independent variables. The transport properties for the fluid are also functions of the fluid state. Generally, the density and temperature are given by

$$\rho = \rho(P, h) \quad 2-41$$

and

$$T = T(P, h) \quad 2-42$$

and the viscosity and thermal conductivity are

$$\mu = \mu(P, T) \quad 2-43$$

and

$$k = k(P, T) , \quad 2-44$$

respectively.

For turbulent flows the Navier-Stokes equations must be augmented with models for the turbulence. For almost all engineering flows the effects of turbulence are usually accounted for by use of empirical correlations for the friction factor and heat transfer coefficient which are valid for turbulent flow conditions. This is the approach used in the COBRA-FLX modeling.

2.1.3 *Averaging Operators*

The fully three-dimensional Navier-Stokes equations given in the previous section are not generally used for engineering analyses of fluid flows in fuel rod arrays. A variety of averaging methods are instead applied to the equations so that a more convenient system of equations is obtained. The methods that are usually applied to the local Navier-Stokes equations for applications to fuel rod arrays include the porous-media approach and the subchannel-geometry approach. The former method distributes the embedded fuel rods into the averaged equations and results in a system of three-dimensional equations for the flow field. The latter method acknowledges the geometry of the fuel rod array and the resulting equations contain directly the geometric features of the rod array. The COBRA-FLX code utilizes the latter averaging method.

Some basic common mathematical operations are needed for either averaging method. The primary objective is to relate the local-instantaneous equations, which apply to the microscopic-level of detail in the flow field, to flow-channel average equations that are more readily useful in engineering analyses. Detailed developments are not given here.

A control volume of the size of the subchannels is shown in Figure 2-3. As shown in the figure, the fluid in the control volume is bounded by a surface that includes both portions of the fuel rods and additional fluid. The fluid within the control volume interacts with both the fuel rods and the fluid at its bounding surfaces. The complete specification of the surface bounding the fluid in the control volume will be given as development of the equations proceeds.

The Gauss theorem relating the volume integral of spatial derivatives to surface integrals is

$$\int_{\text{Vol}_f} \frac{\partial}{\partial x_k} \Psi d\bar{V} = \int_{S_A} \Psi n_k d\bar{A}, \quad 2-45$$

where Vol_f is the control volume occupied by the fluid, S_A is the surface area bounding the control volume, and Ψ is any scalar, vector, or tensor property per unit volume for

the fluid. The Gauss theorem is used to transform the spatial gradients in the local equations given in the previous section. The resulting integration over the surface bounding the control volume gives the transport of the property into and out of the control volume. The specification of the surface area bounding the fluid in the control volume is given in the development of the COBRA-FLX subchannel equations in the next section of this report.

The Reynolds transport theorem is used to relate the integral of a temporal derivative to the derivative of an integral. For the control volume of interest in the present work, the Reynolds transport theorem shows that the order of the derivative and integral operators can be interchanged.

Applying a volume-averaging operator to the local-instantaneous equations in the previous section and using the Gauss theorem gives the following results.

The mass conservation of Equation 2-23 becomes

$$\frac{\partial}{\partial t} \int_{\text{Vol}_f} \rho d\bar{V} + \int_{S_A} \rho (\vec{V} \cdot \vec{n}) d\bar{A} = 0 \quad 2-46$$

The momentum balance of Equation 2-31 becomes

$$\frac{\partial}{\partial t} \int_{\text{Vol}_f} \rho \vec{V} d\bar{V} + \int_{S_A} \rho \vec{V} (\vec{V} \cdot \vec{n}) d\bar{A} = - \int_{S_A} P \vec{n} d\bar{A} + \int_{S_A} (\vec{\tau} \cdot \vec{n}) d\bar{A} + \int_{\text{Vol}_f} \rho \vec{g} d\bar{V} \quad 2-47$$

The enthalpy form of the energy conservation of Equation 2-39 becomes

$$\frac{\partial}{\partial t} \int_{\text{Vol}_f} \rho h d\bar{V} + \int_{S_A} \rho h (\vec{V} \cdot \vec{n}) d\bar{A} = - \int_{S_A} (\vec{q}''' \cdot \vec{n}) d\bar{A} + \int_{\text{Vol}_f} \dot{q}''' d\bar{V} \quad 2-48$$

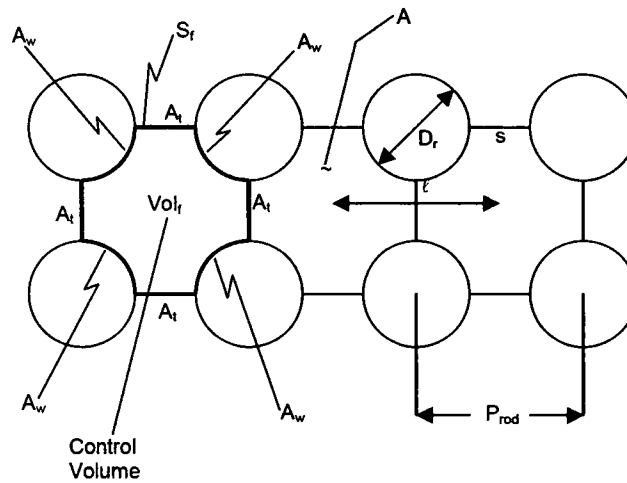
The following simplifying assumptions have been applied to the Equations 2-46, 2-47, and 2-48:

- The flow is at sufficiently low speed such that kinetic and potential energy are small compared to internal thermal energy;
- Work done by the body forces and shear stresses in the energy equation are small compared to surface heat transfer and convective energy transport;
- Heat conduction through the fluid surface is assumed small compared to convective energy transport and heat transfer from solid surfaces;
- The phases are in thermodynamic equilibrium. ($T_l = T_v = T_{sat}$ when both phases are present);
- Gravity is the only significant body force in the momentum equation;
- Viscous shear stresses between fluid elements are assumed small compared to the drag force on solid surfaces;
- The fluid is incompressible but thermally expandable.

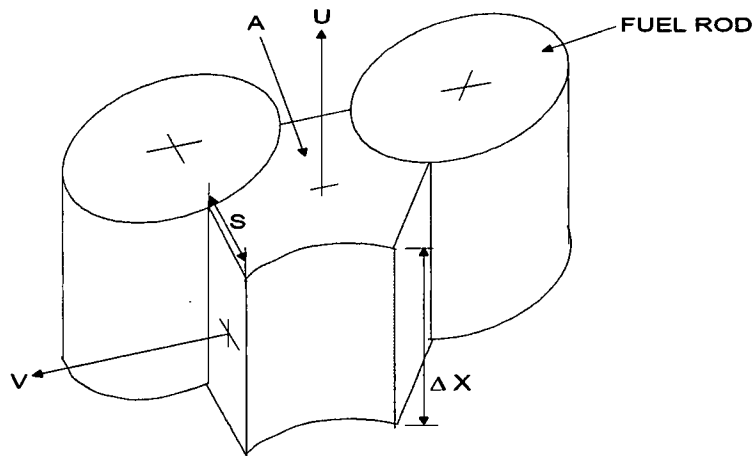
The conservative form of the basic fluid flow equations have been used in the above developments. Generally, the subchannel form of the basic equations used in COBRA-FLX is developed from the conservative formulation. The numerical solution methods generally are based on the transportive form.

The general volume-average results given here are specialized to the rod-array case in the following discussions. The specifications of the surface bounding the fluid and integration of the averaged equations over the area will give the subchannel, centered equation models used in COBRA-FLX.

Figure 2-3: Subchannel Control Volume



(a) Plane View - Square Array



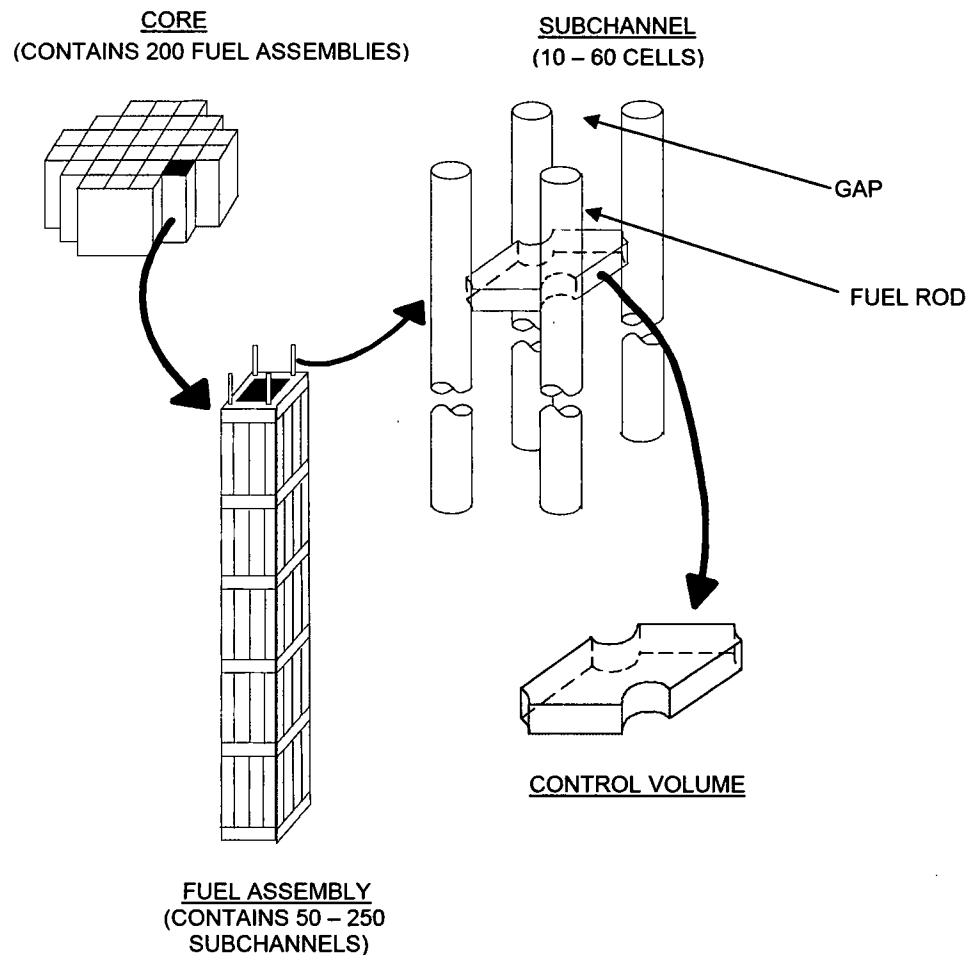
(b) Perspective View - Triangular Array

2.2 Subchannel Formulation of the Basic Equations

In a nuclear reactor core, fluid flow is constrained by the surfaces of closely spaced fuel rods oriented parallel to the primary axial flow direction. On a small scale, the fuel rods

partition the flow area into many small subchannels that communicate laterally by crossflow, momentum exchange and enthalpy exchange through narrow gaps. The control volume for the conservation equations is a segment of a subchannel, as illustrated in Figure 2-4, in relation to the rest of the core.

Figure 2-4: Relation of Subchannel Control Volume to Reactor Core



To derive the subchannel equations, the integral balances given by Equations 2-46, 2-47, and 2-48 are applied to a typical subchannel control volume. Empirical correlations are used where necessary to close the set. The result is a system of subchannel equations which will be numerically solved by applying finite-difference approximations.

The subchannel formulation of the COBRA-FLX basic equations is derived in the following Sections. The equations are obtained from the volume-average equations given in Section 2.1.3.

2.2.1 Fuel Rod Array Geometry

The geometry of the averaging method is shown in Figure 2-3. The size of the averaging volume is of the same scale as a subchannel, so the details of the flow field on a scale smaller than this are not resolved by the modeling. The small scale details needed for applications to rod arrays will be represented by models and engineering correlations (i.e., friction factors, local loss coefficients, heat transfer coefficients, and subchannel-to-subchannel mixing). The subchannel approach is directly analogous to the one-dimensional flow approach used for almost all engineering modeling of fluid flows in simple channels like round tubes.

The major geometric parameters in the subchannel approach are the rod-to-rod spacing or the gap size between the rods, s ; the subchannel-to-subchannel centroid distance, l ; and the flow area of the subchannels in the primary flow direction (see Figure 2-3). The rod diameter, D_r ; rod-to-rod pitch, P_{rod} ; pitch-to-diameter ratio; wetted and heated perimeters; and wetted and heated equivalent diameters will generally enter the empirical correlations for friction factors, heat transfer coefficients, and subchannel mixing.

The geometry of the rod array need not be regular in the coordinate directions (i.e., rectangular and triangular arrays can be handled just as well as square arrays). Special subchannels are usually encountered in practical applications to nuclear reactor cores as subchannels adjacent to array shrouds along the sides and in the corners will be different from centrally-located subchannels. Fuel rod arrays also contain special purpose rods for control and instrumentation purposes. Consequently, the geometric features listed above can vary throughout the array so they are defined as functions of the location within the array.

The fluid control volume is defined by the flow area of the subchannel in the primary flow direction and the axial increment, Δx

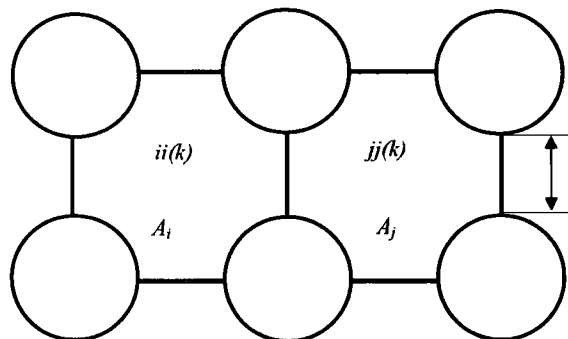
$$\text{Vol}_f = A \Delta x. \quad 2-49$$

If the flow area changes in the axial direction, a suitable average value can be used in the definition of the control volume. The COBRA-FLX code can handle variable flow area.

As shown in Figure 2-3, the surface area bounding the fluid control volume, S_f , is comprised of the wall surfaces of adjacent fuel rods and the interface in the fluid between adjacent subchannels. The wall surface is denoted by A_w and the fluid-to-fluid surface is denoted by S_f . S_f is further delineated as portions in the primary axial flow direction, A , and in the transverse direction perpendicular to the axial direction, A_t . The transverse flow area is associated with each subchannel in the transverse direction that is connected to the subchannel of interest. The flow area for the transverse crossflow is given by the gap spacing times the axial increment

$$A_t = s \Delta x. \quad 2-50$$

Since the orientation of the gap between subchannels is completely arbitrary, a sign convention for the lateral crossflows must be developed. The convention is based on the subchannel numbering scheme used in the COBRA-FLX code. The lateral velocity is directed by its gap such that positive crossflow is by definition an inflow to one subchannel and an outflow from the other. A pair of subchannels denoted by $ii(k)$ and $jj(k)$ are connected by a gap denoted by k ; where $ii(k)$, $jj(k)$, and k are integers. The general approach is shown in Figure 2-5.

Figure 2-5: A Pair of Subchannels

A positive crossflow is from subchannel $ii(k)$ to subchannel $jj(k)$, where $ii(k)$ is the smaller integer. To account for this convention, a switch function (e_{ik}) is defined so that $e_{ik} = 1$ if the subchannel index (i) is smaller than that of its neighbor ($i = ii(k)$) and $e_{ik} = -1$ if the subchannel index (i) is larger than that of its neighbor ($i = jj(k)$).

Therefore, $e_{ik} = 1$ indicates that positive crossflow is out of subchannel i and $e_{ik} = -1$ indicates that positive crossflow is into subchannel i . A specific example is shown in Figure 2-6.

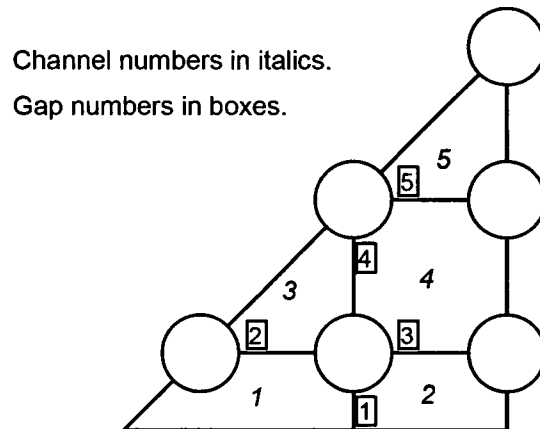
It is assumed that any lateral flow is directed by the gap it flows through and loses its sense of direction after leaving the gap region. That is, the gradient of the flow field properties is not resolved in the transverse direction. This assumption provides the basic character of the subchannel equation system. It allows subchannels to be connected arbitrarily, since no fixed lateral coordinate is required. A fully three-dimensional physical situation may be represented by connecting channels in a three-dimensional array. Since crossflow may exist only between two adjacent channels, no external lateral boundary conditions are required.

The basic assumptions of the mathematical model used in the COBRA-FLX code include:

-
- One-dimensional, two-phase, separated, slip-flow exists in each subchannel during boiling;
 - Turbulent crossflow exists between adjacent subchannels that results in no net flow redistribution;
 - The turbulent crossflow may be superimposed upon a diversion crossflow between subchannels that results from flow redistribution;
 - The two-phase flow structure is fine enough to allow specification of void fraction as a function of enthalpy, pressure, coolant flow rate, axial position, and time;
 - Sonic velocity propagation effects are ignored;
 - The lateral velocity component is assumed to go to zero at the center of the subchannels.

The equations of the fluid mathematical model are derived by using the above assumptions and by applying the general equations of continuity, energy, and momentum to a fluid control volume within an arbitrary subchannel.

The general volume-averaged equations given in the previous section are specialized to the rod-array case in the following sections.

Figure 2-6: Example of Subchannel Numbering

| k | <i>i(k)</i> | <i>j(k)</i> | $e_{i,k}$ | $e_{j,k}$ |
|---|-------------|-------------|-----------|-----------|
| 1 | 1 | 2 | 1 | -1 |
| 2 | 1 | 3 | 1 | -1 |
| 3 | 2 | 4 | 1 | -1 |
| 4 | 3 | 4 | 1 | -1 |
| 5 | 4 | 5 | 1 | -1 |

In an uniform array of rods and channels there are also uniform (input) values for the crossflow resistance C_k , for the turbulent mixing β_m and the lateral momentum

parameter $\frac{s}{l}$. In a non-uniform array of rods and channels, e.g. lumped channels of

different sizes, uniform values for these parameters are not adequate. Therefore, COBRA-FLX has lateral scaling models for the generation of local values for these parameters. The lateral scaling models are based on the geometrical configuration as defined in COBRA-FLX input deck. They are described in the following subsections.

2.2.1.1 Lateral scaling of crossflow resistance factor

The lateral scaling of crossflow resistance is implemented by using the following relation

$$C_k = KIJ \left(\frac{l_k}{l_{REF_KIJ}} \right) \quad 2-51$$

where

C_k is the crossflow resistance for gap k

KIJ is the crossflow resistance for a gap with reference centroid distance. The value of KIJ is assumed to account for both wall friction and the effects of the fuel rod wall curvature as the flow passes between the subchannel gaps.

l_k is the centroid distance for gap k

l_{REF_KIJ} is a reference centroid distance

Equation 2-51 assures that the crossflow resistance is proportional to the number of rod rows between channel centroids.

2.2.1.2 Lateral scaling of turbulent mixing

The lateral scaling of turbulent mixing is implemented by using the following relation

$$\beta_k = \beta \left(\frac{l_{REF_beta}}{l_k} \right) \quad 2-52$$

where

β_k is the turbulent mixing coefficient for gap k

β is the turbulent mixing coefficient for a gap with reference centroid distance

l_k is the centroid distance for gap k

l_{REF_beta} is a reference centroid distance

Equation 2-52 assures that the turbulent mixing is inversely proportional to the number of rod rows between channel centroids.

2.2.1.3 *Lateral scaling of the lateral momentum parameter*

The lateral scaling of the lateral momentum parameter is implemented by using the following relation

$$\left(\frac{s}{l}\right)_{k,j} = \left(\frac{s}{l}\right) \left(\frac{sgap_{k,j}}{l_k}\right) \quad 2-53$$

where

$\left(\frac{s}{l}\right)_{k,j}$ is the local gap width divided by the centroid distance between channels for gap k at elevation j.

$\left(\frac{s}{l}\right)$ is the global gap width to centroid distance ratio, which is automatically set to 1.0, if scaling is applied.

$sgap_{k,j}$ is the local width of gap k at elevation j.

l_k is the centroid distance for gap k.

The setting $\left(\frac{s}{l}\right) = 1.0$ in Equation 2-53 assures that the parameter $\left(\frac{s}{l}\right)_{k,j}$ is computed

locally as the local gap width divided by the centroid distance between the channels adjacent to the gap.

2.2.2 Subchannel Mass Conservation Equation

With the rod-array subchannel geometry and specification of the surface area bounding the subchannel control volume given above, mass conservation of Equation 2-46 becomes

$$\frac{\partial}{\partial t} \int_{\text{Vol}_f} \rho d\bar{V} + \int_A \rho(\vec{V} \cdot \vec{n}) d\bar{A} + \int_{s\Delta x} \rho(\vec{V} \cdot \vec{n}) d\bar{A} = 0 \quad 2-54$$

as there is no fluid flow across the wall surfaces. Performing the integrations in Equation 2-54 gives

$$A\Delta x \frac{\partial}{\partial t} \rho + [(\rho UA)_{x+\Delta x} - (\rho UA)_x] + \sum_{k \in i} e_{ik} \rho V_s \Delta x = 0 \quad 2-55$$

where the summation in the last term on the left-hand side is over all transverse gaps, k , associated with the control volume, Vol_f . Each transverse rod-to-rod gap can have a different gap width specified. The gradient of the mass flow rate in the transverse direction is not resolved and these flows represent sources and sinks for the primary axial flow. The lateral velocity component is assumed to go to zero at the center of the subchannels.

Dividing Equation 2-55 by Δx and taking the limit as Δx approaches zero gives

$$A \frac{\partial}{\partial t} \rho + \frac{\partial}{\partial x} \rho UA + \sum_{k \in i} e_{ik} \rho V_s = 0 \quad 2-56$$

or

$$A \frac{\partial}{\partial t} \rho + \frac{\partial}{\partial x} F + \sum_{k \in i} e_{ik} w = 0, \quad 2-57$$

where F is the mass flow rate of the two-phase mixture in the axial primary direction

$$F = \rho UA \quad 2-58$$

and w is the mass flow per unit length in the lateral direction through the gaps

$$w = \rho V_s . \quad 2-59$$

The axial and lateral flow rates are defined in terms of the average fluxes. Area and volume averages are assumed to be equivalent. The mixture density is defined in terms of the phase densities and vapor volume fraction ($\rho = \alpha\rho_v + (1 - \alpha)\rho_l$); the volume and area averages are assumed to be equal and the phase distribution uniform.

The last term on the left-hand side of Equation 2-57 is the sum over all gap connections of the lateral mass flow rate per unit length. This term is the diversion crossflow mixing, or crossflow, associated with subchannel analysis.

The subchannel application method employs three coolant mass flow rates in the description of the flow field in the rod array. The axial mass flow rate of the coolant, denoted by F , is the main flow of interest. The axial coolant flow is mainly upward and parallel to the rod surfaces and the x -direction is generally assigned to that flow. The flow is taken as positive for vertical upflow in the array. There are two additional mass flow rates that are transverse to the main axial direction and these are responsible for distribution of the coolant across the array.

The transverse mass flows are carried by velocity components normal to the primary flow direction and represent flows between the subchannels. Two mechanisms are considered to create the transverse mass flows: (1) pressure gradients between subchannels that provide the potential for bulk diversion crossflow with net mass exchange, and (2) turbulent fluctuations in the axial flow that provide turbulent mass exchanges between subchannels without net mass exchange. The transverse crossflows are generally small compared to the axial mass flow rate in the absence of major changes in flow channel geometry such as that due to flow blockage.

2.2.2.1 *Diversion Crossflow*

Geometry variations and non-uniform changes in fluid density can establish transverse pressure gradients between subchannels. Geometry variations include fuel rod bowing and swelling and the possibility that design features introduce variations in the subchannel flow area or the axial pressure gradient. Mixing vane spacer grids, for example, are designed to divert flow from one subchannel into another. The fluid density is most greatly affected by the presence of boiling. Variations in the radial and axial heat flux distribution can result in boiling onset in some subchannels while the fluid in adjacent subchannels remains in the subcooled-liquid state. After boiling starts the pressure gradient in the boiling subchannel will differ from that in the non-boiling subchannels. The resulting difference will effect the crossflow between the subchannels.

The diversion crossflow rate is determined by the basic model equations for the fluid flow. The lateral momentum balance equation to be given later is used for this purpose. Diversion crossflow results in a net change in the mass flow rates for the involved subchannels. The diversion crossflow will be denoted by w hereafter.

2.2.2.2 *Turbulent Interchange*

Turbulent interchange is postulated to be associated with turbulent eddies that move between the rod gaps. For the single-phase flow case physics dictates that there is no net exchange of mass between the subchannels. For two-phase boiling flows, this is not the case given the disparate densities of the liquid and vapor phases. However, the assumption made by the COBRA-FLX model of no net mass exchange leads to the exclusion of turbulent interchange in the mass conservation equation. Additionally, while no net mass exchange is assumed, the eddies carry with them momentum and energy and these are available to the subchannels taking part in the exchange. The momentum and energy exchange modeling will be discussed later.

Unlike the diversion crossflow, the turbulent interchange is not obtained from the basic fluid flow equations. An empirical description is used instead and is specified outside

the basic equation framework. The model is the usual approach for subchannel analysis codes such as COBRA-FLX. The turbulent interchange will be denoted by w' hereafter.

2.2.3 Subchannel Momentum Balance Equations

The volume-average momentum balance of Equation 2-47 can be simplified with the specification of the surface area that bounds the fluid control volume. There is no fluid flow across the walls of the fuel rods, so the second term on the left-hand side is of interest only on the fluid surfaces. The pressure gradient, the first term on the right-hand side, contributes both at the solid walls and within the fluid. The viscous shear stresses are not resolved within the fluid in the axial direction so the second term on the right-hand side is represented by the stresses due to the solid fuel rod walls and viscous stresses within the fluid at the interface between subchannels. The last term on the right-hand side is a volumetric source and acts throughout the fluid volume.

Applying the above modeling to Equation 2-47 gives

$$\frac{\partial}{\partial t} \int_{\text{Vol}_f} \rho \bar{V} d\bar{V} + \int_{A+A_s} \rho \bar{V} (\bar{V} \cdot \bar{n}) d\bar{A} = - \int_{A+A_s} P \bar{n} d\bar{A} - \int_{A_w} P \bar{n} d\bar{A} + \int_{A_w} (\bar{\tau} \cdot \bar{n}) d\bar{A} + \int_{A+A_s} (\bar{\tau} \cdot \bar{n}) d\bar{A} + \int_{\text{Vol}_f} \rho \bar{g} d\bar{V} \quad 2-60$$

There are two component directions of interest - the axial primary flow component and the lateral, gap-directed crossflow component. The momentum balance for the axial component will be discussed first. The lateral component, which requires a modified control volume, will be discussed following that.

2.2.3.1 Axial Momentum Equation

The momentum balance for the axial component direction is developed from Equation 2-60 in the following discussion. Descriptions of the pressure and shear forces acting on the control volume and the turbulent momentum mixing are required.

The volume integral of the momentum in the primary flow direction, ρU , is

$$\frac{\partial}{\partial t} \int_{\text{Vol}_f} \rho U d\bar{V} = A \Delta x \frac{\partial}{\partial t} \rho U. \quad 2-61$$

The momentum flux, the second term on the left-hand side, in the axial direction is

$$\int_{A+A_t} \rho \vec{V} (\vec{V} \cdot \vec{n}) d\bar{A} = [(\rho U^2 A)_{x+\Delta x} - (\rho U^2 A)_x] + \sum_{k \in i} e_{ik} \rho U V_s, \quad 2-62$$

where the fluid surface area bounding the control volume has been decomposed into the axial and transverse portions.

The wall and fluid pressure forces in the axial direction sum to give

$$- \int_{A+A_t} P \vec{n} d\bar{A} - \int_{A_w} P \vec{n} d\bar{A} = -A [P_{x+\Delta x} - P_x]. \quad 2-63$$

If the flow area varies in the axial direction an average value can be used.

The viscous shear stresses acting on the fuel rod walls, the third term on the right-hand side of Equation 2-60, are modeled with a friction factor and local loss coefficient as

$$\int_{A_w} (\vec{\tau} \cdot \vec{n}) d\bar{A} = -\frac{1}{2} (f' \Delta x P_w + K_{ll} A) \rho U |U|. \quad 2-64$$

The friction factor, f' , represents the wall shear stress due to the flow parallel to the rods. The local loss coefficient, K_{ll} , represents the effects of local changes in the flow channel geometry. Grid spacers, for example, present obstacles that partially block the flow in the primary flow direction.

The wetted equivalent, or hydraulic, diameter is

$$D_{hy} = \frac{4A}{P_w}, \quad 2-65$$

where P_w is the wetted perimeter for the walls of the fluid subchannel. Equation 2-64 can be written as

$$\int_{A_w} (\bar{\tau} \cdot \bar{n}) d\bar{A} = -\frac{1}{2} \left(\frac{f_w}{D_{hy}} \Delta x + K_{II} \right) \rho U |U| A, \quad 2-66$$

where $f_w = 4f'$.

The viscous stresses acting within the fluid, the fourth term on the right side of Equation 2-60, are modeled as follows. In the axial flow areas at the entrance and exit of the control volume these stresses are neglected as assumed for COBRA-type subchannel codes - the velocity distribution within the fluid is not resolved and the wall-to-fluid friction is the dominant term. The difference between the average fluid velocities in adjacent subchannels, however, produces drag-like stresses at the fluid area between the subchannels. With this modeling, the fourth term becomes

$$\int_{A+A_i} (\bar{\tau} \cdot \bar{n}) d\bar{A} = -C_T \Delta x \sum_{k \in i} w' (\Delta U), \quad 2-67$$

where w' is the turbulent crossflow per unit length at the subchannel interface, ΔU , is the axial velocity difference between the subchannel of interest and an adjacent one, and C_T is a parameter for the modeling. The subchannel velocity difference is

$$\Delta U = \left(\frac{F}{\rho A} \right)_{ii} - \left(\frac{F}{\rho A} \right)_{jj}. \quad 2-68$$

The subchannel-to-subchannel force acts like a viscous shear due to the velocity difference between the subchannels. The COBRA-FLX model for w' is given later.

The volumetric body force, the last term on the right-hand side of Equation 2-60 gives

$$\int_{Vol_f} \rho \bar{g} d\bar{V} = -A \rho \Delta x g \cos \theta, \quad 2-69$$

where the axial component of gravity is evaluated by the angle θ . For $\theta = 0^\circ$ the positive axial flow is vertically upward and gravity opposes the flow. If $\theta = 90^\circ$, the axial flow is horizontal and gravity has no effect.

Putting Equations 2-61 to 2-64, 2-67, and 2-69 into Equation 2-70, dividing through by Δx and taking the limit as Δx approaches zero gives the axial flow momentum balance as

$$A \frac{\partial}{\partial t} \rho U + \frac{\partial}{\partial x} \rho U^2 A + \sum_{k \in i} e_{ik} \rho U V s = -A \frac{\partial P}{\partial x} - \frac{1}{2} \left(\frac{f_w}{D_{hy}} + K_{II} \right) \rho U |U| A - C_T \sum_{k \in i} w^k (\Delta U) - A \rho g \cos \theta \quad 2-70$$

Additional reduction and a few more definitions will be given below for the axial momentum balance of Equation 2-70 when the COBRA-FLX application procedure is outlined.

2.2.3.2 Lateral Momentum Balance

Development of the momentum balance for the lateral flow direction proceeds in the same manner as above. The lateral momentum balance models the diversion crossflow due to a pressure difference between adjacent subchannels. The control volume extends between the centers of two adjacent subchannels and the area available for transverse fluid flow is $s \Delta x$. The distance between the centers of the control volumes is denoted by l and the volume of the lateral-momentum control volume is $V_{LM} = l s \Delta x$.

The first two terms on the right-hand side of Equation 2-60 give the pressure difference between the adjacent subchannels

$$- \int_{A+A_i} P \bar{n} d\bar{A} - \int_{A_w} P \bar{n} d\bar{A} = [P_{I+\Delta l} - P_I] s \Delta x \quad 2-71$$

The fourth term on the right-hand side represents the viscous stresses in the fluid and is neglected as being small. The third term on the right-hand side gives the fluid-to-wall

momentum exchange due to viscosity at the fuel rod walls. It is modeled as an overall loss coefficient, K_G , which accounts for both friction and form drag caused by the area change

$$\int_{A_w} \vec{\tau} \cdot \vec{n} d\vec{A} = -\frac{1}{2} K_G \rho V |V| s \Delta x. \quad 2-72$$

The overall loss coefficient absorbs all the viscous and form drag associated with momentum exchange between the fluid and the wall due to the fluid motion through the gap.

The contribution due to gravity, the last right-hand-side term, is neglected based on the assumption that the primary flow direction is vertical in the rod array and thus the lateral motions are perpendicular to the gravity vector.

The first term on the left-hand side of Equation 2-60, the volume integral, gives

$$\frac{\partial}{\partial t} \int_{V_{LM}} \rho V d\vec{V} = l s \Delta x \frac{\partial}{\partial t} \rho V. \quad 2-73$$

The second term on the left-hand side is the momentum flux contributions to the momentum balance. The component of the momentum flux in the lateral direction due to motion in the lateral direction is assumed to be small and is neglected (i.e., the lateral component of the velocity vector goes to zero at the center of each subchannel). The component due to motion in the axial direction is modeled as

$$\int_A \rho \vec{V} (\vec{V} \cdot \vec{n}) d\vec{A} = [(\rho V U)_{x+\Delta x} - (\rho V U)_x] l s. \quad 2-74$$

Momentum exchange due to turbulent mixing is neglected in the lateral momentum balance.

Putting Equations 2-71 through 2-74 into the general momentum balance of Equation 2-60 gives the momentum balance in the lateral direction

$$s l \Delta x \frac{\partial}{\partial t} \rho V + [(\rho V U)_{x+\Delta x} - (\rho V U)_x] l s = [P_{l+\Delta l} - P_l] s \Delta x - \frac{1}{2} K_G \rho V |V| s \Delta x \quad 2-75$$

Dividing Equation 2-75 by $l \Delta x$ and taking the limit as Δx approaches zero gives the continuous form of the lateral momentum balance

$$s \frac{\partial}{\partial t} \rho V + s \frac{\partial}{\partial x} \rho V U = \frac{s}{l} [P_{l+\Delta l} - P_l] - \frac{1}{2} \frac{s}{l} K_G \rho V |V|. \quad 2-76$$

Additional reduction of the lateral momentum balance is given below when the COBRA-FLX application procedure is outlined.

2.2.4 Subchannel Energy Conservation Equation

Evaluation of the volume-averaged energy conservation Equation 2-48 is as follows.

The first term on the left-hand side is evaluated to be

$$\frac{\partial}{\partial t} \int_{\text{Vol}_l} \rho h d\bar{V} = A \Delta x \frac{\partial}{\partial t} \rho h. \quad 2-77$$

The spatial gradients, the second term on the left-hand side, account for transport between the subchannels due to fluid motion in the axial and lateral directions. The flow area in the axial direction is A and in the lateral directions $s \Delta x$. The integration over the fluid flow surfaces bounding the control volume gives

$$\begin{aligned} \int_{A+A_l} \rho h (\vec{V} \cdot \vec{n}) d\bar{A} &= \int_A \rho h U d\bar{A} + \int_{s\Delta x} \rho h V d\bar{A} \\ &= [(\rho h U A)_{x+\Delta x} + (\rho h U A)_x] + \Delta x \sum_{k \in i} e_{ik} (\rho h V) s \end{aligned} \quad 2-78$$

The conduction term, the first term on the right-hand side of Equation 2-48 gives the energy exchange between the fluid and the fuel rod surfaces. The surface area of a fuel rod facing the fluid in the control volume is the product of the length increment, Δx , its total heated perimeter, P_H , and the fraction, ϕ_{im} , of its total perimeter that actually

faces the control volume. Heat conduction within the fluid is neglected so the surface integral is evaluated over the fuel rod surfaces that bound the fluid control volume

$$- \int_{A_w} (\vec{q} \cdot \vec{n}) d\bar{A} = \Delta x \sum_{m \in i} \phi_{im} P_H q_w'' , \quad 2-79$$

where the summation is over the fuel rod surfaces, m , that bound the subchannel, i , of interest. Each heat transfer surface may have a different total heated perimeter, P_H ; perimeter fraction associated with the subchannel, ϕ_{im} ; and average heat flux, q_w'' .

The heat flux is given by

$$q_w'' = (1 - C_Q) q' / P_H \quad 2-80$$

and Equation 2-79 is

$$- \int_{A_w} (\vec{q} \cdot \vec{n}) d\bar{A} = \Delta x \sum_{m \in i} \phi_{im} (1 - C_Q) q' , \quad 2-81$$

where C_Q is the fraction of the rod power generated directly in the coolant and q' is the specified local linear heating rate for the fuel rod.

The direct deposition of energy into the coolant is a volumetric process and the last integral on the right-hand side gives

$$- \int_{Vol} q''' d\bar{V} = \Delta x \sum_{m \in i} C_Q \phi_{im} q' , \quad 2-82$$

where q' is the local linear heating rate for the fuel rod.

The final contribution to the fluid energy equation is the transport of energy between adjacent subchannels due to turbulent fluctuations in the coolant. As mentioned previously, the turbulent-transport fluid motion is not obtained from any basic equation in COBRA-FLX. The turbulent fluctuations are instead given by empirical modeling.

The turbulent energy exchange model is an empirical model that is not directly related to the basic integral balance equations. A time-fluctuating crossflow per unit length, w' , is computed as a fraction of the average axial flow. The fluctuating crossflow performs an equal mass exchange between adjacent control volumes. The fluctuating crossflow is related to the eddy diffusivity, ε_t , by

$$w' = \varepsilon_t \rho \left(\frac{s}{l} \right). \quad 2-83$$

In COBRA-FLX, w' is calculated with

$$w' = \beta_m s \bar{G}, \quad 2-84$$

where β_m is the turbulent mixing parameter and \bar{G} is the average mass flux in the adjacent subchannels. Other mixing models can be chosen by the user.

The energy transported by the turbulent fluctuations is

$$Q_m = \Delta x \sum_{k \in i} w'(\Delta h), \quad 2-85$$

where Δh is the enthalpy difference between the control volume of interest and an adjacent volume. The energy transport is an energy source term in the energy balance.

Putting Equations 2-77, 2-78, 2-79, 2-82, and 2-85 into the general volume average energy Equation 2-48 gives

$$A \frac{\partial}{\partial t} \rho h + \frac{\partial}{\partial x} \rho U h A + \sum_{k \in i} e_{ik} \rho V h s = \sum_{m \in i} \phi_{im} P_H q_w'' + \sum_{m \in i} C_Q \phi_{im} q - \sum_{k \in i} w'(\Delta h). \quad 2-86$$

This completes the derivation of the general subchannel equations for the fluid flow. In Section 2.2.5 and Section 2.3.2.1, these equations are specialized to the forms used in the COBRA-FLX code.

2.2.5 COBRA-FLX Basic Equations

The general equations given in the previous section are further modified to get the specific formulation used in the COBRA-FLX code.

2.2.5.1 Mass Conservation

The mass conservation Equation 2-57 is in the final form as used in COBRA-FLX, and is repeated here for completeness.

$$A \frac{\partial}{\partial t} \rho + \frac{\partial}{\partial x} F + \sum_{k \in i} e_{ik} w = 0. \quad 2-87$$

2.2.5.2 Momentum Balance Equations

The axial momentum balance of Equation 2-70 is written in terms of axial and lateral mass flow rates and the effective specific volume for momentum. The time derivative, the first term on the left-hand side, is already the axial mass flux. The momentum flux in the axial direction, the second term on the left-hand side is

$$\rho U^2 A = \frac{F^2}{A} v'. \quad 2-88$$

The momentum flux from the lateral mass flow rate, the third term on the left-hand side, is

$$\rho U V_s = \frac{F}{A} w v', \quad 2-89$$

where the specific volume for momentum is (Reference 2-1)

$$v' = \left[\frac{\chi^2}{\alpha_v \rho_v} + \frac{(1-\chi)^2}{(1-\alpha_v) \rho_l} \right]. \quad 2-90$$

The pressure gradient is in its final form. The wall-to-mixture friction and local pressure loss, the second and third terms on the right-hand side, are modified to account for two-

phase flow effects as follows. The wall friction is based on the use of two-phase friction multipliers with the liquid properties as the reference. The local loss uses the specific volume for momentum given just above. With these considerations, the wall-to-mixture momentum exchange is written

$$\frac{1}{2} \left(\frac{f_w}{D_{hy}} + K_{ll}' \right) \rho U^2 A = \frac{1}{2} \left(\frac{f_w}{D_{hy}} \frac{\Phi_{lp}^2}{\rho_l} + K_{ll}' v' \right) \frac{F^2}{A}, \quad 2-91$$

where Φ_{lp}^2 is the two-phase friction multiplier. F^2 is used in place of $F|F|$, since the standard COBRA-FLX does not consider axial flow reversal.

The subchannel-to-subchannel viscous drag and the volumetric forces due to gravity, the fourth and fifth terms on the right-hand side, are in the final forms.

Putting Equations 2-88, 2-89, and 2-91 into the axial momentum balance, Equation 2-70, gives

$$\begin{aligned} \frac{\partial}{\partial t} F + \frac{\partial}{\partial x} \frac{F^2}{A} v' + \sum_{k \in i} e_{ik} \frac{F}{A} w v' = -A \frac{\partial P}{\partial x} - \frac{1}{2} \left(\frac{f_w}{D_{hy}} \frac{\Phi_{lp}^2}{\rho_l} + K_{ll}' v' \right) \frac{F^2}{A} \\ - C_T \sum_{k \in i} w' \left[\left(\frac{F}{\rho A} \right)_i - \left(\frac{F}{\rho A} \right)_j \right] - A \rho g \cos \theta \end{aligned} \quad 2-92$$

Equation 2-92 can be further modified by taking into account that the fluid velocity at each channel i is related to the axial mass flow, specific volume and flow area as follows:

$$U_i = \frac{F_i v_i'}{A_i} \quad 2-93$$

Then the second term of the left side of Equation 2-92 can be replaced via:

$$\frac{\partial}{\partial x} \left(\frac{F^2}{A} v' \right) = \frac{\partial}{\partial x} \left(F^2 \frac{v'}{A} \right) = F^2 \frac{\partial}{\partial x} \left(\frac{v'}{A} \right) + \frac{v'}{A} 2F \frac{\partial F}{\partial x} = F^2 \frac{\partial}{\partial x} \left(\frac{v'}{A} \right) + 2U \frac{\partial F}{\partial x} \quad 2-94$$

Furthermore, using the mass conservation Equation 2-87, we obtain that

$$\frac{\partial}{\partial x} \left(\frac{F^2}{A} v' \right) = F^2 \frac{\partial}{\partial x} \left(\frac{v'}{A} \right) - 2UA \frac{\partial \rho}{\partial t} - 2U \sum_{k \in i} e_{ik} w \quad 2-95$$

Finally, using Equation 2-95 the axial momentum balance equation can be written as

$$\begin{aligned} \frac{\partial}{\partial t} F - 2UA \frac{\partial \rho}{\partial t} - 2U \sum_{k \in i} e_{ik} w + \sum_{k \in i} e_{ik} \frac{F}{A} w v' = -A \frac{\partial P}{\partial x} - \frac{1}{2} \left(\frac{f_w}{D_{hy}} \frac{\Phi_p^2}{\rho_l} + K_{ll} v' \right) \frac{F^2}{A} - F^2 \frac{\partial}{\partial x} \left(\frac{v'}{A} \right) \\ - C_T \sum_{k \in i} w' \left[\left(\frac{F}{\rho A} \right)_i - \left(\frac{F}{\rho A} \right)_j \right] - A \rho g \cos \theta \end{aligned} \quad 2-96$$

The momentum balance in the lateral direction, Equation 2-76, is rewritten as

$$\frac{\partial}{\partial t} w + \frac{\partial}{\partial x} w U = \frac{s}{l} [P_{l+\Delta l} - P_l] - \frac{1}{2} \frac{s}{l} K_G \frac{w|w|}{s^2 \rho} \quad 2-97$$

2.2.5.3 Energy Conservation

Energy conservation of Equation 2-86 is rearranged as follows. The mixture enthalpy in the time derivative, the static enthalpy, is

$$\hat{h} = \frac{1}{\rho} [\alpha_v \rho_v h_v + (1 - \alpha_v) \rho_l h_l] \quad 2-98$$

The axial enthalpy flux is

$$\rho U h = \alpha_v \rho_v U_v h_v + (1 - \alpha_v) \rho_l U_l h_l \quad 2-99$$

and the lateral enthalpy flux is

$$\rho V h = \alpha_v \rho_v V_v h_v + (1 - \alpha_v) \rho_l V_l h_l \quad 2-100$$

These can be written in terms of the flowing quality. If a single value of the flowing quality is to be used, it must be the same in the axial and lateral directions. This

assumption is used in the COBRA-FLX modeling and the mixture enthalpy based on the flowing quality is

$$h = \chi h_v + (1 - \chi)h_l, \quad 2-101$$

which gives the flowing quality

$$\chi = \frac{h - h_l}{h_v - h_l}. \quad 2-102$$

Tong, Reference 2-1, has shown that the static enthalpy and flowing enthalpy are related by

$$\Psi = \frac{\rho}{h_{fg}}(h - \hat{h}), \quad 2-103$$

where h_{fg} is the latent heat of vaporization for saturated conditions. This function is used to eliminate the static enthalpy from the energy equation in favor of the flowing enthalpy. The needed relationship is

$$\frac{\partial \rho \hat{h}}{\partial t} = \left(\rho - h_{fg} \frac{\partial \Psi}{\partial h} \right) \frac{\partial h}{\partial t} + h \frac{\partial \rho}{\partial t}. \quad 2-104$$

With the flowing enthalpy of Equation 2-101, and using Equation 2-104, the energy equation becomes

$$A \left[\left(\rho - h_{fg} \frac{\partial \Psi}{\partial h} \right) \frac{\partial h}{\partial t} + h \frac{\partial \rho}{\partial t} \right] + \frac{\partial}{\partial x} F h + \sum_{k \in i} e_{ki} w h = \sum_{m \in i} \phi_{im} P_H q_w'' + \sum_{m \in i} C_Q \phi_{im} q' - \sum_{k \in i} w' (h_i - h_k) \quad 2-105$$

The transportive form of the energy equation, obtained by combining the mass and energy equations, is

$$A\rho\frac{\partial h}{\partial t} - Ah_{fg}\frac{\partial \Psi}{\partial t} + F\frac{\partial h}{\partial x} + \sum_{k \in i} e_{ki} w h = \sum_{m \in i} \phi_{im} P_H q_w'' + \sum_{m \in i} C_Q \phi_{im} q' - \sum_{k \in i} w'(h_i - h_k) \quad 2-106$$

Equation 2-106 is used in the numerical solution methods in COBRA-FLX.

2.2.5.4 Equation of State

Finally, the equation of state will complete the system of basic equations. All thermodynamic state and transport properties in COBRA-FLX are the saturation properties corresponding to the system pressure. Subcooled liquid properties are calculated at pressure that corresponds to the saturated condition for the given fluid inlet temperature. Superheated vapor properties are available and used for some special applications.

The general equations of state given earlier in Section 2.1.2 reduce to finding the saturation properties corresponding to the pressure and then using the saturation enthalpy to find the density of each phase and the transport properties. Either a reference pressure or a local pressure can be used. In either case, the enthalpy of each phase and the saturation temperature are given by

$$\begin{aligned} h_l &= h_f(P) \\ h_v &= h_g(P) \\ T &= T_{SAT}(P) \end{aligned} \quad 2-107$$

and the phase density is

$$\begin{aligned} \rho_l &= \rho_f(h_l) \\ \rho_v &= \rho_g(h_v) \end{aligned} \quad 2-108$$

and the transport properties are

$$\begin{aligned}\mu_l &= \mu_f(h_l) \\ \mu_v &= \mu_g(h_v) \\ k_v &= k_g(h_v)\end{aligned}\quad 2-109$$

and

$$k_l = k_f(h_l). \quad 2-110$$

The surface tension is

$$\sigma = \sigma(P). \quad 2-111$$

The specific heat at constant pressure for the liquid is

$$C_{pl} = \left(\frac{\partial h_l}{\partial T_l} \right)_p. \quad 2-112$$

The mixture quality used in various correlations, including the DNB correlations is

$$\chi = \frac{h - h_l}{h_v - h_l}. \quad 2-113$$

And, finally, the vapor void fraction is obtained from an empirical correlation that relates the void fraction to the quality and state and transport properties

$$\alpha_v = \alpha(\chi, \rho_v, \rho_l, \sigma, \dots). \quad 2-114$$

This completes the description of the basic equations used in the COBRA-FLX code.

The numerical solution methods are given next and the code finite-difference equations are following that discussion.

2.3 COBRA-FLX Numerical Solution Methodology

COBRA-FLX includes different options for numerical solution of the thermal-hydraulic model equations: a normal upflow solution method, based on either the crossflow or the

pressure drop approximations (to be called SCHEME solution methods) and a solution method, based on the pressure-velocity approximation (to be called PV solution method). Each method iteratively solves the same set of differential equations and uses the same models and correlations for heat transfer, friction, fluid state, and two-phase flow, but the PV method allows reverse and recirculation flows.

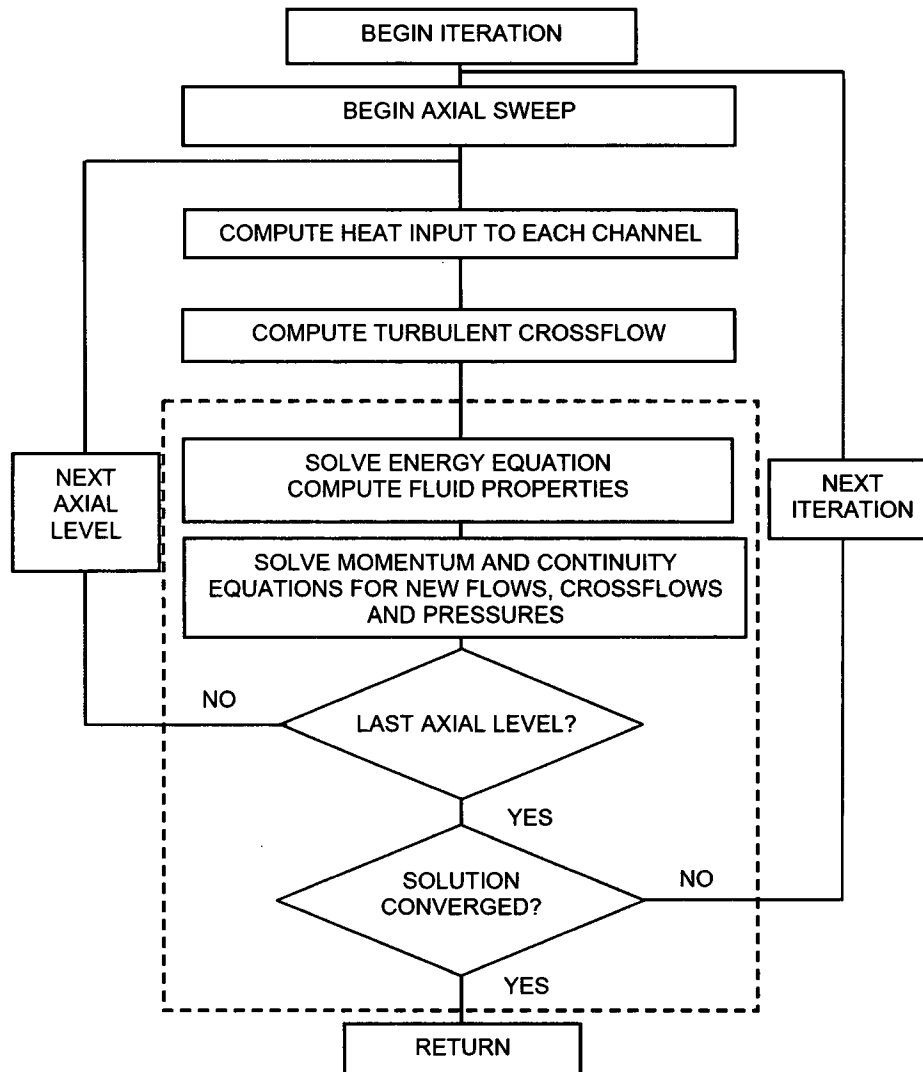
The difference between SCHEME and PV lies in the way the flow and pressure fields are solved. In the crossflow SCHEME logic (Reference 2-2), the lateral momentum equation is solved to obtain crossflows at each axial level. In the pressure drop SCHEME logic, a combination of the axial and lateral momentum equations is solved for the pressure gradient in each channel at an axial level; the new subchannel pressure gradients are used to update the pressure; and the new lateral pressure difference is then applied to the lateral momentum to yield the new crossflows. In both SCHEME logics, the new axial flows are computed with the continuity equation, using the flows at the last axial level and the new crossflows. In PV, tentative axial flows and crossflows are obtained at each level with the respective momentum equations, using the information from the last iteration. The tentative flows and pressures are then adjusted to satisfy continuity by a Newton-Raphson procedure.

All methods should yield the same results. Comparing the crossflow SCHEME logic to the pressure drop SCHEME logic, it should be mentioned that the latter leads to NC (number of subchannels) linear equations, whereas the former leads to system of NG (number of gaps) equations. The comparison of these dimensions gives a survey of the primary computational advantage of the pressure drop SCHEME solution. As NC is generally considerably less than NG, the calculation of the axial pressure differences needs less computational effort than that required by the crossflow solution. This has a strong impact on the CPU time when calculating large bundles, since large systems must be generated and solved several times within the iterative process. However, both SCHEME solutions are faster than the PV solution. Generally, the pressure drop SCHEME solution will be used for most situations. The PV method must be used whenever axial flows are expected to become locally very small or reverse direction at

any time during the simulation, or if the crossflows become larger when compared to the axial flows.

A simplified flow chart of the operations common for all solution methods is shown in Figure 2-7. The overall solution is obtained iteratively by repeatedly sweeping from inlet to exit, solving for the new enthalpies, flows, and pressures at each axial level in turn. One full sweep from inlet to exit constitutes an outer iteration. The solution for subchannel enthalpies and pressures at each axial level during a sweep may also be performed iteratively. In this case one pass over all subchannels is called an inner iteration. In the PV scheme, an additional outer sweep may be made in the opposite direction. The overall solution may be considered converged when the maximum fractional changes in crossflow and axial flow between outer iterations are simultaneously less than the input convergence criteria.

SCHEME and PV methods differ in the method for solution of the energy, momentum and continuity equations for the enthalpy, flow and pressure fields (illustrated in dashed line in Figure 2-7). The details of the SCHEME and the PV solutions are discussed below.

Figure 2-7: General Solution Flow Chart

2.3.1 *SCHEME Solution Methods*

2.3.1.1 *COBRA-FLX Finite-Difference Equations*

The basic equations developed in the previous sections are the continuous differential equations for the model. The application of these equations to the rod array geometry and the finite-difference form of the equations are given here. The finite-difference equations are presented in the form used by both SCHEME solution methods.

2.3.1.1.1 Finite-Difference Application Method

The continuous differential equations are applied to the fuel rod array by dividing the array into subchannels, typically bounded by adjacent rods in the array, and discrete axial increments. The axial increments are Δx in length and there are NDX active increments, or nodes, bounded by NDX+1 axial levels. The axial increment can vary in the axial direction. Additional inactive nodes, node 1 at the inlet and node NDX+2 at the exit, provide locations for specifications of boundary conditions for the numerical solution. The nomenclature and location of the nodes are shown in Figure 2-8.

The axial levels form boundaries through which the nodes are connected at the top and bottom. Level 1 is the inlet boundary and level NDX+1 is the exit boundary. The nodes are located between the level boundaries, (e.g., node 2 is between level 1 and 2 as shown in the Figure 2-8).

Nodes are connected to other nodes in adjacent subchannels in the transverse, or lateral, direction. The rod-to-rod gap is denoted by s and the distance between the centroids of adjacent subchannels is denoted by l . The gap axial index corresponds to the node index, (e.g., the gap connecting axial node number 3 in adjacent subchannels, by gap k , has the flow area $s_3 \Delta x_3$).

The primary dependent variables from the continuous differential equations are the axial mass flow rate, F ; the lateral mass flow rate per unit distance, w ; the mixture density, ρ ; the flowing enthalpy for the mixture, h ; and the pressure, P .

In the code, the variable P is the local pressure minus the exit pressure, $P(x) - P_{\text{exit}}$, so at the exit P is zero. As shown in Figure 2-8, the dependent variables are located at the axial levels between the nodes and are thus indexed by the level number. The axial level will be denoted by the subscript J in the finite-difference equations.

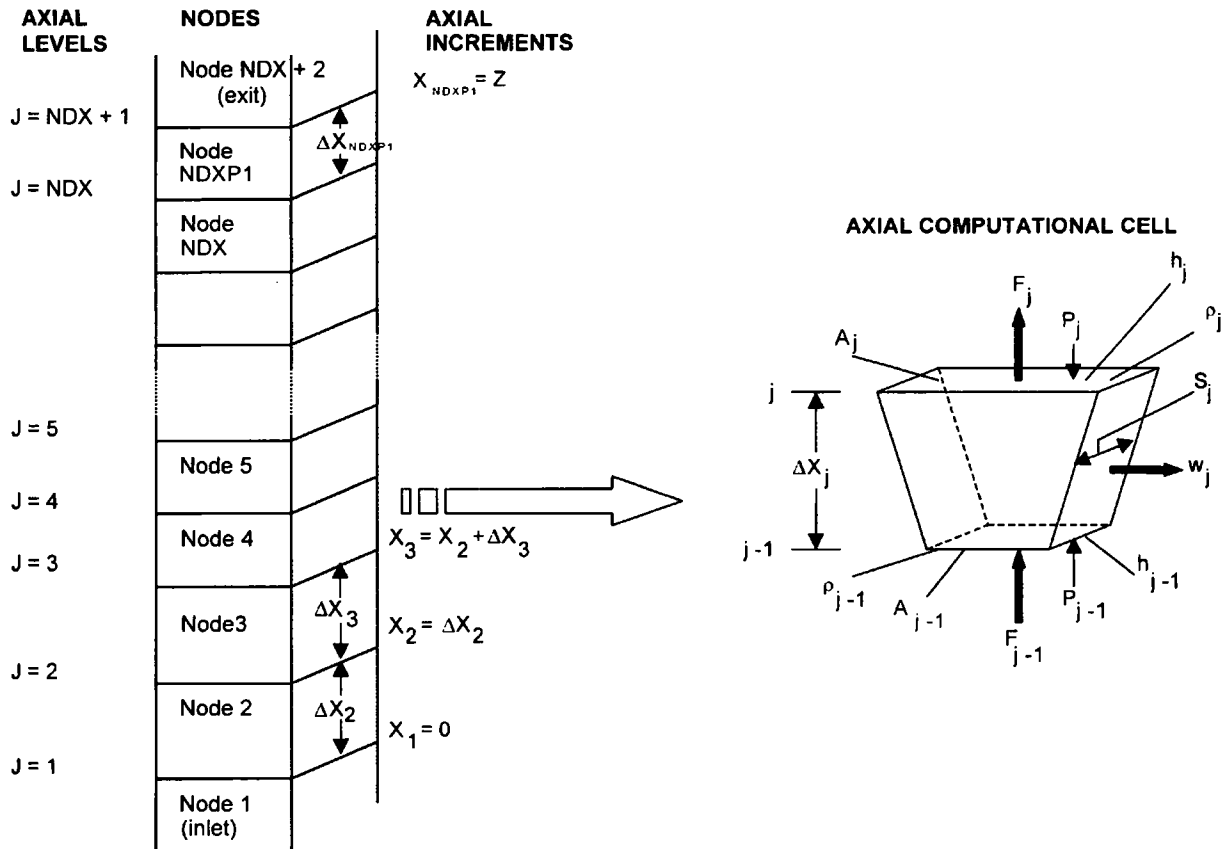
With the above information, the finite-difference equations are developed from the continuous equations in the following discussions.

The finite difference equations are obtained by replacing the partial derivatives in the continuous equations with algebraic differences. The time derivative is approximated by

$$\frac{\partial \Psi}{\partial t} = \frac{\Psi^{n+1} - \Psi^n}{\Delta t}, \quad 2-115$$

where Ψ is any flow field property.

Figure 2-8: Nodal Designation for Channels and Axial Location Indexes



The spatial derivatives, all only in the axial direction for the subchannel equations, are approximated with the donor-cell approach. Generally, a backward difference from level J is used for the spatial gradients in the continuous equations. Additionally, the quantity being transported is computed as that of the donor cell: the cell, or node, from which the fluid is flowing. For example, the finite-difference form of the mass flux derivative in the mass conservation equation is approximated by

$$\frac{\partial \rho U A}{\partial x} = \frac{1}{\Delta x_J} (\rho^* U_J A_J - \rho^* U_{J-1} A_{J-1}), \quad 2-116$$

where ρ^* is the fluid density in the donor cell:

$$\rho^* U_J = \begin{cases} \rho_{J-1} U_J & \text{if } U_J \geq 0 \\ \rho_J U_J & \text{if } U_J < 0 \end{cases} \quad 2-117$$

The mixture mass flow rate, F , is the dependent variable for the mass conservation equation and this gives another finite-difference form

$$\frac{\partial F}{\partial x} = \frac{1}{\Delta x_J} (F_J - F_{J-1}). \quad 2-118$$

Comparing the two approximations of Equations 2-116 and 2-118 shows that the donor-cell density and mixture mass flow rate are related by

$$F_J = \rho^* U_J A_J. \quad 2-119$$

Since the mixture mass flow rate is the dependent variable, and thus a primary solution variable, the axial component of the mixture velocity is calculated from

$$U_J = \frac{F_J}{\rho^* A_J}. \quad 2-120$$

Similar considerations apply for the lateral crossflow, w , the primary solution variable for the transverse momentum balance. The velocity component in the lateral direction is

$$V_J = \frac{w_J}{\rho^* s_J} . \quad 2-121$$

Applying the donor-cell method to the enthalpy transport in the energy equation in the axial and lateral directions gives

$$\frac{\partial Fh}{\partial x} = \frac{1}{\Delta x_J} (F_J h^* - F_{J-1} h^*) \quad 2-122$$

and

$$\sum_{k \in i} e_{ik} w h = \sum_{k \in i} e_{ik} w h^* , \quad 2-123$$

respectively, where h^* is the flowing enthalpy of the donor cell at axial level J .

Turbulent energy and momentum exchange are handled with the switch function, e_{ik} . If adjacent subchannels ii and jj have different enthalpies, the turbulent mixing will cool the hotter subchannel and heat the cooler subchannel. The enthalpy difference $\Delta h = h_{ii} - h_{jj}$ and the switch function alter the sign correctly when the subchannel of interest is ii or jj . The turbulent energy mixing contribution to the energy equation is then

$$\sum_{k \in i} w' \Delta h = \sum_{k \in i} e_{ik} w'_J (h_{ii} - h_{jj})_J . \quad 2-124$$

In the same way, the turbulent momentum mixing contribution to the axial momentum balance is

$$C_T \sum_{k \in i} w' \Delta U = C_T \sum_{k \in i} e_{ik} w'_J (U_{ii} - U_{jj})_J . \quad 2-125$$

The concepts introduced here are used in the development of the finite difference form of the COBRA-FLX subchannel equations in the following paragraphs.

2.3.1.1.2 **Mass Conservation**

The finite-difference form of the mass conservation equation, Equation 2-87, for axial level J is

$$A_J \frac{\Delta x_J}{\Delta t} (\rho^{n+1} - \rho^n) + F_J^{n+1} - F_{J-1}^{n+1} + \Delta x_J \sum_{k \in i} e_{ik} w_J^{n+1} = 0. \quad 2-126$$

When $J = 2$, the boundary condition at the inlet gives the axial mass flow rate for $J = 1$.

Note that all dependent variables in Equation 2-126 are at the new time level, thus forming a fully implicit equation. The axial velocity component is recovered from F_J^{n+1} by use of Equation 2-120.

Furthermore, when Equation 2-126 is divided by Δx_J and represented in a vector form then the finite-difference form as used by the SCHEME solution methods reads:

$$A_J \left\{ \frac{\rho_J^{n+1} - \rho_J^n}{\Delta t} \right\} + \left\{ \frac{F_J^{n+1} - F_{J-1}^{n+1}}{\Delta x_J} \right\} = -[S]^T \{w_J^{n+1}\} \quad 2-127$$

For convenience the notation $[S]^T w_J^{n+1} = \sum_{k \in i} e_{ik} w_J^{n+1}$ is used, where $[S]$ is the matrix with elements (e_{ik}) as described in Section 2.2.1 and the notation $\{a_J\}$ is used to denote the vector with elements a_J at the axial level J , i.e. $\{w_J^{n+1}\}$ represents the vector with elements w_J^{n+1} - the crossflows for all gaps at axial level J and $\{F_J^{n+1}\}$ is the vector with elements F_J^{n+1} - the axial mass flows for all subchannels at axial level J .

2.3.1.1.3 **Axial Momentum Balance**

The finite-difference form for the axial momentum balance, Equation 2-96, for axial level J is

$$\begin{aligned}
& \left(\frac{1}{A_J} \right) \frac{\Delta x_J}{\Delta t} (F_J^{n+1} - F_J^n) - 2U_J^{n+1} \Delta x_J \frac{\rho_J^{n+1} - \rho_J^n}{\Delta t} - 2U_J^{n+1} \Delta x_J \left(\frac{1}{A_J} \right) \sum_{k \in i} e_{ik} w_J^{n+1} + \Delta x_J \left(\frac{1}{A_J} \right) \sum_{k \in i} e_{ik} (U^* w)_J^{n+1} \\
& + (P_J^{n+1} - P_{J-1}^{n+1}) + K'_f (F_J^2)^{n+1} + \rho_J^{n+1} g \Delta x_J \cos \theta_J \\
& + C_{TJ} \Delta x_J \left(\frac{1}{A_J} \right) \sum_{k \in i} e_{ik} (w_J)^{n+1} \left[\left(\frac{F v'}{A} \right)_i^{n+1} - \left(\frac{F v'}{A} \right)_k^{n+1} \right] + \frac{(F_J^2)^{n+1}}{A_J} \left[\left(\frac{v'}{A} \right)_J^{n+1} - \left(\frac{v'}{A} \right)_{J-1}^{n+1} \right] = 0
\end{aligned} \tag{2-128}$$

where

$$K'_f = \frac{1}{2} \Delta x_J \left[\frac{f_w}{D_{hy}} \frac{\rho}{\rho_i} \Phi_p^2 + \frac{K_H}{\Delta x} \right] \left(\frac{1}{\rho_J A_J^2} \right). \tag{2-129}$$

This equation form is needed by the SCHEME solution methods.

Dividing Equation 2-128 by Δx_J and rearranging the terms allows it to be written in the following vector form:

$$\begin{aligned}
& \left\{ \frac{1}{A_J} \frac{F_J^{n+1} - F_J^n}{\Delta t} \right\} - \left\{ 2U_J^{n+1} \frac{\rho_J^{n+1} - \rho_J^n}{\Delta t} \right\} + \left\{ \frac{P_J^{n+1} - P_{J-1}^{n+1}}{\Delta x_J} \right\} = \\
& \{a'_J\} + [A_J]^{-1} \left[[2U_J] [S]^T - [S]^T [U_J^*] \right] \{w_J^{n+1}\}
\end{aligned} \tag{2-130}$$

where the notation given below is used:

$$\{a'_J\} = - \left\{ \left(\frac{F_J^{n+1}}{A_J} \right)^2 \left(\frac{K'_f (A_J)^2}{\Delta x_J} + A_J \frac{\frac{v'_J}{A_J} - \frac{v'_{J-1}}{A_{J-1}}}{\Delta x_J} \right) + \rho_J^{n+1} g \cos \theta \right\} - C_{TJ} [A_J]^{-1} [S]^T [\Delta U] \{w_J^{n+1}\} \tag{2-131}$$

$$\text{and } \Delta U = \left(\frac{F v'}{A} \right)_i^{n+1} - \left(\frac{F v'}{A} \right)_k^{n+1}.$$

Using the definition of K'_f via Equation 2-129 and replacing the density by the specific

volume $v'_J = \frac{1}{\rho_J}$, the following relationship holds:

$$\frac{K'_f(A_J)^2}{\Delta x_J} = \left[\frac{f_W v'_i}{2D_{hy}} \Phi_{ip}^2 + \frac{K_{II} v'}{2\Delta x} \right]_J \quad 2-132$$

For convenience Equation 2-131 may be written in the short form:

$$\{a'_J\} = -\{K_J (F_J^{n+1})^2\} - \{f_J\} \quad 2-133$$

where K_J represents the coefficient of the flow-squared terms and $\{f_J\}$ are the remaining terms of $\{a'_J\}$, i.e.,

$$K_J = \frac{K'_f}{\Delta x_J} + \frac{1}{A_J} \frac{v'_J - v'_{J-1}}{\Delta x_J} = \frac{1}{2} \left[\frac{f_W}{D_{hy}} \frac{\rho}{\rho_l} \Phi_{ip}^2 + \frac{K_{II}}{\Delta x} \right]_J \left(\frac{1}{\rho_J A_J^2} \right) + \frac{1}{A_J} \frac{v'_J - v'_{J-1}}{\Delta x_J} \quad 2-134$$

and

$$\{f_J\} = \rho_J^{n+1} g \cos \theta + C_{TJ} [A_J]^{-1} [S]^T [\Delta U] \{w_J^{n+1}\} \quad 2-135$$

2.3.1.1.4 Lateral Momentum Balance

The finite-difference form for the lateral momentum balance, Equation 2-97, for axial level J is

$$\begin{aligned} & \frac{\Delta x_J}{\Delta l} (w_J^{n+1} - w_J^n) + \left[(wU^*)_J^{n+1} - (wU^*)_{J-1}^{n+1} \right] + \frac{s}{l} \Delta x_J (P_{l+\Delta l}^{n+1} - P_l^{n+1}) \\ & + \frac{1}{2} K_G \Delta x_J \frac{w_J^{n+1} |w_J^{n+1}| s}{s_J^2 \rho_J^{n+1} l} = 0 \end{aligned} \quad 2-136$$

The axial velocity component is not taken directly as the value in the control volume from which the lateral velocity originates. An average value is used instead and is

$$U_J^{*n+1} = \frac{1}{2} (U_{ii}^{n+1} + U_{jj}^{n+1}), \quad 2-137$$

where ii and jj are the adjacent subchannels for which the lateral mass flow is to be determined. This is an effective axial velocity component that is transported laterally between subchannels. Note that for almost all cases the value will approximate the axial velocity value. The fluid density in the denominator of the last term on the left-hand side of Equation 2-136 is determined by the donor-cell method. The density is taken as the value for the subchannel from which the lateral velocity component originates.

The finite-difference form of the lateral momentum balance, Equation 2-136, can be presented in a vector form convenient for the SCHEME solution methods as follows:

$$\left\{ \frac{w_J^{n+1} - w_J^n}{\Delta t} \right\} + \left\{ \frac{U_{J}^{*n+1} w_J^{n+1} - U_{J-1}^{*n+1} w_{J-1}^{n+1}}{\Delta x_J} \right\} + \left(\frac{s}{l} \right) \{ C_J w_J^{n+1} \} = \left(\frac{s}{l} \right) [S] \{ P_{J-1}^{n+1} \} \quad 2-138$$

For this purpose Equation 2-136 is divided by Δx_J and the notation given via Equation 2-139 is used.

$$C_J = \frac{1}{2} K_G \frac{|w_J^{n+1}|}{s_J^2 \rho_J^{n+1}} \quad 2-139$$

The average axial velocity component U_J^{*n+1} is calculated according to Equation 2-137.

2.3.1.1.5 Energy Conservation Equation

The finite-difference form for the transportive form of the energy conservation equation for the mixture, Equation 2-106, for axial level J is

$$\begin{aligned} & A_J \rho_J^n \frac{\Delta x_J}{\Delta t} (h_J^{n+1} - h_J^n) + h_{fg} A_J \frac{\Delta x_J}{\Delta t} (\Psi_J^{n+1} - \Psi_J^n) + F_{J-1}^{n+1} (h_J^{n+1} - h_{J-1}^{n+1}) \\ & + \Delta x_J \sum_{k \in i} e_{ik} w^{n+1} (h_i^{*n+1} - h_k^{n+1}) - \Delta x_J \sum_{m \in i} P_H \phi_{im} q_w^{n+1} - \Delta x_J \sum_{m \in i} C_Q \phi_{im} q^{n+1} \\ & + \Delta x_J \sum_{k \in i} w^{n+1} (h_i^{n+1} - h_k^{n+1}) = 0 \end{aligned} \quad 2-140$$

where all the terms have been moved to the left-hand side.

Furthermore, Equation 2-140 is written in the following vector form needed by the SCHEME solution methods:

$$\left\{ \frac{1}{u_J^n} \frac{h_J^{n+1} - h_J^n}{\Delta t} \right\} + \left\{ \frac{h_J^{n+1} - h_{J-1}^{n+1}}{\Delta x_J} \right\} = \left[F_{J-1}^{n+1} \right]^{-1} \left\{ \left\{ q'_J \right\} - [S]^T [\Delta h_{J-1}] \left\{ w'_{J-1} \right\} - [S]^T [t_{J-1}] [c_{J-1}] + \left[[h_{J-1}] [S]^T - [S]^T [h_{J-1}^*] \right] \left\{ w_{J-1} \right\} \right\} \quad 2-141$$

For this purpose Equation 2-140 is divided by Δx_J and F_{J-1}^{n+1} . Then the first term in equation 2-141 represents the first two terms in the modified Equation 2-140.

The effective enthalpy transport velocity u_J^n may be defined via Equation 2-142. For homogeneous two-phase flows or for single-phase flows Equation 2-142 reduces to $u_J^n = U_J$.

$$u_J^n = \frac{F_J}{A_J \left(\rho_J - h_{fg} \frac{\partial \Psi}{\partial h} \right)} \quad 2-142$$

Furthermore, q'_J represents the heat transfer rate from the fuel surface, i.e.,

$$q'_J = \sum_{m \in i} P_H \phi_{im} q_w'^{n+1} \quad 2-143$$

The thermal conduction between the adjacent subchannels is denoted according to Equation 2-144, i.e.,

$$[S]^T [t_{J-1}] [c_{J-1}] = \sum_{m \in i} C_Q \phi_{im} q'^{n+1} \quad 2-144$$

2.3.1.1.6 Derivation of a Finite-Difference Equation for the Pressure

The conservation equations 2-127, 2-130, 2-138 and 2-141 are going to be combined to achieve the final form of the equations needed for the crossflow and pressure SCHEME solutions.

For convenience the continuity equation 2-127 is written in the following way:

$$\{F_J^{n+1}\} = \{F_{J-1}^{n+1} + \Delta F\} \quad 2-145$$

where

$$\Delta F = -\Delta x_J A_J \left\{ \frac{\rho_J^{n+1} - \rho_J^n}{\Delta t} \right\} - [S]^T \{w_J^{n+1}\} \Delta x_J \quad 2-146$$

After squaring Equation 2-145 the following relationship is obtained:

$$\{(F_J^{n+1})^2\} = \{(F_{J-1}^{n+1})^2 + 2 F_{J-1}^{n+1} \Delta F + (\Delta F)^2\} \quad 2-147$$

which is equivalent to:

$$\{(F_J^{n+1})^2\} = \{(F_{J-1}^{n+1})^2 + (2 F_{J-1}^{n+1} + \Delta F) \Delta F\} \quad 2-148$$

Upon substituting Equation 2-145 into Equation 2-148, the following form is obtained:

$$\{(F_J^{n+1})^2\} = \{(F_{J-1}^{n+1})^2 + (F_J^{n+1} + F_{J-1}^{n+1}) \Delta F\} \quad 2-149$$

The axial mass flow F_J^{n+1} can be calculated with Equation 2-149 using the values from the previous axial level J-1. The value of F_J^{n+1} on the right hand side is unknown but it can be initially estimated and updated through the iterations.

The procedure described above can be applied to the temporal acceleration term in the axial momentum equation 2-130, i.e.,

$$\frac{[A_J]^{-1}}{\Delta t} \{F_J^{n+1} - F_J^n\} = \frac{[A_J]^{-1}}{\Delta t} \{F_J^{n+1} - F_{J-1}^{n+1} + F_{J-1}^{n+1} - F_J^n\} = \frac{[A_J]^{-1}}{\Delta t} \{\Delta F + F_{J-1}^{n+1} - F_J^n\} \quad 2-150$$

Hence, this term can be expressed using the axial mass flow at the previous axial level J-1 via:

$$\frac{[A_J]^{-1}}{\Delta t} \{F_J^{n+1} - F_J^n\} = \frac{[A_J]^{-1} \Delta F}{\Delta t} + [A_J]^{-1} \frac{F_{J-1}^{n+1} - F_J^n}{\Delta t} \quad 2-151$$

Using equations 2-133, 2-146, 2-149 and 2-151 the axial momentum equation 2-130 can be written as an equation for the pressure in the following way:

$$\{P_J^{n+1} - P_{J-1}^{n+1}\} = \{N_J\} \Delta x_J + [R_J] \{w_J^{n+1}\} \Delta x_J \quad 2-152$$

Here,

$$\{N_J\} = -\left\{K_J (F_{J-1}^{n+1})^2\right\} - \{f_J\} - [A_J]^{-1} \left\{\frac{F_{J-1}^{n+1} - F_J^n}{\Delta t}\right\} + [B_J] \left\{\frac{\rho_J^{n+1} - \rho_J^n}{\Delta t}\right\} \quad 2-153$$

and

$$[R_J] = [A_J]^{-1} \left[[B_J] [S]^T - [S]^T [U_J^*] \right] \quad 2-154$$

where for convenience the following notation is used:

$$[B_J] = \left[\frac{\Delta x}{\Delta t} + 2U_J + \Delta x_J K_J A_J (F_J^{n+1} + F_{J-1}^{n+1}) \right] \quad 2-155$$

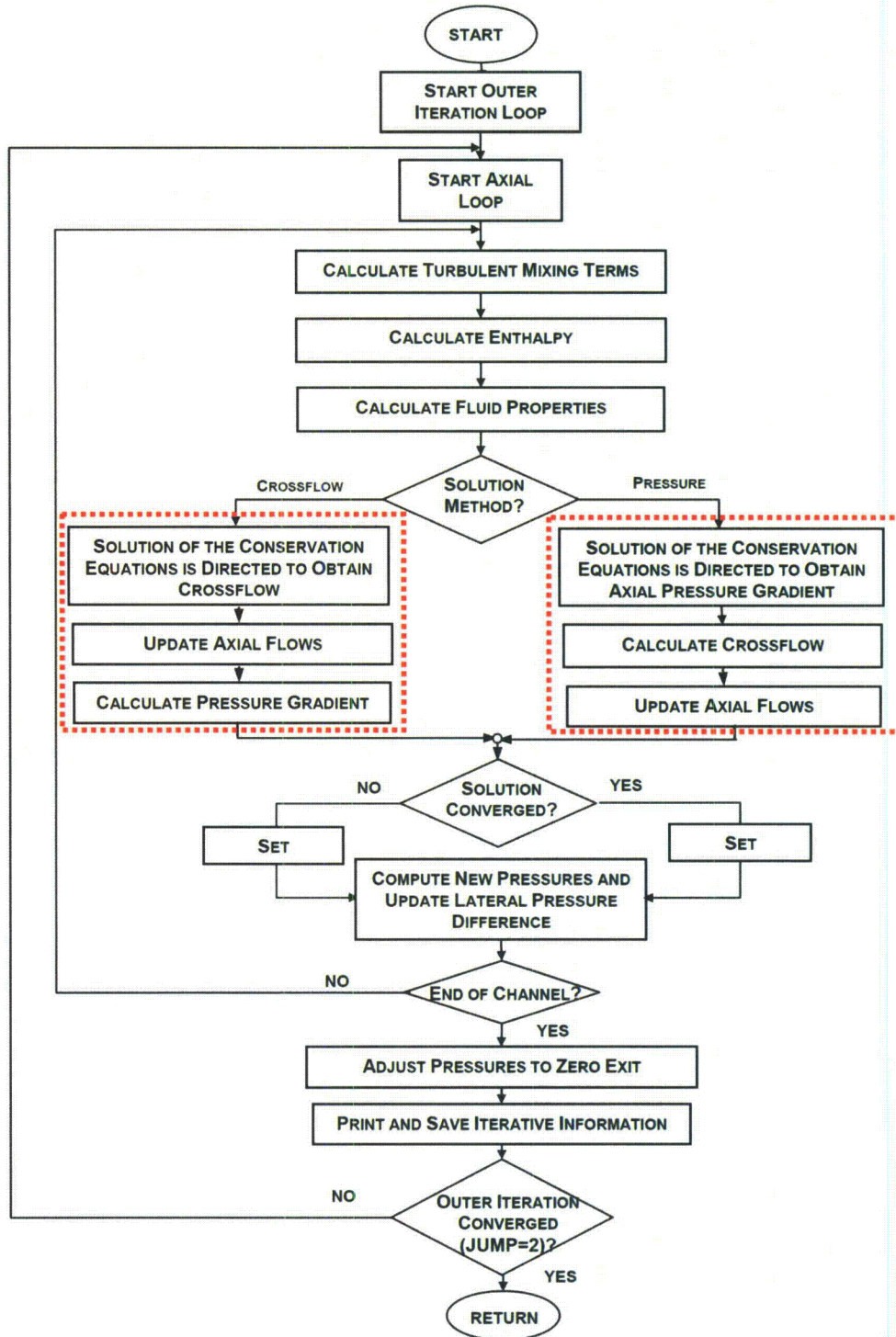
2.3.1.2 General Computational Procedure

The crossflow and pressure SCHEME solution methods solve the same differencing equations, i.e., Equation 2-130, 2-138, 2-152 and 2-141. Both algorithms follow the same general solution procedure as summarized in Figure 2-9.

The main difference between the SCHEME solvers is the order in which the unknown variables are found. The pressure method generates a system of linear equations for the axial pressure differences and then calculates the crossflows. On the other hand the crossflow method is based on the concept of generating a system of linear equations for the crossflow distribution and afterwards calculates the pressure.

The detailed descriptions of the special algorithm parts (placed in dashed-line boxes in Figure 2-9) are given in Section 2.3.1.3 and Section 2.3.1.4. Here, the general computational procedure used by both SCHEME solvers is presented.

Figure 2-9: SCHEME Solutions Sequence



An iterative solution procedure is chosen to account for the strong coupling between the energy and momentum equations. The overall iteration loop is described below.

Since the inlet flow and enthalpy distributions have been specified, the enthalpy can be advanced from axial level $J-1$ to axial level J by solving the mixture enthalpy Equation 2-141 for all enthalpies. The turbulent mixing terms and the fluid properties are then calculated. For the first axial iteration the axial flow F_J^{n+1} is set equal to the axial flow at the previous axial level $J-1$, F_{J-1}^{n+1} ; otherwise the value from the previous axial iteration \tilde{F}_J is used.

Depending on the solution algorithm as explained in Section 2.3.1.3 and 2.3.1.4, the new crossflows w_j^{n+1} and pressure drops $\left(\frac{\Delta P}{\Delta x}\right)_J$ at the current axial level are found.

Using the new crossflows Equation 2-126 is applied to get the new axial flows F_J^{n+1} , i.e.

$$F_J^{n+1} = F_{J-1}^{n+1} - A_J \frac{\Delta x_J}{\Delta t} (\rho^{n+1} - \rho^n) - \Delta x_J \sum_{k \in i} e_{ik} w_j^{n+1} \quad 2-156$$

In order to reduce flow changes between iterations, a damping factor α_m is used according to the equation:

$$F_J^{n+1} = \alpha_m F_J^{n+1} + (1 - \alpha_m) \tilde{F}_J \quad 2-157$$

where \tilde{F}_J is the flow from the previous outer iteration as mentioned above. The pressure is updated by the definition of $\left(\frac{\Delta P}{\Delta x}\right)_J$, that is

$$P_J = P_{J-1} + \left(\frac{\Delta P}{\Delta x}\right)_J \Delta x_J \quad 2-158$$

The solution is unstable if the lateral pressure difference $[S]\{P\} = \{P_{i(k)} - P_{j(k)}\}$ for gap k with adjacent channels $i(k)$ and $j(k)$ in Equation 2-161 (crossflow solution) and

Equation 2-171 (pressure solution) is calculated directly from the current pressure.

Instead $[S]\{P\}$ is calculated as a separate variable SP_J for each gap k and a damping is applied:

$$SP_{J-1} = \alpha_{SP} \left\{ \tilde{SP}_J - \left[\left(\left(\frac{\Delta P}{\Delta x} \right)_J \right)_{i(k)} - \left(\left(\frac{\Delta P}{\Delta x} \right)_J \right)_{j(k)} \right] \Delta x_J \right\} + (1 - \alpha_{SP}) SP_{J-1} \quad 2-159$$

where \tilde{SP}_J is the previous iteration value and α_{SP} is a damping factor.

Note that $[S]\{P_J^{n+1}\}$ is downstream of $[S]\{P_{J-1}^{n+1}\}$; therefore, the iteration allows the downstream pressure difference to be felt at upstream location. At the end of the channels the boundary condition used for the lateral pressure difference is $[S]\{P_J^{n+1}\} = 0$ for uniform exit pressure distribution or $[S]\{P_J^{n+1}\} = P(i(k), J) - P(j(k), J)$ for prescribed non-uniform outlet pressure distribution. In this way a boundary value solution is obtained.

When the calculation reaches the exit, a check is made to see if the axial flow and crossflow distributions have converged at every axial level to the tolerance desired. Otherwise the entire iterative scheme is repeated again, starting at the first axial level and sweeping downstream to the last axial level.

The equations to solve do not require actual pressure since pressure difference is only used in the combined momentum equation. The calculation of pressure is, therefore, only a back solution. It is calculated from Equation 2-152 only in a forward direction. If the solution has converged, the pressures are adjusted for a uniform zero exit pressure in each channel.

Steady state computations are performed first to obtain initial conditions for the transient. As it will be shown in Section 2.3.1.3 and 2.3.1.4, the finite difference equations are stable for large time steps. Hence, those same equations are used for the steady state calculations by setting the time step Δt equal to some arbitrarily large value.

2.3.1.3 Crossflow SCHEME Solution Logic

The finite-differencing equations to be solved by the crossflow SCHEME algorithm are obtained in the previous Section 2.3.1 and given via equations 2-130, 2-138, 2-152 and 2-141. In this section the details of the solution algorithm, i.e. the special crossflow SCHEME algorithm part in a dashed-line box in Figure 2-9 are explained.

As the name of the method states, at first the crossflow is to be determined. For this purpose a linear system of equations for the crossflows is obtained as described below.

The lateral pressure difference between the neighbor subchannels denoted by $[S]\{P_{J-1}^{n+1}\}$ can be written using the pressure equation 2-152 as follows:

$$[S]\{P_{J-1}^{n+1}\} = [S]\{P_J^{n+1}\} - [S]\{N_J\}\Delta x_J - [S][R_J]\{w_J^{n+1}\}\Delta x_J \quad 2-160$$

Substituting this result into the lateral momentum equation 2-138 to eliminate $[S]\{P_{J-1}^{n+1}\}$ gives a system of equations for the crossflows for all gaps at each axial level J which has the form:

$$[M_J]\{w_J^{n+1}\} = \{b_J\} \quad 2-161$$

where

$$[M_J] = \left[\frac{1}{\Delta t} \right] + \left[\frac{U_J^{*n+1}}{\Delta x_J} \right] + \left(\frac{s}{l} \right) [C_J] + \left(\frac{s}{l} \right) [S][R_J]\Delta x_J \quad 2-162$$

and the right hand side is

$$\{b_J\} = \left\{ \frac{w_J^n}{\Delta t} \right\} + \left\{ \frac{U_{J-1}^{*n+1} w_{J-1}^{n+1}}{\Delta x_J} \right\} + \left(\frac{s}{l} \right) [S]\{P_J^{n+1}\} - \left(\frac{s}{l} \right) [S]\{F_J^{n+1}\}\Delta x_J \quad 2-163$$

The matrix $[M_J]$ defined by Equation 2-162 controls the distribution of the crossflow.

The vector $\{b_J\}$ defined by Equation 2-163 contains the crossflow forcing terms.

The first three terms on the right hand side of Equation 2-162 represent diagonal matrices. The first two of them come from the added temporal and spatial acceleration terms and provide additional numerical stability. Reducing Δt and Δx_j leads to more diagonal dominance and thus more numerical stability. The last term on the right side of Equation 2-162 includes a matrix which is singular for any rod bundle problem with a lateral transverse flow loop. The additional terms in Equation 2-162 remove the singularity and allow a unique solution for the crossflow.

For the unknown value of the lateral pressure difference $[S]\{P_J^{n+1}\}$ on the right hand side $\{b_J\}$ (equation 2-163), the previous iterative value $\bar{S}P_J$ is used.

The linear system of equations given by Equation 2-161 is used by the crossflow SCHEME solution method to find the crossflows for all gaps at axial level J . The number of equations to solve at each axial level J is equal to the number of gaps NG . Hence, the size of the matrix $[M_J]$ is $NG \cdot NG$. In COBRA-FLX Equation 2-161 is solved by direct elimination. Next the axial flows and axial pressure gradients are to be determined.

The axial flows F_J^{n+1} are calculated via Equation 2-156 and Equation 2-157 and the lateral pressure difference $SP_{J-1} = [S]\{P_{J-1}^{n+1}\}$ is obtained from Equation 2-160 and Equation 2-159 as explained in the general solution procedure given in Section 2.3.1.2.

The axial pressure gradient $\left\{ \left(\frac{\Delta P}{\Delta x} \right)_J \right\} = \left\{ \frac{P_J^{n+1} - P_{J-1}^{n+1}}{\Delta x_J} \right\}$ is calculated by means of Equation

2-130 as follows:

$$\left\{ \left(\frac{\Delta P}{\Delta x} \right)_J \right\} = \left\{ \frac{P_J^{n+1} - P_{J-1}^{n+1}}{\Delta x_J} \right\} = - \left\{ \frac{1}{A_J} \frac{F_J^{n+1} - F_J^n}{\Delta t} \right\} + \left\{ 2U_J^{n+1} \frac{\rho_J^{n+1} - \rho_J^n}{\Delta t} \right\} + \{a'_J\} + [A_J]^{-1} \left[[2U_J][S]^T - [S]^T [U_J^*] \right] \{w_J^{n+1}\} \quad 2-164$$

Hence, the crossflows, axial mass flows and pressure drops are found using the crossflow SCHEME solver. Afterwards, the algorithm follows the general iterative scheme as described in Section 2.3.1.2.

2.3.1.4 Pressure SCHEME Solution Logic

The finite-differencing equations to be solved by the pressure SCHEME algorithm, typically referred to as the "P" solution, are obtained in Section 2.3.1 and given via Equations 2-130, 2-138, 2-152 and 2-141.

As the name of the method states, at first the pressure gradient is to be determined. For this purpose a linear system of equations for the pressure gradient for all channels at each axial node is obtained as described below.

The lateral momentum equation 2-138 is written for convenience as

$$\{w_J^{n+1}\} = [D_J]^{-1} \{Q_J\} + \left(\frac{s}{l}\right) [D_J]^{-1} [S] \{P_{J-1}^{n+1}\} \quad 2-165$$

where the notations 2-166 and 2-167 are used.

$$[D_J]^{-1} = \left[\frac{1}{\Delta t} + \frac{U_J^{*n+1}}{\Delta x_J} + \left(\frac{s}{l}\right) C_J \right] \quad 2-166$$

$$\{Q_J\} = \left\{ \frac{w_J^n}{\Delta t} + \frac{U_{J-1}^{*n+1} w_{J-1}^{n+1}}{\Delta x_J} \right\} \quad 2-167$$

Considering the pressure gradient $\left(\frac{\Delta P}{\Delta x}\right)_J$ defined via

$$\left(\frac{\Delta P}{\Delta x}\right)_J = \frac{P_J^{n+1} - P_{J-1}^{n+1}}{\Delta x_J} \quad 2-168$$

the pressure at the previous axial level can be expressed using the relationship

$$P_{J-1}^{n+1} = P_J^{n+1} - (P_J^{n+1} - P_{J-1}^{n+1}) = P_J^{n+1} - \left(\frac{\Delta P}{\Delta x} \right)_J \Delta x_J \quad 2-169$$

Dividing by Δx_J and using the notation 2-168, Equation 2-152 becomes

$$\left\{ \left(\frac{\Delta P}{\Delta x} \right)_J \right\} = \{N_J\} + [R_J] \{w_J^{n+1}\} \quad 2-170$$

Taking into account Equation 2-169 the lateral momentum equation 2-165 becomes

$$\{w_J^{n+1}\} = [D_J]^{-1} \{Q_J\} + \left(\frac{s}{l} \right) [D_J]^{-1} [S] \{P_J^{n+1}\} - \left(\frac{s}{l} \right) \Delta x_J [D_J]^{-1} [S] \left\{ \left(\frac{\Delta P}{\Delta x} \right)_J \right\} \quad 2-171$$

Substituting equation 2-171 into Equation 2-170 and rearranging for $\left\{ \left(\frac{\Delta P}{\Delta x} \right)_J \right\}$ yields

$$\left[1 + \left(\frac{s}{l} \right) \Delta x_J [R_J] [D_J]^{-1} [S] \right] \left\{ \left(\frac{\Delta P}{\Delta x} \right)_J \right\} = \{N_J\} + [R_J] [D_J]^{-1} \{Q_J\} + \left(\frac{s}{l} \right) [R_J] [D_J]^{-1} [S] \{P_J^{n+1}\} \quad 2-172$$

The obtained Equation 2-172 can be written in the following matrix form:

$$[M_J] \left\{ \left(\frac{\Delta P}{\Delta x} \right)_J \right\} = \{b_J\} \quad 2-173$$

where

$$[M_J] = \left[1 + \left(\frac{s}{l} \right) \Delta x_J [R_J] [D_J]^{-1} [S] \right] \quad 2-174$$

$$\{b_J\} = \{N_J\} + [R_J] [D_J]^{-1} \left(\{Q_J\} + \left(\frac{s}{l} \right) [S] \{P_J^{n+1}\} \right) \quad 2-175$$

For standard rod bundles, in which each subchannel has four or less adjacent subchannels, it can be shown, that each row of the matrix $[M_J] = (M_{ij})$ has no more than five non-zero elements. Those elements occur when the channel numbers i and j are

such that $j = i$ (diagonal) or j corresponds to the number of a subchannel adjacent to subchannel i . The dimension of $[M_j]$ is $NC \cdot NC$, where NC is the number of subchannels in the bundle. These non-zero elements are determined. The resulting coefficient matrix $[M]$ is stored in compact form containing only the non-zero elements. This matrix is an L-matrix, diagonally dominant, irreducible and sparse.

In COBRA-FLX Equation 2-173 may be solved either by direct elimination or by the method of successive over-relaxation (SOR), as described in the next section.

The linear system of equations 2-173 is used by the pressure SCHEME solution method to find the pressure gradient $\left\{ \left(\frac{\Delta P}{\Delta x} \right)_j \right\}$ for all subchannels at axial location J. As shown in the dashed-line box in Figure 2-9 the axial flows and crossflows are to be determined next. Knowing the pressure gradient, the crossflows are calculated with Equation 2-171. Then the axial flows F_j^{n+1} are calculated via Equation 2-156 and Equation 2-157 and the lateral pressure difference $SP_{j-1} = [S] \{ P_{j-1}^{n+1} \}$ is obtained from Equation 2-159 as explained in the general solution procedure given in Section 2.3.1.2. Hence, the crossflows, axial mass flows and pressure drops are found using the pressure SCHEME solver. Afterwards, the algorithm follows the general iterative scheme as described in Section 2.3.1.2.

2.3.1.4.1 Successive over-relaxation (SOR) method

In problems with a large number of channels the iterative method of successive over-relaxation (SOR) is much more advantageous than the method of direct elimination. The required memory to accommodate the matrix $[M]$ and the computational time are significantly reduced. Using the SOR method it is possible to handle full core subchannel-by-subchannel calculations with more than 60,000 channels.

The linear system to be solved, Equation 2-173 is transformed by dividing each non-zero coefficient by the corresponding central coefficient, so that the diagonal elements all become equal to one:

$$(I + A_{ND})\{x\} = \{b\} \quad 2-176$$

Here the vector $\{x\}$ is the searched pressure gradient $\left(\frac{\Delta P}{\Delta x}\right)$, the matrix $A_{ND} = (a_{ij})$ contains the non-diagonal non-zero elements of the modified matrix and b is the right hand side vector b_j divided by the diagonal elements of the original matrix M_j .

The following iterative scheme for channel i (i varies from 1 to NC) is used by the SOR method:

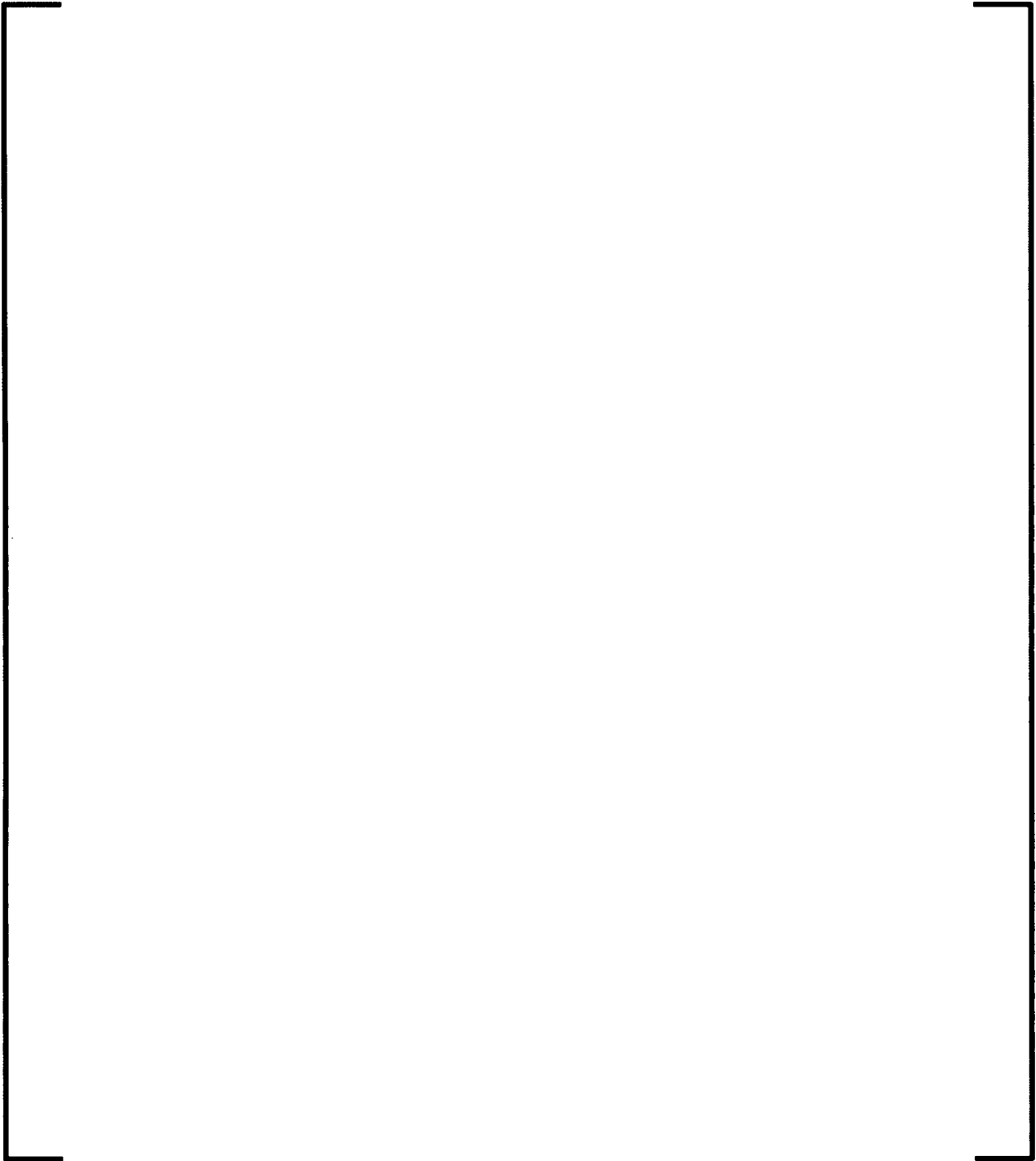
$$x_i = x_i^0 + \omega \left[b_i - x_i^0 - \sum_{j=1, j \neq i}^{NC} (a_{ij} x_j^0) \right] \quad 2-177$$

where x_i^0 denotes the value of the previous iteration of x_i and ω ($1 < \omega < 2$) is the over-relaxation factor.

2.3.1.4.2

[]





2.3.2 *Pressure-Velocity (PV) Solution Method*

This section presents the description of the COBRA-FLX PV numerical solution. This solution method is being provided to allow a more general solution of the subchannel equations. The PV solution option is of particular importance as it can consider applications where the default numerical solution has convergence difficulties or where it fails. The PV solution has the ability to consider reverse and recirculating flows that cannot be considered by the SCHEME solution method.

The PV model retains the same features of the standard pressure-crossflow model and solution options. The mathematical model is the same, but its numerical solution has changed to allow arbitrary flow direction. It also uses a staggered mesh typical for many nuclear reactor thermal-hydraulic analysis codes. The mass and energy control volumes are identical to those of the standard model. The momentum control volumes are staggered.

2.3.2.1 *Thermal-Hydraulic Model Equations*

This section presents the basic subchannel fluid flow equation model for the COBRA-FLX PV solution method. The conversion of the differential equations into the control volume equations that are solved is given in Section 2.3.2.2. The modeling uses the same assumptions and the concepts are not changed: the basic equation set consists of mixture equations of mass, energy and momentum (axial and lateral) and are the same equations solved by the SCHEME solution methods. The relative velocity between the liquid and vapor phases is included by using the void-quality relationships of COBRA-FLX. Subcooled boiling is also included by using the standard COBRA-FLX modeling.

The mixture conservation equations are represented as control volume equations. The approach is to divide the rod bundle cross section into flow subchannels and to divide the length into finite increments. The result is a set of control volumes that represent the flow region of the rod bundle.

The two-phase flow equations have several terms that require additional relationships for closure. They are the various correlations for two-phase flow and friction.

The conservation equations of mass, energy, and momentum are presented here in three-dimensional form. The equations given here are basically those given in Section 2.1.2. The next section presents the control volume equations used for the numerical solution.

2.3.2.1.1 *Mass Conservation*

The mass conservation equation for the two-phase mixture is written as

$$\frac{\partial}{\partial t}((\alpha\rho)_l + (\alpha\rho)_v) + \vec{\nabla} \cdot ((\alpha\rho\vec{V})_l + (\alpha\rho\vec{V})_v) = 0. \quad 2-179$$

The use of α without a subscript is understood to be the vapor fraction α_v and $(1 - \alpha)$ is understood to be the liquid fraction α_l .

The mass conservation equation for the mixture is used in COBRA-FLX without explicit representation of the liquid and vapor components in the mixture and is written as

$$\frac{\partial \rho}{\partial t} + \vec{\nabla} \cdot \rho \vec{V} = 0. \quad 2-180$$

The mixture density is defined by

$$\rho = (\alpha \rho)_l + (\alpha \rho)_v. \quad 2-181$$

The mixture mass flux is

$$G = (\rho \vec{V}) = (\alpha \rho \vec{V})_l + (\alpha \rho \vec{V})_v, \quad 2-182$$

and the mixture velocity is defined

$$\vec{V} = \frac{(\rho \vec{V})}{\rho} \quad 2-183$$

or

$$\vec{V} = \frac{\alpha_v \rho_v \vec{V}_v}{\rho} + \frac{\alpha_l \rho_l \vec{V}_l}{\rho}. \quad 2-184$$

Two components of the velocity vector are of interest in COBRA-FLX: the axial direction component, U , and the lateral component, V , which is normal to the axial component.

2.3.2.1.2 *Fluid Thermal Energy Equation*

The thermal energy equation for the two-phase mixture is written as

$$\frac{\partial}{\partial t} ((\alpha \rho h)_l + (\alpha \rho h)_v) + \vec{\nabla} \cdot ((\alpha \rho \vec{V} h)_l + (\alpha \rho \vec{V} h)_v) - q''' = 0. \quad 2-185$$

The above equation has assumed that the contributions of turbulent and viscous dissipation and mechanical work are small and can be neglected. This is reasonable

since the mechanical work terms are small for typical applications where the pressure changes in space and time are small compared to the absolute pressure.

The total heat source per unit volume is defined as

$$q''' = -\vec{\nabla} \cdot \vec{q}_w'' - \vec{\nabla} \cdot \vec{q}_{mix}'' \quad 2-186$$

It consists of the heat transfer between the fuel rods and the fluid and the turbulent mixing heat transfer between subchannels. The heat transfer is divided into a part passing through the cladding as heat flux and a part deposited directly into the coolant.

The mixture energy equation can be further reduced to

$$\frac{\partial(\rho h)}{\partial t} + \vec{\nabla} \cdot (\rho \vec{V} h) - q''' = 0, \quad 2-187$$

where

$$(\rho h) = (\alpha \rho h)_l + (\alpha \rho h)_v \quad 2-188$$

and

$$(\rho h \vec{V}) = (\alpha \rho h \vec{V})_l + (\alpha \rho h \vec{V})_v \quad 2-189$$

The mixture enthalpy is defined to be the flowing enthalpy. The axial direction mass flux is used to define the mixture enthalpy as

$$h = \frac{(\rho h U)}{(\rho U)}, \quad 2-190$$

which can also be written as

$$h = \frac{(\rho h U)_v}{(\rho U)} h_v + \frac{(\rho h U)_l}{(\rho U)} h_l \quad 2-191$$

The flowing mass fraction of the vapor (flowing quality) is

$$\chi = \frac{(\alpha \rho U)_v}{(\rho U)} \quad 2-192$$

and the flowing mass fraction of the liquid is

$$(1 - \chi) = \frac{(\alpha \rho U)_l}{(\rho U)}. \quad 2-193$$

The vapor volume and mass fractions are, therefore, related by the identity

$$\frac{\alpha}{(1 - \alpha)} = \frac{\rho_l}{\rho_v} \frac{U_l}{U_v} \frac{\chi}{(1 - \chi)}. \quad 2-194$$

This is sometimes referred to as the “void-quality” relationship (Reference 2-3). It is a statement that relates void fraction to the flowing quality through a relationship such as that shown. There are others available as options in the COBRA-FLX model via a user option.

The flowing mass fraction is also seen to satisfy the definition for flowing quality

$$\chi = \frac{h - h_l}{h_v - h_l}. \quad 2-195$$

As a result of the above definitions, the time derivative can be written as

$$\frac{\partial}{\partial t}(\rho h) = \frac{\partial}{\partial t}(\rho h) - (h_{fg}) \frac{\partial \Psi}{\partial t}, \quad 2-196$$

where

$$\Psi = \rho_l \chi (1 - \alpha) - \rho_v (1 - \chi) \alpha. \quad 2-197$$

This term corrects the transient term for relative velocity between the phases (Reference 2-1). The final mixture energy equation in conservative form is

$$\frac{\partial}{\partial t}(\rho h) - (h_{fg}) \frac{\partial \Psi}{\partial t} + \vec{\nabla} \cdot \rho \vec{V} h - q''' = 0. \quad 2-198$$

By factoring the first term and introducing the mixture mass equation and the above definitions, the mixture energy equation can be written in the following transportive (and conservative) form

$$\rho \frac{\partial h}{\partial t} - (h_{fg}) \frac{\partial \Psi}{\partial t} + \vec{\nabla} \cdot \rho \vec{V} h - h \vec{\nabla} \cdot \rho \vec{V} - q''' = 0. \quad 2-199$$

This is the form used for computation because of the ease of defining the flow terms. This form is also flux conservative because it consists of the sum of two conservative equations when the mass balance is satisfied. This form is also desirable because it is much less sensitive to flow errors than the conservative form during the intermediate (not converged) stage of the numerical solution. The mixture energy equation is also the void transport equation in the two-phase regime.

2.3.2.1.3 **Momentum Conservation**

The mixture momentum equation is written as

$$\begin{aligned} & \frac{\partial((\alpha \rho \vec{V})_l + (\alpha \rho \vec{V})_v)}{\partial t} + \vec{\nabla} \cdot ((\alpha \rho \vec{V} \vec{V})_l + (\alpha \rho \vec{V} \vec{V})_v) \\ & + \vec{\nabla} P + \vec{F}_w + \vec{F}_i + \vec{g}((\alpha \rho)_l + (\alpha \rho)_v) = 0 \end{aligned} \quad 2-200$$

This can be further reduced to

$$\frac{\partial}{\partial t}(\rho \vec{V}) + \vec{\nabla} \cdot (\rho \vec{V} \vec{V}) + \vec{\nabla} P + \vec{F}_w + \vec{F}_i + \vec{g} \rho = 0. \quad 2-201$$

By using the previous definitions, (ρV) is ρV ; however, (ρVV) is not the same as ρVV . It is necessary to consider the component directions. For the axial component, define

$$(\rho UU) = (\rho U)^2 v' = (\rho U) \hat{U}, \quad 2-202$$

where

$$\hat{U} = (\rho U)v' \quad 2-203$$

and

$$v' = \frac{\chi^2}{\alpha\rho_v} + \frac{(1-\chi)^2}{(1-\alpha)\rho_l} \quad 2-204$$

is the effective specific volume for momentum (Reference 2-1). Similarly, for the lateral component, define

$$(\rho UV) = (\rho V)\hat{U} \quad 2-205$$

Analogous definitions are applied to the lateral direction momentum equations.

The momentum specific volume is different from the mixture specific volume because of the different velocity of the liquid and vapor phases. Note that the momentum specific volume contains void fraction that is defined by the void-quality relationship as a function of quality. This modeling contains the implicit assumption that the relative motion of the liquid and vapor phases is the same in all coordinate directions. This is also true of the standard, SCHEME, COBRA-FLX formulation.

The wall friction term \bar{F}_w is defined by using a distributed resistance approach as for pipe flow in each of the component directions. This involves the use of a friction factor (f_w), two-phase multiplier (Φ_p^2) and component pressure loss factor (K_{ll}). The turbulent momentum term \bar{F}_l is also included. The formulations are the same as in the standard formulation.

2.3.2.2 Control Volume Equations

The concepts and definitions of the previous discussion can be extended to the formulation of control volume equations that are finite difference analogs to the three

dimensional partial differential equations. Additional assumptions are introduced here to allow some simplification of the equation set.

The control volume is based on the subchannel concept of COBRA-FLX. The approach is to divide the rod bundle cross section into flow subchannels and to divide the length into finite increments. The result is a set of control volumes that represent the flow region of the rod bundle. The same philosophy applies to core analysis where subchannels are represented by some combination of partial and/or full fuel assemblies.

This could be viewed as a macro-micro approach and has similarity to flow in porous media or to one-dimensional flow in pipes. The distinguishing feature is that local distributions within a subchannel are not considered. This eliminates the need for zero slip boundary conditions at solid surfaces. Instead, fluid shear is modeled by using friction factors and heat transfer is modeled by using heat transfer coefficients based on subchannel averaged variables. This is made possible by the validity of the hydraulic diameter concept that allows one-dimensional pipe flow modeling to be applied to axial flow in rod bundle subchannels. This is to be contrasted to a more micro approach where the local distributions are considered in the flow field. That level of two-phase flow modeling is not developed for a micro approach and is considered beyond the scope of COBRA-FLX.

The control volume equations to be presented here are fully implicit by placement of all variables at a new time (note that the "old" time is designated by the superscript n – a lack of superscript n or the use of $n+1$ denotes the "new" time. This allows use of a transient solution procedure with a large time step to obtain a steady-state solution. It also allows transient solutions without large time-step restrictions. There are some practical limits to small time steps because compressible water properties are not included in the model.

2.3.2.2.1 *Nodalization*

The PV nodal treatment uses a standard staggered variable placement where scalars are averages for a control volume and vectors are averages over the boundaries of the

control volume. The flow area relating flow and velocity is placed at the control volume boundary. The result is the coincident placement of the mass and energy cells. The momentum cells are staggered. This is a standard numerical approach (Reference 2-4).

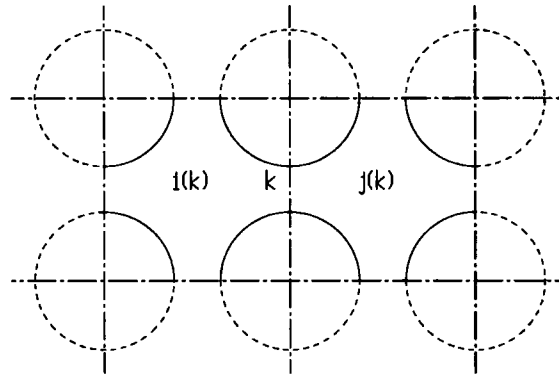
The nodal treatment is identical to that used by SCHEME for mass and energy. The staggered momentum cell treatment is different for PV, but is required for the arbitrary axial flow direction. While the staggered momentum cell introduces numerical definitions different from those used in SCHEME, the subchannel model has not changed.

A. Lateral Nodalization

The lateral nodalization involves the selection of subchannels. While this is rather arbitrary, it must be made consistent with the basic assumptions intended for subchannel analysis. The smallest recommended subchannel is that bounded by rod surfaces and the gaps between rods. Further subdivision cannot be accommodated because closure relationships for fluid-to-fluid shear and heat transfer are not included for that level of detail. Larger channels can be defined that combine several subchannels to model full assemblies used in core analyses.

Lateral bookkeeping for the subchannels and their lateral connection is accomplished by assigning index numbers. Each subchannel is given a number denoted by the index i and its axial location is denoted by the index j . A control volume lateral boundary is denoted by the connection k, j . The control volume axial boundaries are denoted by i, j and $i, j - 1$.

The assignment of the lateral connection number between adjacent subchannels is done in a way that creates a unique ordering. The subchannels are numbered arbitrarily starting with subchannel 1. Connection numbers are assigned sequentially (starting at 1) as higher adjacent subchannel numbers are encountered. Two arrays are created such that for connection k , a subchannel pair is defined by $i(k)$ and $j(k)$ as shown in Figure 2-12.

Figure 2-12: Pair of Interconnected Subchannels

The direction from $i(k)$ to $j(k)$ is taken to be positive if $i(k) < j(k)$.

The derivation of the control volume equations requires consideration of gradient and divergence for transport of mass, energy, and momentum through the faces of the control volumes. This is accomplished by using first-order finite differences in space for the axial and lateral directions. The lateral direction finite differences are expressed by a matrix operator that can be defined simply and compactly. The difference $P_{i(k)} - P_{j(k)}$ represents the pressure drop from $i(k)$ to $j(k)$ and can be expressed by the matrix operation $D_{k,i}P_i$ where

$$D_{k,i} = \begin{bmatrix} 1 & ; & i = i(k) \\ -1 & ; & i = j(k) \\ 0 & ; & \notin k \end{bmatrix}. \quad 2-206$$

Thus, $-D_{k,i}P_i$ is analogous to a lateral pressure gradient where a sum is taken on i .

The transpose $D_{k,i}$ performs an operation that is the divergence in the lateral direction. The sign of $D_{k,i}P_i$ accounts for lateral flow into, or out of, the control volume. The array D is very useful to compact and simplify the notation used in the control volume

equations. The operations of D are performed in the coding by logic using $i(k)$ and $j(k)$ rather than by actual matrix multiplication. The COBRA-FLX code uses arrays $IK(K)$ and $JK(K)$.

Bookkeeping for the connection between fuel rods and subchannels is also included in the lateral direction. The code uses the array $LR(N,L)$ to define the channel number next to rod N for connection L . Up to six connections from a rod to subchannels are allowed. Similarly, the fraction of power from a rod to a subchannel is defined in the code by $PHI(I,L)$. For purposes of the following presentation, let $\varphi_{i,n}$ be the fraction (or multiple) of power from rod n to subchannel i . The total heat transfer to subchannel i can then be written as

$$q_{w_{i,j}} = \sum \varphi_{i,n} q_{w_{n,j}} \quad 2-207$$

or as

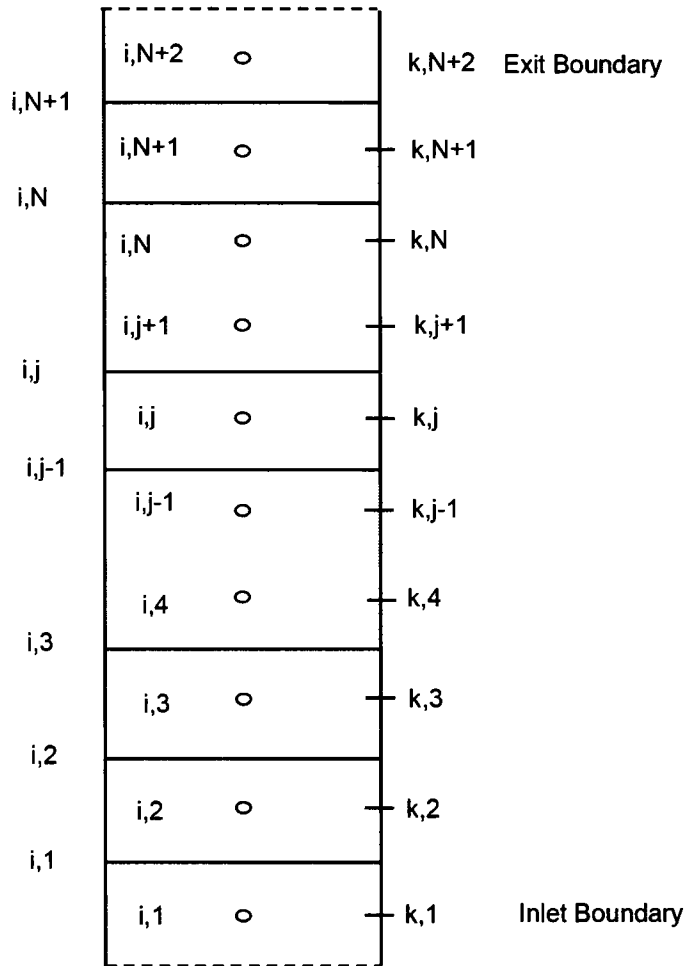
$$q_{w_{i,j}} = \varphi_{i,n} q_{w_{n,j}} \quad 2-208$$

where the sum is understood. In this context, $\varphi_{i,n}$ is similar to $D_{k,i}$ but for the fuel rod to subchannel connection.

B. Axial Nodalization

The second step in nodalization is to divide the channel length into finite lengths. Bookkeeping for the axial node boundaries is accomplished by assigning index numbers. Each subchannel axial location is denoted by the index i,j . The mass and energy control volume axial boundaries are denoted by $i,j-1$ and i,j . The exit boundary is at i,j . Similar index definitions apply to the staggered momentum cells and are defined later. Figure 2-13 illustrates the nodal indexes.

Figure 2-13: Axial Nodal Indices for Control Volumes



2.3.2.2.2 Mass Equation

Figure 2-14 shows the placement of variables on the control volume for the mass equation. The mass conservation equation for a subchannel control volume is

$$\bar{A}_{ij} \Delta x_j \frac{1}{\Delta t} (\rho - \rho^n)_{ij} + (F_{i,j} - F_{i,j-1}) + D_{i,k} W_{k,j} = 0. \quad 2-209$$

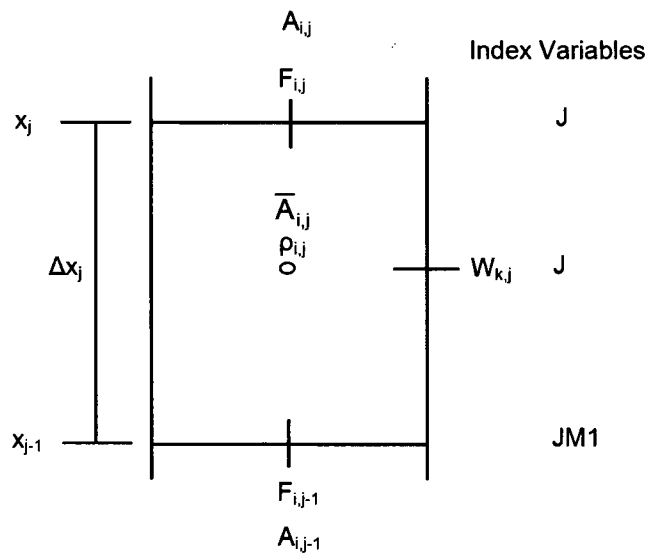
The first term is the mass storage term. The averaged area for the volume is

$$\bar{A}_{i,j} = \frac{1}{2}(A_{i,j-1} + A_{i,j}).$$

2-210

The second term is the divergence of the axial flow. The third term is the divergence of the lateral flow. The crossflow W is the product $w\Delta x$ where w is the crossflow per unit length used within the code ($W(K,J)$).

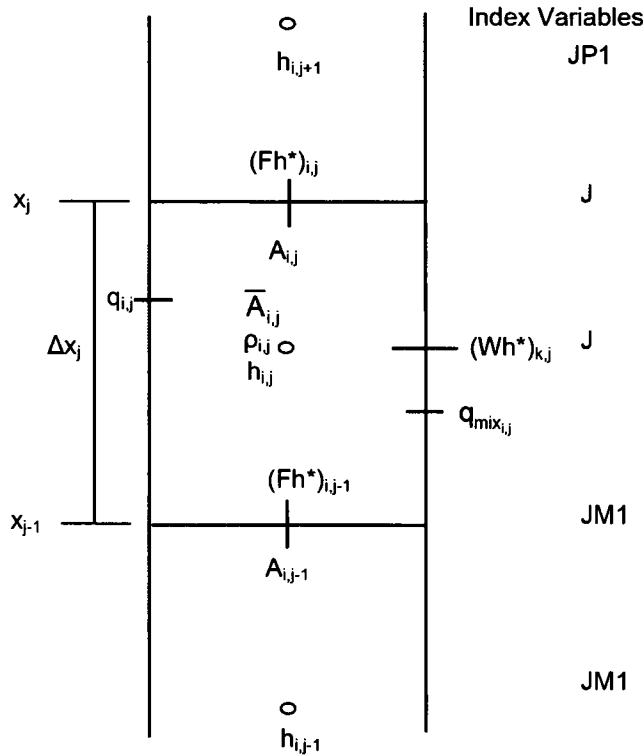
Figure 2-14: Control Volume for Mass Equation



2.3.2.2.3 Energy Equation

Figure 2-15 shows the variable placement for the energy equation.

Figure 2-15: Control Volume for Energy Equation



The control volume form of the mixture energy equation is

$$\begin{aligned} & \bar{A}_{i,j} \Delta x_j \rho_{i,j}^n \frac{1}{\Delta t} (h - h^n) - \bar{A}_{i,j} \Delta x_j (h_{fg}) \frac{1}{\Delta t} (\Psi - \Psi^n)_{i,j} \\ & + (Fh^*)_{i,j} - (Fh^*)_{i,j-1} - h_{i,j} (F_{i,j} - F_{i,j-1}) \\ & + D_{i,k} (Wh^*)_{k,j} - \bar{h}_{i,j} D_{i,k} W_{k,j} - \phi_{i,n} q_{w_{n,j}} + D_{i,k} q_{mix_{k,j}} = 0 \end{aligned} \quad 2-211$$

This form of the energy equation is transportive and also flux-conservative as discussed previously. It is obtained by factoring the temporal term and introducing the mixture mass equation. The divergence terms are readily computed because they consist of naturally occurring terms at the cell boundaries.

The first term is the energy storage term. It uses the same average area as the mass equation. Next is the transient slip correction term (Reference 2-1). Next are the axial

flow terms that define the divergence of the energy flow in the axial direction. This is followed by the lateral flow terms that define the divergence of the energy flow in the lateral direction. The flow terms use donor enthalpies assigned from the direction of the corresponding flows as

$$h_{i,j}^* = \begin{cases} h_{ij} & ; F_{ij} > 0 \\ h_{ij+1} & ; F_{ij} \leq 0 \end{cases} \quad 2-212$$

$$h_{i,j-1}^* = \begin{cases} h_{ij-1} & ; F_{ij-1} > 0 \\ h_{ij} & ; F_{ij-1} \leq 0 \end{cases} \quad 2-213$$

and for the lateral direction

$$h_{k,j}^* = \begin{cases} h_{i(k),j} & ; W_{ki,j} > 0 \\ h_{j(k),j} & ; W_{k,j} \leq 0 \end{cases}. \quad 2-214$$

It should also be noted that the lateral flow is only concerned with a lateral velocity through the gap. There is no specific designation of the coordinate direction for velocities other than lateral. This is a result of the assumptions used for the momentum equations that decouple products of the lateral component velocities.

The heat transfer from the wall and from inter-channel turbulent mixing completes the terms of the energy equation. The heat transfer from the wall consists of contributions from the rods adjacent to a subchannel as indicated by the implied summation over n with $\phi_{i,n}$. The wall heat transfer is split into that due to heat flux and that due to direct moderator heating. The inter-channel turbulent mixing is defined as:

$$q_{mix,k,j} = -W'_{k,j} (h_{j(k),j} - h_{i(k),j}). \quad 2-215$$

W' is the turbulent mixing crossflow and is defined as $W' = w' \Delta x$.

2.3.2.2.4 *Momentum Equation Assumptions*

The three-dimensional momentum equations consist of three equations on a standard coordinate system. The present model retains the common subchannel analysis assumption where the momentum equations are partially decoupled. The flow is assumed to be primarily in the axial direction which allows certain small magnitude cross product momentum flow components to be neglected. To illustrate the assumption, consider the order of magnitude of flow momentum components on the left side of the momentum equations in matrix form:

$$\begin{bmatrix} U*U & U*V & U*W \\ (1*1) & (1*\delta) & (1*\delta) \\ \\ V*U & V*V & V*W \\ (\delta*1) & (\delta*\delta) & (\delta*\delta) \\ \\ W*U & W*V & W*W \\ (\delta*1) & (\delta*\delta) & (\delta*\delta) \end{bmatrix},$$

where U , V , and W are the component velocities. The axial velocity U is of order 1 and the lateral velocities V and W are of order δ . By retaining terms of order 1 and δ , and neglecting terms of order δ^2 , the terms WV , VV , and WW are small and are neglected. The terms UV and UW are important and cannot be neglected. The result of neglecting the small terms is that the V and W component momentum equations can be reduced to a single lateral momentum equation. The result is that the momentum modeling reduces to consideration of two component directions - axial and lateral.

The application of COBRA-FLX PV method to low flows or blockages could lead to situations where the above assumption is not valid. At low flows it is possible for the lateral velocities to be of the same magnitude or greater than the axial velocity. Under those conditions a more complete momentum equation treatment may be required.

2.3.2.2.5 Axial Momentum Equation

The control volume and variable placement for the axial momentum equation is shown in Figure 2-16. Notice the use of a staggered volume centered on flow boundary (i, j) and spanning cells (i, j) and $(i, j + 1)$. The axial mixture momentum equation is written for the staggered control volume in conservative form as

$$\begin{aligned} & \frac{\Delta \hat{x}_j}{\Delta t} (F - F^n)_{i,j} + \left[(\overline{F} \hat{U}^*)_{i,j+1} - (\overline{F} \hat{U}^*)_{i,j} \right] + D_{i,k} \left[(\overline{W} \hat{U}^*)_{k,j} \right] \\ & - W'_{k,j} f_t D_{i,k} \left[\hat{U}_{j(k),j} - \hat{U}_{i(k),j} \right] + \hat{A}_{i,j} (P_{i,j+1} - P_{i,j-1}) \\ & + (\hat{A} K_u F |F|)_{i,j} + (\hat{\rho} \hat{A})_{i,j} \Delta \bar{x}_j g \cos \theta = 0 \end{aligned} \quad 2-216$$

Several geometry definitions are required because of the axially staggered momentum cell. The momentum volume has sub-lengths defined as:

$$\Delta x_+ = f_+ \Delta x_{i,j+1}$$

$$\Delta x_- = f_- \Delta x_{i,j}$$

The interpolation factor f_+ is user defined and $f_- = 1 - f_+$. If $f_+ = 0.5$, the interpolation is that for cell centered pressure on the staggered mesh. If $f_+ = 0.0$, the interpolation is the same as used in SCHEME where the pressure at $j+1$ move down to junction j .

Details of the interpolations are presented later.

At the inlet of the channel $\Delta x_1 = 0$; and, at the exit of the channel $\Delta x_{N+2} = 0$. The length of the control volume is

$$\Delta \bar{x}_j = \Delta x_- + \Delta x_+ \quad 2-217$$

Additional definitions are required for non-uniform area. The areas at the ends of the momentum cell are defined as:

$$\bar{A}_- = \frac{1}{2}(A_{i,j} + A_{i,j-1}) \quad 2-218$$

$$\bar{A}_+ = \frac{1}{2}(A_{i,j+1} + A_{i,j}) \quad 2-219$$

and

$$\bar{A}_{i,j} = \frac{1}{2}(\bar{A}_+ + \bar{A}_-). \quad 2-220$$

The first term of the momentum equation is the temporal acceleration. The initial length for this term is defined as

$$\Delta \hat{x}_j = \Delta \bar{x}_- + \Delta \bar{x}_+ \quad 2-221$$

and is seen to consist of two sub-lengths. For uniform area, $\Delta \bar{x}_- = \Delta x_-$ and $\Delta \bar{x}_+ = \Delta x_+$.

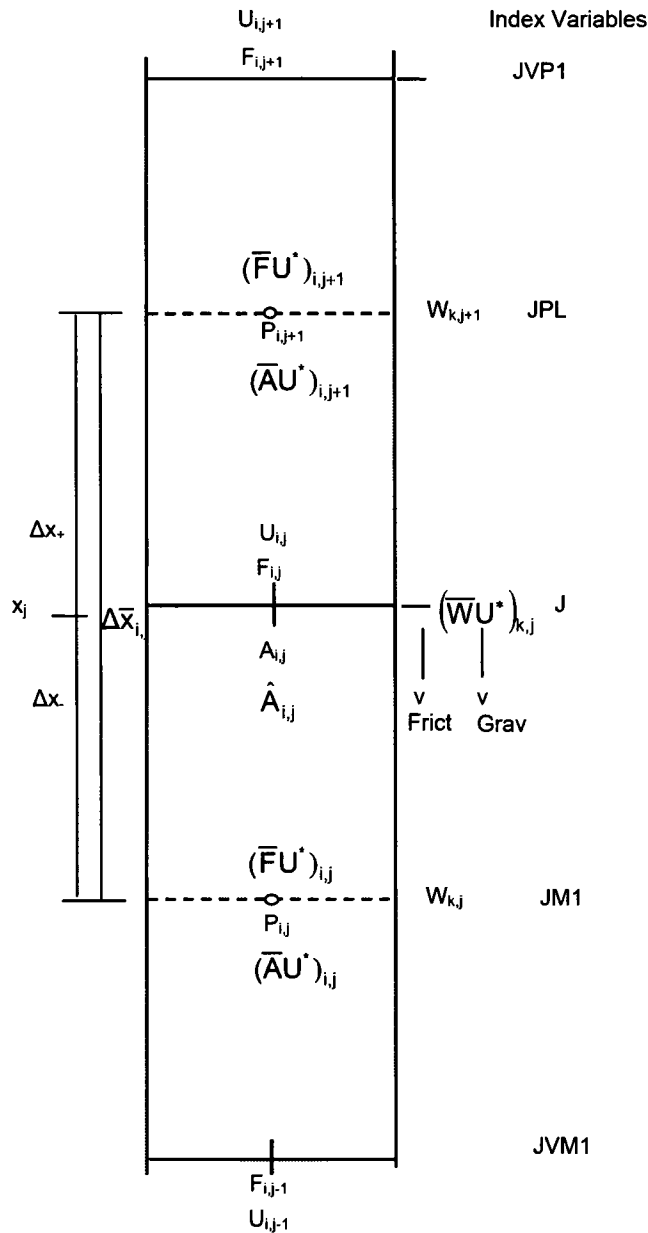
For non-uniform area, the sub-lengths are defined by the integral

$$\Delta \bar{x} = \hat{A} \int \frac{dx}{A}. \quad 2-222$$

The area is assumed to have a linear variation of the form $A = a + bx$ and the integral is

$$\Delta \bar{x} = \hat{A} \frac{1}{b} \ln|a + bx|. \quad 2-223$$

Figure 2-16: Control Volume for Axial Momentum Equation



The sub-lengths are, therefore

$$\Delta \bar{x}_- = \hat{A}_{i,j} \frac{\Delta x_-}{A_{i,j} - \bar{A}_-} \ln \left(\frac{A_{i,j}}{\bar{A}_-} \right) \quad 2-224$$

$$\Delta \bar{x}_+ = \hat{A}_{i,j} \frac{\Delta x_+}{\bar{A}_+ - A_{i,j}} \ln \left(\frac{\bar{A}_+}{A_{i,j}} \right). \quad 2-225$$

The temporal term is modeled here in more detail for non-uniform area than in SCHEME. The modeling is identical for uniform axial area used for licensing analysis.

The third and fourth terms are the spatial acceleration from axial flow. The components are defined as

$$\bar{F}_{i,j} = f_+ F_{i,j} + f_- F_{i,j-1} \quad 2-226$$

$$\bar{F}_{i,j+1} = f_+ F_{i,j+1} + f_- F_{i,j}. \quad 2-227$$

The corresponding velocities at the momentum cell boundaries are defined by donor assignment as

$$\hat{U}_{i,j}^* = \begin{cases} F_{i,j-1} (\bar{v}'/\bar{A})_{ij} & ; \bar{F}_{i,j} > 0 \\ F_{i,j} (\bar{v}'/\bar{A})_{ij} & ; \text{Otherwise} \end{cases} \quad 2-228$$

$$\hat{U}_{i,j+1}^* = \begin{cases} F_{i,j} (\bar{v}'/\bar{A})_{ij+1} & ; \bar{F}_{i,j+1} > 0 \\ F_{i,j+1} (\bar{v}'/\bar{A})_{ij+1} & ; \text{Otherwise} \end{cases} \quad 2-229$$

where

$$\bar{v}'_{ij+1} = f_- \bar{v}''_{ij} + f_+ \bar{v}''_{ij+1} \quad 2-230$$

$$\bar{v}'_{ij} = f_+ \bar{v}''_{ij} + f_- \bar{v}''_{ij-1}$$

SCHEME uses an average of the subchannel velocities and that causes some differences for some applications of the PV model. To provide consistency with SCHEME, PV has a default option to use the average. The user can chose the donor cell velocity approach as defined above.

The fifth and sixth terms are the axial spatial acceleration from lateral flow. The components are defined as

$$\bar{W}_{k,j} = W_{k,j}(\Delta x_+ / \Delta \bar{x}_j) + W_{k,j-1}(\Delta x_- / \Delta \bar{x}_j). \quad 2-231$$

The natural definition of the velocity by donor assignment is

$$\hat{U}_{i,j}^* = \begin{bmatrix} (F\bar{v}'/\bar{A})_{i(k)j} & ; \bar{W}_{k,j} > 0 \\ (F\bar{v}'/\bar{A})_{j(k)j} & ; \text{Otherwise} \end{bmatrix}. \quad 2-232$$

This same definition is used in SCHEME and will be used for PV for numerical solution consistency. There may be some stability issues when using the average.

The last terms are those for pressure gradient, friction and gravity. The average area for those terms is defined as

$$\hat{A}_{i,j} = \frac{1}{\frac{1}{2} \left(\frac{1}{A_+} + \frac{1}{A_-} \right)}. \quad 2-233$$

This definition assures proper pressure drop through area changes. A simple arithmetic average will not give correct results.

The friction coefficient is defined as

$$K_{u_{i,j}} = \frac{1}{2} \frac{1}{A_{i,j}^2} \left(\frac{f_w \Phi_{ip}^2 \bar{v}_l}{D_{hy}} \Delta x + C_D \bar{v}' \right)_{i,j}, \quad 2-234$$

where the averages are defined as

$$\bar{\Phi}_{i,j} = f_+ \Phi_{i,j+1} + f_- \Phi_{i,j} \quad 2-235$$

$$\bar{v}'_{i,j} = f_+ v'_{i,j+1} + f_- v'_{i,j} \quad 2-236$$

$$\bar{v}'_{i,j} = f_+ v'_{i,j+1} + f_- v'_{i,j} \quad 2-237$$

The two-phase friction multiplier is selected by user option and the specific volume for the component pressure loss is also selected by user option.

The average density for the gravity term is defined as

$$\Delta \hat{\rho}_{i,j} = \rho_{i,j} \quad 2-238$$

This definition is used to assign the density to be the same as SCHEME when $f_+ = 0.0$.

It is an approximation to the average value for the momentum cell when $f_+ = 0.5$.

2.3.2.2.6 *Lateral Momentum Equation*

The control volume and variable placement for the lateral momentum equation are shown in

Figure 2-17. The control volume form of the lateral mixture momentum equation is written in conservative form as

$$\Delta y_k \frac{1}{\Delta t} (W - W^n)_{k,j} + (\bar{F} \hat{V}^*)_{k,j} - (\bar{F} \hat{V}^*)_{k,j-1} + \bar{A}_{k,j} (P_{j(k),j} - P_{i(k),j}) + (\bar{A} K_v |W|W)_{k,j} = 0 \quad 2-239$$

where the average axial velocity component is defined as

$$\bar{F}_{k,j} = \frac{1}{2} [F_{i(k),j} + F_{j(k),j}] \quad 2-240$$

In transportive form the lateral momentum balance is written as

$$\begin{aligned} \Delta y_k (\bar{\rho}^n \bar{A})_{k,j} \frac{1}{\Delta t} (V - V^n)_{k,j} + (\bar{F} \hat{V}^*)_{k,j} - (\bar{F} \hat{V}^*)_{k,j-1} \\ - V_{k,j} (\bar{F}_{k,j} - \bar{F}_{k,j-1}) + \bar{A}_{k,j} (P_{j(k),j} - P_{i(k),j}) + (\bar{A} K_v |W|W)_{k,j} = 0 \end{aligned} \quad , \quad 2-241$$

where the mixture velocity in the lateral direction is defined as

$$V_{k,j} = W_{k,j} \left(\frac{1}{\bar{\rho} \bar{A}} \right)_{k,j} . \quad 2-242$$

The transportive form is obtained by factoring the temporal term and introducing the mass equation under the assumption of small lateral velocities as discussed previously. While it is intended to satisfy the mass equation on the momentum cell, some terms are zero as defined by the small crossflow assumptions stated previously.

Several geometry definitions are required because of the laterally staggered momentum cell. The momentum volume is defined to preserve either the global $\left(\frac{s}{l} \right)$ parameter or the local $\left(\frac{s}{l} \right)_{k,j}$ parameter used in the SCHEME modeling. The effective width of the control volume is

$$\bar{S}_{k,j} = \left(\frac{s}{l} \right) \Delta y_k f_k , \quad 2-243$$

where Δy_k is arbitrarily taken to be 1.0 (the value is not important since ratios apply).

The term f_k is a factor that accounts for gaps which are divided by a line of symmetry at a model boundary. For normal gaps (i.e., no symmetry boundary) $f_k = 1.0$. When a gap is bisected by a symmetry boundary, $f_k = 0.5$.

The lateral area for momentum flow is

$$\bar{A}_{k,j} = \bar{S}_{k,j} \Delta x_j . \quad 2-244$$

The first term of the lateral momentum equation is the temporal acceleration. The second term is the lateral spatial acceleration due to the axial flow.

The velocity component in the lateral direction is defined by donor assignment as

$$\hat{V}_{k,j}^* = \begin{cases} \hat{V}_{k,j} & ; \bar{F}_{k,j} > 0 \\ \hat{V}_{k,j+1} & ; \bar{F}_{k,j} \leq 0 \end{cases} \quad 2-245$$

$$\hat{V}_{k,j-1}^* = \begin{cases} \hat{V}_{k,j} & ; \bar{F}_{k,j-1} > 0 \\ \hat{V}_{k,j-1} & ; \bar{F}_{k,j-1} \leq 0 \end{cases} \quad 2-246$$

The velocity used in the donor logic is defined as

$$\hat{V}_{k,j} = W_{k,j} \left(\frac{v'}{A} \right)_{k,j} \quad 2-247$$

There are some small differences between the SCHEME and PV solution. The last two terms to the lateral momentum equation are those for pressure gradient and friction.

The friction coefficient is defined as

$$K_{v_{k,j}} = \frac{K_{ij}}{2 \rho_{k,j}^* (s_{k,j} \Delta x_j f_k)^2}, \quad 2-248$$

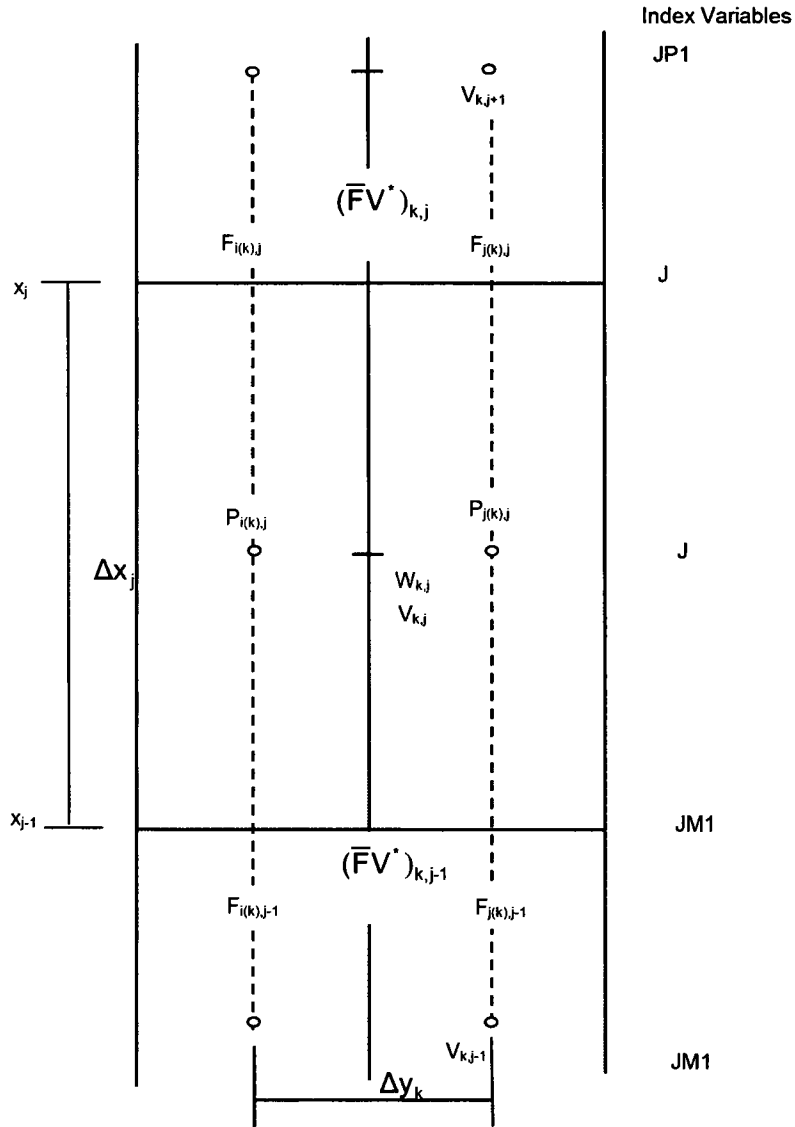
where the friction constant is set to equal the user defined crossflow resistance factor (K_{ij}). Also,

$$|W|_{k,j} = \begin{cases} |W|_{k,j} & ; |W|_{k,j} > 0.001488 \text{ kg}/(s \text{ m}^2) \\ 0.001488 & ; |W|_{k,j} \leq 0.001488 \text{ kg}/(s \text{ m}^2) \end{cases} \quad 2-249$$

The average density is defined as

$$\bar{\rho}_{k,j} = \frac{(\bar{\rho A})_{i(k),j} + (\bar{\rho A})_{j(k),j}}{\bar{A}_{i(k),j} + \bar{A}_{j(k),j}} \quad 2-250$$

Figure 2-17: Control Volume for Lateral Momentum Equation



2.3.2.3 Closure Relationships

The previous conservation equations for mass, energy and momentum have several terms that require additional information (constitutive relations) for closure. The relationships are identical to those of the COBRA-FLX SCHEME option.

2.3.2.3.1 Axial Fluid Friction

The fluid friction modeling in PV is identical to that in SCHEME except that the friction factor is now defined in the laminar regime and donor assignment is used for fluid properties. For turbulent flow the friction factor is defined in the same way as

$$f_{turb} = a Re^b + c, \quad 2-251$$

where the Reynolds number is defined as

$$Re_{i,j} = \left(\frac{F D_{hy}}{A \mu^*} \right)_{i,j}. \quad 2-252$$

Note the donor assignment of viscosity. For laminar flow the friction factor is defined as

$$f_{lam} = \frac{64}{Re}, \quad 2-253$$

with a lower Reynolds number limit of 1.0. The final friction factor is

$$f_w = \max(f_{lam}, f_{turb}). \quad 2-254$$

The max() function eliminates problems of discontinuity between the laminar and turbulent regimes. Since SCHEME cannot get to a low Reynolds number (<2000), this formulation is consistent with SCHEME for licensing analysis. The Reynolds number lower limit of 2000 used in SCHEME does not apply to PV.

The wall viscosity correction to friction factor is an option with PV as it is with SCHEME.

2.3.2.3.2 Lateral Friction

The lateral friction correlation is identical for SCHEME and PV.

2.3.2.3.3 Turbulent Mixing

The turbulent mixing correlation is identical for SCHEME and PV.

2.3.2.4 PV Numerics

The COBRA-FLX PV numerical solution strategy uses a combination of iterative and direct solution. The thermal-hydraulic numerical solution is conceptually split into two parts. The first part solves the momentum and mass equations for the flows and pressure. The second part solves the energy equation and calculates the mixture density from the state equation. Both the flow and energy solutions use the Newton method. The use of the Newton method is of value because it permits a program structure where it is easier to: 1) check the equations being solved; 2) compact the coding; 3) make changes; and 4) monitor convergence.

The solution strategy is an adaptation of the ICE (Reference 2-5) Pressure Velocity method. The primary difference here is being the use of flow rather than velocity. Use of flow has the advantage of simplifying the solution procedure. Flows appear naturally in the conservation equations so they are retained as solution variables. Breaking the flow into its product of density and velocity introduces additional derivatives of density that complicate an already complex solution. The only reason velocity is needed is for use in the momentum convective flow terms.

This section presents a schematic description of the solution procedure as it is programmed. In summary, given initial and boundary conditions, the steady-state solution (or the advancement of the solution one time step) involves a process of iteration and direct matrix solutions. There are two important iteration loops -- outer and inner. The process consists of the following:

(1) Outer Iteration Loop

The outer loop starts with the solution of the energy equations for mixture and phase enthalpies. This solution also defines the quality, void fraction, and mixture density. This is followed by an assignment of momentum specific volumes to nodal boundaries by donor assignment.

This is followed by a solution of the lateral and axial momentum equations. The flows are tentative at this point and subject to correction in the inner loop.

(2) Inner Loop

The inner loop solves the mass equation. This is done by solving for pressure corrections that are then used to update the pressures, axial flows, and crossflows that will drive the solution toward mass conservation.

Iteration continues until convergence of the relative mass error has been achieved or until an iteration limit is reached.

The final step of an outer loop is to save the flows for next outer iteration. Outer iteration continues until the mass error, change in axial flow, and enthalpy convergence criteria are met or until the iteration limits are reached.

2.3.2.4.1 *Newton Solution Method*

Newton's method is used to solve the control volume equations for the PV solution. It is a successive correction procedure that updates a tentative solution such that a residual error is driven to zero. The basic ideas are illustrated for a general function. More specific applications of the method are presented in the following sections.

Consider the equation

$$F(x) = 0 \quad 2-255$$

where x is a solution to the equation. Let \tilde{x} be an initial estimate close to the true solution and let δx be a correction such that the true solution is

$$x = \tilde{x} + \delta x \quad 2-256$$

and

$$F(\tilde{x} + \delta x) = 0. \quad 2-257$$

Expanding the function gives

$$F(\tilde{x}) + \frac{dF(\tilde{x})}{dx} \delta x = 0 \quad 2-258$$

or

$$\left[\frac{dF(\tilde{x})}{dx} \right] \delta x = -F(\tilde{x}). \quad 2-259$$

The right side is the residual error from the initial estimate and the left side contains the coefficient of dF/dx . Solving for δx gives

$$\delta x = -F(\tilde{x}) \left[\frac{dF(\tilde{x})}{dx} \right]^{-1} \quad 2-260$$

When dF/dx is a single value, simple division provides the solution for δx . Given the solution for δx , the tentative value is updated and that value is used as the next tentative solution. The process is repeated until the residual is reduced to an acceptably small value. The Jacobian derivatives can be updated for each iteration to improve convergence although this is not always necessary.

The function can also be a vector function $\vec{F}(\vec{x})$ and then \vec{x} is the solution vector. In that case $[dF/dx]$ is a matrix and the vector $\delta \vec{x}$ is obtained by solution of simultaneous equations.

The Jacobian derivatives provide the “intelligence” to the numerical solution. “Perfect” derivatives can produce the correct solution in one update. In practice, the derivatives are quite approximate and that has an impact on the rate of convergence. Iteration is most rapid when good derivatives are used. Poor convergence or lack of convergence can often be traced to poor derivatives or missing derivatives.

Nonlinear equations can have highly nonlinear or discontinuous Jacobian derivatives and that can lead to numerical difficulties. It is usually important to use derivatives that change slowly during the iteration process. A derivative that flips between two extremes may not produce a converged solution. Successful derivatives will drive the residual to zero.

Newton's method has several advantages over solving a "linearized" equation. The most important is that it solves the nonlinear equation. Solving a linearized equation does not necessarily assure that the nonlinear equation has been solved. Some nonlinear terms can be quite complex and, if errors are made when linearizing, they can be difficult to detect and can lead to erroneous solutions.

The residual is very useful for computation. It is really a statement of the equation being solved and can normally be written in a few lines of a computer program. This provides visibility of the equation and allows easier checking of the program. Monitoring the residual also provides assurance that the solution is actually converging. This is especially important to two phase flow computation to assure conservation of mass, energy and momentum.

Newton's method allows use of a consistent numerical procedure as additional nonlinear terms are brought to a numerical solution. All that need be done is to include the added terms in the residual and Jacobian derivatives.

Newton's method is often used to find roots of equations. In that regard it is possible to obtain multiple solutions to multi valued functions and the solution found depends on the initial x . Most two phase applications do not experience difficulties here because x is normally close to the desired solution which is single valued. An exception to this could occur for situations involving flow instability.

A Newton method is used to solve the control volume equations of the PV solution option. The equations for mixture energy, momentum and mass can be functionally written as the vectors:

Mixture Energy: $E(\tilde{h}, \tilde{F}, \tilde{W}, \tilde{P}) = 0$

Axial Momentum: $M_x(\tilde{h}, \tilde{F}, \tilde{W}, \tilde{P}) = 0$

Lateral Momentum: $M_y(\tilde{h}, \tilde{F}, \tilde{W}, \tilde{P}) = 0$

Mass Continuity: $D(\tilde{h}, \tilde{F}, \tilde{W}, \tilde{P}) = 0$

This represents four equations and four unknowns. The overscore (~) indicates that the variable is treated as a parameter when the equation is solved. Notice that the energy equations depend on the flows (\tilde{F}, \tilde{W}) and that the momentum and continuity (mass) equations depend on the enthalpies (\tilde{h}). Those couplings are important to the numerical approximations used in the solution.

Consider the Newton solution of the above equations in the matrix form:

$$\begin{bmatrix} \frac{\partial E}{\partial h} & \frac{\partial E}{\partial F} & \frac{\partial E}{\partial W} & \frac{\partial E}{\partial P} \\ \frac{\partial M_x}{\partial h} & \frac{\partial M_x}{\partial F} & \frac{\partial M_x}{\partial W} & \frac{\partial M_x}{\partial P} \\ \frac{\partial M_y}{\partial h} & \frac{\partial M_y}{\partial F} & \frac{\partial M_y}{\partial W} & \frac{\partial M_y}{\partial P} \\ \frac{\partial D}{\partial h} & \frac{\partial D}{\partial F} & \frac{\partial D}{\partial W} & \frac{\partial D}{\partial P} \end{bmatrix} \begin{Bmatrix} \delta h \\ \delta F \\ \delta W \\ \delta P \end{Bmatrix} = \begin{Bmatrix} -E \\ -M_x \\ -M_y \\ -D \end{Bmatrix} \quad 2-261$$

The above set represents a very large system of equations and is considered too large for direct solution. As an alternate, it is solved by using a block iteration method.

Because some variables in the equations are treated as parameters, there are zero derivatives in the matrix. As a result, a revised coefficient matrix can be written as:

$$\begin{bmatrix} \frac{\partial E}{\partial h} & 0 & 0 & 0 \\ 0 & \frac{\partial M_x}{\partial F} & 0 & \frac{\partial M_x}{\partial P} \\ 0 & 0 & \frac{\partial M_y}{\partial W} & \frac{\partial M_y}{\partial P} \\ 0 & \frac{\partial D}{\partial F} & \frac{\partial D}{\partial W} & \frac{\partial D}{\partial P} \end{bmatrix} \begin{bmatrix} \delta h \\ \delta F \\ \delta W \\ \delta P \end{bmatrix} = \begin{bmatrix} -E \\ -M_x \\ -M_y \\ -D \end{bmatrix} \quad 2-262$$

Note the zeros. They represent the derivatives with respect to those variables treated as parameters and held constant when the equation is solved. Also note that the matrix divides into four blocks with zeros in the off-diagonal blocks. The diagonal blocks are nonzero and are used in the block iteration procedure. The block at the upper left is the coefficient matrix to solve the energy equations. The block at the lower right is the coefficient matrix to solve the momentum and mass equations for the flow and pressure fields.

The zero blocks in the upper right and lower left do not affect the accuracy of the solution but they can affect the rate of convergence and possibly the stability of the solution. This has relevance to low-flow applications where the gravity and momentum terms can be strongly affected by the mixture density which depends on the energy solution.

Numerical solutions can still be obtained in spite of those zeroed portions of the coefficient matrix. The solution to situations where they become important is to perform the calculation with reduced time steps. Such a provision is included where a time stepping option can be used to achieve steady-state. Under those situations the choice of a sufficiently small time step can create matrix coefficients with enough diagonal dominance to negate the omitted coefficients and drive the solution to convergence. This is viewed as an acceptable compromise to the alternative of solving the full set of equations. Computational experience has been such that low flow situations can be considered by using a smaller time step.

Now consider the solution in each of the diagonal blocks. The energy equation solution is presented first followed by the flow and pressure solutions.

2.3.2.4.2 **Energy Solution**

The energy equation has the functional form

$$E(h) = 0. \quad 2-263$$

The Newton solution form of the energy equations can be written in matrix form as

$$\left[\frac{\partial E}{\partial h} \right] \{ \delta h \} = -\{ E \}, \quad 2-264$$

where δh is the solution vector. This is a formidable matrix system of equations as it involves the solution for enthalpy in all subchannels and at all axial locations. The solution is accomplished by a combination of iteration (outer) and direct solution. The equation is solved at each axial position for the enthalpy in each subchannel as the solution sweeps along the length of the channel. This is done while holding the axial and lateral mixture flows at the latest converged flow solution. The channel is normally swept from the inlet to the exit and a reverse sweep is also performed if a reverse axial flow is detected.

The linear system solved at each level is stored as a banded matrix and solved by Gauss elimination for the incremental vector over the cross section at each axial level j .

The variables are updated by

$$h \leftarrow h + \delta h, \quad 2-265$$

where the left 'arrow' is an update placement equivalent to '=' in FORTRAN. The updated enthalpies are used to define quality, void fraction, and density.

The mixture energy equation for subchannel i at axial location j is written in transportive form as

$$\begin{aligned}
& \bar{A}_{i,j} \rho_{i,j}^n \frac{\Delta x_j}{\Delta t} (h - h^n)_{i,j} - \bar{A}_{i,j} (h_{fg}) \frac{\Delta x_j}{\Delta t} (\Psi - \Psi^n)_{i,j} \\
& + (Fh^*)_{i,j} - (Fh^*)_{i,j-1} - h_{i,j} (F_{i,j} - F_{i,j-1}) \\
& + D_{i,k} (Wh^*)_{k,j} - \bar{h}_{ij} D_{i,k} W_{k,j} - \varphi_{i,n} q_{w_{n,j}} + D_{i,k} q_{mix_{k,j}} = 0
\end{aligned} \tag{2-266}$$

Starting with a zero residual and coefficient matrix, the residual contribution for subchannel i is loaded in as

$$\begin{aligned}
E_{i,j} & \Leftarrow E_{i,j} + \bar{A}_{i,j} \rho_{i,j}^n \frac{\Delta x_j}{\Delta t} (h - h^n)_{i,j} - \bar{A}_{i,j} (h_{fg}) \frac{\Delta x_j}{\Delta t} (\Psi - \Psi^n)_{i,j} \\
& + (Fh^*)_{i,j} - (Fh^*)_{i,j-1} - h_{i,j} (F_{i,j} - F_{i,j-1}) \\
& + D_{i,k} (Wh^*)_{k,j} - \bar{h}_{ij} D_{i,k} W_{k,j} - \varphi_{i,n} q_{w_{n,j}} + D_{i,k} q_{mix_{k,j}}
\end{aligned} \tag{2-267}$$

The residual is initially set to zero and components are accumulated as the various terms are computed. The wall heat transfer is calculated. The contributions to the coefficient matrix diagonal from transient and axial direction flows are

$$\begin{aligned}
\left(\frac{\partial E_i}{\partial h_i} \right)_j & \Leftarrow \left(\frac{\partial E_i}{\partial h_i} \right)_j + \bar{A}_{i,j} \frac{\Delta x_j}{\Delta t} \rho_{i,j}^n + \max \left[- \frac{\bar{A}_{i,j} \Delta x_j (h_{fg}) (\delta \Psi / \delta h)_{i,j}}{\Delta t}, 0 \right] \\
& + \left[\max(F_{i,j}, 0) - \max(-F_{i,j-1}, 0) \right] - (F_{i,j} - F_{i,j-1})
\end{aligned} \tag{2-268}$$

The max() function is applied to the transient slip contribution to assure a positive contribution to the diagonal for stability.

The lateral contributions for the crossflows and turbulent mixing are accumulated by visiting each connection k where contributions are defined for channels $i = i(k)$ and $j = j(k)$. For the $i(k)$ side of connection k , the contribution to the residual is

$$E_{i(k),j} \Leftarrow E_{i(k),j} + W_{k,j} (h_{k,j}^* - h_{i(k),j}) + q_{mix_{k,j}} \tag{2-269}$$

and for the $j = j(k)$ side it is

$$E_{j^{(k)},j} \Leftarrow E_{j^{(k)},j} - W_{k,j} (h_{k,j}^* - h_{j^{(k)},j}) + q_{mix_{k,j}} \quad 2-270$$

The lateral turbulent mixing is defined as

$$q_{mix_{k,j}} = -W'_{k,j} (h_{j^{(k)},j} - h_{i^{(k)},j}). \quad 2-271$$

where the mixing rate is defined as

$$W'_{k,j} = w'_{k,j} \Delta x_j. \quad 2-272$$

The contributions to the coefficient matrix (diagonal and off-diagonal) are:

$$\left(\frac{\partial E_{i^{(k)}}}{\partial h_{i^{(k)}}} \right)_j \Leftarrow \left(\frac{\partial E_{i^{(k)}}}{\partial h_{i^{(k)}}} \right)_j - W_{k,j} \left(1 - \frac{\partial h_{k,j}^*}{\partial h_{i^{(k)},j}} \right) + W'_{k,j} \quad 2-273$$

$$\left(\frac{\partial E_{j^{(k)}}}{\partial h_{j^{(k)}}} \right)_j \Leftarrow \left(\frac{\partial E_{j^{(k)}}}{\partial h_{j^{(k)}}} \right)_j + W_{k,j} \left(1 - \frac{\partial h_{k,j}^*}{\partial h_{j^{(k)},j}} \right) + W'_{k,j} \quad 2-274$$

$$\left(\frac{\partial E_{i^{(k)}}}{\partial h_{j^{(k)}}} \right)_j \Leftarrow \left(\frac{\partial E_{i^{(k)}}}{\partial h_{j^{(k)}}} \right)_j + W_{k,j} \left(1 - \frac{\partial h_{k,j}^*}{\partial h_{j^{(k)},j}} \right) - W'_{k,j} \quad 2-275$$

$$\left(\frac{\partial E_{j^{(k)}}}{\partial h_{i^{(k)}}} \right)_j \Leftarrow \left(\frac{\partial E_{j^{(k)}}}{\partial h_{i^{(k)}}} \right)_j - W_{k,j} \left(1 - \frac{\partial h_{k,j}^*}{\partial h_{i^{(k)},j}} \right) - W'_{k,j}. \quad 2-276$$

The derivatives of the donor enthalpies are defined as

$$\frac{\partial h_{k,j}^*}{\partial h_{i^{(k)},j}} = \begin{bmatrix} 1; & W_{k,j} > 0 \\ 0; & W_{k,j} \leq 0 \end{bmatrix} \quad 2-277$$

$$\frac{\partial h_{k,j}^*}{\partial h_{j^{(k)},j}} = \begin{bmatrix} 1; & W_{k,j} > 0 \\ 0; & W_{k,j} \leq 0 \end{bmatrix}. \quad 2-278$$

2.3.2.4.3 Flow Solution

A Newton solution procedure is also used to solve the mass and momentum equations. The previously presented mass and momentum control volume equations have the functional form

$$\text{Axial Momentum: } M_x(F, \tilde{W}, P) = 0$$

$$\text{Lateral Momentum: } M_y(\tilde{F}, W, P) = 0$$

$$\text{Mass Continuity: } D(F, W, P) = 0$$

where F , W , and P are the solution vectors. As mentioned previously, the enthalpies do not enter the functional form because of the assumed separation of the energy and flow solutions. The variables \tilde{F} and \tilde{W} are those held as parameters for the flow solutions current outer iteration cycle.

The Newton solution form of the equations can be written as the matrix:

$$\begin{bmatrix} \frac{\partial M_x}{\partial F} & 0 & \frac{\partial M_x}{\partial P} \\ 0 & \frac{\partial M_y}{\partial W} & \frac{\partial M_y}{\partial P} \\ \frac{\partial D}{\partial F} & \frac{\partial D}{\partial W} & \frac{\partial D}{\partial P} \end{bmatrix} \begin{Bmatrix} \delta F \\ \delta W \\ \delta P \end{Bmatrix} = \begin{Bmatrix} -M_x \\ -M_y \\ -D \end{Bmatrix} \quad 2-279$$

This system of equations has a block matrix form that allows significant simplification. It will be shown in the following discussion that the matrix elements can be written in the form

$$\begin{bmatrix} [2D] & [2D] & [D] \\ [D] & [0] & [2D] \\ [0] & [D] & [2D] \end{bmatrix}$$

An important feature is the occurrence of diagonal matrices denoted by $[D]$, bi-diagonal matrices denoted by $[2D]$, and the zero-matrices $[0]$. This makes it possible to combine the matrix equations into a single matrix equation that can be solved for δP .

The process is to solve the momentum equations for their respective flows by using the current pressure field as the first step. A result of those solutions is relationships between changes in pressure and flow. Those relationships are combined with the mass equation to produce a pressure correction that is then used to update pressures and flows.

A. Axial Momentum Equation

The axial momentum equation is written in transportive form as

$$\begin{aligned} & \bar{A}_{i,j} \bar{\rho}_{i,j}^n \frac{\Delta x_j}{\Delta t} (U - U^n)_{i,j} + \left[(\bar{F} \hat{U}^*)_{i,j+1} - (\bar{F} \hat{U}^*)_{i,j} \right] + U_{i,j} (\bar{F}_{i,j+1} - \bar{F}_{i,j}) \\ & + D_{i,k} \left[(\bar{W} \hat{U}^*)_{k,j} \right] - U_{i,j} D_{i,k} \left[\bar{W}_{k,j} \right] - W'_{k,j} f_{i,k} D_{i,k} \left[\hat{U}_{j(k),j} - \hat{U}_{i(k),j} \right] + \hat{A}_{i,j} (P_{i,j+1} - P_{i,j}), \\ & + \left(\hat{A} K_u F |F| \right)_{i,j} + \left(\hat{\rho} \hat{A} \right)_{i,j} \Delta x_j g \cos \theta = 0 \end{aligned} \quad 2-280$$

where the several definitions for averages and donor assignments have been made previously. \bar{F} and \bar{W} are held fixed for the current iteration cycle. This equation is solved for the axial flow rates (F) in all subchannels and at all axial levels. This leads to a matrix solution.

The transient term is written in the following form for computational purposes

$$\Delta \hat{x}_j (\bar{A} \bar{\rho}^n)_{i,j} \frac{1}{\Delta t} (U - U^n)_{i,j} = \Delta x_j \frac{1}{\Delta t} \left(\frac{\bar{\rho}^n F}{\bar{\rho}} - F^n \right)_{i,j}. \quad 2-281$$

It is obtained by multiplying top and bottom by the density and applying the definition of the mixture flow (velocity).

The axial momentum equation has the functional form

$$M_x(F, \tilde{W}, P) = 0. \quad 2-282$$

The Newton form of the axial momentum equation is

$$\frac{\partial M_{x_i}}{\partial F} \delta F + \frac{\partial M_{x_i}}{\partial P} \delta P = -M_{x_i} \quad 2-283$$

or

$$\left[\frac{\partial M_{x_i}}{\partial F} \quad \frac{\partial M_{x_i}}{\partial P} \right] \begin{Bmatrix} \delta F \\ \delta P \end{Bmatrix} = -\{M_{x_i}\}. \quad 2-284$$

No derivative of W appears because it is held as a fixed parameter for the current iteration cycle. At this point consider the solution of the momentum equation where the pressure is held at a tentative value subject to later correction; thus, the pressure derivative is zero and

$$\left[\frac{\partial M_{x_i}}{\partial F} \right] \{\delta F\} = -\{M_{x_i}\} \quad 2-285$$

This equation is solved successively at each axial level starting at the inlet. The process described at this point applies for pressure boundary conditions.

It is now necessary to define the residuals and matrix coefficients. This follows the same pattern as the energy equation. Starting with zero residual and coefficient matrix, the residual contribution for subchannel i is

$$M_{x_{i,j}} \Leftarrow M_{x_{i,j}} + \frac{\Delta x_j}{\Delta t} \left(\bar{\rho}^n F / \bar{\rho} - F^n \right)_{i,j} + \left[(\bar{F} \hat{U}^*)_{i,j+1} - (\bar{F} \hat{U}^*)_{i,j} \right] - U_{i,j} (\bar{F}_{i,j+1} - \bar{F}_{i,j}) \\ + \hat{A}_{i,j} (P_{i,j+1} - P_{i,j}) + (\hat{A} K_u F |F|)_{i,j} + (\hat{\rho} \hat{A})_{i,j} \Delta x_j g \cos \theta \quad 2-286$$

The axial flow contribution to the coefficient matrix (diagonal) is

$$\begin{aligned} \left(\frac{\delta M_{x_i}}{\delta F_i} \right)_j &\Leftarrow \left(\frac{\delta M_{x_i}}{\delta F_i} \right)_j + \frac{\Delta x_j}{\Delta t} \left(\bar{\rho}_{i,j}^n / \bar{\rho}_{i,j} \right) + \bar{F}_{i,j+1} \left(\frac{\partial \hat{U}_{i,j+1}^*}{\partial F_{i,j}} - \frac{\partial \hat{U}_{i,j}}{\partial F_{i,j}} \right) \\ &- \bar{F}_{i,j} \left(\frac{\partial U_{i,j}^*}{\partial F_{i,j}} - \frac{\partial U_{i,j}}{\partial F_{i,j}} \right) + \left(\hat{A}K_u \right)_{i,j} \frac{\partial (|F|)}{\partial F_{i,j}} \end{aligned} \quad 2-287$$

The donor velocity derivatives are defined from the phase flow definitions as

$$\left(\frac{\partial \hat{U}_{i,j+1}^*}{\partial F_{i,j}} \right) = \begin{cases} (\bar{v}'/\bar{A})_{i,j+1} & ; \quad \bar{F}_{i,j+1} > 0 \\ 0 & ; \quad \text{Otherwise} \end{cases} \quad 2-288$$

$$\left(\frac{\partial \hat{U}_{i,j}^*}{\partial F_{i,j}} \right) = \begin{cases} (\bar{v}'/\bar{A})_{i,j} & ; \quad \bar{F}_{i,j+1} < 0 \\ 0 & ; \quad \text{Otherwise} \end{cases} \quad 2-289$$

$$\left(\frac{\partial U_{i,j}}{\partial F_{i,j}} \right) = \frac{1}{(\bar{\rho}\bar{A})_{i,j}} \quad 2-290$$

The derivative of the flow in the friction term is defined as

$$\left(\frac{\partial |F|}{\partial F} \right)_{i,j} = \begin{cases} 1|F|_{i,j} & ; \quad \text{Laminar} \\ 2|F|_{i,j} & ; \quad \text{Turbulent} \end{cases} \quad 2-291$$

Only those derivative contributions to the diagonal coefficient at axial level j are included in $\partial M_x / \partial F$. There are also off-diagonal coefficients at levels $j+1$ and $j-1$; however, they are not included because their omission greatly simplifies the matrix computations. Their omission does not affect the accuracy of the solution but it does lead to a slower rate of convergence for the outer iteration than if they were included.

The lateral contributions for the crossflows are accumulated by visiting each connection k , where contributions are defined for subchannels $i=i(k)$ and $j=j(k)$. For connection k , the contribution to the residual is

$$M_{x_{i(k),j}} \Leftarrow M_{x_{i(k),j}} + \bar{W}_{k,j} (\hat{U}_{k,j}^* - U_{i(k),j}) - W'_{k,j} f_t (\hat{U}_{j(k),j}^* - \hat{U}_{i(k),j}) \quad 2-292$$

$$M_{x_{j(k),j}} \Leftarrow M_{x_{j(k),j}} - \bar{W}_{k,j} (\hat{U}_{k,j}^* - U_{j(k),j}) - W'_{k,j} f_t (\hat{U}_{j(k),j}^* - \hat{U}_{i(k),j}) \quad 2-293$$

and the matrix coefficient contributions are:

$$\frac{\partial M_{x_{i(k),j}}}{\partial F_{i(k),j}} \Leftarrow \frac{\partial M_{x_{i(k),j}}}{\partial F_{i(k),j}} + \bar{W}_{k,j} \left(\frac{\partial \hat{U}_{k,j}^*}{\partial F_{i(k),j}} - \frac{\partial U_{i(k),j}}{\partial F_{i(k),j}} \right) + W'_{k,j} f_t \left(\frac{\partial \hat{U}_{i(k),j}}{\partial F_{i(k),j}} \right) \quad 2-294$$

$$\frac{\partial M_{x_{j(k),j}}}{\partial F_{j(k),j}} \Leftarrow \frac{\partial M_{x_{j(k),j}}}{\partial F_{j(k),j}} - \bar{W}_{k,j} \left(\frac{\partial \hat{U}_{k,j}^*}{\partial F_{j(k),j}} - \frac{\partial U_{j(k),j}}{\partial F_{j(k),j}} \right) + W'_{k,j} f_t \left(\frac{\partial \hat{U}_{j(k),j}}{\partial F_{j(k),j}} \right) \quad 2-295$$

$$\frac{\partial M_{x_{i(k),j}}}{\partial F_{j(k),j}} \Leftarrow \frac{\partial M_{x_{i(k),j}}}{\partial F_{j(k),j}} + \bar{W}_{k,j} \left(\frac{\partial \hat{U}_{k,j}^*}{\partial F_{j(k),j}} \right) - W'_{k,j} f_t \left(\frac{\partial \hat{U}_{j(k),j}}{\partial F_{j(k),j}} \right) \quad 2-296$$

$$\frac{\partial M_{x_{j(k),j}}}{\partial F_{i(k),j}} \Leftarrow \frac{\partial M_{x_{j(k),j}}}{\partial F_{i(k),j}} - \bar{W}_{k,j} \left(\frac{\partial \hat{U}_{k,j}^*}{\partial F_{i(k),j}} \right) - W'_{k,j} f_t \left(\frac{\partial \hat{U}_{i(k),j}}{\partial F_{i(k),j}} \right). \quad 2-297$$

The derivatives are defined as

$$\left(\frac{\partial \hat{U}_{k,j}^*}{\partial F_{i(k),j}} \right) = \begin{bmatrix} (v'/A)_{i(k),j} & ; & \bar{W}_{k,j} > 0 \\ 0 & ; & \text{Otherwise} \end{bmatrix} \quad 2-298$$

$$\left(\frac{\partial \hat{U}_{k,j}^*}{\partial F_{j(k),j}} \right) = \begin{bmatrix} (v'/A)_{j(k),j} & ; & \bar{W}_{k,j} < 0 \\ 0 & ; & \text{Otherwise} \end{bmatrix} \quad 2-299$$

$$\left(\frac{\partial U_{i(k),j}}{\partial F_{i(k),j}} \right) = \frac{1}{(\bar{\rho}A)_{i(k),j}} \quad 2-300$$

$$\left(\frac{\partial U_{j(k),j}}{\partial F_{j(k),j}} \right) = \frac{1}{(\bar{\rho}A)_{j(k),j}} \quad 2-301$$

$$\left(\frac{\partial U_i^*}{\partial F_{j(k),j}} \right)_{k,j} = \begin{bmatrix} 1/(\rho^* A)_{j(k),j} & ; & \bar{W}_{i,k,j} < 0 \\ 0 & ; & \text{Otherwise} \end{bmatrix} \quad 2-302$$

This system of equations is solved for δF and provides the flow update

$$F_{i,j} \leftarrow F_{i,j} + \delta F_{i,j} \alpha_x, \quad 2-303$$

where α_x is an acceleration factor. Actually, values less than 1 are normally used; so, it could be called a damping factor.

A result of the above solution is a zero momentum residual (approximately) and there is now a relationship between flow and pressure given by

$$\frac{\partial M_{x_i}}{\partial F} \delta F + \frac{\partial M_{x_i}}{\partial P} \delta P = 0. \quad 2-304$$

$\partial M_{x_i} / \partial P$ is a bi-diagonal matrix with elements given by:

$$\frac{\partial M_{x_{i,j}}}{\partial P_{i,j+1}} = +\hat{A}_{i,j} \quad 2-305$$

$$\frac{\partial M_{x_{i,j}}}{\partial P_{i,j}} = -\hat{A}_{i,j}. \quad 2-306$$

The flow and pressure relationship used for the mass equation solution can now be written as

$$\delta F_{i,j} = -C_{u_{i,j}} (\delta P_{i,j+1} - \delta P_{i,j}), \quad 2-307$$

where

$$C_{u_{i,j}} = \left(\frac{\partial F}{\partial P} \right)_{i,j} = \frac{\hat{A}_{i,j}}{\partial M_{x_{i,j}} / \partial F_{i,j}} \quad 2-308$$

The above presentation is valid for pressure boundary cells and internal cells. The same process applies for boundary cells with flow boundary conditions. The flow is fixed for a flow boundary and the equation to be solved is

$$\frac{\partial M_{x_i}}{\partial P} \delta P = -M_{x_i} \quad 2-309$$

For this case the boundary flow derivatives are set to zero as

$$\frac{\partial M_{x_{i,j}}}{\partial F_{i,j}} = 0 \quad 2-310$$

The pressure derivative for an inlet flow boundary condition is

$$\frac{\partial M_{x_{i,j}}}{\partial P_{i,j}} = -\hat{A}_{i,j} \quad 2-311$$

and, for an exit flow boundary condition, the pressure derivative is

$$\frac{\partial M_{x_{i,j}}}{\partial P_{i,j+1}} = +\hat{A}_{i,j} \quad 2-312$$

The matrix solution for this case provides δP and the pressure is updated as

$$P_{i,j} \leftarrow P_{i,j} + \delta P_{i,j} \quad 2-313$$

B. Lateral Momentum Equation

The lateral momentum equation is written in transportive form as

$$\Delta y_k (\bar{\rho}^n \bar{A})_{k,j} \frac{1}{\Delta t} (V - V^n)_{k,j} + (\bar{F} \hat{V}^*)_{k,j} - (\bar{F} \hat{V}^*)_{k,j-1} - V_{k,j} (\bar{F}_{k,j} - \bar{F}_{k,j-1}) + \bar{A}_{k,j} (P_{j(k),j} - P_{i(k),j}) + (\bar{A} K_v |W|W)_{k,j} = 0 \quad , \quad 2-314$$

where the several definitions for averages and donor assignments have been made previously. \bar{F} and \bar{W} are held fixed for the current iteration cycle.

The transient term is written in the following form for computational purposes

$$\Delta y_k (\bar{\rho}^n \bar{A})_{k,j} \frac{1}{\Delta t} (V - V^n)_{k,j} = \Delta y_k \frac{1}{\Delta t} \left(\frac{\bar{\rho}^n W}{\bar{\rho}} - W^n \right)_{k,j} . \quad 2-315$$

It is obtained by multiplying top and bottom by the density and applying the definition of the mixture crossflow.

The lateral momentum equation has the functional form

$$M_y(\tilde{F}, W, P) = 0 . \quad 2-316$$

The Newton form of the lateral momentum equation is

$$\frac{\partial M_y}{\partial W} \delta W + \frac{\partial M_y}{\partial P} \delta P = -M_y . \quad 2-317$$

No derivative of F appears because it is held as a fixed parameter for the current iteration cycle. At this point consider the solution of the momentum equation where the pressure is held at a tentative value subject to later correction; thus, the pressure derivative is zero and

$$\frac{\partial M_y}{\partial W} \delta W = -M_y . \quad 2-318$$

Now define the residuals and matrix coefficients. The residual is computed for connection k as

$$M_{y_{k,j}} = \Delta y_k \frac{1}{\Delta t} \left(\frac{\bar{\rho}^n W}{\bar{\rho}} - W^n \right)_{k,j} + (\bar{F} \hat{V}^*)_{k,j} - (\bar{F} \hat{V}^*)_{k,j-1} \quad 2-319$$

$$- V_{k,j} (\bar{F}_{k,j} - \bar{F}_{k,j-1}) + \bar{A}_{k,j} (P_{j(k),j} - P_{i(k),j}) + (\bar{A} K_v |W|W)_{k,j}$$

The derivative for the coefficient matrix diagonal is

$$\frac{\partial M_{y_{k,j}}}{\partial W_{k,j}} = \frac{\Delta y_k}{\Delta t} \frac{\bar{\rho}_{k,j}^n}{\bar{\rho}_{k,j}} + \bar{F}_{k,j} \left(\frac{\partial \hat{V}_{k,j}^*}{\partial W_{k,j}} - \frac{\partial V_{k,j}}{\partial W_{k,j}} \right) - \bar{F}_{k,j-1} \left(\frac{\partial \hat{V}_{k,j-1}^*}{\partial W_{k,j}} - \frac{\partial V_{k,j}}{\partial W_{k,j}} \right) \quad 2-320$$

$$+ (\bar{A} K_v)_{k,j} \frac{\partial (|W|W)_{k,j}}{\partial W_{k,j}}$$

This is a diagonal matrix solution because of the dropped momentum terms discussed previously. This equation is solved successively at each axial level starting at the inlet.

The average areas are defined as

$$\bar{A}_{k,j} = \frac{1}{2} (A_{k,j} + A_{k,j+1}) \quad 2-321$$

$$\bar{A}_{k,j-1} = \frac{1}{2} (A_{k,j} + A_{k,j-1}). \quad 2-322$$

The donor densities are defined as

$$\left(\frac{\partial \hat{V}_{k,j}^*}{\partial W_{k,j}} \right) = \begin{bmatrix} (v^*/\bar{A})_{k,j} & ; & \bar{F}_{k,j} > 0 \\ 0 & ; & \text{Otherwise} \end{bmatrix} \quad 2-323$$

$$\left(\frac{\partial \hat{V}_{k,j-1}^*}{\partial W_{k,j}} \right) = \begin{bmatrix} (v^*/\bar{A})_{k,j} & ; & \bar{F}_{k,j-1} < 0 \\ 0 & ; & \text{Otherwise} \end{bmatrix} \quad 2-324$$

$$\left(\frac{\partial V_{k,j}}{\partial W_{k,j}} \right) = \frac{1}{\bar{\rho} \bar{A}_{k,j}}. \quad 2-325$$

The derivative of the flow in the friction term is defined as

$$\left(\frac{\partial |W|}{\partial W} \right)_{k,j} = \begin{bmatrix} 2|W|_{k,j} ; & w_{k,j} > 0.001488 \text{ kg/(m s)} \\ 1|W|_{k,j} ; & \text{Otherwise} \end{bmatrix}. \quad 2-326$$

Only those derivatives at axial level j are included in $\partial M_y / \partial W$. There are also derivatives at levels $j-1$ and $j+1$; however, they are not included in the current solution because their omission greatly simplifies the computations. Their omission does not affect the accuracy of the solution but it does lead to a slower rate of convergence for the outer iteration than if they were included.

Solving for ∂W the crossflow is updated by

$$W_{k,j} \leftarrow W_{k,j} + \delta W_{k,j} \alpha_y. \quad 2-327$$

where α_y is an acceleration factor. Actually values less than 1 are normally used; so, it could be called a damping factor.

A result of the above solution is a zero momentum residual (approximately). There is now a relationship between flow and pressure given by

$$\frac{\partial M_y}{\partial W} \delta W + \frac{\partial M_y}{\partial P} \delta P = 0. \quad 2-328$$

$\partial M_y / \partial P$ is a bi-diagonal matrix with elements given by

$$\frac{\partial M_{y_{k,j}}}{\partial P_{i(k),j}} = -\bar{s}_{k,j} \Delta x_j \quad 2-329$$

$$\frac{\partial M_{y_{k,j}}}{\partial P_{j(k),j}} = +\bar{s}_{k,j} \Delta x_j. \quad 2-330$$

The flow and pressure relationship used in the mass equation solution can now be written as

$$\delta W_{k,j} = -C_{v_{k,j}} (\delta P_{j(k),j} - \delta P_{i(k),j}), \quad 2-331$$

where

$$C_{v_{k,j}} = \left(\frac{\partial W}{\partial P} \right)_{k,j} = \frac{\bar{s}_{k,j} \Delta x_j}{\partial M_{v_{k,j}} / \partial W_{k,j}} \quad 2-332$$

2.3.2.4.4 Mass Equation

The control volume mass balance (mass residual) is written as

$$\bar{A}_{i,j} \Delta x_j \frac{(\rho - \rho^n)_{ij}}{\Delta t} + (F_{ij} - F_{ij-1}) + D_{i,k} W_{k,j} = 0. \quad 2-333$$

The flows are at new time in the mass equation. It has the functional form

$$D(F, W, P) = 0, \quad 2-334$$

where F , W , and P are the solution vectors.

The Newton form of the mass equation is

$$\frac{\partial D}{\partial F} \delta F + \frac{\partial D}{\partial W} \delta W + \frac{\partial D}{\partial P} \delta P = -D. \quad 2-335$$

$\partial D / \partial F$ is a bi-diagonal matrix with elements defined as

$$\frac{\partial D_{ij}}{\partial F_{ij}} = +1 \quad 2-336$$

$$\frac{\partial D_{ij}}{\partial F_{ij+1}} = -1. \quad 2-337$$

$\partial D / \partial W$ is defined as

$$\frac{\partial D}{\partial W} = [D]^T \quad 2-338$$

This matrix has two elements for each connection k at axial level j . For the $i(k)$ side of connection k , the element is

$$\frac{\partial D_{i(k)j}}{\partial W_{k,j}} = D_{i(k),k} = +1 \quad 2-339$$

and for the $j(k)$ side of connection k , it is

$$\frac{\partial D_{j(k)j}}{\partial W_{k,j}} = D_{j(k),k} = -1 \quad 2-340$$

Given that the density has been calculated from the state equation using the tentative pressure, there is also a relationship between density and pressure given by

$$\delta \rho = \frac{\delta \rho}{\delta P} \delta P \quad 2-341$$

This pressure dependence is not currently included in the PV solution.

The previous discussion of the momentum equations has produced equations that relate changes in flow to changes in pressure. Substituting those together with the state relationship into the above Newton form of the mass equation gives the following row of the matrix equation to be solved for a control volume at (i, j) .

$$\begin{aligned} \bar{A}_{ij} \frac{\Delta x_j}{\Delta t} \left(\frac{\partial \rho}{\partial P} \right) \delta P_{ij} - C_{U_{ij}} (\delta P_{ij+1} - \delta P_{ij}) + C_{U_{ij-1}} (\delta P_{ij} - \delta P_{ij-1}) \\ + D_{i,k} C_{V_{kj}} (\delta P_{i(k)j} - \delta P_{j(k)j}) = -D \end{aligned} \quad 2-342$$

The first term is a diagonal element and includes the effect of pressure change on density. It is not contained in the current numerical solution because the fluid is not

compressible. The second and third terms form a tri-diagonal matrix in the axial direction and include the effect of pressure change on the axial flow. The fourth term is generally a full (banded) matrix and includes the effect of pressure change on the lateral flow at axial level j . Direct solution of the entire matrix would require a solution over all control volumes simultaneously and that is a large task. Instead, the solution is done in three parts using an Alternating Direction Implicit (ADI), Successive Over Relaxation (SOR) method.

A. Channel Average Mass Solution

The first part is a solution in the axial direction for the average pressure correction at each axial level. While this is not an SOR step, it is of great value to the overall solution. It takes advantage of the fact that the primary pressure gradient is along the axial length and that the pressure is rather uniform over the cross section. This solution is done by adding the elements of the above equation channel by channel to form a single axial tri-diagonal equation for the average pressure correction at each axial level. All lateral terms cancel. The result of solving the tri-diagonal equation is an array of axial pressure corrections where each is applied uniformly for all channels at the respective axial position; thus,

$$P_{i,j} \leftarrow \tilde{P}_{i,j} + \delta\bar{P}_j. \quad 2-343$$

The axial flows are also updated by

$$F_{i,j} \leftarrow \tilde{F}_{i,j} - C_{U_{i,j}} (\delta\bar{P}_{j+1} - \delta\bar{P}_j). \quad 2-344$$

This is an important calculation that significantly speeds convergence.

B. Mass Solution at each Axial Level - Lateral Direction

The second part of the calculation solves for the pressure correction in the lateral direction. This mass solution is done by solving over the cross section of the bundle

successively at each axial level. In this case the matrix is not tri-diagonal. This computation is valuable when the computation cell is long in the axial direction as compared to the lateral direction such as for subchannel analysis. Given the solution at each level, the pressure update is

$$P_{i,j} \leftarrow \tilde{P}_{i,j} + \delta P_{i,j}. \quad 2-345$$

The axial flows are updated by:

$$F_{i,j} \leftarrow \tilde{F}_{i,j} + C_{U_{i,j}} \delta P_{i,j} \alpha_P \quad 2-346$$

$$F_{i,j-1} \leftarrow \tilde{F}_{i,j-1} + C_{U_{i,j-1}} \delta P_{i,j} \alpha_P. \quad 2-347$$

Notice that only the axial flows at the cell i, j boundaries are updated and that an acceleration factor is used. This is a user definable parameter. A value on the order of 1.8 usually aids convergence. It is typical of SOR methods for elliptic equations. The lateral flows are updated by

$$W_{k,j} \leftarrow \tilde{W}_{k,j} - C_{V_{k,j}} \left(\delta P_{j(k),j} - \delta P_{i(k),j} \right). \quad 2-348$$

An acceleration factor is not used in this direction where the direct solution is performed.

C. Mass Solution along Each Subchannel - Axial Direction

The third part of the calculation solves for the pressure correction along the axial length of each subchannel. In this case the matrix is tri-diagonal. This computation is valuable when the computation cell is long in the lateral direction as compared to the axial direction such as for core wide analysis. Given the solution at each level, the pressure update is as before

$$P_{i,j} \leftarrow \tilde{P}_{i,j} + \delta P_{i,j}. \quad 2-349$$

The axial flows are updated by

$$F_{i,j} \leftarrow \tilde{F}_{i,j} + C_{U_{i,j}} \delta P_{i,j} \quad 2-350$$

$$F_{i,j-1} \leftarrow \tilde{F}_{i,j-1} + C_{U_{i,j-1}} \delta P_{i,j}. \quad 2-351$$

Notice that only the axial flows at the cell i, j boundaries are updated and that an acceleration factor is not used. The lateral flows are updated by

$$W_{k,j} \leftarrow \tilde{W}_{k,j} - C_{V_{k,j}} (\delta P_{j(k),j} - \delta P_{i(k),j}) \alpha_P \quad 2-352$$

Notice that the same acceleration factor is used for the lateral flow update. This is the user definable parameter.

2.3.2.4.5 Solution Procedure and Convergence Criteria

Figure 2-18 shows the PV solution sequence. PV contains the iteration controls and calls all the subroutines significant to the thermal hydraulic solution. Prior to entry to PV, initial conditions and the time dependent boundary forcing functions have been defined.

The first outer iteration step is to solve the mixture energy equations. The solution solved the equations simultaneously over a cross section at each axial level. The quality, void fraction, and mixture density are also defined.

The next iteration step is to assign momentum specific volumes at the boundaries of the mass cells.

The next outer iteration step is to solve the momentum equations and to calculate the tentative axial and lateral flows and related coefficients used in the mass equation solution. The tentative pressure field and the quality, void fraction, and density defined from initial conditions or from the last outer iteration are used as input.

The next outer iteration step is to enter the inner iteration loop to solve the mass equation. This step corrects the pressure and flow fields such that mass conservation is achieved. On the initial iteration, and periodically on subsequent iterations by user option, the axial solution for the average pressure correction and corresponding axial flow correction is performed. This step greatly reduces the number of iterations required for convergence by setting the estimated flow and pressure close to the correct answer. Then, the pressure and flows over the cross section at each axial level are updated. The pressure and flows at each axial level for a single channel are also updated. The inner iteration continues until the mass conservation error decreases to an acceptable value or until the maximum number of iterations is reached.

The next step is to save the flows for the next outer iteration and to determine the fractional change in axial flow used to monitor outer convergence.

The momentum, mass, and energy conservation residuals are monitored and printed during the outer iteration to display the convergence behavior. Convergence of the outer is presently based on three criteria:

1. $(|\delta F|/|F|)_{\max} < \text{allowable relative change in axial flow}$.

The flow in the denominator is limited to not less than 0.002268 kg/s. This is done to keep a reasonable bound on the test for low flow applications.

The fractional change in axial flow is normally the controlling convergence parameter. Convergence of PV to this criterion is slower than SCHEME by about a factor of 4. This is primarily due to the omitted axial off-diagonal derivatives in the momentum equations. Convergence to this criterion can be slowed as the flow decreases and the gravity buoyancy terms become more important. This is further aggravated with boiling flows. Using reduced time steps can improve convergence by adding diagonal dominance to the matrices. Damping can assist with convergence of such cases but it does slow the rate of convergence. When trying to achieve steady-state at low flows, there is a balance between the time step size and the number of steps to achieve steady-state.

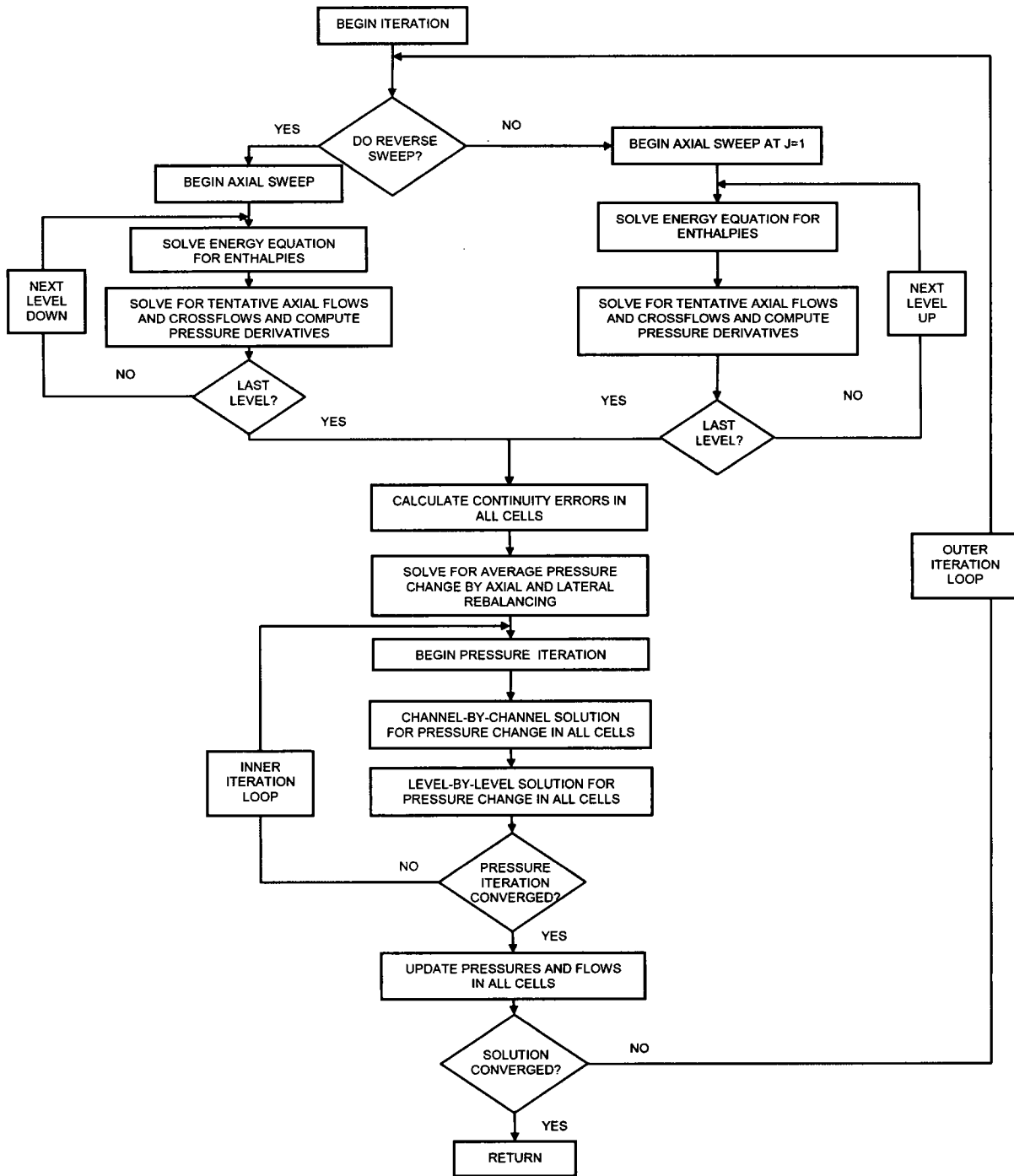
2. $(\overline{\delta h})_{\max} < \text{allowable change in enthalpy} .$

3. $(|D|/|F|)_{\max} < \text{allowable relative mass error per cell} .$

The inner iteration concludes when the third criterion is satisfied or until the maximum iteration limit is reached. The outer iteration continues until all criteria have been met or until the outer iteration limit is reached.

The solution step is completed at the end of the outer iteration; results are printed and the calculation is ended or continues with the next time.

Figure 2-18: PV Solution Sequence



2.4 *Boundary Conditions*

The boundary conditions required in COBRA-FLX help determine the types of problems it can be applied to. They define the “edges” of a problem in steady state and provide the mechanism for driving the solution in a transient. The code has a certain bare minimum of requirements for boundary conditions, but it is as flexible as possible in the manner they are applied. COBRA-FLX requires that the following boundary and operating conditions be specified for each case:

- Inlet enthalpy / Inlet temperature
- Power
- System pressure
- Exit pressure distribution
- Inlet flow rate

2.4.1 *Inlet Enthalpy / Inlet Temperature*

Inlet enthalpy (or inlet temperature) may be uniform or prescribed for each channel separately. If the inlet flow is subcooled or superheated, the inlet temperature may be specified in lieu of enthalpy, and may be either uniform or specified for each channel. Temporal variation in the enthalpy / temperature can be specified under transient conditions.

2.4.2 *Power*

The power describes the energy entering the fluid from the heat structures. It is specified in term of an average surface heat flux (kW/m^2) or a distribution of local node powers is provided via an additional input file. The average power is modified by the axial and radial power profiles input with the rod geometry. Temporal variation in the average power as well as the local node powers can be specified under transient conditions.

The COBRA-FLX power supply model computes the heat source term for the fluid energy equation on a boundary conditions basis. Given the average heat flux and the spatial and temporal power distribution, the heat flux of the n^{th} rod is calculated as

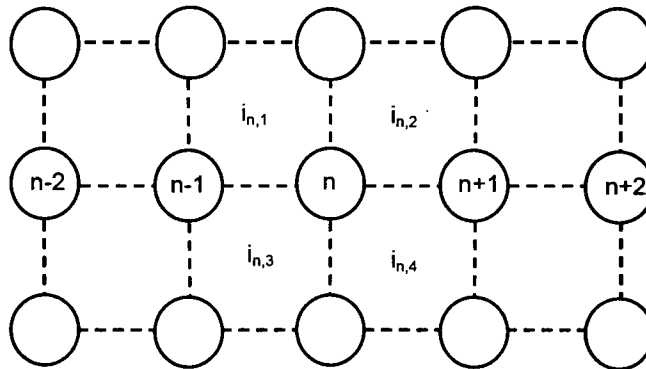
$$q_n'' = \overline{q}'' F_{\text{radial}} F_{\text{axial}} F_{\text{temporal}}, \quad 2-353$$

where \overline{q}'' is the average heat flux, defined as of the power generated in all rods divided by the total surface available for heat transfer to the fluid; F_{radial} is the relative rod power, defined as a ratio of the n^{th} rod power to the power averaged over all rods; F_{axial} is the relative axial heat flux, defined as a ratio of the local heat flux at a given axial elevation to the heat flux averaged over heated length; and F_{temporal} is the power forcing function factor, defined as a ratio of the initial power to the current power ($F_{\text{temporal}} = 1.0$ for steady state calculations).

In COBRA-FLX, one rod can be thermally connected up to six subchannels. Therefore, the heat rate from the rod n to the fluid in the surrounding subchannels will be given as

$$q_n' = \sum_{i=1}^6 \pi D_r \phi_{ni} q_n'', \quad 2-354$$

where i is the subchannel connected to rod n ; ϕ_{ni} is the fraction of rod n 's heated perimeter connected to subchannel i . An example of rod with multiple (four) fluid connections is shown in Figure 2-19.

Figure 2-19: Example of Rod with Multiple Fluid Connections

Having the coolant bulk temperature, T_b , and the heat transfer coefficient, h , defined, the surface temperature of the n^{th} rod is calculated as

$$T_w = \left(\frac{q_n''}{h} + T_b \right). \quad 2-355$$

2.4.3 System Pressure

The system pressure is used to define saturation conditions uniformly throughout the region. Temporal variation in the pressure can be specified under transient conditions.

2.4.4 Exit Pressure Distribution

The standard method is using a uniform pressure at the exits of all subchannels. Additionally, COBRA-FLX has an option to model a non-uniform exit pressure distribution. In this case the difference between the absolute exit pressure and the average exit pressure is to be specified for each relevant channel by input.

2.4.5 Inlet Flow

The inlet flow boundary condition may be specified in term of a uniform mass velocity. Individual subchannel flow fractions can also be specified. Although COBRA-FLX always solves the system of conservation equations in terms of a specified inlet flow, there is an option for splitting the total flow to give equal pressure gradient at the inlet of all subchannels. The total flow may change by the input forcing function on the inlet mass flow.

2.4.6 Transient Forcing Functions

To simulate transients, the inlet enthalpy/temperature, power, system pressure, and inlet flow can vary in time. COBRA-FLX accepts tables of relative (or actual) value of the parameter to be varied versus time. Linear interpolation is used to obtain values between specified time entries. The value of parameter P at time t is computed as

$$P(t) = F(t)P(0), \quad 2-356$$

where $F(t)$ is the interpolated value from the table at time t and $P(0)$ is the steady state value of parameter P . Alternatively, the actual value of the parameter may be used in a table, so that

$$P(t) = F(t), \quad 2-357$$

where $F(t)$ is the interpolated value from the table at time t . Forcing function tables are defined by user input, or they may be read from an external file. Factors entered in the forcing function tables apply to any of the input options available for that parameter. Transient time and the number of time steps in a transient are specified by input. The default is a uniform time step throughout the transient, but the user may select options for non-uniform time steps. The user can let the code select time step automatically to preclude the loss of forcing function details.

2.5 *References*

- 2-1 L. S. Tong, *Boiling Heat Transfer and Two-Phase Flow*, Wiley (1966).
- 2-2 Rowe, D.S., *COBRA IIIC: A Digital computer program for Steady State and Transient Thermal-Hydraulic Analysis of Rod Bundle Nuclear Fuel Elements*, BNWL-1695, March 1973
- 2-3 R. T. Lahey, Jr. and F. J. Moody, *The Thermal-Hydraulics of a Boiling Water Reactor, Second Edition*, American Nuclear Society, 1993.
- 2-4 S. W. Webb and D. S. Rowe, "Modeling Techniques for Dispersed Multiphase Flows," Chapter 19, *Encyclopedia of Fluid Mechanics*, Gulf Publishing Co., Houston TX, 1986.
- 2-5 F. H. Harow and A. A. Amsden, "A Numerical Fluid Dynamics Calculation Method for All Flow Speeds," *Journal of Computational Physics*, Volume 8, No. 2, October 1971.

3.0 CODE STRUCTURE AND FLOW LOGIC DESCRIPTION

The code structure and solution logic are provided in the form of several flow charts. The functional hierarchy in COBRA-FLX is shown in Figure 3-1. The main program COBRA-FLX calls various subroutines to read input and initialize the calculation. The input data is read by subroutine INDAT. The calculation process is controlled by subroutine CALC. At the beginning of each time step, the boundary conditions and forcing functions are established. The overall fluid solution is driven by subroutine CALC_SOLVE and the heat input to the coolant is defined in subroutine HEAT. Result reporting is performed by subroutine EXPRIN. The high-level code solution logic is shown in Figure 3-2. The SCHEME and PV solution algorithms are given in Figure 3-3 and Figure 3-4, respectively.

Figure 3-1: COBRA-FLX Code Structure

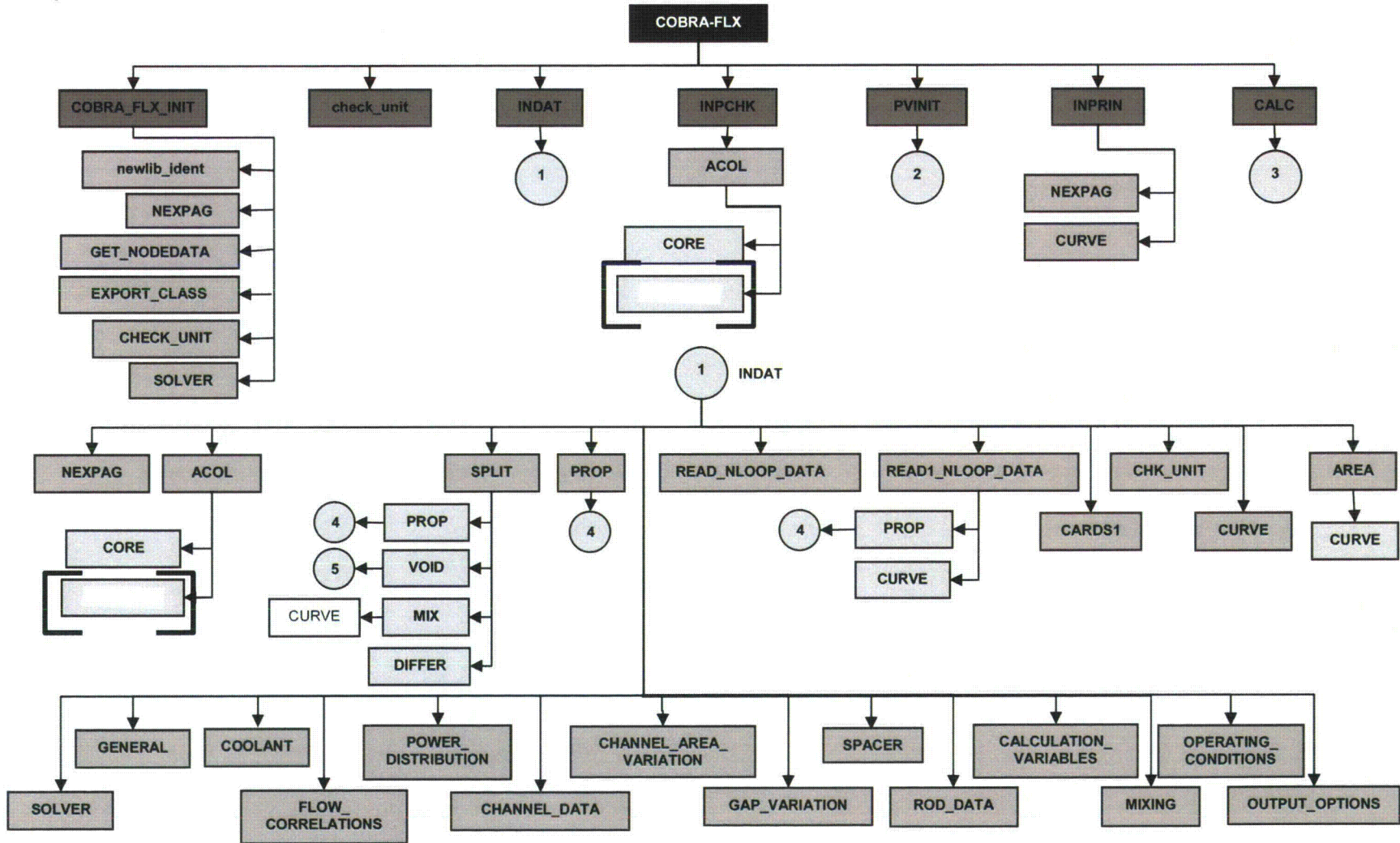


Figure 3-1: COBRA-FLX Code Structure (continued)

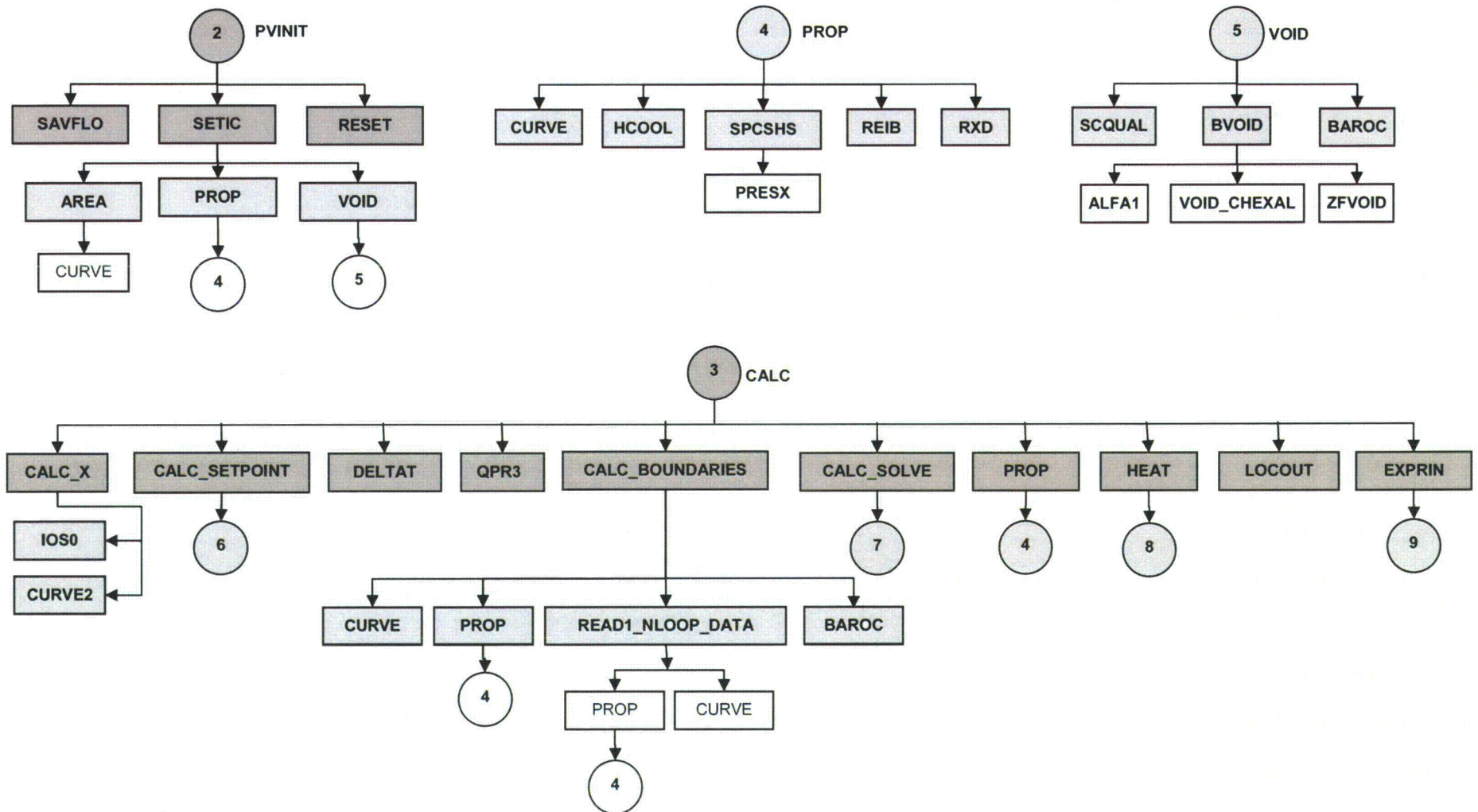


Figure 3-1: COBRA-FLX Code Structure (continued)

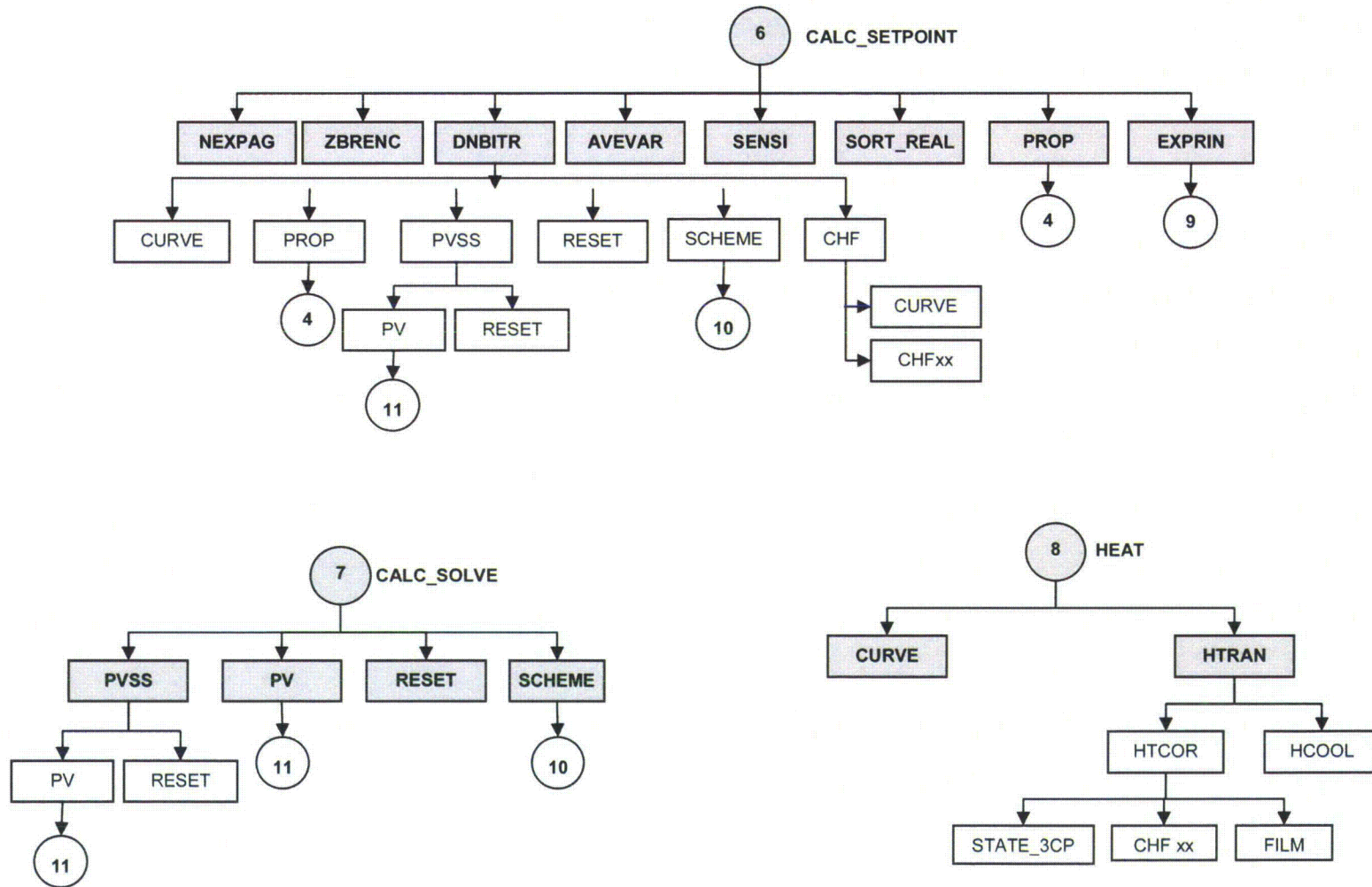


Figure 3-1: COBRA-FLX Code Structure (continued)

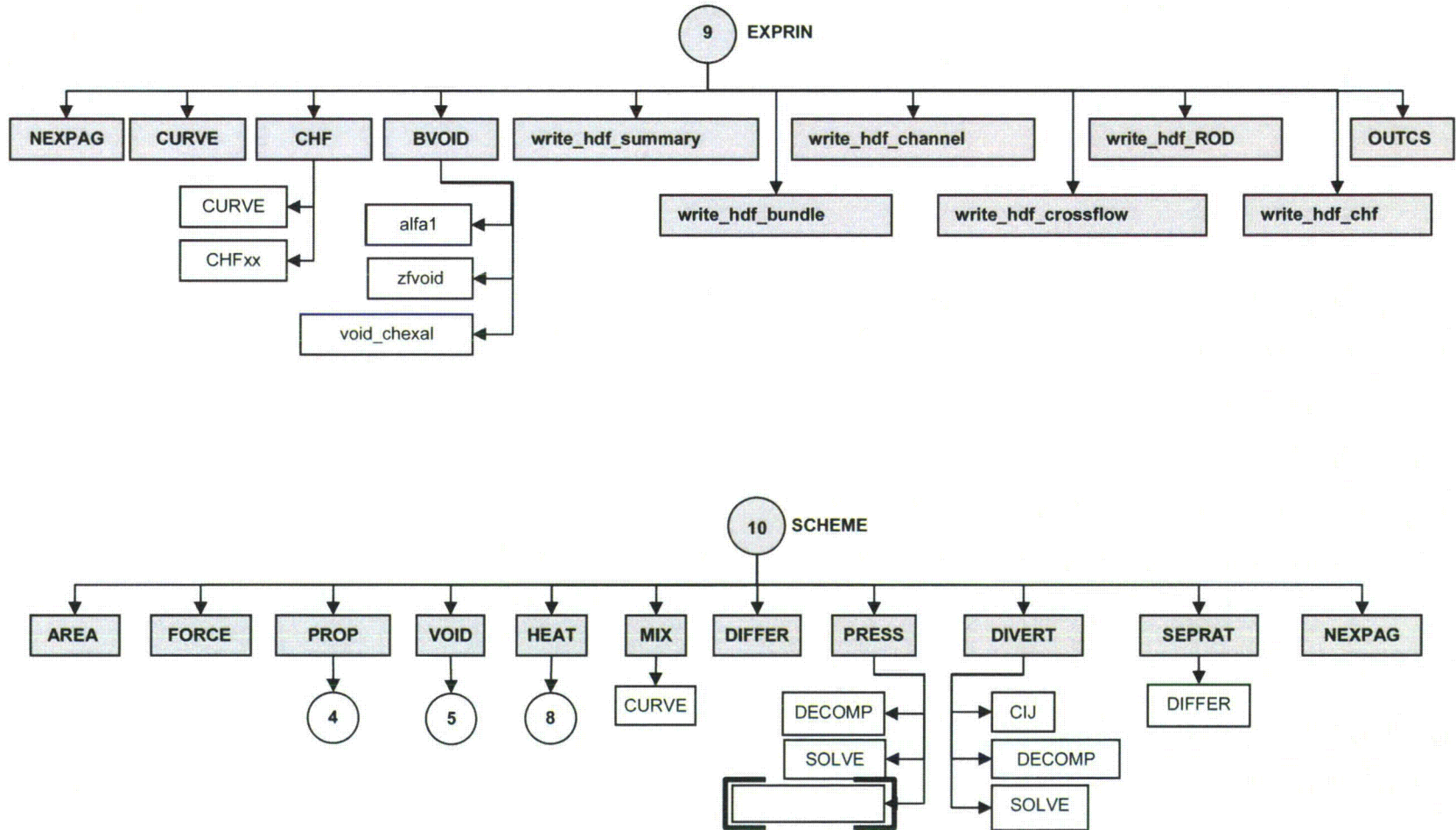


Figure 3-1: COBRA-FLX Code Structure (continued)

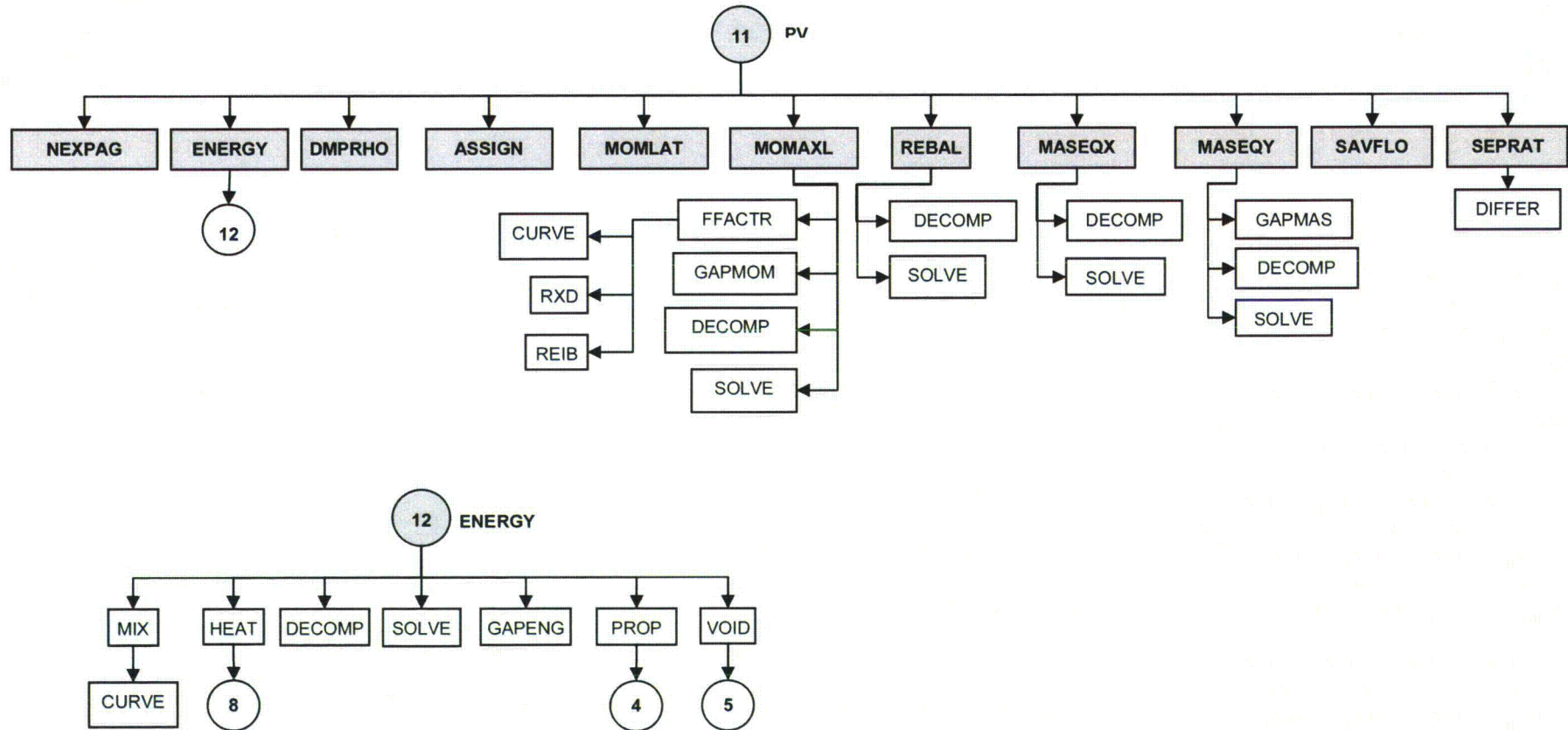


Figure 3-2: COBRA-FLX High Level Solution Logic

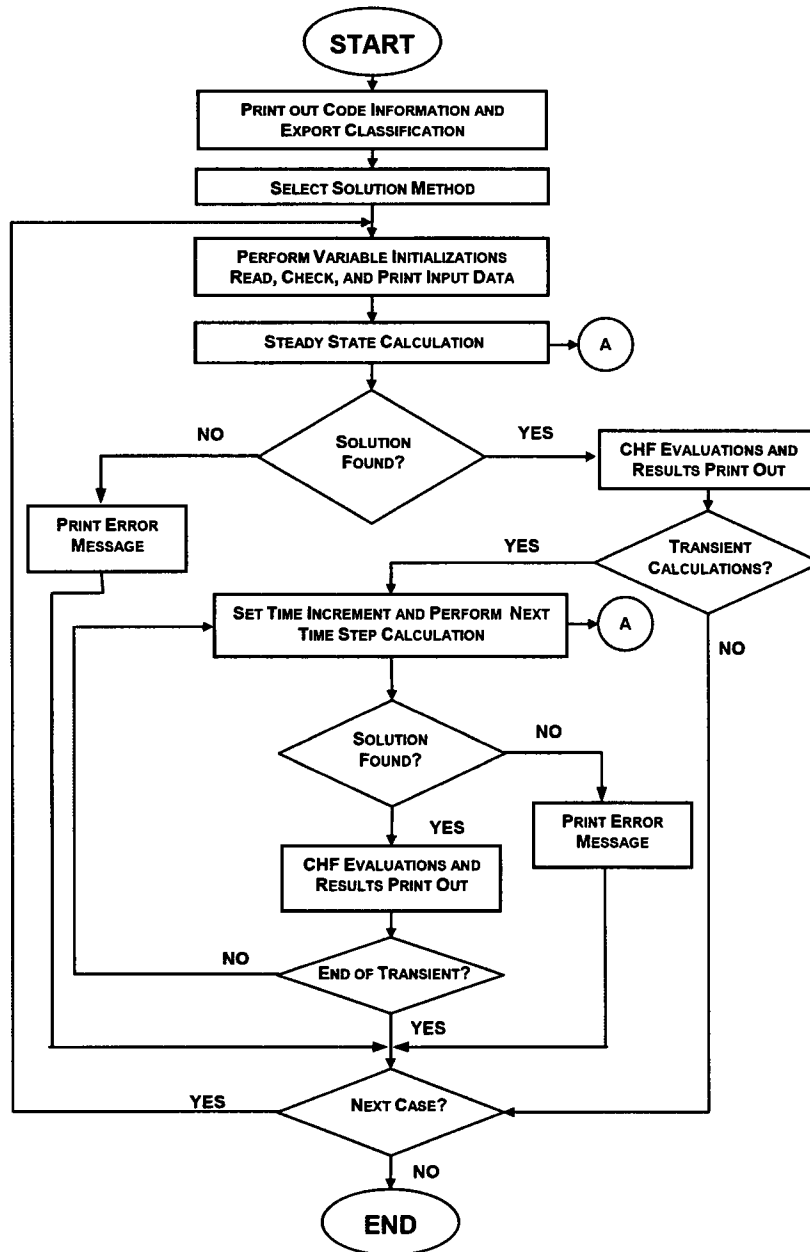


Figure 3-2: COBRA-FLX High Level Solution Logic (continued)

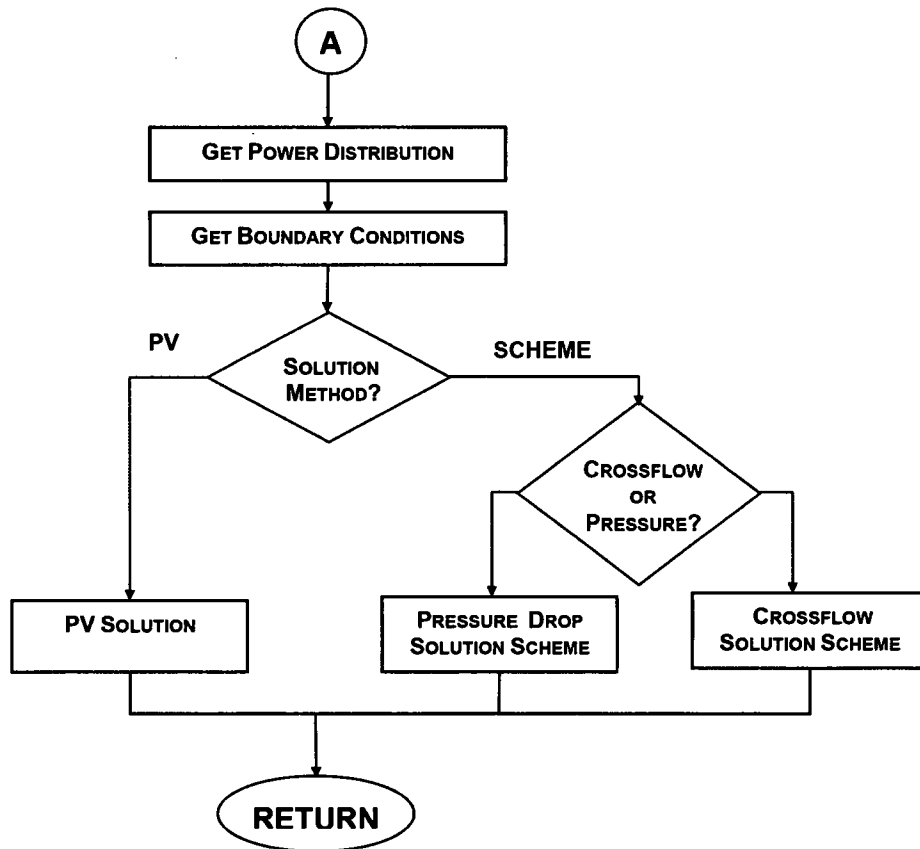


Figure 3-3: SCHEME Solution Logic

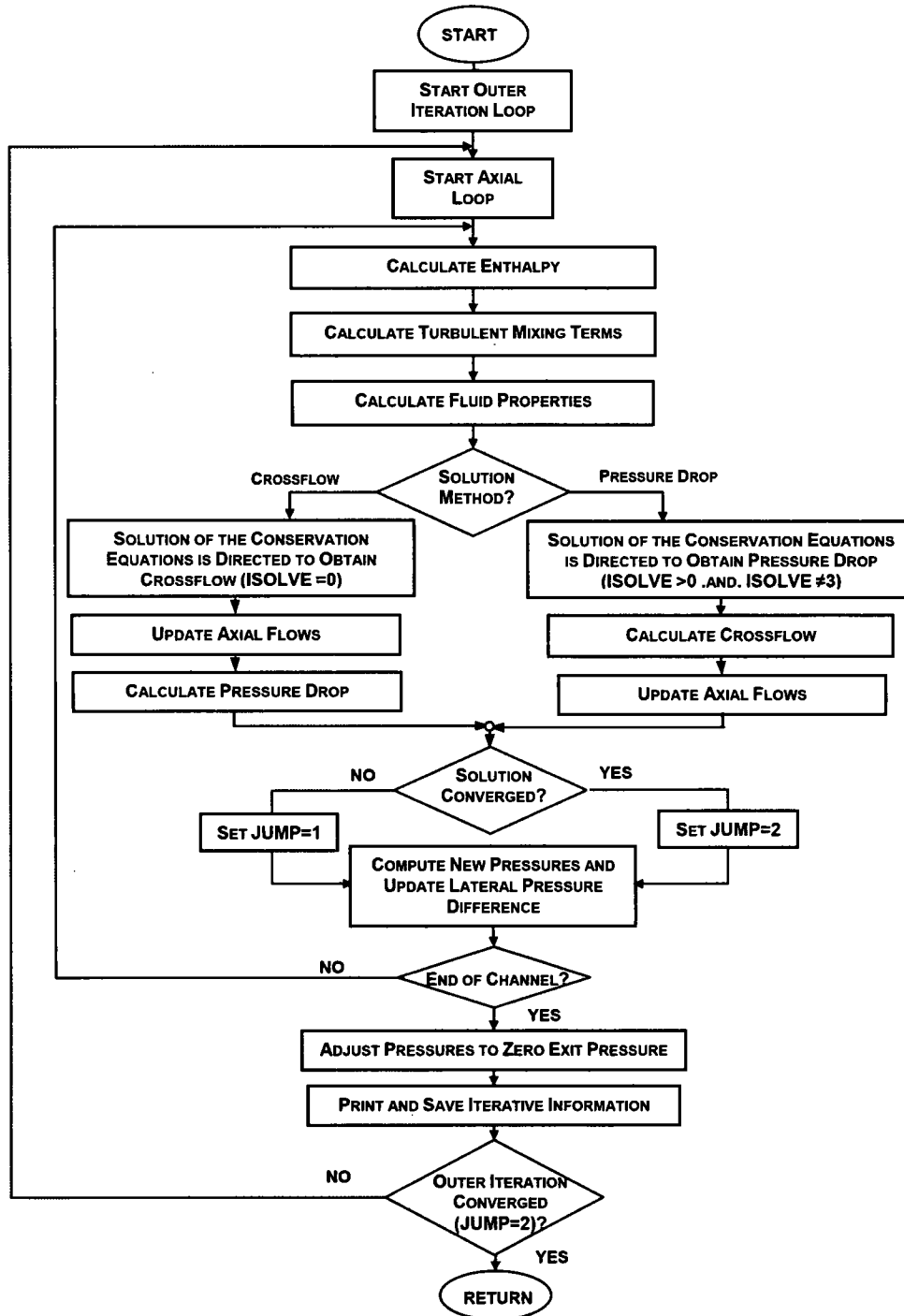
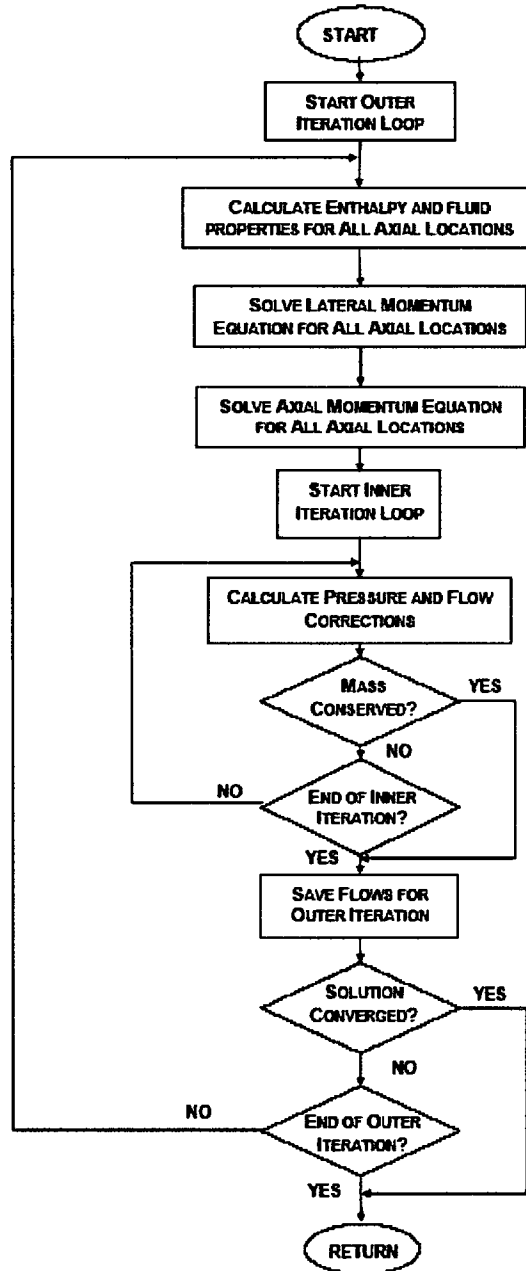


Figure 3-4: Pressure-Velocity (PV) Solution Logic



4.0 SUBROUTINE DESCRIPTION

In Section 4, the COBRA-FLX subroutines and functions are described in alphabetic order. The overall code execution is controlled by the main program COBRA-FLX. Subroutines and functions which are outside the ARCADIA code package (e.g. for the internal fuel rod model and the Card Group 20 input) are not listed.

ACOL (ISOLVE, KMAX, NDX, MZ, NCHAN, NK, IK, JK) – Depending on the selected method for solution of the conservation equations, this subroutine defines the width of the coefficient matrix AAA via the size of the LOCA array.

If the solution is directed to crossflow (ISOLVE = 0), LOCA(K,L), L=1,MZ-1 specifies up to LOCA(K,MZ) boundaries adjacent to the two subchannels that define the boundary K. If the solution of the conservation equations is directed to pressure drop or the pressure-velocity solution method is used (ISOLVE = 1, 3, 4, and >10), LOCA(I,L), L=1,MZ-1 specifies up to LOCA(I,MZ) boundaries adjacent to the subchannel I. ACOL calls subroutine CORE to size the AAA matrix.

| | | |
|------------|--------|--|
| Arguments: | ISOLVE | Indicator of the solution method of conservation equations (input) |
| | KMAX | = Number of gaps if the crossflow solution method is used (input) = Number of subchannels if the pressure drop solution method is used (input) = Maximum of (JK(K) – IK(K)) if the pressure-velocity solution method is used (input) |
| | NDX | Number of axial nodes (input) |
| | MZ | Maximum number of gaps/subchannels adjacent to a gap/subchannel (input) |
| | NCHAN | Number of subchannels (input) |
| | NK | Number of gaps (input) |
| | IK | Identification number of the lower-numbered subchannel adjacent to gap K (input) |
| | JK | Identification number of the higher-numbered subchannel adjacent to gap K (input) |

ACOL is called by subroutines CHAN, INDAT, INPCHK and PREP.

ACOL calls subroutines CORE and [].

ALFA1 (G, X, RL, RG, VL, VG, ALPHA, AK, IKOR) – This subroutine determines the slip ratio and the void fraction using the Chexal-Lellouche correlation.

| | | |
|------------|-------|---|
| Arguments: | G | Mass flux (kg/m^2-s) (input) |
| | X | Quality (-) (input) |
| | RL | Liquid density at saturation (kg/m^3) (input) |
| | RG | Vapor density at saturation (kg/m^3) (input) |
| | VL | Dynamic viscosity of liquid ($kg/m-s$) (input) |
| | VG | Dynamic viscosity of vapor ($kg/m-s$) (input) |
| | ALPHA | Void fraction (-) (output) |
| | AK | Slip ratio (-) (output) |
| | IKOR | = 2 (not used) |

ALFA1 is called by the function BVOID.

AREA (J) – This subroutine calculates the subchannel area and the gap spacing at each axial elevation by using a tabular list of area and gap variations supplied as input. A linear interpolation is used to select values from these tables. If it is requested via input the transverse momentum parameter is calculated based on the local geometry and stored in FACSL(K,J).

AREA modifies the area and hydraulic diameter when wire wraps are present in the subchannel.

| | | |
|------------|---|---|
| Arguments: | J | Axial node index (input) = 1 or NDXP1 if called by INDAT = 1 if called by PREP = J if called by SCHEME and SETIC |
|------------|---|---|

AREA is called by subroutines INDAT, PREP, SCHEME, and SETIC.

AREA calls subroutine CURVE.

ASSIGN – This subroutine assigns the momentum specific volume and density to the momentum cell boundaries for use by the PV-momentum solution. Donor assignment is used in the axial and lateral directions.

Arguments: None

ASSIGN is called by subroutine PV.

AVEVAR (DATA, N, AVE, VAR) – This subroutine calculates the average and the variance of a sample of variables when sensitivity calculations are required.

| | | |
|------------|------|-----------------------------|
| Arguments: | DATA | Sample of variables (input) |
| | N | Sample size (input) |
| | AVE | Sample average (output) |
| | VAR | Sample variance (output) |

AVEVAR is called by subroutine CALC_SETPOINT.

BAROC (IPART, P_SI, Q, GWV, FMULT, PPI) – This subroutine calculates the two-phase friction multiplier using Baroczy's model.

| | | |
|------------|-------|---|
| Arguments: | IPART | Input signal (input) = 1 – enters with pressure and sets the array CORAB = 2 – enters with mass velocity and quality and interpolates in CORAB to obtain the multiplier |
| | P_SI | Pressure (Pa) (input) |
| | Q | Quality (-) (input) |
| | GWV | Mass flux (kg/m^2-s) (input) |
| | FMULT | Two-phase friction multiplier (output) |
| | PPI | Physical property index (output) <i>Not used</i> |

BAROC is called by subroutine VOID and CALC_BOUNDARIES.

Function **BVOID (I, J, TVF, TRHOF)** – This function calculates the bulk void fraction at given quality using different correlations/models. The selection of the correlation/model to be used is done internally according to the input.

| | | |
|------------|-------|--|
| Arguments: | I | Subchannel index (input) |
| | J | Axial level index (input) |
| | TVF | Fluid specific volume (m^3/kg) (input) |
| | TRHOF | Saturated fluid density (kg/m^3) (input) |

BVOID is used by subroutines EXPRIN and VOID.

BVOID calls subroutine ALFA1, ZFVOID, VOID_CHEXAL.

Function **BWFNU (RN, AX, C)** – This function calculates the B&W formulation of the Tong non-uniform heat flux factor (FNU). The used formulation is consistent to the one available in LYNXT.

| | | |
|------------|----|---|
| Arguments: | RN | Rod number (input) |
| | AX | Axial level index (input) |
| | C | C-term in the FNU calculation (in^{-1}) (input) |

BWFNU is used by subroutines CHF50, CHF55, CHF56, CHF57, CHF58, CHF59, CHF60, CHF61, CHF62 and CHF63.

BWFNU calls subroutine CURVE.

CALC – This subroutine controls the overall calculation in the following sequence:

- calls CALC_X to define axial coordinates;
- calls CALC_SETPOINT to perform setpoint and sensitivity calculations if required;
- defines the time step size if transient calculations are to be performed;
- calls QPR3 to obtain 3D power distribution from the file POWER3D if selected by input;
- calls CALC_BOUNDARIES to establish the subchannel boundary conditions and forcing function values;
- calls CALC_SOLVE to start the iteration process using PV or SCHEME solution algorithm;
- sets conditions for the next time step (i.e., stores the obtained solution for using it at the next time step);
- calls LOCOUT to store the coolant conditions into an additional output file if selected by input;
- calls EXPRIN to print out results;

Arguments: none

CALC is called by the main program COBRA-FLX.

CALC calls subroutines CALC_BOUNDARIES, CALC_SETPOINT, CALC_SOLVE, CALC_X, DELTAT, EXPRIN, HEAT, LOCOUT, PROP, and QPR3.

CALC_BOUNDARIES – This subroutine establishes the subchannel boundary conditions and transient forcing functions.

Arguments: none

CALC_BOUNDARIES is called by subroutine CALC.

CALC_BOUNDARIES calls subroutines BAROC, CURVE, PROP, and READ1_NLOOP_DATA.

CALC_SETPOINT – This subroutine performs sensitivity analyses of the operating conditions (system pressure, inlet temperature, mass flow rate, heat flux and hot channel factors) and statistical analyses of the code uncertainties.

Arguments: none

CALC_SETPOINT is called by subroutine CALC.

CALC_SETPOINT calls subroutines AVEVAR, DNBITR, EXPRIN, GASDEV, NEXPAG, PROP, RAN1, SENSI, SORT_REAL and ZBRENC.

CALC_SOLVE – This subroutine begins the iteration process and directs the solution of the conservation equations to PV or SCHEME solution algorithms as selected by input.

Arguments: none

CALC_SOLVE is called by subroutine CALC.

CALC_SOLVE calls subroutines PVSS, PV, RESET, and SCHEME.

CALC_X – This subroutine defines axial coordinates: node lengths, distance from grid, distance from mixing grid and grid spacing of mixing grids.

Arguments: none

CALC_X is called by subroutine CALC.

CALC_X calls subroutine CURVE2 and IOS0.

CALCULATION_VARIABLES (INPUT_STREAM, OUTPUT_STREAM, FLAG) – This subroutine is called by INDAT to read input block **group_9_calculation_variables** for specifying the calculation variables.

| | | |
|------------|---------------|---|
| Arguments: | INPUT_STREAM | XML input |
| | OUTPUT_STREAM | XML output |
| | FLAG | Identifier of the input data set to be read |

This subroutine belongs to the module XML_INPUT_CLASS.

CALCULATION_VARIABLES is called by subroutines CHANNEL_DATA and INDAT.

CARDS1 (PP,TT,VVF,VVG,HHF,HHG,UUF,KKF,SSIGMA,N1,I2) – This subroutine performs the necessary unit conversions of the read physical properties. If the physical properties are to be calculated by polynomials, the interpolation table is also set (not yet in ARTEMIS).

| | | |
|------------|--------|---|
| Arguments: | PP | pressure table (Pa) (input / output) |
| | TT | temperature table (°C) (input) |
| | VVF | liquid specific volume (m^3/kg) (input / output) |
| | VVG | vapor specific volume (m^3/kg) (input / output) |
| | HHF | liquid enthalpy (J/kg) (input / output) |
| | HHG | vapor enthalpy (J/kg) (input / output) |
| | UUF | liquid viscosity (kg/(s m)) (input) |
| | KKF | liquid thermal conductivity (W/(m K)) (input) |
| | SSIGMA | surface tension sigma (N/m) (input) |
| | N1 | if N1 < 0 - indicator for fluid properties (input) if N1 > 0 – number of pressure interpolation steps (input) if N1 = 0 – not yet available in ARTEMIS (input/output) |
| | I2 | constant (input/output) |

CARDS1 is called by subroutine INDAT.

CARDS1 calls functions SATTEM, ROLIQ, HLIQ, HVAP and subroutines HAPROP and SURTEN. (This option is not yet used in ARTEMIS and hence, these functions are not included in this description.)

CHANNEL_AREA_VARIATION (INPUT_STREAM, OUTPUT_STREAM, FLAG) – This subroutine is called by INDAT to read input block **group_5_channel_area_variation**

and **group_5.1_channel_area_variation_data** for specifying the subchannel area variation.

Arguments:

| | |
|---------------|---|
| INPUT_STREAM | XML input |
| OUTPUT_STREAM | XML output |
| FLAG | Identifier of the input data set to be read |

This subroutine belongs to the module XML_INPUT_CLASS.

CHANNEL_AREA_VARIATION is called by subroutine INDAT.

CHANNEL_DATA (INPUT_STREAM, OUTPUT_STREAM, FLAG) – This subroutine is called by INDAT to read input block **group_4_channels** for specifying the subchannel data and the local coupling parameters.

Arguments:

| | |
|---------------|---|
| INPUT_STREAM | XML input |
| OUTPUT_STREAM | XML output |
| FLAG | Identifier of the input data set to be read |

This subroutine belongs to the module XML_INPUT_CLASS.

CHANNEL_DATA is called by subroutine INDAT.

CHANNEL_DATA calls CALCULATION_VARIABLES.

Function **CHECK_UNIT (IUNIT, IMODE)** – This logical function prints the file name that corresponds to unit *iunit* and returns if that file exists.

Arguments:

| | |
|-------|---|
| IUNIT | Unit number (input) |
| IMODE | ≠ 0: check if the file with the associated file name exists and prints out file name (input) = 0: prints out file name |

CHECK_UNIT is used in the main program COBRA-FLX and subroutines COBRA_FLX_INIT and INDAT.

CHF (JEND) – This subroutine searches COBRA-FLX output at the end of each time step for critical heat flux occurrence. The search is made on each rod at a specified

axial location range by considering each rod and the adjacent subchannels. Subroutine CHF uses user-selected functions to calculate the critical heat flux ratios (CHFR). The minimum CHFR is determined; the corresponding subchannel, rod and axial location are also identified.

Arguments:

| | |
|------|--|
| JEND | Number of axial nodes plus one (input) |
|------|--|

CHF is called by the function DNBTR and the subroutine EXPRIN.

CHF calls subroutine CURVE and the functions CHFxx (xx = 1-4, 6-17, 23, 33, 50-64).

Function **CHF1 (N, I, J)** – This function calculates the critical heat flux using the B&W-2 correlation.

Arguments:

| | |
|---|---|
| N | Rod index (input) |
| I | Index of the subchannel adjacent to rod N (input) |
| J | Axial node index (input) |

CHF1 is used in subroutines CHF and HTCOR.

Function **CHF2 (N, I, J)** – This function calculates the critical heat flux using the W-3 correlation.

Arguments:

| | |
|---|---|
| N | Rod index (input) |
| I | Index of the subchannel adjacent to rod N (input) |
| J | Axial node index (input) |

CHF2 is used in subroutines CHF and HTCOR.

Function **CHF3 (N, I, J)** – This function calculates the critical heat flux using the Hench-Levy correlation.

Arguments:

| | |
|---|---|
| N | Rod index (input) |
| I | Index of the subchannel adjacent to rod N (input) |
| J | Axial node index (input) |

CHF3 is used in subroutines CHF and HTCOR.

Function **CHF4 (N, I, J)** – This function calculates the critical heat flux using the CISE-4 correlation.

Arguments:

| | |
|---|---|
| N | Rod index (input) |
| I | Index of the subchannel adjacent to rod N (input) |
| J | Axial node index (input) |

CHF4 is used in subroutines CHF and HTCOR.

Function **CHF6 (N, I, J)** – This function calculates the critical heat flux using the [] correlation.

Arguments:

| | |
|---|---|
| N | Rod index (input) |
| I | Index of the subchannel adjacent to rod N (input) |
| J | Axial node index (input) |

CHF6 is used in subroutines CHF and HTCOR.

Function **CHF7 (N, I, J)** – This function calculates the critical heat flux using the [] correlation.

Arguments:

| | |
|---|---|
| N | Rod index (input) |
| I | Index of the subchannel adjacent to rod N (input) |
| J | Axial node index (input) |

CHF7 is used in subroutines CHF and HTCOR.

Function **CHF8 (N, I, J)** – This function calculates the critical heat flux using the [] correlation.

Arguments:

| | |
|---|---|
| N | Rod index (input) |
| I | Index of the subchannel adjacent to rod N (input) |
| J | Axial node index (input) |

CHF8 is used in subroutines CHF and HTCOR.

Function **CHF9 (N, I, J)** – This function calculates the critical heat flux using the [] correlation.

Arguments:

| | |
|---|---|
| N | Rod index (input) |
| I | Index of the subchannel adjacent to rod N (input) |
| J | Axial node index (input) |

CHF9 is used in subroutines CHF and HTCOR.

Function **CHF10 (N, I, J)** – This function calculates the critical heat flux using the [] correlation.

Arguments:

| | |
|---|---|
| N | Rod index (input) |
| I | Index of the subchannel adjacent to rod N (input) |
| J | Axial node index (input) |

CHF10 is used in subroutines CHF and HTCOR.

Function **CHF11 (N, I, J)** – This function calculates the critical heat flux using the [] correlation.

Arguments:

| | |
|---|---|
| N | Rod index (input) |
| I | Index of the subchannel adjacent to rod N (input) |
| J | Axial node index (input) |

CHF11 is used in subroutines CHF and HTCOR.

Function **CHF12 (N, I, J, ICALL)** – This function calculates the critical heat flux using several correlations for [] correlation.

Arguments:

| | |
|-----|--|
| N | Rod index (input) |
| I | Index of the subchannel adjacent to rod N (input) |
| J | Axial node index (input) |
| ICA | Flag: (input) |
| LL | = 1 if called by CHF for final calculation = 2 if called by HTCOR |

CHF12 is used in subroutines CHF and HTCOR.

CHF12 calls subroutines CURVE.

Function **CHF13 (N, I, J)** – This function calculates the critical heat flux using the [].

Arguments:

| | |
|---|---|
| N | Rod index (input) |
| I | Index of the subchannel adjacent to rod N (input) |
| J | Axial node index (input) |

CHF13 is used in subroutines EXPRIN, CHF and HTCOR.

Function **CHF14 (N, I, J)** – This function calculates the critical heat flux using the [].

Arguments:

| | |
|---|---|
| N | Rod index (input) |
| I | Index of the subchannel adjacent to rod N (input) |
| J | Axial node index (input) |

CHF14 is used in subroutines CHF and HTCOR.

Function **CHF15 (N, I, J)** – This function calculates the critical heat flux using the [].

Arguments:

| | |
|---|---|
| N | Rod index (input) |
| I | Index of the subchannel adjacent to rod N (input) |
| J | Axial node index (input) |

CHF15 is used in subroutines CHF and HTCOR.

CHF15 calls subroutine CURVE.

Function **CHF16 (N, I, J)** – This function calculates the critical heat flux using the [].

Arguments:

| | |
|---|---|
| N | Rod index (input) |
| I | Index of the subchannel adjacent to rod N (input) |
| J | Axial node index (input) |

CHF16 is used in subroutines CHF and HTCOR.

CHF16 calls subroutine CURVE.

Function **CHF17 (N, I, J)** – This function calculates the critical heat flux using the [] correlation.

Arguments:

| | |
|---|---|
| N | Rod index (input) |
| I | Index of the subchannel adjacent to rod N (input) |
| J | Axial node index (input) |

CHF17 is used in subroutines CHF and HTCOR.

CHF17 calls subroutine CURVE.

Function **CHF23 (N, I, J)** – This function calculates the critical heat flux using the [] correlation.

Arguments:

| | |
|---|---|
| N | Rod index (input) |
| I | Index of the subchannel adjacent to rod N (input) |
| J | Axial node index (input) |

CHF23 is used in subroutines CHF and HTCOR.

Function **CHF33 (N, I, J)** – This function calculates the critical heat flux using the [] correlation.

Arguments:

| | |
|---|---|
| N | Rod index (input) |
| I | Index of the subchannel adjacent to rod N (input) |
| J | Axial node index (input) |

CHF33 is used in subroutines CHF and HTCOR.

Function **CHF50 (N, I, J)** – This function calculates the critical heat flux using the ACH-2 correlation with EPR HTP fuel. Application with COBRA-FLX is validated in Appendix C.

Arguments:

| | |
|---|---|
| N | Rod index (input) |
| I | Index of the subchannel adjacent to rod N (input) |
| J | Axial node index (input) |

CHF50 is used in subroutines CHF and HTCOR.

Function **CHF55 (N, I, J)** – This function calculates the critical heat flux using the BWC correlation. Application with COBRA-FLX is validated in Appendix C.

Arguments:

| | |
|---|---|
| N | Rod index (input) |
| I | Index of the subchannel adjacent to rod N (input) |
| J | Axial node index (input) |

CHF55 is used in subroutines CHF and HTCOR.

CHF55 calls subroutine BWFNU.

Function **CHF56 (N, I, J)** – This function calculates the critical heat flux using the BWCMV correlation. Application with COBRA-FLX is validated in Appendix C.

Arguments:

| | |
|---|---|
| N | Rod index (input) |
| I | Index of the subchannel adjacent to rod N (input) |
| J | Axial node index (input) |

CHF56 is used in subroutines CHF and HTCOR.

CHF56 calls subroutine BWFNU.

Function **CHF57 (N, I, J)** – This function calculates the critical heat flux using the BWCMV-A correlation. Application with COBRA-FLX is validated in Appendix C.

Arguments:

| | |
|---|---|
| N | Rod index (input) |
| I | Index of the subchannel adjacent to rod N (input) |
| J | Axial node index (input) |

CHF57 is used in subroutines CHF and HTCOR.

CHF57 calls subroutine BWFNU.

Function **CHF58 (N, I, J)** – This function calculates the critical heat flux using the BWU-Z (Mark-B11) correlation.

Arguments:

| | |
|---|---|
| N | Rod index (input) |
| I | Index of the subchannel adjacent to rod N (input) |
| J | Axial node index (input) |

CHF58 is used in subroutines CHF and HTCOR.

CHF58 calls subroutine BWFNU.

Function **CHF59 (N, I, J)** – This function calculates the critical heat flux using the BWU-Z correlation for the Mark-BW17 with MSMGs. Application with COBRA-FLX is validated in Appendix C.

Arguments:

| | |
|---|---|
| N | Rod index (input) |
| I | Index of the subchannel adjacent to rod N (input) |
| J | Axial node index (input) |

CHF59 is used in subroutines CHF and HTCOR.

CHF59 calls subroutine BWFNU.

Function **CHF60 (N, I, J)** – This function calculates the critical heat flux using the BWU-B11R (Mark-B11) correlation.

Arguments:

| | |
|---|---|
| N | Rod index (input) |
| I | Index of the subchannel adjacent to rod N (input) |
| J | Axial node index (input) |

CHF60 is used in subroutines CHF and HTCOR.

CHF60 calls subroutine BWFNU.

Function **CHF61 (N, I, J)** – This function calculates the critical heat flux using the BWU-Z correlation for the Mark-BW17. Application with COBRA-FLX is validated in Appendix C.

Arguments:

| | |
|---|---|
| N | Rod index (input) |
| I | Index of the subchannel adjacent to rod N (input) |
| J | Axial node index (input) |

CHF61 is used in subroutines CHF and HTCOR.

CHF61 calls subroutine BWFNU.

Main Program COBRA-FLX – COBRA-FLX is the main program. It controls the overall execution of the calculation by performing the following functions:

- calls COBRA_FLX_INIT for files preparation;
- controls input and output by calling LIST_FREE_FORMAT_INPUT, INLIST, INDAT, INPCHK, and INPRIN;
- performs calculations by calling CALC.

Arguments: none

COBRA-FLX calls subroutines COBRA_FLX_INIT, CHECK_UNIT, LIST_FREE_FORMAT_INPUT, INLIST, INDAT, INPCHK, PVINIT, INPRIN, and CALC.

COBRA_FLX_INIT (IOSTAT5, IOSTAT95, INPUT_STREAM, OUTPUT_STREAM) –

This subroutine prints page headers by calling NEXPAG and calls EXPORT_CLASS to print export classification and label text. It also opens input and output files.

Arguments:

| | |
|---------------|---------------------------------------|
| IOSTAT5 | Status of open file 5 (input/output) |
| IOSTAT95 | Status of open file 95 (input/output) |
| INPUT_STREAM | XML input (optional parameter) |
| OUTPUT_STREAM | XML output (optional parameter) |

COBRA_FLX_INIT is called by the main program COBRA-FLX.

COBRA_FLX_INIT calls subroutines EXPORT_CLASS, GET_NODEDATA, CHECK_UNIT, NEXPAG, NEWLIB_IDENT and SOLVER.



COOLANT (INPUT_STREAM, OUTPUT_STREAM) – This subroutine is called by INDAT to read input block **group_1_coolant** for calculation of the physical properties.

| | | |
|------------|---------------|------------|
| Arguments: | INPUT_STREAM | XML input |
| | OUTPUT_STREAM | XML output |

This subroutine belongs to the module XML_INPUT_CLASS.

COOLANT is called by subroutine INDAT.

CORE (NCORE, MSP, NKP, MRSP) – This subroutine sets up the size of the coefficient matrix AAA (NKP, MSP).

| | | |
|------------|-------|------------------------------------|
| Arguments: | NCORE | 1 (fixed) |
| | MSP | Stripe width of AAA matrix (input) |
| | NKP | Number of subchannels (input) |
| | MRSP | =1 <i>Not used</i> |

CORE is called by ACOL.

CURVE (FX, X, F, Y, N, J, ISAVE) – This subroutine performs linear interpolation of tabulated data.

| | | |
|------------|-------|---|
| Arguments: | FX | Quantity to be found (output) |
| | X | Independent variable (input) |
| | F | Input array for the ordinate (monotonic with Y) (input) |
| | Y | Input array for the abscissa (monotonic increase) (input) |
| | N | Number of F(I) or Y(I) values (input) |
| | J | Error signal (output) |
| | ISAVE | Flag =1 or 2 (input) |

CURVE is called by subroutines AREA, BWFNU, CALC_BOUNDARIES, CHF, CHF12, CHF15, CHF16, CHF17, DNBITR, EXPRIN, FFACTR, HEAT, INDAT, INPRIN, MIX, PRECAL, PROP, and READ1_NLOOP_DATA.

CURVE2 (FX, X, F, Y, M1, N1, M, N, JER) – This subroutine performs linear interpolation in the first column of a 2D-array with fixed value of the second column.

Arguments:

| | |
|-----|---|
| FX | Quantity to be found (output) |
| X | Independent variable (input) |
| F | Input array for the ordinate (monotonic with Y, F(1:M, 1:N)) (input) |
| Y | Input array for the abscissa (monotonic increase, Y(1:M, 1:N)) (input) |
| M1 | Actual value of M (input) |
| N1 | Actual value of N (input) |
| M | Size of the first column of F(1:M,1:N) and Y(1:M, 1:N) values (input) |
| N | Size of the second column of F(1:M,1:N) and Y(1:M, 1:N) values (input) |
| JER | Error signal, JER=10 in case of error (output) |

CURVE2 is called by subroutine CALC_X.

DECOMP (NN, IERROR, LMAX, MID, UL, NK) – This subroutine decomposes the banded matrix AAA and stores the diagonal band such that the position (K, L) in the square array becomes (K,(MID-K+L)) in the new array.

Arguments:

| | |
|--------|---|
| NN | Number of unknowns in the linear system of equations (input): = number of subchannels if pressure drop solution method = number of gaps if crossflow solution method = number of subchannels or number of axial nodes increased by 2 depending on the equation to solve if pressure-velocity solution method |
| IERROR | Error signal (output) |
| LMAX | Stripe width of the matrix AAA, e.g. (2×MID -1) (input) |
| MID | Column location for the diagonal elements in banded matrix storage (input) |
| UL | Matrix AAA (input/output) |
| NK | Number of rows in the matrix (input): = number of subchannels if pressure drop solution method = number of gaps if crossflow solution method = number of subchannels or number of axial nodes increased by 2 depending on the equation to solve if pressure-velocity solution method |

DECOMP is called by subroutines DIVERT, ENERGY, MASEQX, MASEQY, MOMAXL, PRESS, and REBAL.

DELTAT (XAR, YAR, NAR, X, DELTAY, DELTAX) – This subroutine is used if the time-step is to be automatically determined by the program. It defines the time step size for transient calculations based on the allowed maximum time changes of inlet flow, inlet enthalpy, pressure, and heat flux. The size of the new time step is defined as the minimum of the four values.

Arguments:

| | |
|--------|---|
| XAR | Time at which the quantity is given (s) (input) |
| YAR | Ratio of the current to the initial value of the given quantity (input) |
| NAR | Transient forcing function indicator for the given quantity (input) |
| X | Current time (s) (input) |
| DELTAY | Relative change in the forcing function for the given quantity (input) |
| DELTAX | New time step size based on the given quantity (s) (output) |

DELTAT is called by subroutine CALC.

DIFFER (IPART, J) – This subroutine is divided into four parts depending on the variable IPART:

- IPART = 1: calculates the right-hand side of the coolant energy equation, which is the steady state value of the enthalpy gradient;
- IPART = 2: calculates the right-hand side of the continuity equation, which is the steady-state value of the flow gradient;
- IPART = 3: calculates the pressure loss coefficient as well as the other components of the pressure gradient without the diversion crossflow terms as defined by the axial momentum equation;
- IPART = 4: calculates the complete pressure gradient including the crossflow terms.

| | | |
|------------|-------|--|
| Arguments: | IPART | Indicator for the calculation to be performed (input): = 1 – RHS of the energy equation = 2 – RHS of the continuity equation (crossflow resistance and the transverse momentum flux term) = 3 – pressure gradient components for the axial momentum equation = 4 – complete pressure gradient including the crossflow terms for the SCHEME crossflow solution method |
| | J | Axial node index (input) |

DIFFER is called by subroutines SCHEME, SEPRAT, and SPLIT.

DIVERT (IPART, J) – This subroutine is divided into two parts depending on the variable IPART:

- IPART = 1: calculates the parameters of the transverse momentum equation. The simultaneous equations for the crossflow solution are generated and solved by calling DECOMP and SOLVE;
- IPART = 2: calculates diversion crossflow based on the pressure drop solution method.

| | | |
|------------|-------|---|
| Arguments: | IPART | Indicator: (input) = 1 – calculate parameters of the transverse momentum equation – generate and solve simultaneous equations for the crossflow solution = 2 – calculates diversion crossflow based on the pressure drop solution method |
| | J | Axial node index (input) |

DIVERT is called by subroutine SCHEME.

DIVERT calls subroutines DECOMP and SOLVE.

DMPRHO (ERRRHX, DRHMAX, IRHMAX, JRHMAX) – This subroutine damps the density changes from the energy equation when the mass flux in the subchannel drops below 40 lbm/sec-ft^2 , i.e. $195.297 \text{ kg/sec-m}^2$. The maximum density change is used to determine the convergence of the iterative process.

| | | |
|------------|--------|---|
| Arguments: | ERRRHX | Maximum relative error in density (output) |
| | DRHMAX | Maximum density change (output) |
| | IRHMAX | Subchannel with maximum relative error (output) |
| | JRHMAX | Axial node with maximum relative error (output) |

DMPRHO is called by subroutine PV.

Function **DNBITR (X)** – This function controls the overall iterative loop when sensitivity calculations are being performed.

| | | |
|------------|---|--|
| Arguments: | X | Monitored quantity during sensitivity calculations (input) |
|------------|---|--|

DNBITR is used in subroutine CALC_SETPOINT.

DNBITR calls subroutines CHF, CURVE, PROP, PVSS, RESET and SCHEME.

ENERGY – This subroutine solves the fluid energy equation for enthalpy at each axial node for the PV algorithm. It uses the flows saved from the previous outer iteration as fixed parameters. The Newton method is used to solve the fully implicit difference equations. The normal solution sweeps from inlet to exit. A reverse sweep is also done if an axial flow reversal exists.

Arguments: none

ENERGY is called by subroutine PV.

ENERGY calls subroutines DECOMP, GAPENG, HEAT, MIX, PROP, SOLVE, and VOID.

EXPORT_CLASS (IOUT, CODENAME, ECCN_STR) – This subroutine prints export classification and label text on the output file.

| | | |
|------------|----------|----------------------------|
| Arguments: | IOUT | Output file 6 (input) |
| | CODENAME | 'COBRA-FLX' (input) |
| | ECCN_STR | '10CFR810.8(c)(3)' (input) |

EXPORT_CLASS is called by subroutine COBRA_FLX_INIT.

EXPRIN – This subroutine calls CHF to perform critical heat flux evaluations. It prints mass and energy balance; subchannel exit summary; bundle average results; subchannel results including DNBR information; crossflow results; rod results and CHF summary. According to the input options, the results are printed to the ASCII output file and/or to HDF output file.

Arguments: none

EXPRIN is called by subroutines CALC and CALC_SETPOINT.

EXPRIN calls subroutines BVOID, CHF, CURVE, NEXPAG, OUTCS, WRITE_HDF_BUNDLE, WRITE_HDF_SUMMARY, WRITE_HDF_CHANNEL, WRITE_HDF_CROSSFLOW, WRITE_HDF_ROD and WRITE_HDF_CHF.

FFACTR (J) – This subroutine calculates the friction factor and the wall viscosity correction for forward and reverse flow for use in the PV solution.

Arguments:

| | |
|---|--------------------------|
| J | Axial node index (input) |
|---|--------------------------|

FFACTR is called by subroutine MOMAXL.

FFACTR calls subroutine CURVE.

FILM (H, ALP, ROV, ROL, VVA, VLA, HD, RHD, TL, TV, TW, TSAT, HFG, CPV, CPL, P, VISV, VISL, BETAV, SIG, IHTR, X) – This subroutine calculates the film boiling heat transfer coefficient.

Arguments:

| | |
|-----|---|
| H | Convection heat transfer coefficient of vapor, (W/m^2-K) (output) |
| ALP | Vapor volume fraction (-) (input) |
| ROV | Vapor density (kg/m^3) (input) |
| ROL | Liquid density (kg/m^3) (input) |
| VVA | Vapor velocity (absolute value) (m/s) (input) |
| VLA | Liquid velocity (absolute value) (m/s) (input) |
| HD | Hydraulic diameter (m) (input) |
| RHD | Reciprocal of hydraulic diameter ($1/HD$) (m^{-1}) (input) |

| | |
|-------|---|
| TL | Liquid temperature (K) (input) <i>Not used</i> |
| TV | Vapor temperature (K) (input) |
| TW | Wall temperature (K) (input) |
| TSAT | Saturation temperature (K) (input) |
| HFG | Latent heat of vaporization (J/kg) (input) |
| CPV | Vapor heat capacity (J/kg-K) (input) |
| CPL | Liquid heat capacity (J/kg-K) (input) <i>Not used</i> |
| P | Pressure (Pa) (input) |
| VISV | Vapor viscosity (kg/m-s) (input) |
| VISL | Liquid viscosity (kg/m-s) (input) <i>Not used</i> |
| BETAV | Variable (K^{-1}) (input) |
| SIG | Surface tension (N/m) (input) |
| IHTR | Indicator of the heat transfer correlation (output) |
| X | Quality (-) (input) |

FILM is called by subroutine HTCOR.

FLOW_CORRELATIONS (INPUT_STREAM, OUTPUT_STREAM) – This subroutine is called by INDAT to read input block **group_2_flow_correlations** for selection of the flow correlations to be used.

| | | |
|------------|---------------|------------|
| Arguments: | INPUT_STREAM | XML input |
| | OUTPUT_STREAM | XML output |

This subroutine belongs to the module XML_INPUT_CLASS.

FLOW_CORRELATIONS is called by subroutine INDAT.

FORCE (J) – This subroutine specifies the forced diversion crossflow. If a forced crossflow is specified, the logical variable FDIV is set to 'TRUE'; otherwise FDIV is set to 'FALSE'. There are two options considered for forced convection crossflow: 1) crossflow forced by wire wraps; and 2) crossflow by a specified flow fraction diverted from one subchannel to an adjacent subchannel.

Arguments:

| | |
|---|--------------------------|
| J | Axial node index (input) |
|---|--------------------------|

FORCE is called by subroutine SCHEME.



GAP_VARIATION (INPUT_STREAM, OUTPUT_STREAM, FLAG) – This subroutine is called by INDAT to read input block **group_6_gap_variation** for specifying the gap spacing variation.

Arguments:

| | |
|---------------|---|
| INPUT_STREAM | XML input |
| OUTPUT_STREAM | XML output |
| FLAG | Identifier of the input data set to be read |

GAP_VARIATION is called by subroutine INDAT.

GAPENG (J, MID) – This subroutine is called by ENERGY to calculate the lateral convective energy flow and turbulent mixing conduction contributions to the energy solution. It loads those contributions to the residual error and the coefficient matrix.

Arguments:

| | |
|-----|--|
| J | Axial node index (input) |
| MID | Column location for banded matrix storage (diagonal) (input) |

GAPENG is called by subroutine ENERGY.

GAPMAS (J, MID) – This subroutine is called by MASEQY to calculate the contribution of the lateral flows to the mass equation solution. It loads those contributions to the residual error and the coefficient matrix.

| | | |
|------------|-----|--|
| Arguments: | J | Axial node index (input) |
| | MID | Column location for banded matrix storage (diagonal) (input) |

GAPMAS is called by subroutine MASEQY.

GAPMOM (J, JMI, JPL, DXM, DXP, MID) – This subroutine is called by MOMAXL to calculate the lateral momentum flow and turbulent momentum contributions to the axial momentum equation. It loads those contributions to the residual error and the coefficient matrix.

| | | |
|------------|-----|--|
| Arguments: | J | Axial node index (input) |
| | JMI | = J (axial node index) (input) |
| | JPL | = (J+1) (input) |
| | DXM | Nodal length of momentum cell associated with JMI (input) |
| | DXP | Nodal length of momentum cell associated with JPL (input) |
| | MID | Column location for banded matrix storage (diagonal) (input) |

GAPMOM is called by subroutine MOMAXL.

Function **GASDEV (IDUM)** – This function generates samples of input variables for the purpose of Monte Carlo simulations (see subroutine CALC_SETPOINT).

| | | |
|------------|------|---|
| Arguments: | IDUM | Large integer currently set to 1308226761 (input) |
|------------|------|---|

GASDEV is used by subroutine CALC_SETPOINT.

GENERAL (INPUT_STREAM, OUTPUT_STREAM) – This subroutine is called by INDAT to read input block **group_0_general** for specification of the case control card: case description.

| | | |
|------------|---------------|------------|
| Arguments: | INPUT_STREAM | XML input |
| | OUTPUT_STREAM | XML output |

This subroutine belongs to the module XML_INPUT_CLASS.

GENERAL is called by subroutine INDAT.

GET_NODEDATA (SYSINFO) – This subroutine is used to get system information.

| | | |
|------------|---------|---|
| Arguments: | SYSINFO | string containing the system information (output) |
|------------|---------|---|

Get_nodedata is called by subroutine Cobra_FLx_init.

Function **HCOOL (N, I, JJ, IREG)** – This function calculates the heat transfer coefficient for the rod N facing subchannel I at axial position JJ.

| | | |
|------------|------|--|
| Arguments: | N | Rod index (input) |
| | I | Subchannel index (input) |
| | JJ | Axial location (input) |
| | IREG | Indicator (output): = 1 – single phase = 2 – two-phase |

HCOOL is called by subroutines HTRAN and PROP.

HEAT (J) – This subroutine calculates the heat input to each subchannel at the axial position J based on the heat flux of the rods. The coolant temperature and heat transfer coefficient are calculated for all rods.

| | | |
|------------|---|--------------------------|
| Arguments: | J | Axial node index (input) |
|------------|---|--------------------------|

HEAT is called by subroutines CALC, ENERGY and SCHEME.

HEAT calls subroutines CURVE and HTRAN.

HTCOR (IHTR, QV, QL, HVFC, HLNb, HLFC, TW, TL, TV, P, ALP, X, ROV, ROL, VW, VL, HD, IHTM, CHFR, CHFF, TSAT, FLUX, NCHF, NN, II, JJ, I3, IZAH, LHSURF) –

This subroutine calculates heat transfer coefficients and/or heat fluxes. It also determines the indicator of the heat transfer regime.

Arguments:

| | |
|------|---|
| IHTR | Indicator of the heat transfer regime (output) |
| QV | Heat flux to vapor (W/m^2) (output) |
| QL | Heat flux to liquid (W/m^2) (output) |
| HVFC | Convection heat transfer coefficient to vapor (W/m^2-K) (output) |
| HLNB | Nucleate boiling heat transfer coefficient (W/m^2-K) (output) |
| HLFC | Convection heat transfer coefficient to liquid (W/m^2-K) (output) |
| TW | Wall temperature (K) (input) |
| TL | Liquid temperature (K) (input) |
| TV | Vapor temperature (K) (input) |
| P | Pressure (Pa) (input) |
| ALP | Vapor volume fraction (-) (input) |
| X | Quality (-) (input) |
| ROV | Vapor density (kg/m^3) (input) |
| ROL | Liquid density (kg/m^3) (input) |
| VV | Vapor velocity (m/s) (input) |
| VL | Liquid velocity (m/s) (input) |
| HD | Hydraulic diameter (m) (input) |
| IHTM | Indicator for rod-to-coolant heat transfer model (input) |
| CHFR | Set to 1.0 or 100. 0 (output) <i>not used</i> |
| CHFF | = RADIA (the relative rod power) if IQP3 is equal to 0 or 1 (i.e. the power distribution is given by POWER3D channel-by-channel file) = 1.0 otherwise (input) |
| TSAT | Saturation temperature (K) (input) |
| FLUX | Heat flux (W/m^2) (input) |
| NCHF | CHF correlation indicator (input) |
| NN | Rod index (input) |
| II | Index of the subchannel adjacent to rod N (input) |

| | |
|--------|--|
| JJ | Axial location (input) |
| I3 | Unit for ASCII output file (I3=6) |
| IZAHL | Index "I" of subchannel in the $lr(nn,l)$ array (input) |
| LHSURF | Logical flag if the heat-transfer-coefficient iterative loop has converged in heat.f90 (input) |

HTCOR is called by subroutine HTRAN.

HTCOR calls subroutines STATE_3CP, FILM and CHFxx (xx = 1-4, 6-17, 23, 33, 50-64).

HTRAN (N, I, JJ, HTC, TLIQ, IHTM, NT, IZAHL, LHSURF) – This subroutine calculates the heat transfer coefficient.

Arguments:

| | |
|--------|--|
| N | Rod index (input) |
| I | Subchannel index (input) |
| JJ | Axial location (input) |
| HTC | Heat transfer coefficient (W/m^2-K) (output) |
| TLIQ | Liquid temperature ($^{\circ}C$) (input) |
| IHTM | Indicator for rod-to-coolant heat transfer model (input) |
| NT | Current time step (input) |
| IZAHL | Index "I" of subchannel in the $lr(nn,l)$ array (input) |
| LHSURF | Logical flag if the heat-transfer-coefficient iterative loop has converged in heat.f90 (input) |

HTRAN is called by subroutine HEAT.

HTRAN calls subroutine HTCOR and HCOOL.

INDAT (INIT, NOPRIN, IDPRGC, INPUT_STREAM, OUTPUT_STREAM) – This subroutine performs an initialization of the variables at the beginning of the calculation and reads the input data.

Arguments:

| | |
|--------|--|
| INIT | Indicator for variables initialization at the beginning of calculation (input) = 1 – initialization = 2 – no initialization |
| NOPRIN | Selector if summary of the input data is printed to the output file (output) = 0 – print summary of input data = 1 – printout is suppressed (not used) |

| | |
|---------------|---|
| IDPRGC | Indicator for type of calculation (input) = 0 – evaluate PANCOS calculations (not used) = 1 – neutron kinetics (not used) = 2 – thermal hydraulics = 3 – coupling of 1&2 = 4 – plant analysis (not used) |
| INPUT_STREAM | XML input |
| OUTPUT_STREAM | XML output |

INDAT is called by the main program COBRA-FLX.

INDAT calls subroutines ACOL, AREA, CURVE, NEXPAG, PROP, READ_NLOOP_DATA, READ1_NLOOP_DATA, SPLIT and the following ARTEMIS required subroutines: SOLVER, GENERAL, FLOW_CORRELATIONS, POWER_DISTRIBUTION, CHANNEL_DATA, CHANNEL_AREA_VARIATION, GAP_VARIATION, SPACER, ROD_DATA, CALCULATION_VARIABLES, MIXING, OPERATING_CONDITIONS, OUTPUT_OPTIONS.

INPCHK – This subroutine searches for input errors if the pressure-velocity solver is selected. Warning messages are given if errors are found but the computation can proceed. The calculation is terminated if a fatal error is found.

Arguments: none

INPCHK is called by the main program COBRA-FLX.

INPCHK calls subroutine ACOL.

INPRIN – This subroutine prepares and prints a summary of input data.

Arguments: none

INPRIN is called by the main program COBRA-FLX.

INPRIN calls subroutines NEXPAG and CURVE.

IOS0 (NAX, ZAXM, IST31, IHILF) – This subroutine defines the test array IHILF to be used for the modification of the Tong factor for the [] CHF correlation.

| | | |
|------------|-------|---|
| Arguments: | NAX | Number of axial nodes (input) |
| | ZAXM | Axial location of the node (<i>m</i>) (input) |
| | IST31 | Distance upstream to the axial location (<i>cm</i>) (input) |
| | IHILF | Array of start nodes for the Tong integral (output) |

IOS0 is called by subroutine CALC_X.

LOCOUT – This subroutine is called to store local coolant conditions in the COOLANT and DNBDATA files.

Arguments: none

LOCOUT is called by subroutine CALC.

MASEQX (MASERR, IMMAX, JMMAX) – This subroutine solves the mass equation for the pressure and flow correction along the core length for each channel (PV solution algorithm). This is done once per inner iteration. It also updates the pressure and flow fields from the calculated pressure correction.

| | | |
|------------|--------|---|
| Arguments: | MASERR | Maximum mass residual (output) |
| | IMMAX | Identification number of the subchannel with maximum mass residual (output) |
| | JMMAX | Identification number of the axial node with maximum mass residual (output) |

MASEQX is called by subroutine PV.

MASEQX calls subroutines DECOMP and SOLVE.

MASEQY (MASERR, IMMAX, JMMAX) – This subroutine solves the mass equation for the pressure and flow correction over the core cross-section at each axial level (PV solution algorithm). It calls subroutine GAPMAS to obtain the lateral contribution to the mass residual. This is done once per inner iteration. It also updates the pressure and flow fields from the calculated pressure correction.

| | | |
|------------|--------|--------------------------------|
| Arguments: | MASERR | Maximum mass residual (output) |
|------------|--------|--------------------------------|

| | |
|-------|---|
| IMMAX | Identification number of the subchannel with maximum mass residual (output) |
| JMMAX | Identification number of the axial node with maximum mass residual (output) |

MASEQY is called by subroutine PV.

MASEQY calls subroutines DECOMP, GAPMAS, and SOLVE.

MIX (J) – This subroutine calculates the contribution of the turbulent mixing to the conservation equations.

Arguments:

| | |
|---|--------------------------|
| J | Axial node index (input) |
|---|--------------------------|

MIX is called by subroutines ENERGY, SCHEME, and SPLIT.

MIX calls subroutine CURVE.

MIXING (INPUT_STREAM, OUTPUT_STREAM, FLAG) – This subroutine is called by INDAT to read input block **group_10_mixing** for specifying the turbulent mixing correlations.

Arguments:

| | |
|---------------|---|
| INPUT_STREAM | XML input |
| OUTPUT_STREAM | XML output |
| FLAG | Identifier of the input data set to be read |

This subroutine belongs to the module XML_INPUT_CLASS.

MIXING is called by subroutine INDAT.

MOMAXL (AXLERR, IXMAX, JXMAX) – This subroutine solves the axial momentum equation for the tentative axial flows using the existing pressure and flows saved from the previous outer iteration. It also calculates the important coefficients used in the mass equation solution.

Arguments:

| | |
|--------|---|
| AXLERR | Maximum axial momentum residual (output) |
| IXMAX | Identification number of the subchannel with maximum axial momentum residual (output) |
| JXMAX | Identification number of the axial node with maximum axial momentum residual (output) |

MOMAXL is called by subroutine PV.

MOMAXL calls subroutines FFACTR, GAPMOM, DECOMP and SOLVE.

MOMLAT (LATERR, KLMAX, JLMAX) – This subroutine solves the lateral momentum equation for the flow field given the existing pressure and flows saved from the previous outer iteration. It also calculates the important coefficients used in the mass equation solution.

Arguments:

| | |
|--------|---|
| LATERR | Maximum lateral momentum residual (output) |
| KLMAX | Identification number of the gap with maximum lateral momentum residual (output) |
| JLMAX | Identification number of the axial node with maximum lateral momentum residual (output) |

MOMLAT is called by subroutine PV.

NEWLIB_IDENT (JOBINFO) – Routine to get system information about the running program.

Arguments:

| | |
|---------|--|
| JOBINFO | String containing the job information (output) |
|---------|--|

newlib_ident is called by subroutine cobra_flx_init.

NEXPAG – This subroutine writes supplementary information on output such as case description, code version, date and time of start of calculation, information about the computer platform, page numbers.

Arguments: none

NEXPAG is called by subroutines COBRA_FLX_INIT, CALC_SETPOINT, EXPRIN, INDAT, INLIST, INPRIN, LIST_FREE_FORMAT_INPUT, PREP, PV, and SCHEME.

OPERATING_CONDITIONS (INPUT_STREAM, OUTPUT_STREAM, FLAG) – This subroutine is called by INDAT to read input block **group_11_operating_conditions** for specifying the operating conditions.

| | | |
|------------|---------------|---|
| Arguments: | INPUT_STREAM | XML input |
| | OUTPUT_STREAM | XML output |
| | FLAG | Identifier of the input data set to be read |

This subroutine belongs to the module XML_INPUT_CLASS.

OPERATING_CONDITIONS is called by subroutine INDAT.

OUTPUT_OPTIONS (INPUT_STREAM, OUTPUT_STREAM, FLAG) – This subroutine is called by INDAT to read input block **group_12_output_options** for specifying the output display options.

| | | |
|------------|---------------|---|
| Arguments: | INPUT_STREAM | XML input |
| | OUTPUT_STREAM | XML output |
| | FLAG | Identifier of the input data set to be read |

OUTPUT_OPTIONS is called by subroutine INDAT.

POWER_DISTRIBUTION (INPUT_STREAM, OUTPUT_STREAM) – This subroutine is called by INDAT to read input block **group_3_power_distribution** for specifying the power distribution.

| | | |
|------------|---------------|------------|
| Arguments: | INPUT_STREAM | XML input |
| | OUTPUT_STREAM | XML output |

This subroutine belongs to the module XML_INPUT_CLASS.

POWER_DISTRIBUTION is called by subroutine INDAT.

PREP (INIT, IDPRGC) – This subroutine is called only after reading COBRA-FLX restart data from the HDF-restart file. It allocates arrays and initializes variables that were not read from the HDF file.

| | | |
|------------|--------|--|
| Arguments: | INIT | Indicator if initialization of variables is to be done (input) |
| | IDPRGC | Indicator for type of calculation (input) |

PREP is called by subroutine PROCESS_INPUT_HDF_THM (ARTEMIS environment).
PREP calls subroutines AREA; NEXPAG; SPLIT:

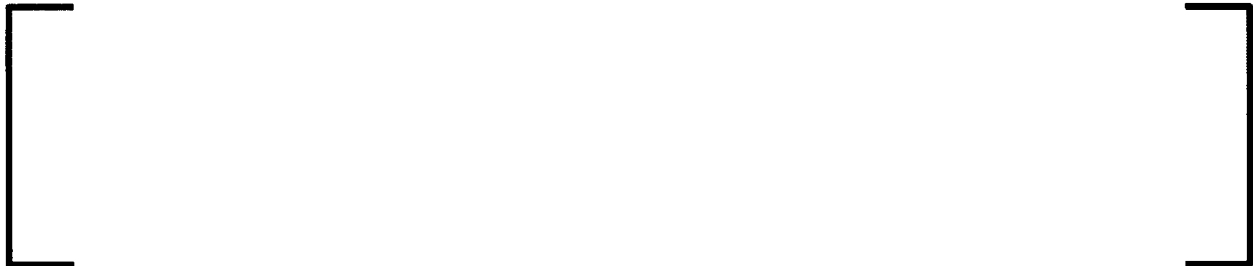
PRESS (J) – This subroutine sets up and solves the system of linear equations for the axial pressure gradient, $A*(DP/DX)=B$ for the pressure solution method. The following linear solvers are available: 1) direct elimination (ISOLVE=1); 2) Successive Over-Relaxation (SOR) method []; and 3) [].

Arguments:

| | |
|---|--------------------------|
| J | Axial node index (input) |
|---|--------------------------|

PRESS is called by subroutine SCHEME.

PRESS calls subroutines DECOMP, SOLVE, and [].



PRESX (PP, HH, VV, TT, II, JJ, ISTART) – This subroutine defines the specific volume and temperature at given pressure and enthalpy using steam tables.

Arguments:

| | |
|--------|--|
| PP | Pressure (<i>psi</i>) (input) |
| HH | Enthalpy (<i>btu/lb</i>) (input) |
| VV | Specific volume (<i>ft³/lb</i>) (output) |
| TT | Temperature (<i>°F</i>) (output) |
| II | Index of the entrée in the pressure table (input) |
| JJ | Index of the entrée in the enthalpy table (input) |
| ISTART | Signal for error message if pressure or/and enthalpy are out of range (output) |

PRESX is called by subroutine SPCSHS.

PROP (IPART, J) – This subroutine consists of two parts. The first calculates the saturated fluid properties at system pressure. The second part calculates all the liquid or superheated fluid properties as functions of temperature.

Arguments:

| | |
|-------|---|
| IPART | Signal for property types to be calculated: (input) = 1 – saturated properties = 2 – liquid properties and parameters (not saturated) |
| J | Axial node index (input) |

PROP is called by subroutines CALC, CALC_BOUNDARIES, CALC_SETPOINT, DNBTR, ENERGY, INDAT, READ1_NLOOP_DATA, SCHEME, SETIC, and SPLIT. PROP calls subroutines CURVE and SPCSHS.

PV – This subroutine is the overall executive for the PV solution algorithm. It advances the solution one time step given the initial and boundary conditions for enthalpy, flow, and pressure. The solution method is based on an adaptation of the Pressure-Velocity method. The method used here considers a solution for pressure and flow rather than a solution for pressure and velocity. An iterative strategy is used for the overall solution. An outer iteration is used to successively update the energy and the pressure and flow fields. An inner iteration is used to obtain the pressure and flow solution such that the mass balance is satisfied. The method of solution separates the energy solution from the pressure and flow solution. This is possible by using a transportive form of the energy equation that is also fully conservative of energy.

Arguments: none

PV is called by subroutines CALC_SOLVE and PVSS.

PV calls subroutines ASSIGN, DMPRHO, ENERGY, MOMAXL, MOMLAT, MASEQX, MASEQY, NEXPAG, REBAL, SAVFLO and SEPRAT.

PVINIT – This subroutine initializes the PV solution algorithm. It calls subroutine SETIC to set the initial conditions.

Arguments: none

PVINIT is called by the main program COBRA-FLX.

PVINIT calls subroutines RESET, SAVFLO, and SETIC.

PVSS – This subroutine provides a time stepping procedure to achieve a transient solution for the steady state problem using the PV algorithm. The old time solution is reset after each time step.

Arguments: none

PVSS is called by subroutines CALC_SOLVE and DNBTR.

PVSS calls subroutines PV and RESET.

QPR3 – This subroutine reads the average nodal fuel powers and/or the average nodal coolant powers from the POWER3D file if required by input. It also prints the average nodal fuel and coolant powers to the output file.

Arguments: none

QPR3 is called by subroutine CALC.

Function **RAN1 (IDUM)** – This function is used in the generation of samples of input variables for the purpose of Monte Carlo simulations.

Arguments:

| | |
|------|-------------------------------------|
| IDUM | Random large integer (input/output) |
|------|-------------------------------------|

RAN1 is used by subroutine CALC_SETPOINT and function GASDEV.

READ_NLOOP_DATA – This subroutine reads the transient operating conditions from the NLOOP file.

Arguments: none

READ_NLOOP_DATA is called by subroutine INDAT.

READ1_NLOOP_DATA (IOSTAT, NCHANI) – This subroutine reads the transient operating conditions and individual temperature and mass flow distribution from the NLOOP file.

Arguments:

| | |
|--------|-------------------------------|
| IOSTAT | Unit status (input) |
| NCHANI | Number of subchannels (input) |

READ1_NLOOP_DATA is called by subroutines CALC_BOUNDARIES and INDAT.
READ1_NLOOP_DATA calls subroutines CURVE and PROP.

REBAL (NINNER) – This subroutine solves the mass equation along the axial direction for a group of subchannels. This is done by adding the mass equations and their matrix coefficients for each subchannel over the cross-section to form an axial tri-diagonal equation for the average axial pressure correction. The correction is applied uniformly to all subchannels at that axial level.

Arguments:

| | |
|--------|---------------------------------|
| NINNER | Current inner iteration (input) |
|--------|---------------------------------|

REBAL is called by subroutine PV.
REBAL calls subroutines DECOMP and SOLVE.

Function **REIB (HKD, REI, IWAHL)** – This function determines the friction factors for smooth and rough subchannels.

Arguments:

| | |
|-------|---|
| HKD | Relative roughness, related to hydraulic diameter (input) |
| REI | Reynolds number (input) |
| IWAHL | Control number for correlation selection (input) |

REIB is used by subroutines FFACTR and PROP.

RESET – This subroutine resets the variables (current to old) to define initial conditions for the next time step.

Arguments: none

RESET is called by subroutines CALC_SOLVE, DNBITR, PVINIT, and PVSS.

ROD_DATA (INPUT_STREAM, OUTPUT_STREAM, FLAG) – This subroutine is called by INDAT to read input block **group_8_rod_data** for specifying the rod data: rod layout, power factors and CHF correlations.

Arguments:

| | |
|---------------|---|
| INPUT_STREAM | XML input |
| OUTPUT_STREAM | XML output |
| FLAG | Identifier of the input set part to be read |

This subroutine belongs to the module XML_INPUT_CLASS.

ROD_DATA is called by subroutine INDAT.

Function **RXD (RE, XXD)** – This function computes the increase of the friction factor in the inlet section, where the flow is not fully developed. The increase is calculated according to Szablewski model as a function of the Reynolds number and the relative inlet length.

| | | |
|------------|-----|-------------------------------|
| Arguments: | RE | Reynolds number (input) |
| | XXD | Relative inlet length (input) |

RXD is used by subroutines FFACTR and PROP.

SAVFLO (ERRFMX, IFMAX, JFMAX, ERRWMX, JWMAX, KWMAX, NCWNEF) – This subroutine saves the current flows for use in the momentum equations. It also monitors the flow deviation used for the outer iteration convergence control. In case of reverse flow encountered at the exit, it sets the donor enthalpy to the average of the enthalpies of the channels with positive flows.

| | | |
|------------|--------|--|
| Arguments: | ERRFMX | Maximum change in the axial flow (output) |
| | IFMAX | Identification number of the subchannel with maximum change in the axial flow (output) |
| | JFMAX | Identification number of the axial node with maximum change in the axial flow (output) |
| | ERRWMX | Maximum change in the lateral flow (output) |
| | JWMAX | Identification number of the axial node with maximum change in the lateral flow (output) |
| | KWMAX | Identification number of the gap with maximum change in the lateral flow (output) |
| | NCWNEF | Indicator if reverse flows are encountered at the exit (output) |

SAVFLO is called by subroutines PV and PVINIT.

SCHEME (JUMP, ETIME) – This subroutine sets up and performs an outer iteration for the solution of the finite difference equations (using either crossflow solution logic or pressure drop solution logic) at each spatial location at a selected time.

| | | |
|------------|-------|--|
| Arguments: | JUMP | Indicator of converged solution (input/output) |
| | ETIME | Current time (input) |

SCHEME is called by subroutines CALC_SOLVE and DNBTR.

SCHEME calls subroutines AREA, DIFFER, DIVERT, FORCE, HEAT, MIX, NEXPAG, PRESS, PROP, SEPRAT, and VOID.

Function **SCQUAL (I, J, TVF)** – This function calculates the subcooled quality as a correction to the equilibrium quality.

Arguments:

| | |
|-----|---|
| I | Channel index (input) |
| J | Axial node index (input) |
| TVF | Liquid specific volume (m^3/kg) (input) |

SCQUAL is used by subroutine VOID.

SENSI – This subroutine prints a summary of the sensitivity calculations if performed.

Arguments: none

SENSI is called by subroutine CALC_SETPOINT.

SEPRAT (IPART, J, JUMP, ACCELP) – Depending on the indicator IPART, this subroutine either calculates the axial pressure gradient in separated channels (e.g. BWR) by calling DIFFER or adjusts the inlet flow rate distribution to obtain equal pressure drop in all separated channels.

Arguments:

| | |
|--------|---|
| IPART | Indicator: (input) = 1 – pressure drop in separated channels (DIFFER) = 2 – adjust inlet flow rate distribution |
| J | Axial node index (input) |
| JUMP | Convergence indicator (output) |
| ACCELP | Damping factor for axial flow (input); <i>not used</i> |

SEPRAT is called by subroutines PV and SCHEME.

SEPRAT calls subroutine DIFFER.

SETIC – This subroutine is used in the PV solution to set the initial conditions for enthalpy, pressure, flow, and crossflow at each axial node for each channel.

Arguments: none

SETIC is called by subroutine PVINIT.

SETIC calls subroutines AREA, PROP, and VOID.

SOLVE (NN, LMAX, MID, UL, X, B, NK) – This subroutine is called after DECOMP to solve the linear system of equations $AAA \cdot X = B$.

Arguments:

| | |
|------|---|
| NN | Number of unknowns in the linear system of equations (input): = number of subchannels if the pressure drop solution method is selected = number of gaps if the crossflow solution method is selected = number of subchannels or number of axial nodes increased by 2 depending on the equation to solve if pressure-velocity solution method |
| LMAX | = $(2 \times \text{MID} - 1)$ (input) |
| MID | MID is the column location for banded (diagonal) matrix (input) |
| UL | Matrix AAA (input) |
| X | Solution vector (output) |
| B | Right hand side vector (input) |
| NK | Number of rows in the matrix (input): = number of subchannels if pressure drop solution method is selected = number of gaps if crossflow solution method is selected = number of subchannels or number of axial nodes increased by 2 depending on the equation to solve if pressure-velocity solution method |

SOLVE is called by subroutines DIVERT, ENERGY, MASEQX, MASEQY, PRESS, and REBAL.

SOLVE calls subroutines AREA, PROP, and VOID.

SOLVER (INPUT_STREAM, OUTPUT_STREAM, FLAG) – This subroutine is called by INDAT to read input block **group_0_solver** for selection of the solution method of conservation equations.

Arguments:

| | |
|---------------|---|
| INPUT_STREAM | XML input |
| OUTPUT_STREAM | XML output |
| FLAG | Identifier of the input data set to be read |

This subroutine belongs to the module XML_INPUT_CLASS.

SOLVER is called by subroutines COBRA_FLX_INIT and INDAT.

SORT_REAL (N, ARR) – This subroutine is used in the sensitivity calculations.

Arguments:

| | |
|-----|----------------------|
| N | Sample size (input) |
| ARR | Limit (input/output) |

SORT_REAL is called by subroutine CALC_SETPOINT.

SPACER (INPUT_STREAM, OUTPUT_STREAM, FLAG) – This subroutine is called by INDAT to read input block **group_7_spacer** for specifying the spacer data.

Arguments:

| | |
|---------------|---|
| INPUT_STREAM | XML input |
| OUTPUT_STREAM | XML output |
| FLAG | Identifier of the input data set to be read |

This subroutine belongs to the module XML_INPUT_CLASS.

SPACER is called by subroutine INDAT.

SPCSHS (I, J, DTWALL, T_SI, HH_SI, HG_SI, PREF_SI) – This subroutine calculates the superheated steam properties.

Arguments:

| | |
|---------|--|
| I | Subchannel index (input) |
| J | Axial node index (input) |
| DTWALL | Wall superheat (°C) (output) |
| T_SI | Fluid temperature (°C) (input) |
| HH_SI | Fluid enthalpy (J/kg) (input) |
| HG_SI | Latent heat of vaporization (J/kg) (input) |
| PREF_SI | Pressure (Pa) (input) |

SPCSHS is called by subroutine PROP.

SPCSHS calls subroutine PRESX.

SPLIT – This subroutine splits the inlet flow to give equal pressure drop across the first node in all subchannels if selected by input. It is assumed that the density does not change along the axial length and that no crossflow occurs.

Arguments: none

SPLIT is called by subroutines INDAT and PREP.

SPLIT calls subroutines DIFFER, MIX, PROP, and VOID.

STATE_3CP (P, TV, TL, ROV, ROL, EV, EL, TSAT, DTSDP, DELDP, DEVDP, DELDT, DEVDT, DRLDP, DRVDP, DRLDT, DRVDT, IOP, IERR) – This subroutine calculates the state dynamic properties of water.

Arguments:

| | |
|-------|---|
| P | Pressure (Pa) (input) |
| TV | Vapor temperature (K) (input) |
| TL | Liquid temperature (K) (input) |
| ROV | Vapor density (kg/m^3) (output) |
| ROL | Liquid density (kg/m^3) (output) |
| EV | Internal energy of vapor (J/kg) (output) |
| EL | Internal energy of liquid (J/kg) (output) |
| TSAT | Saturation temperature (K) (output) |
| DTSDP | Derivative of TSAT vs. P (output) |
| DELDP | Derivative of TL vs. P (output) |
| DEVDP | Derivative of TV vs. P (output) |
| DELDT | Derivative of EL vs. TL (output) |
| DEVDT | Derivative of EV vs. TV (output) |
| DRLDP | Derivative of ROL vs. P (output) |
| DRVDP | Derivative of ROV vs. P (output) |
| DRLDT | Derivative of ROL vs. TL (output) |
| DRVDT | Derivative of ROV vs. TV (output) |
| IOP | Option selector <i>Not used</i> |
| IERR | Error flag (Input variable out of range) (output) |

STATE_3CP is called by subroutine HTCOR.

VOID (J) – This subroutine calculates the subcooled void fraction, bulk void fraction, fluid density, effective specific volume for momentum, two-phase friction gradient multiplier, velocity, and energy transport velocity.

Arguments:

| | |
|---|------------------|
| J | Axial node index |
|---|------------------|

VOID is called by subroutines ENERGY, SCHEME, SETIC, and SPLIT.

VOID calls subroutine BAROC, SCQUAL, and BVOID.

Function **VOID_CHEXAL (I, J, XP, TRHOF)** – This function returns the void fraction for the Chexal–Lellouche void model. It calculates also the void concentration parameters and void drift velocities.

Arguments:

| | |
|-------|---|
| I | Channel number (input) |
| J | Axial node index (input) |
| XP | Flow quality (-) (input) |
| TRHOF | Saturated liquid density (kg/m^3) (input) |

VOID_CHEXAL is used by function BVOID.

WRITE_HDF_SUMMARY (IPART) – This subroutine writes summary information to the HDF output file.

Arguments:

| | |
|-------|--|
| IPART | Indicator of data type to be written (input) |
|-------|--|

This subroutine belongs to the module THM_OUTPUT_CLASS.

WRITE_HDF_SUMMARY is used by subroutine EXPRIN.

WRITE_HDF_BUNDLE – This subroutine writes bundle information to the HDF output file.

Arguments: none

This subroutine belongs to the module THM_OUTPUT_CLASS.

WRITE_HDF_BUNDLE is used by subroutine EXPRIN.

WRITE_HDF_CROSSFLOW – This subroutine writes crossflow results to the HDF output file.

Arguments: none

This subroutine belongs to the module THM_OUTPUT_CLASS.

WRITE_HDF_CROSSFLOW is used by subroutine EXPRIN.

WRITE_HDF_CHANNEL – This subroutine writes results for all channels and axial nodes to the HDF output file.

Arguments: none

This subroutine belongs to the module THM_OUTPUT_CLASS.

WRITE_HDF_CHANNEL is used by subroutine EXPRIN.

WRITE_HDF_CHF – This subroutine writes CHF summary results, CHF results for all channels and axial nodes, CHF summary results at each axial level, and the bundle pressure difference to the HDF output file.

Arguments: none

This subroutine belongs to the module THM_OUTPUT_CLASS.

WRITE_HDF_CHF is used by subroutine EXPRIN.

WRITE_HDF_ROD – This subroutine writes CHF results for all rods and axial nodes to the HDF output file.

Arguments: none

This subroutine belongs to the module THM_OUTPUT_CLASS.

WRITE_HDF_ROD is used by subroutine EXPRIN.

ZBRENC (F, ERRABS, ERRREL, A, B, MAXFN, IERROR) – This subroutine is used for setpoint iterations on power and inlet temperature. It finds the zero of a function $F(X)$ in a given interval.

Arguments:

| | |
|--------|---|
| F | User-specified function $F(X)$ (output) |
| ERRABS | First stopping criterion. A root, B , is accepted if $ABS(F(B)) \leq ERRABS$ (input) |
| ERRREL | Relative error as a second stopping criterion. A root is accepted if the change between two successive approximations to this root is within ERRREL (input) |
| A | Point A , see explanation of argument " B " (input/output) |
| B | Point B (input/output) On input the user must supply two points for which $F(A)$ and $F(B)$ are opposite in sign. On output both, A and B are altered. B will be the best approximation to the root of F . |
| MAXFN | On input MAXFN should contain an upper bound on the number of function evaluations required for convergence. On output MAXFN will contain the actual number of function evaluations used. (input/output) |
| IERROR | Error signal (output) |

ZBRENC is called by subroutine CALC_SETPOINT.

Function **ZFVOID (I, J, TVF, TRHOF)** – This function calculates the void fraction using the Zuber-Findley void-quality equation.

Arguments:

| | |
|-------|---|
| I | Subchannel index (input) |
| J | Axial node index (input) |
| TVF | Liquid specific volume (m^3/kg) (input) |
| TRHOF | Saturated liquid density (kg/m^3) (input) |

ZFVOID is used by subroutine BVOID.

5.0 VERIFICATION AND VALIDATION

COBRA-FLX is a core thermal-hydraulic code capable of predicting the axial and cross flows, and temperature (enthalpy) distributions in confined complex geometries where wall shear forces are more dominant than intra-fluid shear forces. The primary intended application of COBRA-FLX is in rod bundle arrays. Typical applications of COBRA-FLX include core-wide flow and enthalpy predictions, pressure drop predictions, steady-state and transient subchannel calculations, critical heat flux calculations, and Departure from Nucleate Boiling Ratio (DNBR) predictions. COBRA-FLX's solution technique is verified for these types of applications using experimental and parallel code comparisons. The verification of the fluid flow equations, models, and solutions are performed in the following areas.

- Conservation of mass and energy,
- Experimental validation of the fluid flow solution, which comprises the following calculations:
 - a. Inter-Bundle Diversion Cross Flow (IBDCF) test data and COBRA-FLX predictions
 - b. MARGINAN crossflow test data and COBRA-FLX predictions
- Experimental validation of empirical correlations which comprises the following calculation:
 - a. Critical Heat Flux (CHF) correlations
- Verification of the fluid flow and energy solutions using comparisons to NRC approved core thermal-hydraulic subchannel codes for:
 - b. steady-state calculations and
 - c. transient calculations

5.1 Conservation of Mass and Energy

Several core models reflecting a 193 fuel assembly core at full power and full flow were used for quantifying the mass and energy balance errors in COBRA-FLX. The core models consisted of 12 channels, 52 channels, 75 channels, and 7083 channels, respectively, representing the range of model sizes to be used for reload licensing analyses.

Figure 5-1 provides the 12-channel radial node scheme where ten subchannels are modeled individually, the remainder of the fuel assembly is modeled as a single channel and the remainder of the core is modeled as a single channel. The 52-channel model is an extension of the 12-channel model where two more adjacent rows of subchannels are modeled individually to yield a total of 21 subchannels as individual channels. The remainder of the fuel assembly is modeled as a channel while the rest of the fuel assemblies in the core are modeled as individual channels. The 75-channel model is identical to the 52-channel model except that all subchannels in the limiting fuel assembly are modeled as individual channels. The 7083-channel model simulates all the subchannels as individual channels in the 1/8th core model.

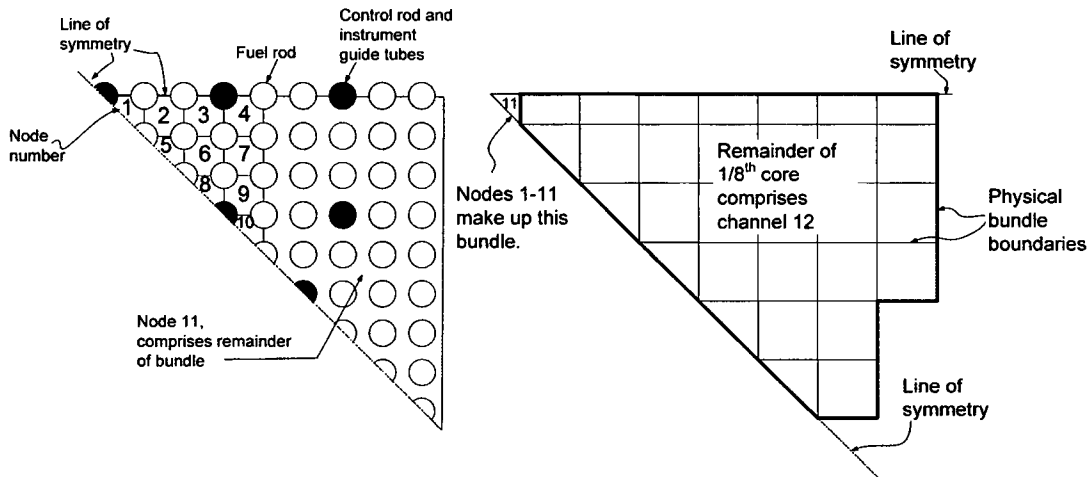
The heat balance error (E_{heat}) is defined as:

$$E_{heat} = \left| \frac{(\sum Mh)_{out} - (\sum Mh)_{in}}{Q_{added}} - 1 \right| \times 100\% \quad 5-1$$

and the mass balance error (E_{mass}) is defined as:

$$E_{mass} = \left| \frac{(\sum M)_{out} - (\sum M)_{in}}{(\sum M)_{in}} \right| \times 100\% \quad 5-2$$

Figure 5-1: Radial Node Scheme for the 12-Channel Model of a 193 Fuel Assembly Core (1/8th Core Symmetry)



The mass and energy balance errors for the four COBRA-FLX core models are shown in Table 5-1.

Table 5-1: Example of COBRA-FLX Heat and Exit Mass Balance Errors

| CORE MODEL | HEAT BALANCE ERROR USING THE P-SOLUTION METHOD (%) | EXIT MASS BALANCE ERROR USING THE P-SOLUTION METHOD (%) | HEAT BALANCE ERROR USING THE PV-SOLUTION METHOD (%) | EXIT MASS BALANCE ERROR USING THE PV-SOLUTION METHOD (%) |
|--------------|--|---|---|--|
| 12-channel | 0.21 | 0.00 | 0.21 | 0.00 |
| 52-channel | 0.47 | 0.00 | 0.47 | 0.00 |
| 75-channel | 0.42 | 0.00 | 0.43 | 0.00 |
| 7083-channel | - | - | 0.22 | 0.00 |

In all cases, the maximum mass flow and enthalpy errors are 0.00%, or less than $1(10)^{-3}\%$, and 0.47% respectively. These calculations utilized the SCHEME-Pressure (P) solution method described in Section 2.3.1.4 and the PV solution method described in Section 2.3.2.

5.2 Experimental Validation of the Fluid Flow Solution

COBRA-FLX's capability to solve fluid flow problems is demonstrated by predicting the measured test data for two experiments.

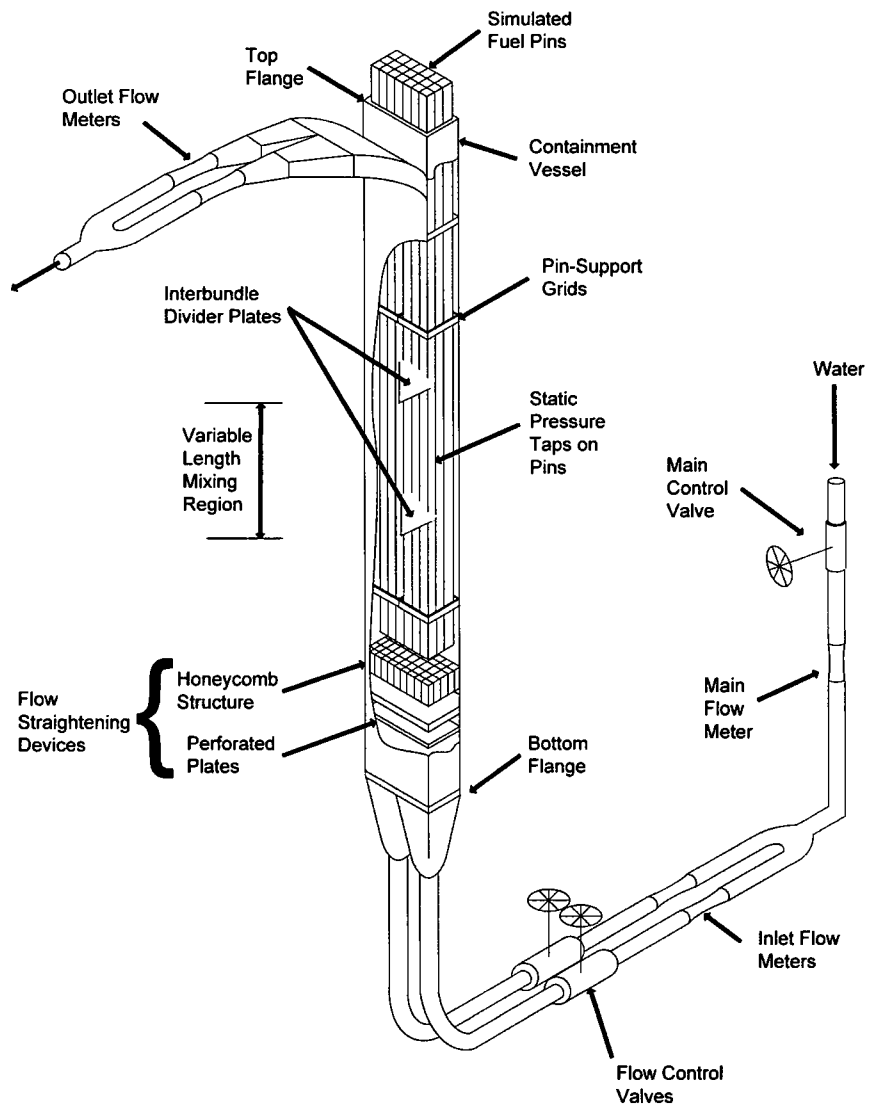
- Inter-Bundle Diversion Crossflow tests (IBDCF),
- MARIGNAN Crossflow tests

These two experiments reflect several Separate Effects Tests (SETs) that are used to demonstrate that the fluid flow solution, on the scale of individual fuel assemblies modeled as channels to the finer scale of individual subchannels modeled as channels, is reliable for use for the type of flow redistributions encountered in core analysis.

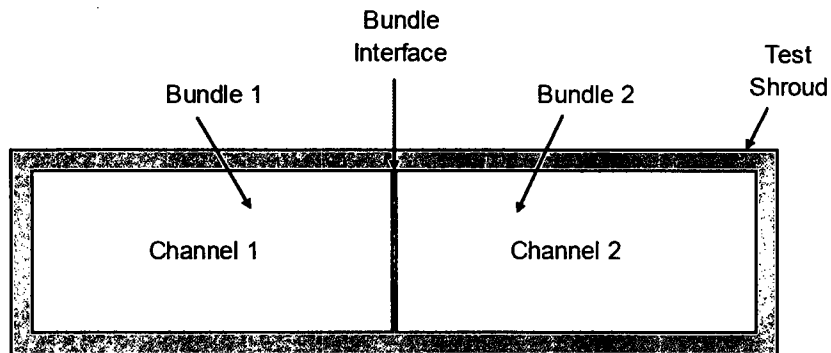
5.2.1 Inter-Bundle Diversion Cross-Flow Tests

Several isothermal cross flow tests were performed using a two-bundle test apparatus. Three spacer grids were positioned within the mixing region shown in the diagram of Figure 5-2. The two bundles were two half-size AREVA 15x15 fuel assemblies, each with an array of 8-by-15 rods to form a total 8-by-30 rod array. The system temperature range was between 85°F and 105°F. In the experiment, incremental pressure measurements along the axial length of the two bundles were taken and the flow distribution was calculated based on the measured pressure profile.

Figure 5-2: Two-Bundle Isothermal Crossflow Test Apparatus for the IBDCF Tests



Fifteen tests were simulated using COBRA-FLX and represent tests 131, 132, 133, 134, 135, 136, 137, 138, 139, 140, 147, 148, 149, 150, and 151. The test simulations differed from each other according to the inlet velocity ratio between the two simulated fuel bundles, identified as Bundles 1 and 2 as shown in Figure 5-3.

Figure 5-3: Cross-Sectional View of IBDCF Test Arrangement

Therefore, where V_1 and V_2 represent the velocities in Bundles 1 and 2 respectively, the ratio V_2/V_1 characterizes the different tests. The velocity ratios, V_2/V_1 , varied from 0.95 (representing a nearly uniform inlet velocity distribution) to 0.0 (representing a flow blockage condition for one bundle). A COBRA-FLX model representing two channels, one channel for each bundle as shown in Figure 5-3, was used to predict the flow redistribution. The tabular comparisons of the COBRA-FLX predictions and test measurements for the twelve tests with inlet velocity ratios greater than 0.49 are shown in Table 5-2 for two numerical solution methods, SCHEME-Pressure (P) and Pressure-Velocity (PV), described in Sections 2.3.1.4 and 2.3.2, respectively. Both solution methods provide good agreement to the test results in Table 5-2 using a typical crossflow resistance factor, K_{ij} , of 0.15.

Table 5-2: Summary of COBRA-FLX Predictions Using the SCHEME-Pressure (P) and Pressure-Velocity (PV) Solution Methods versus Test Values for IBDCF Tests

| IBDCF Test # | Inlet Velocity Ratio (V ₂ / V ₁) | Mean Value of Predicted(V ₂ / V ₁) / Test (V ₂ / V ₁) | | Maximum Value | |
|--------------|---|---|--------------------|-------------------|--------------------|
| | | P solution method | PV solution method | P solution method | PV solution method |
| 134 | 0.500 | 1.001 | 1.001 | 0.929 | 0.929 |
| 139 | 0.501 | 1.001 | 1.001 | 0.930 | 0.930 |
| 148 | 0.497 | 1.001 | 1.001 | 0.926 | 0.926 |
| 133 | 0.752 | 1.005 | 1.005 | 0.972 | 0.972 |
| 138 | 0.750 | 1.005 | 1.006 | 0.972 | 0.972 |
| 149 | 0.751 | 1.004 | 1.005 | 0.970 | 0.970 |
| 132 | 0.900 | 1.006 | 1.007 | 0.992 | 1.023 |
| 137 | 0.901 | 1.006 | 1.007 | 0.991 | 0.991 |
| 150 | 0.905 | 1.005 | 1.006 | 0.991 | 0.991 |
| 131 | 0.951 | 1.006 | 1.007 | 1.022 | 1.027 |
| 136 | 0.946 | 1.006 | 1.007 | 1.018 | 1.022 |
| 151 | 0.954 | 1.004 | 1.005 | 0.991 | 1.017 |

The mean value of the predicted and measured V₁ and V₂ velocity ratios was determined as follows.

$$Mean = \frac{1}{N} \sum_{i=1}^N \left[\frac{\left(\frac{V_2}{V_1} \right)_{COBRA-FLX}}{\left(\frac{V_2}{V_1} \right)_{Test}} \right]_i \tag{5-3}$$

where:

N : Number of axial locations, 37 for these cases

V₂/V₁ : Velocity ratio between bundles 2 and 1

with the subscripts:

COBRA – FLX : predicted using COBRA-FLX

Test : calculated with the experimental pressure measurements

The maximum value reported in Table 5-2 was determined as follows using the Mean defined in Equation 5-3:

$$\text{Maximum} = \frac{\left(\frac{V_2}{V_1}\right)_{COBRA-FLX}}{\left(\frac{V_2}{V_1}\right)_{test}} \quad \text{at} \quad \left\{ \text{Mean} - \left[\frac{\left(\frac{V_2}{V_1}\right)_{COBRA-FLX}}{\left(\frac{V_2}{V_1}\right)_{test}} \right] \right\}_{\max} \quad 5-4$$

The remaining tests, 135, 140, and 147 represent a more severe inlet flow profile with an inlet flow velocity ratio of 0.0. Inlet flow asymmetries of this magnitude require the robustness associated with the PV solution method. The PV solution method provides good agreement, seen in Table 5-3, with the test results demonstrating its reliability for application where significant axial flow asymmetries occur and under low flow conditions.

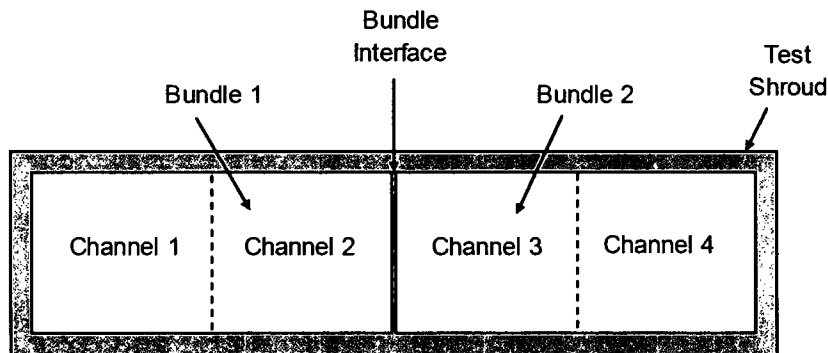
Table 5-3: Summary of COBRA-FLX Predictions Using the Pressure-Velocity (PV) Solution Methods versus Test Values for the Severe Inlet Flow Asymmetry IBDCF DCF Tests

| IBDCF Test # | Inlet Velocity Ratio (V ₂ / V ₁) | Mean Value of Predicted(V ₂ / V ₁) / Test (V ₂ / V ₁) | Maximum Value |
|--------------|---|---|--------------------|
| | | PV solution method | PV solution method |
| 135 | 0.000 | 0.991 | 0.703 |
| 140 | 0.000 | 0.998 | 0.712 |
| 147 | 0.000 | 1.000 | 0.727 |

This agreement was also based on the COBRA-FLX user's selection of an appropriate crossflow resistance factor, K_{ij}, of 4.0 for the severe inlet flow profile conditions. The COBRA-FLX user is responsible to select the appropriate flow solution method and crossflow resistance factor whenever encountering severe flow differences during application.

The robustness for the PV solution method for low flow and reversal flow can be seen by examining Test 147 with an inlet flow velocity ratio of 0.0 where the channel modeling has been modified to use four smaller channels as shown in Figure 5-4.

Figure 5-4: Cross-Sectional View of the IBDCF Test Arrangement Showing the 4 Channel Model Definition



Channels 3 and 4 represented Bundle 2 which had an inlet flow velocity of 0 m/s. The axial flow velocity and the associated crossflow(s) are shown in Figure 5-5,

Figure 5-6, Figure 5-7, and Figure 5-8 for each of the channels for the Test 147 condition. The observation of predicted reverse and recirculating flow can be made within the lowermost 30 cm of the Channel 4 axial flow velocity provided in Figure 5-8. This test simulation and predicted results from Table 5-3 validate the capability of COBRA-FLX to predict reverse and recirculating flow under extreme flow blockages of 100% at the inlet of a fuel bundle.

Figure 5-5: Axial and Crossflow Velocity for Channel 1 of IBDCF Test 147 Using PV Solution Method

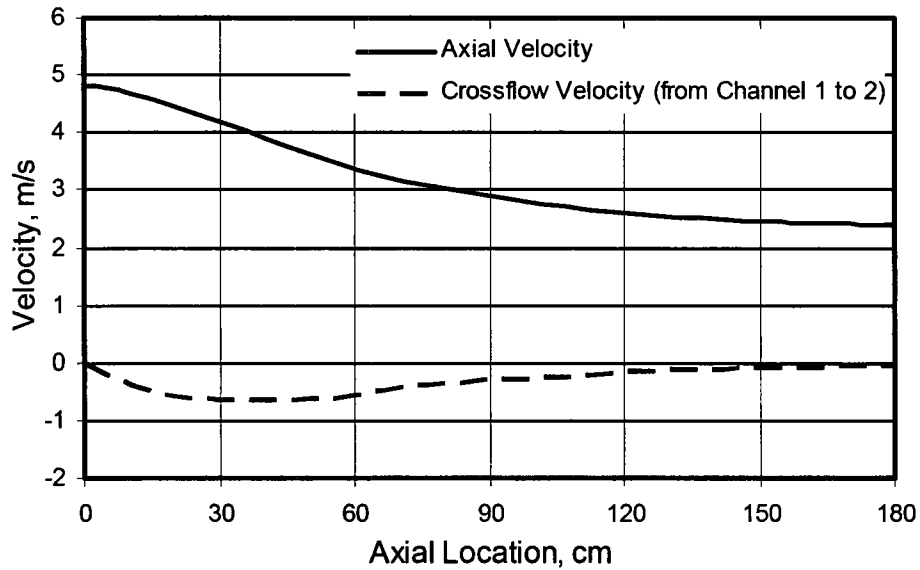


Figure 5-6: Axial and Crossflow Velocity for Channel 2 of IBDCF Test 147 Using PV Solution Method

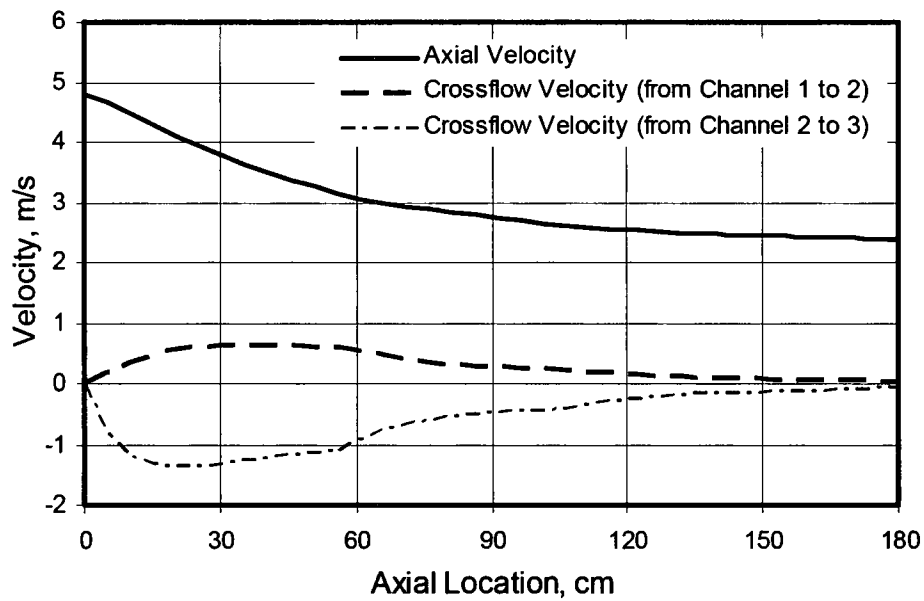


Figure 5-7: Axial and Crossflow Velocity for Channel 3 of IBDCF Test 147 Using PV Solution Method

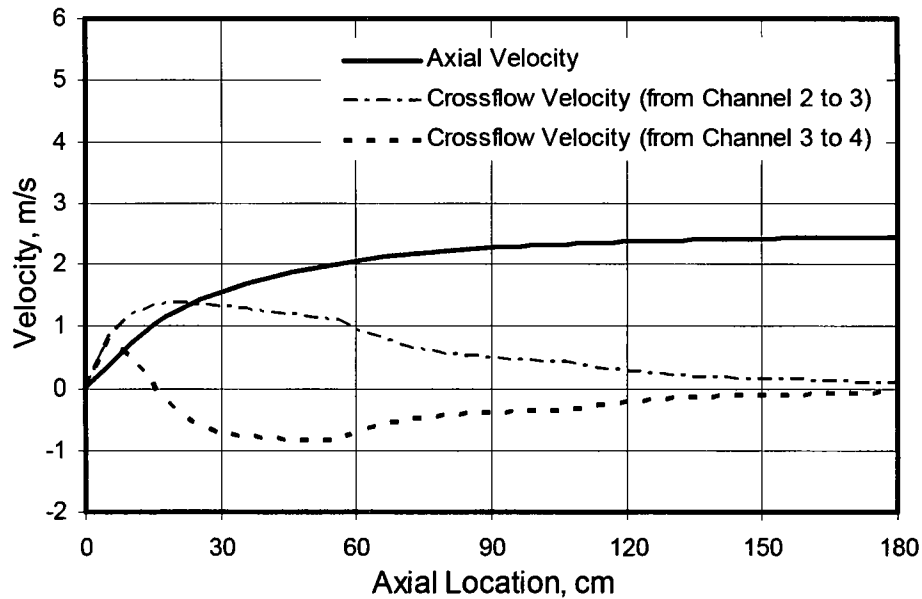
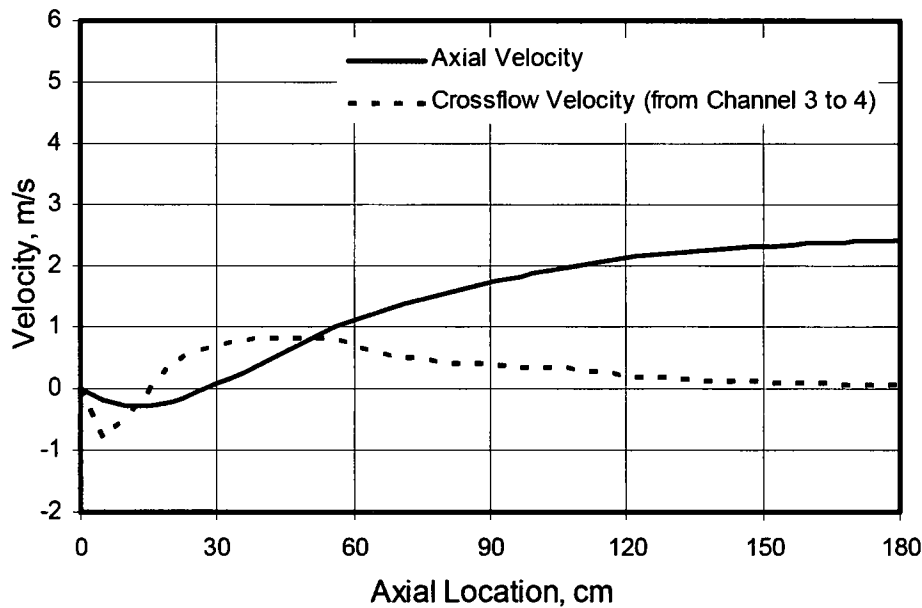


Figure 5-8: Axial and Crossflow Velocity for Channel 4 of IBDCF Test 147 Using PV Solution Method



5.2.2 MARIGNAN Crossflow Tests

Additional benchmarking of the fluid flow solution was performed using the measurements obtained from the MARIGNAN flow experiments performed at the Commissariat à l'Energie Atomique de Cadarache using the Hèrmes T Dual-Assembly Loop. In these isothermal tests two adjacent and hydraulically dissimilar 15x15 AFA-2G fuel assemblies were tested side by side in a common housing. One assembly contained three additional mid-span mixing grids (MSMGs) but was otherwise identical to the other assembly. The MSMG used on production fuel, is a shortened grid with no fuel rod contact and is equipped with mixing vanes.

Laser Doppler velocimetry was used to acquire particle velocities in the axial and transverse direction simultaneously. The lateral view of the two assembly test configuration is shown in Figure 5-9. The location of the velocity measurement positions are shown in Figure 5-10 and Figure 5-11 as shaded circles. Note the Y position above and below the MSMG for the individual measurement sites in the exploded view of Figure 5-11. Measurements were taken at 21 axial locations spanning 410 mm about the center of the third MSMG. At each axial location, velocity measurements were made along adjacent rows of subchannels to a width (x-axis) of four rows from the interface row in both assemblies and the interface row. Therefore, 189 averaged measurements were obtained.

Figure 5-9: MARIGNAN Test Configuration with Two Adjacent Fuel Assemblies with Defined Subchannels (lateral view)

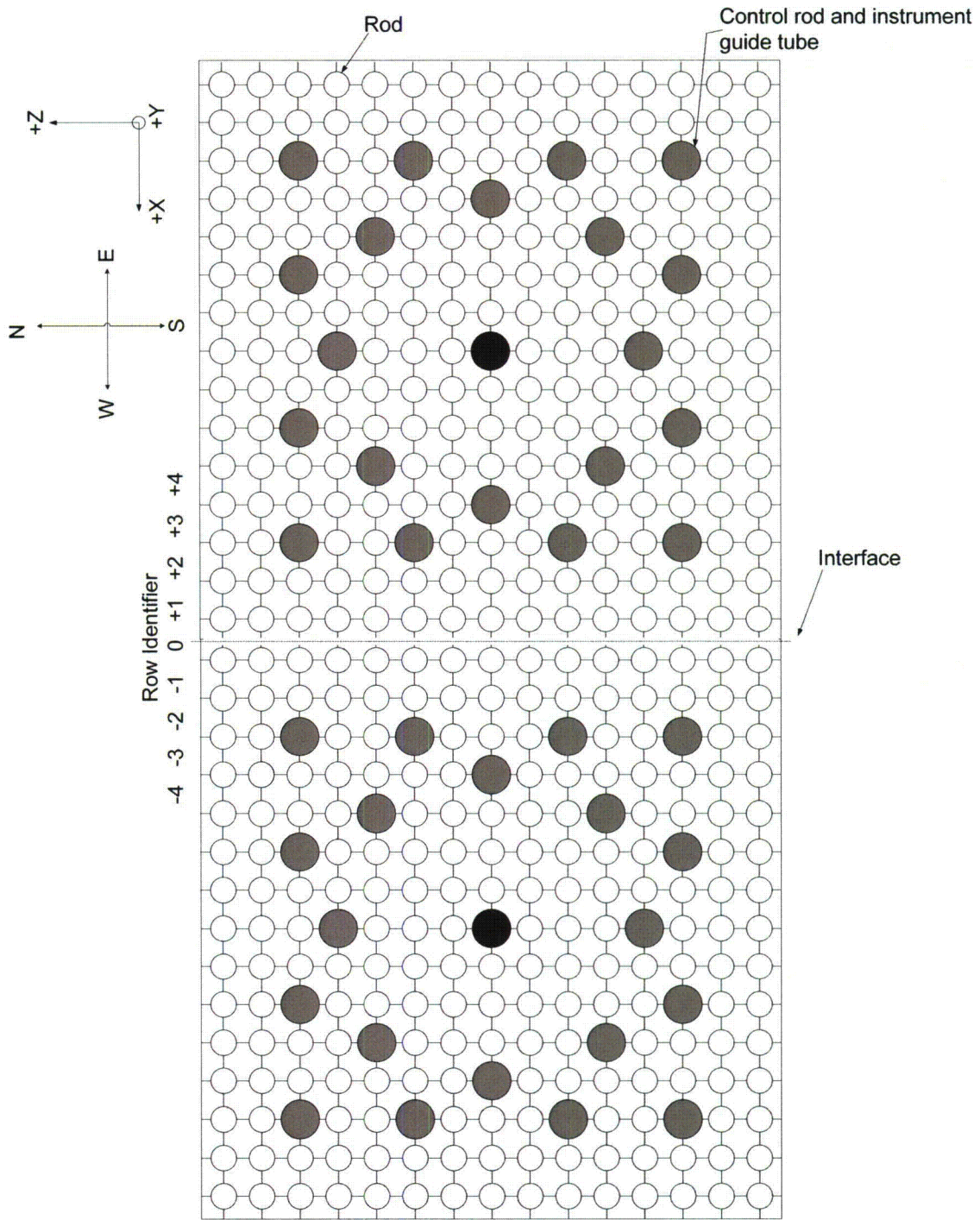


Figure 5-10: Location of the Velocity Measurements in the MARIGNAN Test Configuration (Full View)

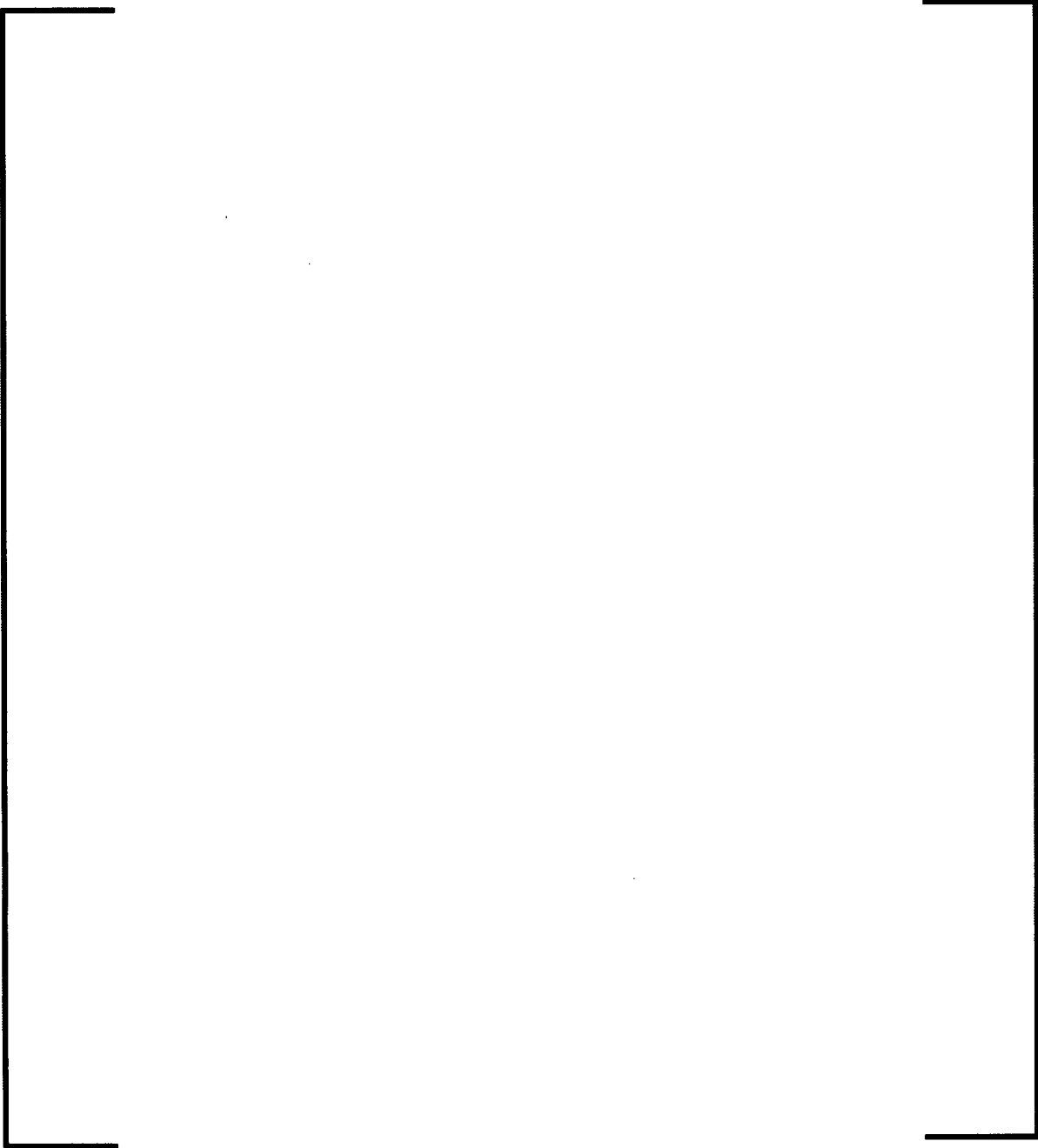
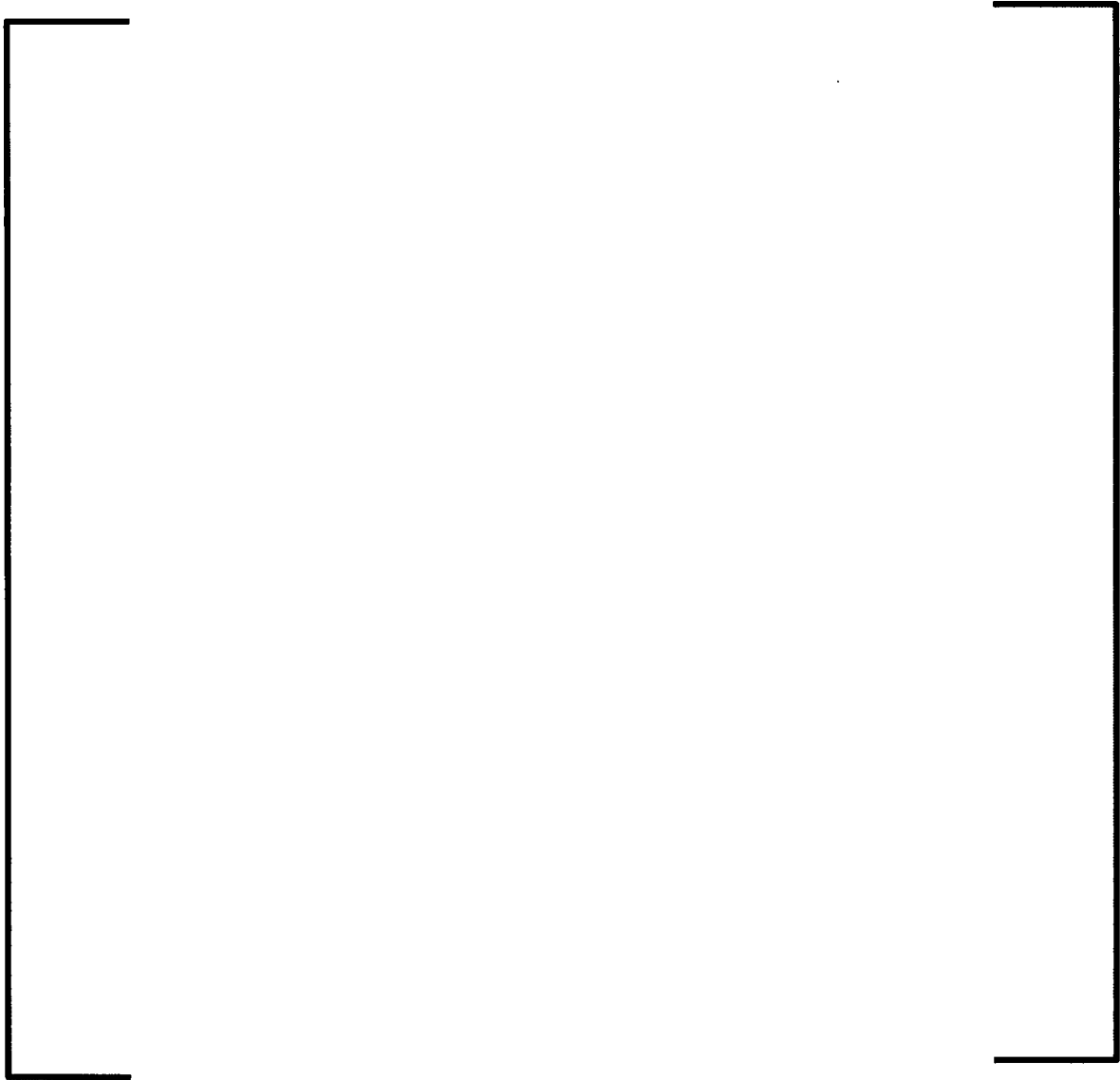


Figure 5-11: Location of the Velocity Measurements in the MARIGNAN Test Configuration (Exploded View)



These flow experiments were modeled using COBRA-FLX to demonstrate its capability to predict the flow redistribution where high induced lateral flows are present resulting in significant variations in the axial flow velocities. This configuration, one assembly containing mid-span mixing grids and the adjacent assembly without such grids, represents one of the most severe cross flow conditions in fuel assembly core thermal-

hydraulic analysis. The COBRA-FLX axial velocity predictions were found to be within 5% of the measured values for 90% of the data. Axial velocity comparisons between MARIGNAN results and COBRA-FLX predictions by subchannel row are shown for four axial positions in Figure 5-12, Figure 5-13, Figure 5-14 and Figure 5-15.

Figure 5-12: Axial Velocity Comparisons by Subchannel Row at the Relative Axial Location of Y= - 200.0 mm in the MARIGNAN Test



Figure 5-13: Axial Velocity Comparisons by Subchannel Row at the Relative Axial Location of $Y = -7.5$ mm in the MARIGNAN Test



Figure 5-14: Axial Velocity Comparisons by Subchannel Row at the Relative Axial Location of $Y = +7.0$ mm in the MARIGNAN Test



Figure 5-15: Axial Velocity Comparisons by Subchannel Row at the Relative Axial Location of Y= +200.0 mm in the MARIGNAN Test



The parameter V/V_{mean} , plotted in the vertical axes in Figure 5-12, Figure 5-13, Figure 5-14, and Figure 5-15, is to be interpreted as:

$$\frac{V}{V_{\text{mean}}}, \text{ where the experimental (Measured) } V_{\text{mean}} = 4.8 \text{ m/s} \quad 5-5$$

These figures show good agreement between measured and predicted axial flow velocities while capturing the general trends in the lateral variation of axial velocities. It is concluded from this agreement that COBRA-FLX is capable of predicting flow redistribution associated with adjacent hydraulically-dissimilar fuel assemblies for core thermal-hydraulic analyses.

5.3 Experimental Validation of Empirical Correlations

COBRA-FLX utilizes various empirical correlations for determining the critical heat flux for a fuel assembly and for completing the necessary system of equations. The AREVA critical heat flux correlations are discussed in Section 5.3.1. The empirical correlations provided in Appendix A serve as a link between some of the governing equations and supply data needed by the governing equations to generate the necessary solutions.

The specific empirical correlations described in Table 1-2 are those within the requested NRC review and will be used for safety-related analyses. They reflect the empirical correlations that have been used within the COBRA 3-CP code and the introduction of the Chexal-Lellouche bulk void correlation. No experimental validation is being presented for these empirical correlation.

5.3.1 Critical Heat Flux Correlations

AREVA has developed several fuel design-specific critical heat flux correlations to support departure from nucleate boiling ratio (DNBR) calculations safety-related reload application analyses. These correlations were developed using NRC approved thermal-hydraulic codes. Appendix C has been included in this report to provide the validation of the correlations for their use with the local conditions predicted using COBRA-FLX.

5.3.2 Validity of Steady-State Critical Heat Flux (CHF) Correlations in Transient Applications

The adequacy of steady-state CHF correlations for analyzing transients has previously been demonstrated in Reference 5-1 using CHF test data from the development of the B&W-2 CHF correlation where rod bundle tests characterized by power, flow, and pressure transients were experimentally simulated. (This demonstration was previously discussed in Appendix G of Reference 5-1). The following classes of transient tests had been performed with various initial conditions.

- Power ramps of a) a single 5% ramp (2% below steady-state CHF to 3% above) and b) a dual ramp totaling 30% (a ramp from 27% below steady-state CHF to steady-state CHF to 2% below, followed by another ramp from 2% below to 3% above),
- Flow coast down transients simulating one or all reactor coolant pumps coasting down, and
- Pressure reduction transients where the pressure decreased approximately at a rate of 20 psi/s.

These calculations, discussed in Appendix G of Reference 5-1 (and quoting Reference 5-2 and Reference 5-3) showed that

- no premature CHF occurred as a result of the power, flow, and pressure transients, and
- the use of instantaneous system pressure, local flow, and quality in a steady-state CHF correlation provided acceptable or conservative results.

LeTourneau and Green, Reference 5-3, have shown that the use of steady-state CHF correlations and instantaneous local conditions provided conservative transient CHF predictions. The transient CHF rod bundle tests performed by AREVA and LeTourneau and Green support the use of instantaneous local conditions and steady-state CHF correlations for predicting transient CHF.

Reference 5-4 contains similar favorable conclusions that are supported by other investigators. Reference 5-5 was quoted in Reference 5-4 which states that there are two known primary problems in the analytical prediction of transient CHF:

- capability and accuracy of the computer codes used to predict the local conditions of flow, quality, and system pressure, and
- use of steady-state CHF correlations.

The first concern is addressed in Section 5.7.2 where COBRA-FLX transient responses are compared to predictions of the NRC approved LYNXT thermal-hydraulic code. Further, the NRC, in Reference 5-6, has approved the use of B&W-2 correlation for transient analysis based on the investigations of Reference for Loss of Coolant Accident (LOCA) calculations.

A RAI response for the LYNXT code review, available on page G-5 of Reference 5-1 quoted several other references in support of the acceptability of using steady-state CHF correlations in transient CHF calculations that include justifications of the use of steady-state correlations for the analysis of a pressure blowdown transient for a variety of inlet conditions, flow coast down, rapid and exponential flow decay, combined flow/pressure transients and flow reversals.

These arguments show that steady-state CHF correlations are applicable in a wide range of flow, power, and pressure transients. It is noted that for the quoted references

in the LYNXT RAI response, the conditions simulated were based on experimental data. The accuracy or conservatism shown in those references had indicated that the steady-state correlation limits were also applicable to transients. AREVA previously supplied proprietary information in Reference 5-7 further defending the applicability of a steady-state CHF correlation for transient application. In conclusion, the use of steady-state CHF correlations and their associated DBNR limits for transient application is appropriate when instantaneous local conditions, as calculated by COBRA-FLX, are used for the derivation of the particular CHF correlation.

5.4 Comparisons of Solution Algorithms (Solution Schemes)

As noted in Section 1, COBRA-FLX has three numerical solution methods noted within the topical report, however, only two of them are technically supported within the report. They are the SCHEME-Pressure (P) solution, formulated to arrive at a system of equations which can be solved for the axial pressure differences, and the Pressure-Velocity (PV) solution to aid in simulating normal flow conditions but also low flow, including flow recirculation, situations such as the steam link break (SLB) transient with no forced pump flow. The SCHEME-Crossflow numerical solution method, discussed in Section 2.3.1.3 is not validated in Section 5.4 since it is not within the request for review and approval discussed in Section 1. The SCHEME-Crossflow solution method, although yielding virtually identical results as SCHEME-Pressure, does require more computational resources. Section 5.4 provides a comparison of calculated subchannel parameters to demonstrate the agreement only between the P and PV numerical solution methods. Earlier in Section 5.2.1, the P and PV solution methods were found in Table 5-2 to provide nearly identical results for inlet flow ratios from 0.95 to 0.50 for adjacent bundles. The comparisons in Section 5.4 examine more typical reactor analysis conditions between the two solution methods.

The comparison of the two COBRA-FLX solution methods will be based on the predictions for a typical 4 pump coast down transient for a 4-loop 193 fuel assembly plant. The core model represents a full core of Mark-BW fuel assemblies for which the BWCMV-A CHF correlation is applicable. The comparison is based on a 12-channel

model as described in Figure 5-1 and extending along the length of the fuel rod with a heated length beginning at 5.1 cm and ending at 370.6 cm.

The transient was analyzed from the initial condition ($t = 0$ seconds) through the first 5 seconds during which a minimum DNBR was observed at 3.4 seconds for both the P and PV solution methods as seen in Figure 5-16. The solution methods resulted in transient minimum DNBR predictions differences of only 0.007 for P and PV solution methods as shown in Table 5-4. Both solution methods predicted the minimum DNBR occurring in the same subchannel and at the same elevation.

Figure 5-16: DNBR Response During a 4 Pump Coastdown Using the P and PV Solution Methods

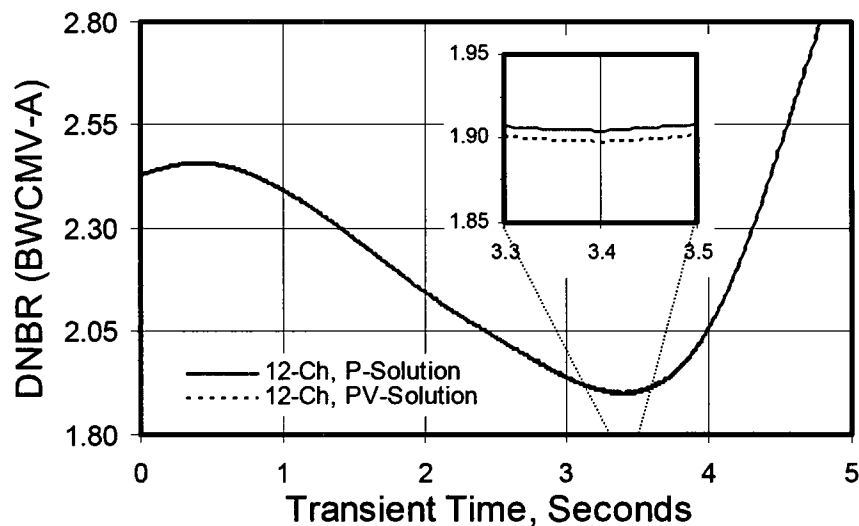
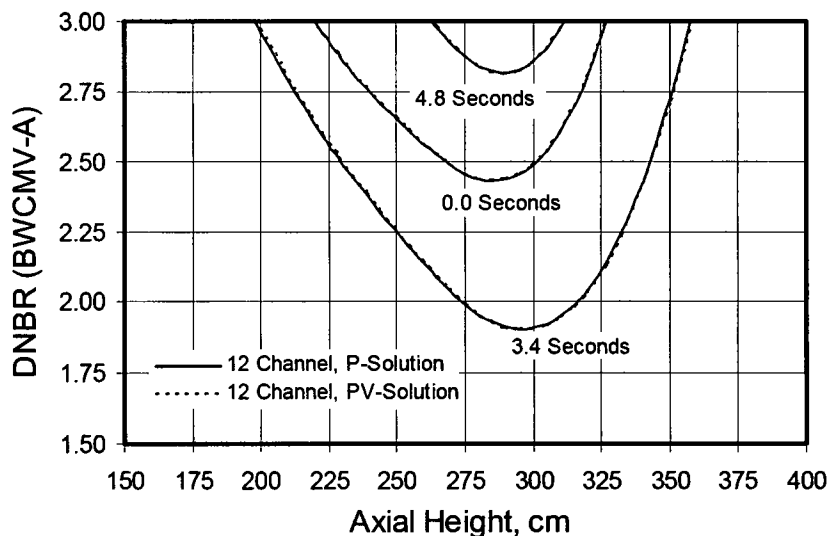


Table 5-4: DNBR Comparison During a 4 Pump Coastdown Using the P and PV Solution Methods

| Time (sec) | PV Solution Method (DNBR) | P Solution Method (DNBR) | Difference |
|--------------------------------------|---------------------------|--------------------------|------------|
| 0.0 (transient initialization) | 2.426 | 2.427 | 0.001 |
| 3.4 (time at transient minimum DNBR) | 1.898 | 1.905 | 0.007 |
| 4.8 (end of evaluation) | 2.811 | 2.816 | 0.005 |

The small axial differences in DNBR predictions between the approximate axial locations of 200 – 350 cm for the three points in time are shown in Figure 5-17.

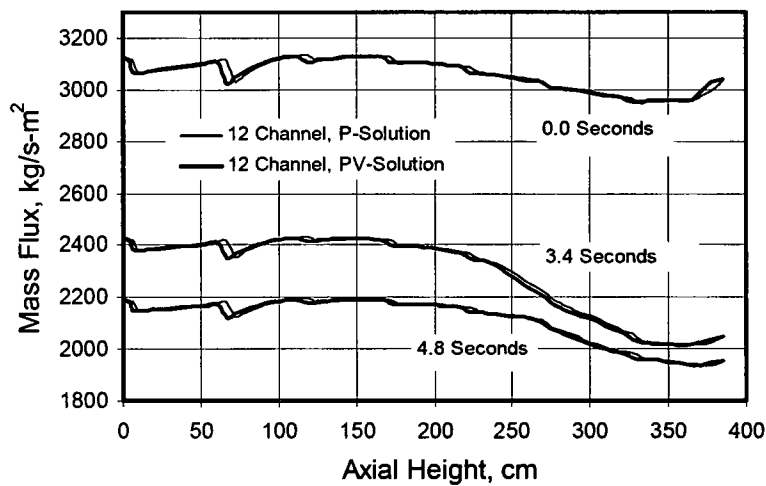
Figure 5-17: DNBR Response During a 4 Pump Coastdown Using the P and PV Solution Methods for the Axial Range of 200 to 350 cm



An examination of the subchannel local conditions for the DNBR-limiting subchannel for both solution methods showed similar good agreement for mass flux in Figure 5-18 for the four pump coastdown. The subchannel mass flux behavior versus axial height in Figure 5-18 shows the PV solution prediction responds earlier to hydraulic resistances

of the spacer grids at several elevations relative to the P solution prediction. This prediction difference is attributed to the PV solution method's use of a staggered mesh to account for the position of the momentum control volumes as discussed throughout Section 2.3.2.

Figure 5-18: DNBR-Limiting Subchannel Mass Flux versus Axial Location at Three Times during a 4 Pump Coastdown for the P and PV Solution Methods



The comparison of the DNBR-limiting subchannel enthalpy for the same three times during the transient is shown in three separate figures for easier comparison.

Figure 5-19: DNBR-Limiting Subchannel Enthalpy versus Axial Location at 0.0 Seconds During a 4 Pump Coastdown for the P and PV Solution Methods

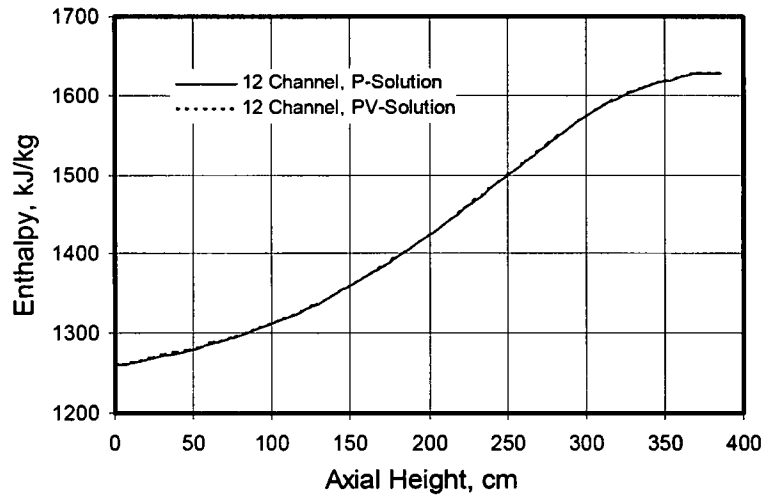


Figure 5-20: DNBR-Limiting Subchannel Enthalpy versus Axial Location at 3.4 Seconds during a 4 Pump Coastdown for the P and PV Solution Methods

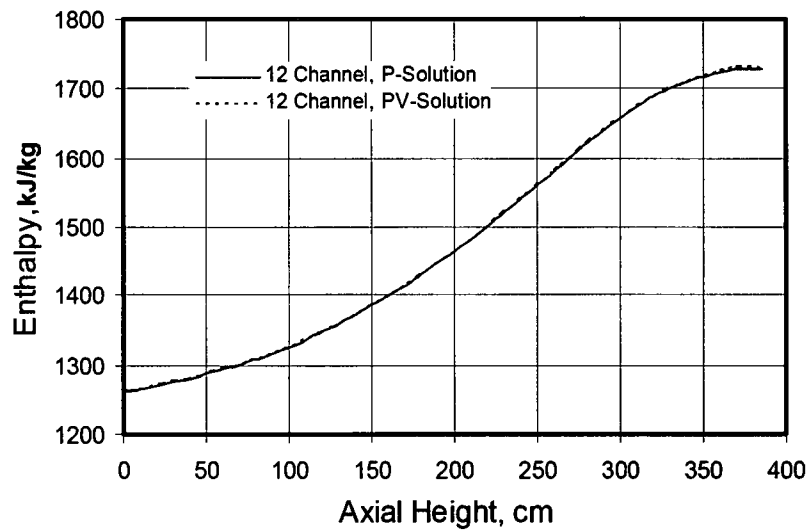
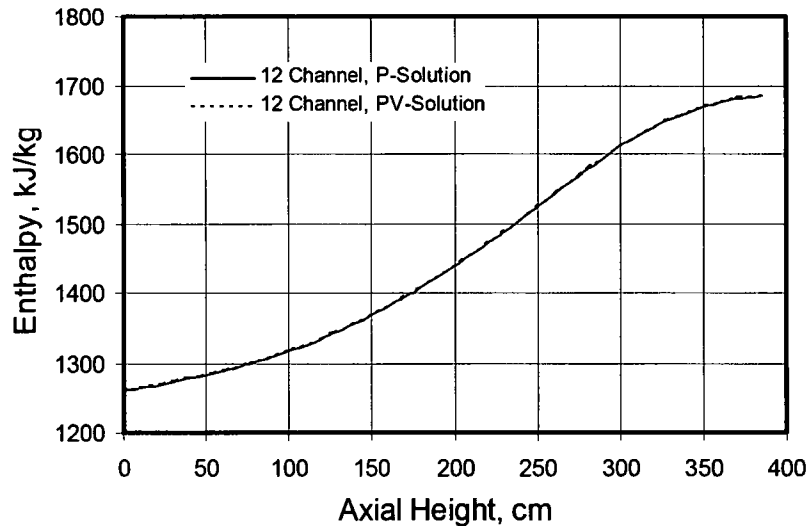


Figure 5-21: DNBR-Limiting Subchannel Enthalpy versus Axial Location at 4.8 Seconds during a 4 Pump Coastdown for the P and PV Solution Methods



The enthalpy predictions in Figure 5-19, Figure 5-20, and Figure 5-21 show good agreement for both solution methods. The supporting enthalpy statistics are supplied in Table 5-5.

Table 5-5: Statistics for the P and PV Based Predictions for Subchannel Enthalpies

| Statistic | Value |
|--|--------|
| Maximum percentage difference in the calculated axial enthalpy | < 0.30 |
| Maximum average percentage difference in the calculated axial enthalpy | < 0.15 |

The predictions for the 4 pump coastdown all support the conclusion that the P and PV solution methods have acceptably small differences. The COBRA-FLX user is responsible to select the appropriate solution method for the type of analysis being performed.

The P solution method has been further improved with the use of a successive over-relaxation method, as discussed in Sections 2.3.1.4.1, []

[], as discussed in Section 2.3.1.4.2. The differences between the results of these SOR methods with the P- solution as opposed to the P solution are insignificantly small. Minimum DNBR differences may change in some applications by as much as 0.001 in DNB ratio. Therefore, the P solution results and conclusions supported by the Section 5.4 validation would be applicable to the SOR methods.

In summary, the P and PV solution methods are shown to provide acceptably consistent results for safety-related analyses. The DNBR predictions using either solution method can be compared to the CHF Design Limit identified in Appendix C. The evaluation of the ACH-2 CHF correlation in Appendix C demonstrates that the same Design Limit is achieved whether the P or PV solution method is used.

5.5 Modeling Size

The versatility of COBRA-FLX allows the user to determine the necessary level of model geometry complexity for simulating the thermal-hydraulic conditions. In DNB analyses, it is necessary to determine local thermal-hydraulic conditions on a subchannel basis and to model a sufficient number of surrounding subchannels to accurately account for proper channel to channel exchanges and for the global power and flow balance. Core regions further from the limiting subchannel can be modeled as groups of subchannels and/or groups of fuel assemblies to decrease the size of the COBRA-FLX model while still maintaining an acceptably consistent prediction of the minimum DNBR performance of the limiting subchannel.

The comparison of model sizes is based upon four core models which are all 1/8th core symmetric. In Figure 5-1, the 12-channel core model is shown where a cluster of individual subchannels (Channels 2 through 10) surround the limiting subchannel (Channel 1). Channel 11 represents the remainder of the fuel assembly, and Channel 12 represents the remainder of the core. The 52-channel model is an extension of the 12-channel model where two more adjacent rows of subchannels are modeled individually to yield a total of 21 subchannels as individual channels. The remainder of

the fuel assembly is modeled as a channel while the rest of the fuel assemblies in the core are modeled as individual channels. The 75-channel model is identical to the 52-channel model except that all subchannels in the limiting fuel assembly are modeled as individual channels. The 7083-channel model simulates all the subchannels as individual channels in the 1/8th core model.

The 4 pump coastdown transient used in Section 5.4 will again be used to quantify the minimum DNBR impact of using various model sizes. Table 5-6 shows the minimum DNBR values for all four model sizes agree well, within 0.005 of each other in minimum DNBR, thereby verifying the model size capability of COBRA-FLX.

Table 5-6: Minimum DNBR Predictions for Various Core Model Sizes for a 4 Pump Coastdown

| Number of Channels Modeled | MDNBR (BWCMV-A) |
|-----------------------------------|----------------------------|
| 12 | 1.957 |
| 52 | 1.956 |
| 75 | 1.954 |
| 7083 | 1.952 |

5.6 Heat Transfer Package

The empirical correlations used with COBRA-FLX, exclusive of the critical heat flux correlations, are provided and discussed in Appendix A. Since the requested review of this topical report is limited to the no-rewetting option, two examples of the user control of no rewetting are shown to verify that COBRA-FLX allows the user to prohibit the return to the nucleate boiling regime once it enters the post-DNB operation. In the first page of Figure C-1, the path in the heat transfer section logic flow chart can be seen where a user-defined input directs whether rewetting is allowed to occur or not. These two cases represent two transients that progress through various heat transfer modes defined in Table 5-7 and extracted from Appendix A.

Table 5-7: COBRA-FLX Heat Transfer Modes

| Region | Heat Transfer Mode |
|---------------------------------------|--------------------|
| Forced convection (liquid) | 1 and 2 |
| Subcooled nucleate boiling | 3 |
| Saturated nucleate boiling | 4 |
| Transition boiling | 5 |
| High flow, high pressure film boiling | 6 |
| High flow, low pressure film boiling | 7 |
| Low flow film boiling | 8 |
| Forced convection (vapor) | 9 and 10 |

The two transients, labeled Transient "A" and "B", were each evaluated with COBRA-FLX with and without rewetting activation. Figure 5-22 and Figure 5-24 show that with no rewetting, the heat transfer mode does not return to a pre-CHF heat transfer condition. Figure 5-23 and Figure 5-25 show the corresponding clad wall temperature response and the impact of no rewetting. Therefore, this demonstrates the COBRA-FLX user control for avoiding rewetting.

Figure 5-22: Transient “A” Progression through Heat Transfer Modes

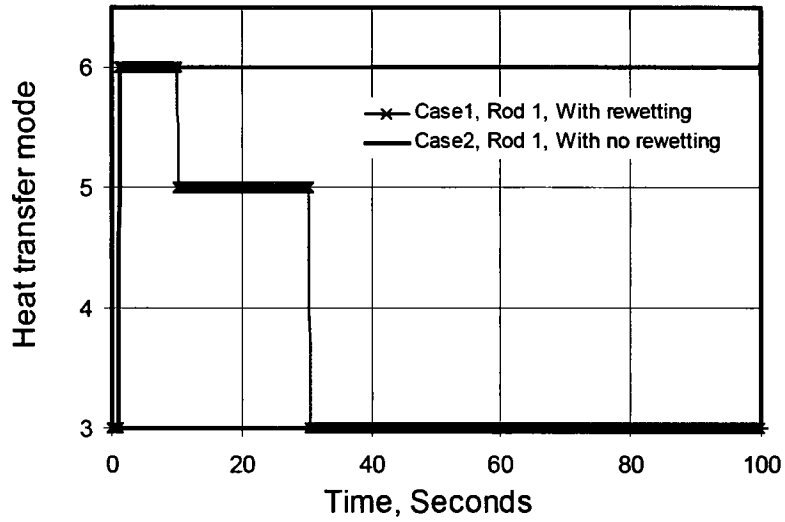


Figure 5-23: Transient “A” Clad Wall Temperature Response

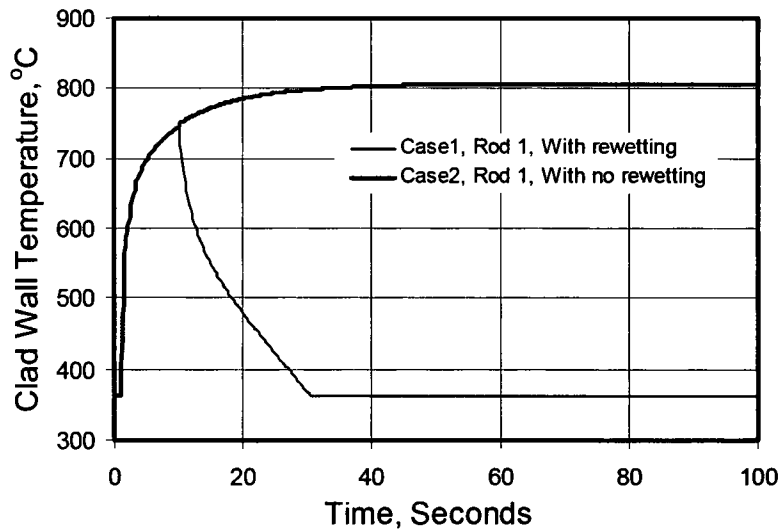


Figure 5-24: Transient “B” Progression through Heat Transfer Modes

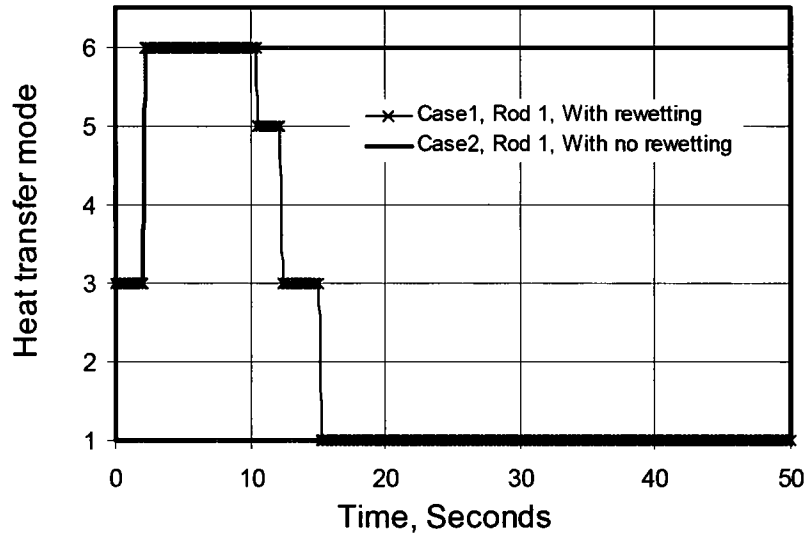
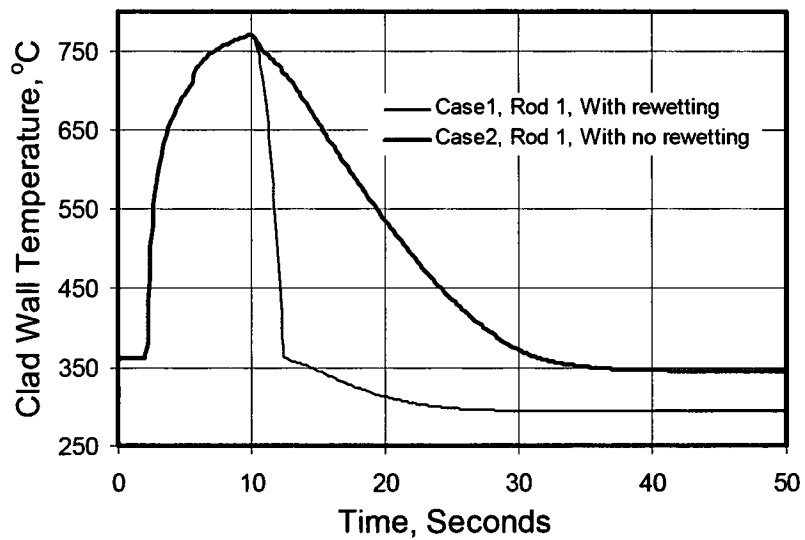


Figure 5-25: Transient “B” Clad Wall Temperature Response



5.7 Comparison of Fluid Flow Solution to Other Subchannel codes

Fluid flow solution comparisons between COBRA-FLX and NRC approved codes LYNXT and XCOBRA-IIIC were performed in both steady-state and transient modes. These comparisons were made using the typical solution algorithms in each code to demonstrate the relative behavior of three AREVA subchannel codes. The corresponding numerical solution algorithms used were the

- SCHEME solution method in XCOBRA-IIIC,
- PV solution method in LYNXT, and
- P and PV solution methods in COBRA-FLX.

Both steady-state and transient comparisons were made using models with identical descriptions of subchannels, axial nodes, peaking patterns, and boundary conditions.

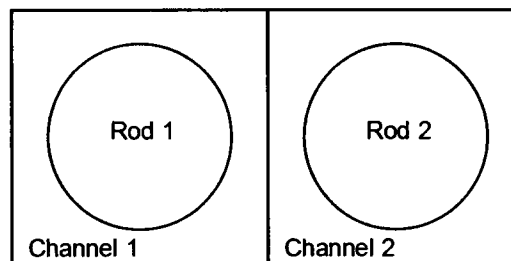
5.7.1 Steady-State Comparisons to Other Codes

The steady-state comparisons were performed using a simple 2-channel model with no crossflow and a 38-channel core model with crossflow. Each comparison has merits and allows observations and conclusions to be made.

5.7.1.1 2-Channel Calculations with No Crossflow

The 2-channel model represents two adjacent fuel assemblies as shown in Figure 5-26. The COBRA-FLX model simulated the entire axial length of identical fuel assemblies of equal power, inlet flow velocity, and hydraulic resistance which results in no lateral crossflow.

Figure 5-26: 2-Channel Model with No Crossflow for Code Comparisons



The axial local coolant properties of Channel 1 (verified to be identical to that of Channel 2) are compared between COBRA-FLX, XCOBRA-IIIC and LYNXT in Figure 5-27 through Figure 5-30 for normalized pressure drop, void fraction, coolant density, and coolant enthalpy, respectively. These comparisons show that COBRA-FLX predictions agree more closely to the LYNXT predictions for these parameters. The more pronounced differences between XCOBRA-IIIC and the other two codes in void fraction and density reflect the impact of the particular void fraction model of XCOBRA-IIIC.

Figure 5-27: Normalized Axial Pressure Drop Comparison for the 2-Channel Model with No Crossflow

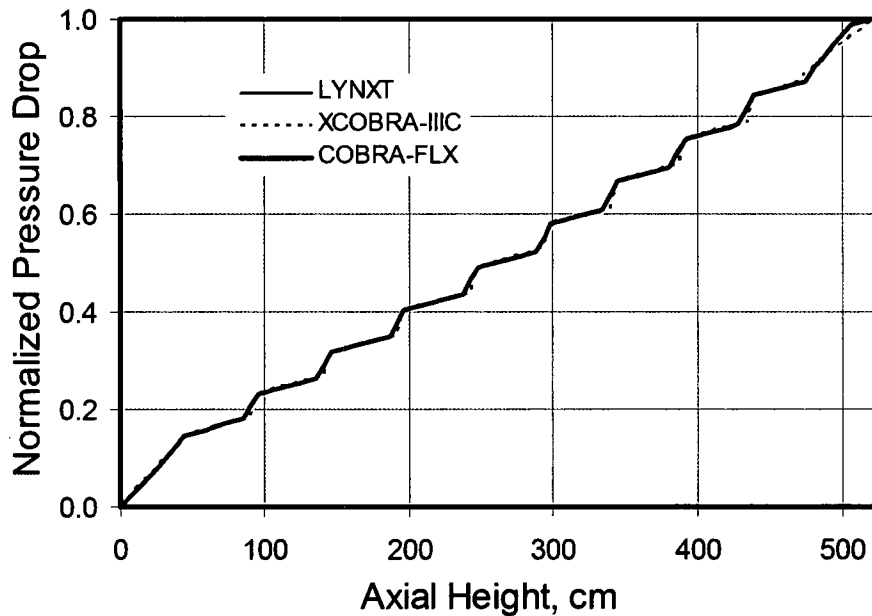


Figure 5-28: Axial Void Fraction Comparison for the 2-Channel Model with No Crossflow

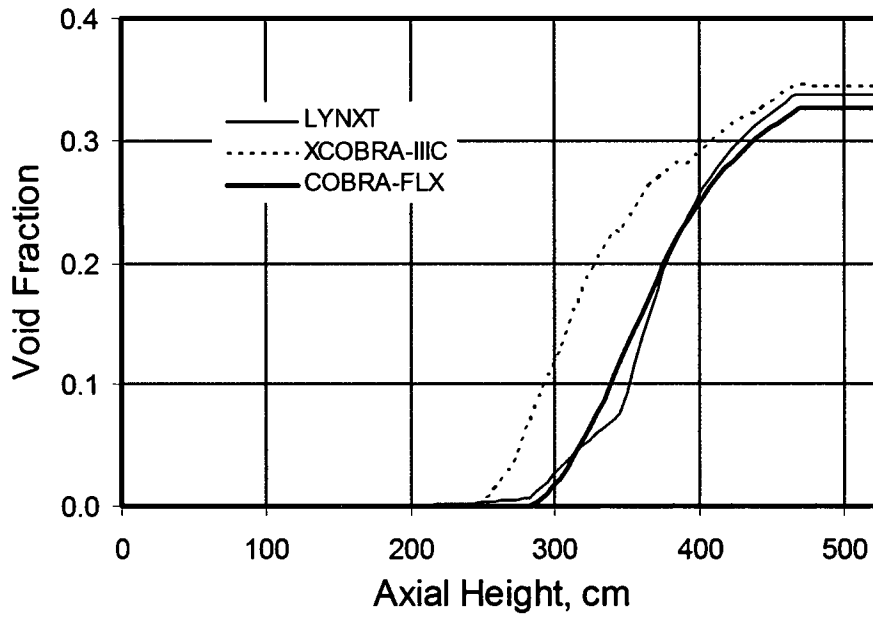


Figure 5-29: Coolant Density Comparison for the 2-Channel Model with No Crossflow

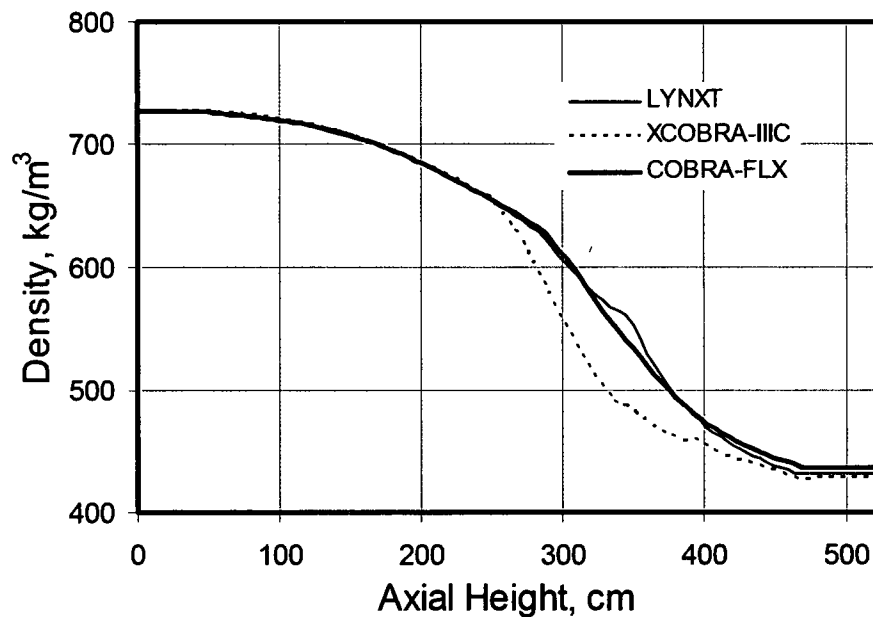
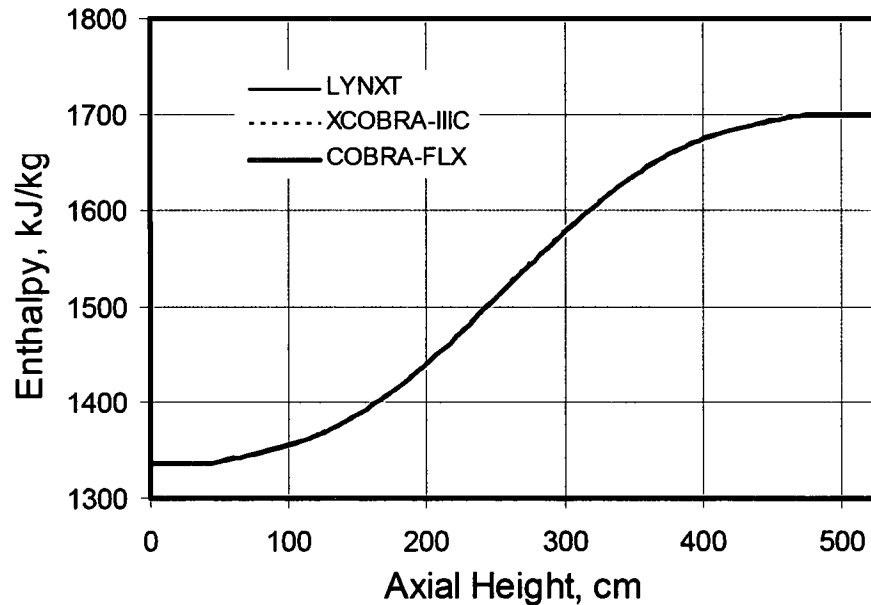


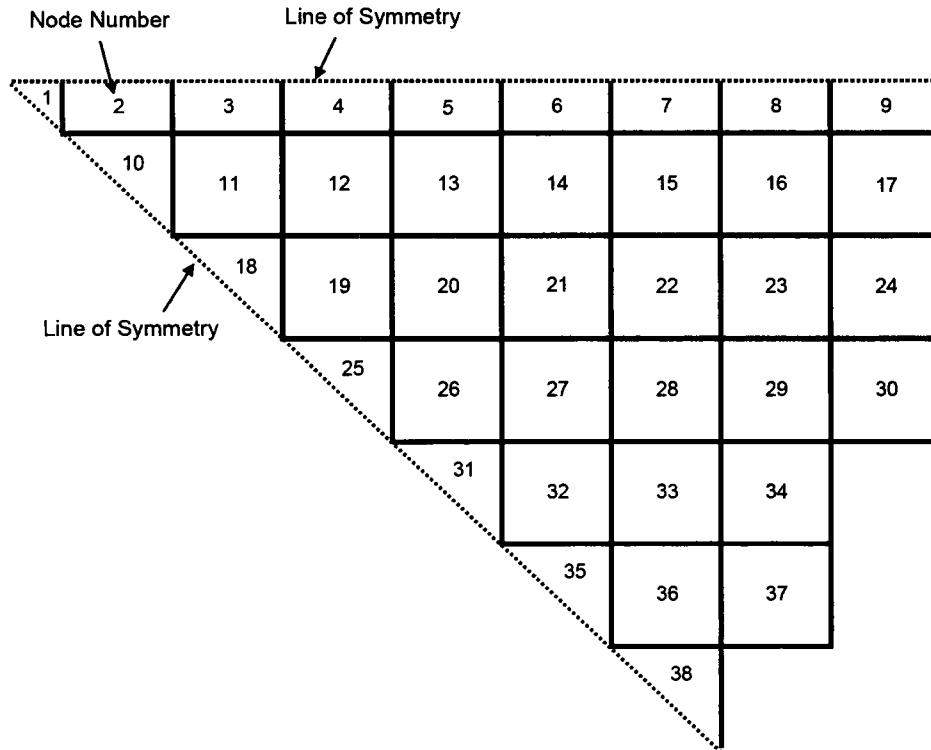
Figure 5-30: Coolant Enthalpy Comparison for the 2-Channel Model with No Crossflow



5.7.1.2 38-Channel Calculations With Crossflow

In order to provide a more representative comparison to what is seen in code applications between COBRA-FLX and the other two codes, a 38-channel core model has been used. This model utilizes a single channel to represent each fuel assembly in a 1/8th symmetric core. A description of radial noding of the model is provided in Figure 5-31. The core model simulates an operational condition at an overpower condition at full flow.

Figure 5-31: Radial Node Scheme for the 38-Channel Model (1/8th Core Symmetry) With Crossflow for Code Comparisons



Each channel is modeled to contain one rod representing the power associated with that portion of an entire fuel assembly. A typical core radial power distribution was used to more closely represent application analyses.

The axial local coolant properties of Channel 1 for all three codes are shown in Figure 5-32, Figure 5-33, and Figure 5-34 for mass velocity, void fraction, and coolant enthalpy, respectively. These comparisons show that COBRA-FLX predictions agree more closely to the LYNXT predictions for these parameters with crossflow occurring for the steady-state condition. Again, the more pronounced differences between XCOBRA-IIIC and the other two codes in void fraction and density reflect the impact of the particular void fraction model of XCOBRA-IIIC.

**Figure 5-32: Mass Velocity Comparison for the 38-Channel Model
With Crossflow**

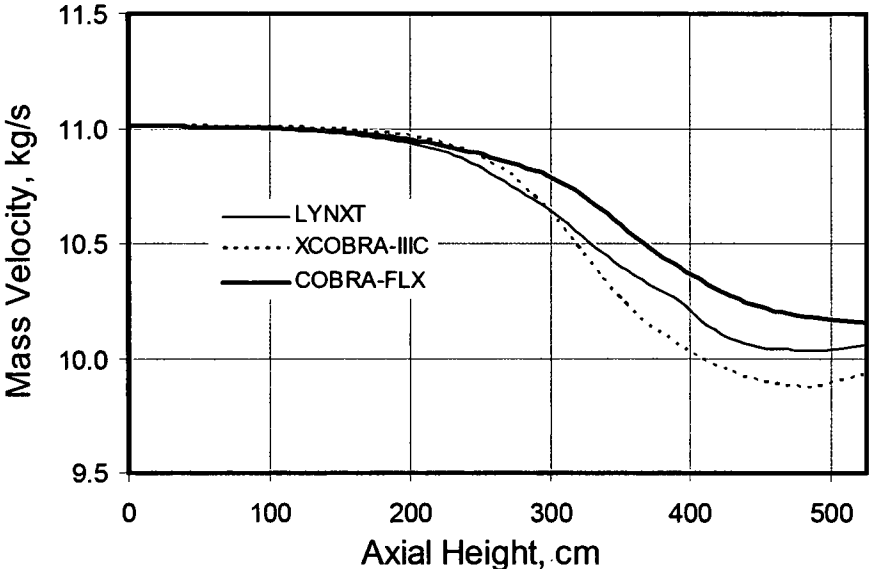


Figure 5-33: Void Fraction Comparison for the 38-Channel Model with Crossflow

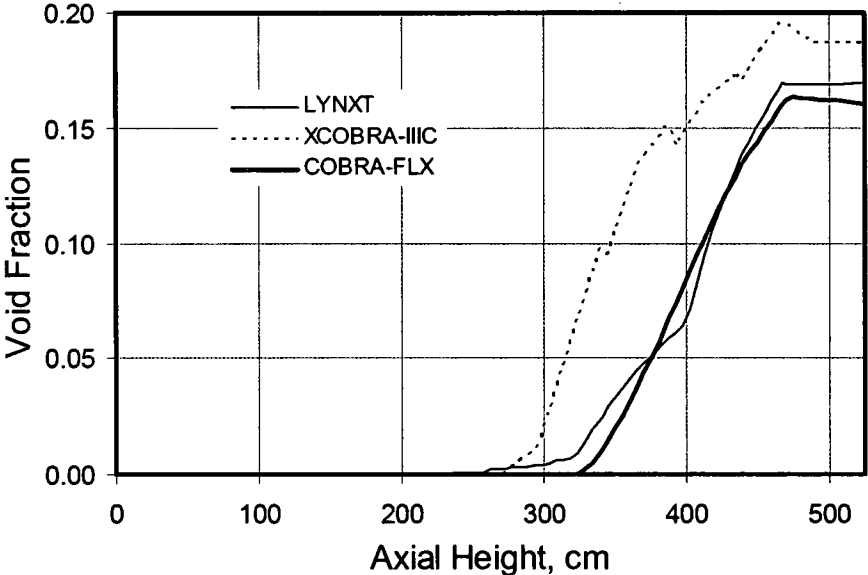
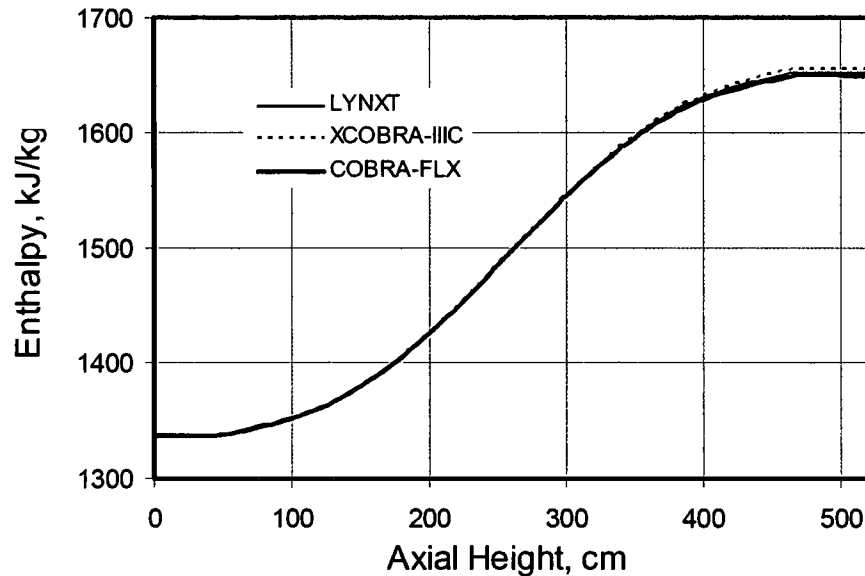


Figure 5-34: Coolant Enthalpy Comparison for the 38-Channel Model with Crossflow

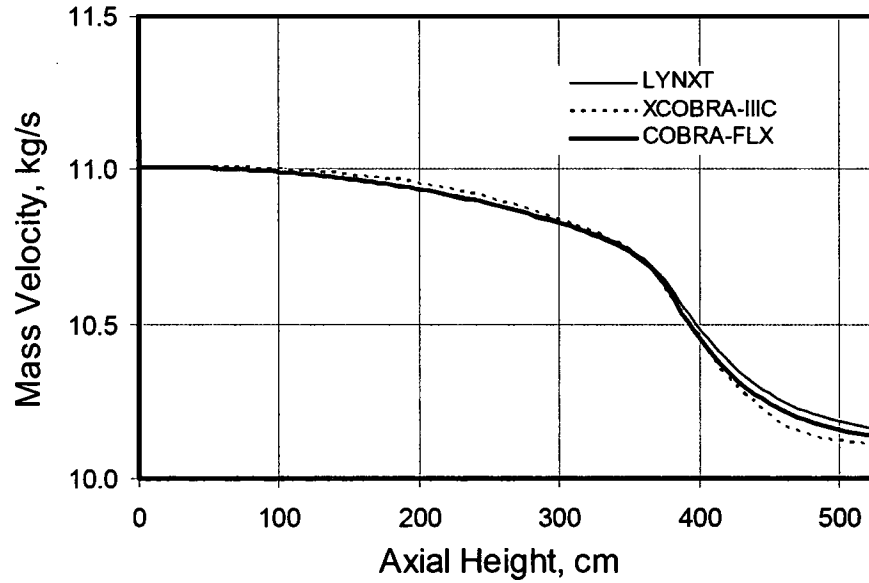


5.7.1.3 Examination of Void Model Impacts Between Codes

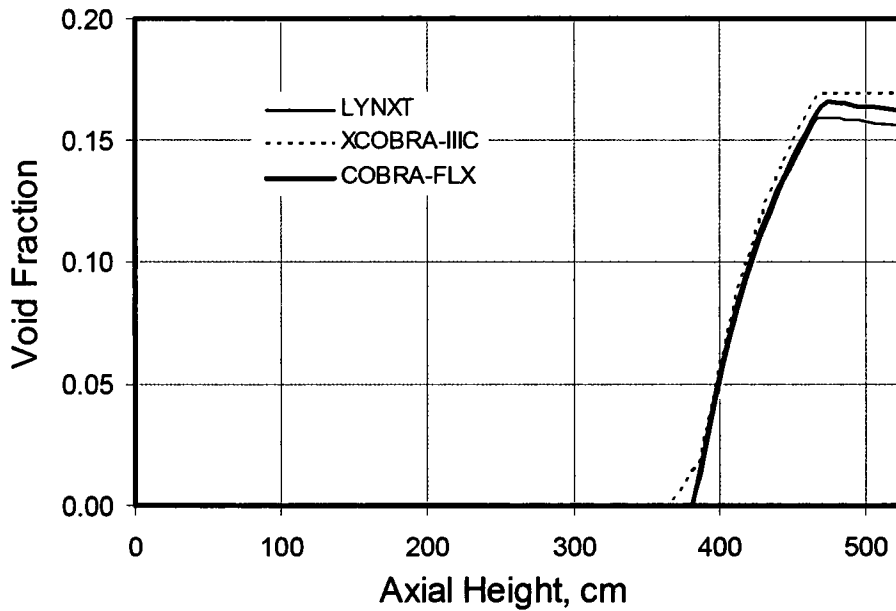
For production application COBRA-FLX would use the empirical correlations from Appendix A, including the Chexal-Lellouche bulk void model, whereas LYNXT uses the B&W void model and XCOBRA-IIIC uses the Levy subcooled void model and homogenous bulk void model. In addition, each code is used with its respective subcooled initiation model, subcooled profile fit, diabatic friction multiplier, and two-phase friction multiplier. If all three codes utilized the same subcooled void formation, void fraction correlation, diabatic friction multiplier, and two-phase friction multiplier, such as those of the homogenous models, COBRA-FLX agrees more closely to LYNXT and XCOBRA-IIIC as seen in Figure 5-35 and Figure 5-36 as compared to local conditions using their respective application void models in Figure 5-32 and

Figure 5-33. These comparisons indicate the void model accounts for the majority of the local condition differences seen earlier in the code to code comparisons.

**Figure 5-35: Mass Velocity Comparison for the 38-Channel Model
Using the Homogenous Void Model**

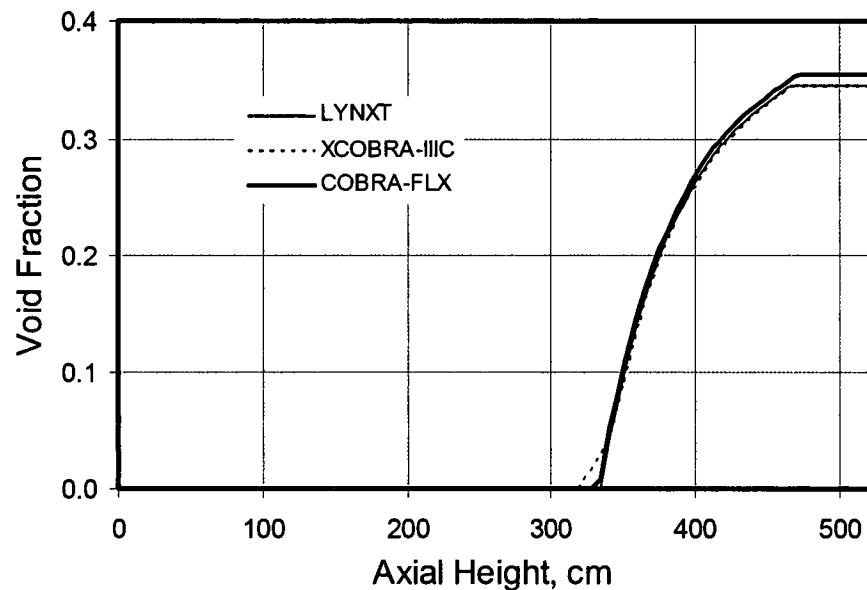


**Figure 5-36: Void Fraction Comparison for the 38-Channel Model
Using the Homogenous Void Model**



The same conclusion can be reached by using the simple 2-channel model with no crossflow. Figure 5-37 shows comparable void fraction agreement as seen above in Figure 5-36 for the 38-channel model when using the homogeneous void model.

Figure 5-37: Void Fraction Comparison for the 2-Channel Model Using the Homogenous Void Model



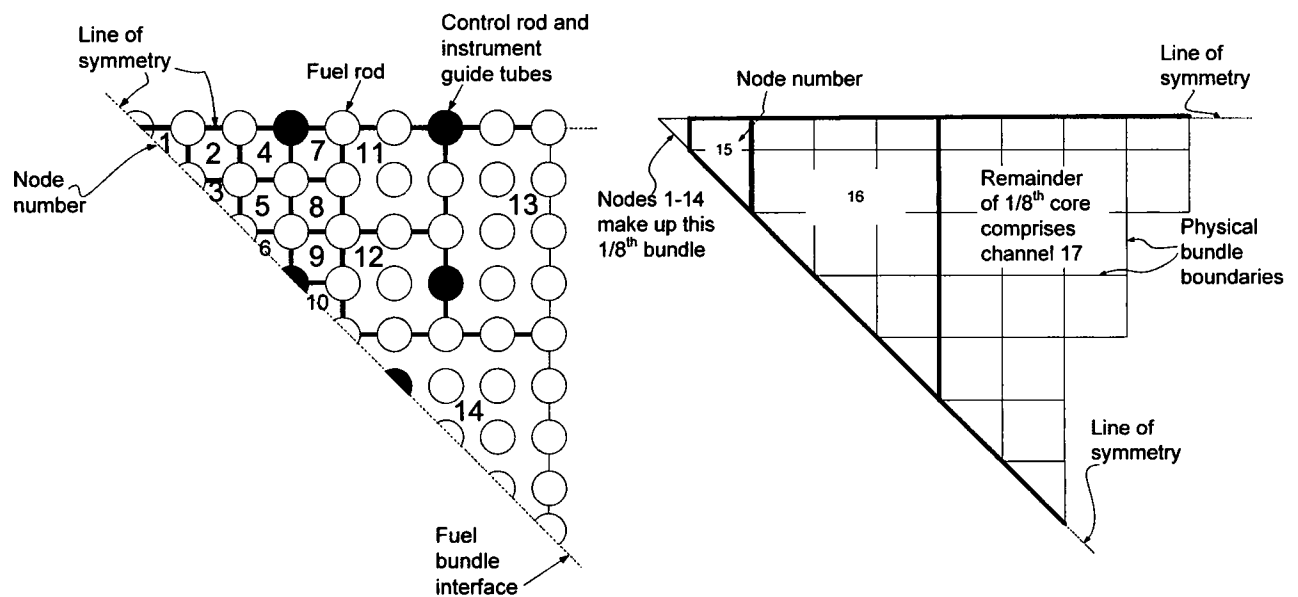
5.7.2 Transient Comparisons with Other Codes

COBRA-FLX predictions are compared to LYNXT predictions for transient DNBR, mass velocity and thermodynamic quality at the MDNBR location in the limiting DNBR channel, as well as their axial variations at several times during the transient. Since the XCOBRA-IIIC code is not approved for transient analysis mode, the COBRA-FLX comparisons are limited to LYNXT. Three transients are used for the comparison.

- 4 pump coastdown transient
- locked rotor transient
- steam line break transient

The 4 pump coastdown and locked rotor transients are evaluated with the 12-channel core model shown in Figure 5-1. The steam line break transient was evaluated using a 17-channel core model for a different reactor design. The radial noding scheme for the 17-channel model is shown in Figure 5-38.

Figure 5-38: Radial Node Scheme for a 17-Channel Model (1/8th Core Symmetry) for the Main Steam Line Break Event



5.7.2.1 4 Pump Coastdown Transient

The COBRA-FLX and LYNXT DNBR predictions for a 4 pump coastdown transient case are shown in Figure 5-39 and Table 5-8 when using the typical code options (e.g., the P solution method for COBRA-FLX and PV solution method for LYNXT and the licensing empirical models). The observed difference in DNBR between the two codes is 0.065.

Figure 5-39: DNBR Comparison for the 12-Channel Model for the 4 Pump Coastdown

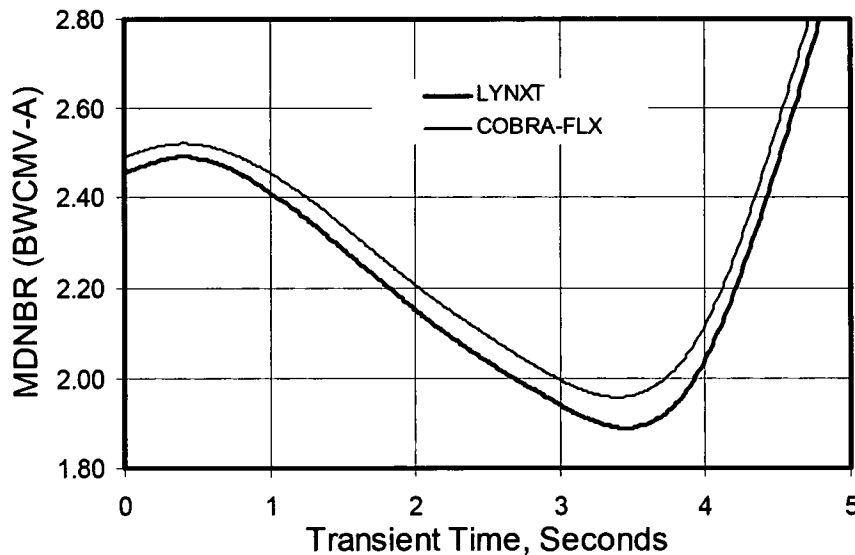


Table 5-8: Summary of DNBR Comparison for the 12-Channel Model for the 4 Pump Coastdown

| Parameter | COBRA-FLX | LYNXT |
|---------------------|-----------|-------|
| MDNBR (BWCMV-A) | 1.958 | 1.890 |
| Time at MDNBR (sec) | 3.40 | 3.43 |

This transient DNBR difference is larger than what was observed for the steady-state comparisons in Section 5.7.1. The local conditions of mass velocity and thermodynamic quality at the time of the minimum DNBR for each code are shown for both codes in Figure 5-40 and Figure 5-41, respectively. The differences observed at the time of the minimum DNBR are representative of the differences observed throughout the transient.

Figure 5-40: Mass Velocity Comparison for the 12-Channel Model for the 4 Pump Coastdown

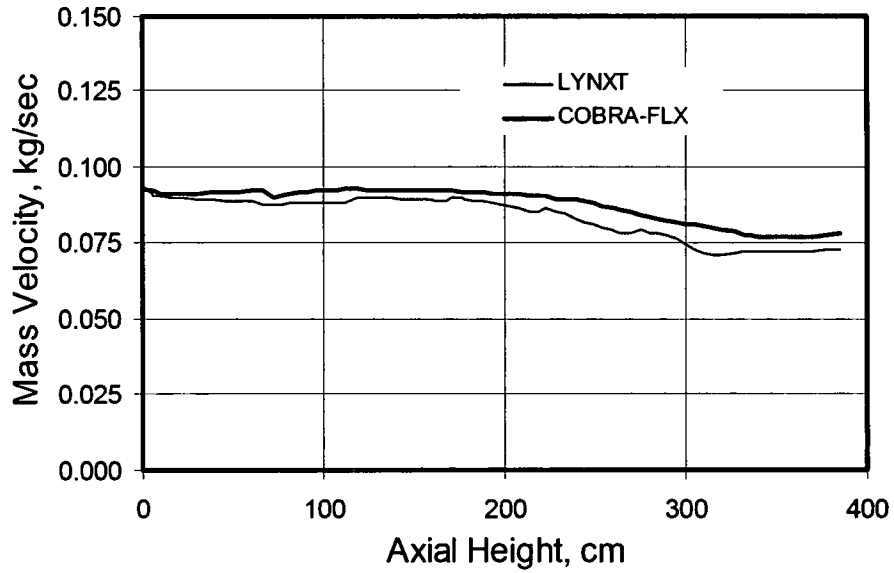
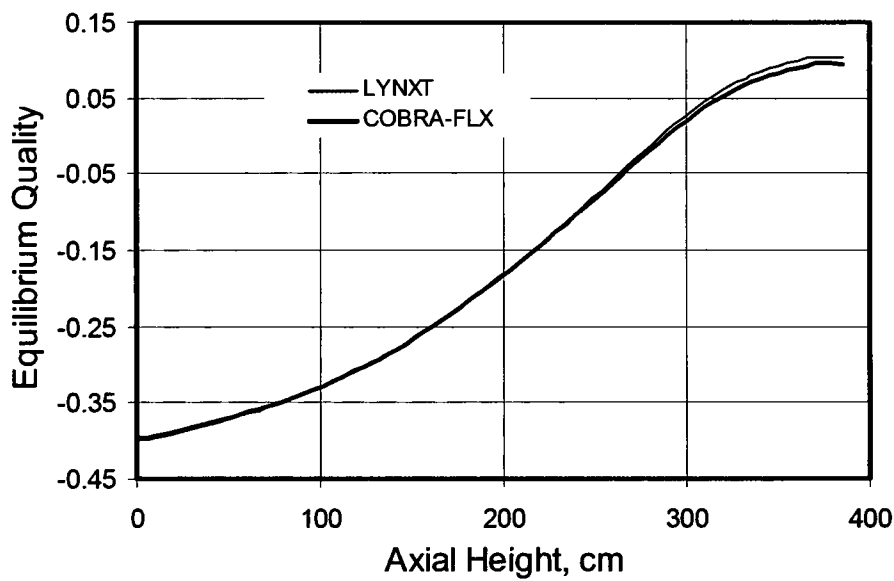


Figure 5-41: Thermodynamic Quality for the 12-Channel Model for the 4 Pump Coastdown



The observed differences between COBRA-FLX and LYNXT were investigated and are attributed to various modeling differences, such as the void fraction models, turbulent momentum factors, and crossflow resistance factor (K_{ij}). A series of COBRA-FLX and LYNXT cases were analyzed. The common starting point, or production cases, was established where both codes analyzed the four pump coastdown event, consistent with the cases in Table 5-8, however, both cases used the PV solution method and an elevated fuel energy deposition factor relative to the value used to support Table 5-8. The acknowledgement of the use of the common solution method and higher energy deposition factor would not affect the conclusions, but rather, only explain why the minimum DNBRs in Table 5-8 are different from those in Table 5-9 for the production case. The investigation showed that the primary attribute for the observed DNB difference is the respective void models for both codes as can be seen in Table 5-9 where both codes utilized the homogeneous void model.

Table 5-9: COBRA-FLX and LYNXT Minimum DNBR Sensitivity to Modeling Parameters for the 4 Pump Coastdown

| | | MDNBR (BWCMV-A) | |
|------------------|--|-----------------|-------|
| Parameter Change | Parameter | COBRA-FLX | LYNXT |
| Individually | Production Case Using the PV Solution Method | 1.899 | 1.846 |
| Individually | Homogenous Void Model for both Codes | 1.920 | 1.922 |
| Individually | Common K_{ij} for both Codes | 1.923 | 1.846 |
| Individually | Common Turbulent Momentum Factor (FTM) | 1.878 | 1.846 |
| Combined | Combined Effect of All Parameters Above | 1.9385 | 1.923 |

The combined effect of using all the noted modeling parameters in Table 5-9 produces DNBR, mass velocity, and thermodynamic quality values that agree well between COBRA-FLX and LYNXT as seen in Figure 5-42, Figure 5-43, and Figure 5-44,

respectively. Therefore, it can be concluded the primary difference in DNBR performance between COBRA-FLX and LYNXT for the 4 pump coastdown is attributed to their respective void models.

Figure 5-42: DNBR Comparison for the Combined Effect of All Modeling Parameters in Table 5-9 for the 4 Pump Coastdown

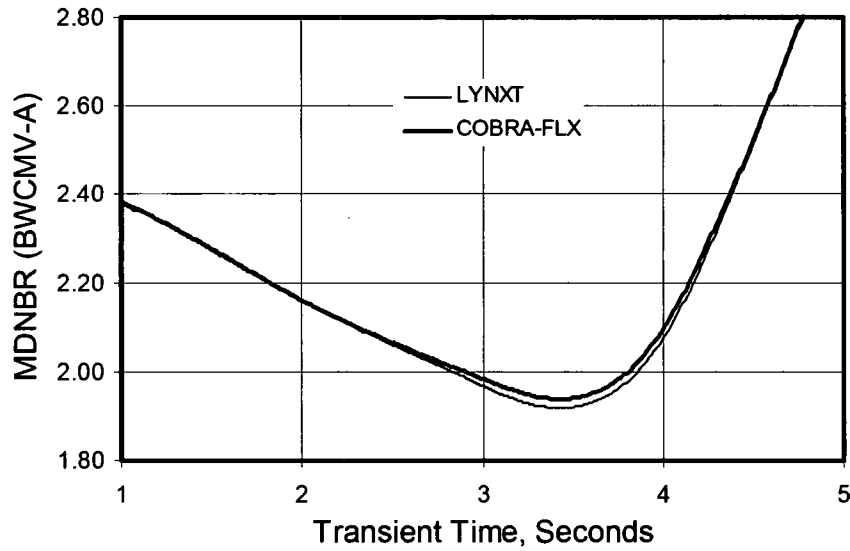


Figure 5-43: Mass Velocity Comparison for the Combined Effect of All Modeling Parameters in Table 5-9 for the 4 Pump Coastdown at the Time of Minimum DNBR

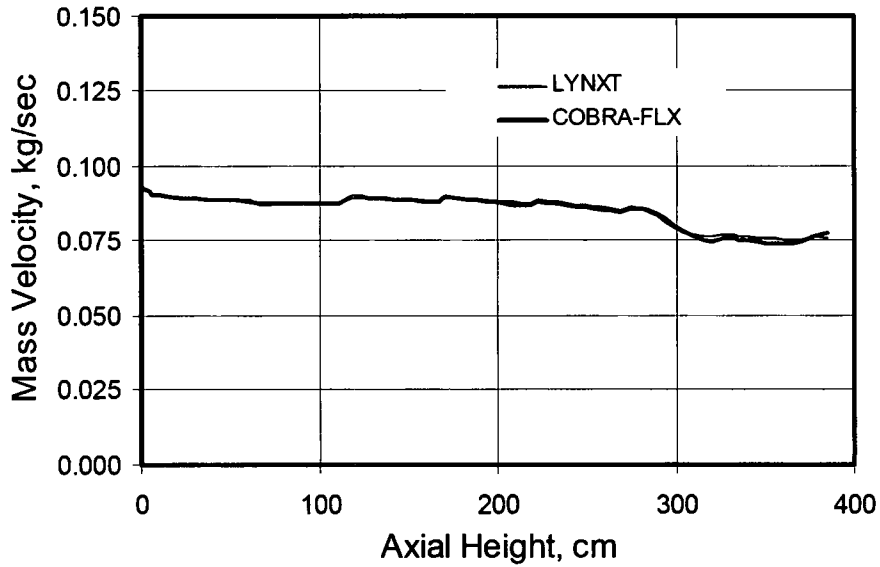
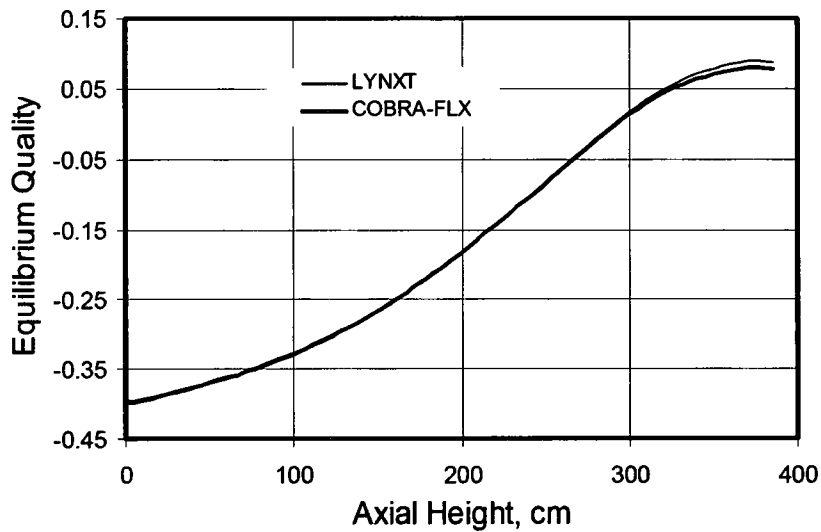


Figure 5-44: Thermodynamic Quality Comparison for the Combined Effect of All Modeling Parameters in Table 5-9 for the 4 Pump Coastdown at the Time of Minimum DNBR



5.7.2.2 Locked Rotor Transient

A locked rotor transient comparison of COBRA-FLX and LYNXT predictions was performed by substituting the earlier 4 pump coastdown forcing function with a locked rotor forcing function. This substitution results in a more abrupt reduction in DNBR as can be seen in Figure 5-45 with a minimum DNBR difference of 0.093 as shown in Table 5-10.

Figure 5-45: DNBR Comparison for the 12-Channel Model for the Locked Rotor

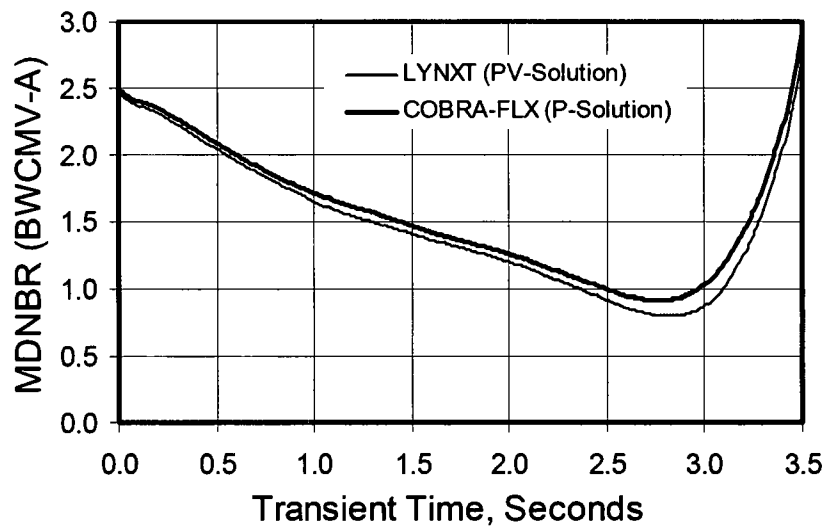


Table 5-10: Summary of DNBR Comparison for the 12-Channel Model for the Locked Rotor

| Parameter | COBRA-FLX | LYNXT |
|---------------------|-----------|-------|
| MDNBR (BWCMV-A) | 0.915 | 0.801 |
| Time at MDNBR (sec) | 2.78 | 2.80 |

Like the 4 pump coastdown transient, the locked rotor transient DNBR difference is larger than what was observed for the steady-state comparisons in Section 5.7.1. The combined effect of using all the noted common modeling parameters in Table 5-9 produces DNBR, mass velocity, and thermodynamic quality values that agree well between COBRA-FLX and LYNXT for the locked rotor event. Table 5-11 shows the good agreement when using all the common parameters in Table 5-9. Therefore, it is concluded the primary difference in DNBR performance between COBRA-FLX and LYNXT for the locked rotor is attributed to their respective void models.

Table 5-11: COBRA-FLX and LYNXT Minimum DNBR Sensitivity to Modeling Parameters for the Locked Rotor

| | | MDNBR (BWCMV-A) | |
|------------------|---|-----------------|-------|
| Parameter Change | Parameter | COBRA-FLX | LYNXT |
| Combined | Combined Effect of All Parameters as in Table 5-9 | 0.944 | 0.918 |

5.7.2.3 Main Steam Line Break Transient

The third transient used to compare the performance between COBRA-FLX and LYNXT is the main steam line break transient. The 17-channel model, shown in Figure 5-38, was used to predict a steady-state condition during the transient. The steady-state condition reflects a large coolant temperature gradient across the core due to the overcooling resulting from the secondary side overcooling of one loop. The PV solution method was used for evaluating the event with both codes. Figure 5-46 shows the COBRA-FLX DNBR behavior versus axial location, at the time of minimum DNBR, matches well with the corresponding LYNXT behavior. The minimum DNBR values also agree well as shown in Table 5-12.

Figure 5-46: DNBR Comparison for the 17-Channel Model for the Main Steam Line Break in the Limiting Subchannel

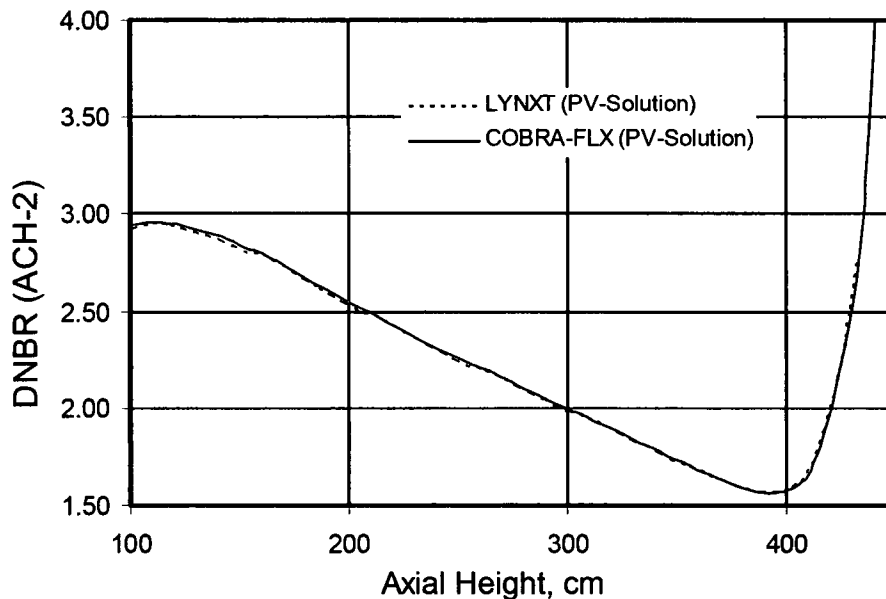


Table 5-12: Summary of DNBR Comparison for the 17-Channel Model for the Main Steam Line Break

| | LYNXT PV-Solution | COBRA-FLX PV-Solution |
|-----------------------------|----------------------|--------------------------|
| MDNBR (ACH-2) | 1.559 | 1.566 |
| Difference in MDNBR | - | -0.007 |
| Axial distance at MDNBR, cm | 395 | 392 |

5.8 Verification and Validation Conclusions

The following conclusions are drawn from the comparative analyses presented in this document:

-
- COBRA-FLX's P and PV numerical solution methods provide acceptable agreement to allow the user the choice of the more suitable method for the analysis application.
 - COBRA-FLX's modeling flexibility to simulate subchannels, groups of subchannels, fuel assemblies, and groups of fuel assemblies within a single model yields consistent results and provides a reliable means to meet the application needs for reload licensing.
 - COBRA-FLX predictions compares reasonably well to NRC-approved codes such as LYNXT and XCOBRA-IIIC, particularly when a common void fraction model is used.
 - Most differences in predictions between COBRA-FLX and LYNXT observed in steady state and transient calculations can be attributed to the fact that COBRA-FLX and LYNXT use different void fraction models. It has been demonstrated that the use of the same void fraction models (homogeneous) and inter-subchannel mass transfer characteristics makes these differences become very small, thereby explaining the differences observed in COBRA-FLX and LYNXT predictions.
 - COBRA-FLX's P and PV solution method has been shown to function as designed for high flow conditions and low flow conditions. The PV solution method has been shown to function as designed for reverse/recirculating flow conditions to support licensing applications.

5.9 *References*

- 5-1 BAW-10156-A, Rev. 1, LYNXT Core Transient Thermal-Hydraulic Program, B&W Fuel Company, August 1993.
- 5-2 BAW-10000A, Correlation of Critical Heat Flux in a Bundle Cooled by Pressurized Water, Babcock & Wilcox, Lynchburg, Virginia, May 1976.
- 5-3 B. W. LeTourneau, S. J. Green, Critical Heat Flux and Pressure Drop Tests with Parallel Upflow of High Pressure Water in Bundles of Twenty ½ in. Rods, Nuclear Science and Engineering, 43, pp.90-104.
- 5-4 BAW-10000, Supplement 1, Correlation of Critical Heat Flux in a Bundle Cooled by Pressurized Water, Supplement 1, Babcock & Wilcox, Lynchburg, Virginia, March 1971.
- 5-5 NUREG/CR-0056, (ANL-78-39), Critical Heat Flux under Transient Conditions: A Literature Survey, Argonne National Laboratory, Argonne, Illinois, June 1978.
- 5-6 Part 50 Appendix K - ECCS Evaluation Models, Chapter 1 – Nuclear Regulatory Commission, Code of Federal Regulations Title 10 – Energy, Office of Federal Register, January 1, 1983.
- 5-7 Letter, J. H. Taylor (B&W) to C. O. Thomas (NRC), Subject: *Request Number Two for Additional Information on BAW-10156*, October 14, 1985.

APPENDIX A: EMPIRICAL CORRELATIONS

A.1 Introduction

The governing equations that are the basis of COBRA-FLX require a series of empirical correlations to complete the necessary system of equations. These empirical correlations serve as a link between some of the governing equations and supply data needed by the governing equations to generate the necessary solutions. Although the Critical Heat Flux (CHF) correlations are empirical equations based on experimental data the description of these correlations is contained in Appendix C of this report.

The various empirical correlations described in Appendix A are:

- water properties
- friction factors (both single- and two-phase)
- void fraction correlation (includes the subcooled boiling inception and subcooled and bulk boiling void fractions)
- heat transfer correlations (includes pre- and post-CHF), and
- the algorithm used for the DNBR iteration scheme.

A.2 Water Properties

The water/steam properties used in COBRA-FLX are based on The International Association for the Properties of Water and Steam (IAPWS) 1997 industrial applications formulation of water and steam properties (IAPWS-IF97) as documented in Reference A-1.

A.3 Friction Factor

The friction factor options are selected using GCC2 in the COBRA-FLX input. The friction factor models selected by the user are the single-phase friction factor and the two-phase multipliers on the single-phase friction factors. The single-phase friction

factor options are described in Section A.3.1 of this appendix and the two-phase options are described in Section A.3.2.

A.3.1 Single-phase Flow

Two basic options are available for the calculation of isothermal friction factors: an input correlation, as described in Section A.3.1.1, and the Lehmann correlation, described in Section A.3.1.2. An adjustment factor for entrance effects is described in Section A.3.1.3. Section A.3.1.4 describes the friction factor adjustments made for low flow situations using the PV algorithm. A wall viscosity correction to the single-phase friction factor is described in Section A.3.1.5.

A.3.1.1 Single-phase Flow

An input friction factor may assume the following form:

$$f_{\text{turb/iso}} = aRe_i^b + c \quad \text{A-1}$$

Since these constants can be influenced by the channel roughness and the channel geometry, up to four different sets of constants that correspond to four different channel types, may be input. In the laminar region the isothermal laminar flow friction factor is defined as follows:

$$f_{\text{lam/iso}} = \frac{64}{Re_i} \quad \text{A-2}$$

A.3.1.2 Lehmann Correlation

As an alternative to the input of the constants in Equation A-1 the correlation of Lehmann, in Reference A-2, may be selected to describe the influence of the surface roughness and of the Reynolds number on the friction factor. Lehmann's correlation has the following form:

$$\frac{l}{\sqrt{f_{turb/iso}}} = -1.94 \log \left[\left(\frac{4.26}{Re_i \sqrt{f_{turb/iso}}} \right)^{1.1} + \left(\frac{\frac{\varepsilon}{D_e}}{3.715} \right)^{1.03} \right] \quad \text{A-3}$$

A.3.1.3 Entrance Effect

In conjunction with the Lehmann correlation there is an option which takes the influence of the entrance effect on the friction factor into account. It is assumed, that the turbulent flow starts developing at each spacer position. The corresponding increase of the friction factor compared to the fully developed friction factor (Lehmann correlation) is calculated according to the method of Szablewski in Reference A-3.

$$f_{RXD} = f_{turb/iso(\text{from Lehmann})} \text{RXD} \left(Re_i, \frac{X_{DG}}{D_e} \right) \quad \text{A-4}$$

The derivation of the Szablewski function in Reference A-3 is shown in Table A-1. The Szablewski function (RXD) exhibits pronounced dependence on the relative entrance length but a weak dependence on the Reynolds number. After 50 X_{DG}/D_e the fully developed region has been reached.

Table A-1: The Szablewski Function RXD as a Function of Relative Entrance Length

| Relative Entrance Length | Szablewski Function RXD | |
|--------------------------|-------------------------|---------|
| | Reynolds Number | |
| X_{DG}/D_e | 100,000 | 500,000 |
| 0.5 | 1.92 | 1.84 |
| 1.0 | 1.70 | 1.60 |
| 5.0 | 1.20 | 1.21 |
| 20.0 | 1.06 | 1.00 |
| 50.0 | 1.00 | 1.00 |

A.3.1.4 Transition from Turbulent Flow to Laminar Flow for the Pressure-Velocity (PV) Solution

In order to satisfy the continuity condition of the friction factor during the transition from turbulent flow to laminar flow, the following procedure is used for the PV solution:

$$f_{PV/iso} = \max(f_{lam/iso}, f_{turb/iso}) \quad A-5$$

where

$f_{PV/iso}$ = isothermal friction factor for the PV algorithm .

The turbulent isothermal friction factors are obtained from Equation A-1 and the equations in Sections A.3.1.2 through A.3.1.3. The laminar isothermal friction factor is from Equation A-2.

A.3.1.5 Wall Viscosity Correction

The isothermal friction factor may be corrected for wall viscosity using the following relationship, in Reference A-4 is as follows:

$$\frac{f}{f_{iso}} = 1 + \frac{P_h}{P_w} \left[\left(\frac{\mu_{wall}}{\mu_{bulk}} \right)^{0.6} - 1 \right] \quad \text{A-6}$$

The wall temperature is calculated from:

$$T_{wall} = T_{bulk} + \frac{q''}{P_h h_{bulk}} \quad \text{A-7}$$

The single phase heat transfer coefficient is calculated from:

$$h_{bulk} = 0.134 Re_i^{0.65} Pr_i^{0.4} \frac{k_i}{D_e} \quad \text{A-8}$$

A.3.2 Two-phase Flow

In two-phase flow, the friction factor is calculated by multiplying the single phase friction factor calculated using the process defined in Section A.3.1 by the two-phase friction multiplier Φ . Several correlations are available for the two-phase friction multiplier. Five are presently included in COBRA-FLX. Section A.3.2.1 describes the homogeneous model. Section A.3.2.2 describes the Armand model from Reference A-5. Section A.3.2.3 describes the Baroczy model of Reference A-6. Section A.3.2.4 describes the Martinelli-Nelson-Jones model of Reference A-7. Section A.3.2.5 describes the polynomial function model.

A.3.2.1 Homogeneous Model

$$\Phi = 1.0 \quad x \leq 0. \quad \text{A-9}$$

$$\Phi = \frac{\rho_f}{\rho_{mixture}} \quad x > 0$$

A.3.2.2 Armand Model

$$\Phi = 1.0 \quad \alpha \leq 0 \quad \text{A-10}$$

$$\Phi = \frac{(1-x)^2}{(1-\alpha)^{1.42}} \quad 0 < \alpha \leq 0.6$$

$$\Phi = \frac{0.478(1-x)^2}{(1-\alpha)^{2.2}} \quad 0.6 < \alpha \leq 0.9$$

$$\Phi = \frac{1.73(1-x)^2}{(1-\alpha)^{1.64}} \quad 0.9 < \alpha < 1.0$$

A.3.2.3 Baroczy Model

$$\Phi = 1.0 \quad \alpha \leq 0 \quad \text{A-11}$$

$$\Phi = \Phi_{lo}^2 \Omega \quad 0 < \alpha < 1.0$$

The two phase multiplier Φ_{lo}^2 is determined at different qualities x as function of the property index PI :

$$PI = \frac{\rho_g}{\rho_f} \left(\frac{\mu_f}{\mu_g} \right)^{0.2} \quad \text{A-12}$$

for a constant mass velocity $G = 1356 \text{ kg}/(\text{m}^2\text{s})$. For any other mass velocity a correction factor Ω is determined, which is a function of the mass velocity G and the property index PI . The functions $\Phi_{lo}^2(x, PI)$ and $\Omega(G, PI)$ are present in tabular form. Actual values are determined by linear interpolation.

A.3.2.4 Martinelli-Nelson-Jones Model

$$\Phi = 1.0 \quad x \leq 0 \quad \text{A-13}$$

$$\Phi = 1.0 + F(G_E, P_E) \left\{ 1.2 \left[\frac{\rho_f}{\rho_g} - 1 \right] x^{0.824} \right\} \quad x > 0$$

The functional relationship of $F(G_E, p_E)$ is as follows, where all the parameters use

British units:

$$F(G_E, p_E) = 1.36 + 0.0005 p_E + 0.1 G_E - 0.000714 p_E G_E \quad G \leq 0.7 \quad \text{A-14}$$

$$F(G_E, p_E) = 1.26 + 0.0004 p_E + \frac{0.119}{G_E} - 0.0002814 \frac{p_E}{G_E} \quad G > 0.7$$

A.3.2.5 Polynomial Function in Quality

$$\Phi = 1.0 \quad x \leq 0. \quad \text{A-15}$$

$$\Phi = a_{\phi,0} + a_{\phi,1}x + a_{\phi,2}x^2 + \dots + a_{\phi,n}x^n \quad x > 0.$$

Up to seven coefficients ($n \leq 6$) are to be supplied as input.

A.4 Void Fraction Correlation

The determination of the void fraction in COBRA-FLX is performed using various empirical models, in both the bulk and subcooled boiling regimes. COBRA-FLX's various bulk boiling void fraction models are described in Section A.4.1. The various subcooled boiling void fraction models are described in Section A.4.2.

A.4.1 Bulk Void

COBRA-FLX has eight options for specifying the bulk void fraction using GCC2's N2. The following sections describe the various bulk void fraction models:

- Section A.4.1.1 – Read in slip ratio model
- Section A.4.1.2 – Homogeneous model
- Section A.4.1.3 – Smith slip ratio model
- Section A.4.1.4 – Polynomial function in quality model
- Section A.4.1.5 – Modified Armand model
- Section A.4.1.6 – Zuber-Findlay model
- Section A.4.1.7 – Chexal-Lellouche model

- Section A.4.1.8 – Chexal-Lellouche model using tables.

A.4.1.1 Read in Slip Ratio

This is the fundamental void-quality relation, as described, for example, in Reference A-8.

$$\alpha = 0.0 \quad x \leq 0. \quad \text{A-16}$$

$$\alpha = \frac{x}{(1-x)S \frac{\rho_g}{\rho_f} + x} \quad x > 0.$$

The slip ratio S is a user-supplied input in G2-2.

A.4.1.2 Homogeneous Model

The slip ratio, S, of the homogeneous void-quality relation is set internally to 1.0.

$$\alpha = 0.0 \quad x \leq 0. \quad \text{A-17}$$

$$\alpha = \frac{x}{(1-x) \frac{\rho_g}{\rho_f} + x} \quad x > 0.$$

A.4.1.3 Smith Slip Ratio Correlation

The slip ratio is calculated according to the correlation given in Reference A-9.

$$\alpha = 0.0 \quad x \leq 0. \quad \text{A-18}$$

$$\alpha = \frac{x}{(1-x)S \frac{\rho_g}{\rho_f} + x} \quad x > 0$$

$$S = 0.4 + 0.6 \left[\frac{0.4 + \left(\frac{\rho_f}{\rho_g} - 0.4 \right) x}{0.4 + 0.6x} \right]^{\frac{1}{2}} \quad \text{A-19}$$

A.4.1.4 Polynomial Function in Quality

Up to seven coefficients, a_n ($0 \leq n \leq 6$) are supplied by the user.

$$\begin{aligned} \alpha &= 0.0 & x &\leq 0. & \text{A-20} \\ \alpha &= a_0 + a_1x + a_2x^2 + \dots + a_nx^n & x &> 0. \end{aligned}$$

A.4.1.5 Modified Armand Model

This is the Armand void correlation, from Reference A-5, as modified by Massena in Reference A-10.

$$\begin{aligned} \alpha &= 0.0 & x &\leq 0. & \text{A-21} \\ \alpha &= \frac{(0.833 + 0.167x)x}{(1-x)\frac{\rho_g}{\rho_f} + x} & x &> 0. \end{aligned}$$

A.4.1.6 Zuber-Findlay Model

This is the generalized drift-flux formula, as derived by Zuber and Findlay in Reference A-11. The vapor void fraction α is given by an algebraic relation that involves the following two parameters:

- the Zuber-Findlay concentration parameter C_0 , and
- the drift velocity parameter V_{gi}

The void fraction is

$$\alpha = \frac{j_g}{C_0(j_g + j_f) + V_{gj}} \quad \text{A-22}$$

where j_g and j_f are the vapor and liquid volumetric flux for void fraction calculations, respectively, given by

$$j_g = \alpha U_g = \frac{x G}{\rho_g} \quad \text{and} \quad j_f = (1 - \alpha) U_f = \frac{(1 - x) G}{\rho_f} \quad \text{A-23}$$

The concentration parameter is $C_0 = \min(C_{01}, C_{02})$ where

$$C_{01} = \left(1.2 - 0.2 \sqrt{\frac{\rho_g}{\rho_f}} \right) (1 - \exp(-18\alpha)) \quad \text{A-24}$$

and

$$C_{02} = \left(1.0 + 0.2 \sqrt{\frac{\rho_g}{\rho_f}} \right) \left(1 - \left(\frac{\alpha - \alpha_0}{1 - \alpha_0} \right)^2 \right) \quad \text{A-25}$$

and

$$\alpha_0 = A_0 + A_1 \left(\sqrt{\frac{\rho_g}{\rho_f}} \right) + A_2 \left(\sqrt{\frac{\rho_g}{\rho_f}} \right)^2 + A_3 \left(\sqrt{\frac{\rho_g}{\rho_f}} \right)^3 \quad \text{A-26}$$

The constants in the Equation A-26 are as follows:

$$A_0 = 0.5881164, \quad A_1 = -1.81701, \quad A_2 = 2.00025 \quad \text{and} \quad A_3 = -3.34398.$$

For $\alpha < \alpha_0$ is $C_0 = C_{01}$.

The drift velocity is given by $V_{gi} = \min(V_{gi1}, V_{gi2})$ where

$$V_{gj1} = 2.9 \left(\frac{\rho_f - \rho_g}{\rho_f^2} \sigma g \right)^{\frac{1}{4}} \quad \text{and} \quad V_{gj2} = \frac{Y}{2.9} \left(1 - \left(\frac{\alpha - \alpha_0}{1 - \alpha_0} \right)^2 \right) \quad \text{A-27}$$

where

$$Y = \max(Y_1, 3.136) \quad \text{A-28}$$

$$Y_1 = b_0 + b_1 \left(\sqrt{\frac{\rho_g}{\rho_f}} \right) + b_2 \left(\sqrt{\frac{\rho_g}{\rho_f}} \right)^2 + b_3 \left(\sqrt{\frac{\rho_g}{\rho_f}} \right)^3 + b_4 \left(\sqrt{\frac{\rho_g}{\rho_f}} \right)^4 + b_5 \left(\sqrt{\frac{\rho_g}{\rho_f}} \right)^5 + b_6 \left(\sqrt{\frac{\rho_g}{\rho_f}} \right)^6$$

The constants in Equation A-28 are as follows:

$$b_0 = 4.72085, \quad b_1 = -17.26736, \quad b_2 = 56.14883, \quad b_3 = 113.21605, \quad b_4 = -1250.603, \\ b_5 = 3039.7669, \quad b_6 = -2431.8228$$

For $\alpha < 0$ is $V_{gj} = V_{gj1}$.

As this system of equations is an implicit one for the void fraction, α , an iterative procedure has been applied to calculate α .

A.4.1.7 Chexal-Lellouche Model

The Chexal-Lellouche void correlation, from Reference A-12, was developed to cover the full range of pressures, flows, void fractions and flow rates for different types of coolants (steam-water, air-water, hydrocarbons and oxygen). The correlation is qualified against several sets of steady-state two-phase/two-component flow test data that cover a wide range of thermodynamic conditions and geometries typical of PWR and BWR fuel assemblies. The correlation is based on a drift flux model and describes the drift flux parameters C_0 and V_{gj} . The key parts of the correlation are explained in the following, a full description is given in the original reference.

The void fraction α is calculated by the drift flux formula

$$\alpha = \frac{j_g}{C_0(j_f + j_g) + V_{gj}} \quad \text{A-29}$$

The volumetric fluxes used in Equation A-29 are consistent with the quality-based volumetric fluxes defined in Equation A-23. When the Equation A-23 quality-based definitions are substituted into Equation A-29 the following equation for the drift flux Chexal-Lellouche void fraction model is obtained:

$$\alpha = \frac{x}{C_0 \left(x + (1-x) \frac{\rho_g}{\rho_f} \right) + \frac{V_{gj} \rho_g}{G}} \quad \text{A-30}$$

The distribution parameter, C_0 , used in Equation A-30 is defined as follows:

$$C_0 = F_r C_{0v} + (1 - F_r) C_{0h} \quad \text{A-31}$$

where

$$F_r = \frac{90^\circ - \theta}{90^\circ} \quad \text{A-32}$$

In Equation A-32 θ is the flow orientation angle measured from the vertical axis ($0^\circ \leq \theta \leq 90^\circ$). The vertical flow distribution parameter, C_{0v} , is defined as follows:

$$C_{0v} = \frac{L}{K_0 + (1 - K_0) \alpha^r} \quad \text{A-33}$$

where the various parameters required for Equation A-33 are defined as follows:

$$L = \frac{1 - \exp(-C_1 \alpha)}{1 - \exp(-C_1)} \quad \text{A-34}$$

$$K_0 = B_1 + (1 - B_1) \left(\frac{\rho_g}{\rho_f} \right)^{1/4} \quad \text{A-35}$$

$$r = \frac{1 + 1.57 \left(\frac{\rho_g}{\rho_f} \right)}{1 - B_1} \quad \text{A-36}$$

The following additional parameters are required to generate the Chexal-Lellouche void fraction predictions:

$$C_1 = 4 \frac{p_{crit}^2}{p(p_{crit} - p)} \quad \text{A-37}$$

$$B_1 = \min(0.8, A_1) \quad \text{A-38}$$

$$A_1 = \frac{1}{1 + \exp\left(-\frac{Re}{60000}\right)} \quad \text{A-39}$$

The Reynolds Number in Equation A-39 is defined as follows:

$$Re = \begin{cases} Re_g & \text{if } Re_g > Re_f \\ Re_f & \text{if } Re_g \leq Re_f \end{cases} \quad \text{A-40}$$

where the local liquid and vapor Reynolds Numbers are defined as follows:

$$Re_f = \frac{j_f \rho_f D_e}{\mu_f} \quad \text{A-41}$$

$$Re_g = \frac{j_g \rho_g D_e}{\mu_g}$$

The drift velocity parameter, V_{gj} , used in Equations A-29 and A-30 are defined as

follows:

$$V_{gj} = V_{gj,0} C_2 C_3 C_4 C_9 \quad \text{A-42}$$

where

$$V_{gj,0} = 1.41 \left[\frac{(\rho_f - \rho_g) \sigma g_c}{\rho_f^2} \right]^{0.25} \quad \text{A-43}$$

$$C_2 = 0.4757 (\ln(\rho_f / \rho_g))^{0.7} \quad \text{for } (\rho_f / \rho_g) \leq 18 \quad \text{A-44}$$

$$C_2 = \begin{cases} 1 & \text{if } C_5 \geq 1 \\ 1/(1 - \exp(-C_5/(1 - C_5))) & \text{if } C_5 < 1 \end{cases} \quad \text{for } (\rho_f / \rho_g) > 18$$

$$C_3 = \max(0.5, 2 \exp(-|Re_f|/60000))$$

$$C_4 = \begin{cases} 1 & \text{if } C_7 \geq 1 \\ 1/(1 - \exp(-C_8)) & \text{if } C_7 < 1 \end{cases}$$

$$C_5 = \sqrt{150/(\rho_f / \rho_g)}$$

$$C_7 = (d_2 / D_e)^{0.6}$$

$$C_8 = C_7 / (1 - C_7)$$

$$C_9 = (1 - \alpha)^{B_1}$$

and d_2 is the normalizing parameter

$$d_2 = 0.09144 \text{ m} \quad \text{A-45}$$

Two important observations on the Chexal-Lellouche void fraction correlation are as follows:

- There are many calculations including exponential functions, power functions and logarithmic functions being evaluated in the process of obtaining the void fraction α . As these calculations are executed up to several million times in a full

core subchannel-by-subchannel calculation, the execution time contributes considerably to the total runtime of a COBRA-FLX calculation.

- Additionally this void correlation is an implicit correlation. The two drift flux parameters C_0 and V_{gj} , as defined in Equations A-31 and A-42, respectively, depend on void fraction α , as L and C_9 , as defined in Equations A-34 and A-44, respectively, are functions of α . Therefore an iterative procedure is needed, resulting in an increased runtime.

Two approaches are available in COBRA-FLX for generating void fractions using the Chexal-Lellouche void fraction model:

- In the first approach the full set of equations is used in an iterative procedure, as described above.
- In the second approach interpolation tables are applied which are based on the data having used the full set of equations. This approach is described in Section A.4.1.8.

To minimize the code execution time the variables to be calculated are sorted into three classes:

- Variables, which depend only on the system pressure or orientation of the channel: $C_1, C_2, C_5, C_6, V_{gj,0}, F_r$. These variables are calculated only once in subroutine PROP ($C_1, C_2, C_5, C_6, V_{gj,0}$) and subroutine INDAT (F_r).
- Variables, which depend on the local coolant conditions or the local channel geometry but not on α : $j_g, j_f, Re_g, Re_f, Re, A_1, B_1, K_0, r, C_3, C_4, C_7, C_8$. These variables are calculated each time the Chexal-Lellouche subroutine VOID_CHEXAL is called.

- Variables, which depend on α : C_0, V_{gj}, α . These variables are recalculated in an iterative loop in subroutine VOID_CHEXAL.

The iteration starts with a first guess applying the homogeneous void correlation, from Equation A-17:

$$\alpha_1 = \frac{x}{(1-x)\frac{\rho_g}{\rho_f} + x} \quad \text{A-46}$$

This α_1 is used to calculate a new $\alpha_2 = f(j_g, j_f, C_0, V_{gj}, \alpha_1)$ applying the Chexal-Lellouche drift-flux formula (Equation A-42). A relaxation formula is applied to get an updated α_3 :

$$\alpha_3 = \omega \alpha_2 + (1-\omega) \alpha_1 \quad \text{A-47}$$

As the sensitivity $\partial\alpha/\partial x$ depends on x and G , the relaxation factor ω is a function of x and G as follows:

$$\omega = \begin{cases} 0.5 & \text{if } x < 0.1 \\ \left\{ \begin{array}{l} 0.5 \\ 1.5 \end{array} \right\} & \text{if } x \geq 0.1 \end{cases} \quad \text{A-48}$$

The iteration continues until $|\alpha_n - \alpha_{n-1}| < 0.00001$ is obtained.

A.4.1.8 Chexal-Lellouche Model Using Tables

By equating the void fraction α calculated by the classical slip ratio relationship according to Section A.4.1.1

$$\alpha = \frac{x}{x + S(1-x)\frac{\rho_g}{\rho_f}} \quad \text{A-49}$$

and the void fraction α calculated by the Chexal-Lellouche formula according to Section A.4.1.7

$$\alpha = \frac{x}{C_0 \left(x + (1-x)\frac{\rho_g}{\rho_f} \right) + \frac{V_{gj}\rho_g}{G}} \quad \text{A-50}$$

then solving for the slip S yields the following:

$$S = C_0 + \frac{x(C_0 - 1)\rho_f}{\rho_g(1-x)} + \frac{V_{gj}\rho_f}{G(1-x)} \quad \text{A-51}$$

A set of slip values is calculated and tabulated as function of three parameters:

- Parameter 1 is the ratio of the volumetric flow rates (VFR) defined as follows:

$$VFR = \frac{x\rho_f}{(1-x)\rho_g} \quad \text{A-52}$$

- Parameter 2 is a property index (PI) defined as follows (consistent with Equation A-12):

$$PI = \frac{\rho_g}{\rho_f} \left(\frac{\mu_f}{\mu_g} \right)^{0.2} \quad \text{A-53}$$

- Parameter 3 is the mass flux, which is defined as follows:

$$G = \frac{\dot{m}}{A} \quad \text{A-54}$$

The values of the natural logarithm of S are stored in a three-dimensional array SR(6,6,9) for six values of the natural logarithm of the parameter mass flux G , six values of the natural logarithm of the parameter “ratio of the volumetric flow rates” VFR and nine values of the natural logarithm of the parameter “property index” PI . The actual natural logarithm of S is evaluated by interpolation/extrapolation of the data of array SR. The actual void fraction α is then calculated from the drift flux formula given above.

A.4.2 Subcooled Void

Subcooled boiling is characterized by correlations for the subcooled boiling initiation and by correlations for the profile fit. This is a classical approach, as described in Reference A-8. COBRA-FLX’s various subcooled boiling initiation and the profile-fit models are described in Sections A.4.2.1 and A.4.2.2, respectively.

A.4.2.1 Subcooled Boiling Initiation

Three different correlations for the subcooled boiling initiation are currently available in COBRA-FLX. Complete suppression of subcooled boiling is also an option. These correlations generate the quality x_d at which bubble departure occurs. The various correlations are: Levy (Section A.4.2.1.1), Saha-Zuber (Section A.4.2.1.2), and a modified Saha-Zuber (Section A.4.2.1.3).

A.4.2.1.1 Levy Correlation

The Levy subcooled boiling initiation model is described in Reference A-13. Levy’s quality at bubble departure is defined as follows:

$$x_d = -\frac{c_{p,i} \Delta T_L}{h_{fg}}$$

A-55

where

$$\Delta T_L = \frac{q''}{h} - QPr_i Y_b \quad 0 < Y_b \leq 5 \quad \text{A-56}$$

$$\Delta T_L = \frac{q''}{h} - 5Q \left[Pr_i + \ln \left(1 + Pr_i \left(\frac{Y_b}{5} - 1 \right) \right) \right] \quad 5 < Y_b \leq 30$$

$$\Delta T_L = \frac{q''}{h} - 5Q \left[Pr_i + \ln(1 + 5Pr_i) + 0.5 \ln \left(\frac{Y_b}{30} \right) \right] \quad Y_b > 30$$

The various additional variables used in Equations A-55 and A-56 are defined as follows:

$$h = 0.023 Re_i^{0.8} Pr_i^{0.4} \frac{k_i}{D_e} \quad \text{A-57}$$

$$Q = \frac{q''}{\rho_f c_{p,i} \left(\frac{\tau_w}{\rho_f} \right)^{0.5}} \quad \text{A-58}$$

$$\tau_w = \frac{fG^2}{8\rho_f} \quad \text{A-59}$$

$$Y_b = \frac{0.015}{\mu} (\sigma D_e \rho_f)^{0.5} \quad \text{A-60}$$

A.4.2.1.2 Saha-Zuber Correlation

The Saha-Zuber subcooled boiling initiation model is described in Reference A-14.

Saha-Zuber's quality at bubble departure is defined as follows:

$$x_d^{SZ} = \begin{cases} \frac{-0.0022 \frac{q'' D_e c_{p,i}}{k_i}}{h_{fg}} & \text{for } Pe < 70000 \\ \frac{-154 \frac{q''}{G}}{h_{fg}} & \text{for } Pe \geq 70000 \end{cases} \quad \text{A-61}$$

A.4.2.1.3 Modified Saha-Zuber Correlation

The modified Saha-Zuber correlation for subcooled boiling initiation allows better agreement between COBRA-FLX and other subchannel codes in use in Europe. In conjunction with the modified Saha-Zuber subcooled boiling initiation correlation, a modification of the Zuber-Staub profile fit is used, as defined in Section A.4.2.2.4.

The modified Saha-Zuber subcooled boiling initiation correlation is based on the Saha-Zuber subcooled boiling initiation correlation defined in Section A.4.2.1.2 and is defined as follows:

$$[\hspace{15em}] \quad \text{A-62}$$

The modified Saha-Zuber subcooled boiling initiation correlation requires an additional parameter which is defined as follows:

$$[\hspace{15em}] \quad \text{A-63}$$

A.4.2.2 Profile-fit Model

The profile-fit model correlates the flowing quality x and the equilibrium quality x_e

$$x_e = \frac{h - h_f}{h_{fg}}$$

A-64

via an equation, which is applied for [], which are defined in Section A.4.2.1. The flowing quality is then used on one of the void fraction models defined in Section A.4.1. There four different profile fits are currently available in COBRA-FLX are as follows:

- Section A.4.2.2.1 – Levy profile-fit model
- Section A.4.2.2.2 – Zuber-Staub profile-fit model
- Section A.4.2.2.3 – Saha-Zuber profile-fit model
- Section A.4.2.2.4 – Modified Zuber-Staub profile-fit model

A.4.2.2.1 Levy Profile-fit Model

The Levy profile-fit model is described in Reference A-13. The model is defined as follows:

$$x = x_e - x_d e^{\left(\frac{x_e - 1}{x_d}\right)}$$

A-65

A.4.2.2.2 Zuber-Staub Profile-fit Model

The Zuber-Staub profile-fit model is described in Reference A-15. The model is defined as follows:

$$x = x_e - x_d \left[1 - \tanh\left(1 - \frac{x_e}{x_d}\right) \right]$$

A-66

A.4.2.2.3 Saha-Zuber profile-fit Model

The Saha-Zuber profile-fit model is described in Reference A-14. The model is defined as follows:

$$x = \frac{x_e - x_d e^{\left(\frac{x_e-1}{x_d}\right)}}{1 - x_d e^{\left(\frac{x_e-1}{x_d}\right)}} \tag{A-67}$$

A.4.2.2.4 Modified Zuber-Staub Profile-fit Model

The Zuber-Staub profile fit, as defined in Equation A-66, is used to generate profile fits for the [

] from Equations A-62 and A-63, respectively). The two profile fits are as follows:

$$\left[\right] \tag{A-68}$$

$$\left[\right] \tag{A-69}$$

[] obtain the final flowing quality for use in Section A.4.1 void fraction models, x_{final} , as follows:

$$\left[\right] \tag{A-70}$$

[], is defined as follows:

$$\left[\right] \tag{A-71}$$

A.5 *Heat Transfer Coefficients*

COBRA-FLX's heat transfer module is based on the module developed by Bjornard and Griffith in Reference A-16 as modified by Jackson and Todreas (in Appendix E of Reference A-17). The flowchart for the heat transfer module is shown in Figure A-1. The variables used in Figure A-1 are defined in Table A-2.

Figure A-1: COBRA-FLX's Heat Transfer Selection Logic Flowchart

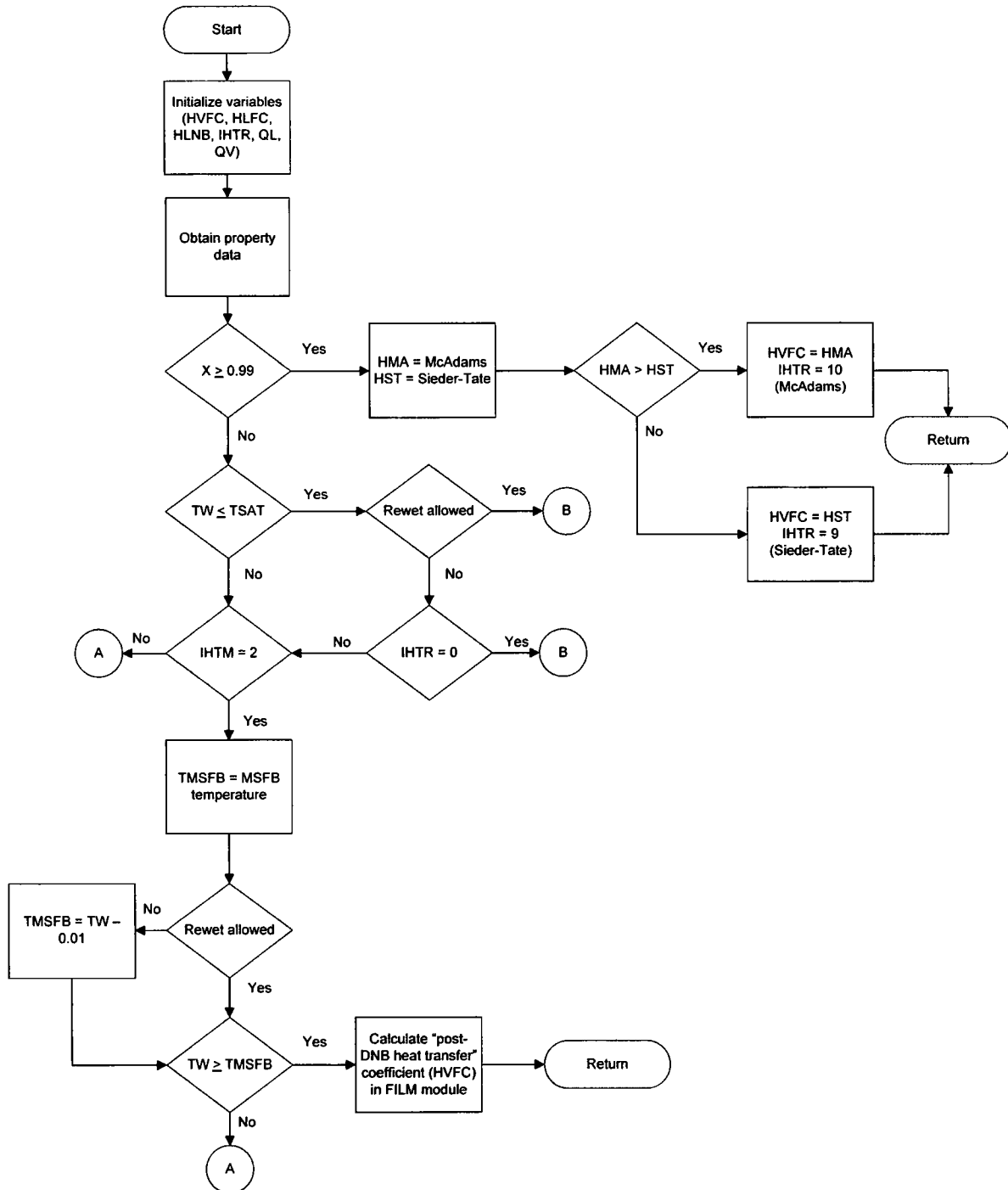


Figure A-1: COBRA-FLX's Heat Transfer Selection Logic Flowchart (continued)

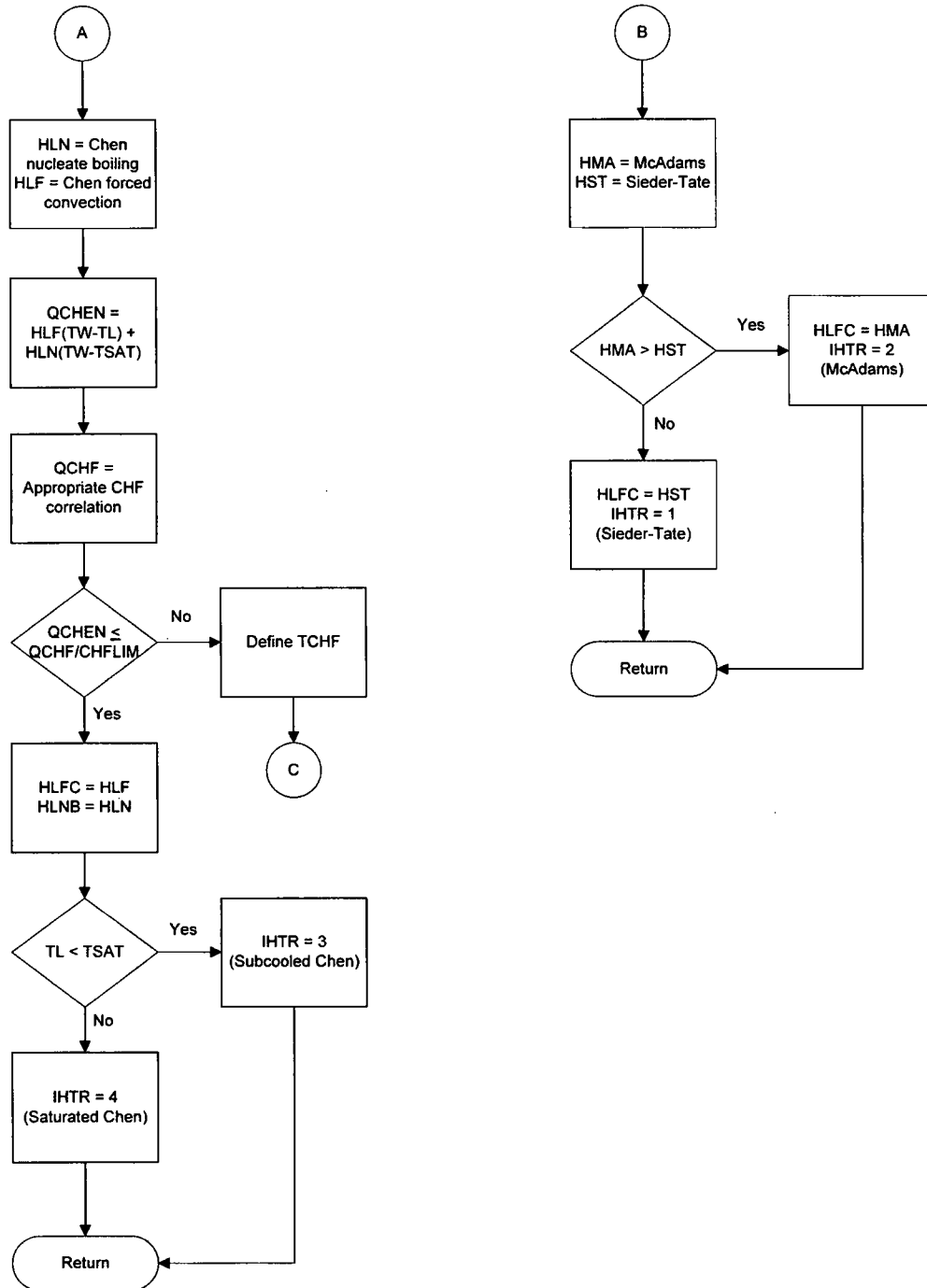


Figure A-1: COBRA-FLX's Heat Transfer Selection Logic Flowchart (continued)

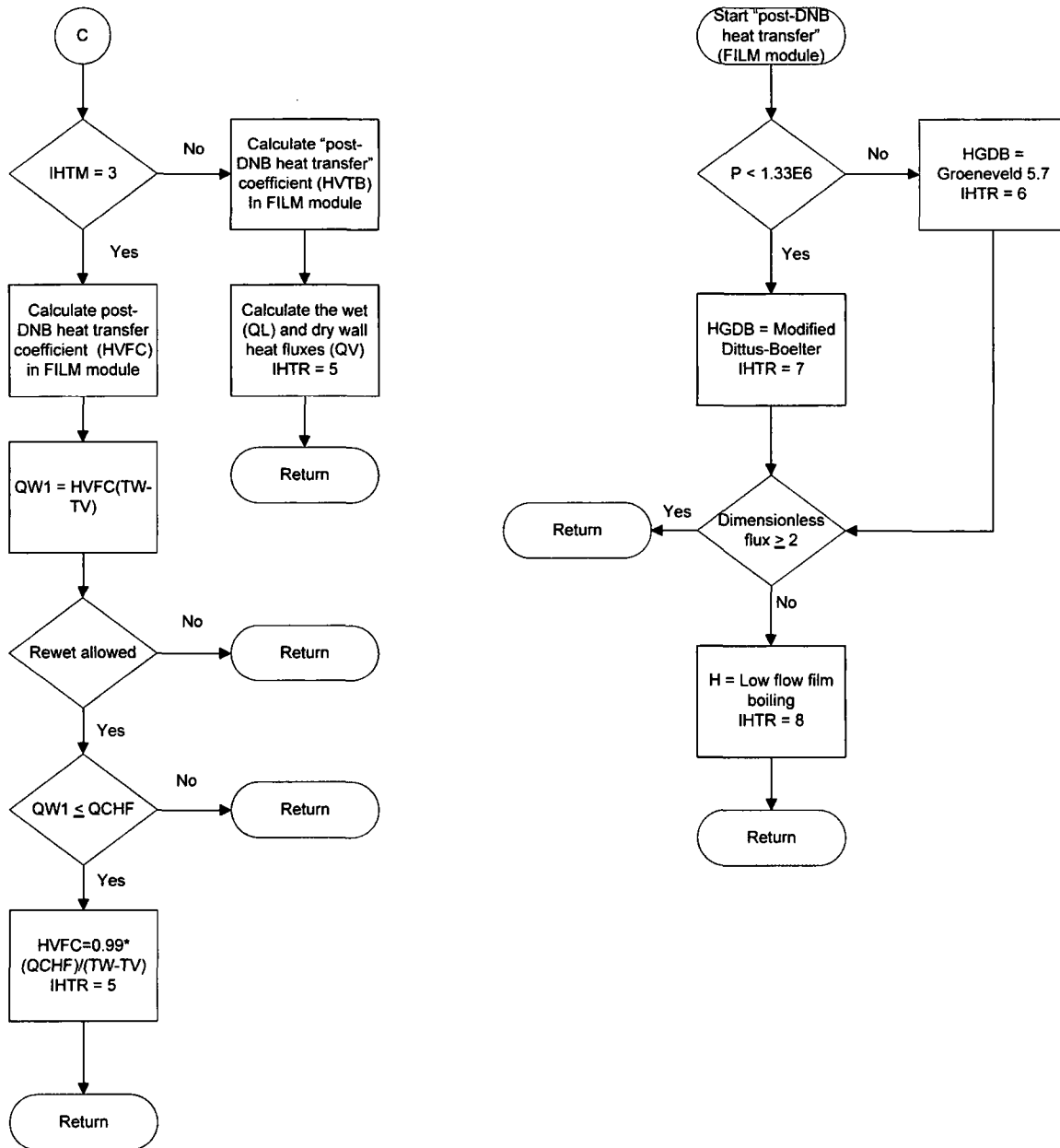


Table A-2: Definition of Variables Used in Figure A-1

| Variable | Description |
|-----------------|---|
| CHFLIM | CHF correlation limit for the user-supplied CHF correlation (input in G3-3) |
| FILM | Module (or subroutine) for generating the film boiling heat transfer coefficients |
| H | Low flow film boiling heat transfer coefficient |
| HGDB | Film boiling heat transfer coefficient |
| HLF | Forced convection component of the Chen nucleate boiling heat transfer |
| HLFC | Heat transfer coefficient to liquid |
| HLN | Nucleate boiling component of the Chen nucleate boiling heat transfer |
| HLNB | Heat transfer coefficient due to nucleate boiling |
| HMA | Heat transfer coefficient based on the McAdams correlation |
| HST | Heat transfer coefficient based on the Sieder-Tate correlation |
| HVFC | Heat transfer coefficient to vapor |
| HVTB | Heat transfer coefficient in transition boiling |
| IHTM | Heat transfer module indicator as input by the user on G8-2e |
| IHTR | Heat transfer mode (modes vary from 1 to 10) |
| P | Pressure |
| QCHEN | Cladding surface heat flux based on the Chen correlation |
| QCHF | Critical heat flux based on the user-defined CHF correlation |
| QL | Heat flux to liquid |
| QV | Heat flux to vapor |
| QW1 | Heat flux based on rewetting |
| TCHF | Cladding surface temperature at Critical Heat Flux |
| TL | Liquid temperature |
| TMSFB | Minimum stable film boiling temperature |
| TSAT | Saturation temperature |
| TV | Vapor temperature |
| TW | Cladding surface temperature |
| X | Quality |

In single-phase forced convection of subcooled liquid or superheated vapor the Figure A-1, based on Reference A-17, uses the maximum of the Sieder-Tate and McAdams heat transfer correlations. Equations A-72 and A-73 describe the Sieder-Tate and McAdams heat transfer coefficients, respectively:

$$h_{ST} = 0.023 \frac{k_i}{D_e} \text{Re}_i^{0.8} \text{Pr}_i^{0.33} \left(\frac{\mu_i}{\mu_{wall}} \right)^{0.14} \quad \text{A-72}$$

$$h_{MA} = 0.13 k_i \left[\frac{\rho_i^2 g \beta_i c_{p,i} (T_{wall} - T_v)}{\mu_i k_i} \right]^{(1/3)} \quad \text{A-73}$$

The nomenclature for these heat transfer correlations is contained in Table A-3. In Equations A-72 and A-73 for the single-phase heat transfer correlation the “i” subscript denotes the liquid condition (l) or the vapor condition (v) and is dependent on the coolant condition.

Table A-3: Definition of Variables Used in Heat Transfer Coefficient Definitions

| Nomenclature | Description and units |
|---|---|
| a, b, c | User-supplied constants for the isothermal friction factor |
| a_n | User-supplied coefficients for the polynomial void fraction as a function of quality |
| $a_{\Phi,n}$ | User-supplied coefficients for the polynomial two-phase multiplier as a function of quality |
| A | Cross sectional flow area, m^2 |
| A_1 | Four coefficients used in the Zuber-Findlay void fraction model |
| A_1 | Reynolds Number dependent parameter used in determining the Chexal-Lellouche fluid parameter |
| b_1 | Seven coefficients used in the Zuber-Findlay void fraction model |
| B_1 | Parameter used in determining the Chexal-Lellouche fluid parameter |
| C | Concentration coefficient for the void fraction models |
| C_0 | Distribution parameter for the Chexal-Lellouche void fraction model |
| C_{0v}, C_{0h} | Distribution parameters for the Chexal-Lellouche void fraction model for vertical and horizontal flow, respectively |
| C_1 | Pressure dependent terms used in determining the Chexal-Lellouche fluid parameter |
| $C_2, C_3, C_4,$ $C_5, C_7, C_8,$ C_9 | Various parameters used in the Chexal-Lellouche drift velocity calculation |
| $c_{p,i}$ | Constant pressure specific heat, $J/(kg-K)$ |
| CHF | Critical Heat Flux condition |
| D_e | Hydraulic diameter based on wetted perimeter, m |
| d_2 | Normalizing diameter for the Chexal-Lellouche void fraction correlation |
| f | Diabatic friction factor |
| f_{iso} | Isothermal friction factor (either laminar or turbulent) |
| $f_{lam/iso}$ | Isothermal laminar friction factor |
| $f_{turb/iso}$ | Isothermal turbulent friction factor |
| F_r | Flow orientation parameter for the Chexal-Lellouche void fraction model |
| g | Acceleration due to gravity, m/s^2 |
| g_c | Gravitational constant |
| G | Mass flux, $kg/(m^2-s)$ or $kg/(m^2-h)$ (as needed by COBRA-FLX) |
| G_E | Mass flux, $Mlb_m/(ft^2-h)$ |
| h_j | Heat transfer coefficient based on correlation j, $W/(m^2-^{\circ}C)$ |
| h_{fg} | Latent heat of vaporization, J/kg |
| j_i | Dimensionless volumetric mass flux for condition i |

**Table A-3: Definition of Variables Used in Heat Transfer Coefficient Definitions
(continued)**

| Nomenclature | Description and Units |
|---------------------|--|
| $J_{i,\alpha}$ | Volumetric mass flux for fluid condition i, m/s |
| k_i | Thermal conductivity for fluid condition i, W/(m-°C) |
| K_0 | Parameter required to generate the Chexal-Lellouche vertical flow distribution parameter |
| L | Chexal-Lellouche fluid parameter |
| \dot{m} | Mass flow rate, kg/h or kg/s (as needed by COBRA-FLX) |
| p | Pressure, N/m ² |
| p_{crit} | Critical pressure, N/m ² |
| p_E | Pressure, psia |
| P_h | Heated perimeter, m |
| P_w | Wetted perimeter, m |
| Pe | Peclet Number |
| PI | Property index |
| Pr_i | Prandtl Number |
| q'' | Heat flux, W/m ² |
| \dot{q} | Linear heat rate, W/m |
| Q | Variable used for the Levy subcooled boiling initiation correlation |
| r | Parameter required to generate the Chexal-Lellouche vertical flow distribution parameter |
| Re_i | Reynolds Number for fluid condition i |
| S | Slip ratio ((vapor velocity)/(liquid velocity)) |
| T_i | Temperature for condition i, °C |
| ΔT_L | Temperature change for the Levy subcooled boiling initiation correlation |
| U_i | Velocity for fluid condition i, m/s |
| V_{gi} | Drift velocity for void fraction calculations, m/s |
| $V_{gi,0}$ | Drift velocity for the Chexal-Lellouche void fraction correlation, m/s |
| $V_{g/1}, V_{g/2}$ | Drift velocity used in the Zuber-Findlay void fraction correlation, m/s |
| V_i | Velocity for fluid condition i, m/s |
| VFR | Volumetric flow rate ratio for the Chexal-Lellouche void fraction correlation |
| w | Weighting function used by the modified Zuber-Staub profile fit correlation |
| x | Flowing quality, dimensionless |
| x_1 | Intermediate flowing quality generated by the modified Zuber-Staub profile fit correlation |

**Table A-3: Definition of Variables Used in Heat Transfer Coefficient Definitions
(continued)**

| Nomenclature | Description and Units |
|---------------------|--|
| x_e | Thermodynamic quality, dimensionless |
| x_{final} | Final flowing quality generated by the modified Zuber-Staub profile fit correlation |
| X_{DG} | Entrance length or distance to upstream spacer grid for Szablewski function, dimensionless |
| Y, Y_1 | Parameters required for the calculation of the Zuber-Findlay void fraction |
| Y_b | Normalized distance from the cladding surface used for the Levy subcooled boiling initiation correlation |
| Greek symbol | |
| α | Void fraction |
| β | Coefficient of thermal volumetric expansion, $1/^\circ\text{C}$ |
| ε | Surface roughness for the Lehmann correlation, m |
| Φ | Two-phase friction multiplier |
| Φ_{lo}^2 | Two-phase multiplier for the Baroczy two-phase friction multiplier correlation |
| μ_i | Dynamic viscosity for fluid condition i, kg/(m-s) |
| ρ_i | Density for fluid condition i, kg/m^3 |
| σ | Surface tension, N/m |
| Ω | Correction for the Baroczy two-phase friction multiplier correlation |
| ω | Relaxation factor for the Chexal-Lellouche void fraction correlation |
| τ_w | Wall shear stress for the Levy subcooled boiling initiation correlation |
| Subscripts | |
| 1, 2, 3 | Subscript on the first three iterations of the void fraction in the Chexal-Lellouche void fraction correlation |
| 5.7 | Groenveld 5.7 heat transfer condition |
| bulk | Bulk coolant condition |
| Chen | Chen nucleate boiling condition |
| CHF | Critical Heat Flux condition |
| DB-mod | Modified Dittus-Boelter condition |
| f | Saturated liquid condition |
| g | Saturated vapor condition |
| FB | Film boiling condition |
| FC | Forced convection single-phase condition |
| HN | Homogeneous nucleation condition |
| i | Fluid condition |

**Table A-3: Definition of Variables Used in Heat Transfer Coefficient Definitions
(continued)**

| Nomenclature | Description and Units |
|---------------------|---------------------------------------|
| LFFB | Low flow film boiling condition |
| mixture | Mixture condition |
| Modified Bromley | Modified Bromley low flow condition |
| MSFB | Minimum Stable film boiling condition |
| MA | McAdams single-phase condition |
| NB | Nucleate boiling condition |
| Rewet | Rewet condition |
| RXD | Szablewski-based friction factor |
| Sat | Saturation condition |
| TB | Transition boiling |
| v | Vapor condition |
| wall | Cladding surface condition |

The Chen nucleate boiling correlation is used to generate the cladding surface heat transfer coefficient when the surface is in nucleate boiling. Chen's correlation, as implemented in COBRA-FLX, uses one of two forms, either subcooled or saturated boiling. The criterion used to determine the region is based on the local coolant conditions. If the local coolant temperature is less than saturation then the heat transfer mode is subcooled nucleate boiling, otherwise the heat transfer mode is saturated nucleate boiling. The heat flux based on the Chen correlation (q''_{Chen}) is defined as follows:

$$q''_{Chen} = q''_{FC} + q''_{NB} = h_{FC}(T_{wall} - T_i) + h_{NB}(T_{wall} - T_{Sat}) \quad A-74$$

If the fluid has a temperature less than saturation the fluid condition is subcooled and the local fluid temperature is used in Equation A-74 to evaluate the forced convection heat flux. If the fluid is saturated the saturation temperature is used in Equation A-74.

The single phase heat transfer coefficient in Equation A-74 (h_{FC}) is defined as follows:

$$h_{FC} = 0.023 \text{Re}_i^{0.8} \text{Pr}_i^{0.4} \frac{k_i}{D_e} F \quad \text{A-75}$$

where F is defined based on the Lockhart-Martinelli parameter (x_u^{-1}) as follows:

$$x_u^{-1} = \left(\frac{x}{1-x} \right)^{0.9} \left(\frac{\rho_f}{\rho_g} \right)^{0.5} \left(\frac{\mu_g}{\mu_f} \right)^{0.1} \quad \text{A-76}$$

$$F = \begin{cases} 1.0 & x_u^{-1} \leq 0.10 \\ 2.35(x_u^{-1} + 0.213)^{0.736} & x_u^{-1} > 0.10 \end{cases} \quad \text{A-77}$$

The nucleate boiling heat transfer coefficient in Equation A-74 (h_{NB}) is defined as follows:

$$h_{NB} = 0.00122(S) \left[\frac{k_f^{0.79} c_{p,f}^{0.45} \rho_f^{0.49}}{\sigma^{0.5} \mu_f^{0.29} h_{fg}^{0.24} \rho_g^{0.24}} \right] (T_{wall} - T_{Sat})^{0.24} (p_{wall} - p)^{0.75} \quad \text{A-78}$$

The suppression factor (S) in Equation A-78 is defined as follows:

$$S = \begin{cases} \left\{ 1 + 0.12(\text{Re}'_{TP})^{1.14} \right\}^{-1} & \text{Re}'_{TP} < 32.5 \\ \left\{ 1 + 0.42(\text{Re}'_{TP})^{0.78} \right\}^{-1} & 32.5 \leq \text{Re}'_{TP} < 70.0 \\ 0.1 & \text{Re}'_{TP} \geq 70.0 \end{cases} \quad \text{A-79}$$

The variable Re'_{TP} used in Equation A-79 is defined as follows:

$$\text{Re}'_{TP} = \frac{G(1 - \max(0, x))D_e}{\mu_f} (F^{1.25})(10^{-4}) \quad \text{A-80}$$

If the coolant is subcooled Equation A-77 is set to 1.0.

In addition to the Chen nucleate boiling calculations when the cladding surface temperature exceeds the saturation temperature the COBRA-FLX heat transfer module

also calculates the minimum stable film boiling temperature (T_{MSFB}). This temperature is as defined in References A-16 and A-17 and is as follows:

$$T_{MSFB} = T_{HN} + (T_{HN} - T_i) \left[\frac{(\rho k c_p)_i}{(\rho k c_p)_{wall}} \right]^{0.5} - \psi \quad \text{A-81}$$

If the rewet option is not allowed the minimum stable film boiling temperature is defined as follows:

$$T_{MSFB} = T_{wall} - 0.01 \quad \text{A-82}$$

The rewet option will not be utilized for U.S. application for safety-related analyses. The COBRA-FLX implementation of the minimum stable film boiling temperature requires the homogeneous nucleation temperature of water (T_{HN}), which is as follows:

$$T_{HN} = \begin{cases} 581.5 + 0.01876(\max(p - 1.0345E5, 0))^{0.5} & , \quad p \leq 68.96E5 \\ 630.37 + 0.00423(p - 68.96E5)^{0.5} & , \quad p > 68.96E5 \end{cases} \quad \text{A-83}$$

The ψ function in Equation A-81 is a function only of pressure and is as follows, as defined in References A-16 and A-17:

$$\psi = \begin{cases} 0.0 & , \quad p \geq 4.827E5 \\ 127.3 - 26.37E-5(p) & , \quad p < 4.827E5 \end{cases} \quad \text{A-84}$$

If the Chen heat flux from Equation A-74 exceeds the critical heat flux (CHF) generated using a user-defined CHF correlation, then post-CHF heat transfer conditions are initiated in COBRA-FLX. The cladding surface temperature at the CHF condition is determined by varying the wall temperature in Equation A-74 until the Chen-based heat flux equals the CHF.

When the cladding surface is in transition boiling one of two different transition boiling heat transfer models is used. One model is based on the methodology outlined in References A-16 and A-17. The other method is based on Stosic's rewet model as

defined in Reference A-18. For both the original method and the method based on Stosic the film boiling heat transfer coefficients, which are defined later, are generated. For the original method from References A-2 and A-3 the transition boiling heat flux is defined as follows:

$$q_{TB}'' = \delta^2 q_{TB}'' + (1 - \delta^2) q_{MSFB}'' \quad A-85$$

where

$$\delta = \left(\frac{T_{MSFB} - T_{wall}}{T_{MSFB} - T_{CHF}} \right) \quad A-86$$

where the MSFB heat flux is based on the appropriate film boiling heat transfer coefficient, the MSFB temperature from Equation A-81 and the vapor temperature. For Stosic's method the appropriate film boiling heat transfer coefficient (h_{FB}) is used to calculate the heat flux as follows:

$$q_{wl}'' = h_{FB} (T_{wall} - T_v) \quad A-87$$

If the heat flux from Equation A-87 is less than the CHF, with rewetting allowed the heat transfer coefficient is calculated as follows:

$$h_{Rewet} = \frac{0.99 q_{CHF}''}{(T_w - T_v)} \quad A-88$$

The film boiling heat transfer calculations are performed for either high or low flow situations based on a dimensionless volumetric flux (j) which is defined as follows (based on the implementation in Reference A-17):

$$j = (j_f)^{0.5} + (j_g)^{0.5} = \left(\frac{G(1-x)}{\{gD_e \rho_f (\rho_f - \rho_g)\}^{1/2}} \right)^{0.5} + \left(\frac{Gx}{\{gD_e \rho_g (\rho_f - \rho_g)\}^{1/2}} \right)^{0.5} \quad A-89$$

For high flow film boiling (as defined by the dimensionless volumetric flux greater than or equal to 2.0) the system pressure is used to select one of two different high-flow film boiling correlations. If the system pressure is greater or equal to than $1.33(10)^6$ N/m² then the following film boiling heat transfer coefficient is used (based on Groenveld 5.7 as defined in References A-16 and A-17):

$$h_{5,7} = 0.052 \left(\frac{k_v}{D_e} \right) \left[\frac{\rho_v D_e}{\mu_v} (V_f + \alpha(V_v - V_f)) \right]^{0.688} (\text{Pr}_v)^{1.26} \left[1 - 0.1 \left\{ (1 - x) \left(\frac{\rho_f}{\rho_v} - 1 \right) \right\}^{0.4} \right]^{-1.06} \quad \text{A-90}$$

If the pressure is less than $1.33(10)^6$ N/m² a modified Dittus-Boelter correlation is used and is as follows, based on References A-16 and A-17:

$$h_{DB-Mod} = 0.023 \left(\frac{k_v}{D_e} \right) \left[\frac{\rho_v D_e}{\mu_v} (V_f + \alpha(V_v - V_f)) \right]^{0.8} (\text{Pr}_v)^{0.4} \quad \text{A-91}$$

If the flow is determined to be low flow (based on the dimensionless volumetric flux less than 2.0, based on Equation A-89 definition) the modified Bromley heat transfer coefficient is defined as follows:

$$h_{Modified\ Bromley} = 0.32 \left[\frac{h_{fg}}{c_{p,v}(T_w - T_{sat})} + 0.5 \right]^{(-1/3)} \left(\frac{T_{sat}}{T_w} \right)^{0.5} \left[\frac{g_c (\rho_f - \rho_v) \rho_v k_v^3 h'_{fg}}{\lambda_c \mu_v} \right]^{(1/3)} (1 - \alpha)^{0.5} \quad \text{A-92}$$

where

$$\lambda_c = 2\pi \left[\frac{\sigma}{\rho_f - \rho_v} \right]^{0.5} \quad \text{A-93}$$

and

$$h'_{fg} = h_{fg} + 0.5c_{p,v}(T_w - T_{sat}) \quad \text{A-94}$$

The low flow film boiling heat transfer coefficient (h_{LFFB}) is determined as follows:

$$h_{LFFB} = (1 - \alpha)h_{\text{Modified Bromley}} + \alpha[\max(h_{FB}, h_{MA})] \quad \text{A-95}$$

where h_{FB} is the appropriate film boiling heat transfer coefficient between Equations A-90 and A-91, which are based on the pressure, and h_{MA} is the McAdams heat transfer coefficient from Equation A-73, which is based on the vapor condition.

A summary of all the heat transfer correlations and the heat transfer mode number are contained in Table A-4.

Table A-4: Summary of Heat Transfer Coefficient/Flux Correlations

| Region | Correlations | Heat Transfer Mode (IHTR) |
|---------------------------------------|--|--|
| Forced convection (liquid) | Maximum of Sieder-Tate (Equation A-72) and McAdams (Equation A-73) | Sieder-Tate (IHTR = 1), McAdams (IHTR = 2) |
| Subcooled nucleate boiling | Subcooled nucleate boiling (Equations A-74 through A-80) | IHTR = 3 |
| Saturated nucleate boiling | Saturated nucleate boiling (Equations A-74 through A-80) | IHTR = 4 |
| Transition boiling | Equations A-85 and A-86 | IHTR = 5 |
| High flow, high pressure film boiling | Equation A-90 | IHTR = 6 |
| High flow, low pressure film boiling | Equation A-91 | IHTR = 7 |
| Low flow film boiling | Equation A-95 | IHTR = 8 |
| Forced convection (vapor) | Maximum of Sieder-Tate (Equation A-72) and McAdams (Equation A-73) | Sieder-Tate (IHTR = 9), McAdams (IHTR = 10) |

A.6 DNBR Iteration Scheme

COBRA-FLX has the capability to vary various boundary conditions internal to the code until user-defined minimum DNBRs are generated. This capability is useful when COBRA-FLX is used to generate reactor setpoints for regions of acceptable operation. The COBRA-FLX option for the DNBR iteration scheme is contained in G11-1a: Setpoint Iteration. COBRA-FLX uses the Van Wijngaarden-Dekker-Brent Method, more commonly called Brent's Method, to vary the boundary condition variables until the target minimum DNBR (DNBLIM input in G11-1a) is attained.

A.7 References

- A-1 W. Wagner, A. Kruse (1998). Properties of Water and Steam - The Industrial Standard IAPWS-IF97 for the Thermodynamic Properties and Supplementary Equations for Other Properties, Springer, Berlin.
- A-2 J. Lehmann, Widerstandsgesetze der turbulenten Strömung in geraden Stahlrohren Gesundheits-Ingenieur, Zeitschrift für angewandte Hygiene und Gesundheitstechnik in Stadt und Land, 82. Jahrgang, 1961, Heft 6.
- A-3 Szablewski, W., Der Einlauf einer turbulenten Rohrströmung, Ingenieur-Archiv, XXI. Band, 1953, S. 323.
- A-4 W.M. Rohsenow, J.A. Clark, Heat Transfer and Pressure Drop Data for High Heat Flux Densities to Water at High Sub-Critical Pressures, Heat Transfer and Fluid Mechanics Institute, Stanford University Press (June 1951).
- A-5 A.A. Armand, The Resistance During the Movement of a Two-Phase System in Horizontal Pipes, Translated by V. Beak, AERE Trans. 828. Izvestiya Vsesojuznogo Teplotekhnicheskogo Instituta (1), pp. 16-23 (1946).
- A-6 Baroczy, C.J., A Systematic Correlation for Two-Phase Pressure Drop, Eighth National Heat Transfer Conference, Los Angeles 1965, Chem. Eng. Progr. Symp. Ser. 64, Vol. 62. p.232.
- A-7 Jones, A.B., Hydrodynamic Stability of a Boiling Channel, KAPL-2170, Knolls Atomic Power Laboratory (1961).
- A-8 Lahey, R.T. & Moody, F.J., The Thermal-Hydraulics of a Boiling Water Nuclear Reactor, Second Edition, American Nuclear Society, 1993
- A-9 Smith, S.L., Void Fractions in Two-Phase Flow: A Correlation based upon an Equal Velocity Head Model, Proc. Instn. Mech. Engrs. 1969-70, Vol 184 Pt 1 No 36.
- A-10 Massena, W.A., Steam-Water Pressure Drop and Critical Discharge Flow - A Digital Computer Program, HW-65706, Hanford Atomic Products Operation, Richland, Washington (June 17, 1960).
- A-11 Zuber, N., Findlay, J.A., Average Volumetric Concentration in two-Phase Flow Systems, Journal of Heat Transfer, pp. 453-468, 1965.
- A-12 B. Chexal, G. Lellouche, J. Horowitz, and J. Healzer, A Void Fraction Correlation for Generalized Applications, Progress in Nuclear Energy, Vol. 27, No. 4, 1992.
- A-13 Levy, S., Forced Convection Subcooled Boiling - Prediction of Vapor Volumetric Fraction, GEAP-5157, General Electric Company (1966).
- A-14 Saha, P. , Zuber, N., Point of Net Vapor Generation and Vapor Void Fraction in Subcooled Boiling, Proc. 5th Int. Heat Transfer Conference, Vol. 4 (1974).
- A-15 N. Zuber, F.W. Staub, G. Bijwaard, Vapor void fraction in subcooled boiling and in saturated boiling systems, Proc. 3rd Int. Heat Transfer Conference, Vol. 5 (1966)
- A-16 Bjornard, T. A.; Griffith, P (1977). PWR Blowdown Heat Transfer. *Symposium on the Thermal and Hydraulic Aspects of Nuclear Reactor Safety, Volume 1 – Light Water Reactors*, American Society of Mechanical Engineers, Atlanta, GA, November 27 - December 2, 1977, pp. 17-39.

-
- A-17 Jackson, J. W.; Todreas, N. E. (1981). COBRA IIIC/MIT-2: A Digital Computer Program for Steady State and Transient Thermal-Hydraulics Analysis of Rod Bundle Nuclear Fuel Elements, MIT-EL 81-018.
- A-18 Z. V. Stosic, On the Frontier of Boiling Curve and Beyond Design of its Origin, *Nuclear Energy for New Europe 2005*, Bled, Slovenia, September 5 – 8, 2005, pages 115.1 through 115.16.

APPENDIX B: COBRA-FLX DEVELOPMENT HISTORY

B.1 History

The lineage of COBRA-FLX as well as the US NRC-approved subchannel codes XCOBRA-IIIC of Reference B-1 and LYNXT of References B-2 and B-3 starts with COBRA-IIIC (Reference B-4). From the basis of COBRA-IIIC the codes deviated. XCOBRA-IIIC is based on COBRA-IIIC. LYNXT is based on COBRA-IV (Reference B-5) which is an extended version of COBRA-IIIC. COBRA-FLX is based on COBRA IIIC/MIT-2 (Reference B-6), which is an extension of the original COBRA-IIIC. Figure B-1 shows the lineage of COBRA-FLX, the two US NRC-approved subchannel codes, and FLICA (which is besides COBRA-FLX, presently used by AREVA in Europe).

The AREVA subchannel codes' common lineage is based on the more than 40 years successful history of the COBRA series of codes, although the codes (specifically COBRA-FLX) have been updated to take advantage of the latest hardware and software developments. The common lineage indicates that the governing equations, many of the empirical correlations (excluding the critical heat flux correlations), general code structure, and general solution algorithms are common between the codes, although the specific code implementations may appear to differ.

B.2 History of COBRA Development

In the 1960's, work was initiated under the sponsorship of a co-operative program between the United States and Canada for the development of heavy water moderated power reactors. This program and its continuations turned out to be one of the most successful scientific development projects in the field of nuclear reactor core analysis, with results eventually applicable from light water moderated reactors to liquid metal cooled fast breeder reactors.

At Battelle Pacific Northwest Laboratory, Richland, Washington, laboratory experiments and analytical work were performed to investigate and describe the fluid flow in rod bundle nuclear fuel assemblies. The first version of the thermal-hydraulic subchannel

analysis code COBRA (Computer Program for Coolant Boiling in Rod Arrays) was presented in 1967 (Reference B-7).

In this appendix, the first version will be referred to as COBRA-I, in order to clearly distinguish it from later versions. The term COBRA will be used to encompass the whole family of codes which originated from this development, or whenever several code versions are addressed (e.g., the AREVA NP COBRA versions).

B.2.1 COBRA Versions Leading to COBRA 3-CP

Figure B-1 provides an overview of the history of COBRA development. This figure does not contain all of the many branches and side lines of development. Instead, it is limited to the direct predecessors of the AREVA NP COBRA-FLX versions of today. These predecessor code versions will be briefly described below.

The basic 1967 COBRA-I version was created to compute coolant flow and enthalpy in the subchannels of rod bundle nuclear fuel assemblies during boiling. Only steady-state calculations were possible. Its most significant new feature was its ability to include mixing from two types of crossflow, i.e., diversion crossflow caused by flow redistribution and a superimposed turbulent crossflow due to random travel of the coolant between adjacent subchannels. The main characteristics of COBRA-I as presented in Reference B-7 are:

- It has the ability to consider both single- and two-phase flow.
- It accounts for thermal mixing between interconnected parallel flow channels which results from both the transport of energy by turbulent crossflow and diversion crossflow.
- It considers the momentum interchanges between adjacent subchannels which result from both turbulent and diversion crossflow.
- It includes the effect of transverse resistance to diversion crossflow.
- It considers an arbitrary layout of fuel rods and flow subchannels and thus allows analysis of most any rod bundle configuration.

-
- It includes arbitrary heat flux distribution by specifying the axial heat flux distribution, relative rod power, and the fraction of rod power to each of the adjacent subchannels.

The COBRA-II version of 1970, besides having a faster and more accurate numerical initial-value solution of the mathematical model, contains the following new features (from Reference B-8):

- It can consider variable subchannel area and gap spacings.
- It can include the effect of subcooled void.
- It can include the effect of forced diversion crossflow produced by flow diverting devices.
- It can include the pressure losses caused by spacing devices.
- It permits non-uniform hydraulic behavior by selecting different subchannel hydraulic characteristics.

The COBRA-III version of 1971 (Reference B-9) responded to the need for transient safety analysis capabilities to predict the behavior of the reactor core and fuel following normal operating transients and potential accident situation. Its corresponding features are:

- It can consider transients of fast to intermediate speed (sonic velocity propagation effects are ignored).
- A simplified transverse momentum equation is used which neglects both the temporal and spatial components of transverse acceleration of crossflow.
- The numerical scheme performs a boundary-value flow solution for both steady state and transients, with inlet enthalpy, inlet mass velocity, and exit pressure as boundary conditions.

The COBRA-IIIC version of 1973 (Reference B-4) removed some limitations which were present in the preceding first transient version. The major improvements are:

- A more complete transverse momentum equation now includes temporal and spatial acceleration of the diversion crossflow.
- Addition of a fuel rod heat transfer model allows calculation of fuel and cladding temperatures during transients by specifying power density.
- Heat transfer correlations are provided to couple the fuel rod model with the subchannel flow analysis.
- Use of the boundary-value flow solution scheme allows enhanced application of the forced crossflow mixing model originally developed for COBRA-II.

At the Massachusetts Institute of Technology, Cambridge, Massachusetts, further COBRA development was based on COBRA-IIIC. Inclusion of several improvements produced the first published COBRA-IIIC/MIT version of 1980 (Reference B-10) which in this appendix shall be designated COBRA-IIIC/MIT-1, with the following new features of major importance:

- Addition of a new fuel rod heat conduction model which includes temperature dependent properties and burnup dependence of the gap heat transfer coefficient.
- Addition of a new heat transfer package, discussed in Appendix A, which covers a broad range of flow regimes and contains a more consistent selection logic.
- Addition of a quality dependent mixing model for two-phase flow.

The COBRA-IIIC/MIT-2 version of 1981 (Reference B-6) basically was a consolidation of the earlier COBRA-IIIC/MIT-1:

- Addition of a new approach combining the original and two new transverse momentum coupling methods, by modifying the transverse momentum equation.
- Improved analysis for cases involving interconnected regions of different size, for enhanced full-core calculations.

B.2.2 Creation and Further Development of COBRA 3-CP

At Siemens/KWU, Erlangen, Germany, further COBRA development was based on COBRA-IIIC/MIT-2. The related code documentation and input description was received from the Massachusetts Institute of Technology, along with the source code.

The initial creation of the new Siemens/KWU code version, called COBRA 3-CP, maintained all the original capabilities of COBRA-IIIC/MIT-2 and included the new features below:

- Implementation of the pressure drop solution method. It increases the computational efficiency of the code, by reducing the number of simultaneous linear equations to be solved and using a successive over-relaxation technique to obtain the solution of these equations. Thus also large problems, such as full pressurized water reactor cores, can be analyzed.
- Input and output in SI-units.
- Free-format input.
- Lehman friction factor correlation.

The main additions leading up to the most recent version of COBRA-FLX can be summarized as follows:

- New fuel rod model, with interface to fuel rod thermal-mechanical response evaluation code, temperature-dependent properties, higher numerical accuracy, burnup-dependent heat transfer coefficient in gap between fuel and cladding, and transient capability.
- Iterative calculation of rod-to-coolant heat transfer coefficient in addition to iteration of fuel temperatures based on convergence of fuel central temperatures.
- Many additional DNB correlations.
- Transverse momentum coupling parameters which can be individually specified for each gap interconnection between subchannels.

- Non-uniform axial node spacing.
- Automatic time step control capability.
- Setpoint iteration capability for temperature and average heat flux at fixed flow.
- Sensitivity calculation according to Siemens Statistical Design Procedure.



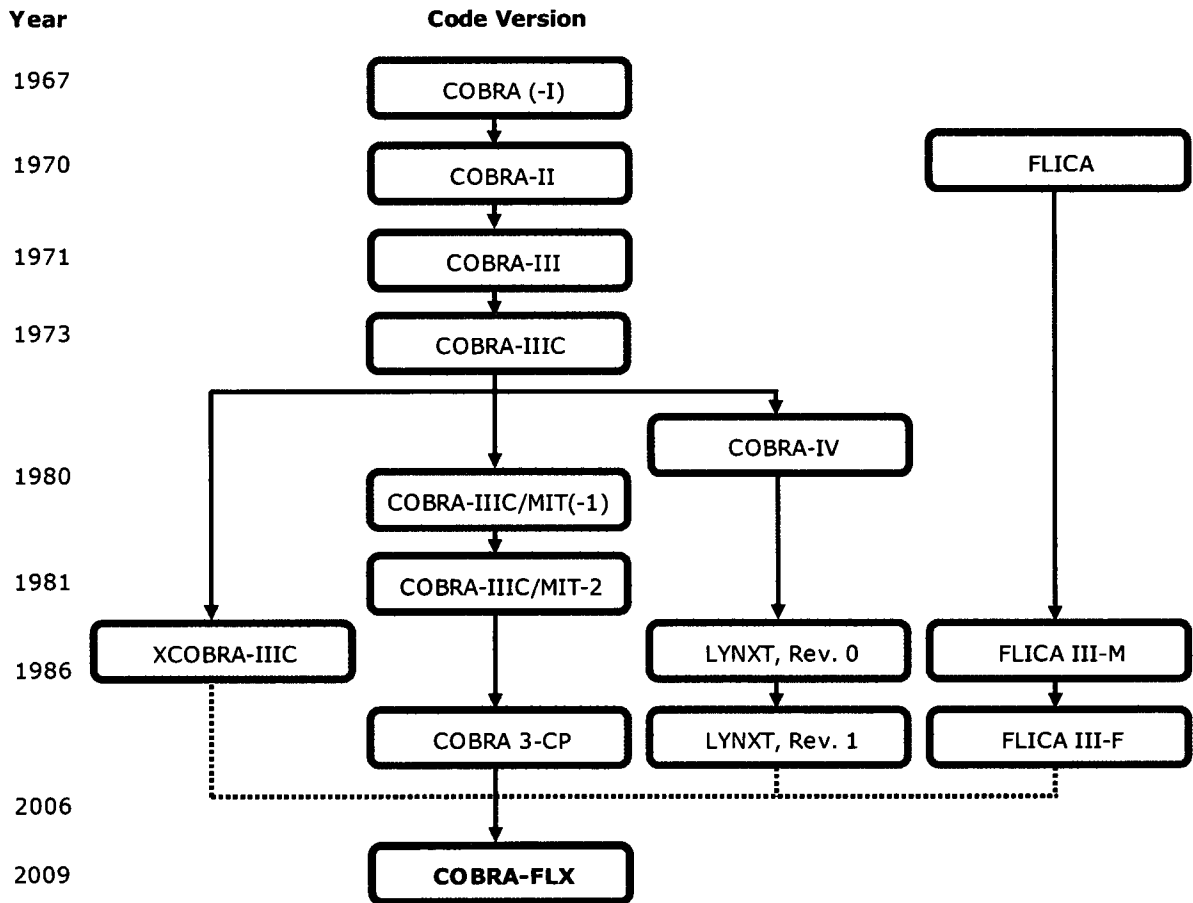
- Chexal-Lellouche void correlation.
- Internal lateral scaling.
- Performance factors to be applied to CHF values calculated by individual correlations

It should be noted that all of the above modifications are additions, [

] or new options. None of the newly generated code versions removed or destroyed any of the capabilities or features that had been included in earlier versions. Instead, new methodologies or improvements were usually programmed such as to supplement the existing options. This aspect is important to note with respect to the continuing validity of previous verification and validation exercises for later COBRA versions.

As discussed in Section 1, the COBRA-FLX code contains numerous parameter options that go beyond those necessary to perform PWR analyses in the U.S. Some capabilities, e.g., fuel rod model, are not within the requested review of COBRA-FLX discussed in Section 1. The inclusion of these capabilities in the code development history of Appendix B is intentional and only for completeness.

Figure B-1: Lineage of the AREVA Subchannel Codes



B.3 References

- B-1 XCOBRA-IIIC: A Computer Code to Determine the Distribution of Coolant Using Steady-State and Transient Core Operation, Siemens Power Corporation, XN-NF-75-21(P)(A), Revision 2, March 1985.
- B-2 LYNXT – Core Transient Thermal-Hydraulic Program, Babcock & Wilcox, BAW-10156-A, February 1986.
- B-3 LYNXT – Core Transient Thermal-Hydraulic Program, B&W Fuel Company, BAW-10156-A, Rev. 1, August 1993.
- B-4 COBRA-IIIC: A Digital Computer Program for Steady-State and Transient Thermal-Hydraulic Analysis of Rod Bundle Nuclear Fuel Elements, Battelle Pacific Northwest Laboratories, BNWL-1695, March 1973.
- B-5 COBRA-IV-I: An Interim Version of COBRA for Thermal-Hydraulic Analysis of Rod Bundle Nuclear Fuel Elements and Cores, Battelle Pacific Northwest Laboratories, BNWL-1962, UC-32, March 1976.
- B-6 COBRA IIIC/MIT-2: A Digital Computer Program for Steady-State and Transient thermal-Hydraulic Analysis of Rod Bundle Nuclear Fuel Elements, Massachusetts Institute of Technology, MIT-EL 81-018, June 1981.
- B-7 Cross-Flow Mixing Between Parallel Flow Channels During Boiling, Part I: COBRA – Computer Program for Coolant Boiling in Rod Arrays, D. S. Rowe, Battelle Pacific Northwest Laboratory, BNWL-371 PT1, March 1967.
- B-8 COBRA-II: A Digital Computer Program for Thermal-Hydraulic Subchannel Analysis of Rod Bundle Nuclear Fuel Elements, D. S. Rowe, Battelle Pacific Northwest Laboratories, BNWL-1229, February 1970.
- B-9 COBRA-III: A Digital Computer Program for Steady State and Transient Thermal-Hydraulic Analysis of Rod Bundle Nuclear Fuel Elements, D. S. Rowe, Battelle Pacific Northwest Laboratories, BNWL-B-82, Interim Report, undated (but not later than July 1971).
- B-10 Reactor Core Thermal-Hydraulic Analysis - Improvement and Application of the Code COBRA-IIIC/MIT, J. N. Loomis, W. D. Hinkle, Massachusetts Institute of Technology, MIT-EL 80-027, September 1980.

APPENDIX C: CRITICAL HEAT FLUX CORRELATION VALIDATION

AREVA has previously developed several critical heat flux (CHF) correlations for determining departure from nucleate boiling ratios (DNBRs) for use with its fuel designs. Each of these correlations have been reviewed and approved by the NRC for reload licensing application within defined ranges and limits using specific thermal-hydraulic subchannel codes. These correlations contain independent variables representing subchannel local coolant conditions, such as thermodynamic quality and mass velocity, previously predicted by either the LYNXT thermal-hydraulic subchannel code (Reference C-1) or the LYNX2 thermal-hydraulic subchannel code (Reference C-20). Consequently, the NRC approval of these CHF correlations has been limited to reload licensing applications for the subchannel local conditions from these codes. Since the subchannel local conditions predicted by COBRA-FLX are similar but not identical to those previously predicted by LYNXT or LYNX2 and used in the defense of the CHF correlations, it is necessary to demonstrate how these CHF correlations can be used in applications based on COBRA-FLX subchannel local conditions.

C.1.1 Validation Process

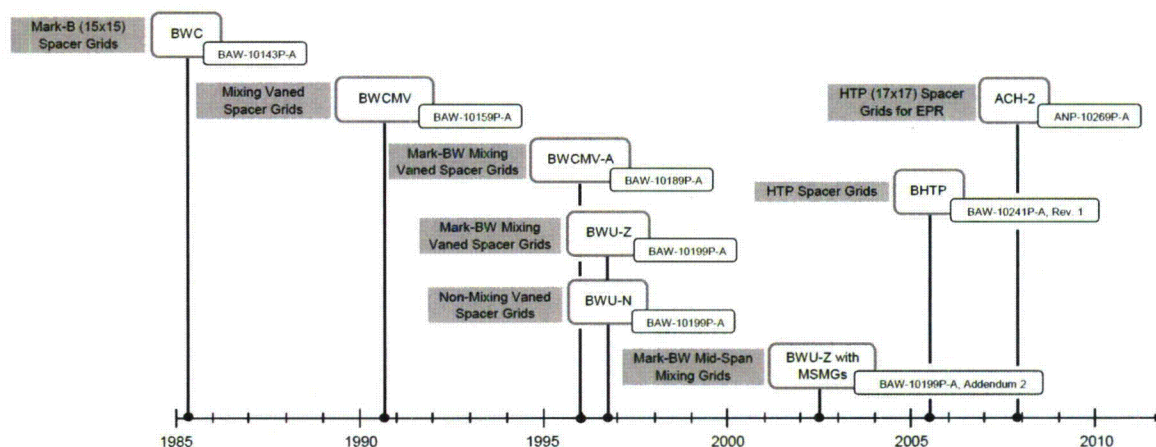
The process used to demonstrate the acceptability of a CHF correlation to be used with COBRA-FLX predicted local conditions is as follows:

- 1) Using the CHF test bundle conditions data base that supported the approved correlation, compute the local subchannel conditions for each test point using COBRA-FLX.
- 2) Using the approved CHF correlation form and coefficients, calculate the measured to predicted (M/P) value for each test point based on the COBRA-FLX local conditions.
- 3) Confirm that no biases are introduced for the independent variables, using M/P values, by examining scatter plots. If biases are introduced, justify the use of the correlation as presently defined.

- 4) Examine a histogram of the M/P CHF values and test for a normal distribution. If the normality of the distribution is acceptable, then the use of the Owen theory for one-sided distributions can be used. If the use of a distribution-free method is necessary to determine a 95/95 design limit, then apply it.
- 5) Determine the CHF correlation design limit using COBRA-FLX local conditions and the method justifiable for the correlation and data base.
- 6) Define the CHF correlation design limit to be used in COBRA-FLX applications based on the computed design limit and considering any appropriate conservative adjustments.

Figure C-1 shows the CHF correlations being validated for COBRA-FLX and the timeline when they were initially justified. These correlations are being validated in order to maintain the ability to provide DNBR predictive capability to support AREVA's customer base.

Figure C-1: Timeline of CHF Correlation Approval and Spacer Grid Applicability



The following sections are dedicated to the validation of the respective CHF correlations.

-
- Section C.2 ACH-2
 - Section C.3 BHTP
 - Section C.4 BWU-Z with Mid-Span Mixing Grids (MSMGs)
 - Section C.5 BWU-Z
 - Section C.6 BWCMV-A
 - Section C.7 BWCMV
 - Section C.8 BWU-N
 - Section C.9 BWC

The nomenclature and imagery used for each correlation in its respective section of Appendix C corresponds to the nomenclature and imagery used in the referenced approved topical report for ease in comparison. However, CHF correlation descriptors within Appendix D and Appendix C may be slightly different. Therefore, Table C-1 provides the identifications used in the other appendices.

Table C-1: CHF Correlation Identifications Throughout the COBRA-FLX Topical Report

| CHF Correlation | Reference(s) | Appendix D Keyword Identification for Card Group 8 | Appendix E Identification | |
|------------------------|---------------------|---|--------------------------------------|----------------|
| ACH-2 | C-2 | ACH_2 | ACH-2 | GCC8: N5=50 |
| BHTP | C-9, C-10 | BHTP | Mark-B HTP | GCC8: N5=53 |
| BWC | C-19 | BWC | BWC | GCC8: N5=55 |
| BWCMV | C-18 | BWCMV | BWCV | GCC8: N5=56 |
| BWCMV-A | C-17 | BWCMV_A | BWCMV-A | GCC8: N5=57 |
| BWU-Z | C-15 | BWU_Z_Mark_BW17_MSMG | BWU-Z (Mark-BW17 MSMG) | GCC8: N5=59 |
| BWU-Z | C-13 | BWU_Z_Mark_BW17 | BWU-Z (Mark-BW17) | GCC8: N5=61 |
| BWU-N | C-13 | BWU_N | BWU-N | GCC8: N5=63 |

A summary is provided in Section C.10 that provides a complete table of the local conditions and Design Limit(s) for all the correlations as supported by COBRA-FLX validation. The results of the validation process are presented in British Units for consistency with the previously approved correlation topical reports. The equivalent International System of Units (SI) values for the correlation local condition range limits are provided in Section C.10 for all the correlations.

C.2 The ACH-2 CHF Correlation

The ACH-2 CHF correlation was developed to support the fuel design for the U.S. EPR. The correlation was approved by the NRC and is documented in Reference C-2. The ACH-2 correlation was developed using [] test data points and further justified

upon the addition of 259 test data points for 14 foot tests as discussed in Sections S.4.0 and S.5.0 of Reference C-2. The verification of the acceptability for using ACH-2 with COBRA-FLX is based on the adequacy of the correlation to represent the data base. A COBRA-FLX-based CHF Design Limit was determined in accordance to Standard Review Plan requirements (Reference C-3) and followed the method described in the ACH-2 topical report.

C.2.1 Measured to Predicted CHF Performance

The [] test points were evaluated using COBRA-FLX to determine the measured to predicted CHF performance of the present ACH-2 CHF correlation. The M/P values were examined for each independent variable and no biases were found to be introduced. The M/P values are shown in Figure C-2 along with the [] limits that are later justified in this section.

Figure C-2: Measured CHF versus Predicted CHF for the ACH-2 CHF Correlation Using COBRA-FLX

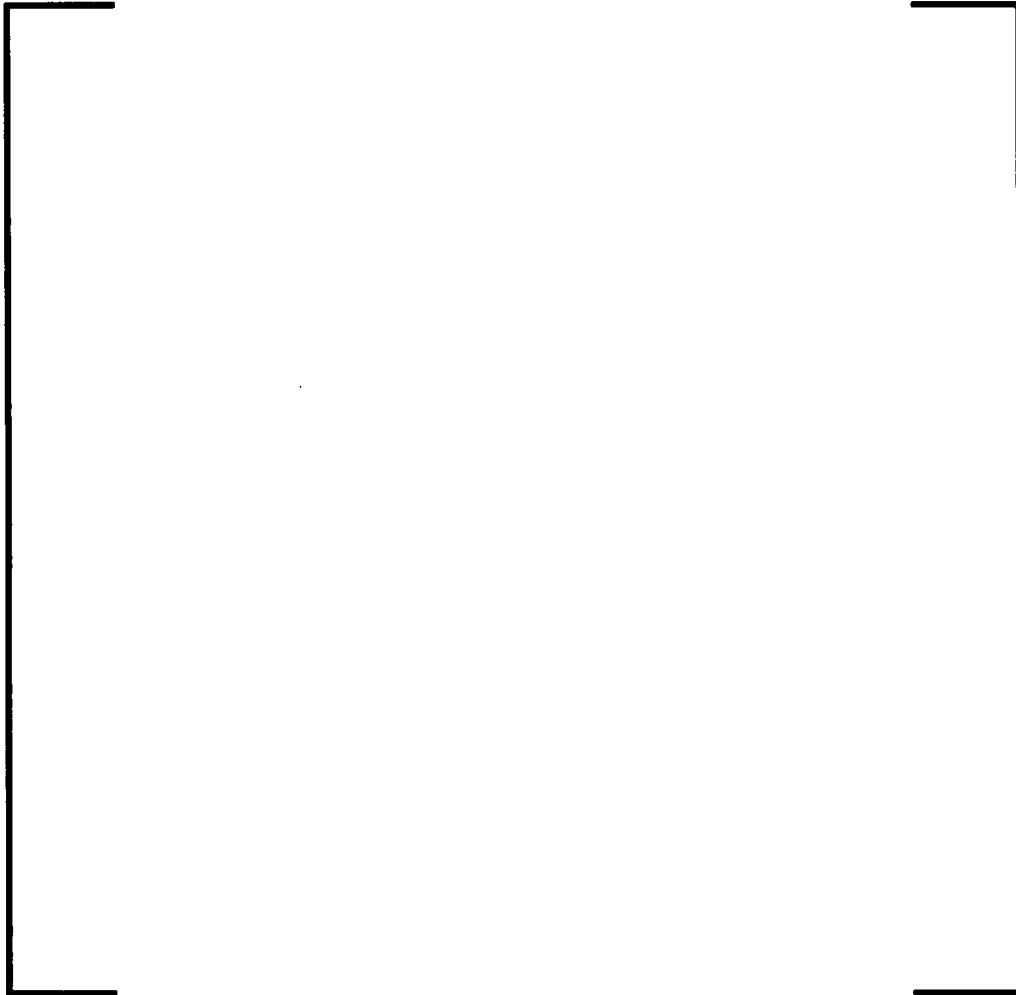


Figure C-3 shows the histogram of the M/P CHF values for the [] data points using COBRA-FLX. As seen by the overlay of the normal distribution (Reference C-4, the distribution has a fairly high value of kurtosis (a higher number of data than expected very close to the mean) but otherwise is a good representation of the expected normality of results. This observation was also made in the ACH-2 topical report.

Figure C-3: Histogram of Measured to Predicted Values for the ACH-2 CHF Correlation Using COBRA-FLX



The ACH-2 correlation was originally justified in Reference C-2 for 14 foot application based on observations and conclusions reached in Section S.4 and S.5 of Reference C-2 regarding the measure to predicted behavior of the original ACH-2 [] test point data base, the inclusion of the [] test point data base for [] data base, and for the [] data base comprised of [] test points. The COBRA-FLX based M/P values for each of these groups of data produced comparable trends observed using the LYNXT based results in Section S.4 of Reference C-2 other than the group M/P values were slightly lower and the group standard deviation values were slightly higher.

C.2.2 Design Limit DNBR

The design limit for departure from nucleate boiling ratio (DNBRL) was calculated to protect 95 percent of the hot pins in the core with 95 percent confidence from departure of nucleate boiling. The DNBRL value based on COBRA-FLX was determined using the same process in the ACH-2 topical report.

Using Owen, from Reference C-5, the DNBRL was found to be [] where:

σ : [], standard deviation of the M/P distribution

N : [], number of data in the correlation data base

nc: [], number of undetermined coefficients in the correlation

Ndf : [], N – 1 – nc, number of degrees of freedom of the optimized correlation

M/P: [], average measured to predicted CHF

$$(\sigma_{\text{limit}})^2 = (\sigma)^2 [(N - 1) / \text{Ndf}]$$

then,

$$\text{DNBRL} = 1.0 / [\text{M/P} - (k_{95/95, N} * \sigma_{\text{limit}})] = [], \text{ based on Owen}$$

Using Sommerville theory (Reference C-6) to any non-parametric distribution (e.g., a distribution which will not pass the standard D prime test for normality, References C-7 and C-8), the DNBRL for a 95/95 criteria was found to be []. For a 95/95 criteria with []. Sorting through the M/P distribution results leads to a [].

$$\text{DNBRL} = []$$

The DNBRL values above using Owen and Sommerville were based on COBRA-FLX calculations and the SCHEME-Pressure (P) solution method described in Section 2.3.1.4. The acceptability of the ACH-2 correlation was also performed using COBRA-FLX with the Pressure-Velocity (PV) solution method described in Section 2.3.2. In Table C-2, the results of the calculations are provided and compared to the original LYNXT results supplied in Section 7 of Reference C-2. The COBRA-FLX based DNBRL values were slightly lower than the LYNXT DNBRL values.

Table C-2: Comparison of COBRA-FLX based and LYNXT based DNBRL Values for the ACH-2 CHF Correlation

The COBRA-FLX based DNBRL values for the inclusion of the [] test point data base for [] data base and for the [] only data base, comprised of [] test points, were comparably lower than the LYNXT based DNBRL values of Section S.5 of Reference C-2.

Table C-2 also shows an insignificantly small difference in the DNBRL values when using the P or PV solution method within COBRA-FLX which is to be expected. This demonstration of the insignificant DNBR difference between the use of the P and PV solution methods, as well as the demonstrations within Section 5, show that it is only necessary to determine and to defend the DNBR Design Limit using one solution method for COBRA-FLX applications. Therefore, the remaining CHF correlations discussed within Appendix C will only be examined using the P solution method. The use of an ACH-2 1.23 DNBR Design Limit for COBRA-FLX applications is deemed acceptable with no changes in the form or coefficients of the correlation shown in Table 5-1 of Reference C-2.

C.2.3 Ranges and Limitations

The application ranges and limitations of the LYNXT based ACH-2 CHF correlation from the ACH-2 topical report will be maintained with the exceptions where the use of COBRA-FLX local conditions warrant a change.

Local Conditions:

Pressure: 284 to 2565 psia

Mass Velocity : 0.950 to 3.061 Mlb/hr-ft²

Thermodynamic Quality at CHF: less than 37%

Fuel Design:

Spacer Grid Type: AREVA NP EPR HTP

Grid Spacing: 18.5 to 20.0 inches

Fuel Rod OD: 0.374 inches

Guide Tube OD: 0.490 inches

Fuel Rod Pitch: 0.496 inches

Application:

Code: COBRA-FLX

DNBRL: 1.23

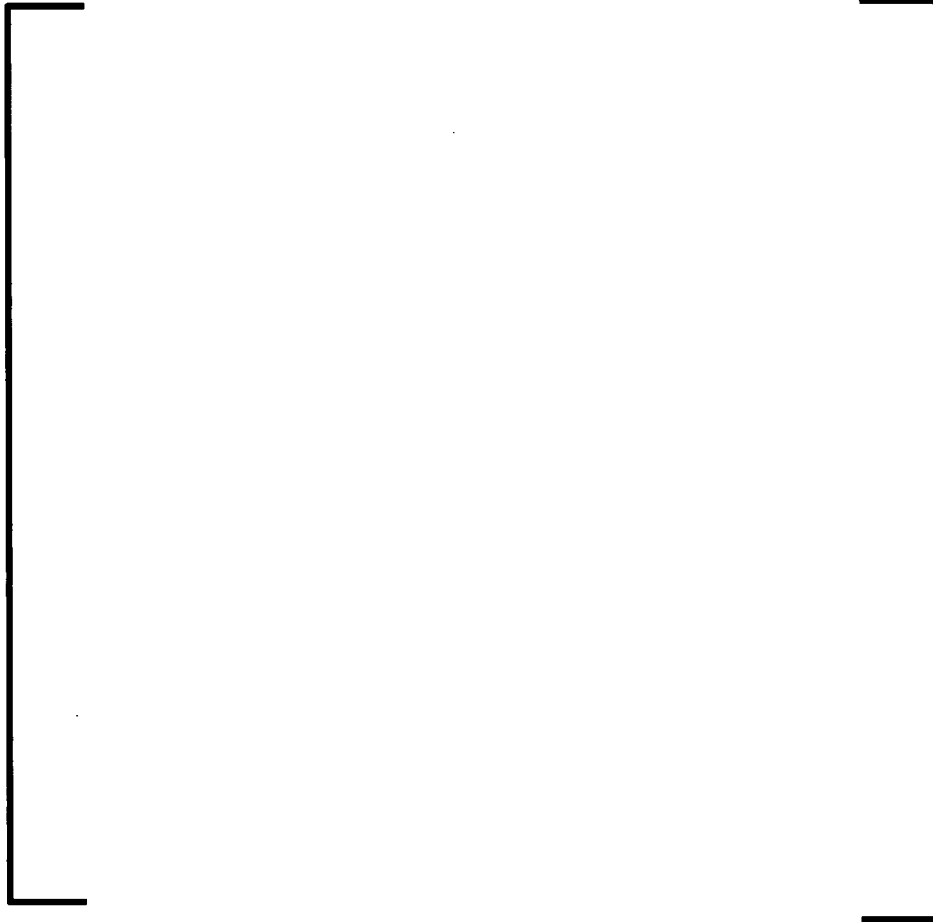
C.3 *The BHTP CHF Correlation*

Section C.3 addresses the acceptability of the BHTP CHF correlation with COBRA-FLX local conditions. The correlation was approved for application to the HTP fuel design using LYNXT local conditions in Reference C-9. The correlation application ranges with LYNXT were extended in Revision 1 of the topical report in Reference C-10. The BHTP correlation was based on the same 1481 CHF test points used earlier to develop the HTP CHF correlation (Reference C-11) for use with the thermal-hydraulic subchannel code XCOBRA-IIIC (Reference C-12). A COBRA-FLX based CHF Design Limit was determined in accordance to Standard Review Plan requirements (Reference C-3) and followed the method described in the BHTP topical report. The verification of the acceptability for using BHTP with COBRA-FLX is based on the adequacy of the correlation to represent the data base.

C.3.1 *Predicted to Measured CHF Performance*

The 1481 test points were evaluated using COBRA-FLX to determine the predicted to measured CHF performance of the present BHTP CHF correlation. The P/M values were examined for each independent variable and no biases were found to be introduced. The P/M values are shown in Figure C-4 along with the [] limits that are later justified in this section.

Figure C-4: Predicted CHF versus Measured CHF for the BHTP CHF Correlation Using COBRA-FLX



A histogram of the P/M CHF values for the [] data points using COBRA-FLX is shown in Figure C-5. A normal distribution is provided for comparison.

The BHTP correlation application range was extended using [] data points as discussed in Section A.3.1 of Reference C-10 with the LYNXT code. These same [] data points were examined using COBRA-FLX and the trends observed were found to be comparable to those obtained using LYNXT. Whereas the LYNXT based BHTP predictions for the range extension were found to be about [] conservative, the COBRA-FLX based predictions were found to be about [] conservative.

Therefore, the extension justification is demonstrated through the comparable behavior of the COBRA-FLX predictions.

Figure C-5: Histogram of Predicted to Measured Values for the BHTP CHF Correlation Using COBRA-FLX



C.3.2 Statistical Design Limit

The design limit for departure from nucleate boiling ratio (DNBRL) was calculated to protect 95 percent of the hot pins in the core with 95 percent confidence from departure of nucleate boiling. The DNBRL value based on COBRA-FLX was determined using the same process in the BHTP topical report.

Using Sommerville theory (Reference C-6) for a distribution-free method, the DNBRL was found to be [] for a 95/95 criteria. [

] Table C-3 provides a comparison of the COBRA-FLX based and LYNXT based DNBRL values.

Table C-3: Comparison of COBRA-FLX Based and LYNXT Based DNBRL Values for the BHTP CHF Correlation

| | |
|--|--|
| | |
|--|--|

No changes are needed in the form or coefficients of the existing BHTP CHF correlation, as defined in Section 2 of Reference C-9, when applied with the DNBR Design Limit of [] using COBRA-FLX local conditions for the HTP fuel design.

C.3.3 Ranges and Limitations

The extension of the BHTP application ranges for system pressure, mass velocity, and thermodynamic quality using LYNXT is discussed in Reference C-10. The use of COBRA-FLX local conditions does not alter the conclusions reached for supporting the range extensions, therefore, the BHTP extensions remain applicable when using COBRA-FLX. Since the mass velocity and thermodynamic quality are code dependent, the values below reflect the use of COBRA-FLX.

Local Conditions:

Pressure: 1385 to 2425 psia

Local Mass Velocity : 0.500 to 3.577 Mlb/hr-ft²

Local Thermodynamic Quality at CHF: up to 51%

Inlet Enthalpy: 383.9 to 644.6 Btu/lb (original range)

258.3 to 644.6 Btu/lb (including range extension)

Fuel Design:

Spacer Grid Type: HTP

Fuel Rod Diameter: 0.360 to 0.440 inches

Fuel Rod Pitch: 0.496 to 0.580 inches

Axial Spacer Span: 10.5 to 26.2 inches

Hydraulic Diameter: 0.4571 to 0.5334 inches

Heated Length: 9.8 to 14.0 feet

Application:

Code: COBRA-FLX

DNBRL: 1.124

C.4 The BWU-Z CHF Correlation for Mark-BW17 Fuel with MSMGs

Section C.4 addresses the acceptability of using the BWU-Z CHF correlation for mid-span mixing grids (MSMGs) with COBRA-FLX local conditions. The BWU-Z correlation is one of several correlations documented in the series of topical reports, (References C-13, C-14, C-15, and C-16) that use the BWU correlation form as shown in Table C-4. This particular BWU-Z correlation is supported by unit cell and guide tube cell CHF test data from Reference C-13 and additional guide tube cell data from Reference C-15. The BWU-Z correlation coefficients are shown in Table 3-1, page 3-5 of Reference C-13 and is supplemented with a [] factor, F_{MSM} from Reference C-15, []

]

Table C-4: Description of CHF Correlation Bases Using the BWU Correlation Form within the BAW-10199 Topical Report Revisions

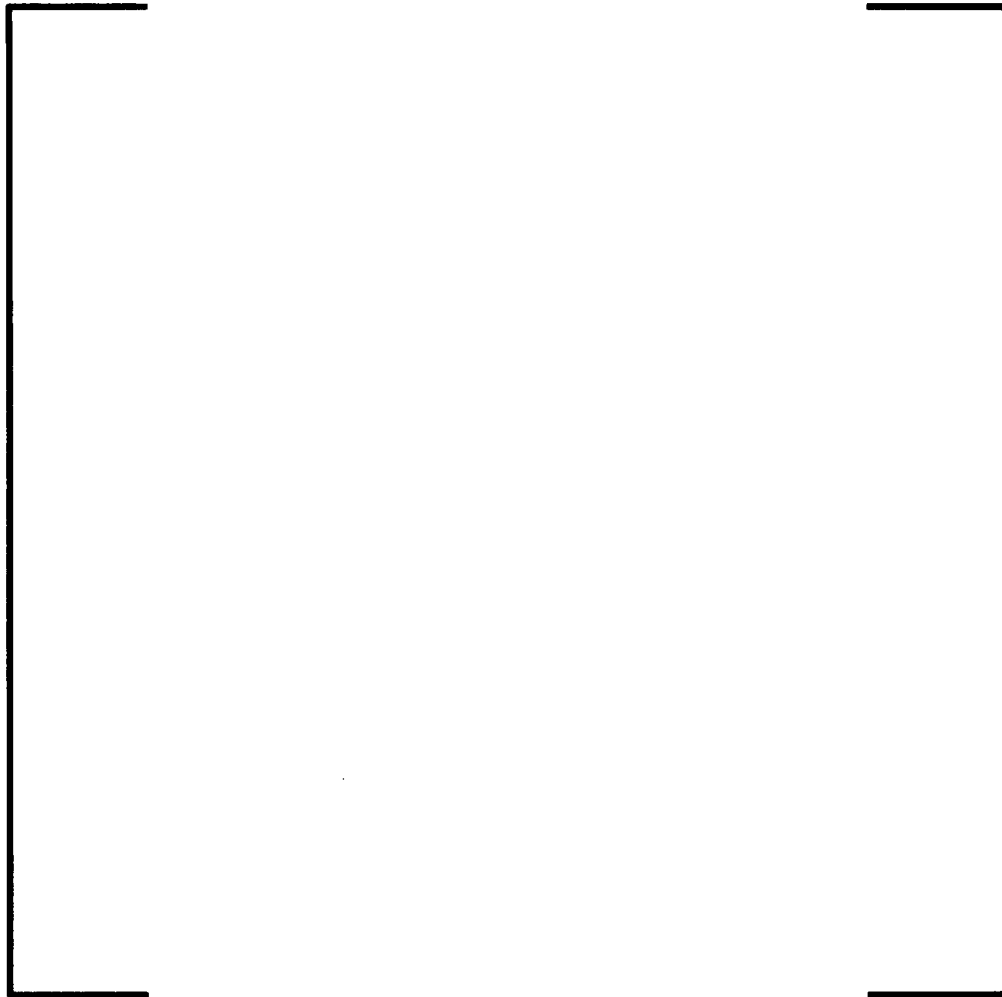
| Reference | Content | SER Date | Correlations | Approved Application |
|-----------|-------------|------------------|-------------------------|--|
| C-13 | Base Report | April 5, 1996 | BWU-I BWU-N BWU-Z | Inconel mixing vane grid or equivalent Non-mixing vane grids Mark-BW17 |
| C-14 | Addendum 1 | April 6, 2000 | BWU-Z | Mark-B11 with F_{B11} Value |
| C-15 | Addendum 2 | March 27, 2002 | BWU-Z | Mark-BW17 with MSMGs with F_{MSM} Value |
| C-16 | Addendum 3 | November 9, 2005 | BWU-Z | Mark-B11 specific correlation, BWU-B11R |

The BWU-Z CHF correlation for MSMGs was justified using a [] test point data base composed of two CHF tests with [] and [] data points, respectively as discussed in the SER of Reference C-15.

C.4.1 Measured to Predicted CHF Performance

The [] test points were evaluated using COBRA-FLX to determine the measured to predicted CHF performance of the present BWU-Z CHF correlation for MSMGs. The M/P values were examined for each independent variable and no biases were found to be introduced. The M/P values are shown in Figure C-6 along with the [] limits that are later justified in this section.

Figure C-6: Measured CHF versus Predicted CHF for the BWU-Z CHF Correlation for Mark-BW17 Fuel with Mid-Span Mixing Grids Using COBRA-FLX



A histogram of the M/P CHF values for the [] data points using COBRA-FLX is shown in Figure C-7. The normality of the distribution is acceptable at a [] level.

Figure C-7: Histogram of Measured to Predicted Values for the BWU-Z CHF Correlation for Mark-BW17 Fuel with Mid-Span Mixing Grids Using COBRA-FLX



C.4.2 Statistical Design Limit

The design limit for departure from nucleate boiling ratio (DNBRL) was calculated to protect 95 percent of the hot pins in the core with 95 percent confidence from departure of nucleate boiling. The DNBRL value based on COBRA-FLX was determined using the same process in the BWU topical report (Reference C-15) for MSMGs.

Using Owen (Reference C-5) the DNBRL was computed to be [] where:

n : [], number of data in the correlation data base

N : [], degrees of freedom, $n-1$

M/P: [], average measured to predicted CHF

$S(M/P,N)$: [], standard deviation of the M/P distribution

$K_{95/95}$ ([]): [], one-sided tolerance factor, (Reference C-5)

then,

$$DNBRL = 1.0 / [M/P - (K_{95/95} * S)] = [], \text{ based on Owen}$$

The application of the BWU-Z CHF correlation for MSMGs would remain the same for the application of the F_{MSM} value when applied to the BWU-Z CHF correlation as discussed on page F-5 of Addendum 2 of Reference C-15 and as follows.

[]

The terms [] are as defined for BWU-Z in Table 3-1 of Reference C-13.

The DNBRL value of [] for COBRA-FLX applications. No changes are needed in the form (Section 1.4 of Reference C-13) or coefficients of the existing BWU-Z CHF correlation for MSMGs, shown in Table 3-1, page 3-5 of Reference C-13 and F_{MSM} value of [] of page F-5 of Reference C-13, when applied with the [] DNBR Design Limit using COBRA-FLX local conditions for pressures greater than 594 psia. []

Table C-5 provides a comparison of the COBRA-FLX based and LYNXT based DNBRL values.

Table C-5: Comparison of COBRA-FLX based and LYNXT based DNBRL Values for the BWU-Z CHF Correlation for the Mark-BW17 Fuel with Mid-Span Mixing Grids

C.4.3 Ranges and Limitations

The ranges and limitations of the BWU-Z CHF correlation for the Mark-BW17 fuel with MSMGs from the LYNXT based SER in Reference C-15 will be maintained with the exceptions where the use of COBRA-FLX local conditions warrant a change for local conditions and the DNBRL values.

Local Conditions:

Pressure: 400 to 2465 psia

Mass Velocity : 0.469 to 3.459 Mlb/hr-ft²

Thermodynamic Quality at CHF: up to 70%

Fuel Design:

Spacer Grid Type: AREVA Mark-BW17

Unit Cell and Guide Tube Cell application

Application:

Code: COBRA-FLX

DNBRL: 1.19 for Pressure > 594 psia

1.66 for $400 \leq$ Pressure \leq 594 psia

C.5 The BWU-Z CHF Correlation for Mark-BW17 Fuel

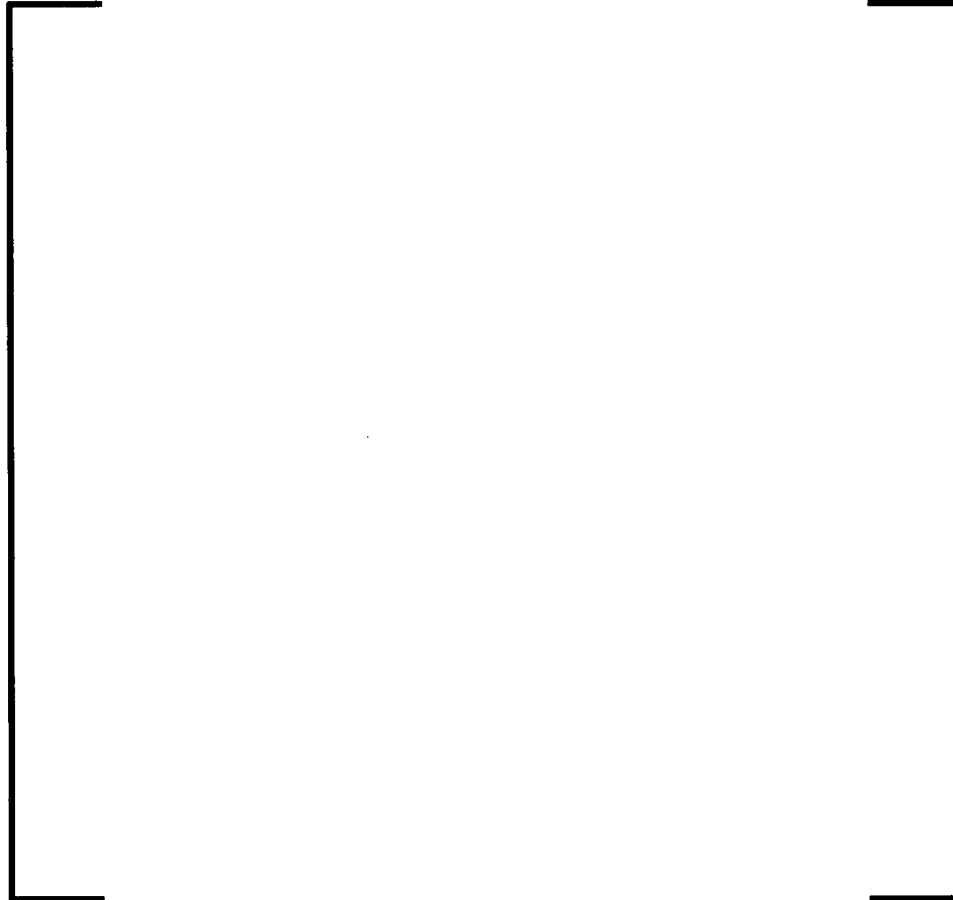
Section C.5 addresses the acceptability of using the BWU-Z CHF correlation for the Mark-BW17 fuel design without MSMGs, labeled only as Mark-BW17. The verification of the acceptability for using BWU-Z, from Reference C-13, with COBRA-FLX is based on the adequacy of the correlation to represent its data base. COBRA-FLX based CHF Design Limits were determined in accordance to Standard Review Plan requirements (Reference C-3) and followed the method described in the BWU topical report.

The BWU-Z correlation is based on the BWU correlation form (discussed in Section 1.4 of Reference C-13) and uses the coefficients shown in Table 3-1, page 3-5 of Reference C-13. The BWU-Z CHF correlation is based on a [] test point data base and possesses DNBR Design Limits that are associated with specific pressure ranges. The response to a Request for Additional Information (RAI) on page D-5 of Reference C-13 provides information regarding the process to define these respective DNBR Design Limits for LYNXT. The determination of the respective DNBR Design Limits using COBRA-FLX local conditions follows the same process.

C.5.1 Measured to Predicted CHF Performance

The [] test points were evaluated using COBRA-FLX to determine the measured-to-predicted CHF performance of the present BWU-Z CHF correlation. The M/P values were examined for each independent variable and no biases were found to be introduced. The M/P values are shown in Figure C-8 along with the [] limits that are later justified in this section.

Figure C-8: Measured CHF versus Predicted CHF for the BWU-Z CHF Correlation for Mark-BW17 Fuel Using COBRA-FLX



A histogram of the M/P CHF values for the [] data points using COBRA-FLX is shown in Figure C-9. The normality of the distribution is acceptable for applying the one-sided tolerance theory of Owen.

Figure C-9: Histogram of Measured to Predicted Values for the BWU-Z CHF Correlation for Mark-BW17 Fuel Using COBRA-FLX



C.5.2 Statistical Design Limit

The design limit for departure from nucleate boiling ratio (DNBRL) was calculated to protect 95 percent of the hot pins in the core with 95 percent confidence from departure of nucleate boiling. The DNBRL value based on COBRA-FLX was determined using the same process in the BWU topical report (Reference C-13) for the BWU-Z CHF correlation for Mark-BW17 fuel.

Using Owen (Reference C-5), the DNBRL was found to be [] for the entire data base where:

n : [], number of data in the correlation data base

N : [], degrees of freedom, []

M/P : [], average measured to predicted CHF

σ_N : [], standard deviation of the M/P distribution corrected for N

K ([]) : [], one-sided tolerance factor, (Reference C-5)

then,

$$DNBRL = 1.0 / [M/P - (K_{95/95} * \sigma_N)] = [\quad]$$

The approved DNBRL values using LYNXT were determined for specific pressure ranges and are discussed in the response to a RAI on page D-5 of Reference C-13. The DNBRL values for COBRA-FLX application, in Table C-6 and based on the values in Table C-5, have been selected to correspond to the same pressure ranges as defined for LYNXT. The “imposed” pressure ranges reflect the application range as defined by the limits of the data base from 400 to 2465 psia. The LYNXT based DNBRL values are provided for comparison in Table C-6.

Table C-6: Individual DNBRL Calculated for Each Pressure Group with the BWU-Z CHF Correlation for the Mark-BW17 Fuel Using COBRA-FLX

| |
|--|
| |
|--|

Table C-7: Pressure Range Dependent Design Limits for the BWU-Z CHF Correlation for the Mark-BW17 Fuel Using COBRA-FLX and LYNXT

| |
|--|
| |
|--|

No changes are needed in the form (Section 1.4 of Reference C-13) or coefficients of the existing BWU-Z CHF correlation (from Table 3-1, page 3-5 of Reference C-13) when

applied with the imposed DNBR Design Limits from Table C-6 using COBRA-FLX local conditions.

C.5.3 Ranges and Limitations

The ranges and limitations of the BWU-Z CHF correlation for the Mark-BW17 fuel from the LYNXT based SER in Reference C-15 will be maintained with the exceptions where the use of COBRA-FLX local conditions warrant a change for local conditions and the DNBR values.

Local Conditions:

Pressure: 400 to 2465 psia
Mass Velocity : 0.328 to 3.535 Mlb/hr-ft²
Thermodynamic Quality at CHF: up to 75%

Fuel Design:

Spacer Grid Type: AREVA Mark-BW17

Application:

Code: COBRA-FLX
DNBR: 1.20 for $1000 < \text{Pressure} \leq 2465$ psia
1.18 for $700 < \text{Pressure} \leq 1000$ psia
1.66 for $400 \leq \text{Pressure} \leq 700$ psia

C.6 The BWCMV-A CHF Correlation

Section C.6 addresses the acceptability of the BWCMV-A CHF correlation with COBRA-FLX local conditions. The correlation was approved for application to the Mark-BW17 fuel assembly design. The correlation was developed using [] CHF test points and is justified in the topical report (Reference C-17). A COBRA-FLX based CHF Design Limit was determined in accordance to Standard Review Plan requirements (Reference C-3) and followed the method described in the BWCMV-A topical report.

[

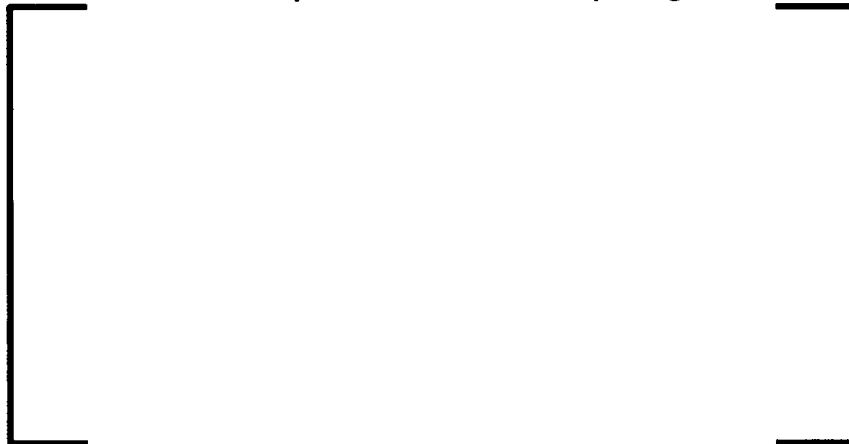
] The measured CHF performance of the Mark-BW17 spacer grid was significantly higher than the performance predicted with the BWCMV CHF correlation as defined in Reference C-18. []

[

]

The verification of the acceptability for using BWCMV-A with COBRA-FLX is based on the adequacy of the correlation to represent the [] point data base reflecting the final [] tests for the Mark-BW17 data base shown in Table 3-4, page 3-10, of Reference C-17 and shown below in Table C-8.

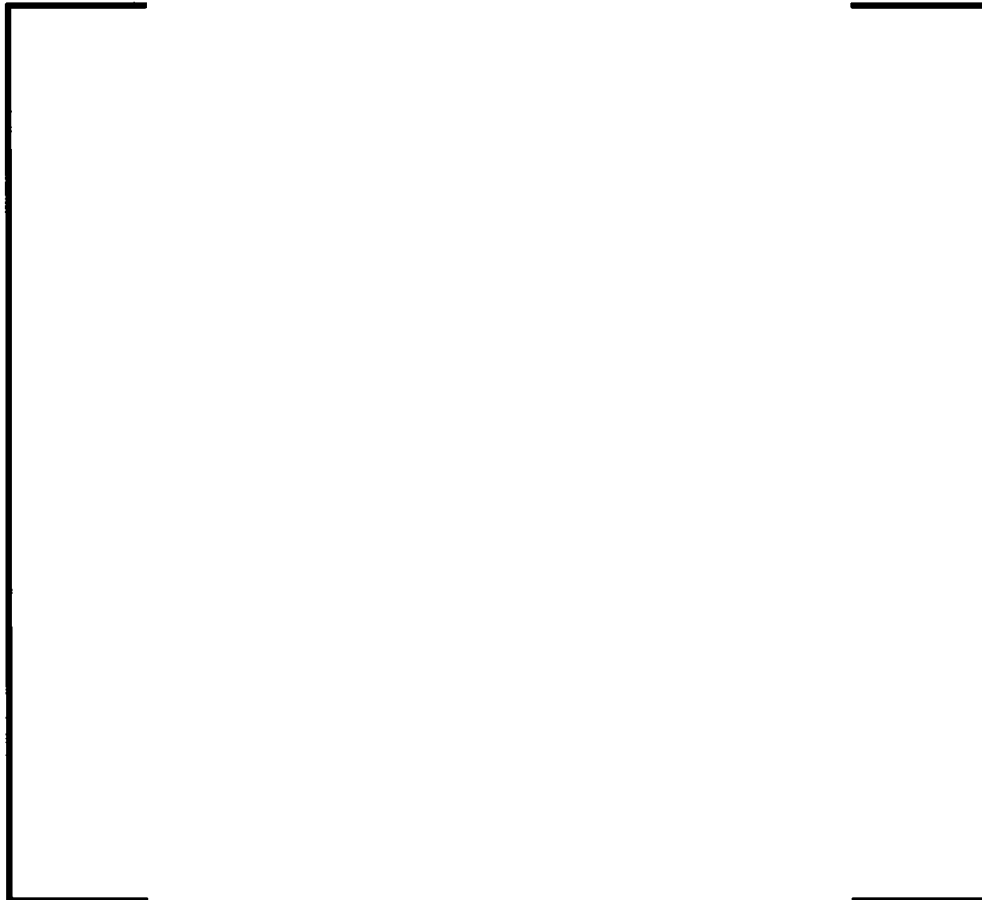
Table C-8: Mark-BW17 Test Program Supporting the BWCMV-A Correlation and the Optimal Effective Grid Spacing



C.6.1 Measured to Predicted CHF Performance

The [] test points were evaluated using COBRA-FLX to determine the measured-to-predicted CHF performance of the present BWCMV-A CHF correlation. The M/P values were examined for each independent variable and no biases were found to be introduced. The M/P values are shown in Figure C-10 along with the [] limits that are later justified in this section.

Figure C-10: Measured CHF versus Predicted CHF for the BWCMV-A CHF Correlation Using COBRA-FLX



A histogram of the M/P CHF values for the [] data points using COBRA-FLX is shown in Figure C-11. The normality of the distribution is acceptable using the D prime test to support the application of the tolerance theory of Owen.

Figure C-11: Histogram of Measured to Predicted Values for the BWCMV-A CHF Correlation Using COBRA-FLX



C.6.2 Statistical Design Limit

The design limit for departure from nucleate boiling ratio (DNBRL) was calculated to protect 95 percent of the hot pins in the core with 95 percent confidence from departure of nucleate boiling. The DNBRL value based on COBRA-FLX was determined using the same process in the BWCMV-A topical report.

Using Owen (Reference C-5), the DNBRL was found to be [] for the entire data base where:

n : [], number of data in the correlation data base

N : [], degrees of freedom

M/P : [], average measured to predicted CHF

$\sigma_{M/P}$: [], standard deviation of the M/P distribution

K ([]) : [], one-sided tolerance factor, (Reference C-5)

then,

$$DNBRL = 1.0 / [M/P - (K_{95/95} * \sigma_{M/P})] = [\quad]$$

No changes are needed in the form or coefficients of the existing BWCMV-A CHF correlation (Section 3 of Reference C-17) when applied with the DNBR Design Limit of [] using COBRA-FLX local conditions for the Mark-BW17 fuel design with and without MSMGs. Table C-9 provides a comparison of the COBRA-FLX based and LYNXT based DNBRL values.

Table C-9: Comparison of COBRA-FLX based and LYNXT based DNBRL Values for the BWCMV-A CHF Correlation

| | |
|--|--|
| | |
|--|--|

C.6.3 Ranges and Limitations

The ranges and limitations of the BWCMV-A CHF correlation from the LYNXT based SER in Reference C-18 will be maintained with the exceptions where the use of COBRA-FLX local conditions warrant a change for local conditions and the DNBRL value

Local Conditions:

- Pressure: 1475 to 2465 psia
- Mass Velocity : 0.900 to 3.535 Mlb/hr-ft²
- Thermodynamic Quality at CHF: <27%

Fuel Design:

- Spacer Grid Type: Mark-BW17
- Hydraulic Diameter: 0.3747 to 0.4637 inches
- Effective Spacing
 - Main Grids []
 - Mid-Span Mixing Grids []

Application:

- Code: COBRA-FLX
- DNBRL: 1.21

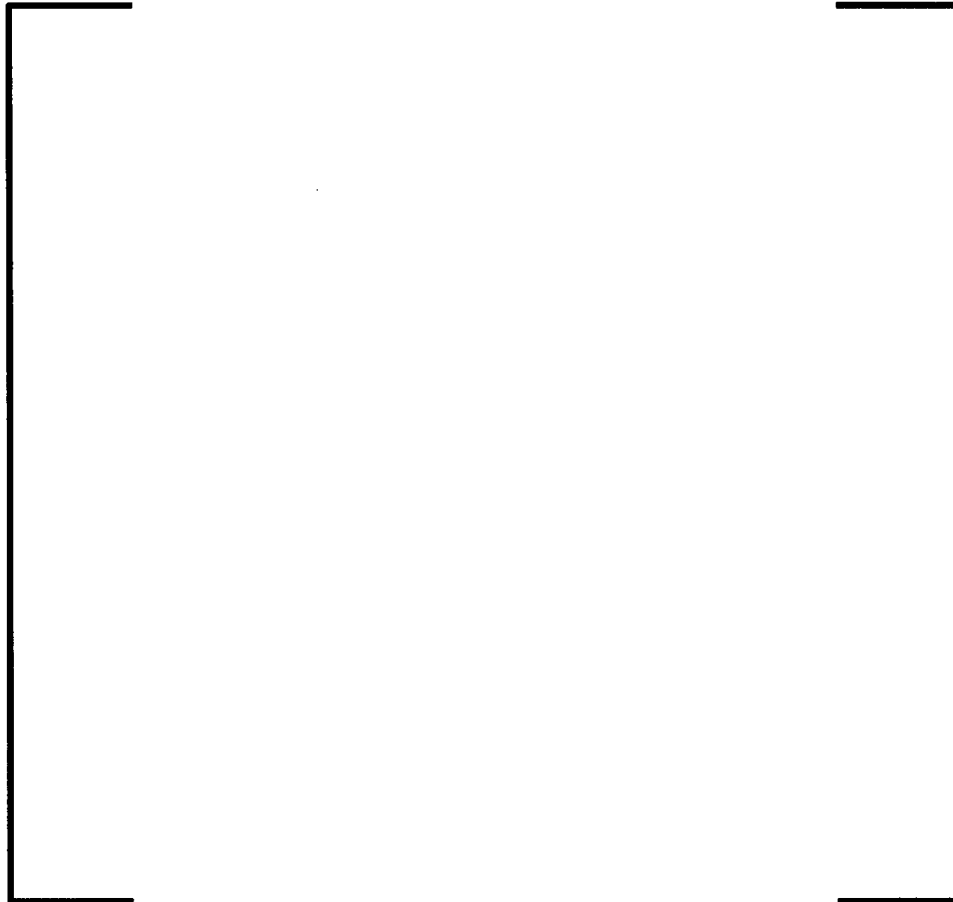
C.7 The BWCMV CHF Correlation

Section C.7 addresses the acceptability of the BWCMV CHF correlation with COBRA-FLX local conditions. The correlation was approved for application to AREVA fuel for 15x15 and 17x17 geometries and the Westinghouse Optimized Fuel Assembly (OFA) design. The correlation was developed using [] CHF test points and is justified in the BWCMV topical report (Reference C-18). The verification of the acceptability for using BWCMV with COBRA-FLX is based on the adequacy of the correlation to represent the CHF test data base. A COBRA-FLX based CHF Design Limit was determined in accordance to Standard Review Plan requirements (Reference C-3) and following the method described in the BWCMV topical report.

C.7.1 Measured to Predicted CHF Performance

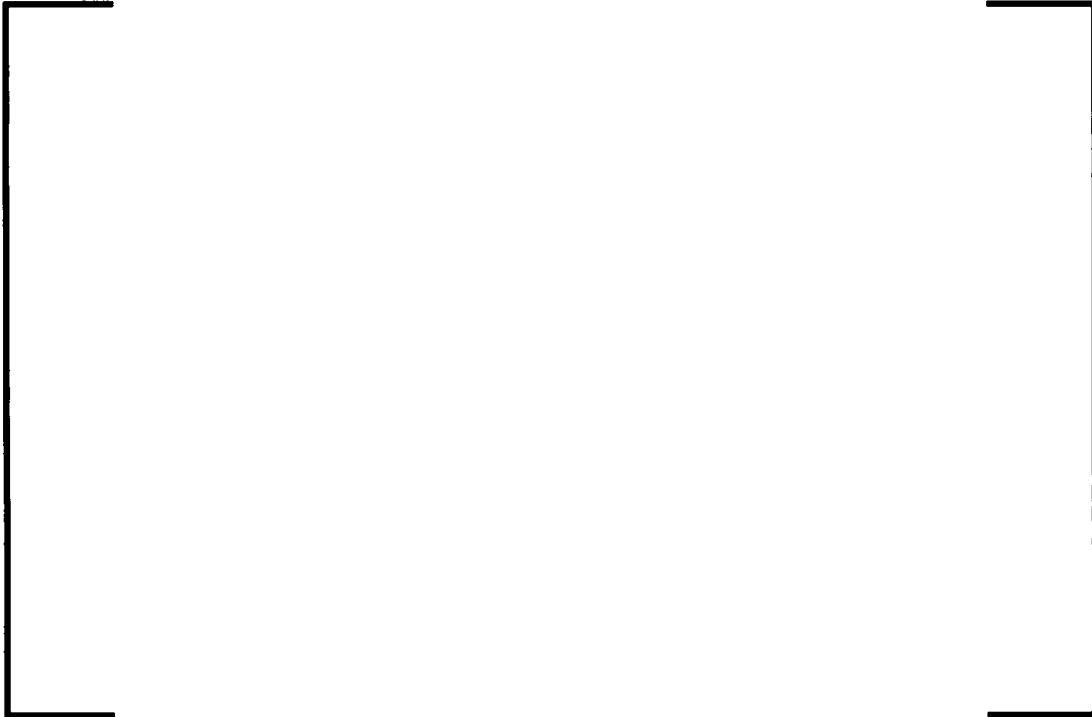
The [] test points were evaluated using COBRA-FLX to determine the measured to predicted CHF performance of the present BWCMV CHF correlation. The M/P values were examined for each independent variable and no biases were found to be introduced. The M/P values are shown in Figure C-12 along with the [] limits that are later justified in this section.

Figure C-12: Measured CHF versus Predicted CHF for the BWCMV CHF Correlation Using COBRA-FLX



A histogram of the M/P CHF values for the [] data points using COBRA-FLX is shown in Figure C-13. The normality of the distribution is acceptable using the D prime test to support the application of the tolerance theory of Owen.

Figure C-13: Histogram of Measured to Predicted Values for the BWCMV CHF Correlation Using COBRA-FLX



C.7.2 Statistical Design Limit

The design limit for departure from nucleate boiling ratio (DNBRL) was calculated to protect 95 percent of the hot pins in the core with 95 percent confidence from departure of nucleate boiling. The DNBRL value based on COBRA-FLX was determined using the same process in the topical report for the BWCMV CHF correlation.

Using Owen (Reference C-5), the DNBRL was found to be [] for the entire data base where:

n : [], number of data in the correlation data base

N : [], degrees of freedom, []

M/P : [], average measured to predicted CHF

$\sigma_{M/P}$: [], standard deviation of the M/P distribution corrected for N

K ([]) : [], one-sided tolerance factor, (Reference C-5)

then,

$$\text{DNBRL} = 1.0 / [M/P - (K_{95/95} * \sigma_{M/P})] = [\quad]$$

No changes are needed in the form or coefficients of the existing BWCMV CHF correlation (Section 4.3 of Reference C-18) when applied with the DNBR Design Limit of [] using COBRA-FLX local conditions for mixing vane fuel. Table C-10 provides a comparison of the COBRA-FLX based and LYNX2 based DNBRL values.

Table C-10: Comparison of COBRA-FLX based and LYNX2 based DNBRL Values for the BWCMV CHF Correlation

| | |
|--|--|
| | |
|--|--|

C.7.3 Ranges and Limitations

The ranges and limitations of the BWCMV CHF correlation for mixing vanned fuel designs from the LYNX2 based SER in Reference C-19 will be maintained with the exceptions where the use of COBRA-FLX local conditions warrant a change for local conditions and the DNBRL value. The BWCMV correlation was approved specifically for the AREVA fuel for 15x15 and 17x17 geometries and the Westinghouse Optimized Fuel Assembly (OFA) design.

Local Conditions:

Pressure: 1485 to 2455 psia
Mass Velocity : 0.981 to 3.672 Mlb/hr-ft²
Thermodynamic Quality at CHF: -22 to +22%

Fuel Design:

Spacer Grid Type: Mixing Vane Grid
Hydraulic Diameter: 0.3747 to 0.5335 inches
Heated Length: 96 to 168 inches
Spacer Grid Spacing: 13 to 32 inches

Application:

Code: COBRA-FLX
DNBRL: 1.22

C.8 The BWU-N CHF Correlation

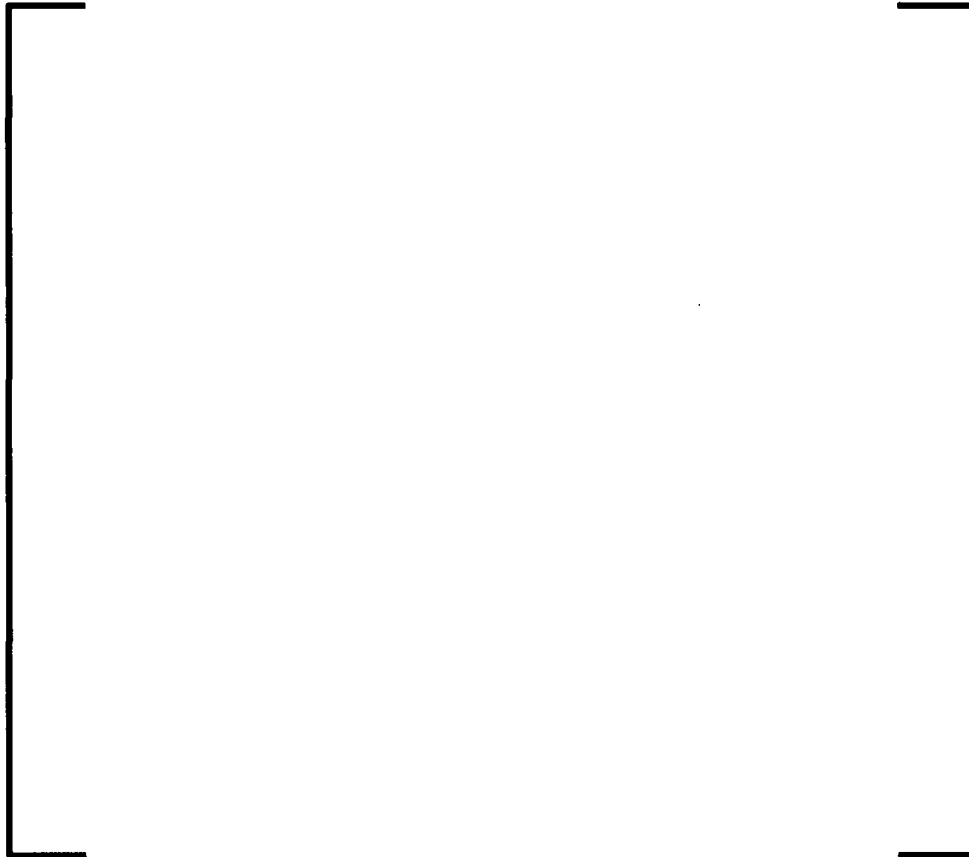
Section C.8 addresses the acceptability of using the BWU-N CHF correlation for non-mixing varied fuel. The verification of the acceptability for using BWU-N (Reference C-13) with COBRA-FLX is based on the adequacy of the correlation to represent the BWU-N data base. COBRA-FLX based CHF Design Limits were determined in accordance to Standard Review Plan requirements (Reference C-3) and followed the method described in the BWU topical report.

The BWU-N correlation is based on the BWU correlation form (discussed in Section 1.4 of Reference C-13) and uses the coefficients shown in Table 3-1, page 3-5 of Reference C-13. The correlation is based on a [] test point data base and possesses DNBR Design Limits that are associated with specific pressure ranges. A re-examination of the CHF test data base with COBRA-FLX revealed that the 1094 point data base contained [] duplicate test points, therefore, the actual data base is composed of just [] test points. Consequently, the validation of the BWU-N correlation for application with COBRA-FLX is shown using only the [] data points. The response to a Request for Additional Information (RAI) on page D-5 of Reference C-13 provides information regarding the process to define these respective DNBR Design Limits for LYNX2. The determination of the respective DNBR Design Limits using COBRA-FLX local conditions follows the same process.

C.8.1 Measured to Predicted CHF Performance

The [] test points were evaluated using COBRA-FLX to determine the measured to predicted CHF performance of the present BWU-N CHF correlation. The M/P values were examined for each independent variable and no biases were found to be introduced. The M/P values are shown in Figure C-14 along with the [] limits that are later justified in this section.

Figure C-14: Predicted CHF versus Measured CHF for the BWU-N CHF Correlation for Non-Mixing Grid Fuel Using COBRA-FLX



A histogram of the M/P CHF values for the [] data points using COBRA-FLX is shown in Figure C-15. The normality of the distribution is acceptable using the D prime test to support the application of the tolerance theory of Owen.

Figure C-15: Histogram of Measure to Predicted Values for the BWU-N CHF Correlation for Non-Mixing Vaned Fuel Using COBRA-FLX



C.8.2 Statistical Design Limit

The design limit for departure from nucleate boiling ratio (DNBRL) was calculated to protect 95 percent of the hot pins in the core with 95 percent confidence from departure of nucleate boiling. The DNBRL value based on COBRA-FLX was determined using the same process in the BWU topical report (Reference C-13) for the BWU-N CHF correlation.

Using Owen (Reference C-5), the DNBRL was found to be [] for the entire data base where:

n : [], number of data in the correlation data base

N : [], degrees of freedom, []

M/P : [], average measured to predicted CHF

σ_N : [], standard deviation of the M/P distribution corrected for N

$K([] : [])$, one-sided tolerance factor, (Reference C-5)

then,

$$DNBRL = 1.0 / [M/P - (K_{95/95} * \sigma_N)] = []$$

The approved DNBRL values using LYNXT were determined for specific pressure ranges and are discussed in the response to a RAI on page D-5 of Reference C-13. The COBRA-FLX based DNBRL values were determined in the same manner and are shown in Table C-11. The DNBRL values for COBRA-FLX application, shown in Table C-13, are selected to correspond to the same pressure ranges as defined for LYNX2. Table C-12 is provided with the statistics associated with the original LYNX2 basis. The "imposed" pressure ranges reflect the application range as defined by the limits of the data base from []. The LYNX2 based DNBRL values are provided for comparison in Table C-13.

Table C-11: Individual DNBRL Calculated for Each Pressure Group with the BWU-N CHF Correlation for Non-Mixing Grids Using COBRA-FLX

| |
|--|
| |
|--|

Table C-12: Individual DNBRL Calculated for Each Pressure Group with the BWU-N CHF Correlation for Non-Mixing Grids Using LYNX2

| |
|--|
| |
|--|

Table C-13: Pressure Range Dependent Design Limits for the BWU-N CHF Correlation for Non-Mixing Grids Using COBRA-FLX and LYNX2



The comparison of Design Limits between COBRA-FLX and LYNX2 in Table C-13 shows some of the largest differences observed in the CHF correlation validation using COBRA-FLX. The casual factors for the larger differences are the following:



The grid intersection CHF test bundle exhibits higher subchannel hydraulic resistances in the wall and corner subchannels (subchannels along the perimeter of a fuel assembly) than those of the grid interior subchannels. This fact has been shared with the NRC during the review of the BWC CHF correlation (page 16-B-14 of Reference C-19) where data from this grid intersection test were initially introduced in a reviewed correlation. This test configuration results in higher crossflow from wall and corner subchannels with the higher powered heater rods than would typically occur for a unit cell test from the higher power heater rod region. The significance of this particular geometry and hydraulic resistance weighs more in the mid-pressure and low-pressure groups for BWU-N as shown in Table C-14.

Table C-14: Influence of the Grid Intersection CHF Test on the BWU-N Data Base



COBRA-FLX's response to this particular test geometry with its [] results in higher M/P values yielding an average M/P notably higher than the average M/P obtained from using LYNX2 local conditions as seen when comparing results between Table C-11 and Table C-12. The standard deviations of the M/P values using COBRA-FLX local conditions were comparable to those obtained using LYNX2 local conditions.

No changes are needed in the form (Section 1.4 of Reference C-13) or coefficients of the existing BWU-N CHF correlation (Table 3-1 of Reference C-13) when applied with the imposed DNBR Design Limits from Table C-13 using COBRA-FLX local conditions.

C.8.3 Ranges and Limitations

The ranges and limitations of the BWU-N CHF correlation for non-mixing vanned fuel from the LYNXT based SER in Reference C-13 will be maintained with the exceptions where the use of COBRA-FLX local conditions warrant a change for local conditions and the DNBRL values.

Local Conditions:

Pressure: 788 to 2616 psia

Mass Velocity : 0.267 to 3.686 Mlb/hr-ft²

Thermodynamic Quality at CHF: less than 70%

Fuel Design:

Spacer Grid Type: Non-mixing Grids

Application:

Code: COBRA-FLX

DNBRL: 1.16 for $1500 < \text{Pressure} \leq 2400$ psia1.16 for $1200 < \text{Pressure} \leq 1500$ psia1.29 for $800 \leq \text{Pressure} \leq 1200$ psia**C.9 The BWC CHF Correlation for 15x15 Geometry**

Section C.9 addresses the acceptability of the BWC CHF correlation for 15x15 geometry with COBRA-FLX local conditions. The BWC correlation was developed in Part 1 of Reference C-19 using 17x17 geometry fuel assemblies with zircaloy spacer grids. The applicability of the correlation to predict the CHF performance for 15x15 geometry fuel assemblies with zircaloy spacer grids was justified in Part 2 of Reference C-19. The 15x15 geometry data base consists of [] CHF test points from three CHF tests representing the guide tube cell geometry, unit cell geometry, and the geometry representing the intersection of four assemblies.

The BWC CHF correlation was initially developed using the LYNX2 thermal-hydraulic subchannel code (Reference C-20). The correlation was extended for application using the LYNXT code in the response to RAI Question 8 in Section E of Reference C-1. The extension of the BWC correlation for COBRA-FLX application on 15x15 geometry only is demonstrated below by examination of the correlation's ability to predict the [] CHF test point data base for the 15x15 geometry fuel. A COBRA-FLX based CHF Design Limit was also determined in accordance to Standard Review Plan requirements (Reference C-3) and following the method described in the BWC topical report.

C.9.1 Measured to Predicted CHF Performance

The [] test points were evaluated using COBRA-FLX to determine the measured to predicted CHF performance of the present BWC CHF correlation. The M/P values were examined for each independent variable and no biases were found to be introduced. The M/P values are shown in Figure C-16 along with the [] limits that are later justified in this section.

**Figure C-16: Predicted CHF versus Measured CHF for the BWC CHF
Correlation for 15x15 Geometry Fuel Using COBRA-FLX**



A histogram of the M/P CHF values for the [] data points using COBRA-FLX is shown in Figure C-17. The normality of the distribution is acceptable using the D prime test to support the application of the tolerance theory of Owen.

Figure C-17: Histogram of Measure to Predicted Values for the BWC CHF Correlation for 15x15 Geometry Fuel Using COBRA-FLX



C.9.2 Statistical Design Limit

The design limit for departure from nucleate boiling ratio (DNBRL, or CHF_{RL} value for BWC) was calculated to protect 95 percent of the hot pins in the core with 95 percent confidence from departure of nucleate boiling. The DNBRL value based on COBRA-FLX was determined using the same process in the BWC topical report.

Using Owen (Reference C-5), the CHFRL was found to be [] for the 15x15 geometry fuel where:

n : [], number of data in the 15x15 geometry data base

N : [], degrees of freedom

M/P : [], average measured to predicted CHF

$\sigma_{M/P}$: [], standard deviation of the M/P distribution

K [] : [], one-sided tolerance factor, (Reference C-5)

then,

$$CHF_{R_L} = 1.0 / [M/P - (K_{95/95} * \sigma_{M/P})] = []$$

No changes are needed in the form or coefficients of the existing BWC CHF correlation (Section 12 of Reference C-19) when applied with the DNBR Design Limit of [] using COBRA-FLX local conditions for the 15x15 geometry fuel with zircaloy grids. Table C-15 provides a comparison of the COBRA-FLX based and LYNXT based DNBRL values.

Table C-15: Comparison of COBRA-FLX based and LYNX2 based DNBRL Values for the BWC CHF Correlation

| | |
|--|--|
| | |
|--|--|

The average M/P value using COBRA-FLX local conditions is [] than the average M/P using the LYNX2 local conditions. The standard deviation is [] for COBRA-FLX than for LYNX2. The [] average M/P value for COBRA-FLX is a result of the grid intersection test previously discussed in Section C.8.2 for the BWU-N CHF correlation. The BWC CHF correlation utilized [] data points for the 15x15 Mark-BZ grid data base representing data for pressures [] and above whereas the BWU-N correlation utilized [] data points for pressure [] and above. The grid intersection CHF test composed [] (from Table C-16) of the data base of the BWC correlation and the Design Limit for BWC using COBRA-FLX was, therefore, also affected by the two casual factors discussed in Section C.8.2. The Design Limit response, a [], to these casual factors for BWC is

comparable to that observed for the Design Limit response for BWU-N, [

], within the common pressure range of approximately 1500 psia and above.

Table C-16: Proportion of the 15x15 BWC Data Base for Each Bundle Test Type



C.9.3 Ranges and Limitations

The ranges and limitations of the BWC CHF correlation for Mark-BZ fuel from the LYNXT based SER in Reference C-19 will be maintained with the exceptions where the use of COBRA-FLX local conditions warrant a change for local conditions and the DNBRL value.

Local Conditions:

Pressure: 1600 to 2600 psia

Mass Velocity : 0.414 to 3.648 Mlb/hr-ft²

Thermodynamic Quality at CHF: -20 to +27%

Fuel Design:

Mark-BZ 15x15 Fuel

Application:

Code: COBRA-FLX

DNBRL: 1.13

C.9.4 Local Conditions and Design Limits Summary

The range limits for the local conditions using COBRA-FLX are provided in Table C-17 along with the corresponding Design Limits.

**Table C-17: Local Conditions and Design Limits for Various Correlations
Using COBRA-FLX**

| CHF Correlation | Parameter | British Units | SI Units |
|------------------------|--|---|--|
| ACH-2 | Pressure Mass Velocity Thermodynamic Quality Design Limit | 284 – 2565 psia 0.950 – 3.061 Mlb/hr-ft ² < 37% 1.23 | 19.6 – 176.9 bar 1288.6 – 4150.8 kg/m ² -s < 37% 1.23 |
| BHTP | Pressure Mass Velocity Thermodynamic Quality Design Limit Inlet Enthalpy (original range) (extension range) | 1385 – 2425 psia 0.500 – 3.577 Mlb/hr-ft ² ≤ 51% 1.124 383.9 to 644.6 Btu/lbm 258.3 to 644.6 Btu/lbm | 95.5 – 167.2 bar 677.8 – 4851.6 kg/m ² -s ≤ 51% 1.124 892.9 to 1499.2 kJ/kg 600.8 to 1499.2 kJ/kg |
| BWU-Z with MSMGs | Pressure Mass Velocity Thermodynamic Quality Design Limits | 400 – 2465 psia 0.469 – 3.459 Mlb/hr-ft ² ≤ 70% 1.19, 594 – 2465 psia 1.66, 400 – 594 psia | 27.6 – 170.0 bar 636.2 – 4691.1 kg/m ² -s ≤ 70% 1.19, 41.0 – 170.0 bar 1.66, 27.6 – 41.0 bar |
| BWU-Z | Pressure Mass Velocity Thermodynamic Quality Design Limits | 400 – 2465 psia 0.328 – 3.535 Mlb/hr-ft ² < 75% 1.20, 1000 – 2465 psia 1.18, 700 – 1000 psia 1.66, 400 – 700 psia | 27.6 – 170.0 bar 444.7 – 4794.4 kg/m ² -s < 75% 1.20, 68.9 – 170.0 bar 1.18, 48.3 – 68.9 bar 1.66, 27.6 – 48.3 bar |
| BWCMV-A | Pressure Mass Velocity Thermodynamic Quality Design Limit | 1475 – 2465 psia 0.900 – 3.535 Mlb/hr-ft ² <27% 1.21 | 101.7 – 170.0 bar 1220.6 – 4794.4 kg/m ² -s <27% 1.21 |
| BWCMV | Pressure Mass Velocity Thermodynamic Quality Design Limit | 1485 – 2455 psia 0.981 – 3.672 Mlb/hr-ft ² -22 to +22% 1.22 | 102.4 – 169.3 bar 1330.7 – 4979.7 kg/m ² -s -22 to +22% 1.22 |
| BWU-N | Pressure Mass Velocity Thermodynamic Quality Design Limits | 788 – 2616 psia 0.267 – 3.686 Mlb/hr-ft ² < 70% 1.16, 1500 – 2400 psia 1.16, 1200 – 1500 psia 1.29, 800 – 1200 psia | 54.3 – 180.4 bar 362.8 – 4999.1 kg/m ² -s < 70% 1.16, 103.4 – 165.5 bar 1.16, 82.7 – 103.4 bar 1.29, 55.2 – 82.7 bar |
| BWC | Pressure Mass Velocity Thermodynamic Quality Design Limit | 1600 – 2600 psia 0.414 – 3.648 Mlb/hr-ft ² -20 to +27% 1.13 | 110.3 – 179.3 bar 562.1 – 4948.2 kg/m ² -s -20 to +27% 1.13 |

C.10 References

- C-1 BAW-10156-A, Rev. 1, LYNXT Core Transient Thermal-Hydraulic Program, B&W Fuel Company, August 1993.
- C-2 ANP-10269P-A, Revision 0, The ACH-2 CHF Correlation for the U.S. EPR, AREVA NP Inc., December 2007.
- C-3 NUREG-800, USNRC Standard Review Plan, U. S. Department of Energy.
- C-4 Bernard Ostle, Statistics in Research, Second Edition, The Iowa State University Press, 1963.
- C-5 D. B. Owen, Factors for One-Sided Tolerance Limits and for Variables Sampling Plans, Sandia Corporation Monograph (SRC-607), March 1963.
- C-6 Paul N. Sommerville, Tables for Obtaining Non-Parametric Tolerance Limits, Annals of Mathematical Statistics, Vol. 29, No. 2, June 1958, pp. 599-601.
- C-7 M. G. Natrella, Experimental Statistics, National Bureau of Standards, 1963.
- C-8 Assessment of the Assumption of Normality, ANSI N15.15, 1974.
- C-9 BAW-10241(P)(A), BHTP DNB Correlation Applied with LYNXT, Framatome ANP, Inc., September 2004.
- C-10 BAW-10241(P)(A), Revision 1, BHTP DNB Correlation Applied with Framatome ANP, Inc., July 2005.
- C-11 EMP-92-153(P)(A) and EMF-92-153(P)(A) Supplement 1, HTTP: Departure From Nucleate Boiling Correlation for High Thermal performance Fuel, Siemens Power Corporation, March 1984.
- C-12 XN-75-21(P)(A), Rev. 2, XCOBRA-IIIC: A Computer Code to Determine the Distribution of Coolant During Steady-State and Transient Core Operation, Exxon Nuclear Company, Inc., March 1985.
- C-13 BAW-10199P-A, The BWU Critical Heat Flux Correlations, Framatome Cogema Fuels, August 1996.
- C-14 BAW-10199P-A, Addendum 1, The BWU Critical Heat Flux Correlations, Framatome Cogema Fuels, December 2000.
- C-15 BAW-10199P-A, Addendum 2, The BWU Critical Heat Flux Correlations, Framatome ANP Inc., June 2002.
- C-16 BAW-10199P-A, Addendum 3, The BWU Critical Heat Flux Correlations, Framatome ANP Inc., November 2005.
- C-17 BAW-10189P-A, CHF Testing and Analysis of the Mark-BW Fuel Assembly Design, Framatome Cogema Fuels, January 1996.
- C-18 BAW-10159P-A, BWCMV Correlation of Critical Heat Flux in Mixing Vane Grid Fuel Assemblies, B&W Fuel Company, July 1990
- C-19 BAW-10143P-A, BWC Correlation of Critical Heat Flux, Babcock & Wilcox, April 1985.
- C-20 BAW-1030-A, LYNX2 – Subchannel Thermal-Hydraulic Analysis Program, Babcock & Wilcox, April 1985.

APPENDIX D: INPUT DESCRIPTION OF KEYWORD BASED FORMAT (KBF)

D.1 *Input Description of Keyword Based Format (KBF)*

This document represents the keyword-based-format (KBF) input description of COBRA-FLX as a thermal-hydraulic module of the ARTEMIS core simulator.

Input Method

Hereafter a brief description of the blocks of the example type is given, in the order in which a KBF file should be typically written, i.e., starting from the artemis block, the thm_input block followed by the blocks dealing with the thermal-hydraulics input.

- **artemis** : This is the block of the first level, which governs the launch of the core of the ARTEMIS code system: the parsing of the tree structure generated from the XML data file.
- **thm_input** : This keyword will indicate to the parser that all keywords of the subtree belong to the THM (i.e. COBRA-FLX).
- **group_0_solver** : Solution method of conservation equations
- **group_0_general** : General description of the case. That input block contains all following input blocks.
- **group_1_coolant** : Physical properties of the coolant
- **group_2_flow_correlations** : Flow correlations
- **group_3_power_distribution** : Power distribution data
- **group_3.2_hot_channel_factors** : Axial heat flux data
- **group_4_channels** : Subchannel data and local coupling parameters
- **group_5_channel_area_variation** : Subchannel area variation
- **group_5.1_channel_area_variation_data** : Subchannel area variation data
- **group_6_gap_variation** : Gap spacing variation
- **group_6.1_gap_variation_data** : Gap spacing variation data
- **group_7_spacer** : Spacer data
- **group_8_rod_data** : Rod layout, power factors, and CHF correlations
- **group_9_calculation_variables** : Calculation variables
- **group_10_mixing** : Turbulent mixing correlations
- **group_11_operating_conditions** : Operating conditions
- **group_12_output_options** : Output display options

Remark: Except groups **group_3.2_hot_channel_factors** , **group_5_channel_area_variation** , **group_5.1_channel_area_variation_data** , **group_6_gap_variation** , **group_6.1_gap_variation_data** and **group_7_spacer** all other groups are mandatory.

The detailed description of each input block, with all available keywords, is given in the following sections. For this purpose a table format is used with the columns:

Name keyword name
Type/Dim. type and dimension
Default default value
O/M indication if the keyword input is Optional (O) or Mandatory (M)
Comment units (if applicable) possible values and description of the keyword

The following notations are chosen for the keyword type (Type) and dimension (Dim.):

"String" means a word;
"Int" means an integer;
"Int(:)" means 1 dimensional array of integers;
"Int(:,:)" means 2 dimensional array of integers;
"Real" means a real number.
"Real(:)" means 1 dimensional array of real numbers.
"Real(:,:)" means 2 dimensional array of real numbers.

Additionally, the corresponding variable names in the COBRA-FLX stand-alone version are given in [...] parenthesis at the last line of the column Comment. In this way, the reader is enabled to search for information in the COBRA-FLX input description.



Input Example

The input is structured into groups according to the KBF specifications which are described and commented as follows:

Input example D.1-1: COBRA-FLX input example

```

artemis {
! This is an ARTEMIS input
thm_input {
! This is an THM input
group_0_solver {
! Definition of the type of solver,
! which will be applied for all succeeding cases,
! which will be specified in group_0_general

```

```

}! end of group_0_solver
group_0_general {
!General description of case no 1.
group_1_coolant {
! Definition of the type of
! coolant and its physical properties
}! end of group_1_coolant
group_2_flow_correlations {
!Definition of the correlation #
!for subcooled void, bulk void etc.
}! end of group_2_flow_correlations
group_3_power_distribution {
! Definition of the axial power profile.
! All rods have the same profile.
}! end of group_3_power_distribution
group_3.2_hot_channel_factors {
!Definition of hot channel factors
}! end of group_3.2_hot_channel_factors
group_4_channels {
!Definition of the channel layout:
flow area [cm2 ], wetted perimeter [cm], heated perimeter [cm], numbers
of the adjacent channels, gap between adjacent channels [cm], centroid
distance between adjacent channels [cm].
} ! end of group_4_channels
group_5_channel_area_variation {
!Definition of the number channels with axial area variation and the
number of axial locations to describe it.
}! end of group_5_channel_area_variation
group_5.1_channel_area_variation_data {
!Definition of the actual data.
!Default value 1.0 is used in this case.
}
group_6_gap_variation {
!Definition of the number gaps with axial gap variation and the number of
axial locations to describe it
} ! end of group_6_gap_variation
group_6.1_gap_variation_data {
!Definition of the actual data.
!Default value 1.0 is used in this case.
} ! end of group_6.1_gap_variation_data
group_7_spacer {
!Definition of type, number, axial locations and loss coefficients of
spacers.
} ! end of group_7_spacer
group_8_rod_data {
!Definition of number and size of rods and chf correlation.
chf_data {
!Definition of supplementary chf data. For the selected correlation not
needed.
} ! end of chf_data
fuel_thermal_properties {
!These data are not needed, if the ARTEMIS FRM is applied.
} ! end of fuel_thermal_properties
fuel_rod_models {
!These data are not needed, if the ARTEMIS FRM is applied.
}

```

```
} ! end of fuel_rod_models
} ! end of group_8_rod_data
group_9_calculation_variables {
!Definition of axial nodding, cross flow parameters, channel length,
iteration criteria, time conditions.
} ! end of group_9_calculation_variables
group_10_mixing {
!Definition of mixing correlation.
} ! end of group_10_mixing
group_11_operating_conditions {
!Definition of the operating conditions (pressure, mass flux, heat flux),
inlet conditions, forcing functions for transient applications.
} ! end of group_11_operating_conditions
group_12_output_options {
!Definition of output control.
} ! end of group_12_output_options
} ! end of group_0_general
} ! end of thm_input

thm_input {
! This is a THM input for the following case 2.
group_0_general {
!General description of case no 2.
!Only the data of group_11_operating_conditions are supposed to be
changed. The data of all other groups remain unchanged
group_11_operating_conditions {
!All data with units ([bar], [kg/(m2 s)]) have to be repeated.
} ! end of group_11_operating_conditions
} ! end of group_0_general
} ! end of thm_input
} ! end of artemis
```

D.1.1 Input block group_0_solver : Solution method of conservation equations

Input example D.1-2: Input block group_0_solver :

```
group_0_solver {
  solver = pressure_sor ;
  omega_sor = 1.8 ;
  ! [
                                     ]
} ! end of group_0_solver
```

This input block is required always, but only once in the Artemis input stream.

Table D-1: Input keywords for COBRA-FLX group_0_solver

| Name | Type Dim. | Default | O/M | Comment (unit, description, etc.) |
|----------------|-----------|---------|-----|--|
| group_0_solver | - | - | M | Starts the input block group_0_solver for selection of the solution method of conservation equations. The block begins with a '{' and ends with a '}'. Note: (1) Input block group_0_solver must be used regardless which input method is chosen. |
| omega_sor | Real | 1.5 | O | Initial relaxation parameter required for the SOR method (solver = pressure_sor (→ p.D-5)) [] input values outside this range will be changed to [] [omega] Note: []. |
| solver | String | - | M | Solution method of conservation equations. [solve] crossflow_gauss - Old version of COBRA IIIC/MIT. The solution of conservation equations is directed to crossflow. |

| | | | |
|--|--|--|--|
| | | | <p>pressure_gauss - The solution of conservation equations is directed to pressure and the resulting system of linear equations is solved by direct elimination.</p> <p>pressure_velocity - Pressure-Velocity (PV) solution method, a more robust algorithm for main steam line break and other low-flow problems.</p> |
| | | | <p>pressure_sor - The solution of conservation equations is directed to pressure and the resulting system of linear equations is solved by successive over-relaxation method SOR. The number of iterations in SOR method is set internally to 1000</p> |
| | | | |
| | | | |

D.1.2 Input block group_0_general : Case control data

Input example D.1-3: Input block group_0_general :

```
group_0_general {
case_description = "First KBF input for the THM, it is a 3x3 case" ;
array_type = arbitrary ;
chf_skip_type = 0 ;
case_number = 1 ;
run = yes ;
input_print_option = all ;

... ! input groups 1 to 12
} ! end of group_0_general
```

This input block is required always

Table D-2: Input keywords for COBRA-FLX group_0_general

| Name | Type Dim. | Default | O/M | Comment (unit, description, etc.) |
|-----------------|-----------|---------|-----|--|
| group_0_general | - | - | M | Starts the input group group_0_general for specification of the case control data: case description. The group begins with a '{' and ends with a '}'. |
| array_type | String | - | M | Selection of the input option. <i>[ipile]</i> arbitrary - For simplified input method (recommended option). pwr_open - For PWR with interconnected channels. (not yet available in KBF) bwr_closed - For BWR with separated channels. (not yet available in KBF) |
| chf_skip_type | Int | - | M | Activation of a CHF calculation. <i>[ipile=-2]</i> 0 - CHF calculation will be performed for all channels. 2 - CHF-calculation is skipped for BWR with separated channels. |
| case_number | Int | - | M | Run identification number. <i>[kase]</i> Note: (1) The value of case_number (→ p.D-7) will be printed at the top of the output headings as a method of identification for the user. The value |

| | | | | |
|---------------------------|--------|---|----------|---|
| | | | | of case_number (→ p.D-7) has no other meaning than the indication it provides of whether or not another case follows. |
| run | String | - | M | Run option. [<i>kase</i>] yes - Calculation continues. no - Calculation stops. |
| input print option | String | - | M | Printing option. [<i>j1</i>] new - Print new input only. all - Print entire input. operating_conditions - Print operating conditions only. channels_spacers_rods - Print table property read in input block group_4_channels (→ p.D-23) , tables grid_loss_coefficient_a (→ p.D-42) , grid_loss_coefficient_b (→ p.D-42) , grid_loss_coefficient_c , (→ p.D-43) and fraction_of_flow_diverted (→ p.D-43) read in group_7_spacer (→ p.D-37) and table property (→ p.D-52) read in group_8_rod_data (→ p.D-43) in the KBF input file. Note: (1) The output generated by option channels_spacers_rods is available only when COBRA-FLX is called from PANBOX. |
| case_description | String | - | M | Alphanumeric information to identify case. [<i>text</i>] |

Note: (1) Input block **group_0_general** (→ p.D-7) contains all remaining input groups 1 to 12.

D.1.3 Input block **group_1_coolant** : Physical properties

Input example D.1-4: Input block **group_1_coolant** :

```
group_1_coolant {
  coolant_name = table;
  !coolant_pressure_steps = 40;
  coolant_properties {
    property_table {
      Axis press (description="coolant property table"; size=30)
    } ! end of property_table pressure (Axis=press; unit=bar) = 102.7
    ...
  }
}
```

```

temperature (Axis=press; unit=Celsius) = 312.90 ...
spec_volume_liquid (Axis=press; unit=dm3/kg) = 1.43108 ...
spec_volume_vapor (Axis=press; unit=dm3/kg) = 17.46331 ...
enthalpy_liquid (Axis=press; unit=kJ/kg) = 1410.20 ...
enthalpy_vapor (Axis=press; unit=kJ/kg) = 2722.98 ...
viscosity_liquid (Axis=press; unit=kg/sm) = 0.0000835 ...
conductivity (Axis=press; unit=W/mKelvin) = 0.5353066 ...
surface_tension (Axis=press; unit=N/m) = 0.0114767 ...
} ! end of coolant_properties
} ! end of group_1_coolant
    
```

This input block is required always.

Table D-3: Input keywords for COBRA-FLX group_1_coolant

| Name | Type Dim. | Default | O/M | Comment (unit, description, etc.) |
|-----------------|-----------|---------|-----|---|
| group_1_coolant | - | - | M | Starts the input group group_1_coolant for calculation of the physical properties. The group begins with a '{' and ends with a '}'. |
| coolant_name | String | - | M | Selection of the method for calculation of the physical properties of the coolant. [<i>nprop</i>] h2o_polynomes - Calculate physical properties at saturation conditions from internal polynoms. table - The physical properties are given in the input block coolant_properties . (→ p.D-11) h2o_taf_ifc67 - TAF: Light water (formulation IFC-67) <div style="border: 1px solid black; height: 100px; width: 100%;"></div> h2o_taf_if97 - TAF97: Light water (Industrial Standard IAPWS-IF97; recommended option for design calculations) Note: (1) CHF calculations with other fluids than light water may require proper correlations; no other provision is made for this than applying Ahmad's scaling laws with chf_correlation = [] in input block |

| group_8_rod_data (→ p.D-43) . | | | |
|--------------------------------------|--------|----|---|
| coolant_pressure_steps | Int | - | <p>O Number of pressure steps generated by polynomial (min=2). <i>[nprop]</i></p> <p>Required if: coolant_name (→ p.D-9) is not table.</p> <p>Note: (1) A table containing coolant_pressure_steps (→ p.D-10) equi-spaced values of pressure from the lowest to the highest pressure in the problem is constructed giving relevant physical properties - at each pressure. Physical properties at intermediate pressures are found by linear interpolation</p> |
| superheated_steam | String | no | <p>O Option for using superheated steam properties. <i>[npress]</i></p> <p>no - Do not use superheated steam properties</p> <p>yes - Use superheated steam properties</p> |

D.1.3.1 Input block `coolant_properties` included in input block group `_1_coolant`

It is required if `coolant_name=table` (→ p.D-8) .

Table D-4: Input keywords for COBRA-FLX `coolant_properties`

| Name | Type Dim. | Default | O/M | Comment (unit, description, etc.) |
|---------------------------------|-----------|---------|-----|---|
| <code>coolant_properties</code> | - | - | O | It includes the definition of <code>property_table</code> (→ p.D-11) and property lists <code>pressure</code> (→ p.D-11) , <code>temperature</code> (→ p.D-11) , <code>spec_volume_liquid</code> (→ p.D-11) , <code>spec_volume_vapor</code> (→ p.D-11) , <code>enthalpy_liquid</code> (→ p.D-12) , <code>enthalpy_vapor</code> (→ p.D-12) , <code>viscosity_liquid</code> (→ p.D-12) , <code>conductivity</code> (→ p.D-12) and <code>surface_tension</code> for providing the physical properties of the coolant. |
| <code>property_table</code> | - | - | O | Definition of the <code>axis_press</code> (→ p.D-11) of <code>property_table</code> for specification of the physical properties to be entered. |
| <code>Axis_press</code> | Int | - | O | Definition of the size of the <code>property_table</code> . (→ p.D-11) <code>size</code> is the number of entries for each coolant property to be specified. [<i>nprop</i>] The definition is: <code>Axis_press(description="coolant property table"; size=...)</code> |
| <code>pressure</code> | Real(:) | - | O | Definition of the list <code>pressure</code> specifying the saturation pressure (bar) of the coolant. [<i>pp</i>] The definition is: <code>pressure (Axis=press; unit=bar) = ...</code> |
| <code>temperature</code> | Real(:) | - | O | Definition of the list <code>temperature</code> specifying the temperature (°C) of the coolant. [<i>tt</i>] The definition is: <code>temperature(Axis=press; unit=Celsius)=...</code> |
| <code>spec volume liquid</code> | Real(:) | - | O | Definition of the list <code>spec_volume_liquid</code> specifying the specific volume of liquid (dm ³ /kg). [<i>vvf</i>] The definition is: <code>spec_volume_liquid (Axis=press; unit=dm3/kg) =...</code> |
| <code>spec_volume_vapor</code> | Real(:) | - | O | Definition of the list <code>spec_volume_vapor</code> |

| | | | | |
|------------------|---------|---|---|---|
| | | | | specifying the specific volume of vapour (dm ³ /kg). <i>[vvg]</i> The definition is: spec_volume_vapor (Axis=press; unit=dm³/kg) =... |
| enthalpy_liquid | Real(:) | - | O | Definition of the list enthalpy_liquid specifying the liquid enthalpy (kJ/kg). <i>[hhf]</i> The definition is: enthalpy_liquid (Axis=press; unit=kJ/kg) =... |
| enthalpy_vapor | Real(:) | - | O | Definition of the list enthalpy_vapor specifying the vapour enthalpy (kJ/kg). <i>[hhg]</i> The definition is: enthalpy_vapor (Axis=press; unit=kJ/kg) =... |
| viscosity_liquid | Real(:) | - | O | Definition of the list viscosity_liquid specifying the liquid viscosity (kg/(m s)). <i>[uuf]</i> The definition is: viscosity_liquid (Axis=press; unit=kg/ms) = ... |
| conductivity | Real(:) | - | O | Definition of the list conductivity specifying the liquid thermal conductivity (W/(m K)). <i>[kkf]</i> The definition is: conductivity (Axis=press; unit=W/mK) =... |
| surface_tension | Real(:) | - | O | Definition of the list surface_tension specifying the surface tension (N/m). <i>[ssigma]</i> The definition is: surface_tension (Axis=press; unit=N/m) =... |

Note:

(1) It is important that the property table defined in the input block **coolant_properties** (→ p.D-11) spans the physical property range of the problem. It must have pressure higher than operating pressure and liquid enthalpy lower than the bundle inlet enthalpy.

The lowest pressure encountered in the problem is defined as that at which the lowest enthalpy would be the saturation value. For example, at 70 bar the saturation enthalpy is 1267.4 kJ/kg. At an inlet subcooling of 242 kJ/kg, the enthalpy would be 1025.4 kJ/kg and this would be the saturation value at a pressure of about 32 bar. Thus, one would require physical property data over the

range 32 bar (or less) to 70 bar in order to include data which cover the enthalpy range.

D.1.4 Input block group_2_flow_correlations : Flow correlations

Input example D.1-5: Input block group_2_flow_correlations :

```

group_2_flow_correlations {
! subcooled_void = no ;
! subcooled_void = Levy ;
subcooled_void = Saha_Zuber ;
! bulk_void = homogeneous ;
! bulk_void = mod_Armand ;
! bulk_void = Smith ;
bulk_void = Chexal_Lellouche_Tables ;
! bulk_void = slip_ratio ;
! slip_ratio = 1.5
! bulk_void = polynomial_quality ;
! npoly_void = 7 ;
! poly_coeff_void (unit=1) = 1.1 1.2 1.3 1.4 1.5 1.6 1.7 ;
! bulk_void = Zuber_Findlay ;
two_phase_friction_multiplier = homogeneous ;
! two_phase_friction_multiplier = Armand ;
! two_phase_friction_multiplier = Baroczy ;
! two_phase_friction_multiplier = Martinelli_Nelson_Jones ;
! two_phase_friction_multiplier = polynomial_quality ;
! npoly_friction_multiplier = 7 ;
! poly_coeff_friction_multiplier (unit=1) = 1.1 1.2 1.3 1.4 1.5 1.6
1.7;
wall_viscosity = not_included ;
! wall_viscosity = included ;
szablewski_correction = not_included ;
! szablewski_correction = included ;
! subcooled_boiling_profile_fit = Levy ;
subcooled_boiling_profile_fit = Zuber_Staub ;
! subcooled_boiling_profile_fit = Saha_Zuber ;
friction_factor {
ff_coefficient_table {
Axis ff_coefficient (description="friction factor coefficient
table"; size=4) ;
} ! end of ff_coefficient_table
ff_coefficient_aa (Axis=ff_coefficient;
unit=1) = 1.1 1.2 1.3 1.4 ;
ff_coefficient_bb (Axis=ff_coefficient; unit=1) = 1.1 1.2 1.3 1.4 ;
ff_coefficient_cc (Axis=ff_coefficient; unit=1) = 0.0 0.0 0.0 0.0 ;
} ! end of friction_factor
} ! end of group_2_flow_correlations

```

This input block is required always.

Table D-5: Input keywords for COBRA-FLX group_2_flow_correlations

| Name | Type Dim. | Default | O/M | Comment (unit, description, etc.) |
|---------------------------|-----------|-------------|-----|---|
| group_2_flow_correlations | - | - | M | Starts the input group group_2_flow_correlations for selection of the flow correlations to be used. The group begins with a '{' and ends with a '}'. |
| subcooled_void | String | no | O | Subcooled void option. [j2] no - No subcooled void. Levy - Levy subcooled void correlation. Saha_Zuber - Saha-Zuber subcooled void correlation. |
| bulk_void | String | homogeneous | O | Bulk void correlation. [j3] homogeneous - Homogeneous model. mod_Armand - Modified Armand model. Smith - Smith slip ratio correlation. slip_ratio - The value of the slip ratio will be given in slip_ratio (→ p.D-15) . polynomial_quality - Polynomial in quality, coefficients will be given in the list poly_coeff_void (→ p.D-16) . Zuber_Findlay - Zuber-Findlay bulk void model. Chexal_Lellouche_Equations - Chexal-Lellouche void correlation using the iterative solution of the formulae. Chexal_Lellouche_Tables - Chexal-Lellouche void correlation using tables with interpolation. |

| | | | | |
|--|--------|--------------|----------|---|
| <code>slip_ratio</code> | Real | - | O | Slip ratio specification. <i>[av(1)]</i> Required if: bulk_void=slip_ratio (→ p.D-14) |
| <code>two_phase_friction_multiplier</code> | String | homogeneous | O | Two-phase friction multiplier. <i>[j4]</i> homogeneous - Homogeneous model. Armand - Armand model. Baroczy - Baroczy model. Martinelli_Nelson_Jones - Martinelli-Nelson-Jones model. polynomial_quality - Polynomial in quality, the coefficients will be given in the list poly_coeff_friction_multiplier (→ p.D-16) . |
| <code>wall_viscosity</code> | String | not_included | O | Wall viscosity correlation option for the wall friction factor. <i>[nviscw]</i> not_included - Wall viscosity not included. included - Wall viscosity included. |
| <code>szablewski correction</code> | String | not_included | O | Szablewski correlation option for the Lehmann friction factor (if it is used). <i>[nszabl]</i> included - Lehmann friction factor uses Szablewski correction (accounts for the increase of friction factor in an inlet section where the flow is not fully developed, in dependence of the Reynolds number and the relative inlet length) not_included - Lehmann friction factor does not use Szablewski correction |
| <code>subcooled_boiling_profile_fit</code> | String | - | M | Subcooled boiling profile fit. Note: This will only be effective when subcooled_void = Levy (→ p.D-14) OR subcooled_void = Saha_Zuber (→ p.D-14) . <i>[j8]</i> Levy - Levy profile fit. Zuber_Staub - Zuber-Staub profile fit. |

| | | | | |
|--------------------------------|---------|---|---|---|
| | | | | <p>Saha_Zuber - Saha-Zuber profile fit.</p> <p>Note: (1) This will only be effective when subcooled_void = Levy (→ p.D-14) or subcooled_void = Saha_Zuber (→ p.D-14) .</p> |
| npoly_void | Int | 7 | O | <p>Number of void fraction polynomial coefficients. The maximal possible number is 7. [nv]</p> <p>Required if: bulk_void=polynomial_quality (→ p.D-14)</p> |
| poly_coeff_void | Real(:) | - | O | <p>Definition of the list poly_coeff_void specifying the void fraction polynomial coefficients if bulk_void = polynomial_quality (→ p.D-14) . [av]</p> <p>The definition is: poly_coeff_void (unit=1) = ...</p> <p>Note: (1) The polynomial is calculated as</p> $\sum_{v=1}^{NV} (AV(v) * x^{(v-1)})$ <p>where x = Quality (0 < x < 1) and NV= npoly_void</p> |
| npoly_friction_multiplier | Int | 7 | O | <p>Number of polynomial coefficients used to calculate the two-phase friction multiplier (polynomial in quality). The maximal possible number is 7. [nf]</p> <p>Required if: two_phase_friction_multiplier = polynomial_quality (→ p.D-15) .</p> |
| poly_coeff_friction_multiplier | Real(:) | - | O | <p>Definition of the list poly_coeff_friction_multiplier specifying the polynomial coefficients used in the calculation of the two-phase friction multiplier. [af]</p> <p>Required if:</p> |

| | | | |
|-------------------------------|----------|----------|---|
| | | | <p>two_phase_friction_multiplier = polynomial_quality (→ p.D-15) .</p> <p>The definition is: poly_coeff_friction_multiplier (unit=1) ...</p> <p>Note: (1) The polynomial is calculated as</p> $\sum_{k=1}^{NF} (AF(k) * x^{k-1})$ <p>where x = Quality (0 < x < 1) and NF= npoly_friction_multiplier</p> |
| <p>friction_factor</p> | <p>-</p> | <p>-</p> | <p>O Input sub-block for the definition of the table ff_coefficient_table (→ p.D-18) and the friction correlation coefficients ff_coefficient_aa (→ p.D-18) , ff_coefficient_bb (→ p.D-18) and ff_coefficient_cc (→ p.D-18) .</p> <p>Required if: The channel definition is provided using group_4_channels (→ p.D-23) , i.e. array_definition=input (→ p.D-25) . Otherwise the friction correlation coefficients are obtained by CoreLib .</p> <p>Note: (1) If the geometry is provided via the input block CoreLib , i.e. array_definition=input (→ p.D-25) on group_4_channels (→ p.D-23) the friction_factor definition here is ignored. The friction correlation coefficients have to be defined for each assembly_type . (2) The friction factor is calculated as (ff_coefficient_aa)*(RE**ff_coefficient_bb) + ff_coefficient_cc , where RE is the Reynolds number for the channel. (3) The sets of constants are numbered sequentially and are associated with the channel type of the same number. Up to 4 channel types and correspondingly, up to 4 sets of constants can be used. Assignment of channel types to individual channels is done in input block group_4_channels (→ p.D-23).</p> |

| | | | |
|-----------------------------|---------|---|---|
| | | | (4) If ff_coefficient_aa < 0 then ff_coefficient_aa is the roughness for the Lehmann friction correlation (μm). |
| ff_coefficient_table | - | - | O Definition of the axis ff_coefficient (\rightarrow p.D-18) of the table ff_coefficient_table for specifying the friction factor coefficients to be entered. |
| Axis ff_coefficient | - | - | O Definition of the size of the table ff_coefficient_table (\rightarrow p.D-18) . size is the number of entries of the friction factor correlation constants for each friction factor coefficient to be specified. The maximal value of size is 4. The definition is: Axis ff_coefficient (description="friction factor coefficient table"; size=...) |
| ff_coefficient_aa | Real(:) | - | O Definition of the list ff_coefficient_aa specifying the constants aa in the friction factor correlation. [aa] The definition is: ff_coefficient_aa (Axis=ff_coefficient; unit=1) = ... |
| ff_coefficient_bb | Real(:) | - | O Definition of the list ff_coefficient_bb specifying the constants bb in the friction factor correlation. [bb] The definition is: ff_coefficient_bb (Axis=ff_coefficient; unit=1) = ... |
| ff_coefficient_cc | Real(:) | - | O Definition of the list ff_coefficient_cc specifying the constants cc in the friction factor correlation. [cc] The definition is: ff_coefficient_cc (Axis=ff_coefficient; unit=1) = ... |

D.1.5 Input block group_3_power_distribution : Power distribution data

Input example D.1-6: Input block group_3_power_distribution :

```
group_3_power_distribution {  
  power_type = table ;  
  heat_flux_table {  
    Axis_fax_z (description="axial heat flux table"; size=2) ;  
  } ! end of heat_flux_table  
  z (Axis=fax_z; unit=1) = 0.0 1.0.;  
  fax (Axis=fax_z; unit=1) = 1.0 1.0 ;  
} ! end of group_3_power_distribution
```

This input block is required always for standalone COBRA-FLX. This block may be omitted in case of coupled calculations (in this case the power is obtained from the neutronics).

Table D-6: Input keywords for COBRA-FLX group_3_power_distribution

| Name | Type Dim. | Default | O/M | Comment (unit, description, etc.) |
|---------------------------------|-----------|---------|-----|--|
| group_3 - power_distribution | - | - | M | Starts the input group group_3_power_distribution for specifying the power distribution. The group begins with a '{' and ends with a '}'. Note: (1) In case of a coupled FLX-THM-FRM calculation the power distribution provided here is neglected. COBRA-FLX uses the power distribution as obtained by the FLX solver. In this case the input example given above may be used. |
| power_type | String | - | M | Power distribution option. [<i>nax, iq3</i>] table - Provides a table with the axial distribution of the specified relative axial heat flux. POWER3D_channel_by_channel - Reads 3-dimensional power data from file POWER3D (channel by channel); the input format being consistent with the power data written to file IF_HOSCAM by the PANBOX code. POWER3D_pin_by_pin - Reads 3-dimensional power data [W] from file POWER3D (pin-by-pin). |
| heat_flux_table | - | - | O | Definition of the axis fax_z (→ p.D-20) for specification of the axial distribution of the heat flux. Required if: power_type = table (→ p.D-20) . |
| Axis fax_z | - | - | O | Definition of the size of the table heat_flux_table (→ p.D-20) providing the axial distribution of the heat flux. size is the number of entries in the lists z (→ p.D-20) and fax (→ p.D-21) and it should be at least 2. <i>[nax]</i> Required if: power_type = table (→ p.D-20) . The definition is: Axis fax_z (description="axial heat flux table"; size=...); |
| z | Real(:) | - | O | Definition of the list z specifying the relative axial |

| | | | | |
|------------|---------|---|----------|---|
| | | | | <p>positions (X/L) at which the relative heat flux will be given. [y]</p> <p>Required if: power_type = table (→ p.D-20) .</p> <p>The definition is: z (Axis=fax_z; unit=1) = 0.0 ... 1.0 ;</p> |
| fax | Real(:) | - | O | <p>Definition of the list fax specifying the relative heat flux (local/average, fax > 0.0), at a given relative axial position z . [axial]</p> <p>Required if: power_type = table (→ p.D-20) .</p> <p>The definition is: fax (Axis=fax_z; unit=1) = ...</p> <p>Note: (1) Data pairs (z, fax) must be specified also at relative position z = 0.0 and z = 1.0. (2) The relative axial heat flux between the points given above is found by using linear interpolation. The user should be extremely careful in choosing the locations he specifies, especially for abrupt changes. If two axial locations are too close, the interpolation routine will produce a DIVIDE BY ZERO type error.</p> |

D.1.6 Input block `group_3.2_hot_channel_factors` : Axial heat flux data

Input example D.1-7: Input block `group_3.2_hot_channel_factors` block:

```
group_3.2_hot_channel_factors {
hot_channel_number = 3 ;
flux_engineering_factor = 1.0 ;
pellet_engineering_factor = 1.0 ;
pin_engineering_factor = 1.0 ;
grid_1_factor = 1.0 ;
grid_2_factor = 1.0 ;
grid_3_factor = 1.0 ;
dnb_limit_indicator = yes ;
dnb_limit = 1.0 ;
} ! end of group_3.2_hot_channel_factors
```

Table D-7: Input keywords for COBRA-FLX `group_3.2_hot_channel_factors`

| Name | Type Dim. | Default | O/M | Comment (unit, description, etc.) |
|--|-----------|---------|-----|--|
| <code>group_3.2_hot_channel_factors</code> | - | - | O | Starts the input group <code>group_3.2_hot_channel_factors</code> for specifying the hot channel factors. The group begins with a '{' and ends with a '}'. |
| <code>hot_channel_number</code> | Int | 0 | O | Number of the hot channel. <i>[ihc]</i> |
| <code>flux_engineering_factor</code> | Real | 1.0 | O | Flux engineering factor. The calculated critical heat fluxes of the rods heating for the hot channel <code>hot_channel_number</code> (→ p.D-22) are divided by <code>flux_engineering_factor</code> <i>[feq]</i> |
| <code>pellet_engineering_factor</code> | Real | 1.0 | O | Hot channel factor for pellet diameter, density and enrichment. The heat input to the hot channel <code>hot_channel_number</code> (→ p.D-22) is multiplied by <code>pellet_engineering_factor</code> without changing the heat fluxes of the adjacent rods, except for calculation of the conditions of subcooled boiling initiation. <i>[fedh1]</i> |
| <code>pin_engineering_factor</code> | Real | 1.0 | O | Hot channel factor for rod diameter, pitch and bowing. It is applied to the specified hot channel <code>hot_channel_number</code> (→ p.D-22) . The channel flow area is divided by <code>pin_engineering_factor</code> . The hydraulic |

| | | | | |
|----------------------------------|--------|-----|---|---|
| | | | | diameter and the heated equivalent diameter are based on the modified flow area. But in the CHF correlations the diameters are based on the unmodified flow areas. <i>[fedh2]</i> |
| <code>grid_1_factor</code> | Real | 1.0 | O | Grid 1 form factor adjustment. It is applied to the spacer loss coefficients <code>grid_loss_coefficients_aa</code> (→ p.D-42) and <code>grid_loss_coefficients_bb</code> (→ p.D-42) read in input block <code>group_7_spacer</code> (→ p.D-37) of the spacers of type 1. <i>[f1grid]</i> |
| <code>grid_2_factor</code> | Real | 1.0 | O | Grid 2 form factor adjustment. It is applied to the spacer loss coefficients <code>grid_loss_coefficients_aa</code> (→ p.D-42) and <code>grid_loss_coefficients_bb</code> (→ p.D-42) read in input block <code>group_7_spacer</code> (→ p.D-37) of the spacers of type 2. <i>[f2grid]</i> |
| <code>grid_3_factor</code> | Real | 1.0 | O | Grid 3 form factor adjustment. It is applied to the spacer loss coefficients <code>grid_loss_coefficients_aa</code> (→ p.D-42) and <code>grid_loss_coefficients_bb</code> (→ p.D-42) read in input block <code>group_7_spacer</code> (→ p.D-37) of the spacers of type 3. <i>[f3grid]</i> |
| <code>dnb_limit_indicator</code> | String | no | O | Indicator for DNB-limit used in the heat transfer calculation. <i>[chf]</i> yes - DNB-limit will be applied in the heat transfer calculation. no - DNB-Limit will not be applied in the heat transfer calculation. |
| <code>dnb_limit</code> | Real | - | O | DNB ratio limit value for the heat transfer. <i>[chflim]</i> Note: (1) This limit value will be applied to all rods/channels. |

D.1.7 Input block `group_4_channels` : Subchannel data and local coupling parameters

Input example D.1-8: Input block `group_4_channels` :

```
group_4_channels {
  number_of_channels_total = 9 ;
```

```

array_definition = input ;
channels (→ p.D-25) {
Axis channel_property (description="channel property") = type number
area wetted_peri heated_peri adj_chan_1 gap_1 distance_1 adj_chan_2
gap_2 distance_2 adj_chan_3 gap_3 distance_3 adj_chan_4 gap_4
distance_4 ;
Axis channel_number (description="number of the channels whose data
are to be read in"; size = 9) ;
System channel_map (description="channel property table") =
channel_property channel_number ;
} ! end of channels
property (System=channel_map; description="channel property table")
=
? type number area wetted_peri heated_peri adj_chan_1 gap_1
distance_1 adj_chan_2 gap_2 distance_2 adj_chan_3 gap_3 distance_3
adj_chan_4 gap_4 distance_4
[
]
number_of_gaps_with_local_coupling_parameters = 3 ;
gaps_with_local_coupling_parameters {
Axis gap_property (description="local multiplier") = number
transverse_momentum crossflow_resistance turbulent_momentum
enthalpy_difference ;
Axis gap_number (description="number of the gaps whose coupling
parameters are to be read in"; size = 3) ;
System gap_map (description="local multiplier table") = gap_property
gap_number ;
} ! end of gaps_with_local_coupling_parameters
property_coupling (System=gap_map;
description="local multiplier table") =
? number transverse_momentum crossflow_resistance turbulent_momentum
enthalpy_difference
[
]
[
]
[
]
} ! end of group_4_channels

```

This input block is required always.

Table D-8: Input keywords for COBRA-FLX group_4_channels

| Name | Type Dim. | Default | O/M | Comment (unit, description, etc.) |
|---|-----------|---------|-----|--|
| group_4_channels | - | - | M | Starts the input group group_4_channels for specifying the subchannel data and the local coupling parameters. The group begins with a '{' and ends with a '}'. |
| array_definition | String | - | M | <p>calculated - The channel geometry is generated internally using CoreLib . The CoreLib input must be provided in geometry and thermal_hydraulics parts of ARTEMIS input block Define_Core .</p> <p>input - The complete geometry is provided in the input blocks channels (→ p.D-26) and property (→ p.D-26) , group_7_spacer (→ p.D-37) and group_8_rods (→ p.D-43) . The number of channels and rods are given by number_of_channels_total (→ p.D-25) and number_of_rods_total (→ p.D-44) respectively.</p> |
| number_of_channels_total | Int | - | O | Total number of channels. <i>[nchan]</i> Required if: array_definition = input (→ p.D-25) |
| number_of_gaps_with_local_coupling_parameters | Int | 0 | O | Number of gaps for which individual local coupling parameters are to be read. Note: (1) If number_of_gaps_with_local_coupling_parameters (→ p.D-25) > 0, the input block gaps_with_local_coupling_parameters (→ p.D-28) and the table property_coupling in group_4_channels (→ p.D-23) are mandatory, otherwise they can be omitted. |

D.1.7.1 Input block channels included in input block group_4_channels

It is required if **array_definition=input** (→ p.D-25) .

Table D-9: Input keywords for COBRA-FLX channels

| Name | Type Dim. | Default | O/M | Comment (unit, description, etc.) |
|-----------------------|-----------|---------|-----|---|
| channels | - | - | O | Definition of the axis channel_property (→ p.D-26) and the axis channel_number (→ p.D-26) connected into the system channel_map = channel_property channel_number (→ p.D-26) . |
| Axis channel_property | String | - | O | Definition of the axis channel_property of the table property (→ p.D-26) specifying the properties of the subchannel identified by number. The definition is: Axis channel_property (description="channel property") = type number area wetted_peri heated_peri adj_chan_1 gap_1 distance_1 adj_chan_2 gap_2 distance_2 adj_chan_3 gap_3 distance_3 adj_chan_4 gap_4 distance_4 |
| Axis channel_number | Int | - | O | Definition of size , i.e. the number of channels whose properties will be read in the table property (→ p.D-26) . The definition is: Axis channel_number (description="number of channels whose data are to be read in", size = ...) |
| System channel map | String | - | O | Defines the coordinate system channel_map required for the property table input. The definition is: System channel_map (description = "channel property table") = channel_property channel_number |
| property | - | - | O | Input of the properties of the number of channels as specified by the size of axis channel_number (→ p.D-26) . The following properties as described in axis channel_property (→ p.D-26) have to be input: Required if: array_definition = input (→ p.D-25) . Properties: type - Subchannel type integer number (equal to 1, 2 , 3 or 4). It defines which of the four sets of friction factor correlation constants specified in input block group_2_flow_correlations (→ p.D-13) shall be applied to this subchannel (given by |

| | | | |
|--|--|--|--|
| | | | <p>number). $[n]$</p> <p>number - Subchannel identification number. $[i]$</p> <p>area - Nominal flow area (cm²). $[ac]$</p> <p>wetted_peri - Wetted perimeter (cm). $[pw]$</p> <p>heated_peri - Heated perimeter (cm). $[ph]$</p> <p>adj_chan_1 - First adjacent subchannel number. $[lc(i,1)]$</p> <p>gap_1 - Nominal gap spacing (cm) of the gap between the channels number and adj_chan_1 $[gaps(i,1)]$</p> <p>distance_1 - Channel centroid-to-centroid distance for the channels number and adj_chan_1 $[dist(i,1)]$</p> <p>adj_chan_2 - Second adjacent subchannel number $[lc(i,2)]$</p> <p>gap_2 - Nominal gap spacing (cm) of the gap between the channels number and adj_chan_2 $[gaps(i,2)]$</p> <p>distance_2 - Channel centroid-to-centroid distance for the channels number and adj_chan_2 $[dist(i,2)]$</p> <p>adj_chan_3 - Third adjacent subchannel number $[lc(i,3)]$</p> <p>gap_3 - Nominal gap spacing (cm) of the gap between the channels number and adj_chan_3 $[gaps(i,3)]$</p> <p>distance_3 - Channel centroid-to-centroid distance for the channels number and adj_chan_3 $[dist(i,3)]$</p> <p>adj_chan_4 - Fourth adjacent subchannel number $[lc(i,4)]$</p> <p>gap_4 - Nominal gap spacing (cm) of the gap between the channels number and adj_chan_4 $[gaps(i,4)]$</p> <p>distance_4 - Channel centroid-to-centroid distance for the channels number and adj_chan_4 $[dist(i,4)]$</p> <p>Note:</p> |
|--|--|--|--|

| | | | |
|--|--|--|--|
| | | | <p>(1) If a line of symmetry splits a gap at the boundary the adjacent subchannel number is given as negative by the user.</p> <p>(2) Up to four sets of subchannel connecting information may be given.</p> <p>(3) If subchannels are input in ascending order, then only higher numbered subchannels need to be identified as connecting.</p> <p>(4) Centroid-to-centroid distances are not required if they are not used in the mixing correlations.</p> <p>(5) <code>adj_chan_1</code>, <code>adj_chan_2</code>, <code>adj_chan_3</code>, and <code>adj_chan_4</code> must be higher than number. If number is greater than <code>adj_chan_1</code>, <code>adj_chan_2</code>, <code>adj_chan_3</code>, or <code>adj_chan_4</code>, the connection will be ignored.</p> |
|--|--|--|--|

D.1.7.2 Input block `gaps_with_local_coupling_parameters` included in input block `group_4_channels`

It is required if `number_of_gaps_with_local_coupling_parameters` (→ p.D-25) > 0.

Table D-10: Input keywords for COBRA-FLX `gaps_with_local_coupling_` parameters

| Name | Type Dim. | Default | O/M | Comment (unit, description, etc.) |
|--|-----------|---------|-----|---|
| <code>gaps_with_local_coupling_parameters</code> | - | - | O | Input block containing the definition of axis gap_property (→ p.D-28) and axis gap_number (→ p.D-28) connected into the system gap_map = gap_property gap_number (→ p.D-29) . |
| <code>Axis gap_property</code> | - | - | O | Axis <code>gap_property</code> specifies the properties for which local coupling parameters will be given. The definition is: Axis gap_property (description="local multiplier") = number transverse_momentum crossflow_resistance turbulent_momentum enthalpy_difference |
| <code>Axis gap_number</code> | Int | - | O | Sets the size of the table property_coupling (→ p.D-29) specifying the individual local coupling parameters of the gaps identified by number. size must be equal to <code>number_of_gaps_with_local_coupling_parameters</code> (→ p.D-25) . The definition is: Axis gap_number (description="number of the |

D.1.8 Input block group_5_channel_area_variation : Channel area variation

Input example D.1-9: Input block group_5_channel_area_variation :

```

group_5_channel_area_variation {
  area_variations {
    Axis axial_locations_av (description="number of axial locations with
area variation"; size = 4) ;
    Axis number_channels_av (description="number of channels with area
variation"; size = 3) ;
    System area_variation_table (description="table of channels and
locations with area variation") = axial_locations_av
number_channels_av
  } ! end of area_variations
  inserting_ramp_av = 1 ;
} ! end of group_5_channel_area_variation

```

Table D-11: Input keywords for COBRA-FLX group_5_channel_area_variation

| Name | Type Dim. | Default | O/M | Comment (unit, description, etc.) |
|--------------------------------|-----------|---------|-----|--|
| group_5_channel_area_variation | - | - | O | Starts the input group group_5_channel_area_variation for specifying the subchannel area variation. The group begins with a '{' and ends with a '}'. Note: (1) If there are no area variations, this input block may be omitted. |
| area_variations | - | - | O | Input block specifying the axes axial_locations_av (→ p.D-30) and number_channels_av (→ p.D-31) connected into the system area_variation_table = axial_locations_av number_channels_av (→ p.D-34). All settings are required for the input block group_5.1_channel_area_variation_data |
| Axis axial_locations_av | Int | - | O | Definition of the size of the table variation_factor_av (→ p.D-32) (see group_5.1_channel_area_variation_data) specifying the axial variation of the channel area. size is the number of axial positions with area variations to be read. [naxl] The definition is: Axis axial_locations_av (description="number of axial locations with area variation"; size ...) |

| | | | | |
|------------------------------------|--------|---|---|--|
| Axis number channels av | Int | - | O | Definition of the size of the table variation_factor_av (→ p.D-32) (see group_5.1_channel_area_variation_data) specifying the axial variation of the channel area. size is the number of subchannels with area variations to be read. <i>[nafact]</i> The definition is: Axis number_channels_av (description="number of channels with area variation"; size = ... |
| inserting_ramp_av | Int | 1 | O | Number of iterations for inserting area variations. If inserting_ramp_av is zero or blank, it is set to 1. <i>[naramp]</i> |
| System area_variation_ table | String | - | O | Defines the coordinate system area_variation_table for the variation_factor_av table definition (see group_5.1_channel_area_variation_data). The definition is: System area_variation_table (description="table of channels and locations with area variation") = axial_locations_av number_channels_av |

D.1.9 Input block group_5.1_channel_area_variation_data :Channel area variation data

Input example D.1-10: Input block group_5.1_channel_area_variation_data block:

```
group_5.1_channel_area_variation_data {
channel_number_av (Axis=number_channels_av; unit=1) = 1 3 5 ;
rel_axial_coordinate_av (Axis=axial_locations_av; unit=1) = 0.0 0.4
0.5 1.0 ;
variation_factor_av (System=area_variation_table;
description="variation table") =
? 1 2 3 4
1 1.0 1.0 1.0 1.0
2 1.0 1.0 1.0 1.0
3 1.0 1.0 1.0 1.0
;
} ! end of group_5.1_channel_area_variation_data
```

Table D-12: Input keywords for COBRA-FLX group_5.1_channel_area_variation_data

| Name | Type Dim. | Default | O/M | Comment (unit, description, etc.) |
|------|--------------|---------|-----|-----------------------------------|
|------|--------------|---------|-----|-----------------------------------|

| | | | | |
|--|---------|---|---|---|
| <code>group_5.1 - channel_area - variation_data</code> | - | - | O | <p>Starts the input group group_5_channel_area_variation_data for specifying the subchannel area variation data. The group begins with a '{' and ends with a '}'.</p> <p>Note: (1) If there are no area variations, this input block may be omitted.</p> |
| <code>channel_number_av</code> | Int(:) | - | O | <p>The list channel_number_av specifies the identification numbers of channels with area variation. It is defined using axis number_channels_av (→ p.D-31) as follows: <i>[nch(nafact)]</i></p> <p>The definition is: channel_number_av (Axis=number_channels_av; unit=1) = ...;</p> |
| <code>rel_axial - coordinate_av</code> | Real(:) | - | O | <p>The list rel_axial_coordinate_av gives the relative axial locations (X/L) with area variation factors to be read. The definition is based on axis axial_locations_av (→ p.D-30) as follows: <i>[axl(naxl)]</i></p> <p>The definition is: rel_axial_coordinate_av (Axis=axial_locations_av; unit=1) = 0.0 ... 0.1 ;</p> <p>Note: (1) Relative positions X/L=0.0 and X/L=1.0 must be specified. (2) Since the code finds the areas between specified axial locations by interpolation, the user should be extremely careful in choosing the locations he specifies, especially for abrupt changes. If two axial locations are too close, the interpolation routine will produce a DIVIDE BY ZERO type error.</p> |
| <code>variation - factor_av</code> | - | - | O | <p>The table variation_factor_av provides the area variation factors (local area/nominal area). The system area_variation_table (→ p.D-31) is used for definition. <i>[afact(nafact,naxl)]</i></p> <p>The definition is: variation_factor_av (System=area_variation_table; description="variation table") =...</p> <p>The total number of channels with area variation is specified by the size of axis number_channels_av (→ p.D-31) and the total number of axial locations with area variation is specified by the size of axis axial_locations_av</p> |

| | | | |
|--|--|--|---|
| | | | (→ p.D-30) (see group_5_channel_area_variation (→ p.D-30)). The identification numbers of the channels with area variation are given in the list channel_number_av (→ p.D-32) . The relative axial locations (X/L) with area variation are set in the list rel_axial_coordinate_av (→ p.D-32) . |
|--|--|--|---|

D.1.10 Input block **group_6_gap_variation** : Gap spacing variation

Input example D.1-11: Input block **group_6_gap_variation** :

```
group_6_gap_variation {
  gap_variations {
    Axis axial_locations_gv (description="number of axial locations with
gap variation"; size = 4) ;
    Axis number_gap_gv (description="number of gap with gap variation";
size = 9) ;
    System gap_variation_table (description="table of gap and locations
with gap variation") = axial_locations_gv number_gap_gv ;
  } ! end of gap_variations inserting_ramp = 1 ;
} ! end of group_6_gap_variation
```

Table D-13: Input keywords for COBRA-FLX group_6_gap_variation

| Name | Type Dim. | Default | O/M | Comment (unit, description, etc.) |
|-------------------------------|-----------|---------|-----|---|
| group_6_- gap_variation | - | - | O | Starts the input group group_6_gap_variation for specifying the gap spacing variation. The group begins with a '{' and ends with a '}'. Note: (1) If there are no gap spacing variations, this input block may be omitted. |
| gap_variations | - | - | O | Definition of axes axial_locations_gv (→ p.D-34) and number_gap_gv (→ p.D-34) connected into a system gap_variation_table = axial_locations_gv (→ p.D-34) number_gap_gv (→ p.D-34) . That is needed for the input block group_6.1_gap_variation_data |
| Axis axial_locations_gv | Int | - | O | Definition of the size of the table variation_factor_gv (see group_6.1_gap_variation_data) specifying the axial variation of the gap spacing. size is the number of axial positions with spacing variations to be read. [<i>ngxl</i>] The definition is: Axis axial_locations_gv (description="number of axial locations with gap variation"; size = ...) |
| Axis number_gap_gv | Int | - | O | Definition of the size of the table variation_factor_gv (→ p.D-36) (see group_6.1_gap_variation_data) specifying the axial variation of the gap spacing. size is the number of gaps with spacing variations to be read. [<i>ngaps</i>] The definition is: Axis number_gap_gv (description="number of gap with gap variation"; size = ...) number_gap_gv = 0 deletes gap variations for succeeding cases. |
| System gap_variation_table | String | - | O | Defines the coordinate system gap_variation_table for the variation_factor_gv (→ p.D-36) table definition (see group_6.1_gap_variation_data): The definition is: System gap_variation_table |

| | | | |
|--|--|--|--|
| | | | (description="table of gap and locations with gap variation") = axial_locations_gv number_gap_gv |
|--|--|--|--|

D.1.11 Input block group_6.1_gap_variation_data :Gap spacing variation data

Input example D.1-12: Input block group_6.1_gap_variation_data block:

```
group_6.1_gap_variation_data {
gap_number_gv (Axis=number_gap_gv; unit=1) = 1 2 3 4 5 6 7 8 9 ;
rel_axial_coordinate_gv (Axis=axial_locations_gv; unit=1) = 0.0 0.4
0.5 1.0 ;
variation_factor_gv (System=gap_variation_table;
description="variation table") =
? 1 2 3 4
1 1.0 1.0 1.0 1.0
2 1.0 1.0 1.0 1.0
3 1.0 1.0 1.0 1.0
4 1.0 1.0 1.0 1.0
5 1.0 1.0 1.0 1.0
6 1.0 1.0 1.0 1.0
7 1.0 1.0 1.0 1.0
8 1.0 1.0 1.0 1.0
9 1.0 1.0 1.0 1.0
;
} ! end of group_6.1_gap_variation_data
```

Table D-14: Input keywords for COBRA-FLX group_6.1_gap_variation_data

| Name | Type Dim. | Default | O/M | Comment (unit, description, etc.) |
|------------------------------|-----------|---------|-----|---|
| group_6.1_gap_variation_data | - | - | O | Starts the input group group_6.1_gap_variation_data for specifying the gap spacing variation data. The group begins with a '{' and ends with a '}'. Note: (1) If there are no gap spacing variations, this input block may be omitted. |
| gap_number_gv | Int(:) | - | O | Definition of the list gap_number_gv specifying the identification numbers of the gaps with spacing variation. The definition is based on the axis number_gap_gv (→ p.D-34) as follows: <i>[ngap(ngaps)]</i> The definition is: gap_number_gv (Axis=number_gap_gv; unit=1) = |

| | | | |
|-------------------------------------|----------------|----------|--|
| <p>rel_axial_ coordinate_gv</p> | <p>Real(:)</p> | <p>-</p> | <p>O Definition of the list rel_axial_coordinate_gv specifying the relative axial locations (X/L) with spacing variation. The definition is based on the axis axial_locations_gv (→ p.D-34) as follows: <i>[gapxl(ngxl)]</i></p> <p>The definition is: rel_axial_coordinate_gv (Axis=axial_locations_gv; unit=1) = ...;</p> <p>Note: (1) Relative positions X/L=0.0 and X/L=1.0 must be specified. (2) Since the code finds the gap spacings between specified axial locations by interpolation, the user should be extremely careful in choosing the locations he specifies, especially for abrupt changes. If two axial locations are too close, the interpolation routine will produce a DIVIDE BY ZERO type error.</p> |
| <p>variation factor gv</p> | <p>-</p> | <p>-</p> | <p>O The table variation_factor_gv provides the gap spacing variation factors (local width/nominal width).</p> <p>The numbers of gaps and axial locations with spacing variation are specified respectively by the size of axis number_gap_gv (→ p.D-34) and by the size of axis axial_locations_gv (→ p.D-34) (see group_6_gap_variation (→ p.D-33)). The identification numbers of the gaps with spacing variation are provided in the list gap_number_gv (→ p.D-35) . The relative axial locations (X/L) with gap spacing variation are given in the list rel_axial_coordinate_gv (→ p.D-36) . <i>[gfact(ngaps,ngxl)]</i></p> <p>The definition is: variation_factor_gv (System=gap_variation_table; description="variation table") =</p> |

D.1.12 Input block group_7_spacer : Spacer data

Input example D.1-13: Input block group_7_spacer :

```

group_7_spacer {
! spacer_type = wire ;
! wire_wrap_pitch = 150.0 ;
! pin_diameter = 1.0 ;
! wire_diameter = 0.12 ;
! REMARK:
! Card Group G7-2 (1 card per gap with 3 different properties)
! and G7-3 (1 card per channel with 1 property) are missing
spacer_type = grid ;
! number_of_iterations_for_ramp = 0 ;
! cross_flow_indicator = calculate ;
! cross_flow_indicator = use_first_case ;
! cross_flow_indicator = write_to_CROSFLOW_and_use ;
! cross_flow_indicator = read_from_CROSFLOW_and_use ;
grid_locations {
Axis grid_location_number (description="number of axial locations
with grids" ; size = 6) ;
}
grid_channel_mapping {
Axis grid_type (description="number of grid types"; size = 2) ;
System grid_mapping (description="grid property table per channel")
= grid_type channel_number ;
}
grid_gap_mapping {
Axis gap_number (description="number of gaps with defined
crossflow"; size = 12) ;
System grid_gap_map (description="grid property table per gap") =
grid_type gap_number ;
}
rel_axial_coordinate_grid (Axis=grid_location_number; unit=1) = 0.01
0.2 0.4 0.6 0.8 0.9 ;
grid_type (Axis=grid_location_number; unit=1) = 1 2 1 2 1 2 ;
grid_loss_coefficient_a (System=grid_mapping;
description="grid loss coefficient a in zeta=a+b*RE**c") =
? 1 2
1 0.6 1.1
2 0.6 1.1
3 0.6 1.1
4 0.6 1.1
5 0.6 1.1
6 0.6 1.1
7 0.6 1.1
8 0.6 1.1
9 0.6 1.1
;
grid_loss_coefficient_b (System=grid_mapping; description="grid loss
coefficient b in zeta=a+b*RE**c") =
? 1 2
1 1.0 1.0
2 1.0 1.0

```

```
3 1.0 1.0
4 1.0 1.0
5 1.0 1.0
6 1.0 1.0
7 1.0 1.0
8 1.0 1.0
9 1.0 1.0
;
grid_loss_coefficient_c (System=grid_mapping; description="grid loss
coefficient c in zeta=a+b*RE**c") =
? 1 2
1 -0.1 -0.1
2 -0.1 -0.1
3 -0.1 -0.1
4 -0.1 -0.1
5 -0.1 -0.1
6 -0.1 -0.1
7 -0.1 -0.1
8 -0.1 -0.1
9 -0.1 -0.1
;
fraction_of_flow_diverted (System=grid_gap_map;
description="fraction of flow diverted from channel i through gap
k") =
? 1 2
1 0.1 0.01
3 0.2 0.02
5 0.3 0.03
7 0.4 0.04
8 0.5 0.05
9 0.6 0.06
10 0.7 0.07
11 0.8 0.08
12 0.9 0.09
;
} ! end of group_7_spacer
```

Table D-15: Input keywords for COBRA-FLX group_7_spacer

| Name | Type Dim. | Default | O/M | Comment (unit, description, etc.) |
|---|-----------|---------|-----|--|
| group_7_spacer | - | - | O | Starts the block group_7_spacer for specifying the spacer data. It begins with a '{' and ends with a '}'. This input block must be always used for including spacer effects. Note: (1) If there are no spacer effects modeled, this input block may be omitted. (2) If the option array_definition = calculated (→ p.D-25) is chosen in group_4_channels (→ p.D-23), the spacer settings are performed internally using CoreLib and group_7_spacer (→ p.D-37) is empty. |
| spacer_type | String | - | O | Spacer type indicator: <i>[j6]</i> wire - Wire wrapped forced diversion crossflow is included. grid - Spacer pressure losses and forced diversion crossflow are included. |
| wire_wrap_pitch | Real | - | O | Wire wrap pitch (cm). <i>[pitch]</i> Required if: spacer_type = wire (→ p.D-39) |
| pin_diameter | Real | - | O | Pin diameter (cm). <i>[dia]</i> Required if: spacer_type = wire (→ p.D-39) |
| wire_diameter | Real | - | O | Wire diameter (cm). <i>[thick]</i> Required if: spacer_type = wire (→ p.D-39) |
| number_of_ - iterations_ - for_ramp | Int | - | O | Number of iterations needed to insert loss coefficients for wire wrap mixing. <i>[nramp]</i> Required if: spacer_type = wire (→ p.D-39) Note: (1) If number_of_iterations_for_ramp (→ p.D-39) < 1 it will be reset to 1 |
| cross_flow_ - indicator | String | - | O | Crossflow solution indicator: <i>[njump]</i> calculate - Solution computed for each case. use_first_case - Use first case solution for all succeeding cases. write_to_CROFLOW_and_use - Write solution |

| | | | | |
|----------------------------------|-----|---|---|--|
| | | | | <p>to tape8 ('CROSFLO') and use for all succeeding cases.</p> <p>read_from_CROSFLOW_and_use - Read solution from tape8 ('CROSFLO') and use for all succeeding cases.</p> <p>Note: (1) If cross_flow_indicator (→ p.D-39) is not set to calculate, the flow condition and the basic problem setup must not change. This option would be normally used for cases involving changes in power or mixing for nonboiling problems.</p> |
| grid_locations | - | - | O | <p>This input block provides the definition of the axis grid_location_number (→ p.D-40) .</p> <p>Required if: spacer_type = grid (→ p.D-39)</p> |
| Axis grid_location_number | Int | - | O | <p>Needed for the input of the lists rel_axial_coordinate_grid (→ p.D-32) and grid_type (→ p.D-41) in case of spacer_type = grid (→ p.D-39) .</p> <p>The size is the total number of axial locations with spacers []. <i>[ngrid]</i></p> <p>The definition is: Axis grid_location_number (description="number of axial locations with grids" ; size =...)</p> |
| grid_channel_mapping | - | - | O | <p>This block contains the definition of the axis grid_type (→ p.D-40) needed for the system grid_mapping (→ p.D-40) .</p> <p>Required if: spacer_type = grid (→ p.D-39)</p> |
| Axis grid_type | Int | - | O | <p>Axis definition needed for the input of the spacer loss coefficient tables grid_loss_coefficient_a, grid_loss_coefficient_b (→ p.D-42) , and grid_loss_coefficient_c (→ p.D-42) . The size is the number of grid types []. <i>[ngridt]</i></p> <p>The definition is: Axis grid_type (description="number of grid types"; size = ...)</p> |
| System grid_mapping | - | - | O | <p>Defines the coordinate system grid_mapping for specifying the tables grid_loss_coefficient_a (→ p.D-42) , grid_loss_coefficient_b (→ p.D-42) and grid_loss_coefficient_c (→ p.D-43) .</p> <p>The definition is: System grid_mapping (description="grid property table per channel") = grid_type channel_number</p> |

| | | | |
|------------------------------------|---------|---|---|
| | | | Note: (1) Axis channel_number (→ p.D-26) is defined in group_4_channels (→ p.D-23) . |
| grid gap mapping | - | - | O Definition of the axis gap_number (→ p.D-28) connected with the axis grid_type (→ p.D-40) into system grid_gap_mapping= grid_type gap_number (→ p.D-41) . Required if: spacer_type = wire (→ p.D-39) |
| Axis gap_number | Int | - | O Axis definition for the table fraction_of_flow_diverted (→ p.D-43) . The size is the number of gaps with forced crossflow. Required if: spacer_type = grid (→ p.D-39) The definition is: Axis gap_number (description="number of gaps with defined crossflow"; size = ...) |
| System grid gap mapping | - | - | O Defines the coordinate system grid_gap_mapping for the table fraction_of_flow_diverted (→ p.D-43) . The definition is: System grid_gap_mapping (description= "grid property table per gap") = grid_type gap_number |
| rel_axial - coordinate_grid | Real(:) | - | O Definition of the list rel_axial_coordinate_grid specifying all relative locations (X/L) where spacers are located. [<i>gridxl</i>] Required if: spacer_type = grid (→ p.D-39) The definition is: rel_axial_coordinate_grid (Axis= grid_location_number; unit=1)= ... Note: (1) Axial spacer positions must not be identical to axial node boundaries specified via axial_node_input (→ p.D-97) in the input block group_9_calculation_variables (→ p.D-95) (possibly random results of internal checks for equality). In particular, specification of exactly the same values as for the relative positions of axial node boundaries must be avoided. (2) Only one spacer grid may be located in a particular axial node, to ensure correct calculation of pressure loss effect. If two or more grids are defined for the same axial node, only the lowermost grid becomes effective, the others are ignored. |
| grid_type | Int(:) | - | O Definition of the list grid_type specifying the |

| | | | |
|--|----------|----------|--|
| | | | <p>spacer type at the corresponding location in the list rel_axial_coordinate_grid (→ p.D-41) . [<i>igrid</i>]</p> <p>Required if: spacer_type = grid (→ p.D-39)</p> <p>The definition is: grid_type (Axis=grid_location_number; unit=1) = ...</p> <p>Note: (1) The list grid_type (→ p.D-41) indicates which of the user-supplied spacer data sets (grid_loss_coefficients_a (→ p.D-42) , grid_loss_coefficients_b (→ p.D-42) , grid_loss_coefficients_c (→ p.D-43)) applies to the spacer at a location. (2) Grid loss coefficients must be provided for every subchannel and spacer type.</p> |
| <p>grid_loss_coefficients_a</p> | <p>-</p> | <p>-</p> | <p>O The table grid_loss_coefficients_a defines the spacer loss coefficient constants A. The number of grid types, for which constants A will be read, is specified by the size of the axis grid_type (→ p.D-40) . The number of channels, for which constants A will be read, is specified by the size of axis channel_number (→ p.D-26) . [<i>cda(nchan,ngridt)</i>]</p> <p>Required if: spacer_type = grid (→ p.D-39)</p> <p>The definition is: grid_loss_coefficient_a (System=grid_mapping; description="grid loss coefficient a in $\zeta = a + b \cdot RE^{**c}$") =</p> <p>If no Reynolds Number dependence is assumed the spacer loss coefficients are $\zeta = A$. If Reynolds Number dependence is assumed the spacer loss coefficients are $\zeta = A + B (Re^c)$.</p> |
| <p>grid_loss_coefficients_b</p> | <p>-</p> | <p>-</p> | <p>O Definition of the Reynolds Number dependent spacer loss coefficient constants B ($\zeta = A + B (Re^c)$) read from the table grid_loss_coefficients_b . The number of grid types, for which constants B will be read, is specified by the size of axis grid_type (→ p.D-40) . The number of channels, for which constants B will be read, is specified by the size of axis channel_number (→ p.D-26) . [<i>cdb(nchan,ngridt)</i>]</p> <p>Required if: spacer_type = grid (→ p.D-39)</p> <p>The definition is: grid_loss_coefficient_b (System=grid_mapping; description="grid loss coefficient b in $\zeta = a + b \cdot RE^{**c}$") =</p> |

| | | | |
|--|----------|----------|---|
| <p><code>grid_loss_ - coefficients_c</code></p> | <p>-</p> | <p>-</p> | <p>O Definition of the Reynolds Number dependent spacer loss coefficient constants C ($\zeta = A + B (Re^c)$) read from the table <code>grid_loss_coefficients_c</code>. The number of grid types, for which constants C will be read, is specified by the size of axis <code>grid_type</code> (→ p.D-40). The number of channels, for which constants C will be read, is specified by the size of axis <code>channel_number</code> (→ p.D-26). <code>[cdc(nchan, ngridt)]</code> Required if: <code>spacer_type = grid</code> (→ p.D-39) The definition is: <code>grid_loss_coefficient_c</code> (System=<code>grid_mapping</code>; description="grid loss coefficient c in $\zeta = a + b * RE^{**c}$") =</p> |
| <p><code>fraction_of_ - flow_diverted</code></p> | <p>-</p> | <p>-</p> | <p>O This table provides the fraction of flow diverted. The number of grid types, for which fractions will be read, is specified by the size of axis <code>grid_type</code> (→ p.D-40). The number of gaps, for which fraction will be read, is specified by the size of axis <code>gap_number</code> (→ p.D-28). <code>[fxflo(nk, ngridt)]</code> Required if: <code>spacer_type = grid</code> (→ p.D-39) The definition is: <code>fraction_of_flow_diverted</code> (System=<code>grid_gap_mapping</code>; description="fraction of flow diverted through gap k")= Note: (1) The forced crossflow has the same sign as the forced flow fraction.</p> |

D.1.13 Input block group_8_rod_data : Rod data

Input example D.1-14: Input block group_8_rod_data :

```
group_8_rod_data {
number_of_rods_total = 9 ;
! number_of_rods_read = 9 ;
number_of_radial_nodes = 0 ;
number_of_fuel_types = 1 ;
chf_correlation = [          ] ;
fuel_rod_model = old_model ;
rods {
Axis rod_property (description="rod_property") = fuel_type number
rod_diameter rod_rel_power adj_channel_1 power_fract_1 adj_channel_2
```

```

power_fract_2 adj_channel_3 power_fract_3 adj_channel_4
power_fract_4 adj_channel_5 power_fract_5 adj_channel_6
power_fract_6 ;
Axis rod number (description="number of the rods whose data are to
be read in"; size = 9) ;
System rod_map (description="rod property table") = rod_property
rod_number ;
} ! end of rods
property (System=rod_map; description="rod property table") =
? fuel_type number rod_diameter rod_rel_power adj_channel_1
power_fract_1 adj_channel_2 power_fract_2 adj_channel_3
power_fract_3 adj_channel_4 power_fract_4 adj_channel_5
power_fract_5 adj_channel_6 power_fract_6
1 rod 1 0.9500 0.98 1 264.0 0 .0 0 .0 0 .0 0 .0 0 .0
2 rod 2 0.9500 0.98 2 264.0 0 .0 0 .0 0 .0 0 .0 0 .0
3 rod 3 0.9500 0.98 3 264.0 0 .0 0 .0 0 .0 0 .0 0 .0
4 rod 4 0.9500 0.98 4 264.0 0 .0 0 .0 0 .0 0 .0 0 .0
5 rod 5 0.9500 1.12 5 264.0 0 .0 0 .0 0 .0 0 .0 0 .0
6 rod 6 0.9500 0.98 6 264.0 0 .0 0 .0 0 .0 0 .0 0 .0
7 rod 7 0.9500 0.98 7 264.0 0 .0 0 .0 0 .0 0 .0 0 .0
8 rod 8 0.9500 0.98 8 264.0 0 .0 0 .0 0 .0 0 .0 0 .0
9 rod 9 0.9500 0.98 9 264.0 0 .0 0 .0 0 .0 0 .0 0 .0
;
! chf_data {
...! input block with data needed by the CHF correlation
! chf_hot_channel_data {
...
! } ! end of chf_hot_channel_data
...
! } ! end of chf_data
! fuel_thermal_properties {
... ! input block for fuel thermal properties ! required only for
COBRA-FLX internal FRM
! } ! end of fuel_thermal_properties
! heat_transfer_model = COBRA_3_CP ;
! heat_transfer_coefficient = new_pre_chf ;
! fuel_rod_models {
... ! required only for COBRA-FLX internal FRM
! } ! end of fuel_rod_models
} ! end of group_8_rod_data
    
```

This input block is required always.

Table D-16: Input keywords for COBRA-FLX group_8_rod_data

| Name | Type Dim. | Default | O/M | Comment (unit, description, etc.) |
|----------------------|-----------|---------|-----|--|
| group_8_rod_data | - | - | M | Starts the input group group_8_rod_data for specifying the rod data: rod layout, power factors and CHF correlations. The group begins with a '{' and ends with a '}'. |
| number_of_rods_total | Int | - | O | Total number of rods. [nrod] |

| | | | | |
|-------------------------------|--------|------|----------|--|
| | | | | Required if: array_definition = input (→ p.D-25) in input block group_4_channels (→ p.D-23) . |
| number_of_rods_read | Int | - | O | Number of rod layout data to be read. |
| number_of_radial_nodes | Int | - | M | <p>Number of radial fuel nodes including the cladding []. <i>[nodesf]</i></p> <p>Note:</p> <p>(1) Setting number_of_radial_nodes = 0 (→ p.D-45) switches off the COBRA-FLX internal fuel rod model. In this case, the surface heat flux is specified as boundary condition for the coolant energy balance also in transient conditions.</p> <p>(2) For coupled COBRA-FLX and ARTEMIS fuel rod model calculations number_of_radial_nodes = 0 (→ p.D-45) . In this case all input needed for the internal COBRA-FLX FRM must be omitted.</p> <p>(3) If a COBRA-FLX internal fuel rod model (different from old_model) will be used then it must be fulfilled that number_of_radial_nodes (→ p.D-45) = fuel_shells + cladding_shells + 1 , where fuel_shells (→ p.D-81) and cladding_shells (→ p.D-81) are also defined in this input block group_8_rod_data (→ p.D-43) .</p> |
| number_of_fuel_types | Int | - | M | <p>Fuel types used. <i>[nfuel]</i></p> <p>Note:</p> <p>(1) number_of_fuel_types (→ p.D-45) should equal 1 if fuel_rod_model (→ p.D-50) is not old_model because the new COBRA-FLX fuel rod model and the PANBOX-model consider only cylindrical fuel geometry.</p> <p>(2) number_of_fuel_types (→ p.D-45) = 1 implies that only cylindrical fuel is used. If number_of_fuel_types (→ p.D-45) = 2 either plate fuel alone or a combination of plate and cylindrical fuel is used (not available in kbf-input).</p> |
| chf_correlation | String | None | O | <p>CHF correlation indicator: <i>[nchf]</i></p> <p>None - No CHF correlation done.</p> <p>BW_2 - The B&W-2 correlation.</p> <p>W_3 - The W-3 correlation See Note below.</p> <p>Hench_Levy - The Hench-Levy correlation.</p> |

| | | | |
|--|--|--|---|
| | | | <p>Cise_4 - The CISE-4 correlation.</p> <p>KWU_table - The KWU CHF look-up table See Note below.</p> |
|--|--|--|---|

| | | | |
|--|--|--|---|
| | | | <p>ACH_2 - The ACH-2 correlation. Additional input is required in block data_ACH_2 (→ p.D-74) for read_limits (→ p.D-74) and</p> |
|--|--|--|---|

| | | | |
|--|--|--|--|
| | | | <p>debug_printing (→ p.D-74) . See Note below.</p> <p>Barnett - The Barnett correlation. Additional input is required in block data_Barnett (→ p.D-71) for heated_length (→ p.D-74) , read_limits (→ p.D-74) and debug_printing (→ p.D-74) .</p> <p>Modified_Barnett - The modified Barnett correlation. Additional input is required in block data_Modified_Barnett (→ p.D-71) for heated_length (→ p.D-74) , read_limits (→ p.D-74) and debug_printing (→ p.D-74) .</p> <p>BHTP - The Mark-B HTP correlation. Additional input is required in block data_BHTP (→ p.D-72) for heated_length (→ p.D-74) , pin_pitch (→ p.D-75) , rod_diameter (→ p.D-75) , read_limits (→ p.D-74) and debug_printing (→ p.D-74) .</p> <p>Biasi - The Biasi correlation. Additional input is required in block data_Biasi (→ p.D-72) for heated_length (→ p.D-74) , read_limits (→ p.D-74) and debug_printing (→ p.D-74) .</p> <p>BWC - The BWC correlation. Additional input is required in block data_BWC (→ p.D-72) for read_limits (→ p.D-74) and debug_printing (→ p.D-74) . See Note below.</p> <p>BWCMV - The BWCMV correlation. Additional input is required in block data_BWCMV (→ p.D-72) for heated_length (→ p.D-74) , read_limits (→ p.D-74) and debug_printing (→ p.D-74) . See Note below.</p> <p>BWCMV_A - The BWCMV-A correlation. Additional input is required in block data_BWCMV_A (→ p.D-72) for heated_length (→ p.D-74) , read_limits (→ p.D-74) and debug_printing (→ p.D-74) , number_of_grid_spacings (→ p.D-75) , grid_spacing_coordinate (→ p.D-75) and grid_spacing (→ p.D-75) . See Note below.</p> <p>BWU_Z_Mark_B11 - The BWU-Z (Mark-B11) correlation. Additional input is required in block data_BWC_Z_Mark_B11 (→ p.D-72) for heated_length (→ p.D-74) , read_limits (→ p.D-</p> |
|--|--|--|--|

| | | | |
|--|--|--|---|
| | | | <p>74) and debug_printing (→ p.D-74) , number_of_grid_spacings (→ p.D-75) , grid_spacing_coordinate (→ p.D-75) and grid_spacing (→ p.D-75) . See Note below.</p> <p>BWU_Z_Mark_BW17_MSMG - The BWU-Z (Mark-BW17 MSMG) correlation. Additional input is required in block data_BWC_Z_Mark_B17_MSMG (→ p.D-73) for heated_length (→ p.D-74) , read_limits (→ p.D-74) and debug_printing (→ p.D-74) , number_of_grid_spacings (→ p.D-75) , grid_spacing_coordinate (→ p.D-75) and grid_spacing (→ p.D-75) . See Note below.</p> <p>BWU_B11R - The BWU-B11R (Mark-B11) correlation. Additional input is required in block data_BWU_B11R (→ p.D-73) for heated_length (→ p.D-74) , read_limits (→ p.D-74) and debug_printing (→ p.D-74) , number_of_grid_spacings (→ p.D-75) , grid_spacing_coordinate (→ p.D-75) and grid_spacing (→ p.D-75) . See Note below.</p> <p>BWU_Z_Mark_BW17 - The BWU-Z (Mark-BW17) correlation. Additional input is required in block data_BWU_Z_Mark_B17 (→ p.D-73) for heated_length (→ p.D-74) , read_limits (→ p.D-74) and debug_printing (→ p.D-74) , number_of_grid_spacings (→ p.D-75) , grid_spacing_coordinate (→ p.D-75) and grid_spacing (→ p.D-75) . See Note below.</p> <p>BWU_I - The BWU-I correlation. Additional input is required in block data_BWU_I (→ p.D-73) for heated_length (→ p.D-74) , read_limits (→ p.D-74) and debug_printing (→ p.D-74) , number_of_grid_spacings (→ p.D-75) , grid_spacing_coordinate (→ p.D-75) and grid_spacing (→ p.D-75) . See Note below.</p> <p>BWU_N - The BWU-N correlation. Additional input is required in block data_BWU_N (→ p.D-73) for heated_length (→ p.D-74) , read_limits (→ p.D-74) and debug_printing (→ p.D-74) . See Note below.</p> |
|--|--|--|---|

| | | | | |
|--|---------------|-----------|----------|--|
| | | | | <p>HTPA - The HTPA correlation. Additional input is required in block data_HTPA (→ p.D-74) for heated_length (→ p.D-74) , pin_pitch (→ p.D-75) , rod_diameter (→ p.D-75) , read_limits (→ p.D-74) and debug_printing (→ p.D-74) . See Note below.</p> <p>Note:</p> <div style="border: 1px solid black; height: 200px; width: 100%;"></div> <p>(3) chf_correlation = ACH_2, BWC, BWCMV, BWCMV_A, BWU_Z_Mark_B11, BWU_Z_Mark_BW17_MSMG, BWU_B11R, BWU_Z_Mark_BW17, BWU_I, BWU_N, HTPA: can be used only if the heat flux is defined via table, i.e. if power_type = table (→ p.D-20) in input block group_3_power_distribution (→ p.D-18) and no transient calculation using COBRA-FLX internal fuel rod model is performed.</p> |
| <p>use_end_of_interval_ - heat_flux</p> | <p>String</p> | <p>no</p> | <p>O</p> | <div style="border: 1px solid black; height: 50px; width: 100%;"></div> <p>yes - Use axial heat flux at node boundaries. no - Use average heat flux in the node.</p> |
| <p>fuel_rod_model</p> | <p>String</p> | <p>-</p> | <p>O</p> | <p>COBRA-FLX internal fuel rod model indicator. <i>[ifrm]</i> old_model - Old model.</p> |

| | | | |
|-------------------|--------|---|---|
| | | | <p>COBRA_3C_MIT_2_equal_distant - COBRA-IIIC/MIT-2 new model; the MATPRO fuel rod model (old input: no centre pellet channel, dishing, Zr-oxide, equidistant radial nodes).</p> <p>PANBOX_1_old_equal_volume - PANBOX-model according [*] (old input: no dishing, Zr-oxide).</p> <p>COBRA_3C_MIT_2_equal_volume - COBRA-IIIC/MIT-2 new model, modified MATPRO fuel rod model (new input: centre pellet channel, dishing, Zr-oxide in block fuel_rod_geometry (→ p.D-84) , radial shells of equal volume (optionally equidistant radial nodes, see temperature_distribution (→ p.D-82)).</p> <p>PANBOX_1_new_qual_volume - PANBOX-model according [*] (new input: centre pellet channel, dishing, Zr-oxide in input block fuel_rod_geometry (→ p.D-84)).</p> <p>Note: (1) fuel_rod_model = COBRA_3C_MIT_2_equal_volume together with temperature_distribution = equal_volumes (→ p.D-82) is strongly recommended for standard applications. (2) By default a summary of the fuel rod data is printed out to the file OUTPUT.</p> |
| rods | - | - | <p>O Definition of the axis rod_property (→ p.D-51) and axis rod_number (→ p.D-52) as well as the system rod_map = rod_property rod_number (→ p.D-52) .</p> <p>Required if: array_definition = input (→ p.D-25)</p> |
| Axis rod_property | String | - | <p>O Definition of the axis rod_property of the table property (→ p.D-52) specifying the properties of the rod identified by number.</p> <p>The definition is: Axis rod_property (description="rod_property") = fuel_type number rod_diameter rod_rel_power adj_channel_1 power_fract_1 adj_channel_2 power_fract_2 adj_channel_3 power_fract_3</p> |

| | | | | |
|-----------------|-----|---|---|--|
| | | | | adj_channel_4 power_fract_4 adj_channel_5 power_fract_5 adj_channel_6 power_fract_6 |
| Axis rod_number | Int | - | O | <p>Definition of the axis rod_number of the table property. size is the number of rods for which data will be read.</p> <p>The definition is: Axis rod_number (description="number of the rods whose data are to be read in"; size= ...)</p> |
| System rod_map | - | - | O | <p>Defines the coordinate system rod_map required for the table property (→ p.D-52) input.</p> <p>The definition is: System rod_map (description="rod property table") = rod_property rod_number</p> |
| property | - | - | O | <p>Table providing the properties of all rods. The number of rods is specified by the size of axis rod_number (→ p.D-52) . The properties as described in the axis rod_property (→ p.D-51) have to be input:</p> <p>Required if: array_definition = input (→ p.D-25)</p> <p>Properties:</p> <p>fuel_type - Rod fuel: 'rod' or 'plate'. [n]</p> <p>number - Rod identification number. [i]</p> <p>rod_diameter - Rod diameter (cm). [dr]</p> <p>rod_rel_power - Relative rod power (Rod power / average rod power). It must be greater than 0. [radia]</p> <p>adj_channel_1 - Number identifier of the first adjacent subchannel to the rod identified by number [lr(i,1)]</p> <p>power_factor_1 - Fraction of rod power going to the above channel adj_channel_1. [phi(i,1)]</p> <p>adj_channel_2 - Number identifier of the second adjacent subchannel to the rod identified by number [lr(i,2)]</p> <p>power_factor_2 - Fraction of rod power going to the above channel adj_channel_2. [phi(i,2)]</p> <p>adj_channel_3 - Number identifier of the third adjacent subchannel to the rod identified by</p> |

| | | | | |
|--------------------------------------|--------|------------|---|---|
| | | | | <p>number $[lr(i,3)]$</p> <p>power_factor_3 - Fraction of rod power going to the above channel <code>adj_channel_3</code>. $[phi(i,3)]$</p> <p>adj_channel_4 - Number identifier of the fourth adjacent subchannel to the rod identified by number $[lr(i,4)]$</p> <p>power_factor_4 - Fraction of rod power going to the above channel <code>adj_channel_4</code>. $[phi(i,4)]$</p> <p>adj_channel_5 - Number identifier of the fifth adjacent subchannel to the rod identified by number $[lr(i,5)]$</p> <p>power_factor_5 - Fraction of rod power going to the above channel <code>adj_channel_5</code>. $[phi(i,5)]$</p> <p>adj_channel_6 - Number identifier of the sixth adjacent subchannel to the rod identified by number $[lr(i,6)]$</p> <p>power_factor_6 - Fraction of rod power going to the above channel <code>adj_channel_6</code>. $[phi(i,6)]$</p> <p>Note: (1) Up to 6 sets of channel number and fraction of rod power going to that channel may be specified for each rod. The sum of the fractional rod powers need not sum up to 1.0 because of the gamma heating. (2) For plate fuel, the rod diameter is the plate thickness and the fraction of power to a channel is the fraction of the circumference required to specify the plate width facing the channel.</p> |
| <code>chf_data</code> | - | - | O | <p>Input block containing all CHF correlation data needed. See input block <code>chf_data</code> (→ p.D-55) .</p> <p>Required if: The selected <code>chf_correlation</code> (→ p.D-45) needs additional input.</p> |
| <code>fuel_thermal_properties</code> | - | - | O | <p>Input block for definition of the fuel thermal properties. Required only for COBRA-FLX internal FRM, i.e. if <code>number_of_radial_nodes</code> (→ p.D-45) > 0 See input block <code>fuel_thermal_properties</code> (→ p.D-77) .</p> |
| <code>heat_transfer_model</code> | String | COBRA_3_CP | O | <p>Definition of the indicator for rod-to-coolant heat transfer model, specifying the heat transfer coefficient. $[ihtcc]$</p> <p>COBRA_3_CP - COBRA-FLX.</p> |

| | | | | |
|--|--------|--------------------------|----------|--|
| | | | | <p>CARO - CARO correlation</p> <p>Note: (1) heat_transfer_model = CARO (→ p.D-53) requires renumbering of rod input data to obtain <code>adj_channel_1 = 1</code> in the table property (→ p.D-52) read in group_8_rod_data (→ p.D-43) - i.e. the first rod must deliver heat to channel 1.</p> |
| <code>heat_transfer_coefficient</code> | String | <code>old_pre_chf</code> | O | <p>Definition of the heat transfer coefficient model. <i>[ihm]</i></p> <p>old_pre_chf - Old model</p> <p>new_pre_chf - New model for pre-CHF conditions</p> <p>new_pre_and_post_chf_BEEST - New model for pre- and post-CHF conditions, according to Bjornard and Griffith (BEEST module); not recommended</p> <p>new_pre_and_post_chf_Stosic - The above model (new_pre_and_post_chf_BEEST) but modified for post-CHF conditions (rewetting), according to Stosic; recommended option.</p> |
| <code>rewetting</code> | String | - | M | <p>Definition of the indicator for rewetting.</p> <p>allowed - Rewetting is allowed.</p> <p>not_allowed - Rewetting is not allowed.</p> |
| <code>fuel_rod_models</code> | - | - | O | <p>Input block for the definition of the fuel rod models. Required only for COBRA-FLX internal FRM See input block fuel_rod_models (→ p.D-80) .</p> |

D.1.13.1 Input block `chf_data` included in input block `group_8_rod_data`

It is required if CHF correlation requiring additional input is chosen, see **chf_correlation** (→ p.D-45) .

Table D-17: Input keywords for COBRA-FLX *chf_data*

| Name | Type Dim. | Default | O/M | Comment (unit, description, etc.) |
|--|-----------|---------|-----|--|
| <i>chf_data</i> | - | - | O | Input block containing all CHF correlation data needed (all described in this table). |
| <i>use_chf_performance_factors</i> | String | no | O | Indicator if performance factors for CHF correlations will be specified via input. [N8] no - Not used. yes - If CHF performance factors are input . The CHF performance factors are 1.0 by default. |
| <i>use_rod_wise_chf_correlations</i> | String | no | O | Indicator if rod-wise CHF correlations will be specified via input. [N9] no - Not used. yes - If rod-wise CHF correlations are specified . |
| <i>use_axially_variable_CHF_correlations</i> | String | no | O | Indicator if node-wise CHF correlations will be specified via input. [N10] no - Not used. yes - If node-wise CHF correlations are specified . |
| <i>chf_correlations_with_performance_factors</i> | String(:) | no | O | List of all CHF correlation names (see chf_correlation (→ p.D-45)) for which chf_performance_factors (→ p.D-55) are specified. [<i>i_chf</i>] Required if: use_chf_performance_factors = yes (→ p.D-55) |
| <i>chf_performance_factors</i> | Real(:) | 1.0 | O | List of the performance factors for the CHF correlations given via the list chf_correlations_with_performance_factors (→ p.D-55) (= multiplier for the critical heat flux). [<i>chf_perf</i>] Required if: use_chf_performance_factors = yes (→ p.D-55) |
| <i>chf_correlation_from_rod_number</i> | Int(:) | - | O | List of the first rod numbers with CHF correlations as specified correspondingly in the list chf_correlation (→ p.D-56) . [<i>ir_n1</i>] Required if: use_rod_wise_chf_correlations |

| | | | | |
|--|-----------|----|---|---|
| | | | | <p>= yes (→ p.D-55)</p> <p>Note:</p> <p>(1) [] The definition is needed for all rods. Multiple and overlapping definitions are allowed. The last definition wins. The definitions are saved for stacked cases.</p> |
| <code>chf_correlation_to_rod_number</code> | Int(:) | - | O | <p>List of the last rod numbers with CHF correlations as specified correspondingly in the list <code>chf_correlation</code> (→ p.D-56) . <code>[ir_n2]</code></p> <p>Required if: <code>use_rod_wise_chf_correlations = yes</code> (→ p.D-55)</p> <p>Note:</p> <p>(1) [] The definition is needed for all rods. Multiple and overlapping definitions are allowed. The last definition wins. The definitions are saved for stacked cases.</p> |
| <code>chf_correlation</code> | String(:) | - | O | <p>List of the used CHF correlations. <code>[nchfref]</code></p> <p>Required if: <code>use_rod_wise_chf_correlations = yes</code> (→ p.D-55) or if <code>use_axially_variable_CHF_correlations = yes</code> (→ p.D-55) it has to be specified in each block <code>rod_type</code> (→ p.D-57) .</p> <p>Note:</p> <p>(1) [] The definition is needed for all rods. Multiple and overlapping definitions are allowed. The last definition wins. The definitions are saved for stacked cases.</p> |
| <code>use_end_of_interval_heat_flux</code> | String(:) | no | O | <p>List of the indicators for all CHF correlations as chosen in the list <code>chf_correlation</code> (→ p.D-56) for [] <code>[chfspc]</code></p> <p>Required if: <code>use_rod_wise_chf_correlations = yes</code> (→ p.D-55) OR <code>use_axially_variable_CHF_correlations = yes</code> (→ p.D-55) and some of the CHF correlations should use the heat flux at the node boundary instead of node average value.</p> |

| | | | | |
|---|---------|---|----------|--|
| | | | | <p>yes - Use axial heat flux at node boundaries.</p> <p>no - Use average heat flux in the node. Note that some CHF correlations always use the heat flux at node boundary. For these CHF correlations this indicator is ignored.</p> |
| <code>rod_type</code> | - | - | O | <p>This block is needed for each axial rod type containing axial regions with different CHF correlations. It contains the definitions of the lists with starting <code>from_x_over_1</code> (→ p.D-57) and ending <code>to_x_over_1</code> (→ p.D-57) relative axial positions with the corresponding list of CHF correlations <code>chf_correlation</code> (→ p.D-56) and list of indicators <code>use_end_of_interval_heat_flux</code> (→ p.D-56) .</p> <p>Required if: use_axially_variable_CHF_correlations = yes (→ p.D-55) .</p> |
| <code>from_x_over_1</code> | Real(:) | - | O | <p>List of all start relative axial positions (<i>X/L</i>) with different CHF correlation. Note that the first value should be 0.0. [<i>x1_chf_ax_type</i>]</p> <p>Required if: use_axially_variable_CHF_correlations = yes (→ p.D-55) for each rod type.</p> |
| <code>to_x_over_1</code> | Real(:) | - | O | <p>List of all end relative axial positions (<i>X/L</i>) with different CHF correlation. Note that the last value should be 1.0. [<i>x2_chf_ax_type</i>]</p> <p>Required if: use_axially_variable_CHF_correlations = yes (→ p.D-55) for each rod type.</p> |
| <code>rod_type - from_rod_number</code> | Int(:) | - | O | <p>List of all first rod numbers with CHF axial type number as correspondingly specified in the list <code>use_rod_type</code> (→ p.D-58) . [<i>it_n1</i>]</p> <p>Required if: use_axially_variable_CHF_correlations = yes (→ p.D-55) .</p> <p>Note: (1) All rods which are not defined in this way, obtain the CHF correlation as defined by <code>chf_correlation</code> (→ p.D-45) of <code>group_8_rod_data</code> (→ p.D-43) . Multiple and overlapping definitions are allowed. The last definition wins. The definitions are saved for stacked cases. []]</p> |

| | | | | |
|-----------------------------------|------|---|---|---|
| | | | | <p>the spacer type. <i>[ispace]</i></p> <p>Required if: chf_correlation = []</p> <p>[]</p> <p>[]</p> <p>[]</p> <p>[]</p> |
| grid_constant | Real | - | O | <p>Spacer grid constant. <i>[xks]</i></p> <p>Required if: chf_correlation = [] (→ p.D-45)</p> <p>If grid_option = [] (→ p.D-58) : Not used.</p> <p>If grid_option = []</p> <p>If grid_option = [] or grid_option = []</p> |
| thermal_diffusion_constant | Real | - | O | <p>Thermal diffusion coefficient for spacer factor (used only in CHF evaluation). <i>[tdc]</i></p> <p>Required if: chf_correlation = []</p> <p>If grid_option = [] (→ p.D-58) : Not used.</p> <p>If grid_option = []</p> |
| [] | - | - | O | [] |

| | | | | |
|---|------|---|---|---|
| | | | | [] |
| [] | - | - | 0 | [] |
| [] | - | - | 0 | [] |
| test_section_type | Real | - | 0 | Test section type. <i>[faktot]</i> Required if: chf_correlation = []. |
| rel_begin_of - heated_length | Real | - | 0 | Begin of heated length (fraction of total length). <i>[xks]</i> Required if: chf_correlation = []. |
| [] | - | - | 0 | [] Required if: chf_correlation = [] |

| | | | | |
|-----------------------------|--------|---|---|---|
| | | | | [] |
| [] | - | - | 0 | [] []] Required if: chf_correlation = [] (→ p.D-45) is used. |
| [] | - | - | 0 | []] Required if: chf_correlation = [] (→ p.D-45) is used. |
| mixing_grids | - | - | 0 | Definition of the axis number_of_mixing_grids (→ p.D-61) for specification of the total number of mixing grids. Required if: chf_correlation = []]. |
| Axis number_of_mixing_grids | Int | - | 0 | Definition of the axis needed for the input of the list mixing_grid_number (→ p.D-61) . The size is the total number of mixing grids. <i>[nmgrid]</i> Required if: chf_correlation = []] The definition is: Axis number_of_mixing_grids (description="number of mixing grids"; size=...) |
| mixing_grid_number | Int(:) | - | 0 | Enumerate in ascending order specifying which of the spacers listed in the axis |

| | | | | |
|--------------------|---------|---|---|---|
| | | | | <p>grid_location_number (→ p.D-40) (see input block group_7_spacer (→ p.D-37)) are mixing grids [<i>mgrid</i>]</p> <p>Required if: chf_correlation = []</p> <p>]</p> <p>The definition is: mixing_grid_number (Axis=number_of_mixing_grids; unit=1) =...</p> |
| grid_height | Real(:) | - | 0 | <p>Grid heights (cm) of all grid types as defined via axis_grid_type (→ p.D-40) on group_7_spacer (→ p.D-37) . [<i>gridht</i>]</p> <p>Required if: chf_correlation = [], []</p> <p>The definition is: grid_height (unit=cm) = ... ;</p> |
| [] | String | - | 0 | <p>[]</p> <p>Required if: chf_correlation = []</p> |
| [] | - | - | 0 | <p>[]</p> <p>Required if: chf_correlation = []</p> |
| [] | Int | - | 0 | <p>[]</p> <p>Required if: chf_correlation = []</p> |

| | | | | |
|---------------------|---------|---|---|---|
| | | | | The definition is: [] |
| [] | Real(:) | - | o | [] Required if: chf_correlation = [] The definition is: [] |
| [] | - | - | o | [] Required if: chf_correlation = [] (→ p.D-45) is used. |
| chf_selector | String | - | o | Select correlation as follows (CHF correlations and CHF look-up tables, especially for [] <i>[irgw]</i>) Required if: chf_correlation = [] |

| | | | | |
|--|--|--|--|--|
| | | | | |
|--|--|--|--|--|

| | | | | |
|--|--------|---|---|--|
| | | | | <p>[</p> <p style="text-align: center;">]</p> <p>Note: (1) Additional information required to choose correction factors for axial heat flux profile, spacer grids, and cold wall effects - see non_uniform_heat_flux_factor (→ p.D-65), spacer_correction_factor (→ p.D-66), and cold_wall_factor. (→ p.D-67) (2) If chf_selector (→ p.D-63) is active, additional information for hottest subchannel provided in input block chf_hot_channel_data (→ p.D-65) is required.</p> |
| chf_hot_channel_data | - | - | O | <p>Optional input block for specification of the hot channel data if chf_correlation =</p> <p>[] (→ p.D-45) .</p> <p>The following keywords are defined here: hc_radial_power_factor (→ p.D-67) , hc_mass_velocity_factor (→ p.D-67) , hc_flow_area (→ p.D-67) , hc_wetted_perimeter (→ p.D-67) , hc_heated_perimeter (→ p.D-68) and hc_ratio_radial_power_factor (→ p.D-68) .</p> |
| non_uniform_ - heat_flux_factor | String | - | O | <p>Selection of correlation for non-linear heat flux profile correction [<i>nonf12</i>]</p> <p>Required if: chf_correlation =</p> <p>[] (→ p.D-45)</p> <p>none - none</p> <p>[] - Tong's Non-uniform heat flux profile correction: []</p> <p>[] - Tong's Non-uniform heat flux profile correction: []</p> <p>[] - Wilson's Non-uniform heat flux profile correction:</p> |

| | | | |
|---------------------------------|---------------|----------|---|
| | | | <p>[]</p> <p>[]</p> <p>[]</p> |
| <p>spacer_correction_factor</p> | <p>String</p> | <p>-</p> | <p>O Selection of correlation for spacer correction factor. [nspf12]</p> <p>Required if: chf_correlation = [] (→ p.D-45)</p> <p>none - none</p> <p>[]</p> <p>thermal_diffusion_coefficient_tong (→ p.D-69), grid_spacing_coefficient, (→ p.D-69) and dnbr_multiplier (→ p.D-69) . Total heated length of bundle used.</p> <p>[]</p> <p>thermal_diffusion_coefficient_tong (→ p.D-69)</p> |

| | | | | |
|----------------------------------|--------|----------|---|--|
| hc_heated_perimeter | Real | - [] | O | Hot-channel heated perimeter (mm). <i>[ponesc]</i> The definition is: hc_heated_perimeter (unit=mm) = ... |
| hc_ratio_radial_ power_factor | Real | 1.0 | O | Ratio of maximum to average radial heat-flux factor of rods around the hot-channel. <i>[trsc]</i> The definition is: hc_ratio_radial_power_factor (unit=1) = ... |
| diameter_selection_1 | String | - | O | Characteristic diameters for CHF-correlation and look-up table application. <i>[idmr(1)]</i> Required if: chf_selector = [] (→ p.D-63) input - Use input value(s) of diameter_1 as characteristic diameter. wetted_diameter - Use equivalent diameter based on wetted perimeter. heated_diameter - Use equivalent diameter based on heated perimeter. |
| diameter_selection_2 | String | - | O | Characteristic diameters for CHF-correlation and look-up table application. <i>[idmr(2)]</i> Required if: chf_selector = [] input - Use input value(s) of diameter_2 as characteristic diameter. wetted_diameter - Use equivalent diameter based on wetted perimeter. heated_diameter - Use equivalent diameter based on heated perimeter. |
| diameter_selection_3 | String | - | O | Characteristic diameters for CHF-correlation and look-up table application. <i>[idmr(3)]</i> Required if: chf_selector = [] input - Use input value(s) of diameter_3 as characteristic diameter. |

| | | | | |
|-----------------------------------|------|---|---|---|
| | | | | Required if: spacer_correction_factor = [] (→ p.D-66) or [] (→ p.D-66) . The definition is: dnbr_multiplier (unit=1) =... |
| [] | - | - | O | Input block for additional information for CHF correlation. Here, the following keywords have to be set: [] Required if: chf_correlation = [] |
| [] | - | - | O | Input block for additional information for CHF correlation. Here, the following keywords have to be set: [] Required if: chf_correlation = [] |
| [] | - | - | O | Input block for additional information for CHF correlation. Here, the following keywords have to be set: [] Required if: chf_correlation = [] |
| lattice_hydraulic_diameter | Real | - | O | Lattice hydraulic diameter (cm) required in the [] (chf_correlation = [] [<i>dhhyd</i>] The definition is: lattice_hydraulic_diameter (unit=cm) = ... |
| bundle_heated_length | Real | - | O | Fuel bundle heated length (cm) required in chf_correlation = [] |

| | | | | |
|--|------|---|---|---|
| | | | | <p>chf_correlation = []</p> <p>The definition is: bundle_heated_length (unit=cm) = ...</p> |
| [] | - | - | O | <p>Input block for additional information for CHF correlation. Here, the following keywords have to be set: []</p> <p>Required if: chf_correlation = [] (→ p.D-45) is used.</p> |
| grid_spacing | Real | - | O | <p>Grid spacing (cm). [<i>spitch</i>]</p> <p>Required if: chf_correlation = []</p> <p>The definition is: grid_spacing (unit=cm) =</p> |
| grid_loss - coeff_ratio_vane - novane | Real | - | O | <p>Ratio of grid pressure loss coefficients (vaned/unvaned). [<i>xkloss</i>]</p> <p>Required if: chf_correlation = []</p> <p>The definition is: grid_loss_coeff_ratio_vane_novane (unit=1) =</p> |
| data_ACH_2 | - | - | O | <p>Input block for additional information for CHF correlation. Here, the following keywords have to be set: read_limits (→ p.D-74) and debug_printing (→ p.D-74) .</p> <p>Required if: chf_correlation = ACH_2 (→ p.D-45) is used.</p> |
| data_Barnett | - | - | O | <p>Input block for additional information for CHF correlation. Here, the following keywords have to be set: heated_length (→ p.D-74) , read_limits (→ p.D-74) and debug_printing (→ p.D-74) .</p> <p>Required if: chf_correlation = Barnett (→ p.D-45) is used.</p> |
| data_Modified_Barnett | - | - | O | <p>Input block for additional information for CHF correlation. Here, the following keywords have to be set: heated_length (→ p.D-74) , read_limits (→ p.D-74) and debug_printing (→ p.D-74) .</p> |

| | | | | |
|----------------------------|---|---|---|---|
| | | | | Required if: chf_correlation = Modified_Barnett (→ p.D-45) is used. |
| data_BHTP | - | - | O | Input block for additional information for CHF correlation. Here, the following keywords have to be set: heated_length (→ p.D-74) , pin_pitch (→ p.D-75) , rod_diameter (→ p.D-75) , read_limits (→ p.D-74) and debug_printing (→ p.D-74) . Required if: chf_correlation = BHTP (→ p.D-45) is used. |
| data_Biasi | - | - | O | Input block for additional information for CHF correlation. Here, the following keywords have to be set: heated_length (→ p.D-74) , read_limits (→ p.D-74) and debug_printing (→ p.D-74) . Required if: chf_correlation = Biasi (→ p.D-45) is used. |
| data_BWC | - | - | O | Input block for additional information for CHF correlation. Here, the following keywords have to be set: read_limits (→ p.D-74) and debug_printing (→ p.D-74) . Required if: chf_correlation = BWC (→ p.D-45) is used. |
| data_BWCMV | - | - | O | Input block for additional information for CHF correlation. Here, the following keywords have to be set: heated_length (→ p.D-74) , read_limits (→ p.D-74) and debug_printing (→ p.D-74) . Required if: chf_correlation = BWCMV (→ p.D-45) is used. |
| data_BWCMV_A | - | - | O | Input block for additional information for CHF correlation. Here, the following keywords have to be set: heated_length (→ p.D-74) , read_limits (→ p.D-74) and debug_printing (→ p.D-74) , number_of_grid_spacings (→ p.D-75) , grid_spacing_coordinate (→ p.D-75) and grid_spacing (→ p.D-75) . Required if: chf_correlation = BWCMV_A (→ p.D-45) is used. |
| data_BWU_Z_Mark_B11 | - | - | O | Input block for additional information for CHF correlation. Here, the following keywords have to be set: heated_length (→ p.D-74) , read_limits (→ p.D-74) and debug_printing (→ p.D-74) , number_of_grid_spacings (→ p.D-75) , grid_spacing_coordinate (→ p.D-75) and |

| | | | | |
|------------------------------------|---|---|---|--|
| | | | | grid_spacing (→ p.D-75) . Required if: chf_correlation = BWU_Z_Mark_B11 (→ p.D-45) is used. |
| data_BWU_Z - Mark_BW17_MSMG | - | - | O | Input block for additional information for CHF correlation. Here, the following keywords have to be set: heated_length (→ p.D-74) , read_limits (→ p.D-74) and debug_printing (→ p.D-74) , number_of_grid_spacings (→ p.D-75) , grid_spacing_coordinate (→ p.D-75) and grid_spacing (→ p.D-75) . Required if: chf_correlation = BWU_Z_Mark_BW17_MSMG (→ p.D-45) is used. |
| data_BWU_B11R | - | - | O | Input block for additional information for CHF correlation. Here, the following keywords have to be set: heated_length (→ p.D-74) , read_limits (→ p.D-74) and debug_printing (→ p.D-74) , number_of_grid_spacings (→ p.D-75) , grid_spacing_coordinate (→ p.D-75) and grid_spacing (→ p.D-75) . Required if: chf_correlation = BWU_B11R (→ p.D-45) is used. |
| data_BWU_Z_Mark_BW17 | - | - | O | Input block for additional information for CHF correlation. Here, the following keywords have to be set: heated_length (→ p.D-74) , read_limits (→ p.D-74) and debug_printing (→ p.D-74) , number_of_grid_spacings (→ p.D-75) , grid_spacing_coordinate (→ p.D-75) and grid_spacing (→ p.D-75) . Required if: chf_correlation = BWU_Z_Mark_BW17 (→ p.D-45) is used. |
| data_BWU_I | - | - | O | Input block for additional information for CHF correlation. Here, the following keywords have to be set: heated_length (→ p.D-74) , read_limits (→ p.D-74) and debug_printing (→ p.D-74) , number_of_grid_spacings (→ p.D-75) , grid_spacing_coordinate (→ p.D-75) and grid_spacing (→ p.D-75) . Required if: chf_correlation = BWU_I (→ p.D-45) is used. |
| data_BWU_N | - | - | O | Input block for additional information for CHF correlation. Here, the following keywords have to be set: read_limits (→ p.D-74) and debug_printing (→ p.D-74) . Required if: chf_correlation = BWU_N (→ p.D- |

| | | | | |
|-----------------------|--------|----|----------|---|
| | | | | 45) is used. |
| data_HTPA | - | - | O | Input block for additional information for CHF correlation. Here, the following keywords have to be set: heated_length (→ p.D-74) , pin_pitch (→ p.D-75) , rod_diameter (→ p.D-75) , read_limits (→ p.D-74) and debug_printing (→ p.D-74) . Required if: chf_correlation = HTPA (→ p.D-45) is used. |
| read_limits | String | no | O | Indicator if CHF correlation limits will be specified via input. [<i>chf_limit</i>] no - The default correlation limits are used. Currently, no alternative option is available . Note: (1) Violation of the pressure, mass velocity, or quality limits will result in a file CHFxx_WARNING (xx is the correlation number) being created and populated for the cases where the limits are violated. This output information is unverified and should not be relied upon for this release of the code. |
| debug_printing | String | no | O | Indicator if debug information is to be printed for the selected CHF correlation. [<i>usdprn</i>] no - No debug printout for this CHF correlation. yes - Debug printout for this CHF correlation . Note: (1) If debug_printing = yes (→ p.D-74) debug information applicable to the CHF correlation of interest is written to the file CHFxx_DEBUG (xx is the correlation number) for the channels specified via chf_correlation (→ p.D-45) . The data is stored in the correlation native units. |
| heated_length | Real | - | O | Fuel bundle heated length (cm) [<i>hlen</i>] Required if: chf_correlation = Barnett, Modified_Barnett, BHTP, Biasi, BWCMV, BWCMV_A, BWU_Z_Mark_B11, BWU_Z_Mark_BW17_MSMG, BWU_B11R, BWU_Z_Mark_BW17, BWU_I, HTPA (→ p.D-45) . The definition is: heated_length (unit=cm) = ... |

| | | | | |
|-------------------------|---------|---|---|---|
| pin_pitch | Real | - | O | Unit cell pin pitch (cm). [ppitch] Required if: chf_correlation = BHTP, HTPA (→ p.D-45) |
| rod_diameter | Real | - | O | Outer rod diameter of a unit cell (cm). [ddr] Required if: chf_correlation = BHTP, HTPA (→ p.D-45) |
| number_of_grid_spacings | Int | 0 | O | Number of grid spacing pairs (max. 50) to be read in the lists grid_spacing_coordinate (→ p.D-75) and grid_spacing (→ p.D-75) . [isgsp] Required if: chf_correlation = BHTP, BWCMV, BWCMV_A, BWU_Z_Mark_B11, BWU_Z_Mark_BW17_MSMG, BWU_B11R, BWU_Z_Mark_BW17, BWU_I, HTPA (→ p.D-45) is used. Note: (1) Totally, number_of_grid_spacings (→ p.D-75) data pairs grid_spacing_coordinate (→ p.D-75) and grid_spacing (→ p.D-75) have to be specified. Data pairs at relative positions $X/L = 0.0$ and $X/L = 1.0$ must be specified. The grid spacing between the points given above is found by using linear interpolation. The user should be extremely careful in choosing the locations he specifies, especially for abrupt changes. |
| grid_spacing_coordinate | Real(:) | - | O | List of the relative axial positions (X/L) . [sgspx] Required if: number_of_grid_spacings (→ p.D-75) is positive. Note: (1) Totally, number_of_grid_spacings (→ p.D-75) data pairs grid_spacing_coordinate (→ p.D-75) and grid_spacing (→ p.D-75) have to be specified. Data pairs at relative positions $X/L = 0.0$ and $X/L = 1.0$ must be specified. The grid spacing between the points given above is found by using linear interpolation. The user should be extremely careful in choosing the locations he specifies, especially for abrupt changes. |
| grid_spacing | Real(:) | - | O | List of the grid spacings (cm) corresponding to the relative axial positions grid_spacing_coordinate (→ p.D-75) . [sgsps] Required if: number_of_grid_spacings (→ p.D-75) is positive. |

| | | | | |
|----------------------------------|-----|---|---|--|
| | | | | <p>Note: (1) Totally, number_of_grid spacings (→ p.D-75) data pairs grid_spacing_coordinate (→ p.D-75) and grid_spacing (→ p.D-75) have to be specified. Data pairs at relative positions $X/L = 0.0$ and $X/L = 1.0$ must be specified. The grid spacing between the points given above is found by using linear interpolation. The user should be extremely careful in choosing the locations he specifies, especially for abrupt changes.</p> |
| <code>first_debug_channel</code> | Int | - | O | <p>An integer that represents the first channel of interest to be printed. <i>[nchans]</i> Required if: debug_printing = yes (→ p.D-74) .</p> |
| <code>last_debug_channel</code> | Int | - | O | <p>An integer that represents the last channel of interest to be printed. <i>[nchanx]</i> Required if: debug_printing = yes (→ p.D-74) .</p> |

D.1.13.2 Input block *fuel_thermal_properties* included in input block *group_8_rod_data*

It is required only for COBRA-FLX internal FRM and **number_of_radial_nodes** (\rightarrow p.D-45) > 0.

Table D-18: Input keywords for COBRA-FLX *fuel_thermal_properties*

| Name | Type Dim. | Default | O/M | Comment (unit, description, etc.) |
|--------------------------------------|-----------|---------|-----|---|
| <i>fuel_thermal_properties</i> | - | - | O | Definition of the fuel thermal properties. |
| <i>fuel_thermal_conductivity</i> | Real | - | O | Fuel thermal conductivity (W/(m K)). [<i>kfuel</i>] The definition is: fuel_thermal_conductivity (unit=W/mK) = ... |
| <i>fuel_specific_heat</i> | Real | - | O | Fuel specific heat (kJ/(kg K)). [<i>cfuel</i>] The definition is: fuel_specific_heat (unit=kJ/kgK) = ... |
| <i>fuel_density</i> | Real | - | O | Fuel density (kg/dm ³). [<i>rfuel</i>] The definition is: fuel_density (unit=kg/dm3) = ... |
| <i>pellet_diameter</i> | Real | - | O | Fuel pellet diameter (cm) (absolute value). [<i>dfuel</i>] The definition is: pellet_diameter (unit=cm) = ... |
| <i>cladding_thermal_conductivity</i> | Real | - | O | Cladding thermal conductivity (W/(m K)). [<i>kclad</i>] The definition is: cladding_thermal_conductivity (unit=W/mK) = ... |
| <i>cladding_specific_heat</i> | Real | - | O | Cladding specific heat (kJ/(kg K)). [<i>cclad</i>] The definition is: cladding_specific_heat (unit=kJ/kgK) = ... |
| <i>cladding_density</i> | Real | - | O | Cladding density (kg/dm ³). [<i>rclad</i>] The definition is: cladding_density (unit=kg/dm3) = ... |
| <i>cladding_thickness</i> | Real | - | O | Cladding thickness (cm). [<i>tclad</i>] |

| | | | | |
|--------------------------------------|---------|---|---|---|
| | | | | The definition is: cladding_thickness(unit=cm) = ... |
| gap_heat_transfer_coefficient | Real | - | O | Gap heat transfer coefficient (kJ/(h cm ² K)) (absolute value). [hgap] The definition is: gap_heat_transfer_coefficient (unit=kJ/hcm2K) = ... |
| radial_power | String | - | O | Definition of the pellet radial power distribution. [dfuel] uniform - Uniform radial heating in the fuel. non_uniform - Nonuniform radial heating in the fuel. |
| relative_radial_position | Real(:) | - | O | Definition of the list of the relative radial positions at which relative power will be read. [rppp] The definition is: relative_radial_position = ... ; Note: (1) Data pairs at relative positions 0.0 and 1.0 must be specified. |
| relative_power | Real(:) | - | O | Definition of the list of relative powers at the positions given in the list relative_radial_position (→ p.D-78) . [qppp0] The definition is: relative_power = ... ; Note: (1) The integrated average over the relative_power (→ p.D-78) values must be 1.0 (there is no internal normalisation). |
| gap_heat_transfer | String | - | O | Definition of the gap heat transfer. [hgap] constant - Constant gap heat transfer coefficient as specified by gap_heat_transfer_coefficient (→ p.D-92) . transient - Gap heat transfer coefficient will vary in time. |
| Axis timesteps | Int | - | O | Definition of the size of the list time_step (→ p.D-79) and the list relative_gap_heat_transfer_coefficient (→ p.D-79) . size is the number of timesteps at which gap heat transfer coefficients will be read (number of transient gap conductance data pairs). [nhgap] |

| | | | | |
|---|---------|---|----------|--|
| | | | | The definition is: Axis timesteps(description="number of timesteps to define the gap_heat_transfer_coefficient"; size = ...) |
| <code>time_step</code> | Real(:) | - | O | Time specification (seconds). <i>[yhgap]</i> The definition is: time_step (Axis=timesteps; unit=s) = ... |
| <code>relative_gap_ - heat_transfer_ - coefficient</code> | Real(:) | - | O | Relative gap conductance (current/initial). <i>[fhgap]</i> The definition is: relative_gap_heat_transfer_coefficient (Axis=timesteps; unit=1) = ... |

D.1.13.3 Input block fuel_rod_models included in input block group_8_rod_data

It is required only for COBRA-FLX internal FRM.

Table D-19: Input keywords for COBRA-FLX fuel_rod_models

| Name | Type Dim. | Default | O/M | Comment (unit, description, etc.) |
|---------------------|-----------|---------|-----|---|
| fuel_rod_models | - | - | O | Input block for the definition of the fuel rod models. |
| material_properties | String | - | O | Definition of the indicator for fuel rod material properties specifying the fuel, Zr and gap material properties. <i>[matpro]</i> Required if: fuel_rod_model (→ p.D-50) is not equal to old_model and number_of_radial_nodes (→ p.D-45) > 0. [] [] [] |
| property_model | String | - | O | Definition of the material properties model. <i>[iprop]</i> Required if: fuel_rod_model (→ p.D-50) is not equal to old_model and number_of_radial_nodes (→ p.D-45) > 0. constant - Properties constant from input. temp_dependent_constant_hgap - U/PuO ₂ and Zr properties are temperature dependent, and gap heat transfer coefficient (h Gap) is constant from input. temp_dependent_calculated_hgap - U/PuO ₂ and Zr properties are temperature dependent, and gap heat transfer coefficient (h Gap) is calculated by models. temp_dependent_interpolated_hgap_CARO - U/PuO ₂ and Zr properties are temperature dependent, and |

| | | | | |
|---------------------------|--------|---|---|--|
| | | | | <p>gap heat transfer coefficient (h_{Gap}) is interpolated vs. temperature from CARO results.</p> <p>temp_dependent_interpolated_hgap_table - U/PuO₂ and Zr properties are temperature dependent, and Gap heat transfer coefficient (h_{Gap}) is interpolated in an input table (see system_gap_heat_transfer_table (→ p.D-92)).</p> <p>Note: (1) property_model = temp_dependent_interpolated_hgap_table (→ p.D-80) is only available when called from PANBOX.</p> |
| Axis fuel_shells | Int | - | O | <p>Definition of the size of the list relative_shell_radius (→ p.D-82). size is the number of radial fuel shells and must satisfy the condition number_of_radial_nodes = number of radial fuel shells + number of radial cladding shells + 1. [iprop]</p> <p>Required if: fuel_rod_model (→ p.D-50) is not equal to old_model and number_of_radial_nodes (→ p.D-45) > 0.</p> <p>The definition is: Axis fuel_shells (description="number of radial fuel shells"; size = ...)</p> |
| shell_distribution | String | - | O | <p>Definition of the fuel shells distribution.</p> <p>Required if: fuel_rod_model (→ p.D-50) is not equal to old_model and number_of_radial_nodes (→ p.D-45) > 0.</p> <p>calculated - The shells distribution will be calculated</p> <p>input - The shells distribution will be read in the list relative_shell_radius (→ p.D-82)</p> |
| cladding_shells | Int | - | O | <p>Number of radial clad cells. [ncc]</p> <p>Required if: fuel_rod_model (→ p.D-50) is not equal to old_model and number_of_radial_nodes (→ p.D-45) > 0.</p> |
| gap_thickness | Real | - | O | <p>Gap thickness (cm) (must be greater than 0.0). [thg]</p> <p>Required if: fuel_rod_model (→ p.D-50) is not equal to old_model and number_of_radial_nodes (→ p.D-45) > 0.</p> <p>The definition is: gap_thickness(unit=cm) = ...</p> |

| | | | | |
|---------------------------------------|---------|------|---|---|
| temperature_ convergence_criterion | Real | 0.01 | O | <p>Fuel rod temperature convergence criterion; if given as 0 it is set to [ϵ] [epsf]</p> <p>Required if: fuel_rod_model (\rightarrow p.D-50) is not equal to old_model and number_of_radial_nodes (\rightarrow p.D-45) > 0.</p> <p>The definition is: temperature_convergence_criterion (unit=1) = ...</p> |
| relative_shell_radius | Real(:) | - | O | <p>Definition of a list of the relative radii to divide fuel pellet radially = $(r_i - r_0)/(r_{\text{Pellet}} - r_0)$; for r_0 see pellet_center_radius (\rightarrow p.D-85) . [rdread]</p> <p>Required if: fuel_rod_model (\rightarrow p.D-50) is not equal to old_model and number_of_radial_nodes (\rightarrow p.D-45) > 0.</p> <p>The definition is: relative_shell_radius (Axis=fuel_shells; unit=1) = ...</p> |
| temperature_ distribution | String | - | O | <p>Definition of the model for calculation of the temperature distribution inside the fuel. [ioldcb]</p> <p>Required if: fuel_rod_model= COBRA_3C_MIT_2_equal_volume (\rightarrow p.D-50) or PANBOX_1_new_equal_volume (\rightarrow p.D-50)</p> <p>equal_volumes - For both the modified new model (fuel_rod_model = COBRA_3C_MIT_2_equal_volume (\rightarrow p.D-50) and the PANBOX model (fuel_rod_model = PANBOX_1_new_equal_volume (\rightarrow p.D-50) the pellet is radially divided into fuel_shells shells of equal volumes. If fuel_rod_model = COBRA_3C_MIT_2_equal_volume (\rightarrow p.D-50) average temperatures between two nodes at r_1 and r_2 are calculated via $T_{av} = (T_1 + T_2)/2$. Heat flux printed out is related to rod diameter (rod_diameter in table property (\rightarrow p.D-26)) although coolant heat-up is calculated from real heat flux using calculated fuel rod geometry if appropriate.</p> <p>equal_distances - This option is included only for strict consistency to older COBRA-FLX versions and should not be used for application purposes. For the PANBOX model</p> |

| | | | | |
|---------------------------------|--------|---|---|---|
| | | | | <p>the pellet is radially divided into fuel_shells shells of equal volumes. For the new model the pellet is divided into nodes with equal distances. If fuel_rod_model = COBRA_3C_MIT_2_equal_volume (→ p.D-50) average temperatures between two nodes at r_1 and r_2 are calculated via $T_{av} = (T_1 + T_2)/2$. Heat flux printed out is related to rod diameter (rod_diameter in table property (→ p.D-26)). Fuel rod data pellet_diameter (→ p.D-77) , cladding_thickness, (→ p.D-77) and gap_thickness (→ p.D-81) , should match rod_diameter in table property (→ p.D-26) , otherwise coolant heat-up is not consistent with fuel rod radial temperature distribution and heat sources.</p> |
| thermal_expansion | String | - | O | <p>Definition of the correction of the fuel pellet and cladding diameter by thermal expansion. Note that use of this option might increase computation time noticeably. [<i>icorad</i>]</p> <p>Required if: fuel_rod_model= COBRA_3C_MIT_2_equal_volume (→ p.D-50) or PANBOX_1_new_equal_volume (→ p.D-50)</p> <p>no - No correction will be applied. yes - Correction will be applied.</p> |
| use_CARO_results | String | - | O | <p>Definition of the use of CARO fuel rod results read from file CAR-INP. [<i>iusca</i>]</p> <p>Required if: fuel_rod_model= COBRA_3C_MIT_2_equal_volume (→ p.D-50) or PANBOX_1_new_equal_volume (→ p.D-50)</p> <p>no - CARO fuel rod results will not be used yes - CARO fuel rod results will be used</p> |
| oxide_thermal_resistance | String | - | O | <p>Definition of the correction of the clad-to-coolant heat transfer for oxide thermal resistance. [<i>iusox</i>]</p> <p>Required if: fuel_rod_model= COBRA_3C_MIT_2_equal_volume (→ p.D-50) or PANBOX_1_new_equal_volume (→ p.D-50)</p> <p>no - No correction will be applied. yes - Correction will be applied.</p> |

| | | | | |
|--|--------|---|---|---|
| <code>gas_pressure</code> | String | - | O | <p>Definition of the calculation of the fuel-to-clad-gap gas pressure after each time step. <i>[icagas]</i></p> <p>Required if: <code>fuel_rod_model=</code> <code>COBRA_3C_MIT_2_equal_volume</code> (→ p.D-50) or <code>PANBOX_1_new_equal_volume</code> (→ p.D-50)</p> <p>.</p> <p>no - No calculation will be performed.</p> <p>yes - Calculation will be performed.</p> |
| <code>use_CARO_axial_heat_flux</code> | String | - | O | <p>Definition of the use of CARO axial heat flux profile; only for comparison to CARO results. <i>[iuscax]</i></p> <p>Required if: <code>fuel_rod_model=</code> <code>COBRA_3C_MIT_2_equal_volume</code> (→ p.D-50) or <code>PANBOX_1_new_equal_volume</code> (→ p.D-50)</p> <p>.</p> <p>no - CARO axial heat flux profile will not be used.</p> <p>yes - CARO axial heat flux profile will be used.</p> |
| <code>use_CARO_radial_heat_flux</code> | String | - | O | <p>Definition of the use of CARO radial heat flux profile; only for comparison to CARO results. <i>[iuscra]</i></p> <p>Required if: <code>fuel_rod_model=</code> <code>COBRA_3C_MIT_2_equal_volume</code> (→ p.D-50) or <code>PANBOX_1_new_equal_volume</code> (→ p.D-50)</p> <p>.</p> <p>no - CARO radial heat flux profile will not be used.</p> <p>yes - CARO radial heat flux profile will be used.</p> |
| <code>fuel_rod_geometry</code> | - | - | O | <p>Input block containing the definition of the fuel rod geometry, i.e. <code>pellet_center_radius</code> (→ p.D-85), <code>pellet_height</code> (→ p.D-85), <code>dishing</code> (→ p.D-85), <code>dishing_depth</code> (→ p.D-85), <code>dishing_radius</code> (→ p.D-85), <code>pellet_shoulder_width</code> (→ p.D-85), <code>pellet_shoulder_height</code> (→ p.D-86), <code>non_reversible_pellet_correction</code> (→ p.D-86), <code>non_reversible_cladding_correction</code> (→ p.D-86) and <code>oxid_thickness</code> (→ p.D-86).</p> <p>Required if: <code>fuel_rod_model =</code> <code>PANBOX_1_old_equal_volume</code>, <code>COBRA_3C_MIT_2_equal_volume</code>, (→ p.D-50)</p> |

| | | | | |
|------------------------------|--------|---|---|---|
| | | | | or PANBOX_1_new_equal_volume (→ p.D-50) . |
| pellet_center_radius | Real | - | O | Pellet center channel radius r_0 (cm). <i>[r0]</i> Required if: fuel_rod_model = PANBOX_1_old_equal_volume, COBRA_3C_MIT_2_equal_volume , (→ p.D-50) or PANBOX_1_new_equal_volume (→ p.D-50) . The definition is: pellet_center_radius (unit=cm) = ... |
| pellet_height | Real | - | O | Pellet height (cm). <i>[h0pel]</i> Required if: fuel_rod_model = COBRA_3C_MIT_2_equal_volume , (→ p.D-50) or PANBOX_1_new_equal_volume (→ p.D-50) . The definition is: pellet_height (unit=cm) = ... |
| dishing_depth | Real | - | O | Center depth of dishing (cm). <i>[hdish]</i> Required if: fuel_rod_model = COBRA_3C_MIT_2_equal_volume , (→ p.D-50) or PANBOX_1_new_equal_volume (→ p.D-50) . The definition is: dishing_depth (unit=cm) = ... |
| dishing_radius | Real | - | O | Dishing radius (cm). <i>[rdish]</i> Required if: fuel_rod_model = COBRA_3C_MIT_2_equal_volume , (→ p.D-50) or PANBOX_1_new_equal_volume (→ p.D-50) . The definition is: dishing_radius (unit=cm) = ... |
| dishing | String | - | O | Definition of the pellet dishing. <i>[idish]</i> Required if: fuel_rod_model = COBRA_3C_MIT_2_equal_volume , (→ p.D-50) or PANBOX_1_new_equal_volume (→ p.D-50) . no - No dishing. one_sided - One-sided dishing only. both_sided - Both-sided dishing. |
| pellet_shoulder_width | Real | - | O | Width of pellet shoulder (cm). <i>[cpel]</i> Required if: fuel_rod_model = |

| | | | | |
|---|------|---|---|---|
| | | | | <p>COBRA_3C_MIT_2_equal_volume, (→ p.D-50) or PANBOX_1_new_equal_volume (→ p.D-50)</p> <p>.</p> <p>The definition is: pellet_shoulder_width (unit=cm) = ...</p> |
| pellet_shoulder_height | Real | - | O | <p>Height of pellet shoulder (cm). [<i>dpe1</i>]</p> <p>Required if: fuel_rod_model = COBRA_3C_MIT_2_equal_volume, (→ p.D-50) or PANBOX_1_new_equal_volume (→ p.D-50)</p> <p>.</p> <p>The definition is: pellet_shoulder_height (unit=cm) = ...</p> <p>Note: (1) Usage of dishing and/or shoulders increases run time considerably because of the iteration of the radial subdivision of the fuel pellet.</p> |
| non_reversible_pellet_correction | Real | - | O | <p>Non-reversible diametral correction of pellet (cm). [<i>dmkorr</i>]</p> <p>Required if: fuel_rod_model = COBRA_3C_MIT_2_equal_volume, (→ p.D-50) or PANBOX_1_new_equal_volume (→ p.D-50)</p> <p>.</p> <p>The definition is: non_reversible_pellet_correction (unit=cm) = ...</p> |
| non_reversible_cladding_correction | Real | - | O | <p>Non-reversible diametral correction of cladding (cm). [<i>dmkorc</i>]</p> <p>Required if: fuel_rod_model = COBRA_3C_MIT_2_equal_volume, (→ p.D-50) or PANBOX_1_new_equal_volume (→ p.D-50)</p> <p>.</p> <p>The definition is: non_reversible_cladding_correction (unit=cm) = ...</p> |
| oxid_thickness | Real | - | O | <p>ZrO thickness(cm). [<i>oxid</i>]</p> <p>Required if: fuel_rod_model = COBRA_3C_MIT_2_equal_volume, (→ p.D-50) or PANBOX_1_new_equal_volume (→ p.D-50)</p> <p>.</p> <p>The definition is: oxid_thickness (unit=cm) = ...</p> |
| fuel_rod_materials | - | - | O | Input block containing the definition of the fuel |

| | | | | |
|--|------|---|---|--|
| | | | | rod materials, i.e. . Required if: property_model (→ p.D-80) is not constant . |
| theoretical_fuel_density_fraction | Real | - | O | Fraction of theoretical density of fuel. [ftd] Required if: property_model (→ p.D-80) is not constant and material_properties = MIT, MATPRO93, (→ p.D-80) and KWU (→ p.D-80) . The definition is: theoretical_fuel_density_fraction (unit=1) = ... |
| volume_fraction_PuO2 | Real | - | O | PuO ₂ fraction by volume (m ³ /m ³). [fpuo2] Required if: property_model (→ p.D-80) is not constant and material_properties = MIT, MATPRO93, (→ p.D-80) and KWU (→ p.D-80) . The definition is: volume_fraction_PuO2 (unit=1) = ... Note: |
| composition_defect | Real | - | O | O/M composition defect of nonstoichiometric fuel (O2pmx = O/M_ratio - 2.0). [o2pmx] Required if: property_model (→ p.D-80) is not constant and material_properties = []. The definition is: composition_defect (unit=1) = ... ; |
| average_burnup | Real | - | O | Average burnup (MWd/kgU). [burn] |

| | | | | |
|-------------------------------------|------|---|---|---|
| | | | | <p>Required if: property_model (\rightarrow p.D-80) is not constant and material_properties = [] .</p> <p>The definition is: average_burnup (unit=MWd/kg) = ...</p> <p>Note: (1) Also in the case of PANBOX (coupled system) calculations with use of nodal burnup values in evaluation of material properties, the input average_burnup (\rightarrow p.D-87) is employed for initialisations. It therefore must have a meaningful value (MWd/kgU).</p> |
| molten_fuel_fraction | Real | - | O | <p>Fraction of molten fuel in pellet (m^3/m^3). [<i>fmolt</i>]</p> <p>Required if: property_model (\rightarrow p.D-80) is not constant and material_properties = []</p> <p>The definition is: molten_fuel_fraction (unit=1) = ...</p> |
| Gd2O3_fraction | Real | - | O | <p>Mass fraction of Gd_2O_3 (kg/kg). [<i>fgd2o3</i>]</p> <p>Required if: property_model (\rightarrow p.D-80) is not constant and material_properties= []</p> <p>The definition is: Gd2O3_fraction (unit=1) = ...</p> |
| fuel_pressure_ - coefficient | Real | - | O | <p>Coefficient of fuel pressure on clad for gap conductance model. [<i>cpr</i>]</p> <p>Required if: property_model = temp_dependent_calculated_hgap (\rightarrow p.D-80), material_properties = [] (\rightarrow p.D-80) and gas_pressure = no, yes. (\rightarrow p.D-84) .</p> <p>The definition is: fuel_pressure_coefficient (unit=1) = ...</p> |
| fuel_pressure_ - exponent | Real | - | O | <p>Exponent for fuel pressure on clad. [<i>expr</i>]</p> <p>Required if: property_model = temp_dependent_calculated_hgap (\rightarrow p.D-80), material_properties = [] (\rightarrow p.D-80) and gas_pressure = no, yes. (\rightarrow p.D-84) .</p> <p>The definition is: fuel_pressure_exponent (unit=1) = ...</p> |
| fuel_pressure | Real | - | O | <p>Fuel pressure on clad for gap conductance</p> |

| | | | | |
|-----------------------------------|------|---|---|---|
| | | | | (bar). [<i>fpress</i>] Required if: property_model = temp_dependent_calculated_hgap , (→ p.D-80) material_properties = [] (→ p.D-80) and gas_pressure = no, yes. (→ p.D-84) . The definition is: fuel_pressure (unit=bar) = ... |
| roughness_weighting_factor | Real | - | O | Weighting factor of clad and fuel roughness. [<i>k</i>] Required if: property_model = temp_dependent_calculated_hgap (→ p.D-80) and material_properties = [] . The definition is: roughness_weighting_factor (unit=1) = ... |
| inner_clad_roughness | Real | - | O | RMS of clad roughness (cm); set to [] if given as zero. [<i>grgh</i>] Required if: property_model = temp_dependent_calculated_hgap (→ p.D-80) and material_properties = [] . The definition is: inner_clad_roughness (unit=cm) = ... |
| fuel_roughness | Real | - | O | RMS of fuel roughness (cm); set to [] if given as zero. [<i>grgf</i>] Required if: property_model = temp_dependent_calculated_hgap (→ p.D-80) and material_properties = [] . The definition is: fuel_roughness (unit=cm) = ... |
| relocation_factor | Real | - | O | Factor for relocation. [<i>a</i>] Required if: property_model = temp_dependent_calculated_hgap (→ p.D-80) and material_properties = [] . The definition is: relocation_factor (unit=1) = ... |

| | | | | |
|----------------------------|------|---|----------|--|
| helium_fraction | Real | - | O | Helium fraction by mole (mol/mol). <i>[gmix(1)]</i> Required if: property_model = temp_dependent_calculated_hgap (→ p.D-80) and material_properties = [] The definition is: helium_fraction (unit=1) = ... |
| argon_fraction | Real | - | O | Argon fraction by mole (mol/mol). <i>[gmix(2)]</i> Required if: property_model = temp_dependent_calculated_hgap (→ p.D-80) and material_properties = [] The definition is: argon_fraction (unit=1) = ... |
| krypton_fraction | Real | - | O | Krypton fraction by mole (mol/mol). <i>[gmix(3)]</i> Required if: property_model = temp_dependent_calculated_hgap (→ p.D-80) and material_properties = [] The definition is: krypton_fraction (unit=1) = ... |
| xenon_fraction | Real | - | O | Xenon fraction by mole (mol/mol). <i>[gmix(4)]</i> Required if: property_model = temp_dependent_calculated_hgap (→ p.D-80) and material_properties = [] The definition is: xenon_fraction (unit=1) = ... |
| nitrogen_fraction | Real | - | O | Nitrogen fraction by mole (mol/mol). <i>[gmix(5)]</i> Required if: property_model = temp_dependent_calculated_hgap (→ p.D-80) and material_properties = [] The definition is: nitrogen_fraction (unit=1) = ... |
| gas_pressure_in_gap | Real | - | O | Pressure of gas mixture in gap (bar). <i>[pgas]</i> Required if: property_model = temp_dependent_calculated_hgap (→ p.D-80) |

| | | | | |
|-------------------------------|------|---|---|---|
| | | | | <p>and material_properties = []</p> <p>The definition is: gas_pressure_in_gap (unit=bar) = ...</p> |
| gas_temperature_in_gap | Real | - | O | <p>Temperature of gas mixture in gap (°C). [<i>tgas</i>]</p> <p>Required if: property_model = temp_dependent_calculated_hgap (→ p.D-80) and material_properties = [] (→ p.D-80) or (material_properties = [] (→ p.D-80) and gas_pressure = yes (→ p.D-84)).</p> <p>The definition is: gas_temperature_in_gap (unit=gradC) = ...</p> |
| gas_plenumvolume | Real | - | O | <p>Volume of fuel rod upper and lower plena (cm³). [<i>volrst</i>]</p> <p>Required if: property_model = temp_dependent_calculated_hgap (→ p.D-80) and material_properties = [] (→ p.D-80) or (material_properties = [] (→ p.D-80) and gas_pressure = yes (→ p.D-84)).</p> <p>The definition is: gas_plenumvolume (unit=cm3) = ...</p> |
| gap_heat_transfer | - | - | O | <p>Definition of the axis burnup (→ p.D-91) and the axis linear_heat_rate (→ p.D-92) connected into the system gap_heat_transfer_table=burnup (→ p.D-92) , linear_heat_rate (→ p.D-92) .</p> <p>Required if: property_model = temp_dependent_interpolated_hgap_table (→ p.D-80)</p> |
| Axis burnup | Int | - | O | <p>Definition of the size of the table gap_heat_transfer_coefficient.size (→ p.D-92) is the number of values in the burnup table. [<i>nbup</i>]</p> <p>Required if: property_model = temp_dependent_interpolated_hgap_table (→ p.D-80)</p> <p>The definition is: Axis burnup (description="number of burnup table values"; size = ...)</p> |

| | | | | |
|--------------------------------|---------|---|---|--|
| Axis linear heat rate | Int | - | O | <p>Definition of the size of the table gap_heat_transfer_coefficient (→ p.D-78) . size is the number of values in the linear heat rate table. <i>[nlhr]</i></p> <p>Required if: property_model = temp_dependent_interpolated_hgap_table (→ p.D-80)</p> <p>The definition is: Axis linear_heat_rate (description="number of linear heat rate table values"; size = ...)</p> |
| System gap_heat_transfer_table | - | - | O | <p>Defines the coordinate system gap_heat_transfer_table for the table gap_heat_transfer_coefficient. (→ p.D-78)</p> <p>Required if: property_model = temp_dependent_interpolated_hgap_table (→ p.D-80)</p> <p>The definition is: System gap_heat_transfer_table (description="gap_heat_transfer table ") = burnup linear_heat_rate</p> |
| burnup_list | Real(:) | - | O | <p>Definition of the list burnup_list for providing burnup (MWd/kg).</p> <p>Required if: property_model = temp_dependent_interpolated_hgap_table (→ p.D-80)</p> <p>The definition is: burnup_list (Axis=burnup; unit=MWd/kg) =...</p> |
| linear_heat_rate_list | Real(:) | - | O | <p>Definition of the list linear_heat_rate_list for providing linear heat rate (W/cm).</p> <p>Required if: property_model = temp_dependent_interpolated_hgap_table (→ p.D-80)</p> <p>The definition is: linear_heat_rate_list (Axis=linear_heat_rate; unit=W/cm) =...</p> |
| gap_heat_transfer_coefficient | - | - | O | <p>Definition of the gap heat transfer coefficients read from the table gap_heat_transfer_coefficient . The number of values in the burnup table is specified by the size of axis burnup (→ p.D-91) . The number of values in the linear heat rate table is specified by the size of axis linear_heat_rate (→ p.D-92) . The burnups are specified in the list burnup_list (→ p.D-92) . The</p> |

| | | | |
|--|-------------|----------|---|
| | | | <p>corresponding linear heat rates are specified in the list linear_heat_rate_list (→ p.D-92) . <i>[hgt(nbup,nlhr)]</i></p> <p>Required if: property_model = temp_dependent_interpolated_hgap_table (→ p.D-80)</p> <p>The definition is: gap_heat_transfer_coefficient (System=gap_heat_transfer_table; description"table of gap_heat_transfer_coefficients") =...</p> |
| <p>coefficient_for_CARO_heat_transfer_model</p> | <p>Real</p> | <p>-</p> | <p>O Definition of a parameter to modify the heat transfer coefficient (HTC) calculated according to the CARO model: $HTC_{effective} = (1.0 + CHTcc) * HTC_{CARO}$. <i>[chtcc]</i></p> <p>Required if: heat_transfer_model=CARO (→ p.D-53)</p> <p>The definition is: coefficient_for_CARO_heat_transfer_model (unit=1) =...</p> |

Note:

A large empty rectangular box with a black border, intended for a note. The box is positioned to the right of the 'Note:' label and occupies most of the page's vertical space.



D.1.14 Input block group_9_calculation_variables : Calculation variables

Input example D.1-15: Input block group_9_calculation_variables :

```

group_9_calculation_variables {
  print_options_1 {
    axial_node_printing = print_every_node ;
    time_step_printing = print_every_time_step ;
    print_bundle_average_results-channel_exit_data-
    bundle_inlet_exit_temperatures = yes ;
    debug_printing = no ;
  } ! end of print_options_1
  axial_node_input = constant ;
  diversion_crossflow_resistance_factor(unit=1) = [      ];
  turbulent_momentum_factor(unit=1) = [      ];
  bundle_length(unit=cm) = 449.73 ;
  bundle_position(unit=deg) = 0.0 ;
  number_of_axial_nodes(unit=1) = 32 ;
  number_of_time_steps(unit=1) = 0 ;
  total_time(unit=s) = 0. ;
  maximum_number_of_iterations(unit=1) = [      ];
  flow_error(unit=1) = [      ];
  crossflow_error(unit=1) = [      ];
  transverse_momentum_parameter(unit=1) = [      ];

```

```

SOR_pressure_error(unit=1) = [      ];
flow_underrelaxation_factor(unit=1) = [      ];
pressure_underrelaxation_factor(unit=1) = [      ];
} ! end of group_9_calculation_variables

```

This input block is required always.

Table D-20: Input keywords for COBRA-FLX group_9_calculation_variables

| Name | Type Dim. | Default | O/M | Comment (unit, description, etc.) |
|-------------------------------|-----------|-----------------------|-----|--|
| group_9_calculation_variables | - | - | M | Starts the input block group_9_calculation_variables for specifying the calculation variables. The block begins with a '{' and ends with a '}'. |
| print_options_1 | - | - | M | Input block for printing option definition. The following keywords have to be set: axial_node_printing (→ p.D-96) , time_step_printing (→ p.D-96) , print_bundle_average_results-channel_exit_data-bundle_inlet_exit_temperatures (→ p.D-97) and debug_printing (→ p.D-97) . |
| axial_node_printing | String | print_every_node | O | Axial printing increment. <i>[nskipx]</i> print_every_node - Every step printed. (Default option.) print_every_other_node - Every other step printed. n - Every n 'th step printed. Note: (1) If axial_node_printing is zero or missing, the code uses print_every_node . |
| time_step_printing | String | print_every_time_step | O | Time step printing increment. <i>[nskipt]</i> print_every_time_step - Every step printed. (Default option.) |

| | | | | |
|---|--------|----------|----------|---|
| | | | | <p>print_every_other_time_step - Every other step printed.</p> <p>n - Every n 'th step printed.</p> |
| <p>print_bundle - average_results - channel_exit_data - bundle_inlet - exit_temperatures</p> | String | - | M | <p>Definition of the printout of bundle average results and channel exit data to file OUTPUT and bundle average inlet and exit temperatures to file DNBDATA (increases run time). <i>[nskip]</i></p> <p>yes - Results printed.</p> <p>no - No results printed.</p> |
| <p>debug_printing</p> | String | no | O | <p>Debug print option. <i>[kdebug]</i></p> <p>no - No debugging information is printed.</p> <p>detailed - A very lengthy debugging printout is provided for each time step of the calculation.</p> <p>iteration_summary_PANBOX - Print the iteration summary when called by the PANBOX code.</p> <p>[</p> <p style="text-align: right;">]</p> <p>Note: (1) The debug option can generate a lot of paper and take a lot of time printing. Therefore it is recommended to use the debug option only when necessary.</p> |
| <p>axial_node_input</p> | String | constant | O | <p>Axial node input. <i>[kaxial]</i></p> <p>constant - Axial nodes of equal length.</p> <p>variable_relative_node_boundaries - Axial nodes with relative positions of axial node boundaries. The relative positions are given using the keyword axial_node_boundaries_relative (→ p.D-98) . This option is not available for PANBOX calculations.</p> <p>variable_absolute_node_boundaries - Axial nodes with absolute positions of axial node</p> |

| | | | | |
|---------------------------------------|---------|---|---|---|
| | | | | <p>boundaries. The absolute positions are given using the keyword axial_node_boundaries (→ p.D-98) . This option is not available for PANBOX calculations.</p> <p>variable_absolute_node_heights - Axial nodes with variable lengths. The axial node lengths are given using the keyword axial_node_heights (→ p.D-98) . This option is not available for PANBOX calculations.</p> <p>panbox - Use the axial division from PANBOX neutronics. number_of_axial_nodes (→ p.D-100) must be greater than or equal to the number of axial nodes in neutronics!</p> <p>artemis - use the axial nodalisation from input block Geometry of input block Define_Core (see ARTEMIS)</p> |
| axial_node_boundaries_relative | Real(:) | - | O | <p>Reads the relative positions of axial node boundaries $[x(:,5)]$</p> <p>Required if: axial_node_input = variable_relative_node_boundaries. (→ p.D-97)</p> <p>The definition is: axial_node_boundaries_relative (unit=1) = ... ;</p> <p>Note: (1) Input of number_of_axial_nodes (→ p.D-100) values, last value must be 1.0; bottom boundary is internally set to zero.</p> |
| axial_node_boundaries | Real(:) | - | O | <p>Reads the positions of the axial node boundaries in [cm]. $[x(:,5)]$</p> <p>Required if: axial_node_input = variable_absolute_node_boundaries. (→ p.D-97)</p> <p>The definition is: axial_node_boundaries (unit=cm) = ... ;</p> <p>Note: (1) Input of number_of_axial_nodes (→ p.D-100) values, the bundle length will be set equal to the last input value; bottom boundary is internally set to zero. The input of bundle_length (→ p.D-99) will be ignored.</p> |
| axial_node_heights | Real(:) | - | O | <p>Reads the axial node lengths in [cm]. $[x(:,5)]$</p> <p>Required if: axial_node_input = variable_absolute_node_heights. (→ p.D-97)</p> |

| | | | | |
|---|--------|----|----------|---|
| | | | | <p>The definition is: axial_node_heights (unit=cm) = ...;</p> <p>Note: (1) Input of number_of_axial_nodes (→ p.D-100) values, the bundle length will be set equal to sum of node lengths; bottom boundary is internally set to zero. The input of bundle_length (→ p.D-99) will be ignored.</p> |
| diversion_crossflow_resistance_factor | Real | - | M | <p>Diversion crossflow resistance factor . <i>[kij]</i></p> <p>The definition is: diversion_crossflow_resistance_factor (unit=1) = ...</p> |
| diversion_crossflow_resistance_scaling | String | no | O | <p>Indicator of internal lateral scaling of the diversion crossflow resistance factor <i>[[scale_kij]</i></p> <p>no - No internal lateral scaling. yes - Internal lateral scaling.</p> <p>Note: (1) Internal lateral scaling according to US NRC requirements (this option is only applicable with number_of_gaps_with_local_coupling_parameters = 0 (→ p.D-25) on group_4_channels (→ p.D-23)): For diversion_crossflow_resistance_scaling = yes (→ p.D-99) , the crossflow resistance is proportional to the number of rod rows between channel centroids, i.e. diversion_crossflow_resistance_factor (→ p.D-99) is multiplied by an internally calculated local factor of DIST / reference_distance (→ p.D-101) (DIST is defined via distance_1, distance_2, distance_3, distance_4 (→ p.D-26))</p> |
| turbulent_momentum_factor | Real | - | M | <p>Turbulent momentum factor. <i>[ftm]</i></p> <p>The definition is: turbulent_momentum_factor (unit=1) = ...</p> |
| bundle_length | Real | - | M | <p>Bundle length (cm). <i>[z]</i></p> <p>The definition is: bundle_length (unit=cm) = ...</p> |
| bundle_position | Real | - | M | <p>Position from vertical (degrees). <i>[theta]</i></p> |

| | | | | |
|--|--------|-----|----------|--|
| | | | | The definition is: bundle_position (unit=deg) = ... |
| number_of_axial_nodes | Int | - | M | Number of axial nodes. <i>[ndx]</i> The definition is: number_of_axial_nodes (unit=1) = ... |
| number_of_time_steps | Int | - | M | Number of time steps. <i>[ndt]</i> The definition is: number_of_time_steps (unit=1) = ... |
| total_time | Real | - | M | Total transient time (sec). <i>[ttime]</i> The definition is: total_time (unit=s) = ... |
| maximum_number_of_iterations | Int | [] | O | Maximum number of iterations. The recommended value is [] <i>[ntries]</i> The definition is: maximum_number_of_iterations (unit=1) = ... |
| flow_error | Real | [] | O | Allowable fraction error in flow form convergence. The recommended value is [] <i>[ferror]</i> The definition is: flow_error (unit=1) = ... |
| transverse_momentum_parameter | Real | - | M | Transverse momentum parameter S/L . <i>[sl]</i> The definition is: transverse_momentum_parameter (unit=1) = ... |
| transverse_momentum_parameter_scaling | String | no | O | Indicator of internal lateral scaling of the transverse momentum parameter. <i>[lscale_sl]</i> no - No internal lateral scaling. yes - Internal lateral scaling. Note: (1) Internal lateral scaling according to US NRC requirements (this option is only applicable with number_of_gaps_with_local_coupling_parameters = 0 (→ p.D-25) on group_4_channels (→ p.D-23)); For transverse_momentum_parameter_scaling = yes (→ p.D-100) , the transverse momentum parameter is internally calculated based on local geometry. |

| | | | | |
|--|------|-----|---|---|
| <code>crossflow_error</code> | Real | [] | O | Crossflow convergence criterion. The recommended value is []. <i>[werror]</i> The definition is: crossflow_error (unit=1) = ... |
| <code>SOR_pressure_error</code> | Real | [] | O | Pressure convergence limit for SOR-method. The recommended value is []. <i>[epsor]</i> Required if: solver = pressure_sor (→ p.D-5) or [] (→ p.D-5) The definition is: SOR_pressure_error (unit=1) = ... |
| <code>flow_underrelaxation_factor</code> | Real | [] | O | Damping factor for axial flow. The recommended value is [] <i>[accelf]</i> The definition is: flow_underrelaxation_factor (unit=1) = ... |
| <code>pressure_underrelaxation_factor</code> | Real | [] | O | Damping factor for lateral difference pressure. The recommended value is []. <i>[accelsp]</i> The definition is: pressure_underrelaxation_factor (unit=1) = ... |
| <code>reference_distance</code> | | - | O | Reference distance (cm) to be used for internal lateral scaling of the diversion crossflow resistance factor KIJ . Reference distance is usually the centroid distance between two fuel rods (rod pitch). <i>[[ref_kij]]</i> Required if: diversion_crossflow_resistance_scaling = yes (→ p.D-99) |

D.1.14.1 Input block `pv_solution_variables` included in input block `group_9_calculation_variables`

It is required if **solver = pressure_velocity** (→ p.D-5).

Table D-21: Input keywords for COBRA-FLX `pv_solution_variables`

| Name | Type Dim. | Default | O/M | Comment (unit, description, etc.) |
|------------------------------------|-----------|---------|-----|---|
| <code>pv_solution_variables</code> | - | - | O | Input block containing the definitions of all |

| | | | | |
|--|------|-----|---|--|
| | | | | <p>solution variables needed for the pressure-velocity solver.</p> <p>Required if: solver = pressure_velocity (→ p.D-5)</p> |
| number_of_steady_state_time_steps | Int | [] | O | <p>Number of time steps of steady_state_time_step (→ p.D-102) for reaching a steady-state solution. A value of one is a normal choice. A value larger than one can be used to run a pseudo transient of number_of_steady_state_time_steps steps to achieve steady-state. A reduced steady_state_time_step would be provided in that case. <i>[nsss]</i></p> |
| steady_state_time_step | Real | [] | O | <p>Time step used to achieve steady state. <i>[dtss]</i></p> <p>Note: (1) Convergence for low flow cases can be difficult and a reduced time step is an option to achieve convergence. Time steps on the order of the Courant step can be used to advantage and a suitable number of time steps would be needed to achieve steady-state. Damping may also be needed (axial_flow_acceleration_factor < 1.0 (→ p.D-103) , lateral_flow_acceleration_factor < 1.0 (→ p.D-103) , density_acceleration_factor < 1.0 (→ p.D-104) or enthalpy_acceleration_factor < 1.0 (→ p.D-104)) especially if the time steps are larger than the Courant time step.</p> |
| min_number_of_steady_state_outer_iterations | Int | [] | O | <p>Minimum number of outer iterations used to achieve steady-state for each steady-state time step. The outer iteration will go at least min_number_of_steady_state_outer_iterations iterations per time step. <i>[itmsss]</i></p> |
| min_number_of_time_step_outer_iterations | Int | [] | O | <p>Minimum number of outer iterations used to achieve a solution at each transient time step. The outer iteration will go at least min_number_of_time_step_outer_iterations iterations per time step. <i>[itmint]</i></p> |
| mass_balance_inner_iterations | Int | [] | O | <p>Maximum number of inner iterations to achieve a mass balance. <i>[maxinr]</i></p> |
| rebalancing_inner_iterations | Int | [] | O | <p>Inner iterations for rebalancing of pressure and flow along the channel length. Rebalancing is done every rebalancing_inner_iterations inner iterations. <i>[irebal]</i></p> |

| | | | |
|--|---------------|-------------------------|---|
| <p>relative_mass_ - conservation_error</p> | <p>Real</p> | <p>[]</p> | <p>0 Maximum allowable relative mass conservation error (C/F) per cell for the inner iteration. C is the mass error per cell (kg/s) and F is the average axial flow (kg/s). This differs for flow_error (→ p.D-100) (dF/F). The relative_mass_conservation_error is the criterion used to measure mass convergence of the inner iteration. flow_error (→ p.D-100) is used to measure the flow convergence of the outer iteration. relative_mass_conservation_error is normally more restrictive. [] [merror]</p> |
| <p>axial_flow_ - acceleration_factor</p> | <p>Real</p> | <p>[]</p> | <p>0 Acceleration factor for axial flow in MOMAXL. A value less than 1 slows the update of the axial flow from MOMAXL. Values [] may be needed for some applications. Reduce steady_state_time_step (→ p.D-102) if damping does not lead to convergence in the steady state solution. [accelx]</p> |
| <p>lateral_flow_ - acceleration_factor</p> | <p>Real</p> | <p>[]</p> | <p>0 Acceleration factor for lateral flow in MOMLAT. A value less than 1 slows the update of the lateral flow from MOMLAT. Values [] may be needed for some applications. Reduce steady_state_time_step (→ p.D-102) if damping does not lead to convergence in the steady state solution. [accely]</p> |
| <p>pressure_ - interpolation_factor</p> | <p>Real</p> | <p>0.0</p> | <p>0 Interpolation factor to locate pressure on staggered mesh. [xfacp] 0.0 - Places the pressure at J+1 at junction J - the same as SCHEME. This is recommended when a high degree of correspondence with SCHEME is desired. 0.5 - Places the pressure at the cell center as in a normal staggered mesh. This is recommended if flow reversals are to be considered.</p> |
| <p>axial_velocity_option</p> | <p>String</p> | <p>scheme_ solution</p> | <p>0 Option flag to select method of assigning axial velocity to the lateral cross flow boundary of the momentum cell in the axial momentum equation. [nustar] scheme_solution - Assigns an average as</p> |

| | | | | |
|--------------------------------|-----|-----|---|--|
| | | | | [] Hence the user must carefully assess the calculation results, especially regarding the flow field. |
| enthalpy_damping_ - iterations | Int | [] | 0 | The enthalpy_acceleration_factor (→ p.D-104) applies to nodal enthalpies after enthalpy_damping_iterations . [damp] Required if: enthalpy_acceleration_factor (→ p.D-104) is used. |

Note:

D.1.15 Input block *group_10_mixing* : Turbulent mixing correlations

Input example D.1-16: Input block *group_10_mixing* :

```
group_10_mixing {
  subcooled_mixing = w_over_gs_constant ;
  two_phase_mixing = subcooled_mixing ;
  thermal_conduction_mixing = no ;
  mixing_coefficient(unit=1) = [      ] ;
  mixing_exponent(unit=1) = [      ] ;
} ! end of group_10_mixing
```

This input block is required only for **array_type = arbitrary** (→ p.D-7) and **array_type = pwr_open** (→ p.D-7) (see **group_0_general** (→ p.D-7)).

Table D-22: Input keywords for COBRA-FLX *group_10_mixing*

| Name | Type Dim. | Default | O/M | Comment (unit, description, etc.) |
|-------------------------|-----------|---------|-----|--|
| <i>group_10_mixing</i> | - | - | O | Starts the input block group_10_mixing for specifying the turbulent mixing correlations. The block begins with a '{' and ends with a '}'. |
| <i>subcooled_mixing</i> | String | - | O | Subcooled mixing correlation indicator: [nscbc] w_over_gs_constant - W/GS = ABETA . |

| | | | | |
|--|--------|-----|-----------------------|--|
| | | | | <p>$w_{over_gs_reynolds} - W/GS = ABETA * RE^{**}BBETA .$</p> <p>$w_{over_gd_reynolds} - W/GD = ABETA * RE^{**}BBETA .$</p> <p>$w_{over_gs_d_aij_reynolds} - W/GS = (D/DIST) * ABETA * RE^{**}BBETA .$</p> <p>beus - Beus mixing model is used.</p> <p>Note: (1) Beta = W/GS where W is the turbulent crossflow. RE is the Reynolds Number. S and D are the gap size and equivalent hydraulic diameter. DIST is the centroid distance between two channels. ABETA (mixing_coefficient (→ p.D-108)) and BBETA (mixing_exponent (→ p.D-108)) are read later in this block.</p> |
| <code>two_phase_mixing</code> | String | - | <input type="radio"/> | <p>Two-phase mixing option: <i>[nbbc]</i></p> <p>subcooled_mixing - Two-phase mixing is the same as for subcooled conditions.</p> <p>n - Read a table with two-phase mixing data. (not yet available in kbf-input)</p> <p>Note: (1) Each pair of two-phase mixing data consists of the steam quality and the corresponding value of Beta.</p> |
| <code>thermal_conduction_mixing</code> | String | [] | <input type="radio"/> | <p>Thermal conduction mixing option: <i>[j5]</i></p> <p>no - No thermal conduction between subchannels</p> <p>yes - Thermal conduction taken into account, read in the thermal conduction geometry factor (not yet available in kbf-input)</p> |
| <code>tm_scaling</code> | String | [] | <input type="radio"/> | <p>Indicator for internal lateral scaling of turbulent mixing coefficient. <i>[lscale_tm]</i></p> <p>no - No internal lateral scaling of the turbulent mixing.</p> <p>yes - If internal lateral scaling of the turbulent mixing will be performed .</p> <p>Note: (1) Internal lateral scaling according to US NRC requirements (this option is only</p> |

| | | | | |
|-------------------------------|--------|---------|----------|---|
| | | | | applicable with subcooled_mixing = w_over_gs_constant, w_over_gs_reynolds, w_over_gd_reynolds, w_over_gs_d_aij_reynolds (→ p.D-106)): For tm_scaling = yes , the turbulent mixing is inversely proportional to the number of rod rows between channel centroids, i.e. the fluctuating crossflow due to turbulent mixing is multiplied by an internally calculated local factor of reference_distance / DIST (see distance_1, distance_2, distance_3, distance_4 (→ p.D-26) in block channels (→ p.D-26)). |
| number_of_mixing_types | Int | 1 | O | Number of gap mixing types to be defined. <i>[nbetai]</i> Required if: mixing_gap_types = individual (→ p.D-108) . |
| mixing_gap_types | String | uniform | O | <i>[nbetai]</i> uniform - If all gaps have the same mixing type. individual - If individual gap mixing types are to be specified. |
| mixing_coefficient | Real | - | O | List of the gap mixing coefficients according to the gap mixing types. <i>[abeta]</i> Required if: The channel definition is provided using group_4_channels (→ p.D-23) , i.e. array_definition=input (→ p.D-25) and subcooled_mixing (→ p.D-106) is not beus . This input is ignored if the mixing correlation coefficients are obtained by CoreLib . The definition is: mixing_coefficient (unit=1) = ... |
| mixing_exponent | Real | - | O | List of the gap mixing exponents according to the gap mixing types. <i>[bbeta]</i> Required if: The channel definition is provided using group_4_channels (→ p.D-23) , i.e. array_definition=input (→ p.D-25) and subcooled_mixing (→ p.D-106) is not beus . This input is ignored if the mixing correlation coefficients are obtained by CoreLib . The definition is: mixing_exponent (unit=1) = ... |
| gaps_with_ | Int | - | O | List of the gap numbers having mixing types |

| | | | | |
|---------------------------------|------|---|---|--|
| <code>mixing_gaptype</code> | | | | other than type 1. To all other gaps (that are not listed here) the mixing type 1 is attached by default. <i>[ig]</i> Required if: <code>mixing_gap_types = individual</code> (→ p.D-108) . |
| <code>mixing_gaptypes</code> | Int | - | ○ | List of the gap mixing types other than type 1 attached to the gaps listed in <code>gaps_with_mixing_gaptype</code> (→ p.D-108) . <i>[idgap1]</i> Required if: <code>mixing_gap_types = individual</code> (→ p.D-108) . |
| <code>reference_distance</code> | Real | - | ○ | Reference distance (cm) to be used for internal lateral scaling of the turbulent mixing. Reference distance is usually the centroid distance between two fuel rods (rod pitch). <i>[ref_beta]</i> Required if: <code>tm_scaling = yes</code> (→ p.D-107) |

D.1.16 Input block `group_11_operating_conditions` : Operating conditions

Input example D.1-17: Input block `group_11_operating_conditions` :

```
group_11_operating_conditions {
! inlet_enthalpy = uniform ;
inlet_temperature = uniform ;
inlet_mass_velocity = uniform ;

exit_pressure(unit=bar) = 157.4 ;
inlet_temperature_value(unit=degC) = 313.9 ;
inlet_mass_velocity_value(unit=kg/sm2) = 3571.29 ;
average_heat_flux(unit=kW/m2) = 637.061 ;
fraction_of_power_generated_in_rod(unit=1) = [      ] ;
bypass_fraction(unit=1) = [      ] ;

pressure_forcing_function {
Axis press_time (description="pressure forcing function"; size=6) ;
} ! end of pressure_forcing_function
p_time (Axis=press_time; unit=s) = 0.0 ...
rel_pressure (Axis=press_time; unit=1) = 1.0 ... ;
! p_time (unit=s) = 0.0 ... ;
! rel_pressure (unit=1) = 1.0 ... ;

! inlet_enthalpy_forcing_function {
! Axis inlet_enthalpy_time (description="inlet_enthalpy forcing
```

```

function"; size=6) ; ! n
! } ! end of inlet_enthalpy_forcing_function
! h_time (Axis=inlet_enthalpy_time; unit=s) = 0.0 ...;
! rel_inlet_enthalpy (Axis=inlet_enthalpy_time; unit=1) = 1.0 ...;

! flow_forcing_function {
! Axis_flow_time (description="flow forcing function"; size=6) ;
! } ! end of flow_forcing_function
! f_time (Axis=flow_time; unit=s) = 0.0 ...;
! rel_flow (Axis=flow_time; unit=1) = 1.0 ...;

! power_forcing_function {
! Axis_power_time (description="power forcing function"; size=6) ;
! } ! end of power_forcing_function
! pow_time (Axis=power_time; unit=s) = 0.0 ...;
! rel_power (Axis=power_time; unit=1) = 1.0 ...;
;
} ! end of group_11_operating_conditions

```

This input block is required always.

Table D-23: Input keywords for COBRA-FLX group_11_operating_conditions

| Name | Type Dim. | Default | O/M | Comment (unit, description, etc.) |
|-------------------------------|-----------|---------|-----|---|
| group_11_operating_conditions | - | - | M | Starts the input block group_11_operating_conditions for specifying the operating conditions. The block begins with a '{' and ends with a '}'. |
| inlet_enthalpy | String | - | O | Inlet enthalpy option indicator. This keyword is read only if the indicator inlet_temperature (→ p.D-110) is not specified. <i>[in]</i> uniform - Inlet enthalpy is given. individual - Read in the individual subchannel inlet enthalpies. All inlet enthalpies are read in the list all_inlet_enthalpies (→ p.D-114). |
| inlet_temperature | String | - | O | Definition of the inlet temperature option indicator. <i>[in]</i> uniform - Inlet temperature is given. individual - Read in the individual subchannel inlet temperatures. All inlet temperatures are read in the list all_inlet_temperatures (→ p.D-114). |
| inlet_mass_velocity | String | - | M | Inlet flow distribution indicator. <i>[ig]</i> |

| | | | | |
|-----------------|--------|------|---|--|
| | | | | <p>uniform - All subchannels are given the same mass velocity.</p> <p>equal_pressure_gradient - Inlet flow is divided to give equal pressure drop in all subchannels.</p> <p>individual - Mass flow factors for each channel read in the list</p> <p>all_mass_flow_fractions (→ p.D-114) .</p> |
| inlet_data | String | none | O | <p>Definition of the transient data to be read from the NLOOP file.</p> <p>none - The file NLOOP is not used.</p> <p>NLOOP_global_data - Only global transient data are read from the file NLOOP .</p> <p>NLOOP_global_local_data - Global and local transient data are read from the file NLOOP .</p> <ul style="list-style-type: none"> • <i>Transient time (s). [ttime];</i> • <i>System pressure at core outlet (bar). [fp/pln];</i> • <i>Core inlet temperature (°C). [fh/tln];</i> • <i>Core inlet mass flux (kg/m²-s). [fg/qln];</i> • <i>(Power generated in pellets and clad)/(total heated area) (kW/m²); equals average heatflux when no fuel rod model is used. [fq/qln];</i> • <i>Relative temperature of subchannel i, T_i (°C)/T_{average} (°C). [tinle];</i> • <i>Relative mass flux of subchannel I, G_i/G_{average}. [finle]</i> <p>Note: (1) Transient data are read from the file NLOOP, if the above condition holds. Tables are set up starting with the first value TIME > NLOOP_skip_time (→ p.D-111) (see below). Initial operating conditions are taken for this time point. Hereafter the tables are normalized. Reading from file NLOOP assigns nonzero values to the transient forcing functions, so inputting stacked transients via file NLOOP requires inputting these values as zero later in this input block. A warning message is printed if more than 10000 time points are available on file NLOOP and only the first 10000 are used for calculation</p> |
| NLOOP_skip_time | Real | - | O | Transient time to be skipped on NLOOP file. |

| | | | | |
|-----------------------------------|------|-----|---|--|
| | | | | <i>[tstart0]</i> The definition is: NLOOP_skip_time(unit=s) = ... |
| exit_pressure | Real | - | O | Operating pressure (bar). <i>[pexit]</i> Required if: inlet_data = none (→ p.D-111) . The definition is: exit_pressure(unit=bar) = ... |
| inlet_temperature_value | Real | - | O | Inlet temperature (°C). <i>[hin]</i> Required if: inlet_data = none (→ p.D-111) . The definition is: inlet_temperature_value(unit=degC) = ... |
| inlet_mass_velocity_value | Real | - | O | Definition of the core inlet mass flux (kg/(m ² s)). <i>[gin]</i> Required if: inlet_data = none (→ p.D-111) and inlet_volumetric_flow_rate (→ p.D-112) is not specified. The definition is: inlet_mass_velocity_value(unit=kg/sm2) = ... |
| inlet_volumetric_flow_rate | Real | - | O | Definition of the core inlet volumetric flow rate (m ³ /s). <i>[vflowin]</i> Required if: inlet_data = none (→ p.D-111) and inlet_mass_velocity_value (→ p.D-112) is not defined. The definition is: inlet_volumetric_flow_rate(unit=m3/s) = ... Note: (1) If the inlet_volumetric_flow_rate (→ p.D-112) is specified the input using the keyword inlet_mass_velocity_value (→ p.D-112) is neglected. Then the inlet mass velocity value is calculated based on (1.0- bypass_fraction (→ p.D-113)), inlet_volumetric_flow_rate (→ p.D-112) , inlet_temperature_value (→ p.D-112) and the total flow area of all sub-channels considered by THM. |
| average_heat_flux | Real | - | O | Average heat flux: (Power generated in fuel rods)/(total surface) (kW/m ²). <i>[aflux]</i> Required if: inlet_data = none (→ p.D-111) . The definition is: average_heat_flux(unit=kW/m2) = ... |
| fraction_of_ | Real | 1.0 | M | Fraction of heat generated in fuel; used to |

| | | | | |
|---|--------|-----|---|--|
| power_generated_- in_rod | | | | <p>calculate power generated in coolant. <i>[fhgfue]</i></p> <p>The definition is: fraction_of_power_generated_- in_rod(unit=1) = ...</p> <p>Note: (1) Total power of system = (power generated in fuel rods)/ fraction_of_power_- generated_in_rod .</p> |
| bypass_fraction | Real | 0.0 | O | <p>Bypass fraction used for vessel temperatures in setpoint calculation or for inlet flow distribution with given volumetric flow rate only. <i>[bypass]</i></p> <p>The definition is: bypass_fraction(unit=1) = ...</p> |
| exit_pressure_- distribution | String | no | O | <p>Indicator if pressure distribution will be specified at the core exit. <i>[-]</i></p> <p>yes - The pressure differences will be specified for selected subchannels.</p> <p>no - No pressure differences will be specified.</p> |
| set_point_iteration | String | - | O | <p>Definition of the setpoint calculation option for the inlet temperature. In case this option is selected, the setpoint parameters have to be specified in the input block set_point_parameters (→ p.D-117) . <i>[in + ispit]</i></p> <p>power - Setpoint iteration = Variation of power.</p> <p>inlet_temperature - Setpoint iteration = Variation of inlet temperature at fixed volumetric flow</p> <p>inlet_temperature_and_sensitivity - Setpoint calculation at which the first setpoint iteration = variation of inlet temperature at fixed volumetric flow is performed followed by sensitivity calculation.</p> <p>none - No setpoint iteration is performed.</p> |
| sensitivity_- calculation | String | no | O | <p>Indicator if sensitivity calculation will be performed. <i>[in + ispit]</i></p> <p>yes - Sensitivity calculation will be performed. Additional parameters have to be specified in input blocks set_point_parameters (→ p.D-116) and sensitivity_parameters (→ p.D-118) .</p> |

| | | | | |
|---|---------|-----|----------|---|
| | | | | no - No sensitivity calculation will be performed. |
| <code>normalize_channel_exit_pressures</code> | String | - | O | Indicator if the pressure differences at the core exit of all sub-channels will be adjusted to achieve zero average outlet pressure difference. <i>[IDPEXIT]</i> Required if: exit_pressure_distribution = yes (→ p.D-113) . no - The pressure differences at core exit will be used as given by input. yes - The pressure differences at core exit will be adjusted. |
| <code>all_inlet_enthalpies</code> | Real(:) | - | O | Inlet enthalpies for all channels in the same order as the channels are numbered. <i>[hinle]</i> Required if: inlet_enthalpy = individual (→ p.D-110) . |
| <code>all_inlet_temperatures</code> | Real(:) | - | O | Inlet temperatures for all channels in the same order as the channels are numbered. <i>[hinle]</i> Required if: inlet_temperature = individual (→ p.D-110) . |
| <code>all_mass_flow_fractions</code> | Real(:) | 1.0 | O | Channel inlet fractions of the total bundle flow are specified for all channels in the same order as the channels are numbered. <i>[fspli]</i> Required if: inlet_mass_velocity = individual (→ p.D-110) . |
| <code>pressure_forcing_function</code> | - | - | O | Definition of the axis_press_time (→ p.D-114) specifying the transient forcing function data pairs for pressure versus time. Each data pair consists of a time specification (seconds) and the relative value (present value/initial value). Required if: inlet_data = none (→ p.D-111) . |
| <code>Axis_press_time</code> | Int | - | O | Definition of the size of the lists p_time (→ p.D-114) and rel_pressure . (→ p.D-115) size is the number of data to be read. <i>[n3/np]</i> The definition is: Axis_press_time (description="pressure forcing function"; size=...) |
| <code>p_time</code> | Real(:) | - | O | Definition of the list p_time providing the time specification (s) for the pressure transient forcing function. <i>[yp]</i> The definition is: p_time (Axis=press_time; unit=s) = ... |

| | | | | |
|--|---------|---|---|---|
| <code>rel_pressure</code> | Real(:) | - | O | Definition of the list <code>rel_pressure</code> providing the relative pressure (current/initial) for the pressure transient forcing function. <i>[fp]</i> The definition is: rel_pressure (Axis=press_time; unit=1) = ... |
| <code>inlet_enthalpy - forcing_function</code> | - | - | O | Definition of the axis <code>inlet_enthalpy_time</code> (→ p.D-115) specifying the transient forcing function data pairs for inlet enthalpy versus time. Each data pair consists of a time specification (seconds) and the relative value (present value/initial value). Required if: <code>inlet_data = none</code> (→ p.D-111) . |
| Axis <code>inlet_enthalpy_time</code> | Int | - | O | Definition of the size of the lists <code>h_time</code> (→ p.D-115) and <code>rel_inlet_enthalpy</code> (→ p.D-115) . <code>size</code> is the number of data to be read. <i>[n4/nh]</i> The definition is: Axis inlet_enthalpy_time (description="inlet_enthalpy forcing function"; size=...) |
| <code>h_time</code> | Real(:) | - | O | Definition of the list <code>h_time</code> providing the time specification (s) for the inlet enthalpy transient forcing function. <i>[yh]</i> The definition is: h_time (Axis=inlet_enthalpy_time; unit=s) = ... |
| <code>rel_inlet_enthalpy</code> | Real(:) | - | O | Definition of the list <code>rel_inlet_enthalpy</code> providing the relative inlet enthalpy (current/initial) for the inlet enthalpy transient forcing function. <i>[fh]</i> The definition is: rel_inlet_enthalpy (Axis=inlet_enthalpy_time; unit=1) = ... |
| <code>flow_forcing_function</code> | - | - | O | Definition of the axis <code>flow_time</code> (→ p.D-115) specifying the transient forcing function data pairs for inlet flow versus time. Each data pair consists of a time specification (seconds) and the relative value (present value/initial value). Required if: <code>inlet_data = none</code> (→ p.D-111) . |
| Axis <code>flow_time</code> | Int | - | O | Definition of the size of the lists <code>f_time</code> (→ p.D-116) and <code>rel_flow</code> (→ p.D-116) . <code>size</code> is the number of data to be read. <i>[ng]</i> The definition is: Axis flow_time (description="flow forcing function"; size=...) |

| | | | | |
|-------------------------------------|---------|---|---|---|
| <code>f_time</code> | Real(:) | - | O | Definition of the list <code>f_time</code> providing the time specification (s) for the inlet flow transient forcing function. <i>[yg]</i> The definition is: f_time (Axis= flow_time; unit=s) =... |
| <code>rel_flow</code> | Real(:) | - | O | Definition of the list <code>rel_flow</code> providing the relative inlet flow (current/initial) for the inlet flow transient forcing function. <i>[fg]</i> The definition is: rel_flow (Axis= flow_time; unit=1) =... |
| <code>power_forcing_function</code> | - | - | O | Definition of the axis <code>power_time</code> specifying the transient forcing function data pairs for heat flux versus time. Each data pair consists of a time specification (seconds) and the relative value (present value/initial value). Required if: <code>inlet_data = none</code> (→ p.D-111) . |
| <code>Axis power_time</code> | Int | - | O | Definition of the size of the lists <code>pow_time</code> (→ p.D-116) and <code>rel_power</code> (→ p.D-116) . <code>size</code> is the number of data to be read. <i>[nq]</i> The definition is: Axis power_time (description="power forcing function"; size=...) |
| <code>pow_time</code> | Real(:) | - | O | Definition of the list <code>pow_time</code> providing the time specification (s) for the heat flux transient forcing function. <i>[yq]</i> The definition is: pow_time (Axis= power_time; unit=s) =... |
| <code>rel_power</code> | Real(:) | - | O | Definition of the list <code>rel_power</code> providing the relative heat flux or power generation (current/initial) for the heat flux transient forcing function. <i>[fq]</i> The definition is: rel_power (Axis= power_time; unit=1) =... Note: (1) If a fuel rod model is specified with <code>group_8_rod_data</code> (→ p.D-43) , <code>rel_power</code> (→ p.D-116) applies no longer to the heat flux, but to the power generation rate. |

D.1.16.1 Input block `set_point_parameters` included in input block `group_11_operating_conditions`

It is required if `set_point_iteration = power`, `inlet_temperature` or `inlet_temperature_and_sensitivity` (→ p.D-113) or `sensitivity_calculation = yes` (→ p.D-113) .

Table D-24: Input keywords for COBRA-FLX set_point_parameters

| Name | Type Dim. | Default | O/M | Comment (unit, description, etc.) |
|---------------------------------|-----------|---------|-----|---|
| set_point_parameters | - | - | O | Input block containing the set-point parameters. [] Required if: set_point_iteration = power, inlet_temperature or inlet_temperature_and_sensitivity (→ p.D-113) |
| heat_flux_lower_limit | Real | - | M | Lower limit of the heat flux interval to be searched (kW/m ²). [xsplow] Required if: set_point_iteration = power (→ p.D-113) |
| heat_flux_upper_limit | Real | - | M | Upper limit of the heat flux interval to be searched (kW/m ²). [xsphgh] Required if: set_point_iteration = power (→ p.D-113) |
| temperature_lower_limit | Real | - | M | Lower limit of the temperature interval to be searched (°C). [xsplow] Required if: set_point_iteration = inlet_temperature or inlet_temperature_and_sensitivity (→ p.D-113) |
| temperature_upper_limit | Real | - | M | Upper limit of the temperature interval to be searched (°C). [xsphgh] Required if: set_point_iteration = inlet_temperature or inlet_temperature_and_sensitivity (→ p.D-113) |
| target_DNBR | Real | - | M | Target DNBR for iteration. [dnblim] Required if: the input block set_point_parameters (→ p.D-117) is used. |
| DNBR_tolerance | Real | - | M | Iteration is stopped if ABS(DNBR-target_DNBR) < DNBR_tolerance . [tollim] Required if: the input block set_point_parameters (→ p.D-117) is used. |
| allowable_number_of_ iterations | Int | - | M | Case is skipped if no convergence is reached after |

| | | | | |
|--|--|--|--|--|
| | | | | allowable_number_of_iterations iterations. <i>[maxfn]</i> Required if: the input block set_point_parameters (→ p.D-117) is used. |
|--|--|--|--|--|

D.1.16.2 Input block *sensitivity_parameters* included in input block group_11_- operating_conditions

It is required if **set_point_iteration = inlet_temperature_and_sensitivity** (→ p.D-113) or **sensitivity_calculation = yes** (→ p.D-113) .

Table D-25: Input keywords for COBRA-FLX *sensitivity_parameters*

| Name | Type Dim. | Default | O/M | Comment (unit, description, etc.) |
|--|-----------|---------|-----|--|
| <i>sensitivity_parameters</i> | - | - | O | Input block containing the sensitivity parameters. <i>[-]</i> Required if: set_point_iteration = inlet_temperature_and_sensitivity (→ p.D-113) or sensitivity_calculation = yes (→ p.D-113) . |
| <i>variation_coefficient_-system_pressure</i> | Real | 0.0 | O | Coefficient of variation for system pressure. <i>[varncs(1)]</i> |
| <i>variation_coefficient_-inlet_temperature</i> | Real | 0.0 | O | Coefficient of variation for inlet temperature. <i>[varncs(2)]</i> |
| <i>variation_coefficient_-mass_flow_rate</i> | Real | 0.0 | O | Coefficient of variation for mass flow rate; may be used to model uncertainty of bypass flow as well as of vessel flow. <i>[varncs(3)]</i> |
| <i>variation_coefficient_-heat_flux</i> | Real | 0.0 | O | Coefficient of variation for heat flux. <i>[varncs(4)]</i> |
| <i>variation_coefficient_-FdeltaH_nuclear</i> | Real | 0.0 | O | Coefficient of variation for F-delta-h nuclear. <i>[varncs(5)]</i> |
| <i>variation_coefficient_-FQ_engineering</i> | Real | 0.0 | O | Coefficient of variation for Fq engineering. <i>[varncs(6)]</i> |
| <i>variation_coefficient_-FdeltaH_engineering1</i> | Real | 0.0 | O | Coefficient of variation for F-delta-h engineering1, will be applied to hot channel (see block group_3.2_hot_channel_factors (→ p.D-22)). <i>[varncs(7)]</i> |

| | | | | |
|--|--------|-----|---|---|
| <code>variation_coefficient_code_uncertainty</code> | Real | 0.0 | O | Coefficient of variation for code uncertainty. [<i>vamcs(8)</i>] |
| <code>variation_coefficient_transient_code_uncertainty</code> | Real | 0.0 | O | Coefficient of variation for transient code uncertainty. [<i>varncs(9)</i>] |
| <code>variation_coefficient_DNB_correlation_uncertainty</code> | Real | 0.0 | O | Coefficient of variation for DNB correlation uncertainty. [<i>vamcs(10)</i>] |
| <code>Monte_Carlo_simulation</code> | String | no | O | Indicator if Monte-Carlo Simulation will be performed. [-] yes - Monte-Carlo Simulation will be performed. In this case the <code>variation_coefficient_DNB_correlation_uncertainty</code> (→ p.D-119) should be positive. no - Monte-Carlo Simulation will not be performed. (not yet available in kbf-input) |

Input block `group_12_output_options` : Output display options

Input example D.1-18: Input block `group_12_output_options` :

```
group_12_output_options {
print_selection = all
! Axis print_channels (description="number of channels whose data
are printed"; size=9) ;
! channels_printed (Axis=print_channels; unit=1) = 1 ...;
! Axis print_rods (description="number of rods whose data are
printed"; size=9) ;
! rods_printed (Axis=print_rods; unit=1) = 1 ...;
! Axis print_fuel_nodes (description="number of fuel nodes whose
data are printed"; size=3) ;
! fuel_nodes_printed (Axis=print_fuel_nodes; unit=1) = 1 ...;
} ! end of group_12_output_options
```

This input block is required always.

Table D-26: Input keywords for COBRA-FLX `group_12_output_options`

| Name | Type Dim. | Default | O/M | Comment (unit, description, etc.) |
|--------------------------------------|-----------|---------|-----|--|
| <code>group_12_output_options</code> | - | - | M | Starts the input block <code>group_12_output_options</code> for specifying the |

| | | | | |
|----------------------------------|--------|-----|---|--|
| | | | | output display options. The block begins with a '{' and ends with a '}'. |
| <code>hdf_write_results</code> | String | yes | O | Indicator if COBRA-FLX results will be written to HDF output file. yes - Print results to HDF file. no - No results are printed to HDF file. |
| <code>write_to_screen</code> | String | no | O | Indicator if COBRA-FLX information will be printed to the screen (or stderr-file). yes - Print control information to the screen. no - No information is printed to the screen. |
| <code>ascii_write_results</code> | String | no | O | Indicator if COBRA-FLX results will be written to ASCII output file. yes - Print results to ASCII file. no - No results are printed to ASCII file. |
| <code>print_selection</code> | String | - | M | Data printout indicator: <i>[nout]</i> channels - Print subchannel data only. channels_crossflows - Print subchannel data and crossflow data table. channels_rods - Print subchannel data and fuel rod data table. all - Print subchannel data, fuel rod data table and crossflow data table. Note: (1) The selected thermal-hydraulics results are printed to the HDF output file for all channels, all rods and all axial nodes (if hdf_write_results = yes (→ p.D-120)). |
| <code>Axis print_channels</code> | Int | - | O | Definition of the size of the list channels_printed (→ p.D-120) . size is the number of channels whose data will be printed to the ASCII output. <i>[npchan]</i> The definition is: Axis print_channels (description="number of channels whose data are printed"; size =...) |
| <code>channels_printed</code> | Int(:) | - | O | Definition of the list channels_printed providing the channel numbers for which results are desired (only ASCII output). <i>[printc]</i> |

| | | | | |
|------------------------------|--------|---|---|---|
| | | | | The definition is: channels_printed (Axis=print_channels; unit=1) =... |
| Axis print_rods | Int | - | O | Definition of the size of the list rods_printed . (→ p.D-121) size is the number of rods whose data will be printed (only ASCII output). [<i>nprod</i>] The definition is: Axis print_rods (description="number of rods whose data are printed"; size =...) |
| rods_printed | Int(:) | - | O | Definition of the list rods_printed providing the rod numbers for which results are desired (only ASCII output). [<i>printr</i>] The definition is: rods_printed (Axis= print_rods; unit=1) =... |
| Axis print_fuel_nodes | Int | - | O | Definition of the size of the list fuel_nodes_printed (→ p.D-121) . size is the number of fuel nodes whose data will be printed. [<i>nprnode</i>] The definition is: Axis print_fuel_nodes (description="number of fuel nodes whose data are printed"; size =...) |
| fuel_nodes_ - printed | Int(:) | - | O | Definition of the list fuel_nodes_printed providing the node numbers for which results are desired. [<i>printn</i>] The definition is: fuel_nodes_printed (Axis= print_fuel_nodes; unit=1) =... |

Note:

- (1) The node numbers are counted such that fuel centerline is node 1 and fuel surface is node N.
- (2) If CHF-data has been calculated, it will be printed out for each of the fuel rods selected plus a summary to identify the rod and channel with the minimum CHF-ratio.
- (3) When called from PANBOX the channel numbers refer rather to fuel assembly numbers than to channels, i.e. specifying a fuel assembly number of an assembly being HOSCAM-nodalized results in the printout of the hot subchannel data within the fuel assembly rather than that of the fuel assembly.

(4) Default rod and channel numbers selected for printout are different for standalone COBRA-FLX and PANBOX: COBRA-FLX prints by default all rods and channels. The coupled system printout is minimal. Printout of all channels and rods is achieved by inputting **debug_printing = detailed** (→ p.D-97) on input block **group_9_calculation_variables** (→ p.D-95) . Type of data printed is still determined by **print_selection** (→ p.D-120) . HOSCAM printout depends on variable NCHHSC in PAN_INP block \$HOSCA:
 NCHHSC = 0: Print data of all hot subchannels and pertaining rods
 NCHHSC>0: Print only data requested for by **rods_printed** (→ p.D-121) or **channels_printed** (→ p.D-120) .

D.2 COBRA-FLX Restart Capability

A restart capability is provided by storing the thermal hydraulics input to the HDF output file. In case of a coupled calculation, no additional settings are required for COBRA-FLX.

A restart capability for THM stand-alone is added, by setting the new keyword **read_restart** to yes. Then all COBRA-FLX input data are read from the restart file (specified in the input block **hdf_options**) instead of the kbf-input file. Then the following **thm_input** block is needed in addition to the **hdf_options** block.

```
thm_input {
  read_restart = yes ;
}
```

Input example D.2: COBRA-FLX restart capability

D.3 Thermal-Hydraulics (COBRA-FLX) Stand-Alone Calculation

The input block needed for a COBRA-FLX stand-alone calculation is **thm_calc**. The calculation is performed based on the input provided in **thm_input** block.

```
thm_calc(ID=1) { }
```

Index of Keywords for KBF and Conventional Formats

| | | | |
|----------|--------------------------------------|------------|--|
| 1 | | | |
| | 10 (G11-1b) | E-77 | |
| A | | | |
| | A (10-CD) | E-97 | |
| | A (19a-FD) | E-105 | |
| | A (37-OC) | E-126 | |
| | A (G8-2n) | E-60 | |
| | AA (25-HM) | E-111 | |
| | AA(1) (25-HM) | E-111 | |
| | AA, BB, CC (G2-1) | E-11 | |
| | ABETA (24-HM) | E-109 | |
| | ABETA (24-HM-2) | E-110 | |
| | ABETA (G10-1) | E-70 | |
| | ABETA (G10-1b) | E-71 | |
| | absolute_energy_error | D-105 | |
| | AC (G4a-1) | E-15 | |
| | AC (G4b-3) | E-18 | |
| | ACCELF (33-HM) | E-121 | |
| | ACCELF (G9-1) | E-64 | |
| | ACCELP (33e-HM) | E-124 | |
| | ACCELP (G9-9) | E-68 | |
| | ACCELSP (33-HM) | E-121 | |
| | ACCELSP (G9-1) | E-64 | |
| | ACCELX (33d-HM) | E-123 | |
| | ACCELX (G9-8) | E-67 | |
| | ACCELY (33d-HM) | E-123 | |
| | ACCELY (G9-8) | E-68 | |
| | ACELF (9-CD-1) | E-97 | |
| | ACELF (G8-2e-1) | E-56 | |
| | AF (27-HM) | E-112 | |
| | AF (G2-3) | E-12 | |
| | AFACT (G5-3) | E-29 | |
| | AFLUX (4-HF) | E-92 | |
| | AFLUX (G11-1) | E-75 | |
| | all_inlet_enthalpies | D-115 | |
| | all_inlet_temperatures | D-115 | |
| | all_mass_flow_fractions | D-115 | |
| | allowable_number_of_iterations | D-120 | |
| | AoneSC (32d-HM-2) | E-118 | |
| | AoneSC (G4b-16) | E-25 | |
| | AoneSC (G8-1c-2) | E-44 | |
| | area_variations | D-30 | |
| | argon_fraction | D-90 | |
| | array_definition | D-25 | |
| | array_type | D-7 | |
| | ascii_write_results | D-123 | |
| | AV (29-HM) | E-113 | |
| | AV (G2-2) | E-11 | |
| | ave+1 (G11-1b) | E-77 | |
| | average_burnup | D-88 | |
| | average_heat_flux | D-113 | |
| | AVTEMP (G11-1.0) | E-75 | |
| | AX_REGIONS (G8-1-3) | E-39 | |
| | AXIAL (5-HF) | E-93 | |
| | AXIAL (G3-1) | E-13 | |
| | axial_flow_acceleration_factor | D-103 | |
| | axial_node_boundaries | D-98 | |
| | axial_node_boundaries_relative | D-98 | |
| | axial_node_heights | D-98 | |
| | axial_node_input | D-97 | |
| | axial_node_printing | D-96 | |
| | axial_velocity_option | D-104 | |
| | Axis axial_locations_av | D-31 | |
| | Axis axial_locations_gv | D-34 | |
| | Axis burnup | D-92 | |
| | Axis channel_number | D-26 | |
| | Axis channel_property | D-26 | |
| | Axis fax_z | D-20 | |
| | Axis ff_coefficient | D-18 | |
| | Axis flow_time | D-117 | |
| | Axis fuel_shells | D-81 | |
| | Axis gap_number | D-29, D-41 | |
| | Axis gap_property | D-28 | |
| | Axis grid_location_number | D-40 | |
| | Axis grid_type | D-40 | |
| | Axis inlet_enthalpy_time | D-116 | |
| | Axis linear_heat_rate | D-92 | |
| | Axis number_channels_av | D-31 | |
| | Axis number_gap_gv | D-34 | |
| | [..... | D-63 | |
| | Axis number_of_mixing_grids | D-62 | |
| | Axis power_time | D-117 | |
| | Axis press | D-11 | |
| | Axis press_time | D-116 | |
| | Axis print_channels | D-123 | |
| | Axis print_fuel_nodes | D-124 | |
| | Axis print_rods | D-123 | |
| | Axis rod_number | D-52 | |
| | Axis rod_property | D-52 | |
| | Axis timesteps | D-79 | |
| | AXL (G5-1) | E-28 | |
| B | | | |
| | B (10-CD) | E-97 | |
| | [..... | E-49 | |
| | BB (25-HM) | E-111 | |
| | BBETA (24-HM) | E-109 | |
| | BBETA (24-HM-2) | E-110 | |
| | BBETA (G10-1) | E-70 | |
| | BBETA (G10-1b) | E-71 | |
| | BLEN (32h-HM) | E-120 | |
| | BLEN (G8-1j) | E-47 | |
| | BRMAX (G11-1.0) | E-75 | |
| | bulk_void | D-14 | |
| | bundle_heated_length | D-70 | |
| | bundle_length | D-100 | |
| | bundle_position | D-100 | |
| | Burn (18a-FD) | E-104 | |
| | Burn (18b-FD) | E-104 | |
| | BURN (19a-FD) | E-105 | |
| | BURN (19-FD) | E-105 | |
| | Burn (G8-2k) | E-58 | |
| | Burn (G8-2l) | E-58 | |
| | BURN (G8-2m) | E-59 | |
| | BURN (G8-2n) | E-60 | |
| | burnup_list | D-92 | |
| | BX (G10-2) | E-71 | |

COBRA-FLX: A Core Thermal-Hydraulic Analysis Code

Topical Report

Appendix D

| | | | |
|--|------------|----------------------------------|------------|
| BYPASS (36-OC1)..... | E-126 | CPR (G8-2m)..... | E-59 |
| BYPASS (G11-1)..... | E-75 | CROSS (G7-2)..... | E-32 |
| bypass_fraction..... | D-114 | cross_flow_indicator..... | D-40 |
| C | | crossflow_error..... | D-101 |
| C (10-CD)..... | E-97 | D | |
| case_description..... | D-8 | D (10-CD)..... | E-97 |
| case_number..... | D-7 | DAMPER (33e-HM)..... | E-123 |
| CC (16-FD)..... | E-101 | DAMPER (G9-9)..... | E-68 |
| CC (25-HM)..... | E-111 | DAMPH (33e-HM)..... | E-124 |
| CCLAD (G4b-13)..... | E-23 | DAMPH (G9-9)..... | E-68 |
| CCLAD (G8-2)..... | E-52 | data_ACH_1..... | D-61 |
| CD (G4b-4)..... | E-19 | data_ACH_2..... | D-71 |
| CD (G7-5)..... | E-33 | data_Barnett..... | D-71 |
| CD0(I,J) (HOS4)..... | E-132 | data_BHTP..... | D-71 |
| CD6(I,J) (HOS4)..... | E-132 | data_Biasi..... | D-72 |
| CDA, CDB, CDC (11-CD)..... | E-98 | data_BWC..... | D-72 |
| CDA,CDB,CDC (G4b-4)..... | E-19 | data_BWCMV..... | D-72 |
| CDA,CDB,CDC (G7-5)..... | E-33 | data_BWCMV_A..... | D-72 |
| CDG (11-CD)..... | E-98 | data_BWU_B11R..... | D-73 |
| CDH(I,J) (HOS4)..... | E-133 | data_BWU_I..... | D-73 |
| CF (16-FD)..... | E-101 | data_BWU_N..... | D-73 |
| CFUEL (G4b-13)..... | E-23 | data_BWU_Z_Mark_B11..... | D-72 |
| CFUEL (G8-2)..... | E-52 | data_BWU_Z_Mark_BW17..... | D-73 |
| channel_number_av..... | D-32 | data_BWU_Z_Mark_BW17_MSMG..... | D-72 |
| channels..... | D-26 | [.....] | D-60 |
| channels_printed..... | D-123 | [.....] | D-60 |
| CHF_AX_TYPE (G8-1-3)..... | E-39 | [.....] | D-60 |
| chf_correlation..... | D-46, D-57 | [.....] | D-61 |
| chf_correlation_from_rod_number..... | D-56 | [.....] | D-61 |
| chf_correlation_to_rod_number..... | D-56 | [.....] | D-70 |
| chf_correlations_with_performance_factors..... | D-56 | data_HTPA..... | D-73 |
| chf_data..... | D-54, D-55 | [.....] | D-59 |
| chf_hot_channel_data..... | D-65 | data_Modified_Barnett..... | D-71 |
| CHF_LIMIT (G8-1m)..... | E-49 | [.....] | D-70 |
| CHF_LIMIT (G8-1n)..... | E-50 | [.....] | D-70 |
| CHF_LIMIT (G8-1o)..... | E-50 | [.....] | D-63 |
| CHF_PERF (G8-1-1)..... | E-38 | [.....] | D-70 |
| chf_performance_factors..... | D-56 | DAUTOG (G11-6.a)..... | E-80 |
| chf_selector..... | D-63 | DAUTOH (G11-5.a)..... | E-80 |
| chf_skip_type..... | D-7 | DAUTOP (G11-4.a)..... | E-79 |
| CHFLIM (G3-3)..... | E-14 | DAUTOQ (G11-7.a)..... | E-81 |
| CHTcc (19b-FD)..... | E-106 | DCHAR(1.3) (32e-HM-1)..... | E-119 |
| CHTcc (G8-2o)..... | E-61 | DCHAR(1.3) (G4b-18)..... | E-26 |
| CITEMP (G11-1.0)..... | E-75 | DCHAR(1.3) (G8-1d-1)..... | E-45 |
| cladding_density..... | D-78 | DDR (G8-1o)..... | E-50 |
| cladding_shells..... | D-81 | debug_printing..... | D-74, D-97 |
| cladding_specific_heat..... | D-77 | density_acceleration_factor..... | D-104 |
| cladding_thermal_conductivity..... | D-77 | DF (16-FD)..... | E-101 |
| cladding_thickness..... | D-78 | DFLUMIN (G11-1.0)..... | E-75 |
| coefficient_for_CARO_heat_transfer_model..... | D-93 | DFUEL (G4b-13)..... | E-23 |
| cold_wall_factor..... | D-67 | DFUEL (G8-2)..... | E-52 |
| COMPI(I) (HOS4)..... | E-132 | DGT(I) (HOS4)..... | E-132 |
| composition_defect..... | D-88 | DHHYD (32g-HM-2)..... | E-120 |
| conductivity..... | D-12 | DHHYD (G8-1g)..... | E-46 |
| coolant_name..... | D-9 | DIA (G7-1)..... | E-32 |
| coolant_pressure_steps..... | D-10 | diameter_1..... | D-69 |
| coolant_properties..... | D-11 | diameter_2..... | D-69 |
| COTEMP (G11-1.0)..... | E-75 | diameter_3..... | D-69 |
| CPel (17d-FD)..... | E-103 | diameter_selection_1..... | D-68 |
| CPel (G8-2h)..... | E-57 | | |
| CPR (19-FD)..... | E-105 | | |

COBRA-FLX: A Core Thermal-Hydraulic Analysis Code

Topical Report

Appendix D

Page D-125

| | | | |
|--|------------|-----------------------------------|-------|
| diameter_selection_2 | D-68 | FAKTOT (32a-HM) | E-115 |
| diameter_selection_3 | D-68 | FAKTOT (32b-HM) | E-115 |
| dishing | D-85 | FAKTOT (G8-1a) | E-41 |
| dishing_depth | D-85 | fax | D-21 |
| dishing_radius | D-85 | fDNBRW (32f-HM-2) | E-119 |
| DIST (G4a-1) | E-15 | fDNBRW (G4b-20) | E-27 |
| DIST (G4b-3) | E-18 | fDNBRW (G8-1e-2) | E-46 |
| diversion_crossflow_resistance_factor | D-99 | FEDH1 (G3-2) | E-13 |
| diversion_crossflow_resistance_scaling | D-99 | FEDH2 (G3-2) | E-13 |
| DMKorc (17d-FD) | E-103 | FEQ (G3-2) | E-13 |
| DMKorc (G8-2h) | E-57 | FERROR (33-HM) | E-121 |
| DMKorr (17d-FD) | E-103 | FERROR (G9-1) | E-64 |
| DMKorr (G8-2h) | E-57 | ff_coefficient_aa | D-18 |
| dnb_limit | D-23 | ff_coefficient_bb | D-18 |
| dnb_limit_indicator | D-23 | ff_coefficient_cc | D-18 |
| DNBLIM (36.1-OC) | E-126 | ff_coefficient_table | D-18 |
| DNBLIM (G11-1a) | E-76 | FG (41-T) | E-128 |
| dnbr_multiplier | D-59, D-70 | FG (G11-6) | E-80 |
| DNBR_tolerance | D-119 | FG (GLN) (NLOOP) | E-74 |
| DNBRMIN (G11-1.0) | E-75 | FGd2O3 (18b-FD) | E-104 |
| DPel (17d-FD) | E-103 | FGd2O3 (G8-2l) | E-58 |
| DPel (G8-2h) | E-57 | FGf12 (32d-HM-2) | E-118 |
| DR (10-CD) | E-97 | FGf12 (G4b-16) | E-25 |
| DR (15-RD) | E-100 | FGf12 (G8-1c-2) | E-44 |
| DR (G4b-3) | E-18 | [] (32f-HM-1) | E-119 |
| DR (G8-1) | E-38 | [] (G4b-19) | E-26 |
| DR0(l) (HOS4) | E-132 | [] (G8-1e-1) | E-45 |
| DTSS (33a-HM) | E-122 | FH (40-T) | E-128 |
| DTSS (G9-5) | E-66 | FH (G11-5) | E-80 |
| DUM (G7-2) | E-32 | FH (TLN) (NLOOP) | E-74 |
| E | | FHGAP (G8-2d) | E-54 |
| EGAP (HOS1) | E-132 | FHGFUE (36-OC1) | E-126 |
| ENEH (35-HM) | E-125 | FHGFUE (G11-1) | E-75 |
| ENEH(K) (G4a-2) | E-16 | FHGFUE (G11-1.0) | E-74 |
| enthalpy_acceleration_factor | D-104 | FINLE (31-HM) | E-113 |
| enthalpy_damping_iterations | D-105 | FINLE(I,2) (NLOOP) | E-74 |
| enthalpy_liquid | D-12 | first_debug_channel | D-76 |
| enthalpy_vapor | D-12 | flow_error | D-100 |
| ENTHMAX (G11-1.0) | E-75 | flow_forcing_function | D-117 |
| EPSF (9-CD) | E-96 | flow_underrelaxation_factor | D-101 |
| EPSF (G8-2e) | E-55 | flux_engineering_factor | D-22 |
| EPSOR (33-HM) | E-121 | FMolt (18a-FD) | E-104 |
| EPSOR (G9-1) | E-64 | FMolt (G8-2k) | E-58 |
| [] | D-63 | FP (39-T) | E-127 |
| [] | D-62 | FP (G11-4) | E-79 |
| [] | D-62 | FP (PLN) (NLOOP) | E-74 |
| exit_pressure | D-112 | FPRESS (19-FD) | E-105 |
| exit_pressure_distribution | D-114 | FPRESS (G8-2m) | E-59 |
| EXPR (19-FD) | E-105 | FPuO2 (18a-FD) | E-104 |
| EXPR (G8-2m) | E-59 | FPuO2 (18b-FD) | E-104 |
| F | | FPuO2 (18-FD) | E-103 |
| f_time | D-117 | FPuO2 (G8-2i) | E-58 |
| F1GRID (G3-2) | E-13 | FPuO2 (G8-2k) | E-58 |
| F2GRID (G3-2) | E-13 | FPuO2 (G8-2l) | E-58 |
| F3GRID (G3-2) | E-13 | FQ (42-T) | E-128 |
| FACFTM(K) (G4a-2) | E-16 | FQ (G11-7) | E-81 |
| FACSL (21-GB) | E-107 | FQ (QLN) (NLOOP) | E-74 |
| FACSL(K) (G4a-2) | E-16 | FRAC (10-CD) | E-97 |
| FACSLK (21-GB) | E-107 | FRAC (G4b-3) | E-18 |
| FACSLK(K) (G4a-2) | E-16 | fraction_of_flow_diverted | D-43 |

COBRA-FLX: A Core Thermal-Hydraulic Analysis Code

Topical Report

Appendix D

Page D-126

| | | | |
|--|------------|---|------------|
| fraction_of_power_generated_in_rod | D-114 | GMIX(3) (19-FD)..... | E-105 |
| FRadF12 (32d-HM-2) | E-118 | GMIX(3) (G8-2m)..... | E-59 |
| FRadF12 (G4b-16) | E-25 | GMIX(3) (G8-2n)..... | E-60 |
| FRadF12 (G8-1c-2) | E-44 | GMIX(4) (19a-FD)..... | E-106 |
| friction_factor | D-17 | GMIX(4) (19-FD)..... | E-105 |
| from_x_over_l | D-58 | GMIX(4) (G8-2m)..... | E-59 |
| FSPLI (G11-3) | E-79 | GMIX(4) (G8-2n)..... | E-60 |
| FTD (18a-FD) | E-104 | GMIX(5) (19a-FD)..... | E-106 |
| FTD (18b-FD) | E-104 | GMIX(5) (G8-2n)..... | E-60 |
| FTD (18-FD) | E-103 | GrgF (19a-FD)..... | E-105 |
| FTD (G8-2i) | E-58 | GrgF (G8-2n)..... | E-60 |
| FTD (G8-2k) | E-58 | GrgH (19a-FD)..... | E-105 |
| FTD (G8-2l) | E-58 | GRGH (19-FD)..... | E-105 |
| FTM (32-HM) | E-114 | GRGH (G8-2m)..... | E-59 |
| FTM (G9-1)..... | E-64 | GrgH (G8-2n)..... | E-60 |
| fuel_density | D-77 | grid_1_factor..... | D-23 |
| fuel_nodes_printed | D-124 | grid_2_factor..... | D-23 |
| fuel_pressure..... | D-89 | grid_3_factor..... | D-23 |
| fuel_pressure_coefficient..... | D-88 | grid_channel_mapping | D-40 |
| fuel_pressure_exponent..... | D-89 | grid_constant..... | D-59 |
| fuel_rod_geometry..... | D-84 | grid_gap_mapping..... | D-41 |
| fuel_rod_materials..... | D-87 | grid_height..... | D-62 |
| fuel_rod_model..... | D-51 | grid_locations | D-40 |
| fuel_rod_models | D-55, D-80 | grid_loss_coeff_ratio_vane_novane..... | D-71 |
| fuel_roughness..... | D-89 | grid_loss_coefficients_a | D-42 |
| fuel_specific_heat..... | D-77 | grid_loss_coefficients_b | D-43 |
| fuel_thermal_conductivity..... | D-77 | grid_loss_coefficients_c | D-43 |
| fuel_thermal_properties..... | D-54, D-77 | grid_option..... | D-59 |
| FXF (G4b-4)..... | E-19 | grid_spacing | D-71, D-75 |
| FXFLO (G7-5)..... | E-33 | grid_spacing_coefficient..... | D-69 |
| G | | grid_spacing_coordinate | D-75 |
| GAP (10-CD) | E-97 | grid_type..... | D-42 |
| gap_heat_transfer | D-79, D-91 | GRIDHT (32g-HM-3) | E-120 |
| gap_heat_transfer_coefficient | D-78, D-93 | GRIDHT (32i-HM-1)..... | E-121 |
| gap_number_gv..... | D-35 | GRIDHT (G8-1h) | E-46 |
| gap_thickness..... | D-81 | GRIDXL (13-CD) | E-99 |
| gap_variations | D-34 | GRIDXL (G4b-6)..... | E-20 |
| GAPREC (20-GB)..... | E-106 | GRIDXL (G7-4)..... | E-33 |
| GAPS (G4a-1) | E-15 | GRIDXL(I) (HOS2)..... | E-132 |
| GAPS (G4b-3)..... | E-18 | group_0_general | D-7 |
| gaps_with_local_coupling_parameters..... | D-28 | group_0_solver | D-5 |
| gaps_with_mixing_gaptype | D-109 | group_1_coolant..... | D-9 |
| GAPXL (G6-1) | E-30 | group_10_mixing..... | D-107 |
| gas_plenumvolume | D-91 | group_11_operating_conditions | D-111 |
| gas_pressure..... | D-84 | group_12_output_options | D-122 |
| gas_pressure_in_gap..... | D-91 | group_2_flow_correlations | D-14 |
| gas_temperature_in_gap..... | D-91 | group_3.2_hot_channel_factors | D-22 |
| Gd2O3_fraction | D-88 | group_3_power_distribution | D-20 |
| GFACT (G6-3)..... | E-30 | group_4_channels | D-25 |
| GIN (36-OC)..... | E-125 | group_5.1_channel_area_variation_data | D-32 |
| GIN (G11-1)..... | E-75 | group_5_channel_area_variation | D-30 |
| GK (G10-3)..... | E-72 | group_6.1_gap_variation_data | D-35 |
| GMIX(1) (19a-FD)..... | E-106 | group_6_gap_variation | D-34 |
| GMIX(1) (19-FD)..... | E-105 | group_7_spacer..... | D-39 |
| GMIX(1) (G8-2m)..... | E-59 | group_8_rod_data | D-45 |
| GMIX(1) (G8-2n)..... | E-60 | group_9_calculation_variables | D-96 |
| GMIX(2) (19a-FD)..... | E-106 | H | |
| GMIX(2) (19-FD)..... | E-105 | h_time..... | D-116 |
| GMIX(2) (G8-2m)..... | E-59 | H0Pel (17d-FD) | E-103 |
| GMIX(2) (G8-2n)..... | E-60 | H0Pel (G8-2h) | E-57 |
| GMIX(3) (19a-FD)..... | E-106 | hc_flow_area | D-67 |

| | | | |
|-----------------------------------|-------|--------------------------------------|-------|
| hc_heated_perimeter..... | D-67 | IFRM (8-CD)..... | E-95 |
| hc_mass_velocity_factor..... | D-67 | IG (30-HM)..... | E-113 |
| hc_radial_power_factor..... | D-67 | IG (G10-1d)..... | E-71 |
| hc_ratio_radial_power_factor..... | D-68 | IGRID (13-CD)..... | E-99 |
| hc_wetted_perimeter..... | D-67 | IGRID (G4b-6)..... | E-20 |
| HCHANS (G8-1r)..... | E-51 | IGRID (G7-4)..... | E-33 |
| HCHANX (G8-1r)..... | E-51 | IGRID(I) (HOS2)..... | E-132 |
| hdf_write_results..... | D-122 | IH (36-OC)..... | E-125 |
| HDish (17d-FD)..... | E-103 | IHTM (8-CD)..... | E-96 |
| HDish (G8-2h)..... | E-57 | IHTM (G8-2e)..... | E-55 |
| heat_flux_lower_limit..... | D-119 | II (22-GB)..... | E-108 |
| heat_flux_table..... | D-20 | IK (G4b-11)..... | E-22 |
| heat_flux_upper_limit..... | D-119 | IMAP (1-CNS)..... | E-88 |
| heat_transfer_coefficient..... | D-54 | IMAP (G4b-1)..... | E-17 |
| heat_transfer_model..... | D-54 | INGAP (G10-1a)..... | E-70 |
| heated_length..... | D-74 | inlet_data..... | D-112 |
| helium_fraction..... | D-90 | inlet_enthalpy..... | D-111 |
| HERROR (33e-HM)..... | E-124 | inlet_enthalpy_forcing_function..... | D-116 |
| HERROR (G9-9)..... | E-68 | inlet_mass_velocity..... | D-111 |
| HG (16-FD)..... | E-101 | inlet_mass_velocity_value..... | D-113 |
| HGAP (G4b-13)..... | E-23 | inlet_temperature..... | D-111 |
| HGAP (G8-2)..... | E-52 | inlet_temperature_value..... | D-113 |
| hgbup (G8-2n-1)..... | E-60 | inlet_volumetric_flow_rate..... | D-113 |
| hglhr (G8-2n-1)..... | E-61 | inner_clad_roughness..... | D-89 |
| hgt (G8-2n-1)..... | E-61 | input_print_option..... | D-8 |
| HHF (G1-2)..... | E-9 | inserting_ramp_av..... | D-31 |
| HHG (G1-2)..... | E-9 | IOLdcb (17c-FD)..... | E-102 |
| HIN (36-OC)..... | E-125 | IOLdcb (G8-2g)..... | E-56 |
| HIN (G11-1)..... | E-75 | IPILE (8-CD)..... | E-95 |
| HINLE (G11-2)..... | E-79 | IPILE (I3)..... | E-7 |
| HLEN (32g-HM-2)..... | E-120 | IPROP (8-CD)..... | E-96 |
| HLEN (G8-1g)..... | E-46 | IPROP (G8-2e)..... | E-55 |
| HLEN (G8-1n)..... | E-50 | IR_N1 (G8-1-2)..... | E-39 |
| HLEN (G8-1o)..... | E-50 | IR_N2 (G8-1-2)..... | E-39 |
| HNR (10-CD)..... | E-97 | IREBAL (33c-HM)..... | E-122 |
| hot_channel_number..... | D-22 | IREBAL (G9-7)..... | E-67 |
| I (15-RD)..... | E-100 | IRGW (32d-HM)..... | E-115 |
| I (G11-1d)..... | E-78 | IRGW (G4b-14)..... | E-23 |
| I (G4a-1)..... | E-15 | IRGW (G8-1c)..... | E-42 |
| I (G4b-3)..... | E-18 | IRUN (G11-8)..... | E-81 |
| I (G5-2)..... | E-29 | ISGSP (G8-1p)..... | E-51 |
| I (G8-1)..... | E-38 | ISOLVE (I2)..... | E-6 |
| I_CHF (G8-1-1)..... | E-38 | ISPACE (32a-HM)..... | E-115 |
| I_CHF (G8-1-4)..... | E-40 | ISPACE (G8-1a)..... | E-41 |
| I_CHF (G8-1aa)..... | E-40 | ISPIT (36.1-OC)..... | E-126 |
| ICAgas (17c-FD)..... | E-103 | ISPIT (G11-1a)..... | E-76 |
| ICAgas (G8-2g)..... | E-57 | ISTART (2-CNS)..... | E-89 |
| ICOrad (17c-FD)..... | E-102 | ISTART (G4b-9)..... | E-21 |
| ICOrad (G8-2g)..... | E-57 | IT_N1 (G8-1-5)..... | E-40 |
| ICROSS (G4b-8)..... | E-21 | IT_N2 (G8-1-5)..... | E-40 |
| IDGAP1 (G10-1d)..... | E-71 | ITAF (23-HM)..... | E-109 |
| IDish (17d-FD)..... | E-103 | ITEXT (G4b-1)..... | E-17 |
| IDish (G8-2h)..... | E-57 | ITMINT (33b-HM)..... | E-122 |
| IDMR(1..3) (32e-HM)..... | E-118 | ITMINT (G9-6)..... | E-67 |
| IDMR(1..3) (G4b-17)..... | E-26 | ITMNSS (33b-HM)..... | E-122 |
| IDMR(1..3) (G8-1d)..... | E-45 | ITMNSS (G9-6)..... | E-67 |
| IDOWN (G4b-8)..... | E-21 | ITMP (14-RD)..... | E-100 |
| IDPEXIT (G11-1c)..... | E-78 | ITP(I,J) (HOS3)..... | E-132 |
| IEND (G4b-9)..... | E-21 | ITS (G11-8)..... | E-81 |
| IFIN (2-CNS)..... | E-89 | ITSI (G11-8)..... | E-81 |
| | | IUSca (17c-FD)..... | E-103 |

COBRA-FLX: A Core Thermal-Hydraulic Analysis Code

Topical Report

Appendix D

Page D-128

| | | | |
|---------------------------------------|-------|---|-------|
| IUSca (G8-2g)..... | E-57 | MAX_N (I2-1)..... | E-6 |
| IUScax (17c-FD)..... | E-103 | MAXFN (36.1-OC)..... | E-126 |
| IUScax (G8-2g)..... | E-57 | MAXFN (G11-1a)..... | E-76 |
| IUScra (17c-FD)..... | E-103 | maximum_number_of_iterations..... | D-100 |
| IUScra (G8-2g)..... | E-57 | MAXINR (33c-HM)..... | E-122 |
| IUSox (17c-FD)..... | E-103 | MAXINR (G9-7)..... | E-67 |
| IUSox (G8-2g)..... | E-57 | MC (I1)..... | E-5 |
| J | | MERROR (33c-HM)..... | E-122 |
| J (10-CD)..... | E-97 | MERROR (G9-7)..... | E-67 |
| j (G11-1b)..... | E-77 | MG (I1)..... | E-5 |
| J (G7-5)..... | E-33 | MGRID (32g-HM-4)..... | E-120 |
| J1 (I3)..... | E-7 | MGRID (32i-HM-2)..... | E-121 |
| J2 (28-HM)..... | E-112 | MGRID (G8-1b)..... | E-42 |
| J3 (28-HM)..... | E-112 | MGRID (G8-1i)..... | E-47 |
| J4 (26-HM)..... | E-111 | MGRID(I) (32c-HM)..... | E-115 |
| J8 (28-HM)..... | E-112 | min_number_of_steady_state_outer_ite- rations..... | D-103 |
| JB (12-CD)..... | E-99 | min_number_of_time_step_outer_ite- rations..... | D-103 |
| JB (G4b-12)..... | E-22 | mixing_coefficient..... | D-109 |
| JB (G4b-7)..... | E-20 | mixing_exponent..... | D-109 |
| JBSTOR (24-HM-3)..... | E-110 | mixing_gap_types..... | D-109 |
| JJ (22-GB)..... | E-108 | mixing_gaptypes..... | D-109 |
| JK (G4b-11)..... | E-22 | mixing_grid_number..... | D-62 |
| K | | mixing_grids..... | D-61 |
| K (19a-FD)..... | E-105 | MN (I1)..... | E-5 |
| K (G4a-2)..... | E-16 | molten_fuel_fraction..... | D-88 |
| K (G6-2)..... | E-30 | momentum_equations_form..... | D-105 |
| K (G7-2)..... | E-32 | Monte_Carlo_simulation..... | D-121 |
| K (G7-5)..... | E-33 | MR (I1)..... | E-5 |
| K (G8-2n)..... | E-60 | MX (I1)..... | E-5 |
| KASE (I3)..... | E-7 | MZ (I1)..... | E-5 |
| KC (16-FD)..... | E-101 | N | |
| KCLAD (G4b-13)..... | E-23 | N (10-CD)..... | E-97 |
| KCLAD (G8-2)..... | E-52 | N (15-RD)..... | E-100 |
| KDEBUG (43-DB)..... | E-129 | N (34-HM)..... | E-124 |
| KF (16-FD)..... | E-101 | N (G1-1)..... | E-9 |
| KFUEL (G4b-13)..... | E-23 | N (G4a-1)..... | E-15 |
| KFUEL (G8-2)..... | E-51 | N (G4b-3)..... | E-18 |
| KIJ (32-HM)..... | E-114 | N (G8-1)..... | E-38 |
| KIJ (G9-1)..... | E-64 | N1 (23-HM)..... | E-108 |
| KKF (G1-2)..... | E-9 | N1 (4-HF)..... | E-92 |
| krypton_fraction..... | D-90 | N1 (G1-1)..... | E-9 |
| KSGrid (32f-HM-2)..... | E-119 | N1 (G4b-1)..... | E-17 |
| KSGrid (G4b-20)..... | E-27 | N1 (GCC4a)..... | E-15 |
| KSGrid (G8-1e-2)..... | E-46 | N1 (GCC4b)..... | E-16 |
| L | | N1 (GCC8)..... | E-35 |
| last_debug_channel..... | D-76 | N1 (IN) (GCC11)..... | E-73 |
| lateral_flow_acceleration_factor..... | D-104 | N1 (IQP3/NAX) (GCC3)..... | E-12 |
| lattice_hydraulic_diameter..... | D-70 | N1 (J2) (GCC2)..... | E-10 |
| LC (G4a-1)..... | E-15 | N1 (J6) (GCC7)..... | E-31 |
| lgauss(j) (G11-1b)..... | E-77 | N1 (NAFACT) (GCC5)..... | E-28 |
| linear_heat_rate_list..... | D-93 | N1 (NGAPS) (GCC6)..... | E-29 |
| LR (15-RD)..... | E-100 | N1 (NOPRIN) (GCC20)..... | E-87 |
| LR (G8-1)..... | E-38 | N1 (NOUT) (GCC12)..... | E-83 |
| LREF_BETA (G10-4)..... | E-72 | N1 (NPROP) (GCC1)..... | E-8 |
| LREF_KIJ (G9-1a)..... | E-65 | N1 (NSCBC) (GCC10)..... | E-69 |
| M | | N1 (NSKIPX) (GCC9)..... | E-63 |
| M (G4b-3)..... | E-18 | N10 (GCC8-cont)..... | E-37 |
| MAAP (G4b-10)..... | E-22 | N2 (23-HM)..... | E-109 |
| mass_balance_inner_iterations..... | D-103 | N2 (G4b-1)..... | E-17 |
| material_properties..... | D-80 | N2 (GCC20)..... | E-87 |
| [.....] | D-6 | | |

COBRA-FLX: A Core Thermal-Hydraulic Analysis Code

Topical Report

Appendix D

Page D-129

| | | | |
|--------------------------|-------|--------------------------|-------|
| N2 (GCC3)..... | E-12 | N6 (GCC12)..... | E-84 |
| N2 (GCC4b)..... | E-16 | N6 (GCC20)..... | E-87 |
| N2 (IG) (GCC11)..... | E-73 | N6 (GCC3)..... | E-13 |
| N2 (J3) (GCC2)..... | E-10 | N6 (GCC4a)..... | E-15 |
| N2 (NAXL) (GCC5)..... | E-28 | N6 (GCC4b)..... | E-17 |
| N2 (NBBC) (GCC10)..... | E-69 | N6 (GCC5)..... | E-28 |
| N2 (NCHAN) (GCC4a)..... | E-15 | N6 (GCC6)..... | E-30 |
| N2 (NGRID) (GCC7)..... | E-31 | N6 (GCC9)..... | E-63 |
| N2 (NGXL) (GCC6)..... | E-29 | N6 (IFRM) (GCC8)..... | E-36 |
| N2 (NPCHAN) (GCC12)..... | E-83 | N6 (J8) (GCC2)..... | E-11 |
| N2 (NPRESS) (GCC1)..... | E-8 | N6 (NQ) (GCC11)..... | E-73 |
| N2 (NROD) (GCC8)..... | E-35 | N6 (NREDGL) (GCC7)..... | E-31 |
| N2 (NSKIPT) (GCC9)..... | E-63 | N7 (23-HM)..... | E-109 |
| N3 (23-HM)..... | E-109 | N7 (GCC1)..... | E-8 |
| N3 (GCC1)..... | E-8 | N7 (GCC10)..... | E-70 |
| N3 (GCC20)..... | E-87 | N7 (GCC12)..... | E-84 |
| N3 (GCC4a)..... | E-15 | N7 (GCC2)..... | E-11 |
| N3 (GCC6)..... | E-29 | N7 (GCC20)..... | E-87 |
| N3 (IHC) (GCC3)..... | E-12 | N7 (GCC3)..... | E-13 |
| N3 (J4) (GCC2)..... | E-10 | N7 (GCC4a)..... | E-15 |
| N3 (J5) (GCC10)..... | E-69 | N7 (GCC4b)..... | E-17 |
| N3 (KDEBUG) (GCC9)..... | E-63 | N7 (GCC5)..... | E-28 |
| N3 (NARAMP) (GCC5)..... | E-28 | N7 (GCC6)..... | E-30 |
| N3 (NGRIDT) (GCC7)..... | E-31 | N7 (GCC7)..... | E-31 |
| N3 (NODESF) (GCC8)..... | E-35 | N7 (GCC8)..... | E-37 |
| N3 (NP) (GCC11)..... | E-73 | N7 (GCC9)..... | E-63 |
| N3 (NPROD) (GCC12)..... | E-83 | N7 (LOCDAT) (GCC11)..... | E-73 |
| N3(NREDGL) (GCC4b)..... | E-17 | N8 (23-HM)..... | E-109 |
| N4 (23-HM)..... | E-109 | N8 (GCC8-cont)..... | E-37 |
| N4 (GCC1)..... | E-8 | N9 (23-HM)..... | E-109 |
| N4 (GCC10)..... | E-69 | N9 (GCC8-cont)..... | E-37 |
| N4 (GCC20)..... | E-87 | [.....] | E-47 |
| N4 (GCC4a)..... | E-15 | NBETA (24-HM-1)..... | E-110 |
| N4 (GCC4b)..... | E-17 | nbup (G8-2n-1)..... | E-60 |
| N4 (GCC5)..... | E-28 | NCC (17-FD)..... | E-101 |
| N4 (GCC6)..... | E-30 | NCC (G8-2e)..... | E-55 |
| N4 (KAXIAL) (GCC9)..... | E-63 | NCF (17-FD)..... | E-101 |
| N4 (LCHF) (GCC3)..... | E-12 | NCF (G8-2e)..... | E-55 |
| N4 (NFUEL) (GCC8)..... | E-35 | NCFI (G8-2a)..... | E-52 |
| N4 (NH) (GCC11)..... | E-73 | NCHAN_DP (G11-1c)..... | E-78 |
| N4 (NPNODE) (GCC12)..... | E-84 | NCHF (32-HM)..... | E-114 |
| N4 (NRAMP) (GCC7)..... | E-31 | NCHF (G4b-1)..... | E-17 |
| N4 (NVISCW) (GCC2)..... | E-10 | NCHFREF (G8-1-2)..... | E-39 |
| N5 (23-HM)..... | E-109 | NCHFTYPE (G8-1-5)..... | E-40 |
| N5 (GCC1)..... | E-8 | NCTYP (8-CD)..... | E-95 |
| N5 (GCC10)..... | E-69 | NCWf12 (32d-HM-1)..... | E-117 |
| N5 (GCC12)..... | E-84 | NCWf12 (G4b-15)..... | E-25 |
| N5 (GCC20)..... | E-87 | NCWf12 (G8-1c-1)..... | E-44 |
| N5 (GCC3)..... | E-12 | ND1X (1-CNS)..... | E-88 |
| N5 (GCC4a)..... | E-15 | ND2X (1-CNS)..... | E-88 |
| N5 (GCC4b)..... | E-17 | NDT (7-MD)..... | E-95 |
| N5 (GCC5)..... | E-28 | NDT (G9-1)..... | E-64 |
| N5 (GCC6)..... | E-30 | NDX (7-MD)..... | E-95 |
| N5 (GCC9)..... | E-63 | NDX (G9-1)..... | E-64 |
| N5 (NCHF) (GCC8)..... | E-35 | NF (27-HM)..... | E-112 |
| N5 (NG) (GCC11)..... | E-73 | NF (G2-3)..... | E-12 |
| N5 (NJUMP) (GCC7)..... | E-31 | NFT (HOS1)..... | E-132 |
| N5 (NSZABL) (GCC2)..... | E-11 | NFUFLT (G4b-1)..... | E-17 |
| N6 (23-HM)..... | E-109 | NFXF (8-CD)..... | E-95 |
| N6 (GCC1)..... | E-8 | NG (38-T)..... | E-127 |
| N6 (GCC10)..... | E-70 | NGAPN (G10-1c)..... | E-71 |

COBRA-FLX: A Core Thermal-Hydraulic Analysis Code

Topical Report

Appendix D

Page D-130

| | | | |
|---|-------|--|-------|
| NGRID (8-CD)..... | E-95 | NSPf12 (G4b-15)..... | E-25 |
| NGRID (G4b-1)..... | E-17 | NSPf12 (G8-1c-1)..... | E-44 |
| NGRID (HOS1)..... | E-132 | NSSS (33a-HM)..... | E-122 |
| NGRIDT (8-CD)..... | E-95 | NSSS (G9-5)..... | E-66 |
| NGRIDT (G4b-1)..... | E-17 | NTHBOX (3-CNS)..... | E-90 |
| NGRIDT (HOS1)..... | E-132 | []..... | E-7 |
| NGROUP (GCC1)..... | E-8 | NTRIES (33-HM)..... | E-121 |
| NGROUP (GCC10)..... | E-69 | NTRIES (G9-1)..... | E-64 |
| NGROUP (GCC11)..... | E-73 | number_of_axial_nodes..... | D-100 |
| NGROUP (GCC12)..... | E-83 | number_of_channels_total..... | D-25 |
| NGROUP (GCC2)..... | E-10 | number_of_fuel_types..... | D-46 |
| NGROUP (GCC20)..... | E-87 | number_of_gaps_with_local_coupling_parameters..... | D-25 |
| NGROUP (GCC3)..... | E-12 | number_of_grid spacings..... | D-75 |
| NGROUP (GCC4a)..... | E-15 | number_of_iterations_for_ramp..... | D-39 |
| NGROUP (GCC4b)..... | E-16 | number_of_mixing_types..... | D-109 |
| NGROUP (GCC5)..... | E-28 | []..... | D-6 |
| NGROUP (GCC6)..... | E-29 | number_of_radial_nodes..... | D-45 |
| NGROUP (GCC7)..... | E-31 | number_of_rods_read..... | D-45 |
| NGROUP (GCC8)..... | E-35 | number_of_rods_total..... | D-45 |
| NGROUP (GCC9)..... | E-63 | number_of_steady_state_time_steps..... | D-102 |
| NGT (HOS1)..... | E-132 | number_of_time_steps..... | D-100 |
| NH (38-T)..... | E-127 | NUSTAR (33d-HM)..... | E-123 |
| NHGAP (G8-2c)..... | E-54 | NUSTAR (G9-8)..... | E-68 |
| nitrogen_fraction..... | D-91 | NV (29-HM)..... | E-113 |
| n1hr (G8-2n-1)..... | E-60 | NV (G2-2)..... | E-11 |
| NLOOP_skip_time..... | D-112 | NVISCW (25-HM)..... | E-111 |
| NMGRID (32c-HM)..... | E-115 | NWRAP (G7-3)..... | E-32 |
| NMGRID (32g-HM-4)..... | E-120 | | |
| NMGRID (32i-HM-2)..... | E-121 | | |
| NMGRID (G8-1b)..... | E-42 | O | |
| NMGRID (G8-1i)..... | E-47 | O2pmx (18a-FD)..... | E-104 |
| NN11 (14-RD)..... | E-99 | O2pmx (18b-FD)..... | E-104 |
| NN22 (14-RD)..... | E-99 | O2pmx (G8-2k)..... | E-58 |
| NN33 (14-RD)..... | E-99 | O2pmx (G8-2l)..... | E-58 |
| NN44 (14-RD)..... | E-99 | omega_sor..... | D-5 |
| nnmc (G11-1b)..... | E-78 | Oxid (17d-FD)..... | E-103 |
| NNonF12 (32d-HM-1)..... | E-117 | Oxid (G8-2h)..... | E-57 |
| NNonF12 (G4b-15)..... | E-24 | oxid_thickness..... | D-86 |
| NNonF12 (G8-1c-1)..... | E-43 | oxide_thermal_resistance..... | D-83 |
| NODESF (8-CD)..... | E-95 | | |
| NODESF (G4b-1)..... | E-17 | P | |
| non_reversible_cladding_correction..... | D-86 | p_time..... | D-116 |
| non_reversible_pellet_correction..... | D-86 | P2 (34-HM)..... | E-124 |
| non_uniform_heat_flux_factor..... | D-65 | P2 (G1-1)..... | E-9 |
| normalize_channel_exit_pressures..... | D-115 | pellet_center_radius..... | D-85 |
| NOUT (44-OO)..... | E-129 | pellet_diameter..... | D-77 |
| NP (38-T)..... | E-127 | pellet_engineering_factor..... | D-22 |
| NPCHAN (44-OO)..... | E-129 | pellet_height..... | D-85 |
| NPNODE (44-OO)..... | E-130 | pellet_shoulder_height..... | D-86 |
| npoly_friction_multiplier..... | D-16 | pellet_shoulder_width..... | D-85 |
| npoly_void..... | D-16 | PEXIT (36-OC)..... | E-125 |
| NPROD (44-OO)..... | E-129 | PEXIT (G11-1)..... | E-75 |
| NPROP (34-HM)..... | E-124 | PEXIT(l) (G11-1d)..... | E-78 |
| NQ (38-T)..... | E-127 | PGAS (19a-FD)..... | E-106 |
| NREDGL (8-CD)..... | E-96 | PGAS (19-FD)..... | E-105 |
| NROW (HOS1)..... | E-132 | PGAS (G8-2m)..... | E-59 |
| NSKIPT (44-OO)..... | E-129 | PGAS (G8-2n)..... | E-60 |
| NSKIPX (44-OO)..... | E-129 | PH (34-HM)..... | E-124 |
| NSOLVE (33e-HM)..... | E-124 | PH (G1-1)..... | E-9 |
| NSOLVE (G9-9)..... | E-68 | PH (G4a-1)..... | E-15 |
| NSPf12 (32d-HM-1)..... | E-117 | PH (G4b-3)..... | E-18 |
| | | PHI (15-RD)..... | E-100 |

COBRA-FLX: A Core Thermal-Hydraulic Analysis Code

Topical Report

Appendix D

Page D-131

| | | | |
|--|------------|---|--------------|
| PHI (G4b-3)..... | E-18 | RADIAL (G4b-5)..... | E-20 |
| PHI (G8-1)..... | E-38 | radial_power..... | D-78 |
| pin_diameter..... | D-39 | RC (16-FD)..... | E-101 |
| pin_engineering_factor..... | D-22 | RCLAD (G4b-13)..... | E-23 |
| pin_pitch..... | D-74 | RCLAD (G8-2)..... | E-52 |
| PITCH (G7-1)..... | E-32 | RDish (17d-FD)..... | E-103 |
| PITCH (HOS1)..... | E-132 | RDish (G8-2h)..... | E-57 |
| poly_coeff_friction_multiplier..... | D-17 | RDread (17a-FD)..... | E-102 |
| poly_coeff_void..... | D-16 | RDread (G8-2f)..... | E-56 |
| PoneSC (32d-HM-2)..... | E-118 | read_limits..... | D-74 |
| PoneSC (G4b-16)..... | E-25 | rebalancing_inner_iterations..... | D-103 |
| PoneSC (G8-1c-2)..... | E-44 | reference_distance..... | D-102, D-110 |
| pow_time..... | D-117 | rel_axial_coordinate_av..... | D-32 |
| power_forcing_function..... | D-117 | rel_axial_coordinate_grid..... | D-41 |
| power_type..... | D-20 | rel_axial_coordinate_gv..... | D-36 |
| PP (G1-2)..... | E-9 | rel_begin_of_heated_length..... | D-61 |
| PPITCH (G8-1o)..... | E-50 | rel_flow..... | D-117 |
| PPTEMP (G11-1.0)..... | E-75 | rel_inlet_enthalpy..... | D-116 |
| pressure..... | D-11 | rel_power..... | D-117 |
| pressure_acceleration_factor..... | D-104 | rel_pressure..... | D-116 |
| pressure_forcing_function..... | D-115 | relative_gap_heat_transfer_coefficient..... | D-79 |
| pressure_interpolation_factor..... | D-104 | relative_mass_conservation_error..... | D-103 |
| pressure_underrelaxation_factor..... | D-101 | relative_power..... | D-78 |
| print_bundle_average_results-channel_exit_data- bundle_inlet_exit_temperatures..... | D-97 | relative_radial_position..... | D-78 |
| print_options_1..... | D-96 | relative_shell_radius..... | D-82 |
| print_selection..... | D-123 | relocation_factor..... | D-90 |
| PRINTC (45-OO)..... | E-130 | rewetting..... | D-55 |
| PRINTN (47-OO)..... | E-130 | RF (16-FD)..... | E-101 |
| PRINTR (46-OO)..... | E-130 | RFUEL (G4b-13)..... | E-23 |
| PRNTC (G12-1)..... | E-84 | RFUEL (G8-2)..... | E-52 |
| PRNTN (G12-3)..... | E-85 | rod_bundle_factor..... | D-69 |
| PRNTR (G12-2)..... | E-85 | rod_diameter..... | D-74 |
| property..... | D-26, D-52 | rod_type..... | D-57 |
| property_coupling..... | D-29 | rod_type_from_rod_number..... | D-58 |
| property_model..... | D-80 | rod_type_to_rod_number..... | D-58 |
| property_table..... | D-11 | rods..... | D-52 |
| pv_solution_variables..... | D-102 | rods_printed..... | D-124 |
| PW (G4a-1)..... | E-15 | roughness_weighting_factor..... | D-89 |
| PW (G4b-3)..... | E-18 | RPPP (G8-2b)..... | E-53 |
| PwoneSC (32d-HM-2)..... | E-118 | RPPP (G8-2b-1)..... | E-54 |
| PwoneSC (G4b-16)..... | E-25 | run..... | D-8 |
| PwoneSC (G8-1c-2)..... | E-44 | S | |
| Q | | sensitivity_calculation..... | D-115 |
| QC (50-NP)..... | E-131 | sensitivity_parameters..... | D-120 |
| QC_BURNI (G8-2a-2)..... | E-53 | set_point_iteration..... | D-114 |
| QC_FAC (G8-2a-1)..... | E-52 | set_point_parameters..... | D-119 |
| QC_LVD (G8-2a-2)..... | E-53 | SGSPS (G8-1q)..... | E-51 |
| QC_MODE (G8-2a-1)..... | E-52 | SGSPX (G8-1q)..... | E-51 |
| QC_PUI (G8-2a-2)..... | E-53 | shell_distribution..... | D-81 |
| QC_U235I (G8-2a-2)..... | E-53 | SL (32-HM)..... | E-114 |
| QC_VOID (G8-2a-2)..... | E-53 | SL (G9-1)..... | E-64 |
| QF (49-NP)..... | E-131 | slip_ratio..... | D-15 |
| QPPPI (G8-2b)..... | E-53 | solver..... | D-5 |
| R | | SOR_pressure_error..... | D-101 |
| R0 (17b-FD)..... | E-102 | spacer_correction_factor..... | D-66 |
| R0 (17d-FD)..... | E-103 | spacer_type..... | D-39 |
| R0 (G8-2h)..... | E-57 | spec_volume_liquid..... | D-11 |
| RADIA (15-RD)..... | E-100 | spec_volume_vapor..... | D-12 |
| RADIA (G8-1)..... | E-38 | SPITCH (32h-HM)..... | E-120 |
| RADIAL (6-HF)..... | E-94 | SPITCH (G8-1j)..... | E-47 |
| | | sqrt(var) (G11-1b)..... | E-78 |

| | | | |
|--|-------|---|------------|
| SSIGMA (G1-2)..... | E-9 | TrSC (32d-HM-2)..... | E-118 |
| steady_state_time_step..... | D-102 | TrSC (G4b-16)..... | E-25 |
| subcooled_boiling_profile_fit..... | D-16 | TrSC (G8-1c-2)..... | E-44 |
| subcooled_mixing..... | D-107 | TSTART0 (G11-1.0)..... | E-74 |
| subcooled_void..... | D-14 | TT (G1-2)..... | E-9 |
| superheated_steam..... | D-10 | TTIME (7-MD)..... | E-95 |
| surface_tension..... | D-12 | TTIME (G9-1)..... | E-64 |
| System_area_variation_table..... | D-31 | TTIME (NLOOP)..... | E-74 |
| System_channel_map..... | D-26 | turbulent_momentum_factor..... | D-99 |
| System_gap_heat_transfer_table..... | D-92 | two_phase_friction_multiplier..... | D-15 |
| System_gap_map..... | D-29 | two_phase_mixing..... | D-108 |
| System_gap_variation_table..... | D-34 | U | |
| System_grid_gap_mapping..... | D-41 | USDPRN (G8-1m)..... | E-49 |
| System_grid_mapping..... | D-41 | USDPRN (G8-1n)..... | E-50 |
| System_rod_map..... | D-52 | USDPRN (G8-1o)..... | E-50 |
| szablewski_correction..... | D-15 | use_axially_variable_CHF_correlations..... | D-56 |
| T | | use_CARO_axial_heat_flux..... | D-84 |
| target_DNBR..... | D-119 | use_CARO_radial_heat_flux..... | D-84 |
| TAVEXI (G11-1.0)..... | E-75 | use_CARO_results..... | D-83 |
| TAVINL (G11-1.0)..... | E-75 | use_chf_performance_factors..... | D-55 |
| TC (16-FD)..... | E-101 | use_end_of_interval_heat_flux..... | D-51, D-57 |
| TCLAD (G4b-13)..... | E-23 | use_rod_type..... | D-59 |
| TCLAD (G8-2)..... | E-52 | use_rod_wise_chf_correlations..... | D-55 |
| TDC (32a-HM)..... | E-115 | UUF (G1-2)..... | E-9 |
| TDC (G8-1a)..... | E-41 | V | |
| TDCW3 (32f-HM-2)..... | E-119 | variation_coefficient_code_uncertainty..... | D-121 |
| TDCW3 (G4b-20)..... | E-27 | variation_coefficient_DNB_correlation_uncer- tainty..... | D-121 |
| TDCW3 (G8-1e-2)..... | E-46 | variation_coefficient_FdeltaH_engineering1..... | D-121 |
| temperature..... | D-11 | variation_coefficient_FdeltaH_nuclear..... | D-121 |
| temperature_convergence_criterion..... | D-82 | variation_coefficient_FQ_engineering..... | D-121 |
| temperature_distribution..... | D-82 | variation_coefficient_heat_flux..... | D-120 |
| temperature_lower_limit..... | D-119 | variation_coefficient_inlet_temperature..... | D-120 |
| temperature_upper_limit..... | D-119 | variation_coefficient_mass_flow_rate..... | D-120 |
| test_section_type..... | D-61 | variation_coefficient_system_pressure..... | D-120 |
| TEXT (G4b-2)..... | E-18 | variation_coefficient_transient_code_uncer- tainty..... | D-121 |
| TEXT (I3)..... | E-7 | variation_factor_av..... | D-33 |
| TGAS (19a-FD)..... | E-106 | variation_factor_gv..... | D-36 |
| TGAS (19-FD)..... | E-105 | VARNCS(1) (G11-1b)..... | E-77 |
| TGAS (G8-2m)..... | E-59 | VARNCS(10) (G11-1b)..... | E-77 |
| TGAS (G8-2n)..... | E-60 | VARNCS(2) (G11-1b)..... | E-77 |
| theoretical_fuel_density_fraction..... | D-87 | VARNCS(3) (G11-1b)..... | E-77 |
| thermal_conduction_mixing..... | D-108 | VARNCS(4) (G11-1b)..... | E-77 |
| thermal_diffusion_coefficient_tong..... | D-69 | VARNCS(5) (G11-1b)..... | E-77 |
| thermal_diffusion_constant..... | D-60 | VARNCS(6) (G11-1b)..... | E-77 |
| thermal_expansion..... | D-83 | VARNCS(7) (G11-1b)..... | E-77 |
| THETA (32-HM)..... | E-114 | VARNCS(8) (G11-1b)..... | E-77 |
| THETA (G9-1)..... | E-64 | VARNCS(9) (G11-1b)..... | E-77 |
| THG (17-FD)..... | E-101 | varncs(j) (G11-1b)..... | E-78 |
| THG (G8-2e)..... | E-55 | viscosity_liquid..... | D-12 |
| THICK (G7-1)..... | E-32 | VOLRST (19-FD)..... | E-105 |
| TIME (G11-1.0)..... | E-75 | VolRst (G8-2m)..... | E-59 |
| time_step..... | D-79 | VolRst (G8-2n)..... | E-60 |
| time_step_printing..... | D-96 | volume_fraction_PuO2..... | D-87 |
| TINLE(I,2) (NLOOP)..... | E-74 | VVF (G1-2)..... | E-9 |
| tm_scaling..... | D-108 | VVG (G1-2)..... | E-9 |
| to_x_over_l..... | D-58 | W | |
| TOLLIM (36.1-OC)..... | E-126 | wall_viscosity..... | D-15 |
| TOLLIM (G11-1a)..... | E-76 | WERROR (33-HM)..... | E-121 |
| total_time..... | D-100 | WERROR (G9-1)..... | E-64 |
| transverse_momentum_parameter..... | D-100 | | |
| transverse_momentum_parameter_scaling..... | D-101 | | |

COBRA-FLX: A Core Thermal-Hydraulic Analysis Code
Topical Report

Appendix D

| | | | |
|-------------------------------|-------|------------------------|-------|
| wire_diameter..... | D-39 | XSPLOW (36.1-OC) | E-126 |
| wire_wrap_pitch..... | D-39 | XSPLOW (G11-1a)..... | E-76 |
| write_to_screen..... | D-122 | Y | |
| X | | Y (5-HF)..... | E-93 |
| X (G9-2)..... | E-66 | Y (G3-1)..... | E-13 |
| X (G9-3)..... | E-66 | YG (41-T) | E-128 |
| X (G9-4)..... | E-66 | YG (G11-6)..... | E-80 |
| X1_CHF_AX_TYPE (G8-1-4) | E-40 | YH (40-T)..... | E-128 |
| X2_CHF_AX_TYPE (G8-1-4) | E-40 | YH (G11-5)..... | E-80 |
| xenon_fraction..... | D-90 | YHGAP (G8-2d)..... | E-54 |
| XFACP (33d-HM) | E-123 | ymc(i) (G11-1b) | E-78 |
| XFACP (G9-8) | E-68 | YP (39-T)..... | E-127 |
| XKLOSS (32h-HM)..... | E-120 | YP (G11-4) | E-79 |
| XKLOSS (G8-1j)..... | E-47 | YQ (42-T) | E-128 |
| XKS (32a-HM) | E-115 | YQ (G11-7)..... | E-81 |
| XKS (32b-HM) | E-115 | Z | |
| XKS (G8-1a)..... | E-41 | z..... | D-21 |
| XQUAL (G10-2) | E-71 | Z (7-MD)..... | E-95 |
| XSPHGH (36.1-OC) | E-126 | Z (G9-1)..... | E-64 |
| XSPHGH (G11-1a)..... | E-76 | | |

APPENDIX E: INPUT DESCRIPTION OF CONVENTIONAL FORMAT

COBRA-FLX, as AREVA’s worldwide core thermal-hydraulic code, possesses numerous analysis features and, particularly, numerous input features that are not required to support U.S. licensing. Therefore, AREVA defines in Table E-1 the key inputs that will be used for U.S. licensing for the requested review and approval.

Table E-1: Roadmap of the Key Inputs for AREVA U.S. Licensing Analyses

| Card Group | Input Identifier | Description | Comments |
|------------|------------------|--|---|
| I1 | | Problem array size identifier | |
| I2 | | Solution method of conservation equations <ul style="list-style-type: none"> • ISOLVE = 1 (solution of the conservation equations is directed to pressure (P-Solution method)) • ISOLVE = 3 (PV-Solution) | Options like ISOLVE = 4 and >10 are used for subchannel-by-subchannel analysis. [] |
| I3 | | Case control card <ul style="list-style-type: none"> • IPILE = 0 | |
| 1 | GCC1 | Physical properties <ul style="list-style-type: none"> • N1 (NPROP) = -7 | This uses IAPWS-IF97 water properties. |
| | G1-1 | Physical property data | |
| | G1-2 | Physical property data | |
| 2 | GCC2 | Flow correlations <ul style="list-style-type: none"> • N1 = 2 (Saha-Zuber subcooled void correlation) • N2 = 8, 9 (Chexal-Lellouche void correlation) • N3 = 0 (homogeneous two-phase friction multiplier) • N4 = 0 (wall viscosity correction not included) • N5 = 0 (Lehmann friction factor with the Szablewski correlation) • N6 = 1 (Zuber-Staub profile fit) | Note that N2 = 9 uses Chexal-Lellouche void correlation using tables with interpolation. This option is advantageous with respect to runtime for large cases, e.g. full core subchannel-by-subchannel calculations. |
| 3 | GCC3 | Axial heat flux | Additional options on an as-needed basis, e.g., G3-3. |
| | G3-1 | Axial heat flux data | |
| | G3-2 | Hot channel factors | |
| 4 | GCC4a | Channel data | |
| | G4a-1 | Subchannel data | |

| Card Group | Input Identifier | Description | Comments |
|------------|------------------------------------|--|--|
| 5 | GCC5 | Subchannel axial area variation | These inputs are used on an as-needed basis. |
| | G5-1 | Axial positions of area variations | |
| | G5-2 | Subchannel number | |
| | G5-3 | Area variation factors | |
| 6 | GCC6 | Crossflow gap axial variation | These inputs are used on an as-needed basis. |
| | G6-1 | Axial positions of crossflow gap variations | |
| | G6-2 | Crossflow gap number | |
| 7 | G6-3 | Crossflow gap variation factors | |
| | GCC7 | Spacer data | |
| | G7-4 | Spacer location and type | |
| 8 | G7-5 | Spacer data sets | |
| | GCC8 | Rod layout, power factors and CHF correlations | N5 (NCHF: CHF Correlation flag) value is either 0 or one from the range 50 through 64. The rest of the options, including the card group GCC8-cont, are used on an case-dependent basis. |
| | G8-1 | Rod layout data | |
| | G8-1* | Performance factors for CHF correlations | Note that the * designates cards G8-1-1 through G8-1-5, and G8-1aa. These inputs are used on a case-dependent basis. |
| | G8-1m | CHF correlation limits and debug options for N5 = 50, 55, and 63 | These inputs are used on an as-needed basis. |
| | G8-1n | CHF correlation limits and debug options for N5 = 51, 52, 54, and 56 to 62. | |
| | G8-1o | CHF correlation limits and debug options for N5 = 53 | |
| | G8-1p | CHF correlation grid spacing input for N5 = 53 and 56 to 62 | |
| G8-1q | CHF correlation grid spacing input | | |
| 9 | G8-1r | CHF correlation channels for debug printout | |
| | GCC9 | Calculation variables | |
| | G9-1 | Calculation variables <ul style="list-style-type: none"> • FTM =1 | KIJ, SL, ACCELF ACCESP, etc. values, and group G9-1a are input on a case dependent basis. |
| G9-1a | Reference distance | | |

| Card Group | Input Identifier | Description | Comments |
|------------|------------------|--|--|
| | G9-2 | Axial node input (relative positions) | These inputs are used on an as-needed basis. Note that either G9-2, or G9-3, or G9-4 have to be entered. |
| | G9-3 | Axial node input (cm) | |
| | G9-4 | Axial node input | |
| | G9-5 | PV-Solution variables | PV-Solution variables are required when I2's ISOLVE =3 and input on a case dependent basis. Default values initially used. |
| | G9-6 | PV-Solution variables | |
| | G9-7 | PV-Solution variables | |
| | G9-8 | PV-Solution variables | |
| | G9-9 | PV-Solution variables | |
| 10 | GCC10 | Mixing correlation constants | Note that cards G10-1 through G10-4 are input on an as-needed basis |
| 11 | GCC11 | Operating conditions | |
| | G11-1 | Operating conditions | Note that cards G11-1 through G11-8 are input on an as-needed basis |
| 12 | GCC12 | Output display options | Note that cards G12-1 through G12-3 are input on an as-needed basis |
| | | Note that the standard COBRA-FLX input file requires a blank card with NGROUP = 0 to start each case | |
| | | Note that the standard COBRA-FLX input file requires a card I3 with KASE = 0 to terminate all calculations | |

COBRA-FLX provides users with the flexibility to supply input values for modeling using three basic formats.

- Conventional Fixed Format
- Conventional Free Format
- Keyword Based Format (KBF)

Each of these formats are described below.

The conventional format for COBRA-FLX is described in Sections E.1 through E.14 and is very similar to that used for LYNXT in Reference E-1 and earlier COBRA derivatives.

The data following the three introductory cards (I1-I3) is broken into card groups in the original COBRA-type input format.

Card groups for original input method:

- Card Group 1 (→ p.E-8): Physical properties
- Card Group 2 (→ p.E-10): Flow correlations
- Card Group 3 (→ p.E-12): Axial heat flux
- Card Group 4 (→ p.E-14): Channel data
- Card Group 5 (→ p.E-28): Subchannel area variation
- Card Group 6 (→ p.E-29): Gap spacing variation
- Card Group 7 (→ p.E-31): Spacer data
- Card Group 8 (→ p.E-34): Rod layout, power factors and CHF correlations
- Card Group 9 (→ p.E-64): Calculation variables
- Card Group 10 (→ p.E-70): Turbulent mixing correlations
- Card Group 11 (→ p.E-74): Operating conditions
- Card Group 12 (→ p.E-85): Output display options
- Card Group 20 (→ p.E-87): Card Group 20 input

The first card in every card group is a group control card designated as GCC_i where *i* is the group number. The group control card reads in the value of **NGROUP** (**NGROUP** = *i*, the card group number) and the integer constants **N1** to **N7**. The variable in parenthesis after each of the integer constants is the variable which will be set equal to the value of the integer. The card numbering system is of the form:

<card group number>-<card position within the group>

For example, card G3-1 is the first card after the group control card in card group 3.

GROUP CONTROL statement is always:

```
read (5,'(8I5)')NGROUP,N1,N2,N3,N4,N5,N6,N7 (for fixed format)
read (5, * )NGROUP,N1,N2,N3,N4,N5,N6,N7 (for free format)
```

Not all values are used in each group.

Free format input is selected by the existence of a file **PRECOB** in the working catalog. If the file **PRECOB** does not exist, the file **INPUT** (fixed format) is used. Only for file **INPUT**, the fixed format information given on the following input cards is relevant. For file **PRECOB**, all input parameters of all card groups are read in free format (*). The free format option is an alternate (recommended) input method for the conventional fixed format. In addition, comment cards may be interspersed with the program input. Comment cards start with a 'c' or 'C' in the first column and are listed on the output file. The width of the input file is limited to 300 characters. Below is the input description for the fixed and free formats. As noted above, the free format feature is for input file **PRECOB**, the fixed format definitions apply only to input file **INPUT**. An example of free format input is provided in Figure E-1.

The keyword based format (KBF) is discussed in Appendix D.

E.1 *Introductory Cards*

E.1.1 *I1: Problem array size*

This card is required always.

Read: **MC, MG, MN, MR, MX, MZ**

Format (**10I5**)

read from subroutine **INDAT**.

| | | |
|----|---|-----------|
| MC | = | Not used. |
| MG | = | Not used. |
| MN | = | Not used. |
| MR | = | Not used. |
| MX | = | Not used. |
| MZ | = | Not used. |

Note: (1) Card I1 must be used regardless of which input method is chosen.

(2) In the COBRA 3-CP 1.mn line of codes, MC through MZ were used to set the array sizes in dynamic storage. Starting with COBRA 3-CP 2.00 (modern, automatic storage allocation implemented), these parameters are no longer needed. None the less, card I1 has been maintained to ensure input file backward compatibility.

E.2 Card Group 1

Physical properties

| | |
|---|-----|
| GCC1: Group control card for card group 1 | E-8 |
| G1-1: Physical properties | E-9 |
| G1-2: Physical properties | E-9 |

E.2.1 GCC1: Group control card for card group 1

This card is required always.

Read: *NGROUP, N1, N2, N3, N4, N5, N6, N7*

Format (2I5)

read from subroutine INDAT.

| | | | |
|-------------|---|----|--|
| NGROUP | = | 1 | Select card group 1. |
| N1 (NPROP) | = | 0 | Calculate physical properties at saturation conditions from internal polynoms. |
| | > | 0 | The physical properties are given in the next N1 cards of type G1-2 (\rightarrow p.E-9) as in the original COBRA. |
| | < | 0 | Physical properties are calculated for operating conditions by KWU TAF routines as follows: |
| | = | -1 | TAF: Light water (formulation IFC-67) |
| | = | -2 | [|
| | | |] |
| | = | -7 | TAF97: Light water (Industrial Standard IAPWS-IF97; recommended option for design calculations) |
| N2 (NPRESS) | = | 0 | Do not use superheated steam properties |
| | > | 0 | Use superheated steam properties |
| N3 | = | | Not used. |
| N4 | = | | Not used. |
| N5 | = | | Not used. |
| N6 | = | | Not used. |
| N7 | = | | Not used. |

*Note: (1) CHF calculations with other fluids than light water may require proper correlations; no other provision is made for this than applying Ahmad's scaling laws with **NCHF = 12** on cards GCC8 (\rightarrow p.E-35) and 32-HM (\rightarrow p.E-116).*

E.2.2 G1-1: Physical properties

This card is required if $N1 \leq 0$ on card GCC1 (\rightarrow p.E-8).

Read: *N, PH, P2, N1*

Format (*I5, 2F10.3, I5*)

read from subroutine **CARDS1**.

| | | |
|----|---|---|
| N | = | Not used. |
| PH | = | Not used. |
| P2 | = | Not used. |
| N1 | = | Number of pressure steps generated by polynomial (min = 2, max = 30). |

E.2.3 G1-2: Physical properties

This card is required if $N1 > 0$ on card GCC1 (\rightarrow p.E-8).

Read: *PP(I), TT(I), VVF(I), VVG(I), HHF(I), HHG(I), UUF(I), KKF(I), SSIGMA(I)*

Format (*E5.2, F5.1, 7F10.0*)

read from subroutine **CARDS1**.

| | | |
|--------|---|---|
| PP | = | Saturation pressure (bar). |
| TT | = | Temperature ($^{\circ}$ C). |
| VVF | = | Liquid specific volume (dm^3/kg). |
| VVG | = | Vapour specific volume (dm^3/kg). |
| HHF | = | Liquid enthalpy (kJ/kg). |
| HHG | = | Vapour enthalpy (kJ/kg). |
| UUF | = | Liquid viscosity (kg/(s m)). |
| KKF | = | Liquid thermal conductivity (W/(m K)). |
| SSIGMA | = | Surface tension (N/m) |

Note: (1) This property table must have pressure higher than operating pressure and liquid enthalpy lower than the bundle inlet enthalpy. For additional details see the discussion following card 34-HM (\rightarrow p.E-126).

(2) A total of $N1$ (card GCC1 (\rightarrow p.E-8)) cards of physical properties must be present. Each card represents a line from the property tables for the coolant (i.e. the steam tables), with all properties being those at the saturated state.

(3) The option to use a user supplied property table is not available in the card group 20 input method (\rightarrow p. E-87).

E.3 Card Group 2**Flow correlations**

| | |
|---|------|
| GCC2: Group control card for card group 2 | E-10 |
| G2-1: Friction factor correlation constants..... | E-11 |
| G2-2: Void fraction polynomial coefficients or slip ratio specification | E-11 |
| G2-3: Two-phase friction multiplier, polynomial in quality | E-12 |

E.3.1 GCC2: Group control card for card group 2

This card is required always.

Read: NGROUP, N1, N2, N3, N4, N5, N6, N7

Format (5I5)

read from subroutine INDAT.

| | | | |
|-------------|---|---|---|
| NGROUP | = | 2 | Select card group 2. |
| N1 (J2) | = | | Subcooled void option. |
| | = | 0 | No subcooled void. |
| | = | 1 | Levy subcooled void correlation. |
| | = | 2 | Saha-Zuber subcooled void correlation. |
| N2 (J3) | = | | Bulk void correlation. |
| | = | 0 | Homogeneous model. |
| | = | 1 | Modified Armand model. |
| | = | 2 | Smith slip ratio correlation. |
| | = | 5 | Read in slip ratio (see card G2-2 (\rightarrow p.E-11)). |
| | = | 6 | Polynomial in quality, coefficients on card G2-2 (\rightarrow p.E-11). |
| | = | 7 | Zuber-Findlay bulk void model. |
| | = | 8 | Chexal-Lellouche void correlation using the iterative solution of the formulae. |
| | = | 9 | Chexal-Lellouche void correlation using tables with interpolation. |
| | | | [|
| | | |] |
| N3 (J4) | = | | Two phase friction multiplier. |
| | = | 0 | Homogeneous model. |
| | = | 1 | Armand model. |
| | = | 2 | Baroczy model. |
| | = | 3 | Martinelli-Nelson-Jones model. |
| | = | 5 | Polynomial in quality, coefficients on card G2-3 (\rightarrow p.E-12). |
| N4 (NVISCW) | = | | Wall viscosity correlation option for the wall friction factor. |
| | = | 0 | Wall viscosity not included. |
| | = | 1 | Wall viscosity included. |

Note: (1) The polynomial is calculated as

$$\sum_{v=1}^{NV} (Av(v) * x^{**v} - 1))$$

where x = Quality ($0 < x < 1$).

E.3.4 G2-3: Two-phase friction multiplier, polynomial in quality

This card is required if $N3 = 5$ on card GCC2 (\rightarrow p.E-10).

Read: NF , ($AF(I)$, $I = 1, 7$)

Format (15, 7E10.5)

read from subroutine **INDAT**.

NF = Number of terms in polynomial (max.7).

AF = 7 Polynomial coefficients.

Note: (1) The polynomial is calculated as

$$\sum_{k=1}^{NF} (AF(k) * x^{** (k - 1)})$$

where x = Quality ($0 < x < 1$).

E.4 Card Group 3

Axial heat flux

| | |
|---|------|
| GCC3: Group control card for card group 3 | E-12 |
| G3-1: Axial heat flux data | E-13 |
| G3-2: Hot channel factors | E-13 |
| G3-3: DNB Limit Value For Heat Transfer..... | E-14 |

E.4.1 GCC3: Group control card for card group 3

This card is required whenever card group 3 is used.

Read: $NGROUP$, $N1$, $N2$, $N3$, $N4$, $N5$, $N6$, $N7$

Format (415)

read from subroutine **INDAT**.

| | | | |
|-----------------|---|---|--|
| $NGROUP$ | = | 3 | Select card group 3. |
| $N1$ (IQP3/NAX) | = | | Number of positions at which the relative axial heat flux will be specified (min = 2, max = 70). |
| $N2$ | = | | Not used. |
| $N3$ (IHC) | = | | Number of hot channel (see card G3-2 (\rightarrow p.E-13)). |
| $N4$ (LCHF) | = | | Indicator for DNB-Limit used in heat transfer calculation (see card G3-3 (\rightarrow p.E-13)). |
| $N5$ | = | | Not used. |
| $N6$ | = | | Not used. |

N7 = Not used.

Note: (1) If $N1 > 1$ NAX is set equal to $N1$.

(2) If $N1 \leq 1$ $IQP3$ is set equal to $N1$ resulting in the read of 3-dimensional power data from file **POWER3D** (channel by channel), the input format being consistent with the power data written to file **IF_HOSCAM** by the **PANBOX** code.

(3) If $N1 = -3$ $IQP3$ is set equal to $N1$ resulting in the read of 3-dimensional power data from file **POWER3D** (pin by pin).

E.4.2 G3-1: Axial heat flux data

This card is required if $N1 > 1$ on card **GCC3** (\rightarrow p. E-12).

Read: $Y(I)$, $AXIAL(I)$, $I = 1, N1$

Format (12F5.3)

read from subroutine **INDAT**.

Y = Relative axial position (X/L).

AXIAL = Relative heat flux (local/average), $AXIAL > 0.0$.

Note: (1) The above data pair format is repeated six times per card, sufficient cards are required to pass $N1$ (card **GCC3** (\rightarrow p. E-12)) data pairs.

(2) Data pairs at relative positions $X/L = 0.0$ and $X/L = 1.0$ must be specified.

(3) The relative axial heat flux between the points given above is found by using linear interpolation. The user should be extremely careful in choosing the locations he specifies, especially for abrupt changes. If two axial locations are too close, the interpolation routine will produce a **DIVIDE BY ZERO** type error.

E.4.3 G3-2: Hot channel factors

This card is required if $N3 > 0$ and $N1 > 1$ on card **GCC3** (\rightarrow p. E-12).

Read: **FEQ**, **FEDH1**, **FEDH2**, **F1GRID**, **F2GRID**, **F3GRID**

Format (6F5.3)

read from subroutine **INDAT**.

FEQ = Flux engineering factor.

FEDH1 = Pellet diameter, density and enrichment.

FEDH2 = Rod diameter, pitch and bowing.

F1GRID = Grid 1 form factor adjustment.

F2GRID = Grid 2 form factor adjustment.

F3GRID = Grid 3 form factor adjustment.

Note: (1) The factors **FEQ**, **FEDH1**, **FEDH2** are applied to the hot channel specified on card **GCC3** (\rightarrow p. E-12).

FEQ: The calculated critical heat fluxes of the rods heating the hot channel are divided by **FEQ**.

FEDH1: The heat input to the hot channel is multiplied by **FEDH1** without changing the

heat fluxes of the adjacent rods, except for calculation of the conditions of subcooled boiling initiation.

FEDH2: The channel flow area is divided by FEDH2. The hydraulic diameter and the heated equivalent diameter are based on the modified flow area. But in the CHF correlations the diameters are based on the unmodified flow areas.

(2) The factor F1GRID is applied to the spacer loss coefficients CD, CDA and CDB (see card G7-5 (→ p.E-33)) of the spacers of type 1, F2GRID to those of type 2, and F3GRID to those of type 3.

E.4.4 G3-3: DNB Limit Value For Heat Transfer

This card is required if $N4 > 0$ and $N1 > 1$ on card GCC3 (→ p. E-12).

Read: **CHFLIM**

Format (F5.3)

read from subroutine **INDAT**.

CHFLIM = DNB Ratio Limit Value For Heat Transfer

Note: (1) This limit value is applied to all rods/channels.

E.5 Card Group 4

Channel data

| | |
|--|------|
| GCC4a: Group control card for card group 4a (if IPILE=0 on card I3) | E-15 |
| G4a-1: Subchannel data | E-15 |
| G4a-2: Local coupling parameters | E-16 |
| GCC4b: Group control card for card group 4b (if IPILE=1 or 2 on card I3) | E-16 |
| G4b-1: Problem specification data | E-17 |
| G4b-2: Alphanumeric data for problem identification | E-18 |
| G4b-3: Hydraulic data | E-18 |
| G4b-4: Spacer data | E-19 |
| G4b-5: Radial power factors | E-20 |
| G4b-6: Grid data | E-20 |
| G4b-7: Channel lists by type | E-20 |
| G4b-8: Array size specifications | E-21 |
| G4b-9: Row declarations | E-21 |
| G4b-10: Channel numbers by row | E-22 |
| G4b-11: Boundary definitions | E-22 |
| G4b-12: Half boundary identification | E-22 |
| G4b-13: Fuel rod thermal specifications | E-23 |
| G4b-14: CHF correlation input: selection of CHF correlation | E-23 |
| G4b-15: CHF correlation input: non-linear profile, spacer grid and cold-wall factor | E-24 |
| G4b-16: CHF correlation input: hot channel data | E-25 |
| G4b-17: CHF correlation input: selection of characteristic diameter | E-26 |
| G4b-18: CHF correlation input: input of characteristic diameter | E-26 |
| G4b-19: CHF correlation input: grid factor for []-correlation | E-27 |
| G4b-20: CHF correlation input: input for Tong's spacer correction | E-27 |

E.5.1 GCC4a: Group control card for card group 4a (if IPILE=0 on card I3)

This card is required if card group 4 is used and **IPILE = 0** on card I3 (→ p.E-6).

Read: **NGROUP, N1, N2, N3, N4, N5, N6, N7**

Format (3I5)

read from subroutine **INDAT**.

| | | | |
|------------|---|---|---|
| NGROUP | = | 4 | Select card group 4 |
| N1 | = | | Number of cards of type G4a-1 (→ p.E-15) containing subchannel data. |
| N2 (NCHAN) | = | | Total number of subchannels. |
| N3 | = | | Number of gaps for which individual local coupling parameters are to be read on cards of type G4a-2 (→ p.E-16). |
| N4 | = | | Not used. |
| N5 | = | | Not used. |
| N6 | = | | Not used. |
| N7 | = | | Not used. |

E.5.2 G4a-1: Subchannel data

This card is required if card group 4 is used and **IPILE = 0** on card I3 (→ p. E-6).

Read: **N, I, AC, PW, PH, LC, GAPS, DIST**

Format (I1, I4, 3E5.0, 4(I5,2E5.0))

read from subroutine **INDAT**.

| | | | |
|------|---|--|---|
| N | = | | Subchannel type number (see notes 7 and 8). |
| I | = | | Subchannel identification number. |
| AC | = | | Nominal flow area (cm ²). |
| PW | = | | Wetted perimeter (cm). |
| PH | = | | Heated perimeter (cm). |
| LC | = | | Adjacent subchannel number (see notes 1 and 6). |
| GAPS | = | | Nominal gap spacing (cm). |
| DIST | = | | Channel centroid-to-centroid distance (see note 4). |

Note: (1) If a line of symmetry splits a gap at the boundary the adjacent subchannel number is given as negative by the user.

(2) Up to four sets of subchannel connecting information may be given.

(3) If subchannels are input in ascending order, then only higher numbered subchannels need to be identified as connecting.

- (4) Centroid-to-centroid distances are not required if they are not used for internal lateral scaling or in the mixing correlations (card G9-1 (\rightarrow p.E-65) or GCC10 (\rightarrow p.E-71)) and may normally be set to zero.
- (5) No channel map is necessary for $IPILE = 0$, since the subchannel interconnections are user supplied.
- (6) LC must be higher than I ; if I is greater than LC , the connection will be ignored.
- (7) For list directed input a value must be specified; if the value is 0 or blank (if formatted input is used) it is automatically set to 1.
- (8) The subchannel type number ($N=1,2,3$, or 4) defines which of the four sets of friction factor correlation constants on card G2-1 (\rightarrow p.E-11) shall be applied to subchannel number I .

E.5.3 G4a-2: Local coupling parameters

This card is required if $N3 > 0$ on GCC4a (\rightarrow p.E-15).

Read: K , $FACSL(K)$, $FACSLK(K)$, $FACFTM(K)$, $ENEH(K)$

Format (I10, 4F13.6)

read from subroutine **INDAT**.

| | | |
|-------------|---|--|
| K | = | Gap number. |
| $FACSL(K)$ | = | Local multiplier to the global transverse momentum parameter SL (\rightarrow p.E-65). |
| $FACSLK(K)$ | = | Local multiplier to the global diversion crossflow resistance factor KIJ (\rightarrow p.E-65). |
| $FACFTM(K)$ | = | Local multiplier to the global turbulent momentum factor FTM (\rightarrow p.E-65). |
| $ENEH(K)$ | = | Local multiplier to the enthalpy difference in the turbulent mixing term of the energy equation, see also card 35-HM (\rightarrow p.E-127). |

Note: (1) A total of $N3$ cards must be given.

(2) []

(3) The factors once defined for individual gaps remain effective for successive runs in the same input file.

E.5.4 GCC4b: Group control card for card group 4b (if $IPILE=1$ or 2 on card I3)

This card is required if card group 4 is used and $IPILE = 1$ or 2 on card I3 (\rightarrow p.E-6).

Read: $NGROUP$, $N1$, $N2$, $N3$, $N4$, $N5$, $N6$, $N7$

Format (I5)

read from subroutine **INDAT**.

| | | | |
|-------------------|---|---|---|
| $NGROUP$ | = | 4 | Select card group 4. |
| $N1$ | = | | Not used. |
| $N2$ | = | | Not used. |
| $N3$ ($NREDGL$) | = | 0 | Reynolds Number independent grid loss coefficients. |

| | | | |
|----|---|---|---|
| | > | 0 | Reynolds Number dependent grid loss coefficients. |
| N4 | = | | Not used. |
| N5 | = | | Not used. |
| N6 | = | | Not used. |
| N7 | = | | Not used. |

*Note: (1) Once this card is read, the new subroutine **CARDS4** is entered for the remaining read statements and data processing of this card group.*

In this case, Card Groups 7 (Spacers) and 8 (Rods) can be omitted.

E.5.5 G4b-1: Problem specification data

*This card is required if **NGROUP = 4** and **IPILE = 1** or **2** on card I3 (→ p. E-6).*

*Read: **N1, N2, NGRID, NGRIDT, NODESF, NFUELT, NCHF, IMAP, ITEXT**
Format (914)
read from subroutine **CARDS4**.*

| | | | |
|--------|---|---|--|
| N1 | = | | Number of channel types (max = 15 , see below). |
| N2 | = | | Total number of channels in problem (see note 2). |
| NGRID | = | | Number of grid positions (max=20). |
| NGRIDT | = | | Number of types of grid (max=10). |
| NODESF | = | | Number of radial nodes on the fuel for center temperature calculation. |
| NFUELT | = | | Number of fuel types. |
| NCHF | = | 0 | No CHF calculations. |
| | = | 1 | B&W-2 CHF correlation. |
| | = | 2 | W-3 correlation. |
| | = | 3 | Hench-Levy correlation. |
| | = | 4 | CISE-4 correlation. |
| | [| | |
| | |] | |
| IMAP | = | | Specify method of presenting gap interconnection data: |
| | = | 1 | See card G4b-8 (→ p.E-21): Array size specifications. |
| | = | 2 | See card G4b-9 (→ p.E-21): Row declarations. |
| | = | 3 | See card G4b-10 (→ p.E-22): Channel numbers by row. |
| | = | 4 | See card G4b-11 (→ p.E-22): Boundary definitions. |
| ITEXT | = | | Number of cards to be read in next which will be printed out as a message. If ITEXT = 0 no message cards are read in. |

Note: (1) Channels are defined as being all of the same type if they have the same geometry, rod dimensions, and grids and only differ in their power. More precisely, the cards G4b-3 (→ p.E-18) and G4b-4 (→ p.E-19), defining the geometry and grids must apply to all channels of

the same type. For example in 1/4-core symmetry data, 1/4, 1/2 and whole channels would be different types.

(2) **NROD** (number of rods) and **NCHAN** (number of channels) are both set to the value of **N2**.

(3) For BWRs (**IPILE = 2** on card I3 (→ p. E-6)) the channels are not connected and the channel map is not required.

(4) With **NCHF** all correlations as listed in **N5 (NCHF)** on card GCC8 (→ p.E-35) can be chosen that require no further input.

E.5.6 G4b-2: Alphanumeric data for problem identification

This card is required if **ITEXT > 0** on card G4b-1 (→ p.E-17).

Read: **TEXT**

Format (20A4)

read from subroutine **CARDS4**.

TEXT = The array **TEXT** (20) is read and immediately printed in a do loop from 1 to **ITEXT**. The idea is that a map of the channel numbering system can be printed as a memory aid in a large problem.

E.5.7 G4b-3: Hydraulic data

This card is required whenever card group 4b is used.

Read: **N, I, FRAC, AC(I), PW(I), PH(I), GAPS(I, 1), DIST(I, 1), DR(I), PHI(I, 1), M**

Format (I1, I4, 8E9.3, I2)

read from subroutine **CARDS4**.

N = Selector for friction factor expression. (Reset to 1 if **N = 0**).

I = Any channel number; preferably the first of the channel type being described.

FRAC = Factor by which **AC, PW** and **PH** should be multiplied. Thus for 1/4 channel, one may set **FRAC = 0.25** and **AC, PW** and **PH** the same as for a whole channel.

AC = Channel flow area (cm²).

PW = Channel wetted perimeter (cm).

PH = Channel heated perimeter (cm).

GAPS = Effective rod gap boundary gap dimensions.

DIST = Centroid-to-centroid channel distance (cm). This is only required for a particular mixing correlation or internal lateral scaling and may normally be set to zero.

DR = Rod diameter (cm).

PHI = Number of rods in channel.

M = Fuel type (reset to 1 if **M = 0**):

= 1 Rod fuel.

= 2 Plate fuel.

*Note: (1) The variable **FRAC** is used to multiply the values for **AC**, **PW**, **PH** and **PHI**. The multiplication of **PHI** poses a potential input error if the value for **RADIAL** on card G4b-5 (\rightarrow p.E-20) is not adjusted to account for this factor.*

*(2) The variable **GAPS** inputs the effective rod gap interconnections between channels. The value of **GAPS** need not be the actual physical dimension of the gap depending on the resistance model used. For assembly to assembly analysis, **GAPS** is the effective rod gap multiplied by the number of gaps in the assembly.*

*(3) **M** indicates which fuel type is being used. **M = 1** indicates rod fuel only; **M = 2** indicates plate fuel or a combination of rod and plate fuel. If **M = 2** data must be provided for rod fuel, giving zeros or blanks if rod fuel is not used.*

E.5.8 G4b-4: Spacer data

This card is required if **NGRID > 0** on card G4b-1 (\rightarrow p.E-17) .

Read: If **NREDGL** (\rightarrow p.E-16) > 0: (**CDA** (**I,L**), **CDB** (**I,L**), **CDC** (**I,L**), **L=1,NGRIDT**), (**FXF** (**L**), **L = 1, NGRIDT**)

Format (**16E5.3**)

read from subroutine **CARDS4**.

If **NREDGL** (\rightarrow p.E-16) = 0: (**CD** (**I,L**), **L = 1, NGRIDT**), (**FXF** (**L**), **L = 1, NGRIDT**)

Format (**16E5.3**)

read from subroutine **CARDS4**.

CD = Spacer loss coefficients.

CDA, CDB, CDC = Reynolds number dependent spacer loss coefficient is $CDA + CDB * RE ** CDC$.

FXF = Fraction of axial flow forced across each boundary (Default = **0.0** because it is not expected that this will be used in reactor problems).

*Note: (1) The spacer loss coefficients are provided first, giving one coefficient or three coefficients for each of the **NGRIDT** grid types (see card G4b-1 (\rightarrow p.E-17)). Following the loss coefficients, a total of **NGRIDT** diversion flow fraction specifications must be provided.*

(2) Note that the same diversion flow fraction is used for all boundaries of the channel at that spacer location.

*(3) Enough cards of this type (G4b-4) must be present to provide $2 * NGRIDT$ or $4 * NGRIDT$ values even if those values are zero or blank.*

*(4) A total of **N1** (card G4b-1 (\rightarrow p.E-17)) pairs of cards G4b-3 and G4b-4 must be provided. Each card pair gives the hydraulic and spacer data for one of the **N1** channel types.*

E.5.9 G4b-5: Radial power factors

This card is required whenever card group 4b is used.

Read: **RADIAL(I)**, **I = 1, NROD**

Format (16E5.3)

read from subroutine **CARDS4**.

RADIAL = Radial power factor for rod **I** which is located in channel **I**. This is defined as the ratio of the rod power to that of the reactor average rod power.

Note: (1) **NROD** is the total number of rods, set to **NCHAN** (total number of channels) which was itself set to **N2** (see card G4b-1 (→ p.E-17)).

(2) One rod exists for each channel and the smeared channels must also have smeared rods. The radial power factor for such smeared rods should be the sum of the factors for each of the unsmeared rods divided by the product of **FRAC** and **PHI** (see card G4b-3 (→ p.E-18)).

(3) If all rods have the same power, **RADIAL(1)** alone may be given and is set negative. This triggers setting (**RADIAL(I); I = 1, NROD**) equal to **1.0**. No importance is attached to the magnitude of **RADIAL(1)** as long as **RADIAL(1) < 0**. In all other cases, a total of **NROD** factors must be given.

E.5.10 G4b-6: Grid data

*This card is required if **NGRID > 0** on card G4b-1 (→ p.E-17).*

Read: (**GRIDXL(I)**, **IGRID(I)**), **I = 1, NGRID**

Format (8(E5.3,15))

read from subroutine **CARDS4**.

GRIDXL = Relative location (X/L) where grids are located.

IGRID = Type of grid at **GRIDXL**.

Note: (1) A total of **NGRID** pairs of data must be provided giving 8 pairs per card.

E.5.11 G4b-7: Channel lists by type

*This card is required if **N1 > 1** on card G4b-1 (→ p.E-17).*

Read: **JB(I)**

Format (20I4)

read from subroutine **CARDS4**.

JB = List of channels of type **I** (**I > 1**).

Note: (1) The first set given is the set of channel numbers for the channels of type 2. The list is terminated by reading in a zero or a blank space. Hence, if the last channel number comes at the end of a card, a blank card must follow in order to give the terminating zero. It is safer to make a habit of punching a final zero. Following type 2, card(s) are read in for those channels in type 3 then type 4 etc. ... up to **N1** types.

- (2) Note that since the channel numbers for type 1 are not read in, it is more economical to select type 1 as that with the majority of channels.
- (3) An internal consistency check is made when reading in **JB(I)**. If a set includes the channel number (**I** in card G4b-3 (→ p.E-18)) for type 1 or does not include that given for its own type in card G4b-3 (→ p.E-18), an appropriate message is printed and the run terminated.
- (4) If **N1 = 1** this card is not used.

E.5.12 G4b-8: Array size specifications

This card is required if **IPILE = 1** on card I3 (→ p. E-6) and **IMAP = 1** on card G4b-1 (→ p.E-17).

Read: **ICROSS, IDOWN**

Format (2I4)

read from subroutine **CARDS4**.

ICROSS = Number of channels across the rectangular channel map.

IDOWN = The number of channels down the side of the rectangular channel map.

Note: (1) For BWRs (**IPILE = 2** on card I3 (→ p. E-6)) the channels are not connected and no channel map is required. For BWRs the next card read in is card G4b-13 (→ p.E-23).

- (2) Note that the maximum value for both **ICROSS** and **IDOWN** is 20.
- (3) The use of this option is only possible when the pattern of channels is rectangular.
- (4) The channel boundaries are established and numbered in the order that is described for card 20-GB (→ p.E-108) of the card group 20 input method (→ p E-87).

E.5.13 G4b-9: Row declarations

This card is required if **IPILE = 1** on card I3 (→ p. E-6) and **IMAP = 2** on card G4b-1 (→ p.E-17).

Read: **ISTART, IEND**

Format (2I4)

read from subroutine **CARDS4**.

ISTART = First channel in each row.

IEND = Last channel in each row.

Note: (1) One of these cards should be given for each row.

- (2) The maximum value of **IEND** is 20 and the maximum number of rows is also 20. If less than 20 rows are to be given, a blank card (or one with two zeros) should be given after the last row.
- (3) See card 2-CNS (→ p.E-91) of the card group 20 input method (→ p. E-87) for additional details.

E.5.14 G4b-10: Channel numbers by row

This card is required if **IPILE = 1** on card I3 (→ p. E-6) and **IMAP = 3** on card G4b-1 (→ p.E-17).

Read: **MAAP (L)**, **L = 1, 20**

Format (2014)

read from subroutine **CARDS4**.

MAAP = The channel numbers of the channels making up a row.

Note: (1) One of these cards should be inputted for each row (maximum 20 rows). The value of **MAAP** represents the channel number with a zero indicating no channel. If less than 20 cards are to be used, the last should be all zeros (i.e. a blank card). The set of cards represents a map of the channel numbering system, which is thus under the control of the user. The boundary numbering is done by the computer.

(2) See card 3-CNS (→ p.E-92) of the card group 20 input method (→ p.E-87) for additional details.

E.5.15 G4b-11: Boundary definitions

This card is required if **IPILE = 1** on card I3 (→ p.E-7) and **IMAP = 4** on card G4b-1 (→ p.E-17).

Read: **IK, JK**

Format (2014)

read from subroutine **CARDS4**.

IK = See notes below.

JK = See notes below.

Note: (1) **IK, JK** are the channel pairs defining each boundary in turn; **NK** = number of boundaries specified. The sets of numbers are read in, 20 to a card, continuing on as many cards as necessary. They are terminated by a zero; if the final channel number is at the end of a card, the zero must be given on the next card (Note that the value of **NK** is not known at the time of reading in **IK, JK**; it is set to the number of pairs read in). Thus, with **IMAP = 4** both channel and boundary numbering are under the control of the user. When listing the subchannel pairs, it is preferable to give the lower number first; this saves the computer reversing the order.

(2) The **IMAP = 4** option can be very cumbersome and should only be used if the other **IMAP**-options won't work.

E.5.16 G4b-12: Half boundary identification

This card is required if **IPILE = 1** on card I3 (→ p. E-6).

Read: **JB (L)**, **L = 1, 20**

Format (2014)

read from subroutine **CARDS4**.

JB = List the identification number pairs for the channels making up each half boundary, i.e. the boundaries that are split by a line of symmetry.

Note: (1) Always terminate with a zero. If there are no half boundaries, give a single card with a zero. The parameter **FACTOR(K)** is set to **1.0** for full boundaries and **0.5** for half boundaries.

(2) The boundary number pairs should be given lowest number first.

E.5.17 G4b-13: Fuel rod thermal specifications

This card is required if **NODESF > 0** on card G4b-1 (→ p.E-17).

Read: **KFUEL(I)**, **CFUEL(I)**, **RFUEL(I)**, **DFUEL(I)**, **KCLAD(I)**, **CCLAD(I)**, **RCLAD(I)**, **TCLAD(I)**, **HGAP(I)**, **I = 1**, **NFUEL**

Format (16E5.3)

read from subroutine **CARDS4**.

| | | |
|-------|---|--|
| KFUEL | = | Fuel thermal conduction (W/(m °C)). |
| CFUEL | = | Fuel specific heat (kJ/(kg °C)) |
| RFUEL | = | Fuel density (kg/dm ³). |
| DFUEL | = | Pellet diameter (cm). |
| KCLAD | = | Cladding thermal conductivity (W/(m °C)). |
| CCLAD | = | Cladding specific heat (kJ/(kg °C)). |
| RCLAD | = | Cladding density (kg/dm ³). |
| TCLAD | = | Cladding thickness (cm). |
| HGAP | = | Fuel-cladding heat transfer coefficient (kJ/(k cm ² °C)). |

E.5.18 G4b-14: CHF correlation input: selection of CHF correlation

This card is required if **NCHF = 12** on card G4b-1 (→ p.E-17).

Read: **IRGW**

Format (I5)

read from subroutine **INDAT**.

| | | |
|------|---|---|
| IRGW | = | Select correlation as follows (CHF correlations and CHF look-up tables, [|
|------|---|---|

]

[

]

Note: (1) If $IRGw < 0$: Additional information of hottest subchannel is required (cf. card G4b-16 (→ p.E-25)).

E.5.19 G4b-15: CHF correlation input: non-linear profile, spacer grid and cold-wall factor

This card is required if $NCHF = 12$ on card G4b-1 (→ p.E-17).

Read: $NNonF12$, $NSPf12$, $NCWf12$

Format (3I10)

read from subroutine *INDAT*.

$NNonF12$ = Select Non-uniform heat flux profile correction correlations:

= 0 none

[

]

[

]

| | | |
|--------|---|---|
| NSPf12 | = | Select spacer correction factor correlations: |
| | = | 0 none |
| | = | 1/2 Tong's Spacer factor for Mixing vane grids including: TDC ($\rightarrow p.E-27$), K_s ($\rightarrow p.E-27$) and f_{DNBR} ($\rightarrow p.E-27$). (Additional Input: see G4b-20 ($\rightarrow p.E-27$)) |
| | | 1: Total heated length of bundle used. |
| | | 2: Heated length up to level J used. |
| | = | 3 Tong's Spacer factor for Mixing vaned grids and non vaned grids including: TDC ($\rightarrow p.E-27$) (Additional Input: see G4b-20 ($\rightarrow p.E-27$)) |
| | = | 4 Spacer grid correction according to Groeneveld et al. (Stockholm, 1995) |
| NCWf12 | = | Select cold wall correction factor correlations: |
| | = | 0 none |
| | = | 1 Tong's cold wall correction factor. (Tong's W3 CHF correlation should be used with equivalent diameter based on the heated perimeter) |

E.5.20 G4b-16: CHF correlation input: hot channel data

This card is required if $NCHF = 12$ on card G4b-1 ($\rightarrow p.E-17$) and if $IRGw$ ($\rightarrow p.E-23$) (on G4b-14 ($\rightarrow p.E-23$)) < 0 .

Read: **FRadF12**, **FGf12**, **AoneSC**, **PwoneSC**, **PoneSC**, **TrSC**

Format (**6F10.5**)

read from subroutine **INDAT**.

| | | |
|---------|---|---|
| FRadF12 | = | Average radial power factor of the rods around the hot-channel. |
| FGf12 | = | Mass velocity factor of hot-channel compared to the average bundle mass velocity. |
| AoneSC | = | Hot-channel flow area (mm^2). |
| PwoneSC | = | Hot-channel wetted perimeter (mm). |
| PoneSC | = | Hot-channel heated perimeter (mm). |

TrSC = Ratio of maximum to average radial heat-flux factor of rods around the hot-channel.

E.5.21 G4b-17: CHF correlation input: selection of characteristic diameter

This card is required if **NCHF = 12** on card G4b-1 ($\rightarrow p.E-17$) and if **IRGw** ($\rightarrow p.E-23$) (on G4b-14 ($\rightarrow p.E-23$)) = **1, 8, 9, 10, 11, 15, 19 or 20**.

Read: If **IRGw** ($\rightarrow p.E-23$) = **1**: **IDMR (1)**, **IDMR (2)**, **IDMR (3)**

Format (**3I10**)

read from subroutine **INDAT**.

If **IRGw** ($\rightarrow p.E-23$) = **8-11,15,19,20**: **IDMR (1)**

Format (**I10**)

read from subroutine **INDAT**.

IDMR (1 . . . 3) = Specifies characteristic diameters for CHF-correlation and look-up table application:

= 1 Use input value(s) on card G4b-18 ($\rightarrow p.E-26$) as characteristic diameters.

= 0 Use equivalent diameter based on wetted perimeter.

< 0 Use equivalent diameter based on wetted perimeter.

E.5.22 G4b-18: CHF correlation input: input of characteristic diameter

This card is required if **NCHF = 12** on card G4b-1 ($\rightarrow p.E-17$), if **IDmr(1..3)** ($\rightarrow p.E-26$) = **1** (respectively, cf. Card G4b-17 ($\rightarrow p.E-26$)) and if **IRGw** ($\rightarrow p.E-23$) (on G4b-14 ($\rightarrow p.E-23$)) = **1, 8, 9, 10, 11, 15, 19 or 20**.

Read: If **IRGw** ($\rightarrow p.E-23$) = **1**: **DCHAR (1)**, **DCHAR (2)**, **DCHAR (3)**

Format (**3F10.5**)

read from subroutine **INDAT**.

If **IRGw** ($\rightarrow p.E-23$) = **8-11,15,19,20**: **DCHAR (1)**

Format (**F10.5**)

read from subroutine **INDAT**.

DCHAR (1 . . 3) = Characteristic diameter(s) (mm) for each of the three boiling regimes [] ($\rightarrow p.E-23$) = **1**) resp. **DCHAR(1)** [], one of the [], or the W3 CHF correlation is selected (**IRGw** ($\rightarrow p.E-23$) = **8, 9, 10, 11, 15, 19 or 20**).

E.5.23 G4b-19: CHF correlation input: grid factor for []-correlation

This card is required if **NCHF = 12** on card G4b-1 (\rightarrow p.E-17) and if **IRGw** (\rightarrow p.E-23) (on G4b-14 (\rightarrow p.E-23)) = 17 or 18 ([]-CHFR-Correlations).

Read: []

Format (F10.5)

read from subroutine **INDAT**.

[]

=

Rod bundle factor:

$F_g = 1$ or defined by user. It depends on grid spacer and sub-channel code. ($F_g = 1$ recommended).

E.5.24 G4b-20: CHF correlation input: input for Tong's spacer correction

This card is required if **NCHF = 12** on card G4b-1 (\rightarrow p.E-17) and if **NSPf12** (\rightarrow p.E-25) (cf. G4b-15 (\rightarrow p.E-24))

[

]

Read: If **NSPf12** (\rightarrow p.E-25) = 1 or 2 (cf. G4b-15 (\rightarrow p.E-24)): **TDCW3**, **KSGrid**, **fDNBRW**

Format (3F10.5)

read from subroutine **INDAT**.

If **NSPf12** (\rightarrow p.E-25) = 3 (cf. G4b-15 (\rightarrow p.E-24)): **TDCW3**

Format (F10.5)

read from subroutine **INDAT**.

TDCW3

=

Thermal Diffusion Coefficient (TDC)

KSGrid

=

Axial grid spacing coefficient (K_s) depending on axial grid spacing

fDNBRW

=

DNBR correction multiplier (f_{DNBR})

E.6 Card Group 5

Subchannel area variation

| | |
|---|------|
| GCC5: Group control card for card group 5 | E-28 |
| G5-1: Axial positions of area variations | E-28 |
| G5-2: Subchannel number | E-29 |
| G5-3: Area variation factors | E-29 |

E.6.1 GCC5: Group control card for card group 5

This card is required whenever card group 5 is used.

Read: *NGROUP*, *N1*, *N2*, *N3*, *N4*, *N5*, *N6*, *N7*

Format (415)

read from subroutine *INDAT*.

| | | | |
|-----------------------------|---|---|--|
| <i>NGROUP</i> | = | 5 | Select card group 5. |
| <i>N1</i> (<i>NAFACT</i>) | = | | Number of subchannels for which area variation data will be given. |
| | = | 0 | Deletes area variation for succeeding cases. |
| <i>N2</i> (<i>NAXL</i>) | = | | Number of axial positions at which area variations will be specified. |
| <i>N3</i> (<i>NARAMP</i>) | = | | Number of iterations for inserting area variations. If N3 is zero or blank, it is set to 1. |
| <i>N4</i> | = | | Not used. |
| <i>N5</i> | = | | Not used. |
| <i>N6</i> | = | | Not used. |
| <i>N7</i> | = | | Not used. |

Note: (1) If there are no area variations, this card group may be omitted.

E.6.2 G5-1: Axial positions of area variations

This card is required whenever card group 5 is used.

Read: *AXL(I)*, *I = 1, N2*

Format (12F5.3)

read from subroutine *INDAT*.

| | | | |
|------------|---|--|---|
| <i>AXL</i> | = | | Relative axial locations (<i>X/L</i>) where area factors are given. |
|------------|---|--|---|

Note: (1) A total of *N2* (see card *GCC5* (→ p.E-28)) relative positions must be specified.

(2) Relative positions *X/L=0.0* and *X/L=1.0* must be specified.

(3) Since the code finds the areas between specified axial locations by interpolation, the user should be extremely careful in choosing the locations he specifies, especially for abrupt changes. If two axial locations are too close, the interpolation routine will produce a **DIVIDE BY ZERO** type error.

E.6.3 G5-2: Subchannel number

This card is required if N1 > 0 on card GCC5 (→ p. E-28).

Read: **I**
 Format (I5)
 read from subroutine **INDAT**.

I = Channel number of channel for which area variation data follow (on cards of type G5-3 (→ p. E-28)).

Note: (1) N1 (on card GCC5 (→ p. E-28)) sets of area variation factors are required. Each set consists of one card G5-2 giving the channel number and one card of type G5-3 (→ p. E-29) to give N2 (on card GCC5 (→ p. E-28)) area variation factors.

E.6.4 G5-3: Area variation factors

This card is required if N1 > 0 on card GCC5 (→ p. E-28).

Read: **AFACT(I,L), L = 1, N2**
 Format (12F5.3)
 read from subroutine **INDAT**.

AFACT = Area variation factors (local area/nominal area).

Note: (1) A total of N2 (on card GCC5 (→ p. E-28)) area variation factors must be provided.

E.7 Card Group 6

Gap spacing variation

| | |
|--|------|
| GCC6: Group control card for card group 6 | E-29 |
| G6-1: Axial positions of gap spacing variations..... | E-30 |
| G6-2: Gap number | E-30 |
| G6-3: Gap spacing variation factors..... | E-30 |

E.7.1 GCC6: Group control card for card group 6

This card is required whenever card group 6 is used.

Read: **NGROUP, N1, N2, N3, N4, N5, N6, N7**
 Format (3I5)
 read from subroutine **INDAT**.

NGROUP = 6 Select card group 6.
 N1 (NGAPS) = Number of gaps for which spacing factors will be given.
 = 0 Deletes gap variations for succeeding cases.
 N2 (NGXL) = Number of axial positions at which gap spacing factors will be specified.
 N3 = Not used.

| | | |
|----|---|-----------|
| N4 | = | Not used. |
| N5 | = | Not used. |
| N6 | = | Not used. |
| N7 | = | Not used. |

Note: (1) If there are no gap spacing variations, this card group may be omitted.

(2) **N1** sets of gap spacing data must be provided. Each set consists of one card G6-2 (\rightarrow p.E-30) giving the number of the selected gap, and **N2** gap variation factors specified on cards of type G6-3 (\rightarrow p.E-30).

E.7.2 G6-1: Axial positions of gap spacing variations

This card is required whenever card group 6 is used.

Read: **GAPXL(L)**, $L = 1, N2$
Format (12F5.3)
read from subroutine **INDAT**.

GAPXL = Relative axial locations (X/L) where gap spacing factors are given.

Note: (1) A total of **N2** (see card GCC6 (\rightarrow p.E-29)) relative positions must be specified, giving 12 values per card.

(2) Relative positions $X/L=0.0$ and $X/L=1.0$ must be specified.

(3) Since the code finds the gap spacings between specified axial locations by interpolation, the user should be extremely careful in choosing the locations he specifies, especially for abrupt changes. If two axial locations are too close, the interpolation routine will produce a **DIVIDE BY ZERO** type error.

E.7.3 G6-2: Gap number

This card is required if **N1 > 0** on card GCC6 (\rightarrow p. E-29).

Read: **K**
Format (I5)
read from subroutine **INDAT**.

K = Gap number.

Note: (1) No sequence is associated with the gap numbers since they are user supplied.

E.7.4 G6-3: Gap spacing variation factors

This card is required if **N1 > 0** on card GCC6 (\rightarrow p. E-29).

Read: **GFACT(K,L)**, $L = 1, N2$
Format (12F5.3)
read from subroutine **INDAT**.

GFACT = Gap spacing variation factors (local gap width/nominal gap width).

Note: (1) 12 Values may be given per card, and sufficient cards must be used to provide all **N2** (on card GCC6 (→ p. E-29)) values.

E.8 Card Group 7

Spacer data

| | |
|---|------|
| GCC7: Group control card for card group 7 | E-31 |
| G7-1: Wire wrap geometry | E-32 |
| G7-2: Gap specification | E-32 |
| G7-3: Wire wrap inventory | E-32 |
| G7-4: Spacer location and type | E-33 |
| G7-5: Spacer data sets | E-33 |

E.8.1 GCC7: Group control card for card group 7

This card is required whenever card group 7 is used.

Read: **NGROUP, N1, N2, N3, N4, N5, N6, N7**

Format (6I5)

read from subroutine **INDAT**.

| | | | |
|-------------|---|---|--|
| NGROUP | = | 7 | Select card group 7. |
| N1 (J6) | = | | Spacer type indicator: |
| | = | 1 | Wire wrapped forced diversion crossflow is included. |
| | = | 2 | Spacer pressure losses and forced diversion crossflow are included. |
| N2 (NGRID) | = | | Total number of spacer locations []. |
| N3 (NGRIDT) | = | | Number of spacer types []. |
| N4 (NRAMP) | = | | Number of iterations to insert loss coefficients for wire wrap mixing. |
| N5 (NJUMP) | = | | Crossflow solution indicator: |
| | = | 0 | Solution computed for each case. |
| | = | 1 | Use first case solution for all succeeding cases. |
| | = | 2 | Write solution to tape8 (= 'CROSFLO') and use for all succeeding cases. |
| | = | 3 | Read solution from tape8 (= 'CROSFLO') and use for all succeeding cases. |
| N6 (NREDGL) | = | 0 | Reynolds Number independent grid loss coefficients |
| | > | 0 | Reynolds Number dependent grid loss coefficients |
| N7 | = | | Not used. |

Note: (1) **N2** relative spacer locations (X/L) and spacer types will be read in on cards of type G7-4 (→ p.E-33) if **N1 = 2**.

(2) **N3** sets of data corresponding to each spacer type will be read in on cards of type G7-5 (→ p.E-33) if **N1 = 2**.

(3) If $N4 < 1$, $N4$ is reset to 1.

(4) $N2$ and $N3$ are not used if $N1 = 1$, $N4$ and $N5$ are not used if $N1 = 2$.

(5) If $N5 > 0$: The flow condition must not change for these cases, nor the basic problem setup. This option would be normally used for cases involving changes in power or mixing for nonboiling problems.

E.8.2 G7-1: Wire wrap geometry

This card is required if $N1 = 1$ on card GCC7 (\rightarrow p.E-31).

Read: **PITCH, DIA, THICK**

Format (8E10.5)

read from subroutine **INDAT**.

| | | |
|-------|---|-----------------------|
| PITCH | = | Wire wrap pitch (cm). |
| DIA | = | Pin diameter (cm). |
| THICK | = | Wire diameter (cm). |

E.8.3 G7-2: Gap specification

This card is required if $N1 = 1$ on card GCC7 (\rightarrow p. E-31).

Read: **K, DUM, (CROSS(L), L = 1, 6)**

Format (15, 10E5.2)

read from subroutine **INDAT**.

| | | |
|-------|---|--|
| K | = | Gap number. |
| DUM | = | Effective fraction of a pitch for forcing crossflow. |
| CROSS | = | Relative pitch lengths identifying the location of wraps crossing through a gap. Up to six positions may be given. |

Note: (1) One card is required for each gap.

(2) The gap numbers are assigned in the order that subchannel pairs are identified in card group 4 (\rightarrow p.E-14).

(3) The sign of the relative pitch length specification gives the direction in which the wrap is crossing. A positive value indicates wraps crossing from I to J where I is less than J ; a negative value for wraps crossing from J to I .

E.8.4 G7-3: Wire wrap inventory

This card is required if $N1 = 1$ on card GCC7 (\rightarrow p. E-31).

Read: **NWRAP(I), I = 1, NCHAN**

Format (10I5)

read from subroutine **INDAT**.

| | | |
|-------|---|--|
| NWRAP | = | Number of wraps contained in each subchannel at the start of the bundle in ascending subchannel order. |
|-------|---|--|

Note: (1) Enough cards must be used to specify the entire wire wrap inventory giving 10 values per card.

E.8.5 G7-4: Spacer location and type

This card is required if **N1 = 2** on card GCC7 (→ p. E-31).

Read: **GRIDXL(I)**, **IGRID(I)**, **I = 1, N2**
 Format (6(E5.2,I5))
 read from subroutine **INDAT**.

GRIDXL = Relative location (X/L) where spacers are located.
 IGRID = Spacer type at the location specified by **GRIDXL**.

Note: (1) For formatted input a total of **N2** sets of the above data must be provided giving six sets per card.

(2) The spacer type indicates which of the user-supplied spacer data sets (see card G7-5 (→ p.E-33)) applies to the spacer at a location.

(3) Axial spacer positions must not be identical to axial node boundaries specified via **N4(KAXIAL)** on card GCC9 (→ p.E-64) (possibly random results of internal checks for equality). In particular, specification of exactly the same values as for the relative positions of axial node boundaries on card G9-2 (→ p.E-67) must be avoided.

(4) Only one spacer grid may be located in a particular axial node, to ensure correct calculation of pressure loss effect. If two or more grids are defined for the same axial node, only the **lowermost** grid becomes effective, the others are ignored.

E.8.6 G7-5: Spacer data sets

This card is required if **N1 = 2** on card GCC7 (→ p. E-31).

Read: If **NREDGL** (→ p.E-31) = 0: **J**, **CD**, **K**, **FXFLO**
 Format (I5, E5.0, I5, E5.0)
 read from subroutine **INDAT**.

If **NREDGL** (→ p.E-31) > 0: **J**, **CDA**, **CDB**, **CDC**, **K**, **FXFLO**
 Format (I5, 3E5.0, I5, E5.0)
 read from subroutine **INDAT**.

J = Subchannel number.
CD = Spacer loss coefficient.
CDA, CDB, CDC = Reynolds Number dependent spacer loss coefficient is $CDA + CDB \cdot RE^{**} CDC$.
K = Connection number of gap through which flow is forced.
FXFLO = Fraction of flow diverted.

Note: (1) If the connection number is zero and the flow fraction is zero, then there is no forced flow diversion.

(2) The forced crossflow has the same sign as the forced flow fraction.

(3) *N3 sets of data must be provided, one set for each spacer type. Each set consists of a card for every subchannel, the cards appearing in sequential subchannel order.*

E.9 Card Group 8

Rod layout, power factors and CHF correlations

| | |
|--|------|
| GCC8: Group control card for card group 8 | E-35 |
| GCC8-cont: Group control continuation card for card group 8..... | E-37 |
| G8-1: Rod layout data | E-38 |
| G8-1-1: Performance factors for CHF correlations | E-38 |
| G8-1-2: Rod-wise CHF correlations | E-39 |
| G8-1-3: Definition of rod-types containing axial regions with different CHF correlations | E-39 |
| G8-1-4: Axial node-wise regions for CHF correlations | E-40 |
| G8-1-5: Assignment of axial CHF rod-types to individual rods..... | E-40 |
| G8-1aa: Control of multiple CHF correlation input | E-41 |
| G8-1a: CHF correlation input | E-41 |
| G8-1b: CHF correlation input | E-42 |
| G8-1c: CHF correlation input: selection of CHF correlation | E-42 |
| G8-1c-1: CHF correlation input: non-linear profile, spacer grid and cold-wall factor | E-43 |
| G8-1c-2: CHF correlation input: hot channel data..... | E-44 |
| G8-1d: CHF correlation input: selection of characteristic diameter | E-45 |
| G8-1d-1: CHF correlation input:input of characteristic diameter | E-45 |
| G8-1e-1: CHF correlation input: grid factor for []-correlation | E-46 |
| G8-1e-2: CHF correlation input: input for Tong's spacer correlation..... | E-46 |
| G8-1g: [] Correlation Geometry Parameters | E-46 |
| G8-1h: Grid Heights | E-47 |
| G8-1i: Mixing Grid Specification | E-47 |
| G8-1j: [] Correlation Input..... | E-47 |
| G8-1k: [] | E-48 |
| G8-1l: Coefficients of the [] correlation | E-50 |
| G8-1m: CHF correlation limits and debug options | E-50 |
| G8-1n: CHF correlation limits and debug options | E-51 |
| G8-1o: CHF correlation limits and debug options | E-51 |
| G8-1p: CHF correlation grid spacing input..... | E-52 |
| G8-1q: CHF correlation grid spacing input..... | E-52 |
| G8-1r: CHF correlation channels for debug printout | E-52 |
| G8-2: Fuel thermal properties | E-53 |
| G8-2a: Nonuniform radial heating in fuel (number of data pairs) | E-53 |
| G8-2a-1: Options for definition of radial power profile..... | E-53 |
| G8-2a-2: Input parameters for calculation of radial power profile | E-54 |
| G8-2b: Nonuniform radial heating in fuel (pellet data) | E-55 |
| G8-2b-1: Nonuniform radial heating in fuel (pellet radii) | E-55 |
| G8-2c: Number of transient gap conductance data pairs..... | E-55 |
| G8-2d: Transient forcing function data pairs for gap conductance versus time | E-56 |

| | |
|---|------|
| G8-2e: Fuel thermal properties | E-56 |
| G8-2e-1: Iteration of Heat Transfer Coefficient | E-57 |
| G8-2f: Fuel rod model (geometry) | E-57 |
| G8-2g: Fuel rod model (model and data selection) | E-57 |
| G8-2h: Fuel rod model (geometry) | E-58 |
| G8-2i: Fuel rod model (fuel material data) | E-59 |
| G8-2k: Fuel rod model (fuel material data) | E-59 |
| G8-2l: Fuel rod model (fuel material data) | E-60 |
| G8-2m: Fuel rod model (gap gas data) | E-60 |
| G8-2n: Fuel rod model (gap gas data) | E-61 |
| G8-2n-1: Fuel rod model (heat transfer coefficient) | E-62 |
| G8-2o: Fuel rod model (heat transfer coefficient) | E-62 |
| CAR_INP: Fuel rod data from file CAR_INP{.KASE} | E-62 |

E.9.1 GCC8: Group control card for card group 8

*This card is required if **IPILE = 0** on card I3 (→ p.E-6) and card group 8 is desired.*

*Read: **NGROUP, N1, N2, N3, N4, N5, N6, N7***

Format (8I5)

*read from subroutine **INDAT**.*

| | | | |
|----------------|---|---|--|
| NGROUP | = | 8 | Select card group 8. |
| N1 | = | | Number of rod layout data to be read (card type G8-1 (→ p.E-38)) |
| N2 (NROD) | = | | Total number of rods. |
| N3 (NODESF) | = | | Number of radial fuel nodes including the cladding (max = 21). NODESF = NCF + NCC + 1 must hold, see card G8-2e (→ p.E-57). Note: NODESF=0 switches off the fuel rod model. In this case, the surface heat flux is specified as boundary condition for the coolant energy balance also in transient conditions. |
| N4 (NFUELTYPE) | = | | Fuel types used. |
| N5 (NCHF) | = | | CHF correlation indicator: |
| | = | 0 | No CHF correlation done. |
| | = | 1 | The B&W-2 correlation. |
| | = | 2 | The W-3 correlation (see Note (4) below). |
| | = | 3 | The Hench-Levy correlation. |
| | = | 4 | The CISE-4 correlation. |

[

]

= 12 [

]

- = 50 The ACH-2 correlation (cf. G8-1m (\rightarrow p.E-50); see Note(10) below).
- = 51 The Barnett correlation (cf. G8-1n (\rightarrow p.E-51)).
- = 52 The modified Barnett correlation (cf. G8-1n (\rightarrow p.E-51)).
- = 53 The Mark-B HTP correlation (cf. G8-1o (\rightarrow p.E-51), G8-1p (\rightarrow p.E-52)).
- = 54 The Biasi correlation (cf. G8-1n (\rightarrow p.E-51)).
- = 55 The BWC correlation (cf. G8-1m (\rightarrow p.E-50); see Note(10) below).
- = 56 The BWCV correlation (cf. G8-1n (\rightarrow p.E-51), G8-1p (\rightarrow p.E-52); see Note(10) below).
- = 57 The BWCMV-A correlation (cf. G8-1n (\rightarrow p.E-51), G8-1p (\rightarrow p.E-52); see Note(10) below).
- = 58 The BWU-Z (Mark-B11) correlation (cf. G8-1n (\rightarrow p.E-51), G8-1p (\rightarrow p.E-52); see Note(10) below).
- = 59 The BWU-Z (Mark-BW17 MSMG) correlation (cf. G8-1n (\rightarrow p.E-51), G8-1p (\rightarrow p.E-52); see Note(10) below).
- = 60 The BWU-B11R (Mark-B11) correlation (cf. G8-1n (\rightarrow p.E-51), G8-1p (\rightarrow p.E-52); see Note(10) below).
- = 61 The BWU-Z (Mark-BW17) correlation (cf. G8-1n (\rightarrow p.E-51), G8-1p (\rightarrow p.E-52); see Note(10) below).
- = 62 The BWU-I correlation (cf. G8-1n (\rightarrow p.E-51), G8-1p (\rightarrow p.E-52); see Note(10) below).
- = 63 The BWU-N correlation (cf. G8-1m (\rightarrow p.E-50); see Note(10) below).
- = 64 The HTPA correlation (cf. G8-1o (\rightarrow p.E-51), G8-1p (\rightarrow p.E-52); see Note(10) below).

N6 (IFRM)

- = Fuel rod model:
- = 0 Old model.
- = 1 COBRA-IIIC/MIT-2 new model; the MATPRO fuel rod model (old input: no centre pellet channel, dishing, Zr-oxide, equidistant radial nodes).
- = 2 PANBOX-model according [*] (old input: no dishing, Zr-oxide).
- = 3 COBRA-IIIC/MIT-2 new model, modified MATPRO fuel rod model (new input: centre pellet channel, dishing, Zr-oxide on card G8-2h (\rightarrow p.E-58), radial shells of equal volume (optionally equidistant radial nodes, see IOLdcb on card G8-2g (\rightarrow p.E-57))).

| | | | |
|----|---|---|--|
| | = | 4 | PANBOX-model according [*] (new input: centre pellet channel, dishing, Zr-oxide on card G8-2h (→ p.E-58)). |
| N7 | = | 0 | Not used. |
| | > | 0 | If continuation card GCC8-cont (→ p.E-37) is read. |

Note: (1) **N6 (IFRM) = 3** together with **IOLdcb = 1** (see card G8-2g (→ p.E-57)) is strongly recommended for standard applications.

(2) **N4 (NFUEL)** should equal **1** if **N6 (IFRM) > 0** because the new fuel rod model and the PANBOX-model only consider cylindrical fuel geometry.

(3) **N4 (NFUEL) = 1** implies that only cylindrical fuel is used. If **N4 (NFUEL) = 2** either plate fuel alone or a combination of plate and cylindrical fuel is used. If **N4 (NFUEL) = 2**, data cards must be provided for both fuel types, leaving blank the cards for cylindrical fuel if that fuel type is not used.

(4) **N5 (NCHF) = 2** should not be used. It is recommended to use **N5 (NCHF) = 7 []** instead of **N5 (NCHF) = 2** (if the W-3 correlation (**N5 (NCHF) = 2**) has been chosen, the user must validate that the **TDC** value in subroutine "CHF" is appropriate).

(5) By default only a summary of the fuel rod data is printed out to the file **OUTPUT**. If **N6 (IFRM) < 0** the detailed fuel rod data is saved to file **RODDATA** (binary file).

(6) [

]

(7) [

]

(8) **N5 (NCHF) = 6,7 and 11**: The characteristic diameter is the actual subchannel hydraulic diameter (see card G4a-1 (→ p.E-15) resp. G4b-3 (→ p.E-18)). Caution: In some cases, this can lead to unrealistic DNB ratios (too high for guide tube subchannels, too low for enlarged subchannels). If the characteristic diameter should be different (e.g. hydraulic diameter of matrix channel for all subchannels even for guide tube, edge and corner channels) please use **N5 (NCHF) = 12** (see above, cf. card G8-1c (→ p.E-42)).

(9) **N5 (NCHF) = 9**: The structure of the [] correlation is defined on card G8-1k (→ p.E-48).

(10) **N5 (NCHF) = 50, 55 to 64**: can be used only if the heat flux is defined via table, i.e. if **N1 > 1** on card GCC3 (→ p.E-12) and no transient calculation using fuel rod model is performed.

E.9.2 GCC8-cont: Group control continuation card for card group 8

This card is required if **N7 > 0** on card GCC8 (→ p.E-35).

Read: **N8, N9, N10**

Format (315)

read from subroutine **INDAT**.

| | | | |
|----|---|---|-----------|
| N8 | = | 0 | Not used. |
|----|---|---|-----------|

| | | | |
|-----|---|---|--|
| | > | 0 | If CHF performance factors are input on card G8-1-1 (\rightarrow p.E-38). The CHF performance factors are 1.0 by default. |
| N9 | = | 0 | Not used. |
| | > | 0 | If rod-wise CHF correlations are specified on card G8-1-2 (\rightarrow p.E-39). |
| N10 | = | 0 | Not used. |
| | > | 0 | If node-wise CHF correlations are specified on card G8-1-3 (\rightarrow p.E-39). |

Note: (1) If **N5 > 0** on card GCC8 (\rightarrow p. E-35) and **N9 > 0** or **N10 > 0** a multiple input of cards for different CHF correlations is possible. In this case G8-1aa (\rightarrow p.E-41) is needed.

E.9.3 G8-1: Rod layout data

This card is required if **N1 > 0** on card GCC8 (\rightarrow p. E-35).

Read: **N, I, DR, RADIA, (LR(L), PHI(L), L = 1, 6)**
 Format (**I1, I4, 2E5.2, 6(I5,E5.2)**)
 read from subroutine **INDAT**.

| | | |
|-------|---|---|
| N | = | Rod type: |
| | = | 1 Rod fuel. |
| | = | 2 Plate fuel. |
| I | = | Rod number. |
| DR | = | Rod diameter (cm). |
| RADIA | = | Relative rod power (Rod power/average rod power). |
| LR | = | Channel number. |
| PHI | = | Fraction of rod power going to the above channel. |

Note: (1) Up to 6 sets of channel number and fraction of rod power going to that channel may be specified for each rod. The sum of the fractional rod powers need not sum up to 1.0 because of the gamma heating.

(2) For plate fuel, the rod diameter is the plate thickness and the fraction of power to a channel is the fraction of the circumference required to specify the plate width facing the channel.

(3) **RADIA** must be greater than 0.

E.9.4 G8-1-1: Performance factors for CHF correlations

This card is required if **N8 > 0** on card GCC8-cont (\rightarrow p.E-37).

Read: **I_CHF, CHF_PERF(I_CHF)**
 Format (**I6, F10.3**)
 read from subroutine **INDAT**.

| | | |
|----------|---|--|
| I_CHF | = | CHF correlation indicator. |
| CHF_PERF | = | Performance factor for CHF correlation with indicator I_CHF (= multiplier for the critical heat flux). |

Note: (1) This card is read until a zero line (i.e. "0 0 0") is encountered.

(2) For each CHF correlation a performance factor can be specified. [] with $N5(NCHF) = 12$ on card GCC8 (\rightarrow p. E-37) are specified as [] on card G8-1c (\rightarrow p.E-42).

E.9.5 G8-1-2: Rod-wise CHF correlations

This card is required if $N9 > 0$ on card GCC8-cont (\rightarrow p. E-37).

Read: **IR_N1**, **IR_N2**, **NCHFREF**
Format (316)
read from subroutine **INDAT**.

IR_N1 = First rod number with CHF correlation number **NCHFREF**.
IR_N2 = Last rod number with CHF correlation number **NCHFREF**.
NCHFREF = CHF correlation indicator for all rods with numbers between **IR_N1** and **IR_N2**.

Note: (1) This card is read until a zero line (i.e. "0 0 0") is encountered.

(2) The number of definitions is limited to [].

(3) This definition is needed for all rods.

(4) Multiple and overlapping definitions are allowed. The last definition wins.

(5) The definitions are saved for stacked cases.

(6) $NCHFREF = 12$ is specified as [] on card G8-1c (\rightarrow p.E-42).

E.9.6 G8-1-3: Definition of rod-types containing axial regions with different CHF correlations

This card and card G8-1-4 (\rightarrow p.E-40) are required if $N10 > 0$ on card GCC8-cont (\rightarrow p. E-37). Card G8-1-5 (\rightarrow p.E-40) is also needed.

Read: **CHF_AX_TYPE**, **AX_REGIONS**
Format (212)
read from subroutine **INDAT**.

CHF_AX_TYPE = Axial CHF rod-type number.
AX_REGIONS = Number of axial regions with different CHF correlations for type **CHF_AX_TYPE**.

Note: (1) The set of cards G8-1-3 (\rightarrow p.E-39) and G8-1-4 (\rightarrow p.E-40) is closed by a zero line (i.e. "0 0" for **CHF_AX_TYPE**, **AX_REGIONS**). At least this zero line is needed in order to apply this option for stacked cases.

(2) **CHF_AX_TYPE** is limited to [].

E.9.7 G8-1-4: Axial node-wise regions for CHF correlations

This card is required if $N10 > 0$ on card GCC8-cont (\rightarrow p. E-37) and for each axial CHF rod-type number $CHF_AX_TYPE > 0$ on card G8-1-3 (\rightarrow p.E-39).

Read: $X1_CHF_AX_TYPE(I)$, $X2_CHF_AX_TYPE(I)$, $I_CHF(I)$, $I = 1$, $AX_REGIONS$
 Format (2F10.5,I6)
 read from subroutine **INDAT**.

$X1_CHF_AX_TYPE=$ Begin of region **I** in terms of relative axial position (**X/L**).
 $X2_CHF_AX_TYPE=$ End of region **I** in terms of relative axial position (**X/L**).
 I_CHF = Number of CHF correlation for region **I**.

Note: (1) $X1_CHF_AX_TYPE = 0.0$ must be present.

(2) $X2_CHF_AX_TYPE = 1.0$ must be present.

(3) $I_CHF = 12$ is specified as [] on card G8-1c (\rightarrow p.E-42).

E.9.8 G8-1-5: Assignment of axial CHF rod-types to individual rods

This card is required if $N10 > 0$ on card GCC8-cont (\rightarrow p. E-37).

Read: IT_N1 , IT_N2 , $NCHFTYPE$
 Format (3I6)
 read from subroutine **INDAT**.

IT_N1 = First rod number with CHF axial type number **NCHFTYPE**.
 IT_N2 = Last rod number with CHF axial type number **NCHFTYPE**.
 $NCHFTYPE$ = Axial type number.

Note: (1) This card is read until a zero line (i.e. "0 0 0" for IT_N1 , IT_N2 , $NCHFTYPE$) is encountered. At least this zero line is needed.

(2) All rods which are not defined in this way, obtain the CHF correlation as defined by **N5** of GCC8 (\rightarrow p. E-37).

(3) Multiple and overlapping definitions are allowed. The last definition wins.

(4) The definitions are saved for stacked cases.

(5) The number of definitions is limited to [].

TDC = If **N5 = 8..10** or **I_CHF = 8..10** : Begin of heated length (fraction of total length).
 Thermal diffusion coefficient for spacer factor (used only in CHF evaluation).
 if **ISPACE = 0** : Not used.
 if **ISPACE = 1,2** : Value according to literature for the different spacer types.

E.9.11 G8-1b: CHF correlation input

This card is required if **N5 = 8..10** on card GCC8 (→ p.E-35) or **I_CHF = 8..10** on card G8-1aa (→ p.E-41).

Read: **NMGRID**, (**MGRID(I)**, **I = 1, NMGRID**)
 Format (10I5)
 read from subroutine **INDAT**.

NMGRID = Number of mixing grids.
 MGRID = Enumerate in ascending order which of the **N2** spacers (see card GCC7 (→ p.E-31)) are mixing grids.

Note: (1) **NMGRID** values required.

E.9.12 G8-1c: CHF correlation input: selection of CHF correlation

This card is required if **N5 = 12** on card GCC8 (→ p. E-35) or **I_CHF = 12** on card G8-1aa (→ p.E-41).

Read: **IRGW**
 Format (I5)
 read from subroutine **INDAT**.

IRGW = Select correlation as follows (CHF correlations and CHF look-up tables, []

| | | |
|---|----|---|
| = | 1 | [|
| = | 2 | |
| = | 12 | |
| = | 3 | |
| = | 13 | |
| = | 4 |] |
| = | 14 | |
| = | 5 | |

= 6
 = 7
 = 16
 = 17
 = 18
 = 19
 = 8
 = 9
 = 10
 = 15
 = 20
 = 11

Note: (1) Additional information on card G8-1c-1 (→ p.E-43) required to choose correction factors for axial heat flux profile, spacer grids, and cold wall effects.

(2) If IRGw < 0: Additional information of hottest subchannel is required (cf. card G8-1c-2 (→ p.E-44)).

E.9.13 G8-1c-1: CHF correlation input: non-linear profile, spacer grid and cold-wall factor

This card is required if N5 = 12 on card GCC8 (→ p. E-35) or I_CHF = 12 on card G8-1aa (→ p.E-41).

*Read: NNonF12, NSPf12, NCWf12
 Format (3I10)
 read from subroutine INDAT.*

NNonF12 = Select Non-uniform heat flux profile correction correlations:

| | | |
|---------|---|---|
| AoneSC | = | Hot-channel flow area (mm ²). |
| PwoneSC | = | Hot-channel wetted perimeter (mm). |
| PoneSC | = | Hot-channel heated perimeter (mm). |
| TrSC | = | Ratio of maximum to average radial heat-flux factor of rods around the hot-channel. |

E.9.15 G8-1d: CHF correlation input: selection of characteristic diameter

This card is required if **N5 = 12** on card GCC8 (→ p. E-35) or **I_CHF = 12** on card G8-1aa (→ p.E-41) and if **IRGW** (→ p. E-42) (on G8-1c (→ p.E-42)) = **1, 8, 9, 10, 11, 15, 19 or 20**.

Read: If **IRGW** (→ p. E-42) = **1**: **IDMR (1) , IDMR (2) , IDMR (3)**
Format **(3I10)**
read from subroutine **INDAT**.

If **IRGW** (→ p. E-42) = **8-11,15,19,20**: **IDMR (1)**
Format **(I10)**
read from subroutine **INDAT**.

| | | |
|-------------------------|---|---|
| IDMR (1 . . . 3) | = | Specifies characteristic diameters for CHF-correlation and look-up table application: |
| | = | 1 Use input value(s) on card G8-1d-1 (→ p.E-45) as characteristic diameters. |
| | = | 0 Use equivalent diameter based on wetted perimeter. |
| | < | 0 Use equivalent diameter based on heated perimeter. |

E.9.16 G8-1d-1: CHF correlation input:input of characteristic diameter

This card is required if **N5 = 12** on card GCC8 (→ p. E-35) or **I_CHF = 12** on card G8-1aa (→ p.E-41), if **IDmr(1...3)** (→ p.E-45) = **1** (respectively, cf. Card G8-1d (→ p.E-45)) and if **IRGW** (→ p. E-42) (on G8-1c (→ p.E-42)) = **1, 8, 9, 10, 11, 15, 19 or 20**.

Read: If **IRGW** (→ p. E-42) = **1**: **DCHAR (1) , DCHAR (2) , DCHAR (3)**
Format **(3F10.5)**
read from subroutine **INDAT**.

If **IRGW** (→ p. E-42) = **8-11,15,19,20**: **DCHAR (1)**
Format **(F10.5)**
read from subroutine **INDAT**.

| | | |
|------------------------|---|---|
| DCHAR (1 . . 3) | = | Characteristic diameter(s) (mm) for each of the three boiling regimes [] IRGW (→ p. E-42) = 1) resp. DCHAR(1) if [] one of the [] or the W3 CHF correlation is selected (IRGW (→ p. E-42) = 8, 9, 10, 11, 15, 19 or 20). |
|------------------------|---|---|

E.9.17 G8-1e-1: CHF correlation input: grid factor for []-correlation

This card is required if **N5 = 12** on card **GCC8** (→ p. E-35) or **I_CHF = 12** on card **G8-1aa** (→ p.E-41) and if **IRGw** (→ p. E-42) (on **G8-1c** (→ p.E-42)) = 17 or 18 []

Read: []
Format (F10.5)
read from subroutine **INDAT**.

[] = Rod bundle factor:
 $F_g = 1$ or defined by user. It depends on grid spacer and sub-channel code. ($F_g = 1$ recommended).

E.9.18 G8-1e-2: CHF correlation input: input for []

This card is required if **N5 = 12** on card **GCC8** (→ p. E-35) or **I_CHF = 12** on card **G8-[]**

Read: If **NSPf12** (→ p. E-43) = 1 or 2 (cf. **G8-1c-1** (→ p.E-43)): **TDCW3**, **KSGrid**, **fDNBRW**
Format (3F10.5)
read from subroutine **INDAT**.

If **NSPf12** (→ p. E-43) = 3 (cf. **G8-1c-1** (→ p.E-43)): **TDCW3**
Format (F10.5)
read from subroutine **INDAT**.

TDCW3 = Thermal Diffusion Coefficient (TDC)
KSGrid = Axial grid spacing coefficient (K_s) depending on axial grid spacing
fDNBRW = DNBR correction multiplier (f_{DNBR})

E.9.19 G8-1g: [] Correlation Geometry Parameters

This card is required if **N5 = 13, 23, 33** on card **GCC8** (→ p. E-43) or **I_CHF = 13, 23, 33** on card **G8-1aa** (→ p.E-41).

Read: **DHHYD**, **HLEN**
Format (8F10.5)
read from subroutine **INDAT**.

DHHYD = Lattice hydraulic diameter (cm).
HLEN = Fuel bundle heated length (cm).

Note: (1) **HLEN** is not used if **N5 = 13 or 33** on card **GCC8** (→ p. E-43) or **I_CHF = 13 or 33** on card **G8-1aa** (→ p.E-41).

E.9.20 G8-1h: Grid Heights

This card is required if **N5 = 13, 15, 16, 23 or 33** on card GCC8 (→ p. E-43) or **I_CHF = 13, 15, 16, 23 or 33** on card G8-1aa (→ p.E-41).

Read: **GRIDHT (I), I = 1, NGRIDT**
Format (8F10.5)
read from subroutine **INDAT**.

GRIDHT = Grid heights (in cm) of grid types according to **NGRIDT** on card GCC7 (→ p.E-31) (**NGRIDT** values).

Note: (1) This card is not used if **N5 = 13 or 33** on card GCC8 (→ p. E-43) or **I_CHF = 13 or 33** on card G8-1aa (→ p.E-41).

E.9.21 G8-1i: Mixing Grid Specification

This card is required if **N5 = 13, 15, 16, 17, 23 or 33** on card GCC8 (→ p.E-35) or **I_CHF = 13, 15, 16, 17, 23 or 33** on card G8-1aa (→ p.E-41).

Read: **NMGRID, (MGRID(I), I = 1, NMGRID)**
Format (10I5)
read from subroutine **INDAT**.

NMGRID = Number of mixing grids.

MGRID = Enumerate in ascending order which of the **N2** spacers (see card GCC7 (→ p.E-31)) are mixing grids.

Note: (1) **NMGRID** values required.

(2) Format of this card is identical to card type G8-1b (→ p.E-42).

E.9.22 G8-1j: XNB Correlation Input

This card is required if **N5 = 14** on card GCC8 (→ p. E-35) or **I_CHF = 14** on card G8-1aa (→ p.E-41).

Read: **SPITCH, XKLOSS, BLEN**
Format (8F10.5)
read from subroutine **INDAT**.

SPITCH = Grid spacing (cm).

XKLOSS = Ratio of grid pressure loss coefficients (vaned/unvaned).

BLEN = Fuel bundle heated length (cm).

Note: (1) The nonuniform heat flux factor is always taken into account unless **N1 (NAX) = 2** is inputted on card GCC3 (→ p.E-12).

E.9.23 G8-1k: []

This card is required if N5 = 9 on card GCC8 (→ p. E-35) or I_CHF = 9 on card G8-1aa (→ p.E-41).

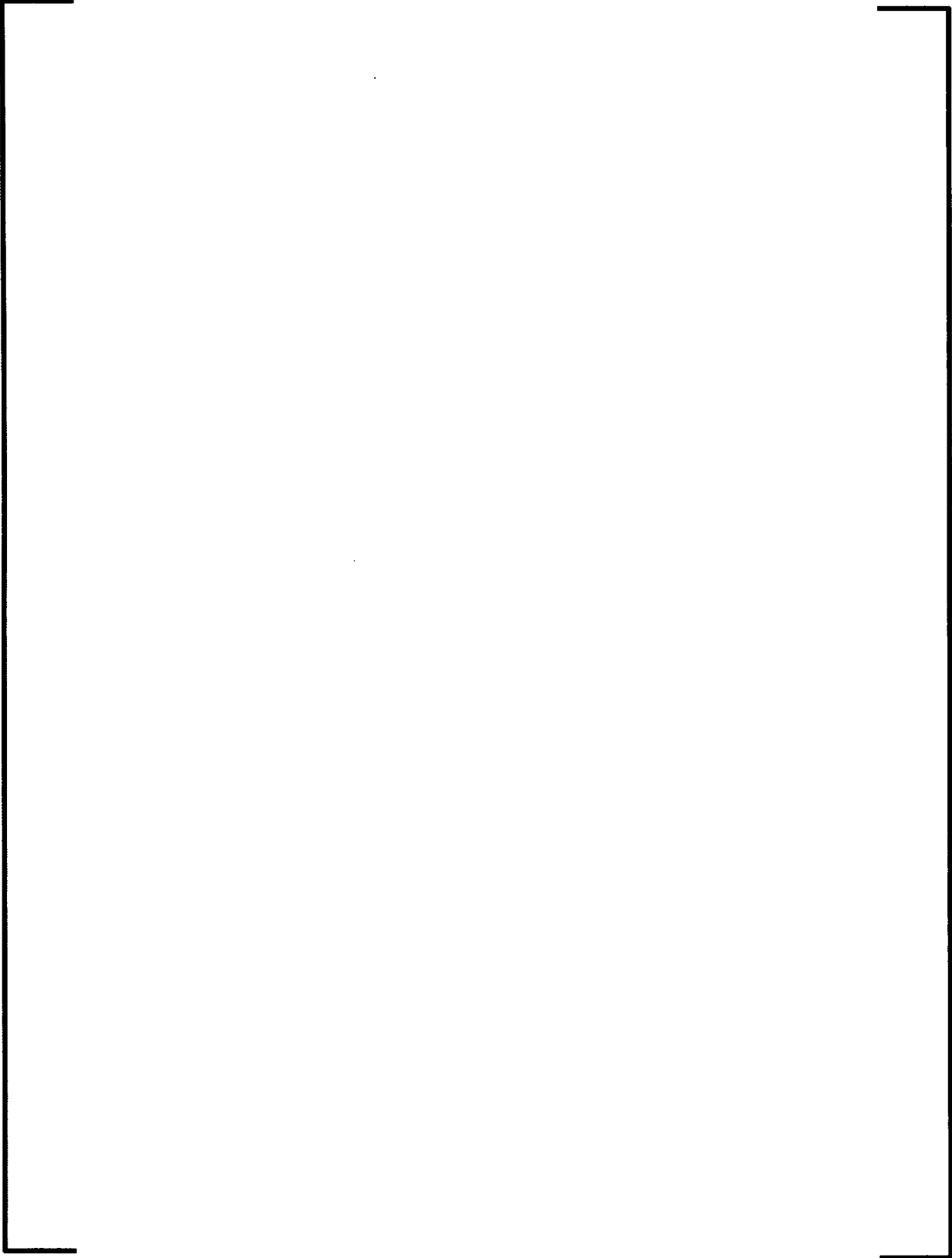
Read: []

Format (A4)

read from subroutine INDAT.

[] = Abbreviation of the [] correlation name (max. 4 characters).

Note: (1) The [] correlation has the following form being equivalent to the [] type of correlation:



[]

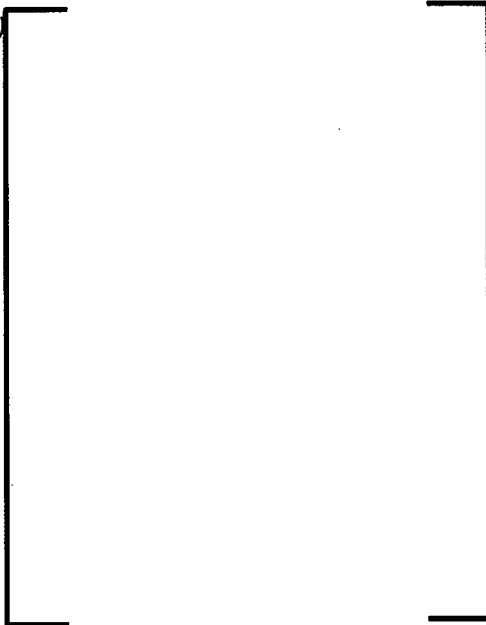
E.9.24 G8-1l: []

This card is required if **N5 = 9** on card GCC8 (→ p.E-35) or **I_CHF = 9** on card G8-1aa (→ p.E-41).

Read: [] (i), i=1,17
 Format (5F10.5)
 read from subroutine **INDAT**.

[]

Note: (1)



E.9.25 G8-1m: CHF correlation limits and debug options

This card is required if **N5 = 50, 55, 63** on card GCC8 (→ p. E-35) or **I_CHF = 50, 55, 63** on card G8-1aa (→ p.E-41).

Read: **CHF_LIMIT, USDPRN**
 Format (2I5)
 read from subroutine **INDAT**.

- CHF_LIMIT = 0 The default correlation limits are used. Currently, no alternative option is available (see note 1).
- USDPRN = 0 No debug printout for this CHF correlation.
- USDPRN = 1 Debug printout for this CHF correlation (see note 2).

Note: (1) Violation of the pressure, mass velocity, or quality limits will result in a file **CHFxx_WARNING** (xx is the correlation number) being created and populated for the cases where the limits are violated.

This output information is unverified and should not be relied upon for this release of the code.

- (2) If **USDPRN = 1** debug information applicable to the CHF correlation of interest is written to the file **CHFxx_DEBUG (xx is the correlation number)** for the channels specified on card **G8-1r** (\rightarrow p.E-52). The data is stored in the correlation native units.

E.9.26 G8-1n: CHF correlation limits and debug options

This card is required if **N5 = 51, 52, 54, 56 to 62** on card **GCC8** (\rightarrow p. E-35) or **I_CHF = 51, 52, 54, 56 to 62** on card **G8-1aa** (\rightarrow p.E-41).

Read: **HLEN, CHF_LIMIT, USDPRN**

Format (**F10.5,2I5**)

read from subroutine **INDAT**.

| | | | |
|-----------|---|---|--|
| HLEN | = | | Fuel bundle heated length (cm). |
| CHF_LIMIT | = | 0 | The default correlation limits are used. Currently, no alternative option is available (see note 1). |
| USDPRN | = | 0 | No debug printout for this CHF correlation. |
| | = | 1 | Debug printout for this CHF correlation (see note 2). |

Note: (1) Violation of the pressure, mass velocity, or quality limits will result in a file **CHFxx_WARNING (xx is the correlation number)** being created and populated for the cases where the limits are violated.
This output information is unverified and should not be relied upon for this release of the code.

- (2) If **USDPRN = 1** debug information applicable to the CHF correlation of interest is written to the file **CHFxx_DEBUG (xx is the correlation number)** for the channels specified on card **G8-1r** (\rightarrow p.E-52). The data is stored in the correlation native units.

E.9.27 G8-1o: CHF correlation limits and debug options

This card is required if **N5 = 53 or 64** on card **GCC8** (\rightarrow p. E-35) or **I_CHF = 53 or 64** on card **G8-1aa** (\rightarrow p.E-41).

Read: **HLEN, PPITCH, DDR, CHF_LIMIT, USDPRN**

Format (**3F10.5,2I5**)

read from subroutine **INDAT**.

| | | | |
|-----------|---|---|--|
| HLEN | = | | Fuel bundle heated length (cm). |
| PPITCH | = | | Unit cell pin pitch (cm). |
| DDR | = | | Outer rod diameter of a unit cell (cm). |
| CHF_LIMIT | = | 0 | The default correlation limits are used. Currently, no alternative option is available (see note 1). |
| USDPRN | = | 0 | No debug printout for this CHF correlation. |
| | = | 1 | Debug printout for this CHF correlation (see note 2). |

Note: (1) Violation of the pressure, mass velocity, or quality limits will result in a file **CHFxx_WARNING (xx is the correlation number)** being created and populated for the

cases where the limits are violated.

This output information is unverified and should not be relied upon for this release of the code.

- (2) If **USDPRN = 1** debug information applicable to the CHF correlation of interest is written to the file **CHFxx_DEBUG** (**xx** is the correlation number) for the channels specified on card **G8-1r** (→ p.E-52). The data is stored in the correlation native units.

E.9.28 G8-1p: CHF correlation grid spacing input

This card is required if **N5 = 53, 56 to 62, 64** on card **GCC8** (→ p. E-35) or **I_CHF = 53, 56 to 62, 64** on card **G8-1aa** (→ p.E-41).

Read: **ISGSP**

Format (I5)

read from subroutine **INDAT**.

ISGSP = Number of grid spacing pairs to be read on card **G8-1q** (→ p.E-52)
(max. 50).

E.9.29 G8-1q: CHF correlation grid spacing input

This card is required if **ISGSP > 0** on card **G8-1p** (→ p.E-52).

Read: **SGSPX(I)**, **SGSPS(I)**, **I=1, ISGSP**

Format (2F10.5)

read from subroutine **INDAT**.

SGSPX = Relative axial position (**X/L**).

SGSPS = Grid spacing (cm).

Note: (1) **ISGSP** (card **G8-1p** (→ p.E-52)) data pairs have to be specified.

(2) Data pairs at relative positions **X/L = 0.0** and **X/L = 1.0** must be specified.

(3) The grid spacing between the points given above is found by using linear interpolation.

The user should be extremely careful in choosing the locations he specifies, especially for abrupt changes.

E.9.30 G8-1r: CHF correlation channels for debug printout

This card is required if **USDPRN = 1** on card **G8-1m** (→ p.E-50), **G8-1n** (→ p.E-51) or **G8-1o** (→ p.E-51).

Read: **HCHANS**, **HCHANX**

Format (2I6)

read from subroutine **INDAT**.

HCHANS = An integer that represents the first channel of interest to be printed.

HCHANX = An integer that represents the last channel of interest to be printed.

Note: (1) CHF correlation specific data are printed for all channels numbered from **HCHANS** to **HCHANX**.

E.9.31 G8-2: Fuel thermal properties

This card is required if $N3 > 0$ on card GCC8 (\rightarrow p. E-35).

Read: **KFUEL(I)**, **CFUEL(I)**, **RFUEL(I)**, **DFUEL(I)**, **KCLAD(I)**, **CCLAD(I)**, **RCLAD(I)**,
TCLAD(I), **HGAP(I)**, $I=1, NFUELT$

Format (9E5.2)

read from subroutine **INDAT**.

| | | |
|-------|---|--|
| KFUEL | = | Fuel thermal conductivity (W/(m K)). |
| CFUEL | = | Fuel specific heat (kJ/(kg K)). |
| RFUEL | = | Fuel density (kg/dm ³). |
| DFUEL | = | Fuel pellet diameter (cm) (absolute value). |
| KCLAD | = | Cladding thermal conductivity (W/(m K)). |
| CCLAD | = | Cladding specific heat (kJ/(kg K)). |
| RCLAD | = | Cladding density (kg/dm ³). |
| TCLAD | = | Cladding thickness (cm). |
| HGAP | = | Gap heat transfer coefficient (kJ/(h cm ² K)) (absolute value). |

Note: (1) Nonuniform radial pellet heating input is read on cards G8-2a (\rightarrow p.E-53) and G8-2b (\rightarrow p.E-55) if negative **DFUEL** is input. Variable gap conductance input is triggered by negative values of **HGAP** (see cards G8-2c (\rightarrow p.E-55) and G8-2d (\rightarrow p.E-56)).

E.9.32 G8-2a: Nonuniform radial heating in fuel (number of data pairs)

This card is required if $DFUEL < 0$ on card G8-2 (\rightarrow p.E-53).

Read: **NCFI**

Format (I5)

read from subroutine **INDAT**.

| | | |
|------|---|--|
| NCFI | = | Number of table value pairs to follow on card G8-2b (\rightarrow p.E-55) or number of values to follow on card G8-2b-1 (\rightarrow p.E-55). |
|------|---|--|

Note: (1) Additional options to define the radial power profile are read on card G8-2a-1 (\rightarrow p.E-53) if negative **NCFI** is input.

E.9.33 G8-2a-1: Options for definition of radial power profile

This card is required if $NCFI < 0$ on card G8-2a (\rightarrow p.E-53).

Read: **QC_MODE**, **QC_FAC**

Format (I5, F10.5)

read from subroutine **INDAT**.

| | | | |
|---------|---|---|---|
| QC_MODE | = | 1 | The radial power profile is read from input. |
| | = | 2 | A core average radial power profile is calculated by subroutine qcalc_e3, using the input parameters on card G8-2a-2 (\rightarrow p.E-54). This profile is used for all nodes. |

E.9.35 G8-2b: Nonuniform radial heating in fuel (pellet data)

This card is required if $NCFI > 0$ on card G8-2a (\rightarrow p.E-53) or $NCFI < 0$ on card G8-2a (\rightarrow p.E-53) and $QC_MODE = 1$ on card G8-2a-1 (\rightarrow p.E-53).

Read: **RPPP, QPPPI**
 Format (12E5.0)
 read from subroutine **INDAT**.

RPPP = Relative radial position.
 QPPPI = Relative heat flux factor.

Note: (1) A total of **abs(NCFI)** (see card G8-2a (\rightarrow p.E-53)) data pairs must be specified.
 (2) Data pairs at relative positions $RPPP = 0.0$ and $RPPP = 1.0$ must be specified.
 (3) For $NCFI > 0$, the integrated average over the QPPPI values must be 1.0 (there is no internal normalisation). For $NCFI < 0$ an internal normalisation is performed.

E.9.36 G8-2b-1: Nonuniform radial heating in fuel (pellet radii)

This card is required if $QC_MODE > 1$ on card G8-2a-1 (\rightarrow p.E-53).

Read: **RPPP(I), I = 1, ABS(NCFI)**
 Format (12E5.0)
 read from subroutine **INDAT**.

RPPP = Relative radial positions where power factors shall be calculated.

Note: (1) Relative positions $RPPP = 0.0$ and $RPPP = 1.0$ must be specified.

(2)[

(3) For $QC_MODE = 2$, the calculated power profile values are printed to the interpreted input section of the output file.

]

E.9.37 G8-2c: Number of transient gap conductance data pairs

This card is required if $HGAP < 0$ on card G8-2 (\rightarrow p.E-53).

Read: **nhgap**
 Format (15)
 read from subroutine **INDAT**.

NHGAP = Number of table value pairs to follow on card G8-2d (\rightarrow p.E-56).

| | | |
|------|---|---|
| NCF | = | Number of radial fuel cells (if NCF is negative ABS(NCF) is used and NCF-1 relative radii are read in by following card G8-2f (→ p.E-57)). |
| NCC | = | Number of radial clad cells. |
| THG | = | Gap thickness (cm) (must be greater than 0.0). |
| EPSF | = | Fuel rod temperature convergence criterion; if given as 0 it is set to the default [] Recommended value [] For EPSF < 0.0 see card G8-2e-1. (→ p.E-57) |

Note: (1) **IHTM** different than zero requires renumbering of rod input data (see card G8-1 (→ p.E-38)) to obtain **LR(1,1) = 1** - i.e. the first rod must deliver heat to channel 1.

(2) **NODESF = NCF + NCC + 1** (see card GCC8 (→ p.E-35)) must hold.

(3) **THG** must be non-zero.

(4) **IPROP = n04** is only available when called from PANBOX

(5) **IHTM < 0** assures that no rewetting is possible once post-DNB regime is entered.

E.9.40 G8-2e-1: Iteration of Heat Transfer Coefficient

This card is required if **EPSF < 0.0** on card G8-2e (→ p.E-53).

Read: **ACELF**

Format (F10.2)

read from subroutine **INDAT**.

| | | |
|-------|---|---|
| ACELF | = | Damping factor for iteration of heat transfer coefficient (Default: ACELF = []). |
|-------|---|---|

E.9.41 G8-2f: Fuel rod model (geometry)

This card is required if **NCF < 0** on card G8-2e (→ p. E-53).

Read: **RDread(I), I = 1, NCF-1**

Format (8F10.2)

read from subroutine **INDAT**.

| | | |
|--------|---|---|
| RDread | = | NCF-1 relative radii to divide fuel pellet radially = $(r_i - r_0)/(r_{\text{Pellet}} - r_0)$; for r_0 see card G8-2h (→ p.E-58). |
|--------|---|---|

E.9.42 G8-2g: Fuel rod model (model and data selection)

This card is required if **N6 = 3** or **4** on card GCC8 (→ p.E-35).

Read: **IOldcb, ICorad, IUSca, IUSox, ICAgas, IUScax, IUScra**

Format (7I5)

read from subroutine **INDAT**.

| | | |
|--------|---|---|
| IOldcb | = | 1 For both the modified new model (IFRM=3) and the PANBOX model (IFRM=4) the pellet is radially divided into NCF (see card G8-2e (→ p. E-53)) shells of equal volumes. |
|--------|---|---|

| | | |
|--------|-----|--|
| | | <p>If IFRM = 3 average temperatures between two nodes at r_1 and r_2 are calculated via $T_{av} = (T_1 + T_2)/2$. Heat flux printed out is related to rod diameter DR (see card G8-1 ($\rightarrow p.E-38$)) although coolant heat-up is calculated from real heat flux using calculated fuel rod geometry if appropriate.</p> |
| | = 0 | <p>This option is included only for strict consistency to older COBRA-FLX versions and should not be used for application purposes. For the PANBOX model (IFRM = 2 or 4) the pellet is radially divided into NCF (see card G8-2e ($\rightarrow p.E-56$)) shells of equal volumes. For the new model (IFRM = 1 or 3) the pellet is divided into nodes with equal distances. If IFRM = 1 or 3 average temperatures between two nodes at r_1 and r_2 are calculated via $T_{av} = (T_1 + T_2)/2$. Heat flux printed out is related to rod diameter DR (see card G8-1 ($\rightarrow p.E-38$)). Fuel rod data DFUEL, TCLAD (see card G8-2 ($\rightarrow p.E-53$)) and THG (see card G8-2e ($\rightarrow p.E-56$)) should match DR, otherwise coolant heat-up is not consistent with fuel rod radial temperature distribution and heat sources.</p> |
| ICOrad | = | Correct fuel pellet and cladding diameter by thermal expansion, yes (1) or no (0). Note that use of this option might increase computation time noticeably. |
| IUSca | = | Use CARO fuel rod results read from file CAR-INP ($\rightarrow p.E-62$), yes (1) or no (0). |
| IUSox | = | Correct clad-to-coolant heat transfer for oxide thermal resistance, yes (1) or no (0). |
| ICAgas | = | Calculate fuel-to-clad-gap gas pressure after each time step, yes (1) or no (0). |
| IUScax | = | Use CARO axial heat flux profile, yes (1) or no (0); only for comparison to CARO results. |
| IUScra | = | Use CARO radial heat flux profile, yes (1) or no (0); only for comparison to CARO results. |

E.9.43 G8-2h: Fuel rod model (geometry)

This card is required if **N6 = 2, 3** or **4** on card GCC8 ($\rightarrow p.E-35$).

Read: If **N6 = 2** (on card GCC8 ($\rightarrow p.E-35$)): **R0**

Format (**F10.2**)

read from subroutine **INDAT**.

If **N6 = 3** or **4** (on card GCC8 ($\rightarrow p.E-35$)): **R0**, **H0Pel**, **HDish**, **RDish**, **IDish**, **CPel**,

DPel, **DMKorr**, **DMKorc**, **Oxid**

Format (**4F10.2**, **I5**, **5F10.2**)

read from subroutine **INDAT**.

| | | |
|-------|---|--|
| R0 | = | Pellet center channel radius r_0 (cm). |
| H0Pel | = | Pellet height (cm). |
| HDish | = | Center depth of dishing (cm). |

| | | |
|--------|---|---|
| RDish | = | Dishing radius (cm). |
| IDish | = | 0 No dishing. |
| | = | 1 One-sided dishing only. |
| | = | 2 Both-sided dishing. |
| CPel | = | Width of pellet shoulder (cm). |
| DPel | = | Height of pellet shoulder (cm). |
| DMKorr | = | Non-reversible diametral correction of pellet (cm). |
| DMKorc | = | Non-reversible diametral correction of cladding (cm). |
| Oxid | = | ZrO thickness(cm). |

Note: (1) Usage of dishing (IDish, HDish and RDish > 0) and/or shoulders (CPel and DPel > 0) increases run time considerably because of the iteration of the radial subdivision of the fuel pellet.

E.9.44 G8-2i: Fuel rod model (fuel material data)

This card is required if IPROP > 0 and MATPRO = 0 on card G8-2e (→ p.E-56).

Read: FTD, FPuO2

Format (2F10.2)

read from subroutine INDAT.

| | | |
|-------|---|--|
| FTD | = | Fraction of theoretical density of fuel. |
| FPuO2 | = | PuO ₂ fraction by volume (m ³ /m ³). |

E.9.45 G8-2k: Fuel rod model (fuel material data)

This card is required if IPROP > 0 and MATPRO = 1 on card G8-2e (→ p. E-56).

Read: FTD, FPuO2, O2pmx, Burn, FMolt

Format (5F10.2)

read from subroutine INDAT.

| | | |
|-------|---|---|
| FTD | = | Fraction of theoretical density of fuel. |
| FPuO2 | = | PuO ₂ fraction by volume (m ³ /m ³). |
| O2pmx | = | O/M composition defect of nonstoichiometric fuel (O2pmx = O/M_ratio - 2.0). |
| Burn | = | Average burnup (MWd/kgU). |
| FMolt | = | Fraction of molten fuel in pellet (m ³ /m ³). |

Note: (1) Also in the case of PANBOX (coupled system) calculations with use of nodal burnup values in evaluation of material properties, the input BURN is employed for initialisations. It therefore must have a meaningful value (MWd/kgU).

E.9.46 G8-2i: Fuel rod model (fuel material data)

This card is required if $IPROP > 0$ and $MATPRO = 2$ on card G8-2e (\rightarrow p. E-56).

Read: **FTD**, **FPuO2**, **FGd2O3**, **O2pmx**, **Burn**

Format (5F10.2)

read from subroutine **INDAT**.

| | | |
|---------------|---|---|
| FTD | = | Fraction of theoretical density of fuel. |
| FPuO2 | = | PuO ₂ fraction by volume (m ³ /m ³). |
| FGd2O3 | = | Mass fraction of Gd ₂ O ₃ (kg/kg). |
| O2pmx | = | O/M composition defect of nonstoichiometric fuel (O2pmx = O/M_ratio - 2.0). |
| Burn | = | Average burnup (MWd/kgU). |

Note: [

]

(2) Also in the case of PANBOX (coupled system) calculations with use of nodal burnup values in evaluation of material properties, the input **BURN** is employed for initialisations. It therefore must have a meaningful value (MWd/kgU).

E.9.47 G8-2m: Fuel rod model (gap gas data)

This card is required if $IPROP = 2$ and $MATPRO = 0$ on card G8-2e (\rightarrow p. E-56).

Read: If **ICAgas = 0** (on card G8-2g (\rightarrow p.E-57)): **BURN**, **CPR**, **EXPR**, **FPRESS**, **GRGH**, **GMIX(1)**, **GMIX(2)**, **GMIX(3)**, **GMIX(4)**, **PGAS**

Format (10F10.2)

read from subroutine **INDAT**.

If **ICAgas = 1** (on card G8-2g (\rightarrow p.E-57)): **BURN**, **CPR**, **EXPR**, **FPRESS**, **GRGH**, **GMIX(1)**, **GMIX(2)**, **GMIX(3)**, **GMIX(4)**, **PGAS**, **TGAS**, **VolRst**

Format (12F10.2)

read from subroutine **INDAT**.

| | | |
|---------------|---|---|
| BURN | = | Burnup (MWd/kgU). |
| CPR | = | Coefficient of fuel pressure on clad for gap conductance model. |
| EXPR | = | Exponent for fuel pressure on clad. |
| FPRESS | = | Fuel pressure on clad for gap conductance (bar). |
| GRGH | = | RMS of fuel and clad roughness (cm); set to [] if given as zero. |

| | | |
|----------|---|--|
| GMIX (1) | = | Helium fraction by mole (mol/mol). |
| GMIX (2) | = | Argon fraction by mole (mol/mol). |
| GMIX (3) | = | Krypton fraction by mole (mol/mol). |
| GMIX (4) | = | Xenon fraction by mole (mol/mol). |
| PGAS | = | Pressure of gas mixture in gap (bar). |
| TGAS | = | Temperature of gas mixture in gap (°C). |
| VolRst | = | Volume of fuel rod upper and lower plena (cm ³). |

*Note: (1) Also in the case of PANBOX (coupled system) calculations with use of nodal burnup values in evaluation of material properties, the input **BURN** is employed for initialisations. It therefore must have a meaningful value (MWd/kgU).*

E.9.48 G8-2n: Fuel rod model (gap gas data)

This card is required if **IPROP = 2** and **MATPRO = 1** or **2** on card G8-2e (→ p. E-56).

Read: **BURN, K, GrgH, GrgF, A, GMIX(1), GMIX(2), GMIX(3), GMIX(4), GMIX(5), PGAS, TGAS, VolRst**

Format (13F10.2)

read from subroutine **INDAT**.

| | | |
|----------|---|--|
| BURN | = | Burnup (MWd/kgU). |
| K | = | Weighting factor of clad and fuel roughness. |
| GrgH | = | RMS of clad roughness (cm); set to [] if given as zero. |
| GrgF | = | RMS of fuel roughness (cm); set to [] if given as zero. |
| A | = | Factor for relocation. |
| GMIX (1) | = | Helium fraction by mole (mol/mol). |
| GMIX (2) | = | Argon fraction by mole (mol/mol). |
| GMIX (3) | = | Krypton fraction by mole (mol/mol). |
| GMIX (4) | = | Xenon fraction by mole (mol/mol). |
| GMIX (5) | = | Nitrogen fraction by mole (mol/mol). |
| PGAS | = | Pressure of gas mixture in gap (bar). |
| TGAS | = | Temperature of gas mixture in gap (°C). |
| VolRst | = | Volume of fuel rod upper and lower plena (cm ³). |

*Note: (1) Also in the case of PANBOX (coupled system) calculations with use of nodal burnup values in evaluation of material properties, the input **BURN** is employed for initialisations. It therefore must have a meaningful value (MWd/kgU).*

E.9.49 G8-2n-1: Fuel rod model (heat transfer coefficient)

These cards are required if *IPROP = n04* on card G8-2e (→ p. E-56)

Read: *nbup, nlhr*
 Format (2I5)
 read from subroutine *INDAT*.

nbup = number of burnup table values
nlhr = number of linear heat rate table values

Read: (*hgbup(i), i=1, nbup*)
 Format (10F10.2)
 read from subroutine *INDAT*.

hgbup = burnup table values defining rectangular grid for heat transfer coefficient values (must be ascending) [MWd/kgU]

Read: (*hglhr(i), i=1, nlhr*)
 Format (10F10.2)
 read from subroutine *INDAT*.

hglhr = linear heat rate table values defining rectangular grid for heat transfer coefficient values (must be ascending) [W/cm]

Read: (*hgt(i, j), i=1, nbup, j=1, nlhr*)
 Format (10F10.2)
 read from subroutine *INDAT*.

hgt = gap heat transfer values [kW/m²/K]

E.9.50 G8-2o: Fuel rod model (heat transfer coefficient)

This card is required if *IHTCC = 1* on card G8-2e (→ p. E-56)

Read: *CHTcc*
 Format (F10.2)
 read from subroutine *INDAT*.

CHTcc = parameter to modify the heat transfer coefficient (HTC) calculated according to the CARO model:
 $HTC_{effective} = (1.0 + CHTcc) * HTC_{CARO}$

E.9.51 CAR_INP: Fuel rod data from file CAR_INP{.KASE}

This file is required if fuel rod material property data and geometry should be corrected by local results from a detailed fuel rod thermal-mechanical response evaluation model (e.g. Code CARO-E, RODEX, etc.). At least *UISca = 1* (see card G8-2g (→ p. E-57)) required.

a. Identification of run for CAR_INP-file generation (lines #2-3):

C 6186P11442 06/12/95 15:02:44 nhp45 9000/715 A A.09.01 gid=608 u=bethke
 C CAR_LOC 1.00: Copyright (C) Siemens AG 1995 Mon Jun 12 15:02:30 MESZ 1995

b. File identification from CARO-LOCA Interface (lines #7-8):

```
C CARO-E1.8 ( STAND : 07/02/95 )
nhp48 54B0 07/04/95 10:10:03 HP-715
C *KKP-2 *ND *LG2 **BE 16 *UO2*neuer BS*neue GEO*Duplx *KKP-2,UO2,
100d
```

c. File identification from CARO-Result (lines #12-13):

```
C CARO-E1.8 ( STAND : 07/02/95 )
nhp48 0A1B 11/04/95 10:40:10 HP-715
C *KKP-2 *ND *LG2 **BE 16 *UO2*neuer BS*neue GEO*Duplx *KKP-2,UO2
```

d. Fuel rod thermal-mechanical response results (starting from line #14):**1. Rec. (Format (5F10.5):**

Mole fractions $[\text{mol/mol}]$ of Helium, Argon, Krypton, Xenon and Nitrogen.

2. Rec. (Format (8F10.5):

Volumes of lower plenum, upper plenum, annulus, cracks, dishings, center channel, porosity $[\text{mm}^3]$ and gap gas pressure $[\text{bar}]$.

3. Rec. (Format (2I5, 4F10.5):

Number of axial nodes, number of radial nodes, heated length of fuel-rod thermal-mechanical response evaluation model calculation $[\text{m}]$, rod outer diameter $[\text{mm}]$, pellet outer diameter $[\text{mm}]$ and dishing-radius $[\text{mm}]$.

4. Rec. (Format (12F10.5):

For each axial node (cf. 3. Rec.):

Diameter-correction pellet and cladding $[\%]$ related to the average cladding diameter (irreversible deformation), pellet center channel radius $[\text{mm}]$, linear power rate $[\text{W/cm}]$, burnup $[\text{MWd/KgU}]$, gap heat transfer coefficient $[\text{kW}/(\text{K m}^2)]$, average cladding temperature $[\text{°C}]$ and thickness of oxide $[\mu\text{m}]$.

For each radial node (cf. 3. Rec.):

Relative inner radius of radial nodes $= (r_i - r_{\text{center}})/(r_{\text{Pellet}} - r_{\text{center}}) [-]$, fuel pellet porosity $[-]$, deficit of density $[-]$, local burnup $[\text{MWd/KgU}]$, power per volume $[\text{W}/\text{mm}^3]$ and radial temperature $[\text{°C}]$.

5. Rec. (Format (12F10.5):

For each axial node (cf. 3. Rec.):

Number of temperature table nodes, table of average fuel rod temperatures $[\text{°C}]$ and gap heat transfer coefficients $[\text{kW}/(\text{K m}^2)]$.

Note: (1) Optionally filename extension **{.KASE}** can be used to identify one data file for each run identified by identification-number **KASE** (see card I3 (→ p.E-7)); if no file **CAR_INP{.KASE}** exists the general file **CAR_INP** is used.

(2) If neither **CAR_INP{.KASE}** nor **CAR_INP** exists in the current working directory **IUSca** (see card G8-2g (→ p.E-57)) is set to zero and fuel rod average values from cards G8-2h (→ p.E-58), G8-2i (→ p.E-59), G8-2k (→ p.E-59), G8-2l (→ p.E-60), G8-2m (→ p.E-60) and G8-2n (→ p.E-61) are used.

E.10 Card Group 9
Calculation variables

| | |
|---|------|
| GCC9: Group control card for card group 9 | E-64 |
| G9-1: Calculation variables | E-65 |
| G9-1a: Reference distance | E-67 |
| G9-2: Axial node input | E-67 |
| G9-3: Axial node input | E-67 |
| G9-4: Axial node input | E-68 |
| G9-5: PV-Solution Variables | E-68 |
| G9-6: PV-Solution Variables | E-68 |
| G9-7: PV-Solution Variables | E-69 |
| G9-8: PV-Solution Variables | E-69 |
| G9-9: PV-Solution Variables | E-70 |

E.10.1 GCC9: Group control card for card group 9

This card is required whenever card group 9 is used.

Read: **NGROUP, N1, N2, N3, N4, N5, N6, N7**
Format (515)
read from subroutine **INDAT**.

| | | | |
|--------------------|---|----|--|
| NGROUP | = | 9 | Select card group 9. |
| N1 (NSKIPX) | = | | Axial printing increment. |
| | = | 1 | Every step printed. |
| | = | 2 | Every other step printed. |
| | = | n | Every n 'th step printed. |
| N2 (NSKIPT) | = | | Time step printing increment. (Same function as N1 above, except that it is used to select the time step printouts by N2). |
| | < | 0 | Printout of bundle average results and channel exit data to file OUTPUT and bundle average inlet and exit temperatures to file DNBDATA (increases run time). |
| N3 (KDEBUG) | = | | Debug print option. |
| | = | 0 | No debugging information is printed. |
| | = | 1 | A very lengthy debugging printout is provided for each time step of the calculation. |
| | = | -1 | Print the iteration summary when called by the PANBOX code. |

| | | | |
|-------------|---|----|--|
| | = | -2 | Print CPU time of preselected subroutines to screen and output. [] |
| N4 (KAXIAL) | = | | Axial node input. |
| | = | 0 | NDX (→ p.E-65) nodes of equal length |
| | > | 0 | Read in axial nodes (see G9-2 (→ p.E-67), G9-3 (→ p.E-67) and G9-4 (→ p.E-68)). This option is not available for PANBOX calculations. |
| | < | 0 | Use the axial division from PANBOX neutronics. NDX (→ p. E-65) must be greater than or equal to the number of axial nodes in neutronics! |
| N5 | = | | Not used. |
| N6 | = | | Not used. |
| N7 | = | | Not used. |

Note: (1) If N1 or N2 are given as zero or blank, the code resets them to 1.

(2) The debug option can generate a lot of paper and take a lot of time printing. Therefore it is recommended to use the debug option only when necessary.

(3) See card 44-00 (→ p.E-131) of the card group 20 input method (→ p.E-87) for additional details.

E.10.2 G9-1: Calculation variables

This card is required whenever card group 9 is used.

Read: KIJ, FTM, Z, THETA, NDX, NDT, TTIME, NTRIES, FERROR, SL, WERROR, EPSOR, ACCELF, ACCELSF

Format (4E5.2, 2I5, E5.2, I5, 6E5.2)

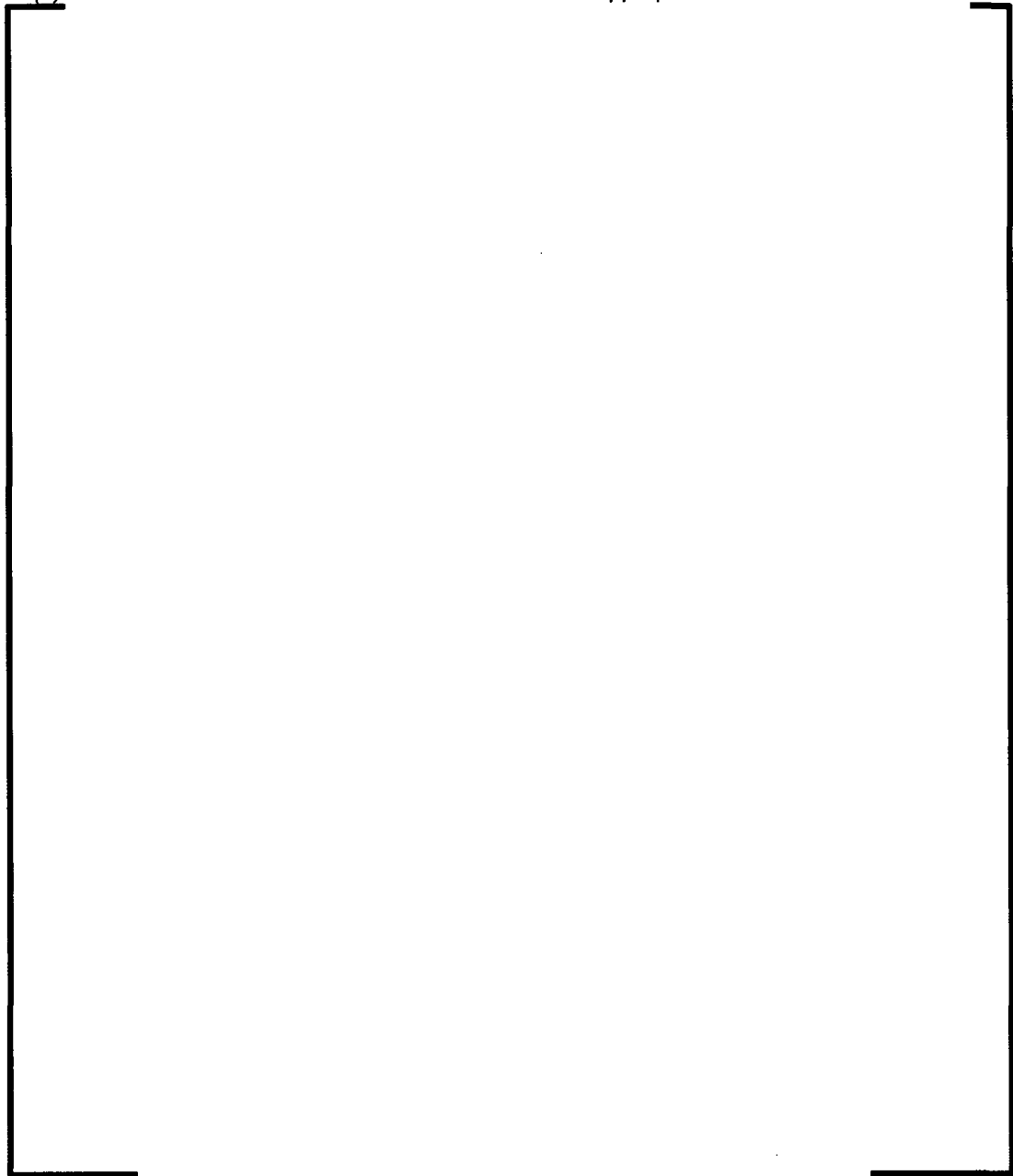
read from subroutine INDAT.

| | | |
|--------|---|---|
| KIJ | = | Diversion crossflow resistance factor (see Note (7) below). |
| FTM | = | Turbulent momentum factor. |
| Z | = | Bundle length (cm). |
| THETA | = | Position from vertical (degrees). |
| NDX | = | Number of axial nodes. |
| NDT | = | Number of time steps. |
| TTIME | = | Total transient time (sec). |
| NTRIES | = | Maximum number of iterations. |
| FERROR | = | Allowable fraction error in flow form convergence. |
| SL | = | Transverse momentum parameter S/L (see Note (7) below). |
| WERROR | = | Crossflow convergence criterion. |

| | | |
|---------|---|---|
| EPSOR | = | Pressure convergence limit for SOR -method; if ISOLVE (\rightarrow p.E-6) \leq 3, EPSOR is not used. |
| ACCELF | = | Damping factor for axial flow. |
| ACCELSP | = | Damping factor for lateral difference pressure. |

Note: (1) Default values are: **NTRIES** = [], **FERROR** = [], **WERROR** = [], **EPSOR** = [], **ACCELF** = [], **ACCELSP** = []

(2) The default values for the calculation variables are appropriate for most cases.



(7) Internal lateral scaling according to US NRC requirements (this option is only applicable with $N3 = 0$ on GCC4a (\rightarrow p.E-15):

For $KIJ < 0$, the crossflow resistance is proportional to the number of rod rows between channel centroids, i.e. $abs(KIJ)$ is multiplied by an internally calculated local factor of $DIST/LREF_KIJ$ (cf. cards G4a-1 (\rightarrow p.E-15) and G9-1a (\rightarrow p.E-67))

For $SL < 0$, the transverse momentum parameter is internally calculated based on local geometry.

E.10.3 G9-1a: Reference distance

This card is required if $KIJ < 0$ on card G9-1 (\rightarrow p.E-65).

Read: **LREF_KIJ**

Format (E10.5)

read from subroutine **INDAT**.

LREF_KIJ = Reference distance (cm) to be used for internal lateral scaling of the diversion crossflow resistance factor **KIJ**.
Reference distance is usually the centroid distance between two fuel rods (rod pitch).

E.10.4 G9-2: Axial node input

This card is required if $N4 = 1$ on card GCC9 (\rightarrow p.E-64).

Read: **X(I,5)**, $I = 2, NDX+1$

Format (10F5.5)

read from subroutine **INDAT**.

X = Relative positions of axial node boundaries.

Note: (1) Input **NDX** (see card G9-1 (\rightarrow p.E-65)) values, last value must be **1.0**; bottom boundary is internally set to zero.

E.10.5 G9-3: Axial node input

This card is required if $N4 = 2$ on card GCC9 (\rightarrow p. E-64).

Read: **X(I,5)**, $I = 2, NDX+1$

Format (10F5.5)

read from subroutine **INDAT**.

X = Positions of axial node boundaries (cm).

Note: (1) Input **NDX** values, bundle length **Z** (see card G9-1 (\rightarrow p.E-65)) will be set equal to $X((NDX + 1),5)$; bottom boundary is internally set to zero.

E.10.6 G9-4: Axial node input

This card is required if **N4 = 3** on card **GCC9** (\rightarrow p. E-64).

Read: **X(I,5)**, **I = 2, NDX+1**

Format (**10F5.5**)

read from subroutine **INDAT**.

X = Axial node lengths (cm).

Note: (1) Input **NDX** values, bundle length **Z** (see card **G9-1** (\rightarrow p.E-65)) will be set equal to sum of node lengths.

E.10.7 G9-5: PV-Solution Variables

This card is required if **ISOLVE = 3** on card **I2** (\rightarrow p.E-6).

Read: **NSSS**, **DTSS**

Format (**15,E10.0**)

read from subroutine **INDAT**.

NSSS = Number of time steps of **DTSS** for reaching a steady-state solution. **NSSS = 1** is a normal choice. **NSSS > 1** can be used to run a pseudo transient of **NSSS** steps to achieve steady-state. A reduced time step **DTSS** would be provided in that case. (Default = 1).

DTSS = Time step used to achieve steady state. []

Note: (1) Convergence for low flow cases can be difficult and a reduced time step is an option to achieve convergence. Time steps on the order of the Courant step can be used to advantage and a suitable number of time steps would be needed to achieve steady-state. Damping may also be needed (**ACCELX < 1.0** on card **G9-8** (\rightarrow p.E-69), **ACCELY < 1.0** on card **G9-8** (\rightarrow p.E-69), **DAMPER < 1.0** on card **G9-9** (\rightarrow p.E-70)) especially if the time steps are larger than the Courant time step.

E.10.8 G9-6: PV-Solution Variables

This card is required if **ISOLVE = 3** on card **I2** (\rightarrow p.E-6).

Read: **ITMNSS**, **ITMINT**

Format (**2I5**)

read from subroutine **INDAT**.

ITMNSS = Minimum number of outer iterations used to achieve steady-state for each steady-state time step. The outer iteration will go at least **ITMNSS** iterations per time step []

ITMINT = Minimum number of outer iterations used to achieve a solution at each transient time step. The outer iteration will go at least **ITMINT** iterations per time step []

E.10.9 G9-7: PV-Solution Variables

This card is required if **ISOLVE = 3** on card I2 (→ p. E-6).

Read: **MAXINR**, **IREBAL**, **MERROR**

Format (2I5,E10.0)

read from subroutine **INDAT**.

| | | |
|--------|---|--|
| MAXINR | = | Maximum number of inner iterations to achieve a mass balance [] |
| IREBAL | = | Inner iterations for rebalancing of pressure and flow along the channel length. Rebalancing is done every IREBAL inner iterations [] |
| MERROR | = | Maximum allowable relative mass conservation error (C/F) per cell for the inner iteration. C is the mass error per cell (kg/s) and F is the average axial flow (kg/s). This differs for FERROR (dF/F) (on card G9-1 (→ p. E-65)). MERROR is the criterion used to measure mass convergence of the inner iteration. FERROR is used to measure the flow convergence of the outer iteration. MERROR is normally more restrictive. ([]) |

E.10.10 G9-8: PV-Solution Variables

This card is required if **ISOLVE = 3** on card I2 (→ p. E-6).

Read: **ACCELX**, **ACCELY**, **XFACP**, **NUSTAR**

Format (3E10.0,I10)

read from subroutine **INDAT**.

| | | |
|--------|-------|--|
| ACCELX | = | Acceleration factor for axial flow in MOMAXL. A value less than 1 slows the update of the axial flow from MOMAXL. Values [] may be needed for some applications. Reduce DTSS if damping does not lead to convergence in the steady state solution ([]). |
| ACCELY | = | Acceleration factor for lateral flow in MOMLAT. A value less than 1 slows the update of the lateral flow from MOMLAT. Values [] may be needed for some applications. Reduce DTSS if damping does not lead to convergence in the steady state solution ([]). |
| XFACP | = | Interpolation factor to locate pressure on staggered mesh. |
| | = 0.0 | Places the pressure at J+1 at junction J – the same as SCHEME . This is recommended when a high degree of correspondence with SCHEME is desired. |
| | = 0.5 | Places the pressure at the cell center as in a normal staggered mesh. This is recommended if flow reversals are to be considered. |

| | | |
|--------|---|--|
| NUSTAR | = | Option flag to select method of assigning axial velocity to the lateral cross flow boundary of the momentum cell in the axial momentum equation. |
| | = | 0 Assigns an average as done in the SCHEME solution. NUSTAR assigns a donor value and may be more stable in some applications. |
| | = | 1 Allows to also calculate reverse flow. |

E.10.11 G9-9: PV-Solution Variables

This card is required if ISOLVE = 3 on card I2 (→ p. E-6).

Read: **DAMPER, ACCELP, HERROR, NSOLVE, DAMPH**

Format (3E10.0,2I10)

read from subroutine **INDAT**.

| | | |
|--------|---|---|
| DAMPER | = | Acceleration factor for either nodal density or nodal enthalpy. The use depends on the value of DAMPH . If DAMPH is zero, then DAMPER is applied to the nodal density during the outer iterations. If DAMPH is greater than zero, DAMPER is applied to the nodal enthalpies in ENERGY after DAMPH iterations. |
| ACCELP | = | Acceleration factor on nodal pressures used in MASEQX and MASEQY. A value less than 1.0 will slow the pressure and subsequent flow convergence ([]). |
| HERROR | = | Absolute nodal energy error (J/kg) ([]). |
| NSOLVE | = | Selects between conservative and transportive forms of the momentum equations. |
| | = | 0 The conservative form of the momentum equations is used. |
| | = | 1 The transportive form (factors the temporal term in the conservative form and substitutes the mass equation) is used. |
| DAMPH | = | Switch for DAMPER : |
| | = | 0 DAMPER is applied to nodal densities. |
| | > | 0 DAMPER applies to nodal enthalpies after DAMPH iterations. |

Note: (1) Typically, NSOLVE = 1 will produce converged solution for low flow or reverse flow conditions when NSOLVE = 0 will fail to converge. NSOLVE = 0 will produce results most similar to SCHEME.

E.11 Card Group 10

Turbulent mixing correlations

| | |
|---|------|
| GCC10: Group control card for card group 10 | E-71 |
| G10-1: Mixing correlation constants | E-72 |
| G10-1a: Mixing data input | E-72 |
| G10-1b: Mixing data input | E-72 |
| G10-1c: Mixing data input | E-73 |
| G10-1d: Mixing data input | E-73 |
| G10-2: Two-phase mixing data | E-73 |

| | |
|---|------|
| G10-3: Thermal conduction geometry factor | E-73 |
| G10-4: Reference distance | E-74 |

E.11.1 GCC10: Group control card for card group 10

This card is required whenever card group 10 is used.

Card group 10 is not needed for IPILE (\rightarrow p.E-6)= 2.

Read: **NGROUP**, **N1**, **N2**, **N3**, **N4**, **N5**, **N6**, **N7**

Format (4I5)

read from subroutine **INDAT**.

| | | | |
|------------|---|----|---|
| NGROUP | = | 10 | Select card group 10. |
| N1 (NSCBC) | = | | Subcooled mixing correlation indicator: |
| | = | 0 | W/GS = ABETA. |
| | = | 1 | W/GS = ABETA * RE**BBETA. |
| | = | 2 | W/GD = ABETA * RE**BBETA. |
| | = | 3 | W/GS = (D/DIST) * ABETA * RE**BBETA. |
| | = | 4 | Beus mixing model is used. |
| N2 (NBBC) | = | | Two-phase mixing option: |
| | = | 1 | Two-phase mixing is the same as for subcooled conditions. |
| | > | 1 | Read in N2 pairs of data for a table of two-phase mixing data (see card G10-2 (\rightarrow p.E-73)). |
| N3 (J5) | = | | Thermal conduction mixing option: |
| | = | 0 | No thermal conduction between subchannels |
| | = | 1 | Thermal conduction taken into account, read in the thermal conduction geometry factor (see card G10-3 (\rightarrow p.E-73)). |
| N4 | = | 0 | No internal lateral scaling of the turbulent mixing. |
| | > | 0 | If internal lateral scaling of the turbulent mixing will be performed (see Note (5) below) . |
| N5 | = | | Not used. |
| N6 | = | | Not used. |
| N7 | = | | Not used. |

Note: (1) **Beta = W/GS** where **W** is the turbulent crossflow. **RE** is the Reynolds-number. **S** and **D** are the gap size and equivalent hydraulic diameter. **DIST** is the centroid distance between two channels. **ABETA** and **BBETA** are read in on card G10-1 (\rightarrow p.E-72).

(2) Each pair of two-phase mixing data consists of the steam quality and the corresponding value of **Beta**.

(3) The maximum value for **N2** is 130.

(4) Negative values of **N1** allow input of individual mixing values for selected gaps (see cards G10-1a (\rightarrow p.E-72), G10-1b (\rightarrow p.E-72), G10-1c (\rightarrow p.E-73), G10-1d (\rightarrow p.E-73)).

(5) Internal lateral scaling according to US NRC requirements (this option is only applicable with $N1 = 0, 1, 2, 3$):
 For $N4 > 0$, the turbulent mixing is inversely proportional to the number of rod rows between channel centroids, i.e. the fluctuating crossflow due to turbulent mixing is multiplied by an internally calculated local factor of $LREF_BETA/DIST$ (cf. cards G10-4 (\rightarrow p.E-74) and G4a-1 (\rightarrow p.E-15)).

E.11.2 G10-1: Mixing correlation constants

This card is required if $N1 = 0, 1, 2$ or 3 on card GCC10 (\rightarrow p.E-71).

Read: **ABETA, BBETA**

Format (2F5.3)

read from subroutine **INDAT**.

ABETA = Subcooled mixing correlation constants (see card GCC10 (\rightarrow p.E-71) for the correlations).

BBETA = Subcooled mixing correlation constants (see card GCC10 (\rightarrow p.E-71) for the correlations).

E.11.3 G10-1a: Mixing data input

This card is required if $N1 < 0$ on card GCC10 (\rightarrow p.E-71).

Read: **INGAP**

Format (I5)

read from subroutine **INDAT**.

INGAP = Number of mixing types []

Note: (1) Negative values of **INGAP** allow to specify individual gaptypes for each gap.

E.11.4 G10-1b: Mixing data input

This card is required if $N1 < 0$ on card GCC10 (\rightarrow p.E-71).

Read: **ABETA, BBETA**

Format (2F5.3)

read from subroutine **INDAT**.

ABETA = Mixing constants.

BBETA = Mixing constants.

Note: (1) Repeat **Abs(INGAP)** times (see card G10-1a (\rightarrow p.E-72)).

E.11.5 G10-1c: Mixing data input

This card is required if $INGAP < 0$ on card G10-1a (\rightarrow p.E-72).

Read: **NGAPN**

Format (I5)

read from subroutine **INDAT**.

NGAPN = Number of cards to follow.

E.11.6 G10-1d: Mixing data input

This card is required if $INGAP < 0$ on card G10-1a (\rightarrow p.E-72).

Read: **IG, IDGAP1 (IG)**

Format (2I5)

read from subroutine **INDAT**.

IG = Number of gap.

IDGAP1 = Gap type.

Note: (1) Repeat **NGAPN** times.

(2) Gaps not enumerated are set to default-type **IDGAP1 = 1**.

E.11.7 G10-2: Two-phase mixing data

This card is required if $N2 > 1$ on card GCC10 (\rightarrow p. E-71).

Read: **XQUAL (I), BX (I), I = 1, N2**

Format (12F5.3)

read from subroutine **INDAT**.

XQUAL = Steam quality.

BX = Corresponding value of **Beta = W/GS**.

Note: (1) **N2** (see card GCC10 (\rightarrow p. E-71)) pairs of data must be provided on cards of this type giving six pairs per card.

E.11.8 G10-3: Thermal conduction geometry factor

This card is required if $N3 = 1$ on card GCC10 (\rightarrow p. E-71).

Read: **GK**

Format (F5.3)

read from subroutine **INDAT**.

GK = Thermal conduction geometry factor.

Note: (1) $GK > 0.0$ activates the term accounting for thermal conduction mixing between subchannels in the energy balance equation. The thermal conduction coefficient is determined as a function of the subchannel geometry and the average fluid thermal conductivity of two interconnected subchannels. This coefficient is then multiplied by GK . Hence $GK = 1.0$ leaves the coefficient unchanged, $GK > 1.0$ increases the thermal

mixing, $0.0 < GK < 1.0$ reduces it. $GK = 0.0$ eliminates the thermal conduction mixing term (same effect as $N3 = 0$ on card GCC10 (→ p. E-71)).

E.11.9 G10-4: Reference distance

This card is required if $N4 > 0$ on card GCC10 (→ p. E-71).

Read: **LREF_BETA**

Format (**E10.5**)

read from subroutine **INDAT**.

LREF_BETA = Reference distance (cm) to be used for internal lateral scaling of the turbulent mixing.
Reference distance is usually the centroid distance between two fuel rods (rod pitch).

E.12 Card Group 11

Operating conditions

| | |
|--|------|
| GCC11: Group control card for card group 11 | E-74 |
| NLOOP: Transient data from file NLOOP (unit 96) | E-75 |
| G11-1.0: Transient parameters with transient data read from file NLOOP | E-76 |
| G11-1: Operating conditions | E-77 |
| G11-1a: Setpoint iteration | E-77 |
| G11-1b: Sensitivity calculation | E-78 |
| G11-1c: Number of channels with given pressure difference at the outlet | E-80 |
| G11-1d: Channels with given pressure difference at the outlet | E-80 |
| G11-2: Inlet temperature or enthalpy | E-80 |
| G11-3: Channel mass velocity factors | E-81 |
| G11-4.a: Automatic time step control | E-81 |
| G11-4: Transient forcing function data pairs for pressure versus time | E-81 |
| G11-5.a: Automatic time step control | E-81 |
| G11-5: Transient forcing function data pairs for inlet enthalpy or inlet temperature versus time | E-82 |
| G11-6.a: Automatic time step control | E-82 |
| G11-6: Transient forcing function data pairs for inlet flow versus time | E-82 |
| G11-7.a: Automatic time step control | E-82 |
| G11-7: Transient forcing function data pairs for heat flux versus time | E-83 |
| G11-8: Write local coolant conditions to files COOLANT (tape77) and DNBDATA (tape9) | E-83 |

E.12.1 GCC11: Group control card for card group 11

This card is required whenever Card Group 11 is used.

Read: **NGROUP, N1, N2, N3, N4, N5, N6, N7**

Format (**B15**)

read from subroutine **INDAT**

NGROUP = 11 Select card group 11.

| | | |
|-------------|---|--|
| N1 (IN) | = | Inlet enthalpy option indicator. |
| | = | 0 Inlet enthalpy is given. |
| | = | 1 Inlet temperature is given. |
| | = | 2 Read in the individual subchannel inlet enthalpies. |
| | = | 3 Read in the individual subchannel inlet temperatures. |
| | = | 5 Inlet temperature, setpoint calculation. |
| N2 (IG) | = | Inlet flow distribution indicator. |
| | = | 0 All subchannels are given the same mass velocity. |
| | = | 1 Inlet flow is divided to give equal pressure drop in all subchannels. |
| | = | 2 Mass velocity factors for each channel read in on card G11-3 (→ p.E-81). |
| N3 (NP) | = | Pressure transient forcing function indicator. |
| N4 (NH) | = | Inlet enthalpy or temperature forcing function. Which inlet variable is chosen is indicated by N1 (IN) above. |
| N5 (NG) | = | Inlet flow transient forcing function indicator. |
| N6 (NQ) | = | Heat flux transient forcing function indicator. |
| N7 (LOCDAT) | = | Store local coolant conditions on tape (see card G11-8 (→ p.E-83)). |

*Note: (1) Each of the variables **N3**, **N4**, **N5** and **N6** gives the number (**max=10000**) of tabular data pairs to be read in for each transient forcing function. Each data pair consists of a time specification (seconds) and the relative value (present value/initial value) for the parameter in question. If any of these option numbers are zero or blank, the corresponding forcing function data is not read in and is excluded from the calculations.*

E.12.2 NLOOP: Transient data from file NLOOP (unit 96)

*This card is required if **NDT > 0** on card G9-1 (→ p.E-65) and **N3 .. N6 = 0** on card GCC11 (→ p.E-74).*

*Read: If **N1 (IN) > 0** (on card GCC11 (→ p. E-74)): **TTIME**, **FP**, **FH**, **FG**, **FQ***

Format (5G12.5)

*read from subroutine **READ_NLOOP_DATA***

*If **N1 (IN) < 0** (on card GCC11 (→ p. E-74)): **TTIME**, **PLN**, **TLN**, **GLN**, **QLN**, (**TINLE(I,2)**, **I = 1, NCHAN**), (**FINLE(I,2)**, **I = 1, NCHAN**)*

Format ()*

*read from subroutine **READ1_NLOOP_DATA***

| | | |
|--------------|---|---|
| TTIME | = | Transient time (s). |
| FP (PLN) | = | System pressure at core outlet (bar). |
| FH (TLN) | = | Core inlet temperature (°C). |
| FG (GLN) | = | Core inlet mass flux (kg/(m ² s)). |
| FQ (QLN) | = | (Power generated in pellets and clad)/(total heated area) (kW/m ²); equals average heatflux when no fuel rod model is used. |
| TINLE (I, 2) | = | Relative temperature of subchannel i : (T _i (°C))/(T _{average} (°C)) . |

FINLE (I, 2) = Relative mass flux of subchannel i : G_i/G_{average} .

Note: (1) Transient data are read from the file **NLOOP**, if the above condition holds. Tables are set up starting with the first value **TIME > TSTART0**. Initial operating conditions are taken for this time point. Hereafter the tables are normalized as with standard input on files **INPUT** and **PRECOB**. Reading from file **NLOOP** assigns nonzero values to the transient indicators **NP**, **NH**, **NG** and **NQ**, so inputting stacked transients via file **NLOOP** requires inputting these values as zero on card **GCC11** (\rightarrow p.E-74). A warning message is printed if more than 10000 time points are available on file **NLOOP** and only the first 10000 are used for calculation.

(2) If **N1 < 0** on card **GCC11** (\rightarrow p. E-74) individual channel inlet temperature factors and inlet flow factors are read from file **NLOOP**. If **N1 = -3** or **N2 = 2** individual temperatures and channel flows are obtained respectively by multiplying the average temperature **TLN** with **TINLE(I,2)** and the mass flux **GLN** with **FINLE(I,2)**.

E.12.3 G11-1.0: Transient parameters with transient data read from file NLOOP

This card is required if **NDT > 0** on card **G9-1** (\rightarrow p.E-65) and **N3 .. N6 = 0** on card **GCC11** (\rightarrow p. E-74).

Read: **TSTART0**, **FHGFUE**

Format (2F10.5)

read from subroutine **INDAT**.

TSTART0 = Skip **TSTART0** seconds of transient on unit 96.

FHGFUE = Fraction of heat generated in fuel and clad.

Write: **TIME**, **DNBRMIN**, **PPTEMP**, **AVTEMP**, **CITEMP**, **COTEMP**, **TAVINL**, **TAVEXI**, **ENTHMAX**, **DFLUMIN**, **BRMAX**

Format (11G15.5)

written by subroutine **EXPRIN** to unit 9, file **DNBDATA**.

TIME = Transient time (s).

DNBRMIN = Minimum DNBR.

PPTEMP = Peak pellet central temperature ($^{\circ}$ C).

AVTEMP = Peak pellet average temperature ($^{\circ}$ C).

CITEMP = Peak clad inner temperature ($^{\circ}$ C).

COTEMP = Peak clad outer temperature ($^{\circ}$ C).

TAVINL = Coolant average inlet temperature ($^{\circ}$ C).

TAVEXI = Coolant average exit temperature ($^{\circ}$ C).

ENTHMAX = Maximum Fuel Enthalpy (kJ/kg).

DFLUMIN = Heat Flux at Location of Minimum DNBR (kW/m²).

BRMAX = Maximum heat transfer regime indicator occurring (-).

Note: (1) Fuel rod temperatures **PPTEMP**, **AVTEMP**, **CITEMP** and **COTEMP** as well as **ENTHMAX** and **DFLUMIN** are omitted if not calculated; **TAVINL**, **TAVEXI** are omitted if not demanded for by **N2 (NSKIPT)** on card **GCC9** (\rightarrow p.E-64) resp. **44-00** (\rightarrow p.E-131).

E.12.4 G11-1: Operating conditions

This card is required whenever card group 11 is used.

Read: **PEXIT, HIN, GIN, AFLUX, FHGFUE, BYPASS**

Format (6F10.0)

read from subroutine **INDAT**.

| | | | |
|--------|---|---|---|
| PEXIT | = | | Operating pressure (bar). |
| HIN | = | | Depends on value of N1 on card GCC11 (\rightarrow p. E-74): if N1 = 0 : Inlet enthalpy (kJ/kg); if N1 = 1 : Inlet temperature ($^{\circ}$ C). |
| GIN | > | 0 | Core inlet mass flux (kg/(m ² s)). |
| | < | 0 | Depends on value of N1 on card GCC11 (\rightarrow p. E-74): if N1 = 0,1 : Core inlet volumetric flow rate (m ³ /s); if N1 = 5 : Core inlet velocity (m/s). |
| AFLUX | = | | Average heat flux: (Power generated in fuel rods)/(total surface) (kW/m ²). |
| FHGFUE | = | | Fraction of heat generated in fuel []; used to calculate power generated in coolant. Note: Total power of system = (power generated in fuel rods)/FHGFUE |
| BYPASS | = | | Bypass fraction []. Only used for vessel temperatures in setpoint calculation or for inlet flow distribution with given volumetric flow rate for GIN . |

Note: (1) Card is skipped if card G11-1.0 (\rightarrow p.E-76) has already been read.

(2) **PEXIT** < 0 allows to specify the pressure distribution at the core outlet. If **PEXIT** < 0 the operating pressure (bar) is set to **abs(PEXIT)**. The pressure differences at the core exit are given relative to this pressure using G11-1c (\rightarrow p.E-80) and G11-1d (\rightarrow p.E-80).

E.12.5 G11-1a: Setpoint iteration

This card is required if **N1** = 5 on card GCC11 (\rightarrow p.E-74).

Read: **ISPIT, XSPLOW, XSPHGH, DNBLIM, TOLLIM, MAXFN**

Format (I5, 4F10.5, I5)

read from subroutine **INDAT**.

| | | | |
|--------|---|-----|---|
| ISPIT | = | 1 | Setpoint iteration = Variation of power. |
| | = | 2 | Setpoint iteration = Variation of inlet temperature at fixed volumetric flow given by reference conditions on card G11-1 (\rightarrow p.E-77). |
| | = | 11 | Perform sensitivity calculation; see card G11-1b (\rightarrow p.E-78). (1) |
| | = | -11 | First perform setpoint iteration as for ISPIT=2 , then perform sensitivity calculation as for ISPIT=11 . |
| XSPLOW | = | | Lower limit of interval to be searched if ISPIT = 1: kW/m ² , ISPIT = 2: $^{\circ}$ C. (2) |

| | | |
|--------|---|---|
| XSPHGH | = | Upper limit of interval to be searched if ISPIT = 1: kW/m ² , ISPIT = 2: °C. (2) |
| DNBLIM | = | Target DNBR for iteration. |
| TOLLIM | = | Iteration is stopped if ABS(DNBR-DNBLIM) < TOLLIM . |
| MAXFN | = | Case is skipped if no convergence is reached after MAXFN iterations. |

Note: (1) For **N1 = 5** on card G11-1 (→ p.E-77) negative values of **GIN** are interpreted as velocity (m/s).

(2) For a fast convergence it is recommended to input the initial interval (**XSPLOW**, **XSPHGH**) as small as possible and bracketing (and thus guaranteeing convergence in a finite number of steps) the final value; if the initial guesses do not bracket the limit value, a secant approximation is tried. Convergence can only be achieved if **FERROR**, **WERROR** (card G9-1 (→ p.E-65)) and **TOLLIM** are well balanced.

(3) Results of setpoint iteration are printed out and the same data together with minimum **DNBR** are written to **DNBDATA** (unit 9) in the format **10G13.6**:
TINV, Vessel inlet temperature (°C)
TOUTV, Vessel outlet temperature (°C)
(TOUTV+TINV)/2., Vessel average temperature (°C)
TOUTV-TINV, Vessel temperature rise (°C)
(ENGOUT-ENGIN)*10⁻⁶, Core power (MW)
PEXIT*10⁻⁵, Operating pressure (bar)
DNBMIN, Minimum **DNBR** reached during iteration
OFFSET, Axial power offset

E.12.6 G11-1b: Sensitivity calculation

This card is required if **ABS(ISPIT) = 11** on card G11-1a (→ p.E-77).

Read: **VARNCS (1)**, **VARNCS (2)**, **VARNCS (3)**, **VARNCS (4)**, **VARNCS (5)**, **VARNCS (6)**,
VARNCS (7), **VARNCS (8)**, **VARNCS (9)**, **VARNCS (10)**

Format (**6F10.5**)

read from subroutine **INDAT**.

| | | |
|------------|---|---|
| VARNCS (1) | = | Coefficient of variation for system pressure. |
| VARNCS (2) | = | Coefficient of variation for inlet temperature. |
| VARNCS (3) | = | Coefficient of variation for mass flow rate; may be used to model uncertainty of bypass flow as well as of vessel flow. |
| VARNCS (4) | = | Coefficient of variation for heat flux. |
| VARNCS (5) | = | Coefficient of variation for F-delta-h nuclear. |
| VARNCS (6) | = | Coefficient of variation for Fq engineering. |
| VARNCS (7) | = | Coefficient of variation for F-delta-h engineering1, will be applied to hot channel (see card GCC3 (→ p.E-12)). |
| VARNCS (8) | = | Coefficient of variation for code uncertainty. |
| VARNCS (9) | = | Coefficient of variation for transient code uncertainty. |

VARNCS (10) = Coefficient of variation for **DNB** correlation uncertainty.

*Note: (1) Although results can be obtained with any input, this option has been established for use with **PRECOB** input only (see the code manual). [*

*]. Calculations are performed with the operating conditions given on card G11-1 (→p.E-77) as a reference value, i.e. no iteration is performed. Input unwanted calculations as **VARNCS(I) = 0**.*

*(2) **VARNCS(10) > 0** triggers a Monte Carlo simulation with positive values of **VARNCS(I)** corresponding to a normal and negative values to a square distribution.*

*(3) Simulation input as well as results are appended to the setpoint iteration data (see card G11-1a (→p.E-77)) written to unit 9, file **DNBDATA**.*

Write: 10

Format (I5)

*written from subroutine **EXPRIN** to unit 9, file **DNBDATA**.*

10 = 10 Number of input variables.

Write: j, lgauss(j), ave+1, sqrt(var), varncs(j)

Format (I5, I5, 3F10.5)

*written from subroutine **EXPRIN** to unit 9, file **DNBDATA**.*

j = Number of input variable.

lgauss(j) = 1 (true): Gauss distribution.

= 0 (false): Rectangle distribution.

ave+1 = Sample average.

sqrt(var) = Sample variance.

varncs(j) = Input variance.

*Write: **nnmc***

Format (I5)

*written from subroutine **EXPRIN** to unit 9, file **DNBDATA**.*

nnmc = Monte Carlo simulation sample size (=3000).

*Write: **ymc(i)***

Format (F10.5)

*written from subroutine **EXPRIN** to unit 9, file **DNBDATA**.*

ymc(i) = Normalized sample **DNBR**; repeated **nnmc** times.

E.12.7 G11-1c: Number of channels with given pressure difference at the outlet

This card is required if **PEXIT** < 0 on card G11-1 (→ p.E-77).

Read: **NCHAN_DP**, **IDPEXIT**

Format (16,11)

read from subroutine **INDAT**.

| | | | |
|-----------------|---|---|--|
| NCHAN_DP | = | | Total number of channels for which the pressure difference will be read. |
| IDPEXIT | = | 0 | The pressure differences at core exit will be used as given by input. |
| | > | 0 | The pressure differences at core exit of all subchannels will be adjusted to achieve zero average outlet pressure difference (i.e. average outlet pressure PEXIT). |

E.12.8 G11-1d: Channels with given pressure difference at the outlet

This card is required if **PEXIT** < 0 on card G11-1 (→ p.E-77).

Read: **I**, **PEXIT(I)**

Format (16,F10.3)

read from subroutine **INDAT**.

| | | | |
|-----------------|---|--|---|
| I | = | | Channel number for which the pressure difference is read. |
| PEXIT(I) | = | | The pressure difference (bar) at core exit for subchannel number I . |

Note: (1) This card is read **NCHAN_DP** times (see card G11-1c (→ p.E-80)).

E.12.9 G11-2: Inlet temperature or enthalpy

This card is required if **N1** = 2 or 3 on card GCC11 (→ p.E-74)

Read: (**HINLE(I)**), **I** = 1, **NCHAN**)

Format (12E5.0)

read from subroutine **INDAT**.

| | | | |
|--------------|---|--|--|
| HINLE | = | | Depends on value of N1 on card GCC11 (→ p.E-74): if N1 = 2 : Channel inlet enthalpies (kJ/kg). if N1 = 3 : Channel inlet temperatures (°C). |
|--------------|---|--|--|

Note: (1) These inlet variable values must be specified in the order that the channels are numbered and sufficient cards must be used to supply all the values called for (one per channel).

E.12.10 G11-3: Channel mass velocity factors

This card is required if $N2 = 2$ on card GCC11 (\rightarrow p. E-74).

Read: (FSPLI(I), I = 1, NCHAN)
Format (12E5.0)
read from subroutine INDAT.

FSPLI = Channel mass velocity factors (12 per card) if formatted input,
channel inlet fraction of total bundle flow if free formatted input.

Note: (1) These factors are inputted in the same order as the channels are numbered.

E.12.11 G11-4.a: Automatic time step control

This card is required if $N3 < 0$ on card GCC11 (\rightarrow p. E-74).

Read: DAUTOP
Format (E5.0)
read from subroutine INDAT.

DAUTOP = Relative change in pressure forcing function.

E.12.12 G11-4: Transient forcing function data pairs for pressure versus time

This card is required if $ABS(N3) > 1$ on card GCC11 (\rightarrow p. E-74).

Read: YP, FP
Format (12E5.0)
read from subroutine INDAT.

YP = Time specification (s).
FP = Relative pressure (current/initial).

Note: (1) A total of $N3$ data pairs must be provided giving 6 per card (for formatted input).

E.12.13 G11-5.a: Automatic time step control

This card is required if $N4 < 0$ on card GCC11 (\rightarrow p. E-74).

Read: DAUTOH
Format (E5.0)
read from subroutine INDAT.

DAUTOH = Relative change in temperature (enthalpy) forcing function.

E.12.14 G11-5: Transient forcing function data pairs for inlet enthalpy or inlet temperature versus time

This card is required if $ABS(N4) > 1$ on card GCC11 (\rightarrow p. E-74).

Read: **YH, FH**

Format (**12E5.0**)

read from subroutine **INDAT**.

| | | |
|----|---|---|
| YH | = | Time specification (s). |
| FH | = | Relative parameter value (current/initial). Depends on value of N1 on card GCC11 (\rightarrow p.E-74): if N1 = 0 : relative enthalpy given; if N1 = 1 : relative temperature given. |

Note: (1) A total of **N4** data pairs must be provided giving 6 per card.

E.12.15 G11-6.a: Automatic time step control

This card is required if $N5 < 0$ on card GCC11 (\rightarrow p. E-74).

Read: **DAUTOG**

Format (**E5.0**)

read from subroutine **INDAT**.

| | | |
|--------|---|--|
| DAUTOG | = | Relative change in mass flux forcing function. |
|--------|---|--|

E.12.16 G11-6: Transient forcing function data pairs for inlet flow versus time

This card is required if $ABS(N5) > 1$ on card GCC11 (\rightarrow p. E-74).

Read: **YG, FG**

Format (**12E5.0**)

read from subroutine **INDAT**.

| | | |
|----|---|--|
| YG | = | Time specification (s). |
| FG | = | Relative inlet flow (current/initial). |

Note: (1) A total of **N5** data pairs must be provided giving 6 per card (for formatted input).

E.12.17 G11-7.a: Automatic time step control

This card is required if $N6 < 0$ on card GCC11 (\rightarrow p. E-74).

Read: **DAUTOQ**

Format (**E5.0**)

read from subroutine **INDAT**.

| | | |
|--------|---|--|
| DAUTOQ | = | Relative change in power (heat flux) forcing function. |
|--------|---|--|

Note: (1) Time step is the minimum determined from the relative changes specified.

E.12.18 G11-7: Transient forcing function data pairs for heat flux versus time

This card is required if **ABS(N6) > 1** on card GCC11 (→ p. E-74).

Read: **YQ, FQ**

Format (12E5.0)

read from subroutine **INDAT**.

YQ = Time specification (s).

FQ = Relative heat flux/power generation (current/initial).

Note: (1) A total of **N6** data pairs must be provided giving 6 per card (for formatted input); if a fuel rod model is specified with card group 8 (→ p.E-34) **FQ** applies no longer to the heat flux, but to the power generation rate.

E.12.19 G11-8: Write local coolant conditions to files COOLANT (tape77) and DNBDATA (tape9)

This card is required if **N7.NE. 0** and if **N1 = 0 or 1** on card GCC11 (→ p. E-74).

Read: **ITS, ITSI, IRUN**

Format (8I5)

read from subroutine **INDAT**.

ITS = Test section number.

ITSI = Test section variant (less or equal 10).

IRUN = Run number.

Note: (1) If **N7 = 1** on card GCC11 (→ p. E-74) format of data on file **COOLANT** is:

First record:

ITS, ITSI, IRUN, NCHAN, NDX, PAGET, IERROR

Next **NDX+1** records: Channel enthalpies (kJ/kg) at axial node **J**

H(I,J)*10⁻³, I=1, NCHAN

Next **NDX+1** records: Channel pressure drops (bar) at axial node **J**

P(I,J)*10⁻⁵, I=1, NCHAN

Next **NDX+1** records: Channel mass fluxes (kg/(m² s)) at axial node **J**

F(I,J)/AREAX(I,J), I=1, NCHAN

(4) If **N7 = 2** on card **GCC11** (→ p. E-74) the following information is written to file **MIXDATA**,

First record, format **(A)**:

PAGET

Second record, format **(10I10)**:

ITS, ITSI, IRUN, NCHAN, NDX, IMAX, IERROR

Third record, format **(10E12.5)**:

ABETAI(I), BBETAI(I), I = 1, IMAX

Fourth record, only for uniform inlet temperature/enthalpy, format **(10E12.5)**:

GIN, PREF, TIN, ENGADD_FR, AFLUX

Fifth record, format **(10E12.5)**:

T(I), F(I), I = 1, NCHAN at the bundle exit

The newly introduced variables denote the following:

IMAX: Total number of mixing types

IERROR: Error indicator

ABETAI(I), BBETAI(I): Mixing constants for mixing type *I*

ENGADD_FR: Energy added from fuel rods (kW)

T(I), F(I): Coolant temperature (degrees centigrade) and mass flow (kg/s) at the outlet of channel *I*

E.13 Card Group 12

Output display options

| | |
|---|------|
| GCC12: Group control card for card group 12 | E-85 |
| G12-1: Subchannel numbers | E-86 |
| G12-2: Fuel rod numbers | E-87 |
| G12-3: Node numbers | E-87 |

E.13.1 GCC12: Group control card for card group 12

This card is required whenever card group 12 is used.

Read: **NGROUP, N1, N2, N3, N4, N5, N6, N7**

Format **(5I5)**

read from subroutine **INDAT**.

| | | | |
|--------------------|---|----|--|
| NGROUP | = | 12 | Select card group 12. |
| N1 (NOUT) | = | | Data printout indicator: |
| | = | 0 | Print subchannel data only. |
| | = | 1 | Print subchannel data and crossflow data table. |
| | = | 2 | Print subchannel data and fuel rod data table. |
| | = | 3 | Print subchannel data, fuel rod data table and crossflow data table. |
| N2 (NPCHAN) | = | | Subchannel data printout indicator: |
| | = | 0 | All subchannel data printed. |
| | > | 0 | Read in N2 subchannel numbers for which results are desired (see card G12-1 (→ p.E-86)). |
| N3 (NPROD) | = | | Fuel rod data printout indicator: |
| | = | 0 | Data of all rods printed if called for by N1 . |

| | | | |
|-------------|---|---|--|
| | > | 0 | Read in N3 rod numbers for which results are desired (see card G12-2 (→ p.E-87)). |
| | < | 0 | Read in ABS(N3) rod numbers for which results are desired (see card G12-2 (→ p.E-87)). Additionally the detailed fuel node temperature data is printed. |
| N4 (NPNODE) | = | | Fuel node printout indicator: |
| | = | 0 | Temperature printed for all nodes if called for by N3 . |
| | > | 0 | Read in N4 node numbers for which results are desired (see card G12-3 (→ p.E-87)). |
| N5 | = | | Not used. |
| N6 | = | | Not used. |
| N7 | = | | Not used. |

*Note: (1) If CHF-data has been calculated, it will be printed out for each of the fuel rods selected by **N3** and card(s) G12-2 (→ p.E-87) plus a summary to identify the rod and channel with the minimum CHF-ratio.*

(2) When called from PANBOX the channel numbers refer rather to fuel assembly numbers than to channels, i.e. specifying a fuel assembly number of an assembly being HOSCAM-nodalized results in the printout of the hot subchannel data within the fuel assembly rather than that of the fuel assembly.

*(3) Default rod and channel numbers selected for printout are different for standalone COBRA-FLX and PANBOX:
COBRA-FLX prints by default all rods and channels. The coupled system printout is minimal. Printout of all channels and rods is achieved by inputting **KDEBUG = -1** on card GCC9 (→ p.E-64).*

*Type of data printed is still determined by **NOU**T on GCC 12. HOSCAM printout depends on variable **NCHHSC** in PAN_INP block \$HOSCA:*

***NCHHSC = 0**: Print data of all hot subchannels and pertaining rods*

***NCHHSC>0**: Print only data requested for by NPROD or NPCHAN > 0*

E.13.2 G12-1: Subchannel numbers

*This card is required if **N2 > 0** on card GCC12 (→ p.E-85).*

*Read: **PRNTC(I)**, I = 1, N2*

Format (36I2)

*read from subroutine **INDAT**.*

PRNTC = Channel numbers for which results are desired.

*Note: (1) A total of **N2** channel numbers must be specified giving 36 per card (for formatted input).*

E.13.3 G12-2: Fuel rod numbers

This card is required if $N3 > 0$ on card GCC12 (→ p.E-85).

Read: **PRNTR(I)**, $I = 1, N3$

Format (36I2)

read from subroutine **INDAT**.

PRNTR = Rod numbers for which results are desired.

Note: (1) A total of $N3$ rod numbers must be specified giving 36 per card (for formatted input).

E.13.4 G12-3: Node numbers

This card is required if $N4 > 0$ on card GCC12 (→ p. E-85).

Read: **PRNTN(I)**, $I = 1, N4$

Format (36I2)

read from subroutine **INDAT**.

PRNTN = Node numbers for which results are desired.

Note: (1) A total of $N4$ node numbers must be specified giving 36 per card (for formatted input).

(2) The node numbers are counted such that fuel centerline is node 1 and fuel surface is node N.

E.14 Card Group 20**Card Group 20 Input**

| | | |
|---------|--|-------|
| E.14.1 | GCC20: Group control card for card group 20..... | E-89 |
| E.14.2 | 1-CNS: Channel map parameter | E-90 |
| E.14.3 | 2-CNS: Channel map..... | E-91 |
| E.14.4 | 3-CNS: Channel map..... | E-92 |
| E.14.5 | 4-HF: Heat flux specification..... | E-94 |
| E.14.6 | 5-HF: Heat flux profile..... | E-95 |
| E.14.7 | 6-HF: Rod power factors..... | E-96 |
| E.14.8 | 7-MD: Miscellaneous data | E-97 |
| E.14.9 | 8-CD: Channel Indicators | E-97 |
| E.14.10 | 9-CD: Fuel rod temperature convergence | E-98 |
| E.14.11 | 9-CD-1: Iteration of Heat Transfer Coefficient | E-99 |
| E.14.12 | 10-CD: Channel data for type I..... | E-99 |
| E.14.13 | 11-CD: Grid data for channel type I..... | E-100 |
| E.14.14 | 12-CD: Channels making up type I..... | E-101 |
| E.14.15 | 13-CD: Grid positions | E-101 |
| E.14.16 | 14-RD: Indicators..... | E-101 |
| E.14.17 | 15-RD: Rod layout information | E-102 |
| E.14.18 | 16-FD: Fuel temperature data | E-103 |
| E.14.19 | 17-FD: Fuel thermal properties..... | E-103 |
| E.14.20 | 17a-FD: Fuel rod model (geometry) | E-104 |

| | | |
|---------|--|-------|
| E.14.62 | 33-HM: Convergence criteria..... | E-123 |
| E.14.63 | 33a-HM: PV-Solution Variables..... | E-124 |
| E.14.64 | 33b-HM: PV-Solution Variables..... | E-124 |
| E.14.65 | 33c-HM: PV-Solution Variables..... | E-124 |
| E.14.66 | 33d-HM: PV-Solution Variables..... | E-125 |
| E.14.67 | 33e-HM: PV-Solution Variables..... | E-126 |
| E.14.68 | 34-HM: Physical properties..... | E-126 |
| E.14.69 | 35-HM: Coupling parameters..... | E-127 |
| E.14.70 | 36-OC: Steady state operating conditions..... | E-127 |
| E.14.71 | 36-OC1: Operating conditions..... | E-128 |
| E.14.72 | 36.1-OC: Setpoint iteration..... | E-128 |
| E.14.73 | 37-OC: Inlet enthalpy distribution..... | E-128 |
| E.14.74 | 38-T: Transient indicators..... | E-129 |
| E.14.75 | 39-T: Pressure transient forcing function..... | E-129 |
| E.14.76 | 40-T: Inlet enthalpy transient forcing function..... | E-130 |
| E.14.77 | 41-T: Inlet flow transient forcing function..... | E-130 |
| E.14.78 | 42-T: Channel power transient forcing function..... | E-130 |
| E.14.79 | 43-DB: Debug option..... | E-131 |
| E.14.80 | 44-OO: Output printing..... | E-131 |
| E.14.81 | 45-OO: Channels to be printed..... | E-132 |
| E.14.82 | 46-OO: Rods to be printed..... | E-132 |
| E.14.83 | 47-OO: Fuel nodes to be printed..... | E-132 |
| E.14.84 | 48-NP: This card is obsolete..... | E-132 |
| E.14.85 | 49-NP: Fuel nodal powers..... | E-133 |
| E.14.86 | 50-NP: Coolant nodal powers..... | E-133 |
| E.14.87 | GCC: End input data and start calculation..... | E-133 |

E.14.1 GCC20: Group control card for card group 20

This card is required whenever the card group 20 input method is used.

Read: **NGROUP**, **N1**, **N2**, **N3**, **N4**, **N5**, **N6**, **N7**

Format (**14I5**)

read from subroutine **INDAT**.

| | | | |
|-------------|---|----|--|
| NGROUP | = | 20 | Select card group 20. |
| N1 (NOPRIN) | = | | Printing trigger, NOPRIN , set to N1 . |
| | = | 0 | Standard COBRA IIIC printing obtained as well as "new" printout. |
| | = | 1 | Standard COBRA printing suppressed. |
| N2 | = | | Not used. |
| N3 | = | | Not used. |
| N4 | = | | Not used. |
| N5 | = | | Not used. |
| N6 | = | | Not used. |

N7 = Not used.

Note: (1) If **NGROUP = 0**, this acts as a trigger to stop reading input data and to start the hydraulic calculation (e.g. after card 49-NP (→ p.E-133)).

(2) In the older input methods, the remaining input data was divided into as many as 12 groups and a group control card, card type GCC was provided at the start of each data group. These older methods are described in the original input. In the latest method, all of the data has been consolidated into one card group. To select this input method, the value of **NGROUP** on the group control card is set to 20 and thus this card group is called card group 20.

E.14.2 1-CNS: Channel map parameter

This card is required whenever card group 20 is used.

Read: **IMAP, ND1X, ND2X**

Format (*)

read from subroutine **CARD20**.

IMAP = Selects method for reading channel map into array **NTHBOX (ND1X,ND2X)** :

= 1 Go to card 4-HF (→ p.E-94).

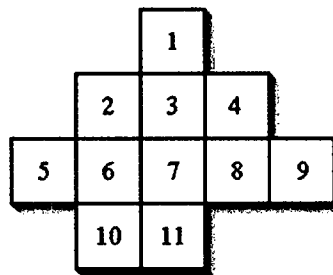
= 2 Go to card 2-CNS (→ p.E-91).

= 3 Go to card 3-CNS (→ p.E-92).

ND1X = The number of channels across the longest row of the channel numbering map (max = **25**).

ND2X = The number of rows in the channel numbering map.

Note: (1) In COBRA IIIc/MIT, the channel numbering system is contained in the array **NTHBOX (ND1X,ND2X)** with a zero for each non-channel. This array is later used to define the interaction between adjacent channels. Thus a channel map:



would be presented in **NTHBOX (5,4)** as

```

0 0 1 0 0
0 2 3 4 0
5 6 7 8 9
0 10 11 0 0
  
```

The method of inputting the channel map into **NTHBOX** and the dimensions for **NTHBOX** are provided on this card. **IMAP = 1, 2 or 3** indicates the input method while **ND1X** and **ND2X** carry the appropriate dimensions.

If $IMAP = 1$, there are assumed to be $ND1X \cdot ND2X$ channels numbered sequentially along each row and column by column to give a rectangular matrix. Thus, if cards GCC20 (\rightarrow p.E-89) and 1-CNS are given as in Figure G20-F1(b) with $IMAP = 1$, $ND1X = 4$ and $ND2X = 3$, the resulting channel map would be that shown in figure G20-F1(a):

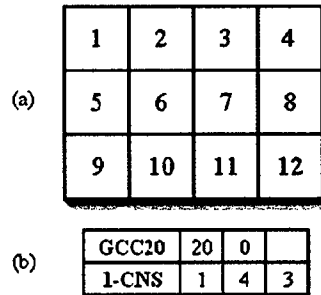


Figure G20-F1: Channel map and required cards using $IMAP = 1$

E.14.3 2-CNS: Channel map

This card is required if $IMAP = 2$ on card 1-CNS (\rightarrow p.E-90).

Read: **ISTART, IFIN**
Format (*)
read from subroutine **CARD20**.

ISTART = Position in row where sequential channel numbering is to begin.
IFIN = Position in row where sequential channel numbering ends.

Note: (1) A total of $ND2X$ (see card 1-CNS (\rightarrow p.E-90)) cards of this type are read sequentially, one for each row of the channel map. Each card gives the column numbers in the row where channel numbering should begin and end. Channel identification numbers are then placed sequentially in each column from the first position (**ISTART**) to the last (**IFIN**) inclusively.
For example, $ISTART = 3$, $IFIN = 6$ would imply a row,
 $0 \ 0 \ (N+1) \ (N+2) \ (N+3) \ (N+4) \ 0 \ 0$
 where channel N was the last channel in the previous row and $ND1X = 8$.
 To input the channel map shown in figure G20-F2(a) using $IMAP = 2$, card types GCC20 (\rightarrow p.E-89), 1-CNS (\rightarrow p.E-90) and 2-CNS would be given as shown in figure G20-F2(b).

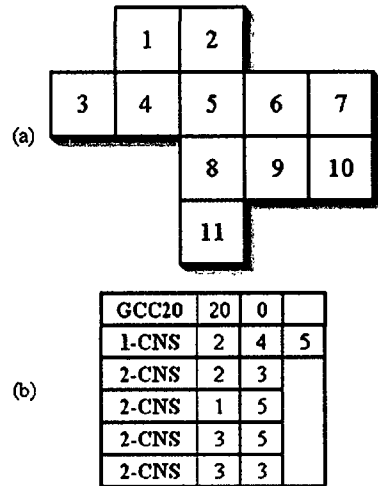


Figure G20-F2: Channel map and required cards using **IMAP = 2**

E.14.4 3-CNS: Channel map

This card is required if **IMAP = 3** on card 1-CNS (→ p.E-90).

Read: (**NTHBOX** (**ND1,ND2**), **ND1 = 1, ND1X**), **ND2 = 1, ND2X**
 Format (*)
 read from subroutine **CARD20**.

NTHBOX = Channel identification number for every channel appearing on this row of the channel numbering map. Channels are specified from left to right across the row.

Note: (1) One card of type 3-CNS (→ p.E-92) must be given for each of the **ND2X** rows in the channel numbering map. Each row of **NTHBOX** must start on a new card.

(2) Note that **ND1X** must not exceed 25.

(3) All **ND1X** columns in the row must be given a channel identification number. A zero (or blanks) may be given for columns which do not represent a channel.

(4) The **IMAP = 3** option allows the user to specify the values of the array **NTHBOX** directly. This flexibility permits the user to create and use channel maps which are not necessarily sequential.

To input the channel map of figure G20-F3(a) (the same as figure G20-F2(a) (→ p.E-91))

using **IMAP = 3** instead of **IMAP = 2** requires the cards illustrated in figure G20-F3(b).

IMAP = 3 could be used either to specify a particular numbering system or when there are two channels in the same row separated by a "zero" or "non-channel".

In the simplified method (i.e. **IPILE = 0**) channel maps as shown in figure G20-F4(a) may be required. Only **IMAP = 3** is adequate for inputting this kind of array. The cards needed are illustrated in figure G20-F4(b).

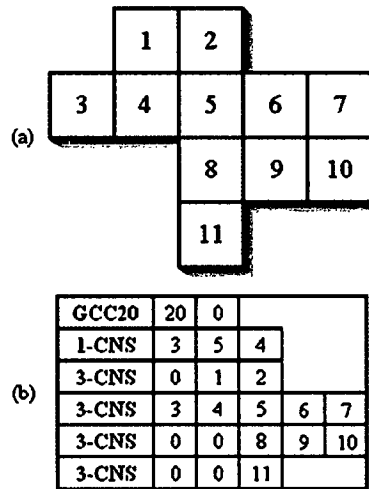


Figure G20-F3: Channel map and required cards using **IMAP = 3**

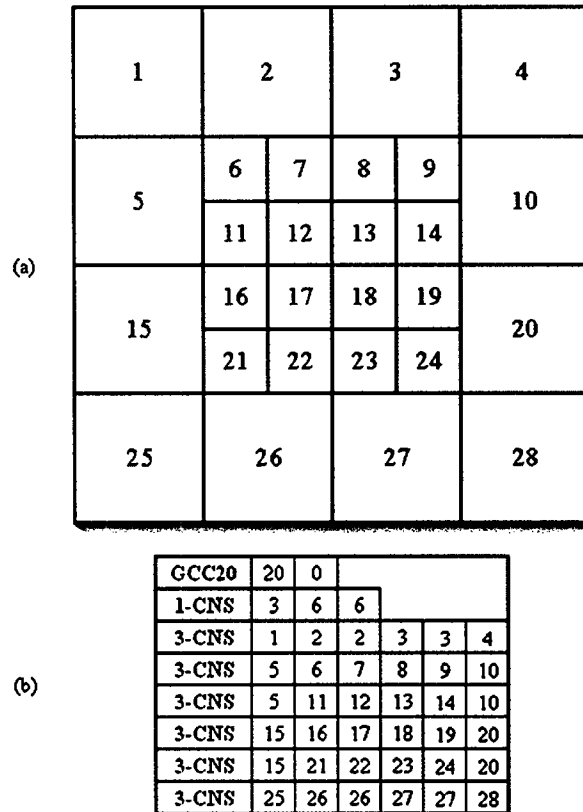


Figure G20-F4: Channel map and required cards for which only the **IMAP = 3** option will work

E.14.5 4-HF: Heat flux specification

This card is required whenever card group 20 is used.

Read: **N1, AFLUX**

Format (*)

read from subroutine **CARD20**.

- N1 = 0 Trigger to read average nodal fuel powers after rest of data (cards 48-NP ($\rightarrow p.E-132$) through 49-NP ($\rightarrow p.E-133$)). **NAX** is set to **0** and **IQP3** is set to **0**.
- = 1 Trigger to read average nodal fuel and coolant powers after rest of data (cards 48-NP ($\rightarrow p.E-132$) through 50-NP ($\rightarrow p.E-133$)). **NAX** is set to **0** and **IQP3** is set to **1**.
- > 1 Number of axial points at which heat flux profile will be given on following card 5-HF ($\rightarrow p.E-95$) (max = **30**). **NAX** is set to **N1** and **IQP3** is set to **2**.

- AFLUX = Reactor average heat flux (kW/m²). If **N1 = 0** or **1**, the value of **AFLUX** is irrelevant and may be given as zero.

Note: (1) If the value of **N1** is set to **0** or **1**, the input of the nodal power factors is post-poned and the remainder of the card may be blank.

E.14.6 5-HF: Heat flux profile

This card is required if **N1 > 1** on card 4-HF (→ p.E-94).

Read: **Y(I)**, **AXIAL(I)**, **I = 1, N1**
 Format (*)
 read from subroutine **CARD20**.

Y = Normalized axial position along channel (x/L); $0 \leq Y \leq 1.0$
AXIAL = Relative heat flux (local/average) corresponding to **Y**.

Note: (1) Both the position and the heat flux are specified as relative values with the average heatflux being supplied on card 4-HF (→ p.E-94).

(2) To input the relative axial heat flux profile illustrated in table G20-T1 and figure G20-F5 the card types 4-HF (→ p.E-94) and 5-HF have to be entered as illustrated in figure G20-F6:

| | | | | | | | | | | | |
|----------------------|-------|-------|-------|-------|-------|-------|-------|-------|-------|-------|-------|
| Rel. axial position | 0.00 | 0.05 | 0.10 | 0.15 | 0.20 | 0.25 | 0.30 | 0.35 | 0.40 | 0.45 | 0.50 |
| Rel. axial heat flux | 0.100 | 0.175 | 0.250 | 0.350 | 0.450 | 0.575 | 0.700 | 0.900 | 1.100 | 1.250 | 1.400 |
| Rel. axial position | 0.55 | 0.60 | 0.65 | 0.70 | 0.75 | 0.80 | 0.85 | 0.90 | 0.95 | 1.00 | |
| Rel. axial heat flux | 1.520 | 1.640 | 1.660 | 1.680 | 1.590 | 1.500 | 1.275 | 1.050 | 0.710 | 0.350 | |

Table G20-T1: Data for figures G20-F5 and G20-F6

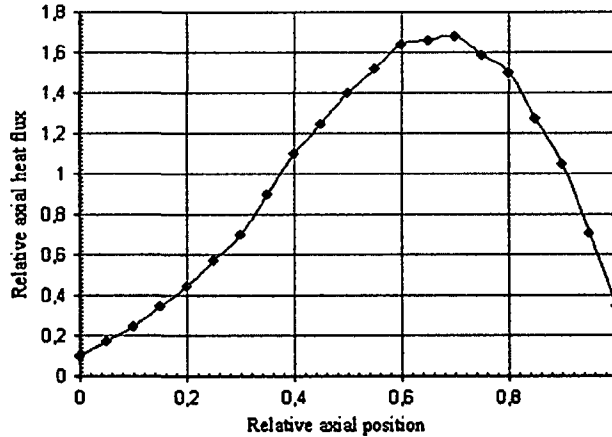


Figure G20-F5: Axial heat flux profile

| | | | | | | | | | | | | | | | | | | | | | | |
|-------------|------|-------|------|-------|------|-------|------|-------|------|-------|------|-------|------|-------|--|--|--|--|--|--|--|--|
| 4-HF | 21 | 547.0 | | | | | | | | | | | | | | | | | | | | |
| 5-HF | 0.00 | 0.100 | 0.05 | 0.175 | 0.10 | 0.250 | 0.15 | 0.350 | 0.20 | 0.450 | 0.25 | 0.575 | 0.30 | 0.700 | | | | | | | | |
| 5-HF | 0.35 | 0.900 | 0.40 | 1.100 | 0.45 | 1.250 | 0.50 | 1.400 | 0.55 | 1.520 | 0.60 | 1.640 | 0.65 | 1.660 | | | | | | | | |
| 5-HF | 0.70 | 1.680 | 0.75 | 1.590 | 0.80 | 1.500 | 0.85 | 1.275 | 0.90 | 1.050 | 0.95 | 0.710 | 1.00 | 0.350 | | | | | | | | |

Figure G20-F6: Cards of type 4-HF (→ p.E-94) and 5-HF to input the data of table G20-T1 resp. figure G20-F5

E.14.7 6-HF: Rod power factors

This card is required if $N1 > 1$ on card 4-HF (\rightarrow p.E-94).

Read: **RADIAL(I)**, $I = 1, NCHAN$

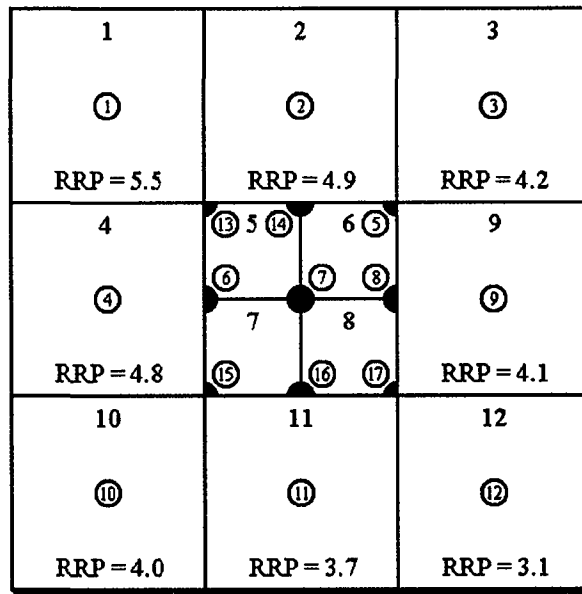
Format (*)

read from subroutine **READIN/CARD20**.

RADIAL = Relative rod power(local/average).

Note: (1) **NCHAN** = number of channels in problem. It is set to the highest value of the channel map array **NTHBOX**; see cards 1-CNS (\rightarrow p.E-90) through 3-CNS (\rightarrow p.E-92).

(2) In the simplified method (**IPILE** = 0) some subchannels are lumped together to create one channel, while others are treated as individual subchannels (see figure G20-F7). Each composite channel can be visualized as having only one rod which generates the entire power input into that channel. In order to reduce the input data, the power given to such a channel for its rod is specified here, while rods that share their power with several channels will be described on card 14-RD (\rightarrow p.E-101).



RRP= Relative rod power 5= Channel-no. ⑤ = Rod-no.

Figure G20-F7: Channel map using lumped channel configuration and relative rod powers (RRP); Note that it is assumed that the RRP-calculation has accounted for the values of **FRAC** and **HNR** (see card 10-CD (\rightarrow p.E-99)).

This system of entering the data reduces the cards required in the presentation requiring only that the lumped channel has the same identification number as its rod.

To input the relative rod power (RRP) for the configuration shown in figure G20-F7, card 6-HF should have the actual relative rod power for channels 1-4, zero for channels 5-8 and the actual values for channels 9-12, as shown below.

| | | | | | | | | | | | | |
|-------------|-----|-----|-----|-----|-----|-----|-----|-----|-----|-----|-----|-----|
| 6-HF | 5.5 | 4.9 | 4.2 | 4.8 | 0.0 | 0.0 | 0.0 | 0.0 | 4.1 | 4.0 | 3.7 | 3.1 |
|-------------|-----|-----|-----|-----|-----|-----|-----|-----|-----|-----|-----|-----|

(3) The relative rod power is calculated as the total energy added to the channel from all rods divided by the average heat flux value **AFLUX** (see card 4-HF (\rightarrow p.E-94)), the product of the channel geometry fraction **FRAC** and the number of heated rods **HNR** (see card 10-CD (\rightarrow p.E-99)); in equation form:

$$RRP = \text{TOTAL POWER TO CHANNEL} / (\text{AFLUX} \cdot \text{FRAC} \cdot \text{HNR})$$

(4) The power given to channels 5, 6, 7 and 8 from rods 5-8 and 13-17 will be specified later in card 15-RD (\rightarrow p.E-102).

E.14.8 7-MD: Miscellaneous data

This card is required whenever card group 20 is used.

Read: **Z**, **NDX**, **NDT**, **TTIME**

Format (*)

read from subroutine **CARD20**.

| | | |
|--------------|---|--|
| Z | = | Channel length (cm). |
| NDX | = | Number of axial intervals. |
| NDT | = | Number of time steps: |
| | = | 0 Steady state only. |
| | > | 0 Steady state and transient. |
| TTIME | = | Total duration of transient (s); the length of each time step is set to TTIME/NDT . |

E.14.9 8-CD: Channel Indicators

This card is required whenever card group 20 is used.

Read: **IPILE**, **NCTYPE**, **NGRID**, **NGRIDT**, **NODESF**, **NFXF**, **IFRM**, **IHTM**, **IPROP**, **NREDGL**

Format (*)

read from subroutine **CHAN**.

| | | |
|---------------|---|---|
| IPILE | = | 0 For simplified method. |
| | = | 1 For PWR with interconnected channels. |
| | = | 2 For BWR with separated channels. |
| | = | -2 For BWR with separated channels; CHF-calculation is skipped for subchannels with friction factor selector = 2 (card 10-CD (\rightarrow p.E-99)). |
| NCTYP | = | Number of channel types to be read in; controls reading of cards 10-CD (\rightarrow p.E-99) through 12-CD (\rightarrow p.E-101). |
| NGRID | = | Number of grid positions (max = 10). |
| NGRIDT | = | Number of grid types for each channel (max = 5). |
| NODESF | = | Number of radial fuel nodes including the cladding (max = 21). NODESF = NCF + NCC + 1 must hold, see card 17-FD (\rightarrow p.E-103). Note: NODESF=0 switches off the fuel rod model. In this case, the surface heat flux is specified as boundary condition for the coolant energy balance also in transient conditions. |
| NFXF | = | Number of 'forced flow' types; if not in use set to 0.0 . |
| IFRM | = | Fuel rod model: |

| | | | |
|--------|---|-----|---|
| | = | 0 | Old model. |
| | = | 1 | COBRA IIIc MIT2 new model; the MATPRO fuel rod model (old input: no centre pellet channel, dishing, Zr-oxide, equidistant radial nodes). |
| | = | 2 | PANBOX-model according [*] (old input: no dishing, Zr-oxide). |
| | = | 3 | COBRA IIIc MIT2 new model; modified MATPRO fuel rod model (new input: centre pellet channel, dishing, Zr-oxide on card 17d-FD (\rightarrow p.E-105), radial shells of equal volume (optionally equidistant radial nodes, see IOLdcb on card 17c-FD (\rightarrow p.E-104))). |
| | = | 4 | PANBOX-model according [*] (new input: centre pellet channel, dishing, Zr-oxide on card 17d-FD (\rightarrow p.E-105)). |
| IHTM | = | nxx | Indicator for rod-to-coolant heat transfer model, n (= IHTCC) specifying the heat transfer coefficient: n (= IHTCC) = 0 : COBRA-FLX. n (= IHTCC) = 1 : CARO correlation. |
| | = | n00 | Old model. |
| | = | n01 | New model for pre-CHF conditions. |
| | = | n02 | New model for pre- and post-CHF conditions, according to Bjornard and Griffith (BEEST module); not recommended. |
| | = | n03 | Model n02 but modified for post-CHF conditions (rewetting), according to Stosic; recommended option. |
| IPROP | = | nxx | Indicator for fuel rod material properties, n (= MATPRO) specifying the fuel, Zr and gap material properties: n (= MATPRO) = 0 : Original COBRA 3-C-MIT. n (= MATPRO) = 1 : MATPRO '93 (not allowed for commercial application, science only). n (= MATPRO) = 2 : Siemens-KWU fuel rod properties. |
| | = | n00 | Properties constant from input. |
| | = | n01 | U/PuO ₂ and Zr properties temperature dependent, $h_{\text{Gap}} = \text{const.}$ |
| | = | n02 | Gap heat transfer coefficient (h_{Gap}) is calculated by models. |
| | = | n03 | Gap heat transfer coefficient (h_{Gap}) is interpolated vs. temperature from CARO results. |
| NREDGL | = | 0 | Reynolds Number independent grid loss coefficients. |
| | > | 0 | Reynolds Number dependent grid loss coefficients. |

Note: (1) [*] [

]

E.14.10 9-CD: Fuel rod temperature convergence

This card is required if **NODESF > 0** and either **IFRM > 1** or **IHTM > 0** on card 8-CD (\rightarrow p.E-97).

Read: **EPSF**

Format (*)

read from subroutine **CHAN**.

EPSF = Fuel rod convergence criterion; if **EPSF** is given as zero, it is set to the []

Note: (1) If $EPSF > 0$: Additional input for iteration of heat transfer coefficient is required (see card 9-CD-1 (\rightarrow p.E-99))

E.14.11 9-CD-1: Iteration of Heat Transfer Coefficient

This card is required if $EPSF < 0$ on card 9-CD (\rightarrow p.E-98).

Read: **ACELf**

Format (*)

read from subroutine **CHAN**.

ACELf = Damping factor for iteration of heat transfer coefficient []

E.14.12 10-CD: Channel data for type I

This card is required whenever card group 20 is used.

Read: **N, J, FRAC, GAP, HNR, DR, A, B, C, D**

Format (*)

read from subroutine **CHAN**.

N = Friction indicator to select friction factor for channel (card 25-HM (\rightarrow p.E-113)); nominal value = 1, max = 4.

J = Indicator to define **A, B, C** and **D** below:

 = 1 The area and perimeters are user supplied.

 = 2 The area and perimeters are calculated from the user supplied dimensions.

FRAC = Amount by which channel area, wetted and heated perimeters and number of heated rods are to be multiplied (see below); if **FRAC > 1.0** relative rod powers will also be multiplied.

GAP = Effective rod gap for interconnection between channels; if **IPILE = 0** (card 8-CD (\rightarrow p.E-97)) this value may be given as zero since the individual gap sizes will be read in later.

HNR = Number of heated rods in fuel assembly.

DR = Diameter of heated rods (cm).

A = If **J = 1** : Channel flow area (cm²);
if **J = 2** : Number of unheated rods (e.g. control rods).

B = If **J = 1** : Channel wetted perimeter (cm);
if **J = 2** : Diameter of unheated rods (cm).

C = If **J = 1** : Channel heated perimeter (cm);
if **J = 2** : Width of square assembly (cm).

D = If **J = 1** : Not used;
if **J = 2** : Radius of channel corners (cm).

Note: (1) The values for channel area, heated and wetted perimeters and the number of heated rods are multiplied by **FRAC**. Thus, if a line of symmetry divides a channel so that it is a half channel, the data for a whole channel may be given and **FRAC** set to 0.5.

Alternatively, data for a single channel may be given and **FRAC** set to e.g. 4 to obtain the parameters for a smeared group of 4 channels. If **FRAC** is given as zero it is reset to 1.0.

(2) **GAP** is the "effective" gap between assemblies. For no internal resistance to mixing within an assembly, **GAP** can be considered as the gap between individual rods multiplied with the number of gaps. The result then is reduced according to the chosen internal resistance model.

(3) The card group 20 input method achieves considerable simplification of the input data by allowing the information for similar channels to be input only once. Two channels are of the same type if the data called for on cards 10-CD and 11-CD (→ p.E-100) is identical for both channels.

The value of **NCTYP** on card 8-CD (→ p.E-97) indicates the number of channel types in the problem. One group of cards 10-CD and 11-CD (→ p.E-100) must be provided for the first channel type and one group of cards 10-CD through 12-CD (→ p.E-101) must be present for each of the remaining channel types. The data for each channel type will then be read sequentially by type number ($I = 1, NCTYP$).

Cards 10-CD and 11-CD (→ p.E-100) describe the geometry and grid locations for channel type I while card 12-CD (→ p.E-101) specifies which channels are of this type. Since any channels which do not have their type declared specifically on a 12-CD (→ p.E-101) card are assumed to be of type 1, no 12-CD (→ p.E-101) card should be given for the first channel type. The best economy is achieved if type 1 is defined as that type which contains the majority of channels.

As an example, if **NCTYPE** = 3 on card 8-CD (→ p.E-97), the cards needed to input data for these 3 channel types are illustrated in figure G20-F8.

| | | | | | | | | | | |
|-------|-------|--------|-------|-----|------|------|--------|--------|--------|--|
| 10-CD | 1.0 | 1.0 | 1.0 | 0.0 | 1.0 | 0.44 | 0.1834 | 1.382 | 1.382 | |
| 11-CD | 1.105 | 0.4605 | 1.015 | | | | | | | |
| 10-CD | 1.0 | 1.0 | 1.0 | 0.0 | 0.85 | 0.44 | 0.2309 | 1.695 | 1.178 | |
| 11-CD | 1.105 | 0.4605 | 1.015 | | | | | | | |
| 12-CD | 2 | 6 | 9 | | | | | | | |
| 10-CD | 1.0 | 1.0 | 1.0 | 0.0 | 0.4 | 0.44 | 0.0918 | 0.9083 | 0.5496 | |
| 11-CD | 1.105 | 0.4605 | 1.015 | | | | | | | |
| 12-CD | 4 | 8 | | | | | | | | |

Figure G20-F8: The arrangement of cards 10-CD through 12-CD (→ p.E-101) to input channel data for three different channel types.

E.14.13 11-CD: Grid data for channel I

This card is required if **NGRID** > 0 on card 8-CD (→ p.E-97).

Read: **If (NREDGL > 0): CDA(L), CDB(L), CDC(L), L=1, NGRIDT**
Format (*)
read from subroutine **CHAN**.

If (NREDGL = 0): CDG(L), L = 1, NGRIDT
Format (*)
read from subroutine **CHAN**.

CDG = Single phase grid loss coefficient for each grid type.

CDA, CDB, CDC = Reynolds number dependent grid loss coefficient is $CDA + CDB * RE ** CDC$

E.14.14 12-CD: Channels making up type I

This card is required if **NCTYP** > 1 on card 8-CD (\rightarrow p.E-97) and for channels of type I with $2 \leq I \leq$ **NCTYP**.

Read: **JB(L)**, **L** = 1, 150

Format (*)

read from subroutine **CHAN**.

JB = Channel identification numbers for channels of type I.

Note: (1) The channels of type I are listed on one or more cards. The numbers up to the first zero are taken as the relevant channels. To avoid typing 150 values, input can be terminated by "/" after the first zero. The zero must be given since it acts as a trigger.

(2) Next card read is:

Card 13-CD (\rightarrow p.E-101) if **I** = **NCTYP**;

Card 10-CD (\rightarrow p.E-99) if **I** < **NCTYP**.

E.14.15 13-CD: Grid positions

This card is required if **NGRID** > 0 on card 8-CD (\rightarrow p.E-97).

Read: **GRIDXL(I)**, **IGRID(I)**, **I** = 1, **NGRID**

Format (*)

read from subroutine **CHAN**.

GRIDXL = Fractional distance up channel (x/L) at which each grid is located ($0 \leq$ **GRIDXL** \leq 1.0).

IGRID = Grid type; the coefficients for each type of grid were read in on card 11-CD (\rightarrow p.E-100).

Note: (1) If **NGRID** > 0 a list of the grids, their positions and types is required.

(2) Axial grid positions must not be identical to axial node boundaries (possibly random results of internal checks for equality).

(3) Only one spacer grid may be located in a particular axial node, to ensure correct calculation of pressure loss effect. If two or more grids are defined for the same axial node, only the **uppermost** grid becomes effective, the others are ignored.

E.14.16 14-RD: Indicators

This card is required if **IPILE** = 0 on card 8-CD (\rightarrow p.E-97).

Read: **NN11**, **NN22**, **NN33**, **NN44**, **ITMP**

Format (*)

read from subroutine **CHAN**.

NN11 = Number of cards of rod layout data to be read.

NN22 = Total number of rods.

NN33 = Number of radial fuel nodes including the cladding.

NN44 = Fuel type specification:

| | | | |
|------|---|---|--|
| | = | 1 | Cylindrical fuel only. |
| | = | 2 | Plate fuel or combination of plate and cylindrical fuel. |
| ITMP | = | | Transverse momentum coupling parameter indicator: |
| | = | 0 | FACSL and FACSLK (see card 21-GB (\rightarrow p.E-109)) are set to 1.0 for all gaps. |
| | = | 1 | FACSL and FACSLK are read in on card 21-GB (\rightarrow p.E-109) for each gap. |

Note: (1) In the simplified method (**IPILE** = 0 on card 8-CD (\rightarrow p.E-97)) the power addition to each channel from every rod must be specified for every channel which was not set as a lumped channel on card 6-HF (\rightarrow p.E-96). The cards 14-RD and 15-RD (\rightarrow p.E-102) are used to input the necessary rod data starting the read in of this data.

(2) **NN44** should be 1 if **IFRM** = 1 (card 8-CD (\rightarrow p.E-97)) because the new fuel rod model considers cylindrical geometry only.

(3) A description of the transverse momentum models available in COBRA-FLX is given in the report on COBRA IIIC/MIT-2 (MIT-EL 81-018, June 1981)

E.14.17 15-RD: Rod layout information

This card is required if **IPILE** = 0 on card 8-CD (\rightarrow p.E-97) and **NN11** > 0 on card 14-RD (\rightarrow p.E-101).

Read: **N**, **I**, **DR(I)**, **RADIA(I)**, **LR(I,L)**, **PHI(I,L)**, **L = 1, 6**

Format (*)

read from subroutine **CHAN**.

| | | | |
|-------|---|---|---|
| N | = | | Fuel rod type: |
| | = | 1 | Indicates rod fuel. |
| | = | 2 | Indicates plate fuel. |
| I | = | | Identification number of rod. |
| DR | = | | Rod diameter (cm). |
| RADIA | = | | Relative rod power (rod power/average rod power). |
| LR | = | | Adjacent channel number. |
| PHI | = | | Fraction of the rod power to that channel. |

Note: (1) This block is repeated 6 times (**L** = 1, 6).

(2) If **NN11** on card 14-RD (\rightarrow p.E-101) is greater than zero, a total of **NN11** cards of type 15-RD must be provided. Each card gives rod type, identification number, diameter, relative power and adjacent channel numbers with fraction of rod power going to that channel for one rod. One card for every rod considered is required.

E.14.18 16-FD: Fuel temperature data

This card is required if **NODESF > 0** on card 8-CD (\rightarrow p.E-97).

Read: **KF(I)**, **CF(I)**, **RF(I)**, **DF(I)**, **KC(I)**, **CC(I)**, **RC(I)**, **TC(I)**, **HG(I)**, **I = 1**,
NN44

Format (*)

read from subroutine **CHAN**.

| | | |
|----|---|--|
| KF | = | Fuel thermal conductivity (W/(m K)). |
| CF | = | Fuel specific heat (kJ/(kg K)). |
| RF | = | Fuel density (kg/dm ³). |
| DF | = | Pellet diameter (cm). |
| KC | = | Clad thermal conductivity (W/(m K)). |
| CC | = | Clad specific heat (kJ/(kg K)). |
| RC | = | Clad density (kg/dm ³). |
| TC | = | Clad thickness (cm). |
| HG | = | Fuel to clad heat transfer coefficient (kJ/(h cm ² K)). |

Note: (1) Fuel temperature data must be given even when **IPROP > 0** on card 8-CD (\rightarrow p.E-97).

(2) Card type 16-FD gives the thermal properties of the fuel and clad. Whenever **NODESF > 0** (card 8-CD (\rightarrow p.E-97)) a total of **NN44** cards (card 14-RD (\rightarrow p.E-101)) of type 16-FD are required. If **NN44 = 2**, the first card gives data for the cylindrical fuel and can be blank if no cylindrical fuel is used. The second card gives data for the plate fuel only.

(3) All user supplied quantities should apply to the "hot" case since no adjustment is made for thermal expansion.

E.14.19 17-FD: Fuel thermal properties

This card is required if **NODESF > 0** and if **IFRM > 0** on card 8-CD (\rightarrow p.E-97).

Read: **NCF**, **NCC**, **THG**

Format (*)

read from subroutine **CHAN**.

| | | |
|-----|---|--|
| NCF | = | Number of radial fuel cells (if NCF is negative ABS(NCF) is used and NCF-1 relative radii are read in by following card 17a-FD (\rightarrow p.E-104)). |
| NCC | = | Number of radial clad cells. |
| THG | = | Gap thickness (cm) (must be greater than 0.0). |

Note: (1) **NODESF = NCF + NCC + 1** (see card 8-CD (\rightarrow p.E-97)) must hold.

(2) **THG** must be non-zero.

E.14.20 17a-FD: Fuel rod model (geometry)

This card is required if $NCF < 0$ on card 17-FD ($\rightarrow p.E-103$).

Read: $RDread(I)$, $I = 1$, $NCF-1$

Format (*)

read from subroutine **CHAN**.

$RDread = NCF-1$ relative radii to divide fuel pellet radially = $(r_1 - r_0)/(r_{Pellet} - r_0)$;
for r_0 see card 17b-FD ($\rightarrow p.E-104$) resp. card 17d-FD ($\rightarrow p.E-105$).

E.14.21 17b-FD: Fuel rod model (geometry)

This card is required if $IFRM = 2$ on card 8-CD ($\rightarrow p.E-97$).

Read: $R0$

Format (*)

read from subroutine **CHAN**.

$R0 =$ Pellet center channel radius r_0 (cm).

E.14.22 17c-FD: Fuel rod model (model and data selection)

This card is required if $IFRM = 3$ or 4 on card 8-CD ($\rightarrow p.E-97$).

Read: $IOLdcb$, $ICOrad$, $IUSca$, $IUSox$, $ICAgas$, $IUScax$, $IUScra$

Format (*)

read from subroutine **CHAN**.

$IOLdcb = 1$ · For both, the modified new model and the PANBOX-model the pellet is radially divided into **NCF** (see card 17-FD ($\rightarrow p.E-103$)) shells of equal volumes.
· If $IFRM = 3$ average temperatures between two nodes at r_1 and r_2 are calculated by integration between r_1 and r_2 .
· Heat flux printed out is related to rod diameter **DR** (see card 15-RD ($\rightarrow p.E-102$)) although coolant heat-up is calculated from real heat flux using calculated fuel rod geometry if appropriate.

$IOLdcb = 0$ · This option is included only for strict consistency to older COBRA-FLX versions and should not be used for application purposes.
· For the PANBOX-model ($IFRM = 2$ or 4) the pellet is radially divided into **NCF** (see card 17-FD ($\rightarrow p.E-103$)) shells of equal volumes. For the new model ($IFRM = 1$ or 3) the pellet is divided into nodes with equal distances.
· If $IFRM = 1$ or 3 average temperatures between two nodes at r_1 and r_2 are calculated via $T_{av} = (T_1 + T_2)/2$.
· Heat flux printed out is related to rod diameter **DR** (see card 15-RD ($\rightarrow p.E-102$)). Fuel rod data **DF**, **TC** (see card 16-FD ($\rightarrow p.E-103$)) and **THG** (see card 17-FD ($\rightarrow p.E-103$)) should match **DR**, otherwise coolant heat-up is not consistent with fuel rod radial temperature distribution and heat sources.

$ICOrad =$ Correct fuel pellet and cladding diameter by thermal expansion, yes (1) or no (0). Note that use of this option might increase computation time noticeably.

| | | |
|--------|---|---|
| IUSca | = | Use CARO fuel rod results read from file CAR-INP (\rightarrow p.E-62), yes (1) or no (0). |
| IUSox | = | Correct clad-to-coolant heat transfer for oxide thermal resistance, yes (1) or no (0). |
| ICAgas | = | Calculate fuel-to-clad-gap gas pressure after each time step, yes (1) or no (0). |
| IUScax | = | Use CARO axial heat flux profile, yes (1) or no (0); only for comparison to CARO results. |
| IUScra | = | Use CARO radial heat flux profile, yes (1) or no (0); only for comparison to CARO results. |

E.14.23 17d-FD: Fuel rod model (geometry)

This card is required if **IFRM = 3 or 4** on card 8-CD (\rightarrow p.E-97).

Read: **R0, HOPel, HDish, RDish, IDish, CPel, DPel, DMKorr, DMKorc, Oxid**
Format (*)
read from subroutine **CHAN**.

| | | |
|--------|---|---|
| R0 | = | Pellet center channel radius r_0 (cm). |
| HOPel | = | Pellet height (cm). |
| HDish | = | Center depth of dishing (cm). |
| RDish | = | Dishing radius (cm). |
| IDish | = | 0 No dishing. |
| | = | 1 One-sided dishing only. |
| | = | 2 Both-sided dishing. |
| CPel | = | Width of pellet shoulder (cm). |
| DPel | = | Height of pellet shoulder (cm). |
| DMKorr | = | Non-reversible diametral correction of pellet (cm). |
| DMKorc | = | Non-reversible diametral correction of cladding (cm). |
| Oxid | = | ZrO thickness(cm). |

Note: (1) Usage of dishing (**IDish, HDish and RDish > 0**) and/or shoulders (**CPel and DPel > 0**) increases run time considerably because of the iteration of the radial subdivision of the fuel pellet.

E.14.24 18-FD: Fuel rod model (fuel material data)

This card is required if **NODESF > 0, IPROP > 0** and **MATPRO = 0** on card 8-CD (\rightarrow p.E-97).

Read: **FTD, FPuO2**
Format (*)
read from subroutine **CHAN**.

| | | |
|-------|---|--|
| FTD | = | Fraction of theoretical density of fuel. |
| FPuO2 | = | PuO ₂ fraction by volume (m ³ /m ³). |

E.14.25 18a-FD: Fuel rod model (fuel material data)

This card is required if **NODESF > 0**, **IPROP > 0** and **MATPRO = 1** on card 8-CD (→ p.E-97).

Read: **FTD**, **FPuO2**, **O2pmx**, **Burn**, **FMolt**

Format (*)

read from subroutine **CHAN**.

| | | |
|-------|---|--|
| FTD | = | Fraction of theoretical density of fuel. |
| FPuO2 | = | PuO ₂ fraction by volume (m ³ /m ³). |
| O2pmx | = | O/M-ratio of nonstoichiometric fuel. |
| Burn | = | Average burnup (MWd/kgU). |
| FMolt | = | Fraction of molten fuel in pellet (m ³ /m ³). |

Note: (1) Also in the case of PANBOX (coupled system) calculations with use of nodal burnup values in evaluation of material properties, the input **BURN** is employed for initialisations. It therefore must have a meaningful value (MWd/kgU).

E.14.26 18b-FD: Fuel rod model (Fuel material data)

This card is required if **NODESF > 0**, **IPROP > 0** and **MATPRO = 2** on card 8-CD (→ p.E-97).

Read: **FTD**, **FPuO2**, **FGd2O3**, **O2pmx**, **Burn**

Format (*)

read from subroutine **CHAN**.

| | | |
|--------|---|--|
| FTD | = | Fraction of theoretical density of fuel. |
| FPuO2 | = | PuO ₂ fraction by volume (m ³ /m ³). |
| FGd2O3 | = | Mass fraction of Gd ₂ O ₃ (kg/kg). |
| O2pmx | = | O/M-ratio of nonstoichiometric fuel. |
| Burn | = | Average burnup (MWd/kgU). |

Note: (1)[

]

(2) Also in the case of PANBOX (coupled system) calculations with use of nodal burnup values in evaluation of material properties, the input **BURN** is employed for initialisations. It therefore must have a meaningful value (MWd/kgU).

E.14.27 19-FD: Fuel rod model (gap gas data)

This card is required if **NODESF > 0**, **IPROP = 2** and **MATPRO = 0** on card 8-CD (\rightarrow p.E-97).

Read: If **ICAgas = 0** (on card 17c-FD (\rightarrow p.E-104)): **BURN**, **CPR**, **EXPR**, **FPRESS**, **GRGH**, **GMIX(1)**, **GMIX(2)**, **GMIX(3)**, **GMIX(4)**, **PGAS**

Format (*)

read from subroutine **CHAN**.

If **ICAgas = 1** (on card 17c-FD (\rightarrow p.E-104)): **BURN**, **CPR**, **EXPR**, **FPRESS**, **GRGH**, **GMIX(1)**, **GMIX(2)**, **GMIX(3)**, **GMIX(4)**, **PGAS**, **TGAS**, **VOLRST**

Format (*)

read from subroutine **CHAN**.

| | | |
|----------|---|---|
| BURN | = | Burnup (MWd/kgU). |
| CPR | = | Coefficient of fuel pressure on clad for gap conductance model. |
| EXPR | = | Exponent for fuel pressure on clad. |
| FPRESS | = | Fuel pressure on clad for gap conductance (bar). |
| GRGH | = | RMS of fuel and clad roughness (cm); set to $1.5 \cdot 10^{-5}$ microinches if given as zero. |
| GMIX (1) | = | Helium fraction by mole (mol/mol). |
| GMIX (2) | = | Argon fraction by mole (mol/mol). |
| GMIX (3) | = | Krypton fraction by mole (mol/mol). |
| GMIX (4) | = | Xenon fraction by mole (mol/mol). |
| PGAS | = | Pressure of gas mixture in gap (bar). |
| TGAS | = | Temperature of gas mixture in gap ($^{\circ}$ C). |
| VOLRST | = | Total volume of fuel rod upper and lower plenum (cm ³) |

Note: (1) The four elements of **GMIX** must sum up to 1.0.

(2) Also in the case of PANBOX (coupled system) calculations with use of nodal burnup values in evaluation of material properties, the input **BURN** is employed for initialisations. It therefore must have a meaningful value (MWd/kgU).

E.14.28 19a-FD: Fuel rod model (gap gas data)

This card is required if **NODESF > 0**, **IPROP = 2** and **MATPRO = 1** or **2** on card 8-CD (\rightarrow p.E-97).

Read: **BURN**, **K**, **GrgH**, **GrgF**, **A**, **GMIX(1)**, **GMIX(2)**, **GMIX(3)**, **GMIX(4)**, **GMIX(5)**, **PGAS**, **TGAS**

Format (*)

read from subroutine **CHAN**.

| | | |
|------|---|--|
| BURN | = | Burnup (MWd/kgU). |
| K | = | Weighting factor of clad and fuel roughness. |
| GrgH | = | RMS of clad roughness (cm); set to $1.5 \cdot 10^{-5}$ microinches if given as zero. |

| | | |
|----------|---|--|
| GrgF | = | RMS of fuel roughness (cm); set to $1.5 \cdot 10^{-5}$ microinches if given as zero. |
| A | = | Factor for relocation. |
| GMIX (1) | = | Helium fraction by mole (mol/mol). |
| GMIX (2) | = | Argon fraction by mole (mol/mol). |
| GMIX (3) | = | Krypton fraction by mole (mol/mol). |
| GMIX (4) | = | Xenon fraction by mole (mol/mol). |
| GMIX (5) | = | Nitrogen fraction by mole (mol/mol). |
| PGAS | = | Pressure of gas mixture in gap (bar). |
| TGAS | = | Temperature of gas mixture in gap (°C). |

Note: (1) Also in the case of PANBOX (coupled system) calculations with use of nodal burnup values in evaluation of material properties, the input BURN is employed for initialisations. It therefore must have a meaningful value (MWd/kgU).

E.14.29 19b-FD: Fuel rod model (heat transfer coefficient)

This card is required if IHTCC = 1 on card 8-CD (→ p.E-97)

Read: **CHTcc**

Format (*)

read from subroutine **CHAN**.

| | | |
|-------|---|--|
| CHTcc | = | Coefficient for heat transfer model according to CARO heat transfer calculation. |
|-------|---|--|

E.14.30 20-GB: Effective rod gap

This card is required if IPILE = 0 on card 8-CD (→ p.E-97).

Read: **GAPREC (I)**, I = 1, **NK**

Format (*)

read from subroutine **CHAN**.

| | | |
|--------|---|---|
| GAPREC | = | Effective rod gap for interconnection between channels. |
|--------|---|---|

*Note: (1) **NK** is the total number of gap interconnections.*

(2) In order to specify a gap for each boundary the gaps are entered in the same order as the boundaries are established. In general the boundaries are established by going from left to right in each row and from top to bottom between two consecutive rows. As an example consider the channel map of figure G20-F9 and the resulting channel pair - boundary number combinations of table G20-T2.

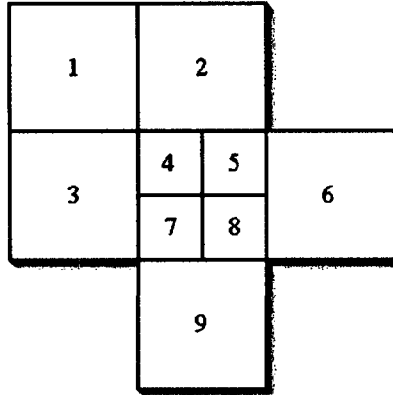


Figure G20-F9: Channel map on which table G20-T2 is based

| Channel pair making up boundary | | | | | | | | | | | | | |
|---------------------------------|-----|-----|-----|-----|-----|-----|-----|-----|-----|-----|-----|-----|-----|
| 1-2 | 1-3 | 2-4 | 2-5 | 3-4 | 4-5 | 5-6 | 4-7 | 5-8 | 3-7 | 7-8 | 8-6 | 7-9 | 8-9 |
| 1 | 2 | 3 | 4 | 5 | 6 | 7 | 8 | 9 | 10 | 11 | 12 | 13 | 14 |
| Boundary number | | | | | | | | | | | | | |

Table G20-T2: Channel pair - boundary number combinations based on channel map G20-F9

E.14.31 21-GB: Transverse momentum coupling parameters

This card is required if **IPILE = 0** on card 8-CD (→ p.E-97) and **ITMP = 1** on card 14-RD (→ p.E-101).

Read: **FACSL(I)**, **FACSLK(I)**, **I = 1, NK**
 Format (*)
 read from subroutine **CHAN**.

- FACSL** = Coupling parameter for gap I (multiplier to SL (→ p.E-116)). May be set equal to the ratio of the number of inter-rod gaps at the boundary between the two regions separated by gap I, divided by the number of rows separating the centroids of the two inter-connected regions.
- FACSLK** = Second type of coupling parameter (multiplier to KIJ (→ p.E-116)). May be set equal to the number of inter-rod gaps at the boundary of the two regions separated by gap I.

Note: (1) **NK** is the total number of gap interconnections.

(2) If **IPILE = 0** on card 8-CD (→ p.E-97) and **ITMP = 1** on card 14-RD (→ p.E-101) cards of type 21-GB are required to provide the transverse momentum coupling parameter for each boundary. These parameters should appear in the same order as the boundaries are established.

(3) The suggestions given in the descriptions above are for use of the Weisman approach for transverse momentum modeling. Alternatively, the Chiu approach could be used. See the written COBRA IIIC/MIT-2-Manual Section I.6 for description of both methods. **FACSL** corresponds to $(Ng/Nr)_{ij}$ and **FACSLK** corresponds to $(Nr)_{ij}$.

E.14.32 22-GB: PWR half-boundaries

This card is required if **IPILE = 1** on card 8-CD (\rightarrow p.E-97).

Read: **II(L), JJ(L), L = 1, N**
Format (*)
read from subroutine **CHAN**.

- II = II(L) and JJ(L) are the channel identification numbers which define the L-th "half-boundary."
- JJ = II(L) and JJ(L) are the channel identification numbers which define the L-th "half-boundary."

Note: (1) Card 22-GB should be used whenever **IPILE = 1**. This card contains the channel pairs which define half-boundaries. A half-boundary is any channel boundary cut by a line of symmetry. Figure G20-F10 shows a channel map in which half-boundaries are specified by the channel pairs 1 and 5, 5 and 8, 8 and 10 (Note that only half of the channel map is numbered since only one half will be analyzed by the code). If there are no half-boundaries in the problem, a blank card is still required.

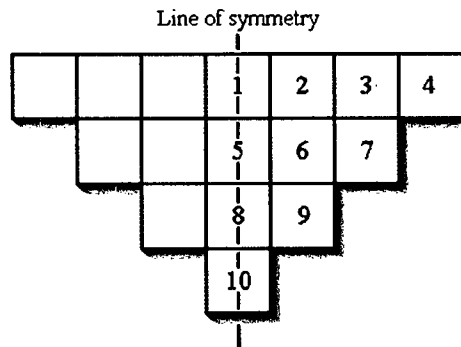


Figure G20-F10: Channel map with half-boundaries defined by channel pairs (1;5), (5;8) and (8;10)

- (2) The list of half-boundaries is terminated by a zero (**II(N) = 0**). If the list is finished at the end of a card, a blank card should follow to provide the zero-trigger.
- (3) If **IPILE = 0** the true rod spacing should have been set using card type 20-GB (\rightarrow p.E-108).

E.14.33 23-HM: Hydraulic model Indicators

This card is required whenever card group 20 is used.

Read: **N1, N2, N3, N4, N5, N6, N7, N8, N9, ITAF**
Format (*)
read from subroutine **MODEL**.

- N1 = Mixing indicator:
- = 0 **B = W/(G*S) = 0.02.**

| | | | |
|------|---|----|---|
| | = | 1 | $B = W/(G*S) = ABETA * RE^{**}BBETA.$ |
| | = | 2 | $B = W/(G*D) = ABETA * RE^{**}BBETA.$ |
| | = | 3 | The new mixing model is used. |
| N2 | = | . | Single phase friction indicator. |
| N3 | = | | Two phase friction indicator. |
| N4 | = | | Void indicator. |
| N5 | = | | Inlet flow indicator. |
| N6 | = | | Parameter indicator. |
| N7 | = | | Iteration indicator. |
| N8 | = | | Physical property indicator. |
| N9 | = | | Coupling parameter in the mixing term of the energy equation. |
| ITAF | > | 0 | Select KWU steamtables and use fluid properties for operating pressure (see also card GCC1 ($\rightarrow p.E-8$)). |
| | = | -1 | Use this option if other fluid properties than that of liquid water are desired. The fluid properties have to be specified with card group 1 ($\rightarrow p.E-8$) before starting the card group 20 input. |

Note: (1) COBRA-FLX contains a preset hydraulic model with many optional variations. Card 23-HM contains the indicators which select the various options. If all variables **N1 - N9** are zero, (i.e. a blank card) the preset model is used unchanged and the next card read will be card 36-OC ($\rightarrow p.E-127$).

(2) The parameters **N2 - N9** are merely "yes-no"-triggers for the hydraulic model options. Any value given greater than zero indicates that a particular option will be used and that the appropriate cards of input will be provided. Since no other significance is attached to the values of **N2 - N9**, only the values **0** and **1** should be used to avoid confusion.

(3) The Beus mixing model is described in the report on COBRA IIIC/MIT-2 (MIT-EL 81-018, June 1981), Section II.2.g.1.

(4) The preset model is defined in the following card descriptions.

(5) **N9 = 0** means that no coupling parameter will be used.

E.14.34 24-HM: Mixing model

This card is required if **N1 = 1** or **2** on card 23-HM ($\rightarrow p.E-110$).

Read: **ABETA**, **BBETA**

Format (*)

read from subroutine **MODEL**.

ABETA = See card 23-HM ($\rightarrow p.E-12$).

BBETA = See card 23-HM ($\rightarrow p.E-12$).

Note: (1) If **N1 = 0**, then **ABETA = 0.02**, **BBETA = 0.0** and $W/(G*S) = ABETA*(RE^{**}BBETA)$.

(2) Thermal conduction between channels is suppressed for all **N1**.

- (3) *W* is the mixing rate,
RE is an average Reynolds number for the gap,
S is the gap width,
D is an average hydraulic parameter,
G is the mass flux.

E.14.35 24-HM-1: Mixing model

This card is required if *N1* = -1 or -2 on card 23-HM (→ p.E-110).

Read: **NBETA**

Format (*)

read from subroutine **MODEL**.

NBETA = Number of different mixing gap types.

E.14.36 24-HM-2: Mixing model

This card is required if *N1* = -1 or -2 on card 23-HM (→ p.E-110).

Read: **ABETA**, **BBETA**

Format (*)

read from subroutine **MODEL**.

ABETA = See card 23-HM (→ p.E-12).

BBETA = See card 23-HM (→ p.E-12).

Note: (1) Repeat this card **NBETA** times (see card 24-HM-1 (→ p.E-112)); except for the first repetition card 24-HM-3 (→ p.E-112) is required.

E.14.37 24-HM-3: Mixing model

This card is required if *N1* = -1 or -2 on card 23-HM (→ p.E-110) and if card 24-HM-2 (→ p.E-112) has already been read the second time.

Read: **JBSTOR** (150)

Format (*)

read from subroutine **MODEL**.

JBSTOR = Numbers of gaps to which **ABETA** and **BBETA** (see card 24-HM (→ p.E-111)) are assigned.

Note: (1) See also card 24-HM-2 (→ p.E-112); the read may be terminated by a slash. All gaps not enumerated explicitly are assigned the values of **ABETA** and **BBETA** first read.

E.14.38 25-HM: Single phase friction model

This card is required if $N2 > 0$ on card 23-HM (\rightarrow p.E-110).

Read: **NVISCW**, **AA(N)**, **BB(N)**, **CC(N)**, $N = 1, 4$

Format (*)

read from subroutine **MODEL**.

| | | | |
|--------|---|---|--|
| NVISCW | = | 1 | Wall viscosity correction to the single phase friction factor is required. |
| | = | 0 | Wall viscosity correction to the single phase friction factor is not required. |
| AA(1) | < | 0 | Selects Lehmann friction factor correlation. |
| AA | = | | The single phase friction factor is calculated as $AA*(RE**BB)+CC$, where RE is the Reynolds number. |
| BB | = | | The single phase friction factor is calculated as $AA*(RE**BB)+CC$, where RE is the Reynolds number. |
| CC | = | | The single phase friction factor is calculated as $AA*(RE**BB)+CC$, where RE is the Reynolds number. |

Note: (1) Up to four sets of constants may be specified, one for each friction type.

(2) The friction factor defined by **AA(N)**, **BB(N)** and **CC(N)** is applied to the channels with that value of **N** on card 11-CD (\rightarrow p.E-100). If all channels have the same friction factor, **N** is given as **1** on card 10-CD (\rightarrow p.E-99) for all channel types and only **AA(1)**, **BB(1)** and **CC(1)** are given.

(3) If $N2 = 0$, **NVISCW** is set to **0** and the smooth tube friction factor is used, i.e. **AA = 0.184**, **BB = 0.2** and **CC = 0.0** for all $N = 1, 4$.

(4) If $AA(1) < 0$, $|AA(1)|$ is the roughness for the Lehmann friction correlation (μ m).

E.14.39 26-HM: Two-phase friction model

This card is required if $N3 > 0$ on card 23-HM (\rightarrow p.E-110).

Read: **J4**

Format (*)

read from subroutine **MODEL**.

| | | | |
|----|---|---|---|
| J4 | = | | Two-phase friction multiplier: |
| | = | 0 | Homogeneous model. |
| | = | 1 | Armand model. |
| | = | 2 | Baroczy model. |
| | = | 3 | Martinelli-Nelson-Jones model. |
| | = | 5 | Polynomial in quality, coefficients on card 27-HM (\rightarrow p.E-114). |

Note: (1) If $N3 = 0$, **J4** is set to **0**.

E.14.40 27-HM: Two-phase friction polynomial

This card is required if **J4 = 5** on card 26-HM (\rightarrow p.E-113).

Read: **NF**, **AF(L)**, **L = 1**, **NF**

Format (*)

read from subroutine **MODEL**.

NF = Number of terms in polynomial (max = 7).

AF = Polynomial coefficients.

Note: (1) If the **J4 = 5** option is selected (see card 26-HM (\rightarrow p.E-113)), the two-phase friction multiplier will be calculated as:

$$\sum_{k=1}^{NF} (AF(k) \cdot x^{k-1})$$

where **x** = quality ($0 \leq x \leq 1$).

E.14.41 28-HM: Void fraction model

This card is required if **N4 > 0** on card 23-HM (\rightarrow p.E-110).

Read: **J2**, **J3**, **J8**

Format (*)

read from subroutine **MODEL**.

J2 = Subcooled void indicator:
 = 0 No subcooled void.
 = 1 Levy subcooled void correlation.
 = 2 Saha-Zuber subcooled void correlation.

J3 = Slip ratio indicator:
 = 0 Slip ratio is set to 1.
 = 1 Armand slip ratio correlation.
 = 2 Smith slip ratio correlation.
 = 5 Slip ratio given (on card 29-HM (\rightarrow p.E-115)).
 = 6 Void fraction as a polynomial in quality, coefficients given on card 29-HM (\rightarrow p.E-115).
 = 7 Zuber-Findlay bulk void model.

J8 = Subcooled boiling profile fit.
 Note: This will only be effective in combination with **J2 > 0**.
 = 0 Levy profile fit.
 = 1 Zuber-Staub profile fit.
 = 2 Saha-Zuber profile fit.

Note: (1) If **N4 = 0**, **J2** and **J3** are both set to 0.

E.14.42 29-HM: Void fraction polynomial coefficients or slip ratio specification

This card is required if **J3 = 5** or **6** on card 28-HM (\rightarrow p.E-114).

Read: **NV**, **AV(L)**, **L = 1**, **NV**

Format (*)

read from subroutine **MODEL**.

NV = Number of terms in polynomial (max = 7).

AV = Polynomial coefficients.

Note: (1) For **J3 = 5**, **NV** should be set to 1 and only one value of **AV** read in. The slip ratio is taken as **AV(1)**.

(2) For **J3 = 6**, up to 7 values of **AV** may be read in and the void fraction is calculated as a polynomial in **x**, namely:

$$\sum_{v=1}^{NV} (AV(v) * x^{*(v-1)})$$

where **x** = quality ($0 \leq x \leq 1$).

E.14.43 30-HM: Inlet flow model

This card is required if **N5 > 0** on card 23-HM (\rightarrow p.E-110).

Read: **IG**

Format (*)

read from subroutine **MODEL**.

IG = Inlet flow indicator:
 = 0 Same inlet mass velocity for all channels.
 = 1 Inlet mass velocities for channels calculated to give same inlet pressure gradient.
 = 2 Inlet mass velocities given on cards of type 31-HM (\rightarrow p.E-115).

Note: (1) If **N5 = 0**, **IG** is set to 0.

E.14.44 31-HM: Inlet flow distribution

This card is required if **IG = 2** on card 30-HM (\rightarrow p.E-115).

Read: **FINLE(I,1)**, **I = 1**, **NCHAN**

Format (*)

read from subroutine **MODEL**.

FINLE = Inlet mass velocity ratio for each channel (local/average). One value is required for every channel, given in the same order as the channels are numbered.

E.14.45 32-HM: Parameters

This card is required if N6 > 0 on card 23-HM (→ p.E-110).

Read: **NCHF, KIJ, FTM, SL, THETA**

Format (*)

read from subroutine **MODEL**.

| | | |
|-------|---|---|
| NCHF | = | CHF correlation indicator: |
| | = | 0 No CHF correlation done. |
| | = | 1 The B and W-2 correlation. |
| | = | 2 The W-3 correlation. |
| | = | 3 The Hench-Levy correlation. |
| | = | 4 The CISE-4 correlation. |
| | = | 6 [] |
| | = | 7 [] |
| | = | 8 [] |
| | = | 10 [] |
| | = | 11 [] |
| | = | 12 [] |
| | = | 13 [] |
| | = | 14 [] |
| | = | 15 [] |
| | = | 16 [] |
| | = | 17 [] |
| | = | 23 [] |
| | = | 33 [] |
| KIJ | = | Cross-flow resistance coefficient, k. |
| FTM | = | Turbulent momentum factor, f_t . |
| SL | = | Transverse momentum factor, S/L. |
| THETA | = | Inclination of channel to vertical / [Degrees]. |

Note: (1) If **N6 = 0**, **NCHF** is set to 0, **KIJ** to 0.0, **FTM** to 0.0 and **THETA** to 0.0 (i.e. vertical).

(2) If **NCHF = 5** then **IHTM** on card 8-CD (→ p.E-97) must equal 2.

(3) If **NCHF = 13, 23, 33** additionally cards 32g-HM-2 (→ p.E-122), 32g-HM-3 (→ p.E-122) and 32g-HM-4 (→ p.E-122) are required.

- = 1
- = 2
- = 12
- = 3
- = 13
- = 4
- = 14
- = 5
- = 6
- = 7
- = 16
- = 17
- = 18
- = 19
- = 8
- = 9
- = 10
- = 15
- = 20
- = 11

*Note: (1) If $IRGw < 0$: Additional information of hottest subchannel is required (cf. card 32d-HM-2
(→ p.E-120)).*

E.14.50 32d-HM-1: CHF correlation input: non-linear profile, spacer grid and cold-wall factor

This card is required if **NCHF = 12** on card 32-HM (→ p.E-116).

Read: **NNonF12, NSPf12, NCWf12**

Format (3110)

read from subroutine **MODEL**.

| | | | |
|---------|---|-----|---|
| NNonF12 | = | | Select Non-uniform heat flux profile correction correlations: |
| | = | 0 | none |
| | = | 1 |] |
| | = | 2 | |
| | = | 3 | |
| | = | 4/5 | |
| | = | | |
| | = | 6 | |
| | = | 7 | |
| | = | 8 | |
| | = | 9 | |
| | = | | |
| NSPf12 | = | | Select spacer correction factor correlations: |
| | = | 0 | none |
| | = | 1/2 |] |
| | = | | |
| | = | 3 | |
| | = | 4 | |
| | = | | |
| NCWf12 | = | | Select cold wall correction factor correlations: |
| | = | 0 | none |
| | = | 1 | [|
| | | |] |

E.14.51 32d-HM-2: CHF correlation input: hot channel data

This card is required if $NCHF = 12$ on card 32-HM ($\rightarrow p.E-116$) and if $IRGw$ ($\rightarrow p.E-117$) (on 32d-HM ($\rightarrow p.E-117$)) < 0 .

Read: $FRadF12$, $FGf12$, $AoneSC$, $PwoneSC$, $PoneSC$, $TrSC$
 Format (6F10.5)
 read from subroutine **MODEL**.

| | | |
|-----------|---|---|
| $FRadF12$ | = | Average radial power factor of the rods around the hot-channel. |
| $FGf12$ | = | Mass velocity factor of hot-channel compared to the average bundle mass velocity. |
| $AoneSC$ | = | Hot-channel flow area (mm^2). |
| $PwoneSC$ | = | Hot-channel wetted perimeter (mm). |
| $PoneSC$ | = | Hot-channel heated perimeter (mm). |
| $TrSC$ | = | Ratio of maximum to average radial heat-flux factor of rods around the hot-channel. |

E.14.52 32e-HM: CHF correlation input: selection of characteristic diameter

This card is required if $NCHF = 12$ on card 32-HM ($\rightarrow p.E-116$) and if $IRGw$ ($\rightarrow p.E-117$) (on 32d-HM ($\rightarrow p.E-117$)) = 1, 8, 9, 10, 11, 15, 19 or 20.

Read: If $IRGw$ ($\rightarrow p.E-117$) = 1: $IDMR(1)$, $IDMR(2)$, $IDMR(3)$
 Format (3I10)
 read from subroutine **MODEL**.

If $IRGw$ ($\rightarrow p.E-117$) = 8-11,15,19,20: $IDMR(1)$
 Format (I10)
 read from subroutine **MODEL**.

| | | |
|---------------|---|--|
| $IDMR(1...3)$ | = | Specifies characteristic diameters for CHF-correlation and look-up table application: |
| | = | 1 Use input value(s) on card 32e-HM-1 ($\rightarrow p.E-121$) as characteristic diameters. |
| | = | 0 Use equivalent diameter based on wetted perimeter. |
| | < | 0 Use equivalent diameter based on wetted perimeter. |

E.14.53 32e-HM-1: CHF correlation input: input of characteristic diameter

This card is required if **NCHF = 12** on card 32-HM (\rightarrow p.E-116), if **IDmr(1...3)** (\rightarrow p.E-120) = 1 (respectively, cf. Card 32e-HM (\rightarrow p.E-120)) and if **IRGw** (\rightarrow p.E-117) (on 32d-HM (\rightarrow p.E-117)) = 1, 8, 9, 10, 11, 15, 19 or 20.

Read: If **IRGw** (\rightarrow p.E-117) = 1: **DCHAR(1)**, **DCHAR(2)**, **DCHAR(3)**

Format (3F10.5)

read from subroutine **MODEL**.

If **IRGw** (\rightarrow p.E-117) = 8-11,15,19,20: **DCHAR(1)**

Format (F10.5)

read from subroutine **MODEL**.

DCHAR(1..3) = Characteristic diameter(s) (mm) for each of the three boiling regimes [] **IRGw** (\rightarrow p.E-117) = 1) resp. **DCHAR(1)** [], one of the [] or the W3 CHF correlation is selected (**IRGw** (\rightarrow p.E-117) = 8, 9, 10, 11, 15, 19 or 20).

E.14.54 32f-HM-1: CHF correlation input: grid factor for []

This card is required if **NCHF = 12** on card 32-HM (\rightarrow p.E-116) and if **IRGw** (\rightarrow p.E-117) (on 32d-HM (\rightarrow p.E-117)) = 17 or 18 []

Read: []

Format (F10.5)

read from subroutine **MODEL**.

[] = Rod bundle factor:
F_g = 1 or defined by user. It depends on grid spacer and sub-channel code. (**F_g** = 1 recommended).

E.14.55 32f-HM-2: CHF correlation input: input for [

].

Read: If **NSPff12** (\rightarrow p.E-119) = 1 or 2 (cf. 32d-HM-1 (\rightarrow p.E-119)): **TDCW3**, **KSGrid**, **fDNBRW**

Format (3F10.5)

read from subroutine **MODEL**.

If **NSPff12** (\rightarrow p.E-119) = 3 (cf. 32d-HM-1 (\rightarrow p.E-119)): **TDCW3**

Format (F10.5)

read from subroutine **MODEL**.

TDCW3 = Thermal Diffusion Coefficient (TDC)
KSGrid = Axial grid spacing coefficient (**K_s**) depending on axial grid spacing
fDNBRW = DNBR correction multiplier (**f_{DNBR}**)

E.14.56 32g-HM-2: [] Correlation Geometry Parameters

This card is required if **NCHF = 13, 23, 33** on card 32-HM (→ p.E-116).

Read: **DHHYD, HLEN**

Format (*)

read from subroutine **MODEL**.

DHHYD = Lattice hydraulic diameter (cm).

HLEN = Fuel bundle heated length (cm).

Note: (1) **HLEN** is not used if **NCHF = 13 or 33** on card 32-HM (→ p.E-116).

E.14.57 32g-HM-3: [] Correlation Grid Heights

This card is required if **NCHF = 13, 23, 33** on card 32-HM (→ p.E-116).

Read: **GRIDHT(I), I = 1, NGRIDT**

Format (*)

read from subroutine **MODEL**.

GRIDHT = Grid heights (in cm) of grid types according to **NGRIDT** on card 8-CD (→ p.E-97) (**NGRIDT** values).

Note: (1) This card is not used if **NCHF = 13 or 33** on card 32-HM (→ p.E-116).

E.14.58 32g-HM-4: [] Correlation Mixing Grid Specification

This card is required if **NCHF = 13, 23, 33** on card 32-HM (→ p.E-116).

Read: **NMGRID, (MGRID(I), I = 1, NMGRID)**

Format (*)

read from subroutine **MODEL**.

NMGRID = Number of mixing grids.

MGRID = Enumerate in ascending order which of the **NGRID** spacers (see card 8-CD (→ p.E-97)) are mixing grids.

Note: (1) **NMGRID** values required.

E.14.59 32h-HM: [] Correlation Input

This card is required if **NCHF = 14** on card 32-HM (→ p.E-116).

Read: **SPITCH, XKLOSS, BLEN**

Format (*)

read from subroutine **MODEL**.

SPITCH = Grid spacing (cm).

XKLOSS = Ration of grid pressure loss coefficients (vaned/unvaned).

BLEN = Fuel bundle heated length (cm).

E.14.63 33a-HM: PV-Solution Variables

This card is required if **ISOLVE = 3** on card I2 (→ p.E-6).

Read: **NSSS, DTSS**

Format (*)

read from subroutine **MODEL**.

NSSS = Number of time steps of **DTSS** for reaching a steady-state solution. **NSSS = 1** is a normal choice. **NSSS > 1** can be used to run a pseudo transient of **NSSS** steps to achieve steady-state. A reduced time step **DTSS** would be provided in that case. ([]).

DTSS = Time step used to achieve steady state. ([]).

Note: (1) Convergence for low flow cases can be difficult and a reduced time step is an option to achieve convergence. Time steps on the order of the Courant step can be used to advantage and a suitable number of time steps would be needed to achieve steady-state. Damping may also be needed (**ACCELX < 1.0** on card 33d-HM (→ p.E-125), **ACCELY < 1.0** on card 33d-HM (→ p.E-125), **DAMPER < 1.0** on card 33e-HM (→ p.E-126)) especially if the time steps are larger than the Courant time step.

E.14.64 33b-HM: PV-Solution Variables

This card is required if **ISOLVE = 3** on card I2 (→ p. E-6).

Read: **ITMNSS, ITMINT**

Format (*)

read from subroutine **MODEL**.

ITMNSS = Minimum number of outer iterations used to achieve steady-state for each steady-state time step. The outer iteration will go at least **ITMNSS** iterations per time step ([]).

ITMINT = Minimum number of outer iterations used to achieve a solution at each transient time step. The outer iteration will go at least **ITMINT** iterations per time step ([]).

E.14.65 33c-HM: PV-Solution Variables

This card is required if **ISOLVE = 3** on card I2 (→ p. E-6).

Read: **MAXINR, IREBAL, MERROR**

Format (*)

read from subroutine **MODEL**.

MAXINR = Maximum number of inner iterations to achieve a mass balance ([]).

| | | |
|--------|---|---|
| IREBAL | = | Inner iterations for rebalancing of pressure and flow along the channel length. Rebalancing is done every IREBAL inner iterations ([]). |
| MERROR | = | Maximum allowable relative mass conservation error (C/F) per cell for the inner iteration. C is the mass error per cell (kg/s) and F is the average axial flow (kg/s). This differs for FERROR (dF/F) (on card 33-HM (→ p.E-123)). MERROR is the criterion used to measure mass convergence of the inner iteration. FERROR is used to measure the flow convergence of the outer iteration. MERROR is normally more restrictive. ([]) |

E.14.66 33d-HM: PV-Solution Variables

This card is required if **ISOLVE = 3** on card I2 (→ p. E-6).

Read: **ACCELX**, **ACCELY**, **XFACP**, **NUSTAR**

Format (*)

read from subroutine **MODEL**.

| | | |
|--------|---|--|
| ACCELX | = | Acceleration factor for axial flow in MOMAXL. A value less than 1 slows the update of the axial flow from MOMAXL. Values [] may be needed for some applications. Reduce DTSS if damping does not lead to convergence in the steady state solution ([]). |
| ACCELY | = | Acceleration factor for lateral flow in MOMLAT. A value less than 1 slows the update of the lateral flow from MOMLAT. Values [] may be needed for some applications. Reduce DTSS if damping does not lead to convergence in the steady state solution ([]). |
| XFACP | = | Interpolation factor to locate pressure on staggered mesh. |
| | = | 0.0 Places the pressure at J+1 at junction J – the same as SCHEME . This is recommended when a high degree of correspondence with SCHEME is desired. |
| | = | 0.5 Places the pressure at the cell center as in a normal staggered mesh. This is recommended if flow reversals are to be considered. |
| NUSTAR | = | Option flag to select method of assigning axial velocity to the lateral cross flow boundary of the momentum cell in the axial momentum equation. |
| | = | 0 Assigns an average as done in the SCHEME solution. NUSTAR assigns a donor value and may be more stable in some applications. |
| | = | 1 Allows to also calculate reverse flow |

E.14.67 33e-HM: PV-Solution Variables

This card is required if **ISOLVE = 3** on card I2 (→ p. E-6).

Read: **DAMPER**, **ACCELP**, **HERROR**, **NSOLVE**, **DAMPH**

Format (*)

read from subroutine **MODEL**.

| | | |
|---------------|---|--|
| DAMPER | = | Acceleration factor for either nodal density or nodal enthalpy. The use depends on the value of DAMPH . If DAMPH is zero, then DAMPER is applied to the nodal density during the outer iterations. If DAMPH is greater than zero, DAMPER is applied to the nodal enthalpies in ENERGY after DAMPH iterations. |
| ACCELP | = | Acceleration factor on nodal pressures used in MASEQX and MASEQY . A value less than 1.0 will slow the pressure and subsequent flow convergence ([]). |
| HERROR | = | Absolute nodal energy error (J/kg) ([]). |
| NSOLVE | = | Selects between conservative and transportive forms of the momentum equations. |
| | = | 0 The conservative form of the momentum equations is used. |
| | = | 1 The transportive form (factors the temporal term in the conservative form and substitutes the mass equation) is used. |
| DAMPH | = | Switch for DAMPER : |
| | = | 0 DAMPER is applied to nodal densities. |
| | > | 0 DAMPER applies to nodal enthalpies after DAMPH iterations. |

Note: (1) Typically, **NSOLVE = 1** will produce converged solution for low flow or reverse flow conditions when **NSOLVE = 0** will fail to converge. **NSOLVE = 0** will produce results most similar to **SCHEME**.

E.14.68 34-HM: Physical properties

This card is required if **N8 > 0** on card 23-HM (→ p.E-110).

Read: **NPROP**, **N**, **PH**, **P2**

Format (*)

read from subroutine **MODEL**.

| | | |
|--------------|---|--|
| NPROP | = | Number of pressure points in physical property table to interpolate between (min = 2 , max = 30). |
| N | = | Trigger for evaluation of PH : |
| | = | 2 The value of PH is lowest pressure in problem. |
| | = | 1 The value of PH is lowest enthalpy in problem. |
| PH | = | If N = 2 : Lowest pressure in problem (bar). If N = 1 : Lowest enthalpy in problem (kJ/kg) from which the lowest pressure will be calculated (see below). |
| P2 | = | Highest pressure in problem (bar). |

Note: (1) From this card, a table containing **NPROP** equi-spaced values of pressure from **PH** to **P2** is constructed giving relevant physical properties - calculated from polynomial expressions - at each pressure. Physical properties at intermediate pressures are found by linear interpolation.

(2) It is important that the table spans the physical property range of the problem. The lowest pressure encountered in the problem is defined as that at which the lowest enthalpy would be the saturation value. For example, at 70 bar the saturation enthalpy is 1267.4 kJ/kg. At an inlet subcooling of 242 kJ/kg, the enthalpy would be 1025.4 kJ/kg and this would be the saturation value at a pressure of about 32 bar. Thus, one would require physical property data over the range 32 bar (or less) to 70 bar in order to include data which cover the enthalpy range.

(3) To avoid translating the lowest enthalpy into pressure, the option of giving the enthalpy is included. The program translates this value to a pressure which is safely below that required using the expression in Imperial units:

$p = 6 \cdot h^3 \cdot (h - 1.35) / (h - 0.35)$ where p = calculated pressure (psia), $h = 0.01 \cdot H$ and H = enthalpy (Btu/lb). Finally, the pressure p is converted into [Pa].

(4) The option to use a user supplied property table is available using card group 1 (\rightarrow p.E-12) of the old COBRA input method. This option is especially useful for coolants other than water.

E.14.69 35-HM: Coupling parameters

This card is required if **N9** > 0 on card 23-HM (\rightarrow p.E-110).

Read: **ENEH**, **K** = 1, **NK**

Format (*)

read from subroutine **MODEL**.

ENEH = Coupling parameter introduced in the mixing term of the energy conservation equation.
The calculated enthalpy difference will be multiplied by **ENEH(K)**.

Note: (1) **NK** is the total number of gap interconnections.

(2) The coupling parameters should be entered in the same order as the inter-channel gaps are numbered. The numbering order is described on card 20-GB (\rightarrow p.E-108).

E.14.70 36-OC: Steady state operating conditions

This card is required whenever card group 20 is used.

Read: **IH**, **HIN**, **GIN**, **PEXIT**

Format (*)

read from subroutine **OPERA**.

IH = Inlet enthalpy indicator.

HIN = Depends on the value of **IH**:
If **IH** = 0 : Inlet enthalpy (kJ/kg).
If **IH** = ± 1 : Inlet temperature ($^{\circ}$ C).
If **IH** = ± 2 : Not used, set to zero. Inlet enthalpies for each channel given on cards of type 37-OC (\rightarrow p.E-128).
If **IH** = ± 3 : Not used, set to zero. Inlet temperatures for each

| | | |
|-------|---|--|
| | | channel given on cards of type 37-OC (\rightarrow p.E-128). If $IH = \pm 5$: Inlet temperature ($^{\circ}C$); setpoint calculation. |
| GIN | = | Average inlet mass velocity (kg/(sec m ²)). |
| PEXIT | = | System pressure (bar). |

Note: (1) If the values of IH are negative, the next card read will be 36-OC1 (\rightarrow p.E-128).

E.14.71 36-OC1: Operating conditions

This card is required if $IH < 0$ on card 36-OC (\rightarrow p.E-127).

Read: **FHGFUE, BYPASS**

Format (*)

read from subroutine **OPERA**.

| | | |
|--------|---|--|
| FHGFUE | = | Fraction of heat generated in fuel. |
| BYPASS | = | Bypass flow (fraction of GIN on card 36-OC (\rightarrow p.E-127)). |

E.14.72 36.1-OC: Setpoint iteration

This card is required if $IH = \pm 5$ on card 36-OC (\rightarrow p.E-127).

Read: **ISPIT, XSPLow, XSPHGH, DNBLIM, TOLLIM, MAXFN**

Format (*)

read from subroutine **OPERA**.

| | | |
|--------|---|---|
| ISPIT | = | Type of setpoint iteration: |
| | = | 1 Variation of power. |
| | = | 2 Variation of inlet temperature at fixed volumetric flow given by reference conditions on card 36-OC (\rightarrow p.E-127). |
| XSPLow | = | Lower limit of interval to be searched: If $ISPIT = 1$: kW/m ² , if $ISPIT = 2$: $^{\circ}C$. |
| XSPHGH | = | Upper limit of interval to be searched: If $ISPIT = 1$: kW/m ² , if $ISPIT = 2$: $^{\circ}C$. |
| DNBLIM | = | Target DNBR for iteration. |
| TOLLIM | = | Iteration is stopped if ABS(DNBR - DNBLIM) < TOLLIM . |
| MAXFN | = | Case is skipped if no convergence is reached after MAXFN calculations. |

E.14.73 37-OC: Inlet enthalpy distribution

This card is required if $IH = 2$ or 3 on card 36-OC (\rightarrow p.E-127).

Read: **A(I), I = 1, NCHAN**

Format (*)

read from subroutine **READIN/OPERA**.

| | | |
|---|---|--|
| A | = | Depends on value of IH on card 36-OC (\rightarrow p.E-127): If $IH = 2$: Inlet enthalpies for each channel (kJ/kg). If $IH = 3$: Inlet temperatures for each channel ($^{\circ}C$). |
|---|---|--|

E.14.74 38-T: Transient indicators

This card is required whenever card group 20 is used.

Read: **NP, NH, NG, NQ**

Format (*)

read from subroutine **OPERA**.

| | | |
|----|---|--|
| NP | = | Number of points at which pressure transient forcing function data points will be given (see card 39-T (\rightarrow p.E-129); max = 30). |
| NH | = | Number of points at which inlet enthalpy transient forcing function data pairs will be given (see card 40-T (\rightarrow p.E-130); max = 30). |
| NG | = | Number of points at which inlet flow transient forcing function data pairs will be given (see card 41-T (\rightarrow p.E-130); max = 30). |
| NQ | = | Number of points at which channel power transient forcing function data pairs will be given (see card 42-T (\rightarrow p.E-130); max = 30). |

Note: (1) If only steady state calculations are required, card 38-T (\rightarrow p.E-129) is given as a blank card and cards 39-T (\rightarrow p.E-129) through 42-T (\rightarrow p.E-130) are omitted.

(2) COBRA-FLX handles transient analysis by using transient forcing functions. These forcing functions simulate transient behavior by allowing the user to specify up to thirty (30) parameter data pairs - relative value and transient time - for pressure, inlet enthalpy, inlet flow and channel power. Parameter values between two specified time points are then found by linear interpolation.

If any parameter is being held constant, the corresponding indicator should be left blank and the respective transient forcing function cards are omitted.

Cards 39-T (\rightarrow p.E-129) through 42-T (\rightarrow p.E-130) are all of the same format and carry the data time specification (seconds from the start of the analysis) and the ratio of transient value to steady state value for the parameter in question at that time. Each card carries a maximum of seven (7) data pairs and sufficient cards must be provided to supply all the data pairs called for by the value of the indicators above. Since all transients must start at time 0 and the full steady state value of all parameters, the first data pair must be time = 0 and relative value = 1.

E.14.75 39-T: Pressure transient forcing function

This card is required if NP > 1 on card 38-T (\rightarrow p.E-129).

Read: **YP(I), FP(I), I = 1, NP**

Format (*)

read from subroutine **READIN/OPERA**.

| | | |
|----|---|---|
| YP | = | Time (sec). |
| FP | = | Ratio of transient to steady state pressure at time YP. |

Note: (1) YP(1), FP(1) should be given as 0.0 and 1.0 respectively.

(2) The value of FP at a time intermediate between two values of YP is found by linear interpolation.

E.14.76 40-T: Inlet enthalpy transient forcing function

This card is required if $NH > 1$ on card 38-T (\rightarrow p.E-129).

Read: $YH(I)$, $FH(I)$, $I = 1$, NH

Format (*)

read from subroutine **READIN/OPERA**.

YH = Time (sec).

FH = Ratio of transient to steady state enthalpy or temperature (depending on the value of IH on card 36-OC (\rightarrow p.E-127)) at time YH.

Note: (1) $YH(1)$, $FH(1)$ should be given as **0.0** and **1.0** respectively.

(2) The value of FH at a time intermediate between two values of YH is found by linear interpolation.

E.14.77 41-T: Inlet flow transient forcing function

This card is required if $NG > 1$ on card 38-T (\rightarrow p.E-129).

Read: $YG(I)$, $FG(I)$, $I = 1$, NG

Format (*)

read from subroutine **READIN/OPERA**.

YG = Time (sec).

FG = Ratio of transient to steady state average mass velocity at time YG.

Note: (1) $YG(1)$, $FG(1)$ should be given as **0.0** and **1.0** respectively.

(2) The value of FG at a time intermediate between two values of YG is found by linear interpolation.

E.14.78 42-T: Channel power transient forcing function

This card is required if $NQ > 1$ on card 38-T (\rightarrow p.E-129) and $IQP3 = 2$ on card 4-HF (\rightarrow p.E-94).

Read: $YQ(I)$, $FQ(I)$, $I = 1$, NQ

Format (*)

read from subroutine **READIN/OPERA**.

YQ = Time (s).

FQ = Ratio of transient to steady state channel power at time YQ.

Note: (1) $YQ(1)$, $FQ(1)$ should be given as **0.0** and **1.0** respectively.

(2) The value of FQ at a time intermediate between two values of YQ is found by linear interpolation.

E.14.79 43-DB: Debug option

This card is required whenever card group 20 is used.

Read: **KDEBUG**

Format (*)

read from subroutine **TABLES**.

| | | |
|--------|---|-------------------------------|
| KDEBUG | = | Debug option: |
| | = | 0 Normal - no test printing. |
| | = | 1 Debug - with test printing. |

Note: (1) The debug option can generate massive amounts of output and should be used only when necessary.

E.14.80 44-OO: Output printing

This card is required whenever card group 20 is used.

Read: **NSKIPX, NSKIPT, NOUT, NPCHAN, NPROD, NPNODE**

Format (*)

read from subroutine **TABLES**.

| | | |
|--------|---|---|
| NSKIPX | = | Axial print option: |
| | = | 0 Every axial step is printed. |
| | = | 1 Every axial step is printed. |
| | = | n Every n-th axial step is printed. |
| NSKIPT | = | Time step printing increment (Function is the same as NSKIPX , except that it is used to select the time step printouts by ABS(NSKIPT)). |
| | < | 0 Printout of bundle-averaged results to file OUTPUT and bundle average inlet and exit temperatures to file DNBDATA (increases run time). |
| NOUT | = | Data printout indicator: |
| | = | 0 Print subchannel data only. |
| | = | 1 Print subchannel data and crossflow data table. |
| | = | 2 Print subchannel data and fuel rod data table. |
| | = | 3 Print subchannel data, fuel rod data table and crossflow data table. |
| NPCHAN | = | Subchannel data printout indicator: |
| | = | 0 All subchannel data printed. |
| | > | 0 Read in N2 subchannel numbers for which results are desired (see card 45-OO (\rightarrow p.E-132)). |
| NPROD | = | Fuel rod data printout indicator: |
| | = | 0 Data of all rods printed if called for by N1 . |
| | > | 0 Read in NPROD rod numbers for which results are desired (see card 46-OO (\rightarrow p.E-132)). |

| | | | |
|--------|---|---|--|
| | < | 0 | Read in NPROD rod numbers for which results are desired (see card 46-OO (\rightarrow p.E-132)). Additionally the detailed fuel node temperature data is printed. |
| NPNODE | = | | Fuel node printout indicator: |
| | = | 0 | Temperature printed for all nodes if called for by NOUT . |
| | > | 0 | Read in NPNODE node numbers for which results are desired (see card 47-OO (\rightarrow p.E-132)). |

Note: (1) Radial fuel nodes are numbered such that rod center = 1 and the rod outer surface = (NODESF + 1) (for NODESF see card 8-CD (\rightarrow p.E-97)).

E.14.81 45-OO: Channels to be printed

This card is required if **NPCHAN** > 0 on card 44-OO (\rightarrow p.E-131).

Read: **PRINTC** (I), I = 1, **NPCHAN**
Format (*)
read from subroutine **TABLES**.

PRINTC = Identification number of channels to be printed.

E.14.82 46-OO: Rods to be printed

This card is required if **NPROD** > 0 on card 44-OO (\rightarrow p.E-131).

Read: **PRINTR** (I), I = 1, **NPROD**
Format (*)
read from subroutine **TABLES**.

PRINTR = Identification number of rods to be printed.

E.14.83 47-OO: Fuel nodes to be printed

This card is required if **NPNODE** > 0 on card 44-OO (\rightarrow p.E-131).

Read: **PRINTN** (I), I = 1, **NPNODE**
Format (*)
read from subroutine **TABLES**.

PRINTN = Radial fuel nodes to be printed;

Note: (1) Radial fuel nodes are numbered such that rod center = 1 and the rod outer surface = (NODESF + 1) (for NODESF see card 8-CD (\rightarrow p.E-97)).

E.14.84 48-NP: This card is obsolete.

Note: (1) DNB-ratios are calculated as critical/channel average heat flux. Only the first out of six rods specified on card G8-1 (\rightarrow p.E-38) delivers heat to the coolant channel. When specifying **IQP3** = 0 or 1, DNB-ratios are multiplied by **RADIA** on card G8-1 (\rightarrow p.E-38). Thus **RADIA** should be inputted as maximum rod to channel average heat flux to account for radially nonuniform heating of a coolant channel.

E.14.85 49-NP: Fuel nodal powers

This card is required if **IQP3 = 0** on card 4-HF (→ p.E-94) (or note on card GCC3 (→ p.E-12)).

Read: **QF(I, J)**

Format (**10F10.5**)

read from subroutine **QPR3**.

QF = Fuel nodal powers (MW).

Note: (1) **NCHAN** (number of channels) values are read by core layers (**NDX**, see card 7-MD (→ p.E-97)), starting at the bottom layer, 10 values for a group of 10 channels on each line (or less than 10 on last **NDX** of lines depending on **NCHAN**). Cards are read from file **POWER3D**. One set is read for each time step starting with 0 seconds.

E.14.86 50-NP: Coolant nodal powers

This card is required if **IQP3 = 0** on card 4-HF (→ p.E-94) (or note on card GCC3 (→ p. E-12)).

Read: **QC(I, J)**

Format (**10F10.5**)

read from subroutine **QPR3**.

QC = Coolant nodal powers (MW).

Note: (1) **NCHAN** (number of channels) values are read by core layers (**NDX**, see card 7-MD (→ p.E-97)), starting at the bottom layer, 10 values for a group of 10 channels on each line (or less than 10 on last **NDX** of lines depending on **NCHAN**). Cards are read from file **POWER3D**. One set is read for each time step starting with 0 seconds.

E.14.87 GCC: End input data and start calculation

This card is required always.

Read: **BLANK CARD**

Format (no Format)

read from subroutine .

Note: (1) At this point in the calculation, control returns to reading card GGC. If **NGROUP = 1-12** more input data are read in the original COBRA format (→ p.E-8, these later data overwriting what has already been read in. If **NGROUP = 0** calculation starts.

(2) If **N1 = 0** or **1** on card 4-HF (→ p.E-94) additional nodal power must be provided here. This additional data is read in from subroutine **QPR3** after the start of the calculations.

E.15 Card Group HOSCAM**Radial and Axial Nodalization Input**

| | |
|---|-------|
| HOS1: HOSCAM Dimensions | E-134 |
| HOS2: Spacer Grid Definitions..... | E-134 |
| HOS3: Fuel Rod Types | E-134 |
| HOS4: Fuel Rod Geometries and Pressure Loss Coefficients..... | E-134 |

E.15.1 HOS1: HOSCAM Dimensions

Read: *NROW, NGT, NFT, NGRID, NGRIDT, EGAP, PITCH*

| | | |
|--------|---------|---|
| NROW | integer | Number of fuel rods in a row of the fuel assembly. |
| NGT | integer | Number of guide tubes per fuel assembly. |
| NFT | integer | Number of fuel types in core. |
| NGRID | integer | Number of grids in active length. |
| NGRIDT | integer | Number of grid types along active length. |
| EGAP | real | Additional gap at edge of fuel assembly (cm). |
| PITCH | real | Fuel rod pitch within fuel assembly (cm); the fuel rod assembly pitch is NROW*PITCH+EGAP . |

Note: (1) If compositions are available, **NFT** refers rather to the total number of composition types than to the number of fuel types

E.15.2 HOS2: Spacer Grid Definitions

Read: *GRIDXL(I), IGRID(I), I = 1, NGRID*

| | | |
|-----------|---------|---|
| GRIDXL(I) | real | Relative position of grid within active length. |
| IGRID(I) | integer | Type of grid at position I. |

E.15.3 HOS3: Fuel Rod Types

Read: *ITP(I,J), I = 1, NX; J = 1, NY*

| | | |
|----------|---------|------------------------------|
| ITP(I,J) | integer | Fuel type at position (I,J). |
|----------|---------|------------------------------|

Note: (1) **NX** and **NY** refer to the neutronics node numbers in the x and y directions.

(2) This card is only read, if no compositions are available on the nuclear data base (file **NK_PWR**).

E.15.4 HOS4: Fuel Rod Geometries and Pressure Loss Coefficients

Read: *COMPI(I), DR0(I), DGT(I), CD0(I,J), CD6(I,J), CDH(I,J), J = 1, NGRIDT*

| | | |
|----------|---------|--|
| COMPI(I) | integer | Composition number for fuel type I. |
| DR0(I) | real | Fuel rod diameter for fuel type I (cm). |
| DGT(I) | real | Guide tube diameter for fuel type I (cm). |
| CD0(I,J) | real | Fuel assembly pressure loss coefficient for fuel type I and grid type J. |

| | | | | |
|------------|------|--|---|---|
| CD6 (I, J) | real | [|] | pressure loss coefficient for fuel type I and grid type J. |
| CDH (I, J) | real | Hot channel pressure loss coefficient for fuel type I and grid type J. | | |

*Note: (1) Cards HOS4 are read **NFT** (→ p.E-134) times.*

*(2) If compositions are available, data pertain rather to composition number **COMP(I)** than to fuel type I.*

*(3) Composition numbers **COMPI(I)** are ignored if no compositions are available on nuclear data base **NK_PWR**.*

*(4) Failure to specify all compositions numbers will result in printout of missing assignments on file **COB_OUT** and subsequent program stop.*

Figure E-1: Example Input Using Free Format

(Instructional notes, in italics, are provided in this figure. They are not present in the actual COBRA-FLX input.)

Record of the input check

The following information is always printed:

- selected solver
- overview on the main parameters as read from all input blocks
- information about the problem size, e.g. number of channels, gaps, rods, axial nodes

```

file connected with unit 95 is: /uf7/nrl/2009/cases2/32-9125510-001/AppendixA/PRECOB
10497P18699 03/08/10 14:02:08 fl22 x86 64 Linux 2.6.18-164.e cobra-flx_2.05R1 2009-06-16 13:43:56
COBRA-FLX: Copyright (C) AREVA NP 2005
0free format input on tape 95
0
C Four Pump Coastdown (4PCD)
C Note that in order to run the COBRA-FLX, the input deck must be renamed as PRECOB
C **Blank Cards are not needed after card groups but are there for visual separation**
C I1 (Introductory Card 1): Problem Array Size
C =====
C MC MG MN MR MX MZ
  83 158 0 92 31 30

C I2 (Introductory Card 2): Solution Method
C =====
C OMEGA ISOLVE
  6000 1

C I3 (Introductory Card 3): Case Control
C =====
C IPILE KASE J1 TITLE
  0 +1 1 '4PCD 12 Channel Model P-solution'

C GCC1 (Card Group 1): Physical Properties
C =====
C NGROUP N1 N2 N3 N4 N5 N6 N7
  1 -7 0 0 0 0 0 0

C G1-1: Physical Properties
C -----
C N PH P2 NP
  1 30.00 170.00 30

C GCC2 (Card Group 2): Flow Correlations
C =====
C N1 (J2) = 2, Saha-Zuber subcooled void correlation
C N2 (J3) = 8, Chexal-Lellouche void correlation using the iterative solution to the formula
C N3 (J4) = 0, Homogeneous model two phase friction multiplier
C N4 (NVISCW) = 1, Wall viscosity included
C N5 (NSZABL) = 0, Lehmann friction factor uses Szablewski correlation
C N6 (J8) = 1, Zuber-Staub profile fit
C N7 = 0, Not used

C NGROUP N1 N2 N3 N4 N5 N6 N7
  2 2 8 0 1 0 1 0

```

PAGE 3

C G2-1: Friction factor correlation constants

C-----
C
C []

C GCC3 (Card Group 3): Axial Heat Flux Data

C-----
C
C NGROUP N1 N2 N3 N4 N5 N6 N7
 3 70 0 1 0 0 0 0

C G3-1: Axial heat flux data

C-----
C Y AXIAL
0.00000 0.00001
0.01251 0.05000
0.01261 0.41797
0.02542 0.41923
0.05929 0.43183
0.09881 0.46450
0.13834 0.51660
0.17236 0.57610
0.19763 0.62813
0.22398 0.68858
0.23715 0.72085
0.25033 0.75429
0.26350 0.78874
0.27668 0.82406
0.28986 0.86007
0.30752 0.90914
0.32230 0.95065
0.32938 0.97060
0.34256 1.00771
0.35573 1.04467
0.36891 1.08130
0.38208 1.11745
0.39526 1.15295
0.40843 1.18763
0.42161 1.22135
0.43478 1.25396
0.44266 1.27287
0.45744 1.30705
0.46113 1.31530
0.47431 1.34378
0.48748 1.37064
0.50066 1.39580
0.51383 1.41916
0.52701 1.44065
0.54018 1.46022
0.55336 1.47782
0.56653 1.49343
0.57792 1.50530
0.59270 1.51851
0.59289 1.51865
0.60606 1.52832
0.61924 1.53608
0.63241 1.54201
0.64559 1.54621
0.65876 1.54880
0.67194 1.54992

0.68511 1.54850
0.69829 1.53935
0.71317 1.51735
0.72795 1.48208
0.73781 1.45096
0.75099 1.40017
0.76416 1.33955
0.77734 1.27027
0.79051 1.19384
0.80369 1.11202
0.81686 1.02680
0.83004 0.94027
0.84832 0.82211
0.86310 0.73168
0.86957 0.69440
0.88274 0.62384
0.89592 0.56199
0.90909 0.51022
0.92227 0.46960
0.93544 0.44071
0.94862 0.42365
0.96113 0.41797
0.96213 0.05000
1.00000 0.00001

C G3-2: Hot Channel Factors

C -----
C FEQ FEDH1 FEDH2 F1GRID F2GRID F3GRID
C 1.0 1.0 1.0 1.0 1.0 1.0

C GCC4 (Card Group 4): Subchannel Data

C -----
C NGROUP N1 N2 N3 N4 N5 N6 N7
C 4 12 12 0 0 0 0 0

C G4a-1: Subchannel Data

C -----
C
C
C

C GCC5 (Card Group 5): Subchannel area variation (not used)
C GCC6 (Card Group 6): Gap spacing variation (not used)

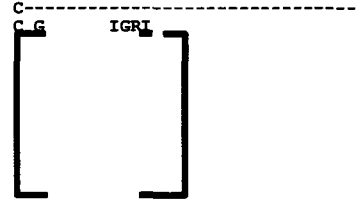
C GCC7 (Card Group 7): Spacer Data

C -----
C NGROUP N1 N2 N3 N4 N5 N6 N7
C 7 2 8 4 0 0 0 0

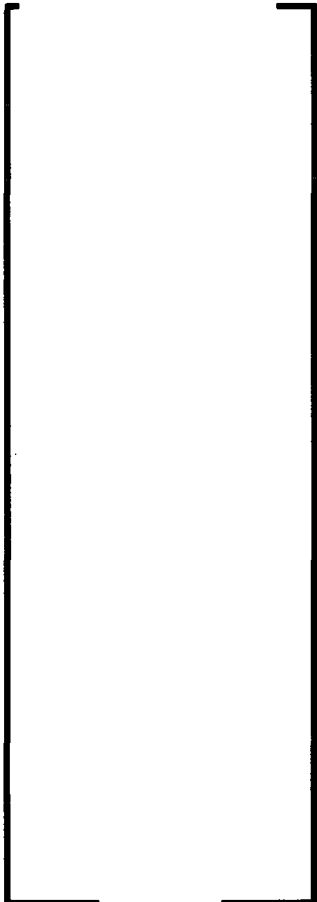
C Grid Type 1
C Grid Type 2
C Grid Type 3
C Grid Type 4



C G7-4: Spacer location and type



C G7-5: Spacer data sets are used





C GCC8 (Card Group 8) : Rod Layout Data

| NGROUP | N1 | N2 | N3 | N4 | N5 | N6 | N7 |
|--------|----|----|----|----|----|----|----|
| 8 | 14 | 14 | 0 | 1 | 57 | 0 | 0 |

C G8-1: Rod Layout Data

| | d-chan | d-chan | d-chan | d-chan | d-chan | d-chan |
|---|--------|--------|--------|--------|--------|--------|
| 1 | . | | | | | |

C G8-1n: CHF Correlation limits and debug options

| HLEN | CHF_Limit | USDPRN |
|------|-----------|--------|
| [] | | 0 0 |

C G8-1p: CHF Correlation grid spacing input

C ISGSP
2

C G8-1q: CHF Correlation grid spacing input

| SGSPX | SGSPS |
|-------|-------|
| [] | [] |

C GCC9 (Card Group 9) : Calculation Variables

| NGROUP | N1 | N2 | N3 | N4 | N5 | N6 | N7 |
|--------|----|----|----|----|----|----|----|
| 9 | 1 | 1 | 0 | 1 | 0 | 0 | 0 |

C G9-1: Computational variables

```

C-----
C Internal lateral scaling comments:
C For KIJ < 0, Crossflow resistance is multiplied by an internal factor of DIST/LREF KIJ.
C For SL < 0, The transverse momentum parameter is internally calculated based on local geometry.

```

```

C KIJ   FTM   Z   THETA   NDX   NDT   TTIME
[       ]
C NTRIES  FERROR  SL  WERROR  EPSOR  ACCELF  ACCELSF
[       ]

```

```

C G9-1a: Reference distance
C-----
C LREF_KIJ
[       ]

```

```

C G9-2: Axial Node Input
C-----

```

- C X
- 0.012602
- 0.012609
- 0.015803
- 0.025422
- 0.039526
- 0.059289
- 0.079051
- 0.098814
- 0.118577
- 0.138340
- 0.158103
- 0.172364
- 0.187148
- 0.197628
- 0.210804
- 0.223979
- 0.237154
- 0.250329
- 0.263505
- 0.276680
- 0.289855
- 0.307516
- 0.322300
- 0.329381
- 0.342556
- 0.355731
- 0.368906
- 0.382082
- 0.395257
- 0.408432
- 0.421607
- 0.434783
- 0.442661
- 0.457443
- 0.461133
- 0.474308
- 0.487484
- 0.500659
- 0.513834
- 0.527009
- 0.540184
- 0.553360

0.566535
0.577918
0.592702
0.592885
0.606061
0.619236
0.632411
0.645586
0.658762
0.676657
0.685112
0.698287
0.713168
0.727951
0.737813
0.750988
0.764163
0.777339
0.790514
0.803689
0.816864
0.830040
0.848319
0.863103
0.869565
0.882740
0.895916
0.909091
0.922266
0.935441
0.948617
0.961133
0.961199
0.961792
0.978261
1.000000

C GCC10 (Card Group 10): Mixing Parameters

C
=====

| NGROUP | N1 | N2 | N3 | N4 | N5 | N6 | N7 |
|--------|----|----|----|----|----|----|----|
| 10 | 1 | 1 | 0 | 1 | 0 | 0 | 0 |

C G10-1: Mixing correlation constants

C-----
C ABETA BBETA
[]

C G10-4: Reference distance

C-----
C LREF BETA
[]

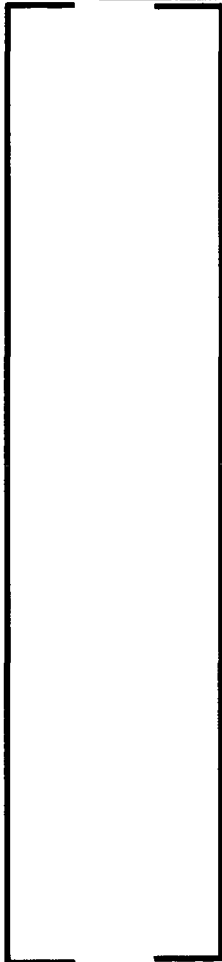
C GCC11 (Card Group 11): Operating Conditions

C
=====

| NGROUP | N1 | N2 | N3 | N4 | N5 | N6 | N7 |
|--------|----|----|-----|-----|-----|-----|----|
| 11 | 1 | 2 | 101 | 101 | 101 | 101 | 0 |

C CARD G11-1: OPERATING CONDITIONS

C-----
C PEXIT[BAR] HIN[degC] GIN[m^3/sec] AFLUX[kW/m^2] FHGFUE BYPASS

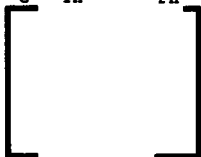


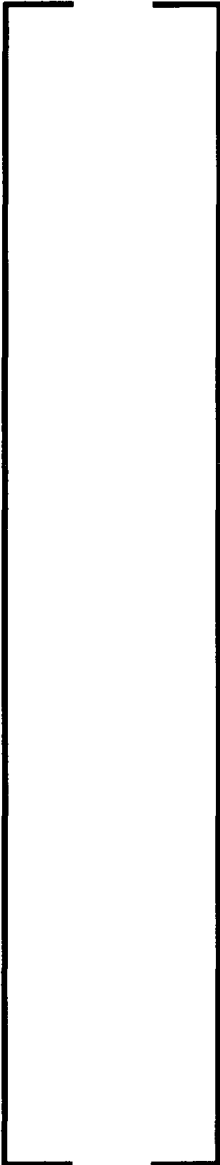
C CARD G11-5: Inlet enthalpy forcing function

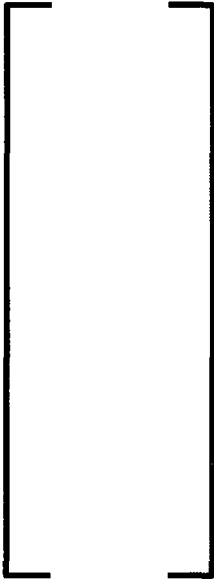
C

YH

FH





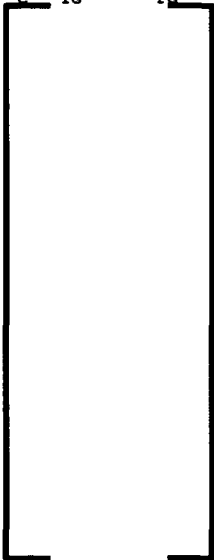


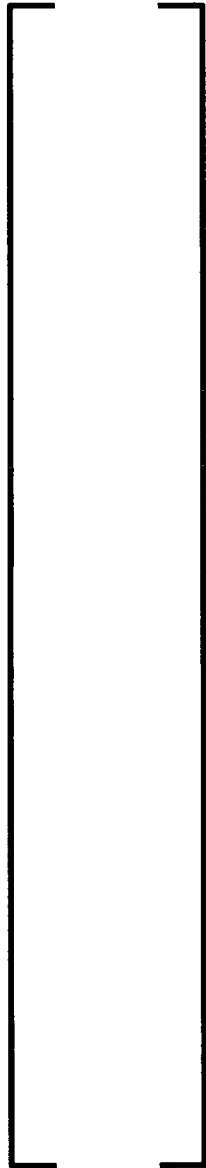
C CARD G11-6: Flow forcing function

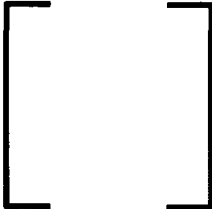
C-----

C YG

FG



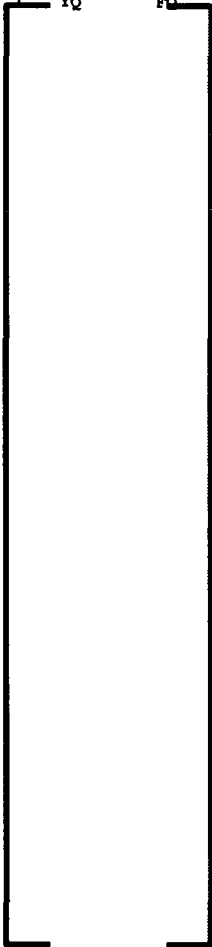


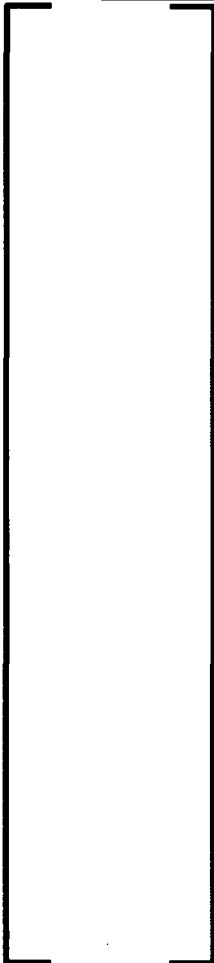


C CARD G11-7: Heat flux forcing function

C YQ

FQ





C GCC12 (Card Group 12): Output Display Options

C =====
C NGROUP N1 N2 N3 N4 N5 N6 N7
 12 3 0 0 0 0 0 0

C Finished reading case 1
C Note that standard card group with NGROUP=0 must terminate each case

C =====
C 0 0 0 0 0 0 0

C =====

C End Case 1

=====

=====

=====

C End of all input. Note that Group I3 with KASE=0 must terminate the COBRA-FLX input deck
0 0 0/

E.16 *References*

- E-1 BAW-10156-A, Rev. 1, LYNXT Core Transient Thermal-Hydraulic Program, B&W Fuel Company, August 1993.

APPENDIX F: OUTPUT DESCRIPTION

Appendix F describes the structure of the output files of COBRA-FLX as a thermal-hydraulic module of the ARTEMIS core simulator, i.e. the ASCII output file (artemis_output) and the HDF (hierarchical data format) output file (artemis_out.hdf). The information written to both files can vary depending on user input options. By default ASCII output is disabled and HDF output is enabled. An overview of the file contents is given in Table F-1.

Appendix F also includes an example of the COBRA-FLX output file, shown in Figure F-1, that corresponds to the input file from Figure E-1.

Table F-1: Overview of COBRA-FLX Output File Content

| Information | ASCII output file | HDF output file |
|---|---|---|
| Image of the input keyword-based format (KBF) file | always printed by ARTEMIS | always printed by ARTEMIS |
| Record of input check | always printed | printed together with the interpreted input in group <i>thm_input</i> |
| Fluid property table | always printed | always printed in group <i>thm_input/group_01_coolant/coolant_properties</i> |
| Interpreted input | always printed | always printed in group <i>thm_input</i> |
| Record of iteration | always printed | not available only the total number of axial iterations is printed if COBRA-FLX HDF output is enabled |
| Mass balance and energy balance | printed if COBRA-FLX ASCII output is enabled | printed if COBRA-FLX HDF output is enabled information stored in the group <i>summary_results/mass_energy_balance</i> |
| Channel exit conditions | printed if COBRA-FLX ASCII output is enabled | not available as separated information |
| Bundle averaged results | printed as requested by user if COBRA-FLX ASCII output is enabled | printed if COBRA-FLX HDF output is enabled bundle averaged results are written for all axial nodes |
| Channel results | printed as requested by user if COBRA-FLX ASCII output is enabled | printed if COBRA-FLX HDF output is enabled the results are printed for all channels and all axial nodes |
| Cross flow results | printed as requested by user if COBRA-FLX ASCII output is enabled | printed if COBRA-FLX HDF output is enabled the cross flows are printed for all gaps and all axial nodes |
| Rod results | printed as requested by user if COBRA-FLX ASCII output is enabled | printed if COBRA-FLX HDF output is enabled the results are printed for all rods and all axial nodes |
| Critical heat flux (CHF) summary (if CHF correlation is selected) | CHF channel and axial results are printed as requested by user if COBRA-FLX ASCII output is enabled | printed if COBRA-FLX HDF output is enabled CHF results are printed for all channels and axial nodes in the group <i>chf_channel_results</i> CHF axial results are printed for all axial nodes in the group <i>chf_axial_results</i> |

F.1 COBRA-FLX ASCII Output Description

The COBRA-FLX ASCII output file is named artemis_output. More detailed information on the file content is provided in this section.

Image of the input KBF (keyword-based format) file

This information is always printed by ARTEMIS.

Record of input check

The following information is always printed:

- selected solver
- overview on the main parameters as read from all input blocks
- information about the problem size, e.g. number of channels, gaps, rods, axial nodes

Fluid property table

This information is always printed. The water properties are either input or calculated at the initial operating conditions according to the selected steam tables.

Interpreted input

This information is always printed. The following data is given according to the input:

- friction factor correlations and two-phase flow correlations
- heat flux distribution and engineering factors for the hot channel
- subchannel geometrical data (area, channel type, wetted, heated and hydraulic perimeters, adjacent channels, gap lengths and centroid distances) and gap information (related channel numbers and coupling parameters)
- spacer data
- rod geometrical data (diameter, radial power factor, adjacent channels and corresponding fraction of power)
- selected CHF correlation
- summary of power distribution information
- calculation parameters
- mixing correlations

- operating conditions

Record of iteration

This information is always printed. Here, the axial and crossflow errors variation during the outer iterations are given.

Mass balance and energy balance

The following information is always printed:

- inlet and outlet mass flow and the total mass flow error [kg/s]
- inlet and outlet flow energy and energy error [kW]

Channel exit conditions

The following results are always printed for all channels at the last axial node:

- channel number [-]
- enthalpy [kJ/kg]
- temperature [°C]
- density [kg/dm³]
- equilibrium quality [-]
- void fraction [-]
- flow [kg/s]
- mass flux [kg/(s m²)]

Bundle averaged results

This information is always printed for steady state calculations. In case of transient calculation the bundle averaged results are printed for the transient time steps if selected by input. The axial nodes at which the results are printed can be also specified by the user. The results printed at the selected axial locations are:

- axial distance [cm]
- pressure loss [bar]
- enthalpy [kJ/kg]
- temperature [°C]

- density [kg/dm³]
- equilibrium quality [-]
- void fraction [-]
- flow [kg/s]
- mass flux [kg/(s m²)]

Channel results (as requested by user)

These results are always printed. The user may specify via input the channels and axial nodes for which the information is printed. The following results are printed for each selected channel:

- axial distance [cm]
- pressure loss [bar]
- enthalpy [kJ/kg]
- temperature [°C]
- density [kg/dm³]
- equilibrium quality [-]
- void fraction [-]
- flow [kg/s]
- mass flux [kg/(s m²)]
- minimum departure of nucleate boiling ratio (MDNBR) [-]
- rod number belonging to the channel and corresponding to MDNBR [-]
- Tong factor corresponding to MDNBR [-]
- CHF correlation number
- CHF correlation name
- CHF correlation type (typically DNBR)

Cross flow results (as requested by user)

These results are printed only if requested by the user. The axial nodes for which the information is printed may be selected via input.

Rod results (as requested by user)

These results are printed only if requested by the user. The rod numbers and axial nodes for which the information is printed may be selected via input. For each selected rod the selected CHF correlation number and type is written first. Afterwards the following results are printed:

- axial distance [cm]
- heat flux [kW/m²]
- DNBR [-] – minimum DNBR over the adjacent channels to the rod
- Tong factor corresponding to the DNBR value [-]
- channel number belonging to the rod and corresponding to DNBR [-]

Critical heat flux (CHF) summary

This information is printed only if a CHF correlation is selected. Two tables of results are provided to the output, i.e. CHF summary at all axial nodes and CHF summary for all channels.

The CHF summary at each axial node includes:

- axial distance [cm]
- heat flux [kW/m²]
- MDNBR – minimum DNBR over all channels at the axial node [-]
- rod number corresponding to the MDNBR [-]
- channel number corresponding to the MDNBR [-]
- CHF correlation number corresponding to the MDNBR [-]
- CHF correlation name corresponding to the MDNBR [-]

The CHF summary for all channels includes:

- axial distance at which the MDNBR is reached for each channel [cm]
- heat flux corresponding to the MDNBR reached for the channel [kW/m²]
- MDNBR – minimum DNBR over all axial nodes for the channel [-]
- rod number belonging to the channel and corresponding to the MDNBR [-]
- channel number [-]
- CHF correlation number corresponding to the MDNBR [-]

- CHF correlation name corresponding to the MDNBR [-]

Finally, a line containing the global MDNBR and the corresponding rod, channel and node number is printed along with the pressure loss [bar].

F.2 COBRA-FLX HDF Output Description

All thermal hydraulics data are stored in the HDF output file under the group *thermal_hydraulics*. They are structured into several sub-groups as described in Section F.2.1. The different data types along with the used abbreviations are listed in Table F-2.

Table F-2: COBRA-FLX Data Types and Abbreviations for HDF Output

| Type Abbreviation | Description |
|-------------------|-------------------------------------|
| G | (Sub-)Group |
| S | String |
| rsp | Real Single Precision |
| rdp | Real Double Precision (not used) |
| isp | Integer Single Precision |
| idp | Integer Double Precision (not used) |
| L | Logical |

If the datum stored is available in the source code the corresponding variable name is also provided in parenthesis at the end of the description given in the following tables supplied in Section F.2.

F.2.1 Group *thermal_hydraulics*

All input and output data for COBRA-FLX are stored into the group *thermal_hydraulics*. The group *thermal_hydraulics* is saved to calculation points *CalculationPoint_xxxxx* (for any xxxxx = 00000 - 99999) stored to the ARTEMIS HDF output file.

For a standalone COBRA-FLX calculation each calculation point corresponds to a different steady-state case. For transient calculations each calculation point contains

the results at a particular time-step. The calculation points are consecutively numbered during the simulation.

The sub-groups that can be present in the group *thermal_hydraulics* are listed in Table F-3. The input data is stored into the group *thm_input*. The remaining sub-groups, i.e. *summary_results*, *bundle_averaged_results*, *channel_results*, *crossflow_results*, *chf_channel_results*, *chf_axial_results* and *rod_results* contain the COBRA-FLX results as selected via the input options.

Table F-3: Sub-groups in Group *thermal_hydraulics*

| Name | HDF-Group | Type | Dimension(s) | Unit | Description |
|-------------------------|--------------------|------|--------------|------|--|
| thm_input | thermal_hydraulics | G | - | - | COBRA-FLX input data (currently, all data needed for THM restart). This group is written only into CalculationPoint_00000. |
| summary_results | thermal_hydraulics | G | - | - | Summary results about mass and energy balance, setpoint iteration (if performed), number of outer iterations, current time and global data |
| bundle_averaged_results | thermal_hydraulics | G | - | - | Bundle averaged results for all axial nodes |
| channel_results | thermal_hydraulics | G | - | - | Channel results for all subchannels and all axial nodes |
| crossflow_results | thermal_hydraulics | G | - | - | Cross flows for all gaps and axial nodes |
| chf_channel_results | thermal_hydraulics | G | - | - | Global critical heat flux (CHF) information for each channel |
| chf_axial_results | thermal_hydraulics | G | - | - | Global CHF information for each axial node |
| rod_results | thermal_hydraulics | G | - | - | Rod results for all rods and all axial nodes |

F.2.1.1 Group *thm_input*

This group is currently written only in the initial calculation point

CalculationPoint_00000. It is part of the group *thermal_hydraulics*. It contains the complete COBRA-FLX input stored in sub-groups according to the KBF input blocks.

All data set after reading and interpreting the input is also stored here. The *thm_input* group includes the following sub-groups:

- *group_0_solver*
- *group_0_general*
- *group_01_coolant*
- *group_02_flow_correlations*
- *group_03_power_distribution*
- *group_04_channel_data*
- *group_05_channel_area_variation*
- *group_06_gap_variation*
- *group_07_spacer*
- *group_08_rod_data*
- *group_09_calculation_variables*
- *group_10_mixing*
- *group_11_operating_conditions*
- *group_12_output_options.*

The detailed description of the stored data is provided in the extensive Table F-4.

Table F-4: Description of Stored Data in Group *thm_input*

| Name | HDF-Group | Type | Dimension(s) | Unit | Description |
|--------------------------------|------------------|------|--------------|------|--|
| group_0_solver | thm_input | G | - | - | Solver input options |
| solver | group_0_solver | isp | - | - | Solution method (isolve) |
| [] | group_0_solver | rsp | - | - | [] |
| [] | group_0_solver | isp | - | - | [] |
| [] | group_0_solver | isp | - | - | [] |
| group_0_general | thm_input | G | - | - | General input options |
| case_description | group_0_general | S | - | - | Text description of the test case (text) |
| array_type | group_0_general | isp | - | - | Array type (j7, ipile) |
| ihext | group_0_general | isp | - | - | Indicator of negative ipile |
| case_number | group_0_general | isp | - | - | Run identification number (kase) |
| input_print_option | group_0_general | isp | - | - | Input print option (j1) |
| group_01_coolant | thm_input | G | - | - | Coolant properties |
| itaf | group_01_coolant | isp | - | - | Physical properties indicator |
| nprop | group_01_coolant | isp | - | - | Total number of pressure interpolation steps for physical properties (nprop) |

| Name | HDF-Group | Type | Dimension(s) | Unit | Description |
|-------------------------------|----------------------------|------|--------------|--------------------|---|
| superheated_steam | group_01_coolant | isp | - | - | Superheated steam properties indicator (npress) |
| coolant_properties | group_01_coolant | G | - | - | Coolant properties table |
| pressure | coolant_properties | rsp | 1 | Pa | Saturation pressure (pp) |
| temperature | coolant_properties | rsp | 1 | °C | Temperature |
| spec_volume_liquid | coolant_properties | rsp | 1 | m ³ /kg | Liquid specific volume |
| spec_volume_vapor | coolant_properties | rsp | 1 | m ³ /kg | Vapour specific volume |
| enthalpy_liquid | coolant_properties | rsp | 1 | J/kg | Liquid enthalpy |
| enthalpy_vapor | coolant_properties | rsp | 1 | J/kg | Vapour enthalpy |
| viscosity_liquid | coolant_properties | rsp | 1 | kg/(m s) | Liquid viscosity |
| conductivity | coolant_properties | rsp | 1 | W/(m K) | Liquid thermal conductivity |
| surface_tension | coolant_properties | rsp | 1 | N/m | Surface tension |
| ccp | coolant_properties | rsp | 1 | J/(kg K) | Heat capacity |
| group_02_flow_correlations | thm_input | G | - | - | Flow correlations parameters |
| subcooled_void | group_02_flow_correlations | isp | - | - | Subcooled void option (j2) |
| bulk_void | group_02_flow_correlations | isp | - | - | Bulk void correlation (j3) |
| two_phase_friction_multiplier | group_02_flow_correlations | isp | - | - | Two phase friction multiplier (j4) |
| wall_viscosity | group_02_flow_correlations | isp | - | - | Wall viscosity correlation (nviscw) |

| Name | HDF-Group | Type | Dimension(s) | Unit | Description |
|--------------------------------|-----------------------------|------|--------------|------|--|
| szablewski_correction | group_02_flow_correlations | isp | - | - | Indicator for Szablewski correction of Lehmann friction factor (nzabl) |
| subcooled_boiling_profile_fit | group_02_flow_correlations | isp | - | - | Subcooled boiling profile fit (j8) |
| ff_coefficient_aa | group_02_flow_correlations | rsp | 1 | - | Friction factor correlation constant AA |
| ff_coefficient_bb | group_02_flow_correlations | rsp | 1 | - | Friction factor correlation constant BB |
| ff_coefficient_cc | group_02_flow_correlations | rsp | 1 | - | Friction factor correlation constant CC |
| npoly_void | group_02_flow_correlations | isp | - | - | Number of void fraction polynomial coefficients (nv) (optional) |
| slip_ratio | group_02_flow_correlations | rsp | - | - | Slip ratio (av(1)) (optional) |
| poly_coeff_void | group_02_flow_correlations | rsp | 1 | - | 7 void fraction polynomial coefficients (av) (optional) |
| npoly_friction_multiplier | group_02_flow_correlations | isp | - | - | Number of two phase friction polynomial coefficients (nf) (optional) |
| poly_coeff_friction_multiplier | group_02_flow_correlations | rsp | 1 | - | 7 two phase friction polynomial coefficients (af) (optional) |
| group_03_power_distribution | thm_input | G | - | - | Power distribution |
| nax | group_03_power_distribution | isp | - | - | Number of axial positions with specified axial heat flux (nax) |
| iqp3 | group_03_power_distribution | isp | - | - | Power type specification (iqp3) |
| y | group_03_power_distribution | rsp | 1 | - | Relative axial positions (X/L) with specified axial heat flux (y) |

| Name | HDF-Group | Type | Dimension(s) | Unit | Description |
|---------------------------|-----------------------------|------|--------------|------|--|
| axial | group_03_power_distribution | rsp | 1 | - | Relative axial heat flux specified (local/average) (axial) |
| axmax | group_03_power_distribution | rsp | - | - | Maximum of the axial shapes for power distribution (axmax) |
| sumax | group_03_power_distribution | rsp | - | - | Average of the axial shapes for power distribution (sumax) |
| sumphr | group_03_power_distribution | rsp | - | m | Total heated perimeter calculated from rod data (sumphr) |
| sumrp | group_03_power_distribution | rsp | - | m | Internal parameter used for power distribution (sumrp) |
| offset | group_03_power_distribution | rsp | - | - | offset |
| hot_channel_factors | group_03_power_distribution | G | - | - | Hot channel factors |
| hot_channel_number | hot_channel_factors | isp | - | - | Hot channel number (ihc) |
| flux_engineering_factor | hot_channel_factors | rsp | - | - | Hot channel flux engineering factor (feq) |
| pellet_engineering_factor | hot_channel_factors | rsp | - | - | Hot channel pellet engineering factor (fedh1) |
| pin_engineering_factor | hot_channel_factors | rsp | - | - | Hot channel pin engineering factor (fedh2) |
| grid_1_factor | hot_channel_factors | rsp | - | - | Hot channel spacer loss coefficient factor (f1grid) |
| grid_2_factor | hot_channel_factors | rsp | - | - | Hot channel spacer loss coefficient factor (f2grid) |
| grid_3_factor | hot_channel_factors | rsp | - | - | Hot channel spacer loss coefficient factor (f3grid) |
| dnb_limit_indicator | hot_channel_factors | L | - | - | Indicator of DNB-Limit (lchf) |
| dnb_limit | hot_channel_factors | rsp | - | - | DNB ratio limit for heat transfer (chflim) |

| Name | HDF-Group | Type | Dimension(s) | Unit | Description |
|-----------------------|-----------------------|------|--------------|----------------|---|
| group_04_channel_data | thm_input | G | - | - | Channel data |
| array_definition | group_04_channel_data | S | - | - | Indicator if the thermal hydraulics data is read via input or calculated via CoreLib (array_def) |
| an | group_04_channel_data | rsp | 1 | m ² | Nominal flow area (an) |
| dist | group_04_channel_data | rsp | 2 | m | Channel centroid to centroid distance dist(i,:) |
| eneh | group_04_channel_data | rsp | 1 | - | Gap local multiplier to enthalpy difference in energy equation turbulent mixing term (eneh), only if nk>0 |
| facftm | group_04_channel_data | rsp | 1 | - | Gap local multiplier to global turbulent momentum factor FTM (facftm) , only if nk>0 |
| facsl | group_04_channel_data | rsp | 2 | - | Gap local multiplier to global transverse momentum parameter S/L (facsl) , only if nk>0 |
| facslk | group_04_channel_data | rsp | 1 | - | Gap local multiplier to global diversion cross flow resistance KIJ (facslk) , only if nk>0 |
| facto | group_04_channel_data | rsp | 1 | - | Gap factor (facto) , only if nk>0 |
| gaps | group_04_channel_data | rsp | 2 | m | Nominal gap spacings gaps(i,:) belonging to channel i , only if nk>0 |
| lscale_inp | group_04_channel_data | L | - | - | Indicator for lateral scaling via input , only if nk>0 |
| lscale_sl | group_04_channel_data | L | - | - | Indicator for lateral scaling of parameter SL, only if nk>0 |

| Name | HDF-Group | Type | Dimension(s) | Unit | Description |
|--------------------------|-----------------------|------|--------------|----------------|--|
| lscale_kij | group_04_channel_data | L | - | - | Indicator for lateral scaling of crossflow resistance factor KIJ, only if nk>0 |
| lref_kij | group_04_channel_data | rsp | - | m | Characteristic distance for lateral scaling of the crossflow resistance factor, only if nk>0 |
| hperi | group_04_channel_data | rsp | 1 | m | Heated perimeter (hperi) |
| lc | group_04_channel_data | isp | 2 | - | Neighbour channels lc(i,:) to channel i |
| number_of_channels_total | group_04_channel_data | isp | - | - | Total number of sub-channels (nchan) |
| nk | group_04_channel_data | isp | - | - | Total number of gaps (nk) |
| ntype | group_04_channel_data | isp | - | - | Subchannel type (ntype) |
| perim | group_04_channel_data | rsp | 1 | m | Wetted perimeter (perim) |
| atotal | group_04_channel_data | rsp | - | m ² | Total sub-channel area (atotal) |
| dhyd | group_04_channel_data | rsp | 1 | m | Sub-channel hydraulic diameters (dhyd) |
| gapn | group_04_channel_data | rsp | 1 | m | Gap length (gapn) |
| ik | group_04_channel_data | isp | 1 | - | First sub-channel number belonging to a gap (ik) |
| jk | group_04_channel_data | isp | 1 | - | Second sub-channel number belonging to a gap (jk) |
| lengt | group_04_channel_data | rsp | 1 | m | Centroid distance for each gap (lengt) |

| Name | HDF-Group | Type | Dimension(s) | Unit | Description |
|---------------------------------|---------------------------------|------|--------------|------|--|
| phtot | group_04_channel_data | rsp | - | m | Total heated sub-channels perimeter (phtot) |
| group_05_channel_area_variation | thm_input | G | - | - | Channel variation parameter |
| naxl | group_05_channel_area_variation | isp | - | - | Number of axial positions with specified area variation (naxl) |
| nafact | group_05_channel_area_variation | isp | - | - | Number of channels with specified area variation factors (local/nominal area) (nafact) |
| naramp | group_05_channel_area_variation | isp | - | - | Number of iterations for inserting the area variation (naramp) |
| axl | group_05_channel_area_variation | rsp | 1 | - | Relative axial locations (X/L) with specified area variation (axl) (optional) |
| affect | group_05_channel_area_variation | rsp | 2 | - | Area variation factors (local/nominal area) (affect) (optional) |
| idare | group_05_channel_area_variation | isp | 1 | - | Parameter internally used for channel area variation (idare) (optional) |
| nch | group_05_channel_area_variation | isp | 1 | - | Parameter internally used for channel area variation (nch) (optional) |
| group_06_gap_variation | thm_input | G | - | - | Gap variations |
| ngxl | group_06_gap_variation | isp | - | - | Number of axial positions with specified gap variation (ngxl) |
| ngaps | group_06_gap_variation | isp | - | - | Number of gaps with variation (ngaps) |
| gapxl | group_06_gap_variation | rsp | 1 | - | Relative axial locations (X/L) with specified gap variation (gapxl) (optional) |

| Name | HDF-Group | Type | Dimension(s) | Unit | Description |
|----------------------------|------------------------|------|--------------|------|---|
| gfact | group_06_gap_variation | rsp | 2 | - | Gap variation factors (local/nominal area) (gfact) (optional) |
| idgap | group_06_gap_variation | isp | 1 | - | Parameter internally used for gap variation (idgap) (optional) |
| ngap | group_06_gap_variation | isp | 1 | - | Gap numbers with given spacing variation (ngap) (optional) |
| group_07_spacer | thm_input | G | - | - | Spacer parameters |
| spacer_type | group_07_spacer | isp | - | - | Spacer type indicator (j6) |
| ngrid | group_07_spacer | isp | - | - | Total number of spacer locations (ngrid) |
| ngridt | group_07_spacer | isp | - | - | Number of spacer types (ngridt) |
| number_iterations_for_ramp | group_07_spacer | isp | - | - | Number of iterations for inserting loss coefficients for wire wrap mixing (nramp) |
| cross_flow_indicator | group_07_spacer | isp | - | - | Crossflow solution indicator (njump) |
| jump | group_07_spacer | isp | - | - | Crossflow solution indicator (jump) |
| wire_wrap_pitch | group_07_spacer | rsp | - | m | Wire wrap pitch (pitch) (optional) |
| pin_diameter | group_07_spacer | rsp | - | m | Pin diameter (dia) (optional) |
| wire_diameter | group_07_spacer | rsp | - | m | Wire diameter (thick) (optional) |
| gridxl | group_07_spacer | rsp | 1 | - | Relative locations (X/L) of spacers (gridxl) (optional) |
| igrd | group_07_spacer | isp | 1 | - | Spacer types at locations gridxl (igrd) (optional) |
| grid_loss_coefficient_a | group_07_spacer | rsp | 2 | - | Spacer loss coefficient (cda) (optional) |

| Name | HDF-Group | Type | Dimension(s) | Unit | Description |
|---------------------------|-------------------|------|--------------|------|--|
| grid_loss_coefficient_b | group_07_spacer | rsp | 2 | - | Spacer loss coefficient (cdb) (optional) |
| grid_loss_coefficient_c | group_07_spacer | rsp | 2 | - | Spacer loss coefficient (cdc) (optional) |
| fraction_of_flow_diverted | group_07_spacer | rsp | 2 | - | Fraction of flow diverted (fxflo) (optional) |
| group_08_rod_data | thm_input | G | - | - | Rod data |
| fuel_rod_model | group_08_rod_data | isp | - | - | COBRA-FLX fuel rod model indicator (ifrm) |
| heat_transfer_model | group_08_rod_data | isp | - | - | Heat transfer coefficient correlation (ihtcc) |
| heat_transfer_coefficient | group_08_rod_data | isp | - | - | Rod-to-coolant heat transfer model (ihtm) |
| number_of_rods_total | group_08_rod_data | isp | - | - | Total number of rods (nrod) |
| number_of_radial_nodes | group_08_rod_data | isp | - | - | Total number of radial fuel nodes including cladding (nodesf) |
| number_of_fuel_types | group_08_rod_data | isp | - | - | Number of fuel types (nfuel) |
| property_model | group_08_rod_data | isp | - | - | Fuel rod material properties model (iprop) |
| acelf | group_08_rod_data | rsp | - | - | Damping factor for heat transfer coefficient iteration (acelf) |
| material_properties | group_08_rod_data | isp | - | - | Material properties (matpro) (optional) |
| fuel_shells | group_08_rod_data | isp | - | - | Number of radial fuel shells (ncf) (optional) |
| cladding_shells | group_08_rod_data | isp | - | - | Number of radial cladding shells (ncc) (optional) |
| gap_thickness | group_08_rod_data | rsp | - | m | Gap thickness (thg) (optional) |

| Name | HDF-Group | Type | Dimension(s) | Unit | Description |
|-----------------------------------|-------------------------|------|--------------|-------------------|--|
| temperature_convergence_criterion | group_08_rod_data | rsp | - | - | Temperature convergence criterion (epsf) (optional) |
| temperature_distribution | group_08_rod_data | isp | - | - | Indicator for temperature distribution (ioldcb) (optional) |
| thermal_expansion | group_08_rod_data | isp | - | - | Thermal expansion indicator (icorad) (optional) |
| use_CARO_results | group_08_rod_data | isp | - | - | Indicator for using CARO results (iusca) (optional) |
| oxide_thermal_resistance | group_08_rod_data | isp | - | - | Indicator for oxide thermal resistance (iusox) (optional) |
| gas_pressure | group_08_rod_data | isp | - | - | Indicator for considering gas pressure (icagas) (optional) |
| use_CARO_heat_flux | group_08_rod_data | isp | - | - | Indicator for using the CARO heat flux (iuscax) (optional) |
| fuel_thermal_properties | group_08_rod_data | G | - | - | Fuel thermal properties (optional) |
| fuel_thermal_conductivity | fuel_thermal_properties | rsp | - | W/(m K) | Fuel thermal conductivity (kfuel) |
| fuel_specific_heat | fuel_thermal_properties | rsp | - | J/(kg K) | Fuel specific heat (cfuel) |
| fuel_density | fuel_thermal_properties | rsp | - | kg/m ³ | Fuel density (rfuel) |
| pellet_diameter | fuel_thermal_properties | rsp | - | m | Pellet diameter (dfuel) |
| cladding_thermal_conductivity | fuel_thermal_properties | rsp | - | W/(m K) | Cladding thermal conductivity (kclad) |
| cladding_specific_heat | fuel_thermal_properties | rsp | - | J/(kg K) | Cladding specific heat (cclad) |
| cladding_density | fuel_thermal_properties | rsp | - | kg/m ³ | Cladding density (rclad) |

| Name | HDF-Group | Type | Dimension(s) | Unit | Description |
|-------------------------------|-------------------------|------|--------------|----------------------|---|
| cladding_thickness | fuel_thermal_properties | rsp | - | m | Cladding thickness (tclad) |
| gap_heat_transfer_coefficient | fuel_thermal_properties | rsp | - | W/(m ² K) | Gap heat transfer coefficient (hgap) |
| rods | group_08_rod_data | G | - | - | Rods description |
| d | rods | rsp | 1 | m | Rod diameter (d) |
| idfue | rods | isp | 1 | - | Fuel rod type (idfue) |
| radia | rods | rsp | 1 | - | Relative rod power (local/average) (radia) |
| lr | rods | isp | 2 | - | Subchannel numbers belonging to given rod (lr) |
| phi | rods | rsp | 2 | - | Fraction of power going to adjacent channels (phi) |
| chf_data | group_08_rod_data | G | - | - | CHF data input information |
| chf_correlation | chf_data | isp | - | - | CHF correlation indicator (nchf) |
| number_of_chf_correlations | chf_data | isp | - | - | Total number of CHF correlations used for this case (nnn_case) |
| chf_correlations | chf_data | isp | 2 | - | CHF correlation indicator (rod,node) (n_chf), only if number_of_chf_correlations > 0 |
| l_chfspc | chf_data | L | 1 | - | Indicator how DNBR is computed (lchfspc) , only if number_of_chf_correlations > 0 |
| case_chf_correlations | chf_data | isp | 1 | - | All numbers of the CHF correlations used for this case (chf_case), only if number_of_chf_correlations > 0 |

| Name | HDF-Group | Type | Dimension(s) | Unit | Description |
|-------------------------------|------------------------|------|--------------|------|--|
| chf_performance_factors | chf_data | rsp | 2 | - | Performance factors (correlation, 1(irgw)) for CHF correlations (chf_perf) , only if number_of_chf_correlations > 0 |
| chf_mixing_grids | chf_data | L | 1 | - | Indicator for mixing grids (correlation) for CHF correlations (l_mg) , only if number_of_chf_correlations > 0 |
| number_of_mixing_grids | chf_data | isp | 1 | - | Number of mixing grids (CHF correlation) for CHF correlations (n_mgrid) , only if number_of_chf_correlations > 0 |
| mixing_grid_number | chf_data | isp | 2 | - | Spacer numbers that are mixing grids for CHF correlation(m_grid(:,i_chf)) , only if number_of_chf_correlations > 0 |
| mixing_grid_height | chf_data | rsp | 2 | m | Mixing grid heights for grid types and CHF correlations (grid_ht(i_chf,type)) , only if number_of_chf_correlations > 0 |
| [] | chf_data | G | - | - | [] is selected and contains special data needed for it. |
| grid_option | [] | isp | - | - | Spacer grid option (ispace) |
| dnbr_multiplier | [] | rsp | - | - | DNBR multiplier/Test section type (factot_7) |
| grid_constant | [] | rsp | - | - | Spacer grid constant (xks_7) |
| thermal_diffusion_coefficient | [] | rsp | - | - | Thermal diffusion coefficient for spacer factor used in CHF evaluation (tdc_7) |

| Name | HDF-Group | Type | Dimension(s) | Unit | Description |
|----------------------------|-----------|------|--------------|------|---|
| [] | chf_data | G | - | - | This group is available [] is selected and contains special data needed for it. |
| test_section_type | [] | rsp | - | - | DNBR multiplier/Test section type (faktot_8) |
| rel_begin_of_heated_length | [] | rsp | - | - | Spacer grid constant (xks_8) |
| [] | chf_data | G | - | - | This group is available if [] CHF correlation is selected and contains special data needed for it. |
| [] | [] | S | - | - | [])] |
| [] | [] | rsp | 1 | - | [] |
| test_section_type | [] | rsp | - | - | DNBR multiplier/Test section type (faktot_9) |
| rel_begin_of_heated_length | [] | rsp | - | - | Spacer grid constant (xks_9) |
| [] | chf_data | G | - | - | [] is selected and contains special data needed for it. |
| test_section_type | [] | rsp | - | - | DNBR multiplier/Test section type (faktot_10) |
| rel_begin_of_heated_length | [] | rsp | - | - | Spacer grid constant (xks_10) |

| Name | HDF-Group | Type | Dimension(s) | Unit | Description |
|------------------------------------|-----------|------|--------------|------|---|
| hc_heated_perimeter | [] | rsp | - | m | Hot-channel heated perimeter (ponesc) |
| hc_ratio_radial_power_factor | [] | rsp | - | - | Ratio of maximum to average radial heat flux factor of the rods around the hot channel (trsc) |
| characteristic_diameter_selection | [] | isp | 1 | - | Flags for characteristic diameters used for CHF-correlation (idmr) |
| thermal_diffusion_coefficient_tong | [] | rsp | - | - | Thermal diffusion coefficient for Tong spacer correlation (tdcw3) |
| grid_spacing_coefficient | [] | rsp | - | - | Axial grid spacing coefficient depending on axial grid spacing (ksgrid) |
| dnbr_multiplier | [] | rsp | - | - | DNBR correction multiplier (fdnbrw) |
| rod_bundle_factor | [] | rsp | - | - | Rod bundle factor (fgpg) |
| [] | chf_data | G | - | - | This group is available if [] CHF correlation is selected and contains special data needed for it. |
| lattice_hydraulic_diameter | [] | rsp | 1 | m | Lattice hydraulic diameter (dhhyd13) |
| bundle_heated_length | [] | rsp | - | m | Fuel bundle heated length (hlen13) |

| Name | HDF-Group | Type | Dimension(s) | Unit | Description |
|-----------------------------------|-----------|------|--------------|------|---|
| [] | chf_data | G | - | - | This group is available if [] CHF correlation is selected and contains special data needed for it. |
| grid_spacing | [] | rsp | - | m | Grid spacing (spitch) |
| grid_loss_coeff_ratio_vane_novane | [] | rsp | - | - | Ratio of grid pressure loss coefficients (vaned/unvaned) (xkloss) |
| bundle_heated_length | [] | rsp | - | m | heated length (blen) |
| [] | chf_data | G | - | - | This group is available if [] CHF correlation is selected and contains special data needed for it. |
| lattice_hydraulic_diameter | [] | rsp | 1 | m | Lattice hydraulic diameter (dhhyd23) |
| bundle_heated_length | [] | rsp | - | m | Fuel bundle heated length (hlen23) |
| [] | chf_data | G | - | - | This group is available if [] CHF correlation is selected and contains special data needed for it. |
| lattice_hydraulic_diameter | [] | rsp | 1 | m | Lattice hydraulic diameter (dhhyd33) |
| bundle_heated_length | [] | rsp | - | m | Fuel bundle heated length (hlen33) |
| data_ACH_2 | chf_data | G | - | - | This group is available if ACH-2 CHF correlation is selected and contains special data needed for it. |

| Name | HDF-Group | Type | Dimension(s) | Unit | Description |
|-----------------------|-----------------------|------|--------------|------|--|
| debug_printing | data_ACH_2 | isp | - | - | Indicator for CHF correlation debug output (usdprn50) |
| first_debug_channel | data_ACH_2 | isp | - | - | First channel for CHF correlation debug output (hchans50) |
| last_debug_channel | data_ACH_2 | isp | - | - | Last channel for CHF correlation debug output (hchanx50) |
| read_limits | data_ACH_2 | isp | - | - | Indicator for CHF correlation limits (ach2_limit) |
| data_Barnett | chf_data | G | - | - | This group is available if Barnett CHF correlation is selected and contains special data needed for it. |
| heated_length | data_Barnett | rsp | - | m | Fuel bundle heated length (hlen_barn) |
| debug_printing | data_Barnett | isp | - | - | Indicator for CHF correlation debug output (usdprn51) |
| first_debug_channel | data_Barnett | isp | - | - | First channel for CHF correlation debug output (hchans51) |
| last_debug_channel | data_Barnett | isp | - | - | Last channel for CHF correlation debug output (hchanx51) |
| read_limits | data_Barnett | isp | - | - | Indicator for CHF correlation limits (barn_limit) |
| data_Modified_Barnett | chf_data | G | - | - | This group is available if Modified-Barnett CHF correlation is selected and contains special data needed for it. |
| heated_length | data_Modified_Barnett | rsp | - | m | Fuel bundle heated length (hlen_mbrn) |
| debug_printing | data_Modified_Barnett | isp | - | - | Indicator for CHF correlation debug output (usdprn52) |

| Name | HDF-Group | Type | Dimension(s) | Unit | Description |
|---------------------|-----------------------|------|--------------|------|---|
| first_debug_channel | data_Modified_Barnett | isp | - | - | First channel for CHF correlation debug output (hchans52) |
| last_debug_channel | data_Modified_Barnett | isp | - | - | Last channel for CHF correlation debug output (hchanx52) |
| read_limits | data_Modified_Barnett | isp | - | - | Indicator for CHF correlation limits (mbrn_limit) |
| data_BHTP | chf_data | G | - | - | This group is available if BHTP CHF correlation is selected and contains special data needed for it. |
| heated_length | data_BHTP | rsp | - | m | Fuel bundle heated length (hlen_bhtp) |
| pin_pitch | data_BHTP | rsp | - | m | Unit cell pin pitch (ppitch_bhtp) |
| rod_diameter | data_BHTP | rsp | - | m | Outer rod diameter of a unit cell (ddr_bhtp) |
| debug_printing | data_BHTP | isp | - | - | Indicator for CHF correlation debug output (usdprn53) |
| first_debug_channel | data_BHTP | isp | - | - | First channel for CHF correlation debug output (hchans53) |
| last_debug_channel | data_BHTP | isp | - | - | Last channel for CHF correlation debug output (hchanx53) |
| read_limits | data_BHTP | isp | - | - | Indicator for CHF correlation limits (bhtp_limit) |
| data_Biasi | chf_data | G | - | - | This group is available if Biasi CHF correlation is selected and contains special data needed for it. |
| heated_length | data_Biasi | rsp | - | m | Fuel bundle heated length (hlen_bias) |
| debug_printing | data_Biasi | isp | - | - | Indicator for CHF correlation debug output (usdprn54) |

| Name | HDF-Group | Type | Dimension(s) | Unit | Description |
|---------------------|------------|------|--------------|------|--|
| first_debug_channel | data_Biasi | isp | - | - | First channel for CHF correlation debug output (hchans54) |
| last_debug_channel | data_Biasi | isp | - | - | Last channel for CHF correlation debug output (hchanx54) |
| read_limits | data_Biasi | isp | - | - | Indicator for CHF correlation limits (bias_limit) |
| data_BWC | chf_data | G | - | - | This group is available if BWC CHF correlation is selected and contains special data needed for it. |
| debug_printing | data_BWC | isp | - | - | Indicator for CHF correlation debug output (usdprn55) |
| first_debug_channel | data_BWC | isp | - | - | First channel for CHF correlation debug output (hchans55) |
| last_debug_channel | data_BWC | isp | - | - | Last channel for CHF correlation debug output (hchanx55) |
| read_limits | data_BWC | isp | - | - | Indicator for CHF correlation limits (bwc_limit) |
| data_BWCMV | chf_data | G | - | - | This group is available if BWC-MV CHF correlation is selected and contains special data needed for it. |
| heated_length | data_BWCMV | rsp | - | m | Fuel bundle heated length (hlen_bwcv) |
| debug_printing | data_BWCMV | isp | - | - | Indicator for CHF correlation debug output (usdprn56) |
| first_debug_channel | data_BWCMV | isp | - | - | First channel for CHF correlation debug output (hchans56) |
| last_debug_channel | data_BWCMV | isp | - | - | Last channel for CHF correlation debug output (hchanx56) |

| Name | HDF-Group | Type | Dimension(s) | Unit | Description |
|---------------------|---------------------|------|--------------|------|--|
| read_limits | data_BWCMV | isp | - | - | Indicator for CHF correlation limits (bwcv_limit) |
| data_BWCMV_A | chf_data | G | - | - | This group is available if BWC-MV-A CHF correlation is selected and contains special data needed for it. |
| heated_length | data_BWCMV_A | rsp | - | m | Fuel bundle heated length (hlen_bwca) |
| debug_printing | data_BWCMV_A | isp | - | - | Indicator for CHF correlation debug output (usdprn57) |
| first_debug_channel | data_BWCMV_A | isp | - | - | First channel for CHF correlation debug output (hchans57) |
| last_debug_channel | data_BWCMV_A | isp | - | - | Last channel for CHF correlation debug output (hchanx57) |
| read_limits | data_BWCMV_A | isp | - | - | Indicator for CHF correlation limits (bwca_limit) |
| data_BWU_Z_Mark_B11 | chf_data | G | - | - | This group is available if BWU-Z Mark-B11 CHF correlation is selected and contains special data needed for it. |
| heated_length | data_BWU_Z_Mark_B11 | rsp | - | m | Fuel bundle heated length (hlen_bwz1) |
| debug_printing | data_BWU_Z_Mark_B11 | isp | - | - | Indicator for CHF correlation debug output (usdprn58) |
| first_debug_channel | data_BWU_Z_Mark_B11 | isp | - | - | First channel for CHF correlation debug output (hchans58) |
| last_debug_channel | data_BWU_Z_Mark_B11 | isp | - | - | Last channel for CHF correlation debug output (hchanx58) |
| read_limits | data_BWU_Z_Mark_B11 | isp | - | - | Indicator for CHF correlation limits (bwz1_limit) |

| Name | HDF-Group | Type | Dimension(s) | Unit | Description |
|---------------------------|---------------------------|------|--------------|------|--|
| data_BWU_Z_Mark_BW17_MSMG | chf_data | G | - | - | This group is available if BWU-Z Mark-BW17 MSMG correlation is selected and contains special data needed for it. |
| heated_length | data_BWU_Z_Mark_BW17_MSMG | rsp | - | m | Fuel bundle heated length (hlen_bwzm) |
| debug_printing | data_BWU_Z_Mark_BW17_MSMG | isp | - | - | Indicator for CHF correlation debug output (usdprn59) |
| first_debug_channel | data_BWU_Z_Mark_BW17_MSMG | isp | - | - | First channel for CHF correlation debug output (hchans59) |
| last_debug_channel | data_BWU_Z_Mark_BW17_MSMG | isp | - | - | Last channel for CHF correlation debug output (hchanx59) |
| read_limits | data_BWU_Z_Mark_BW17_MSMG | isp | - | - | Indicator for CHF correlation limits (bwzm_limit) |
| data_BWU_B11R | chf_data | G | - | - | This group is available if BWU-B11R correlation is selected and contains special data needed for it. |
| heated_length | data_BWU_B11R | rsp | - | m | Fuel bundle heated length (hlen_bwub) |
| debug_printing | data_BWU_B11R | isp | - | - | Indicator for CHF correlation debug output (usdprn60) |
| first_debug_channel | data_BWU_B11R | isp | - | - | First channel for CHF correlation debug output (hchans60) |
| last_debug_channel | data_BWU_B11R | isp | - | - | Last channel for CHF correlation debug output (hchanx60) |
| read_limits | data_BWU_B11R | isp | - | - | Indicator for CHF correlation limits (bwub_limit) |
| data_BWU_Z_Mark_BW17 | chf_data | G | - | - | This group is available if BWU-Z Mark-BW17 correlation is selected and contains special data needed for it. |

| Name | HDF-Group | Type | Dimension(s) | Unit | Description |
|---------------------|----------------------|------|--------------|------|---|
| heated_length | data_BWU_Z_Mark_BW17 | rsp | - | m | Fuel bundle heated length (hlen_bwuz) |
| debug_printing | data_BWU_Z_Mark_BW17 | isp | - | - | Indicator for CHF correlation debug output (usdprn61) |
| first_debug_channel | data_BWU_Z_Mark_BW17 | isp | - | - | First channel for CHF correlation debug output (hchans61) |
| last_debug_channel | data_BWU_Z_Mark_BW17 | isp | - | - | Last channel for CHF correlation debug output (hchanx61) |
| read_limits | data_BWU_Z_Mark_BW17 | isp | - | - | Indicator for CHF correlation limits (bwuz_limit) |
| data_BWU_I | chf_data | G | - | - | This group is available if BWU-I correlation is selected and contains special data needed for it. |
| heated_length | data_BWU_I | rsp | - | m | Fuel bundle heated length (hlen_bwui) |
| debug_printing | data_BWU_I | isp | - | - | Indicator for CHF correlation debug output (usdprn62) |
| first_debug_channel | data_BWU_I | isp | - | - | First channel for CHF correlation debug output (hchans62) |
| last_debug_channel | data_BWU_I | isp | - | - | Last channel for CHF correlation debug output (hchanx62) |
| read_limits | data_BWU_I | isp | - | - | Indicator for CHF correlation limits (bwui_limit) |
| data_BWU_N | chf_data | G | - | - | This group is available if BWU-N correlation is selected and contains special data needed for it. |
| debug_printing | data_BWU_N | isp | - | - | Indicator for CHF correlation debug output (usdprn63) |

| Name | HDF-Group | Type | Dimension(s) | Unit | Description |
|--------------------------------|--------------------------------|------|--------------|------|--|
| first_debug_channel | data_BWU_N | isp | - | - | First channel for CHF correlation debug output (hchans63) |
| last_debug_channel | data_BWU_N | isp | - | - | Last channel for CHF correlation debug output (hchanx63) |
| read_limits | data_BWU_N | isp | - | - | Indicator for CHF correlation limits (bwun_limit) |
| data_HTPA | chf_data | G | - | - | This group is available if HTPA CHF correlation is selected and contains special data needed for it. |
| heated_length | data_HTPA | rsp | - | m | Fuel bundle heated length (hlen_htpa) |
| pin_pitch | data_HTPA | rsp | - | m | Unit cell pin pitch (ppitch_htpa) |
| rod_diameter | data_HTPA | rsp | - | m | Outer rod diameter of a unit cell (ddr_htpa) |
| debug_printing | data_HTPA | isp | - | - | Indicator for CHF correlation debug output (usdprn64) |
| first_debug_channel | data_HTPA | isp | - | - | First channel for CHF correlation debug output (hchans64) |
| last_debug_channel | data_HTPA | isp | - | - | Last channel for CHF correlation debug output (hchanx64) |
| read_limits | data_HTPA | isp | - | - | Indicator for CHF correlation limits (htpa_limit) |
| group_09_calculation_variables | thm_input | G | - | - | Calculation variables |
| axial_node_printing | group_09_calculation_variables | isp | - | - | Axial printing increment (nskipx) |
| time_step_printing | group_09_calculation_variables | isp | - | - | Time step printing increment (nskipt) |
| debug_printing | group_09_calculation_variables | isp | - | - | Debug print option (kdebug) |

| Name | HDF-Group | Type | Dimension(s) | Unit | Description |
|---------------------------------------|--------------------------------|------|--------------|---------|---|
| axial_node_input | group_09_calculation_variables | isp | - | - | Axial node input (kaxial) |
| diversion_crossflow_resistance_factor | group_09_calculation_variables | rsp | - | - | Diversion crossflow resistance factor KIJ |
| turbulent_momentum_factor | group_09_calculation_variables | rsp | - | - | Turbulent momentum factor (ftm) |
| bundle_length | group_09_calculation_variables | rsp | - | m | Bundle length (z) |
| bundle_position | group_09_calculation_variables | rsp | - | degrees | Position from vertical (theta) |
| elev | group_09_calculation_variables | rsp | - | - | cos(theta) (elev) |
| number_of_axial_nodes | group_09_calculation_variables | isp | - | - | Number of axial nodes (ndx) |
| dx | group_09_calculation_variables | rsp | - | m | Node length for equidistant axial nodes (dx) |
| ndxp1 | group_09_calculation_variables | isp | - | - | Number of axial nodes + 1 (ndxp1) |
| number_of_time_steps | group_09_calculation_variables | isp | - | - | Number of time steps (ndt) |
| dt | group_09_calculation_variables | rsp | - | s | Time step size (dt) |
| total_time | group_09_calculation_variables | rsp | - | s | Total transient time (ttime) |
| maximum_number_of_iterations | group_09_calculation_variables | rsp | - | - | Maximum number of outer iterations (ntries) |
| flow_error | group_09_calculation_variables | rsp | - | - | Convergence criterion for flow (maximum allowable fraction error in flow form convergence) (ferror) |
| transverse_momentum_parameter | group_09_calculation_variables | rsp | - | - | Transverse momentum parameter S/L (sl) |

| Name | HDF-Group | Type | Dimension(s) | Unit | Description |
|---------------------------------|--------------------------------|------|--------------|------|---|
| crossflow_error | group_09_calculation_variables | rsp | - | - | Cross flow convergence criterion (werror) |
| SOR_pressure_error | group_09_calculation_variables | rsp | - | - | SOR pressure convergence criterion (epsor) |
| flow_underrelaxation_factor | group_09_calculation_variables | rsp | - | - | Damping factor for axial flow (accelf) |
| pressure_underrelaxation_factor | group_09_calculation_variables | rsp | - | - | Damping factor for lateral pressure difference (accelsp) |
| x | group_09_calculation_variables | rsp | 2 | | Axial node information: x(:,1) - axial height (m) x(:,2) - distance from grid (m) x(:,3) - distance from mixing grid (m) x(:,4) - grid spacing of mixing grids (m) x(:,5) - node length (m) x(:,6) - grid spacing of mixing grids SPC (m) x(:,7) - relative axial height (-) |
| PV-solution | group_09_calculation_variables | G | - | - | Pressure-Velocity solution input information |
| nsss | PV-solution | isp | - | - | Number of time steps of size dtss for reaching steady state (nsss) |
| dtss | PV-solution | rsp | - | s | Time step size for reaching steady state (dtss) |
| itmNSS | PV-solution | isp | - | - | Minimum number of outer iterations for achieving steady state (itmNSS) |
| itmint | PV-solution | isp | - | - | Minimum number of outer iterations/time-step for transient solution (itmint) |
| maxinr | PV-solution | isp | - | - | Max number of inner iterations for mass balance (maxinr) |

| Name | HDF-Group | Type | Dimension(s) | Unit | Description |
|--------|-------------|------|--------------|------|---|
| irebal | PV-solution | isp | - | - | Number of inner iterations for rebalancing of pressure and flow along the channel length (irebal) |
| merror | PV-solution | rsp | - | - | Maximum allowable relative mass conservation error per cell for the inner iteration (merror) |
| accelx | PV-solution | rsp | - | - | Acceleration factor (accelx) |
| accely | PV-solution | rsp | - | - | Acceleration factor (accely) |
| xfacp | PV-solution | rsp | - | - | Pressure interpolation factor (xfacp) |
| xfacm | PV-solution | rsp | - | - | Interpolation factor (xfacm) |
| nustar | PV-solution | rsp | - | - | Flag (nustar) |
| damper | PV-solution | rsp | - | - | Acceleration factor (damper) |
| accelp | PV-solution | rsp | - | - | Acceleration factor (accelp) |
| herror | PV-solution | rsp | - | J/kg | Absolute energy error (herror) |
| nsolve | PV-solution | isp | - | - | Momentum equation form (nsolve) |
| damp | PV-solution | rsp | - | - | Switch for DAMPER (damp) |
| mflowx | PV-solution | rsp | - | - | Flag (mflowx) |
| mflowy | PV-solution | rsp | - | - | Flag (mflowy) |
| masx | PV-solution | rsp | - | - | Flag (masx) |
| masy | PV-solution | rsp | - | - | Flag (masy) |
| iterss | PV-solution | isp | - | - | Flag (iterss) |

| Name | HDF-Group | Type | Dimension(s) | Unit | Description |
|---------------------------|-----------------|------|--------------|------|--|
| group_10_mixing | thm_input | G | - | - | Mixing correlations |
| subcooled_mixing | group_10_mixing | isp | - | - | Subcooled mixing correlation (nscbc) |
| two_phase_mixing | group_10_mixing | isp | - | - | Two phase mixing option (nbbc) |
| thermal_conduction_mixing | group_10_mixing | isp | - | - | Thermal conduction mixing option (j5) |
| mixing_coefficient | group_10_mixing | rsp | - | - | Subcooled mixing correlation constant (abeta) |
| mixing_exponent | group_10_mixing | rsp | - | - | Subcooled mixing correlation constant (bbeta) |
| abetag | group_10_mixing | rsp | 1 | - | Subcooled mixing correlation constant for each gap (abetag), stored only if nk>0 |
| bbetag | group_10_mixing | rsp | 1 | - | Subcooled mixing correlation constant for each gap (bbetag), stored only if nk>0 |
| lscale_tm | group_10_mixing | L | - | - | Indicator for lateral scaling of turbulent mixing (lscale_tm), stored only if nk>0 |
| lref_beta | group_10_mixing | rsp | - | m | Reference distance for lateral scaling of turbulent mixing (lref_beta) |
| ingap | group_10_mixing | isp | - | - | Number of mixing types (ingap) |
| ngapn | group_10_mixing | isp | - | - | Number of gaps with mixing type different than the default (first) mixing type (ngapn) |
| idgap1 | group_10_mixing | isp | 1 | - | Gap type number (idgap1), stored only if nk>0 |
| xqual | group_10_mixing | rsp | - | - | Steam quality (xqual) |

| Name | HDF-Group | Type | Dimension(s) | Unit | Description |
|-------------------------------|-------------------------------|------|--------------|-------------------|--|
| bx | group_10_mixing | rsp | - | - | beta (bx) |
| gk | group_10_mixing | rsp | - | - | Thermal conduction geometry factor (gk) |
| group_11_operating_conditions | thm_input | G | - | - | Operating conditions |
| in | group_11_operating_conditions | isp | - | - | Inlet temperature/enthalpy option indicator (in) |
| ispit | group_11_operating_conditions | isp | - | - | Setpoint iteration indicator (ispit) |
| inlet_mass_velocity | group_11_operating_conditions | isp | - | - | Inlet flow distribution indicator (ig) |
| inlet_volumetric_flow_rate | group_11_operating_conditions | rsp | - | m ³ /s | Core inlet volumetric flow rate (vflowin), only if in=0 or in=1 |
| np | group_11_operating_conditions | isp | - | - | Pressure transient forcing function indicator (np) |
| nh | group_11_operating_conditions | isp | - | - | Inlet enthalpy/temperature transient forcing function indicator (nh) |
| ng | group_11_operating_conditions | isp | - | - | Inlet flow transient forcing function indicator (ng) |
| nq | group_11_operating_conditions | isp | - | - | Heat flux transient forcing function indicator (nq) |
| locdat | group_11_operating_conditions | isp | - | - | Indicator for storing local coolant conditions on tape (locdat) |
| exit_pressure | group_11_operating_conditions | rsp | - | Pa | Operating pressure (pexit) |
| inlet_enthalpy_value | group_11_operating_conditions | rsp | - | J/kg | Inlet enthalpy (hin) |
| inlet_temperature_value | group_11_operating_conditions | rsp | - | °C | Inlet temperature (tin) |

| Name | HDF-Group | Type | Dimension(s) | Unit | Description |
|------------------------------------|-------------------------------|------|--------------|-----------------------|--|
| inlet_mass_velocity_value | group_11_operating_conditions | rsp | - | kg/(m ² s) | Core inlet mass flux (gin) |
| vvin | group_11_operating_conditions | rsp | - | m ³ /kg | Core inlet specific volume (vvin) |
| average_heat_flux | group_11_operating_conditions | rsp | - | W/m ² | Average heat flux (aflux) |
| fraction_of_power_generated_in_rod | group_11_operating_conditions | rsp | - | - | Fraction of heat generated in fuel (fhgfue) |
| bypass_fraction | group_11_operating_conditions | rsp | - | - | Bypass fraction (bypass) |
| pref | group_11_operating_conditions | rsp | - | Pa | Reference pressure (pref) |
| nchan_dp | group_11_operating_conditions | isp | - | - | Number of channels with non-zero exit pressure difference (nchan_dp) |
| exit_pressure_differences | group_11_operating_conditions | rsp | 1 | Pa | Exit pressure differences for all channels (dpexit), stored only if nchan_dp > 0 |
| hinle | group_11_operating_conditions | rsp | 1 | J/kg | Inlet enthalpy (hinle) |
| tinle | group_11_operating_conditions | rsp | 2 | °C | Inlet temperature (tinle) by channel. The second dimension allows 3 values with only the first value used in ARTEMIS coupled calculations. |
| finle | group_11_operating_conditions | rsp | 2 | kg/s | Inlet mass flow (finle) by channel. The second dimension allows 3 values with only the first value used in ARTEMIS coupled calculations. |
| p_time | group_11_operating_conditions | rsp | 1 | s | Time for pressure forcing function (yp) |

| Name | HDF-Group | Type | Dimension(s) | Unit | Description |
|-------------------------|-------------------------------|------|--------------|------|---|
| rel_pressure | group_11_operating_conditions | rsp | 1 | - | Pressure forcing function (fp) |
| h_time | group_11_operating_conditions | rsp | 1 | s | Time for enthalpy/temperature forcing function (yh) |
| rel_enthalpy | group_11_operating_conditions | rsp | 1 | - | Enthalpy/temperature forcing function (fh) |
| f_time | group_11_operating_conditions | rsp | 1 | s | Time for inlet flow forcing function (yg) |
| rel_flow | group_11_operating_conditions | rsp | 1 | - | Inlet flow forcing function (fg) |
| pow_time | group_11_operating_conditions | rsp | 1 | s | Time for heat flux/power forcing function (yq) |
| rel_power | group_11_operating_conditions | rsp | 1 | - | Heat flux/power forcing function (fq) |
| setpoint_iteration | group_11_operating_conditions | G | - | - | Setpoint iteration parameters, only if ispit > 0 (not yet available in HDF) |
| group_12_output_options | thm_input | G | - | - | Output options |
| ascii_write_results | group_12_output_options | L | - | - | ASCII data printout indicator (artemis_ascii_results) |
| hdf_write_results | group_12_output_options | L | - | - | HDF data printout indicator (artemis_hdf_results) |
| write_to_screen | group_12_output_options | L | - | - | Data printout to screen indicator (artemis_stderr) |
| print_selection | group_12_output_options | isp | - | - | Data printout indicator (nout) |
| npchan | group_12_output_options | isp | - | - | Sub-channel data printout indicator (npchan) |
| nprod | group_12_output_options | isp | - | - | Fuel rod data printout indicator (nprod) |

| Name | HDF-Group | Type | Dimension(s) | Unit | Description |
|--------------------|-------------------------|------|--------------|------|--|
| npnode | group_12_output_options | isp | - | - | Fuel node printout indicator (npnode) |
| channels_printed | group_12_output_options | isp | 1 | - | Subchannel numbers to print data for (prntc) |
| rods_printed | group_12_output_options | isp | 1 | - | Fuel rod numbers to print data for (prntr) |
| fuel_nodes_printed | group_12_output_options | isp | 1 | - | Fuel rod nodes numbers to print data for (prntn) |

F.2.1.2 Group summary_results

This group contains summary information and the sub-groups *mass_energy_balance*, *setpoint_iteration* and *chf_summary*. The detailed description of the stored data is provided in Table F-5.

Table F-5: Description of Stored Data in Group *summary_results*

| Name | HDF-Group | Type | Dimension(s) | Unit | Description |
|----------------------------|---------------------|------|--------------|-------------------|---|
| case number | summary_results | isp | - | - | Case number (kase) |
| time | summary_results | rsp | - | s | Time (etime) |
| number_axial_iterations | summary_results | isp | - | - | Number of axial iterations (iterat) |
| bundle_pressure_difference | summary_results | rsp | - | bar | Bundle pressure difference (avgdp) |
| mass_energy_balance | summary_results | G | - | - | Mass and energy balance information |
| mass_flow_in | mass_energy_balance | rsp | - | kg/s | Mass flow in (floin) |
| mass_flow_out | mass_energy_balance | rsp | - | kg/s | Mass flow out (floout) |
| flow_energy_in | mass_energy_balance | rsp | - | W | Flow energy in (engin) |
| flow_energy_out | mass_energy_balance | rsp | - | W | Flow energy out (engout) |
| energy_added | mass_energy_balance | rsp | - | W | Energy added (engadd) |
| fuel_rod_model_error | mass_energy_balance | rsp | - | W | COBRA-FLX fuel rod model error (fmerr) |
| setpoint_iteration | summary_results | G | - | - | Summary results about setpoint iteration calculations |
| vessel_inlet_mass_flow | setpoint_iteration | rsp | - | kg/s | Vessel inlet mass flow (floin/(1.-bypass)) |
| vessel_inlet_flow | setpoint_iteration | rsp | - | m ³ /s | Vessel inlet flow (vessel inlet mass flow/rho) |
| core_power | setpoint_iteration | rsp | - | W | Core power (engout-engin) |
| core_outlet_pressure | setpoint_iteration | rsp | - | Pa | Core outlet pressure (pexit) |
| vessel_inlet_temp | setpoint_iteration | rsp | - | °C | Vessel inlet temperature (tinv) |

| Name | HDF-Group | Type | Dimension(s) | Unit | Description |
|--------------------------------|--------------------|------|--------------|------|---|
| vessel_outlet_temp | setpoint_iteration | rsp | - | °C | Vessel outlet temperature (toutv) |
| vessel_average_temp | setpoint_iteration | rsp | - | °C | Vessel average temperature $0.5(t_{inv} + t_{outv})$ |
| vessel_temp_rise | setpoint_iteration | rsp | - | °C | Vessel temperature rise (toutv-tinv) |
| dnbmin | setpoint_iteration | rsp | - | - | min DNB (dnbmin) |
| offset | setpoint_iteration | rsp | - | - | Offset (offset) |
| chf_summary | summary_results | G | - | - | CHF summary information |
| global_min_dnbr | chf_summary | rsp | - | - | Minimum DNBR of all channels |
| global_rod_number_min_dnbr | chf_summary | isp | - | - | Rod number with the minimum DNBR |
| global_channel_number_min_dnbr | chf_summary | isp | - | - | Channel number with the minimum DNBR |
| global_axial_position_min_dnbr | chf_summary | isp | - | - | Axial position with the minimum DNBR |

F.2.1.3 Group bundle_averaged_results**Table F-6: Description of Stored Data in Group *bundle_averaged_results***

| Name | HDF-Group | Type | Dimension(s) | Unit | Description |
|---------------------|-------------------------|-------------|---------------------|-----------------------|--|
| total_axial_area | bundle_averaged_results | rsp | 1 | m ² | Total axial area at each printed axial distance (atot) |
| axial_distance | bundle_averaged_results | rsp | 1 | m | Axial distance |
| pressure_difference | bundle_averaged_results | rsp | 1 | Pa | Bundle averaged pressure difference |
| enthalpy | bundle_averaged_results | rsp | 1 | J/kg | Bundle averaged enthalpy |
| coolant_temperature | bundle_averaged_results | rsp | 1 | °C | Bundle averaged coolant temperature |
| coolant_density | bundle_averaged_results | rsp | 1 | kg/m ³ | Bundle averaged coolant density |
| equilibrium_quality | bundle_averaged_results | rsp | 1 | - | Bundle averaged equilibrium quality |
| void_fraction | bundle_averaged_results | rsp | 1 | - | Bundle averaged void fraction |
| coolant_mass_flow | bundle_averaged_results | rsp | 1 | kg/s | Bundle averaged coolant mass flow |
| coolant_mass_flux | bundle_averaged_results | rsp | 1 | kg/(m ² s) | Bundle averaged coolant mass flux |

F.2.1.4 Group crossflow_results**Table F-7: Description of Stored Data in Group *crossflow_results***

| Name | HDF-Group | Type | Dimension(s) | Unit | Description |
|-------------|-------------------|-------------|---------------------|-------------|---|
| ik_channel | crossflow_results | isp | 1 | - | Channel ik belonging to a gap k (ik(k)) |
| jk_channel | crossflow_results | isp | 1 | - | Channel jk belonging to a gap k (jk(k)) |
| crossflows | crossflow_results | rsp | 2 | kg/(m.s) | Crossflow through gap k (w(k,j)) |

F.2.1.5 Group channel_results**Table F-8: Description of Stored Data in Group *channel_results***

| Name | HDF-Group | Type | Dimension(s) | Unit | Description |
|---------------------|-----------------|------|--------------|-----------------------|--|
| channel_area | channel_results | rsp | 2 | m ² | Channel area at all axial nodes (areax(i,j)) |
| enthalpy | channel_results | rsp | 2 | J/kg | Enthalpy (h(i,j)) |
| pressure_difference | channel_results | rsp | 2 | Pa | Pressure difference |
| coolant_temperature | channel_results | rsp | 2 | °C | Coolant temperature |
| density | channel_results | rsp | 2 | kg/m ³ | Two-phase density (rho(i,j)) |
| equilibrium_quality | channel_results | rsp | 2 | - | Equilibrium quality (h(i,j)-hf)/hfg |
| void_fraction | channel_results | rsp | 2 | - | Void fraction |
| mass_flow | channel_results | rsp | 2 | kg/s | Coolant mass flow (f(i,j)) |
| mass_flux | channel_results | rsp | 2 | kg/(m ² s) | Coolant mass flow rate (f(i,j)/areax(i,j)) |
| min_dnbr | channel_results | rsp | 2 | - | Minimum DNB ratio for channel and axial position (mdnbrij(i,j)) |
| rod_number_mdnbr | channel_results | isp | 2 | - | Rod number with minimum DNBR for channel and axial position (ndnbrij(i,j)) |
| tong_factor | channel_results | rsp | 2 | - | Tong factor |

F.2.1.6 Group *chf_channel_results***Table F-9: Description of Stored Data in Group *chf_channel_results***

| Name | HDF-Group | Type | Dimension(s) | Unit | Description |
|-------------------------|---------------------|-------------|---------------------|------------------|--|
| min_dnbr_channel | chf_channel_results | rsp | 1 | - | For each channel - the minimal DNB ratio |
| axial_height_min_dnbr | chf_channel_results | rsp | 1 | m | For each channel - the axial height where a minimum DNB ratio occurs |
| heat_flux_min_dnbr | chf_channel_results | rsp | 1 | W/m ² | For each channel - the heat flux corresponding to the minimum DNB ratio |
| axial_position_min_dnbr | chf_channel_results | isp | 1 | - | For each channel - the axial node where a minimum DNB ratio occurs |
| rod_number_min_dnbr | chf_channel_results | isp | 1 | - | For each channel - the rod number corresponding to the minimum DNB ratio |

F.2.1.7 Group *chf_axial_results***Table F-10: Description of Stored Data in Group *chf_axial_results***

| Name | HDF-Group | Type | Dimension(s) | Unit | Description |
|----------------------------|-------------------|------|--------------|------------------|--|
| axial_nodalisation | chf_axial_results | rsp | 1 | m | Axial nodalisation |
| channel_number_mdnbr_axial | chf_axial_results | isp | 1 | - | Channel number with minimum DNB ratio at each axial position ($mcfr(j)$) |
| heat_flux_mdnbr_axial | chf_axial_results | rsp | 1 | W/m ² | Heat flux corresponding to the minimum DNB ratio at each axial position |
| mdnbr_axial | chf_axial_results | rsp | 1 | - | Minimum DNB ratio at each axial position j ($mchfr(j,1)$) |
| rod_number_mdnbr_axial | chf_axial_results | isp | 1 | - | Rod number with minimum DNB ratio at each axial position j ($mcfr(j,1)$) |
| max_boiling_regime | chf_axial_results | rsp | 1 | - | Maximum boiling regime indicator at each axial position j ($mchfr(j,3)$) (Remark: COBRA-FLX internal fuel rod model only, i.e. $nodesf > 0$) |
| max_clad_temperature | chf_axial_results | rsp | 1 | °C | Maximum cladding outer temperature at each axial position j ($mchfr(j,2)$) (Remark: COBRA-FLX internal fuel rod model only) |
| rod_max_clad_temperature | chf_axial_results | isp | 1 | - | Rod number with maximum cladding outer temperature at each axial position j ($mcfr(j,2)$) (Remark: COBRA-FLX internal fuel rod model only) |
| rod_max_boiling_regime | chf_axial_results | isp | 1 | - | Rod number with maximum boiling regime indicator at each axial position j ($mcfr(j,3)$) (Remark: COBRA-FLX internal fuel rod model only) |

F.2.1.8 Group rod_results

Table F-11: Description of Stored Data in Group *rod_results*

| Name | HDF-Group | Type | Dimension(s) | Unit | Description |
|----------------------|------------------|-------------|---------------------|------------------|--|
| heat_flux | rod_results | rsp | 2 | W/m ² | Heat flux (flux(rod,j)) |
| channel_number_mdnbr | rod_results | isp | 2 | - | Channel number with minimum DNBR for rod and axial position (cchan(n,j)) |
| dnbr | rod_results | rsp | 2 | - | DNB ratio (chfr(n,j)) |
| tong_factor | rod_results | rsp | 2 | - | Tong factor |

Figure F-1: Example of ASCII Output File

(Instructional notes, in italics, are provided in this figure. They are not present in the actual COBRA-FLX output.)

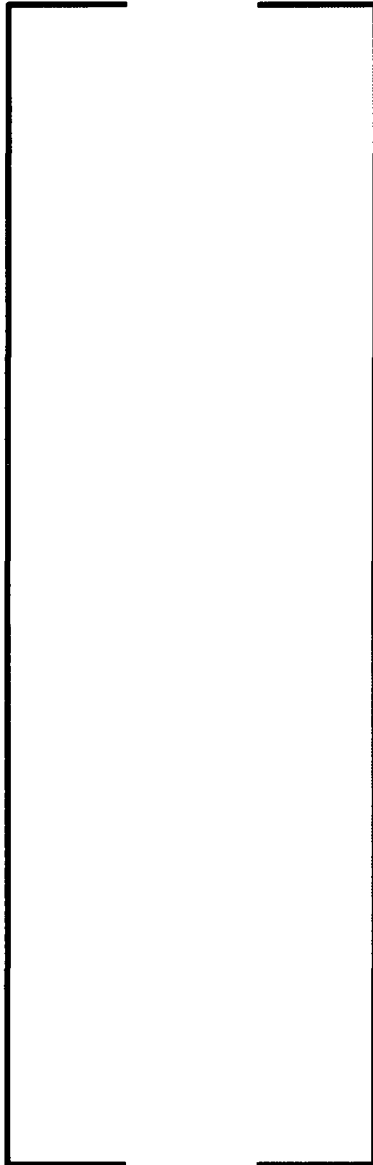
Interpreted input

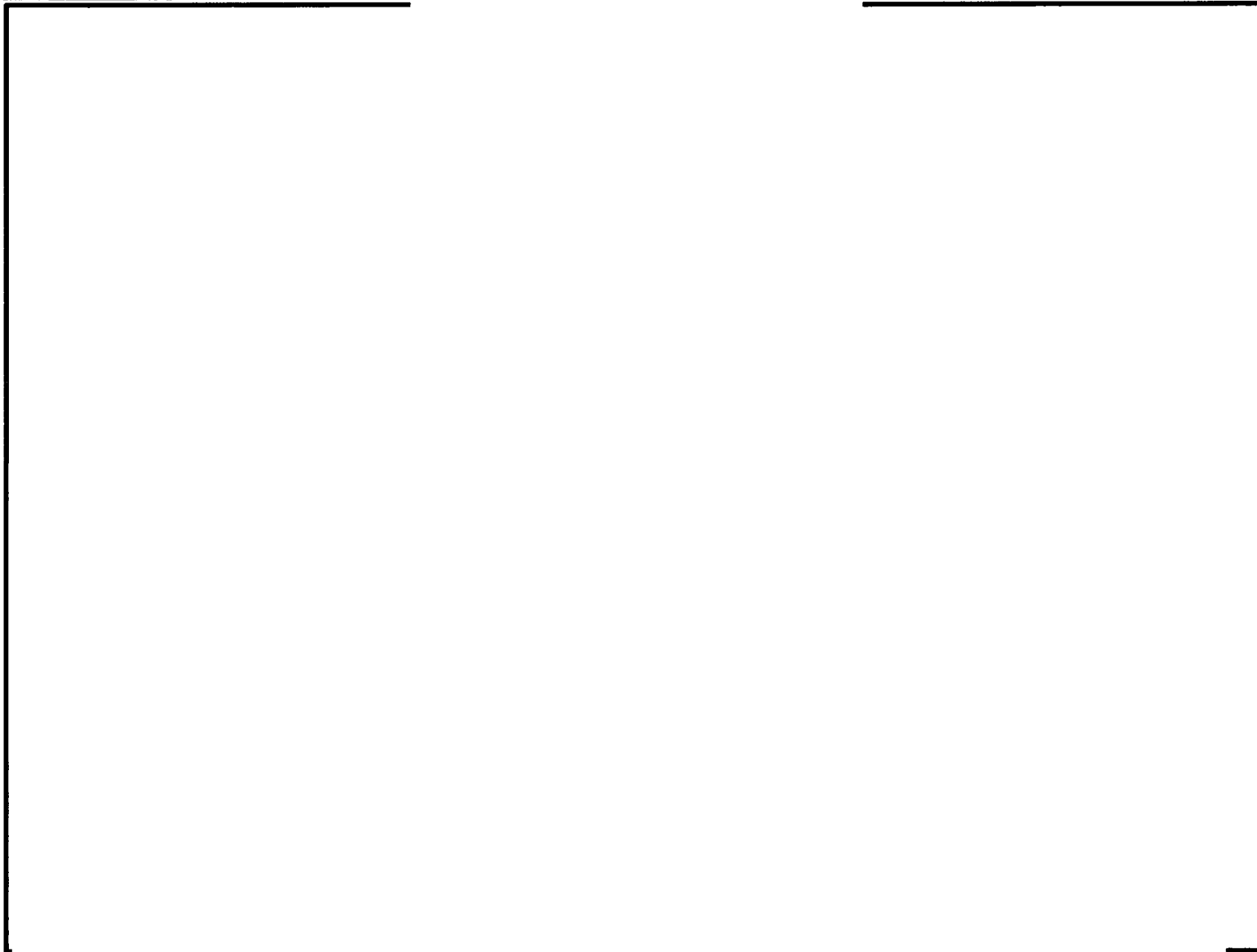
The following data is given according to the input:

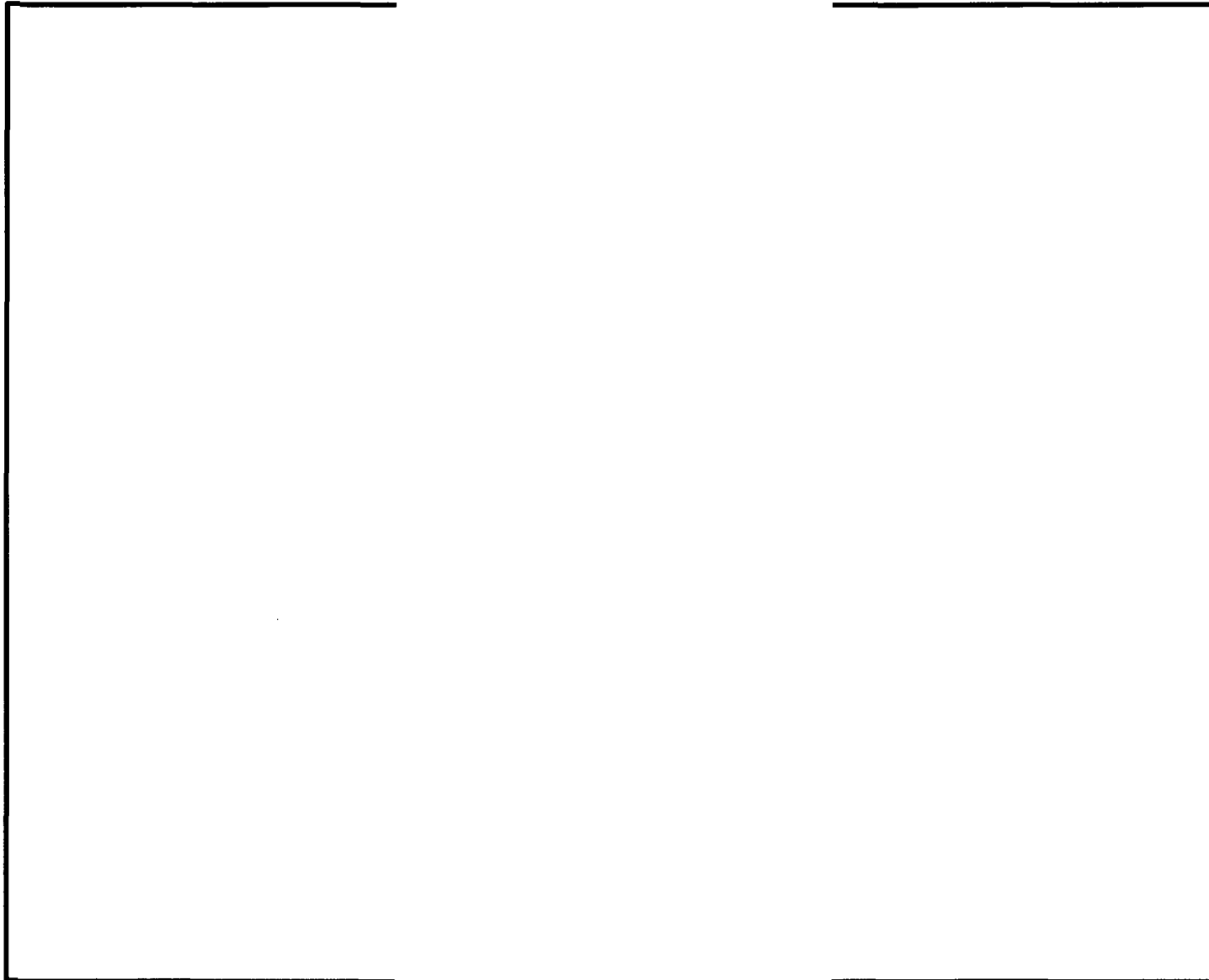
- *friction factor correlations and two-phase flow correlations*
- *heat flux distribution and engineering factors for the hot channel*
- *subchannel geometrical data (area, channel type, wetted, heated and hydraulic perimeters, adjacent channels, gap lengths and centroid distances)*
- *and gap information (related channel numbers and coupling parameters)*
- *spacer data*
- *rod geometrical data (diameter, radial power factor, adjacent channels and corresponding fraction of power)*
- *selected CHF correlation*
- *summary of power distribution information*
- *calculation parameters*
- *mixing correlations*
- *operating conditions*

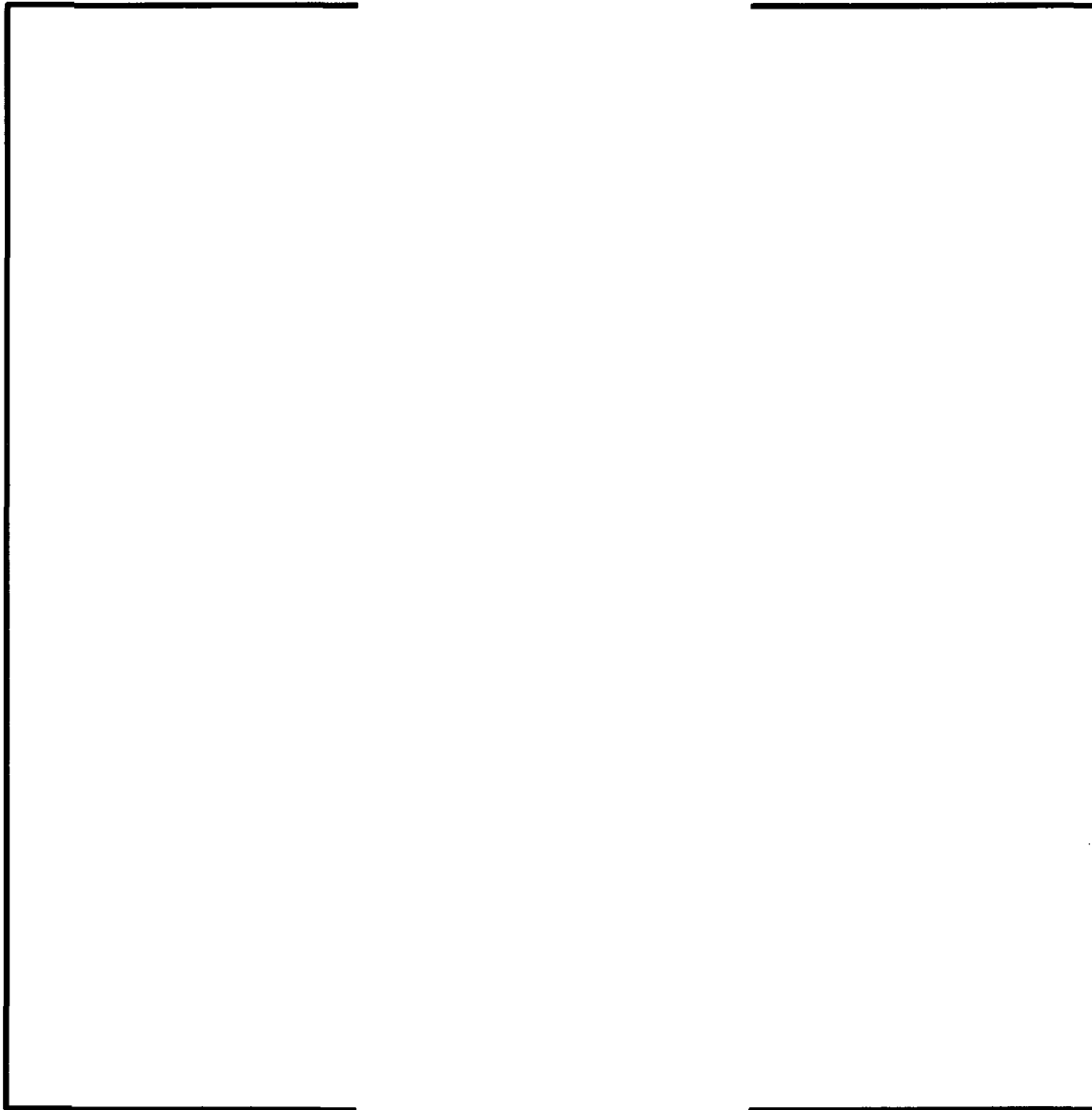


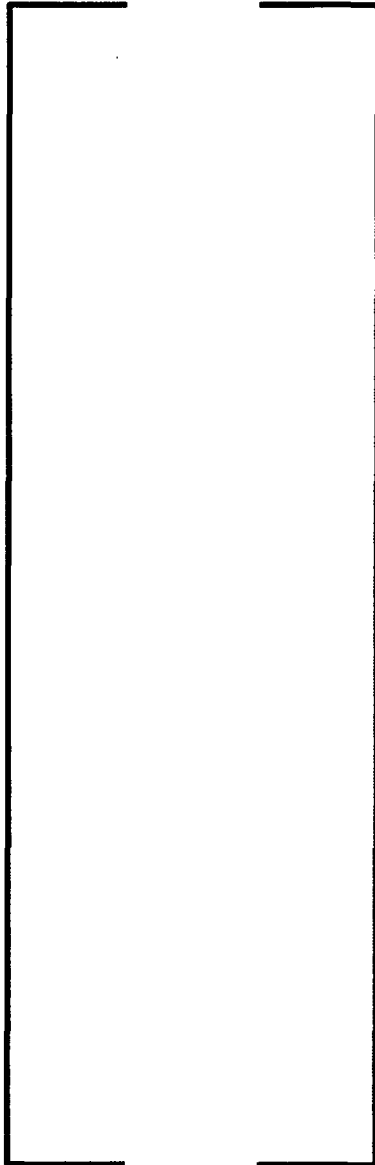


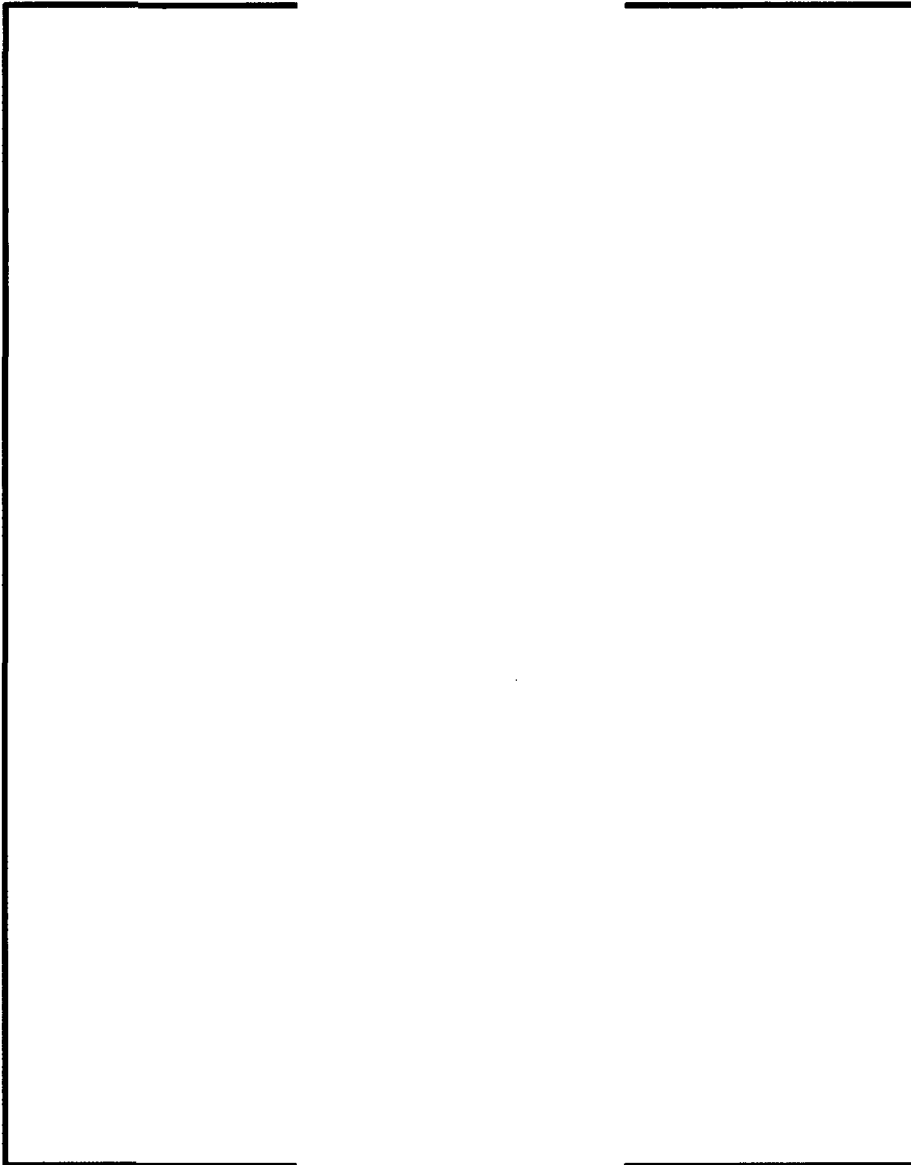


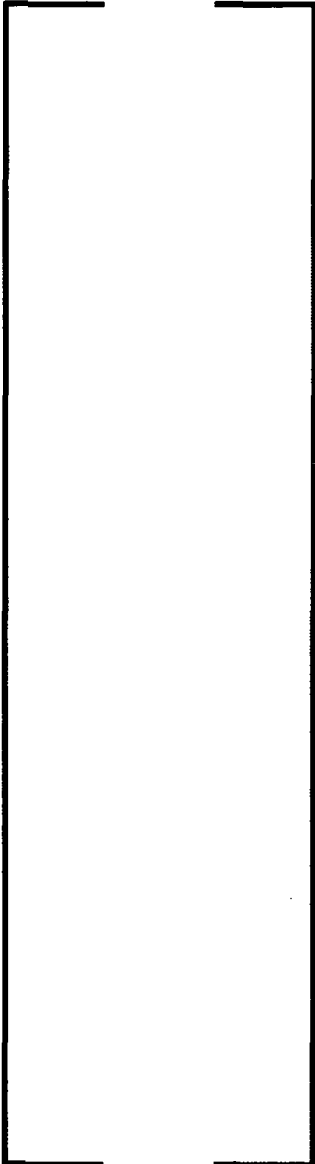


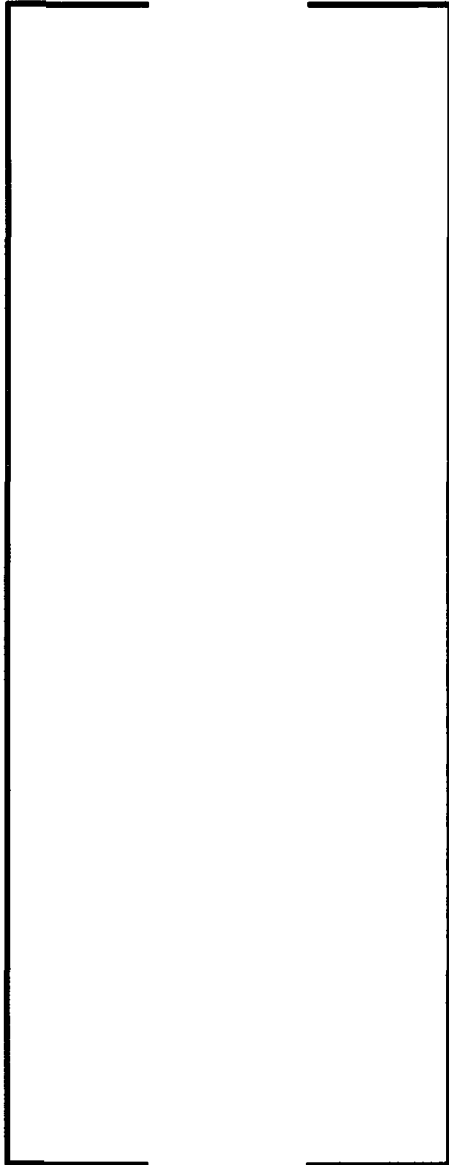


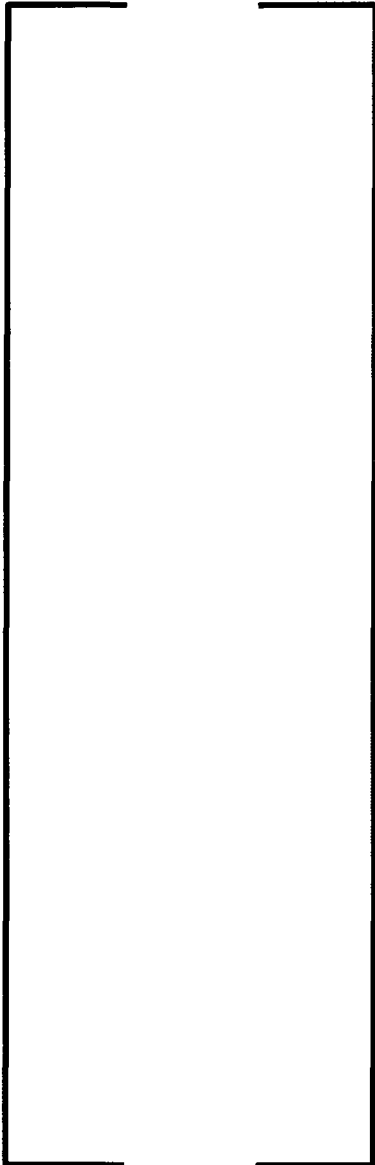


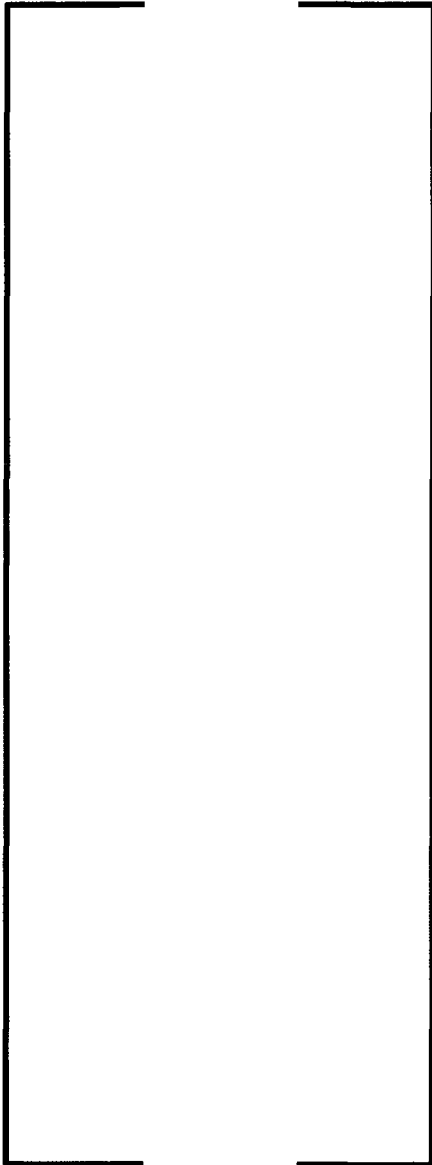


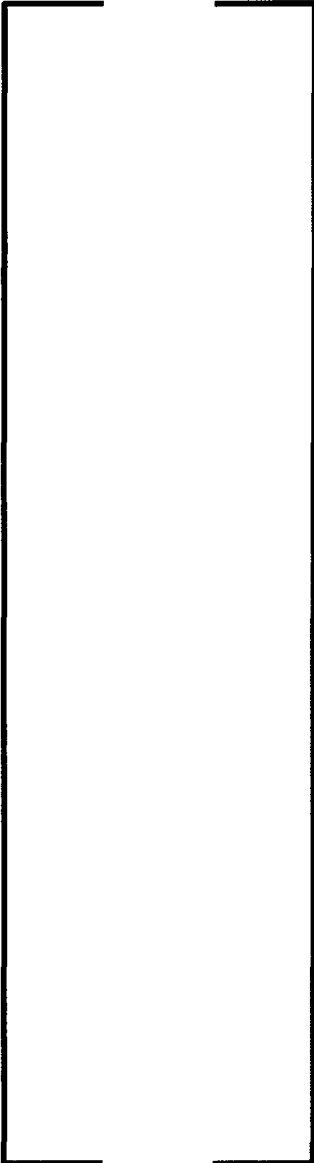


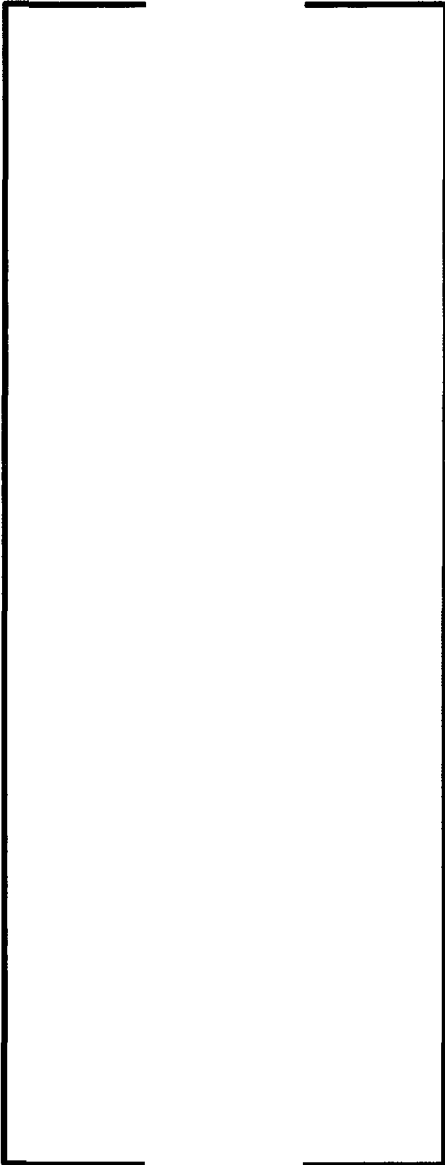


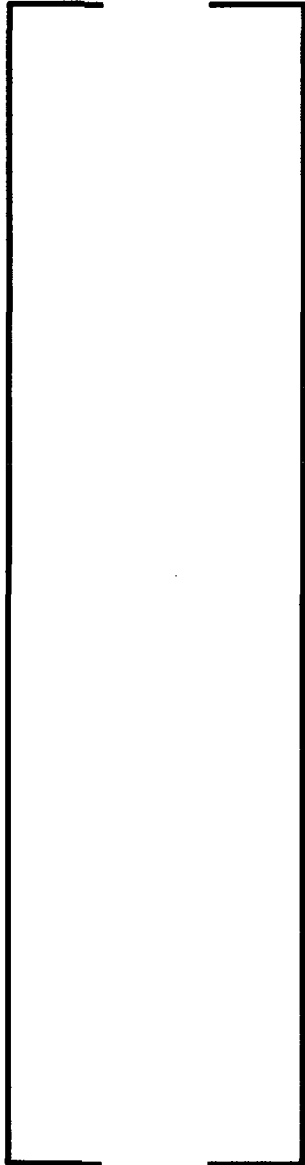




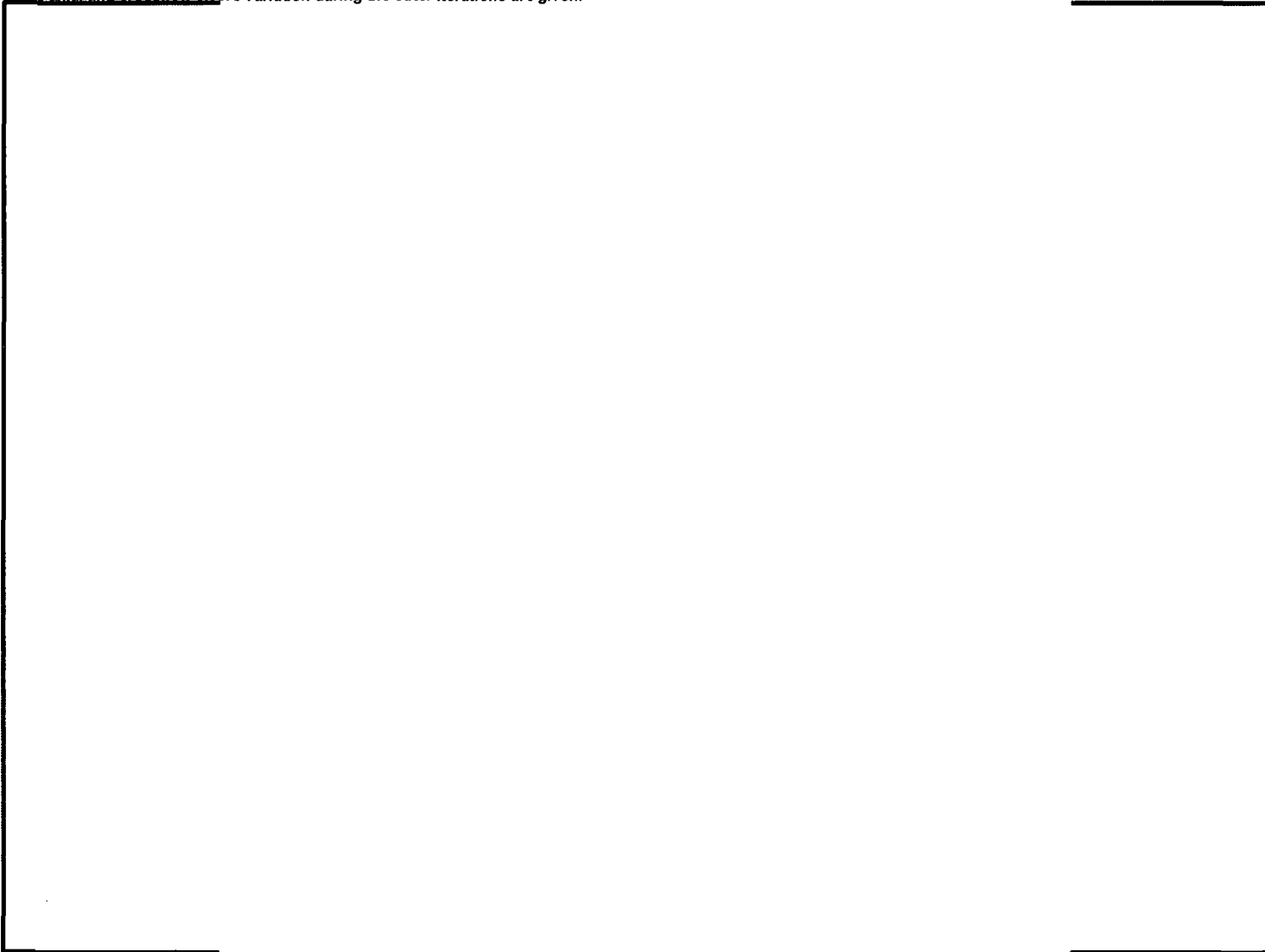


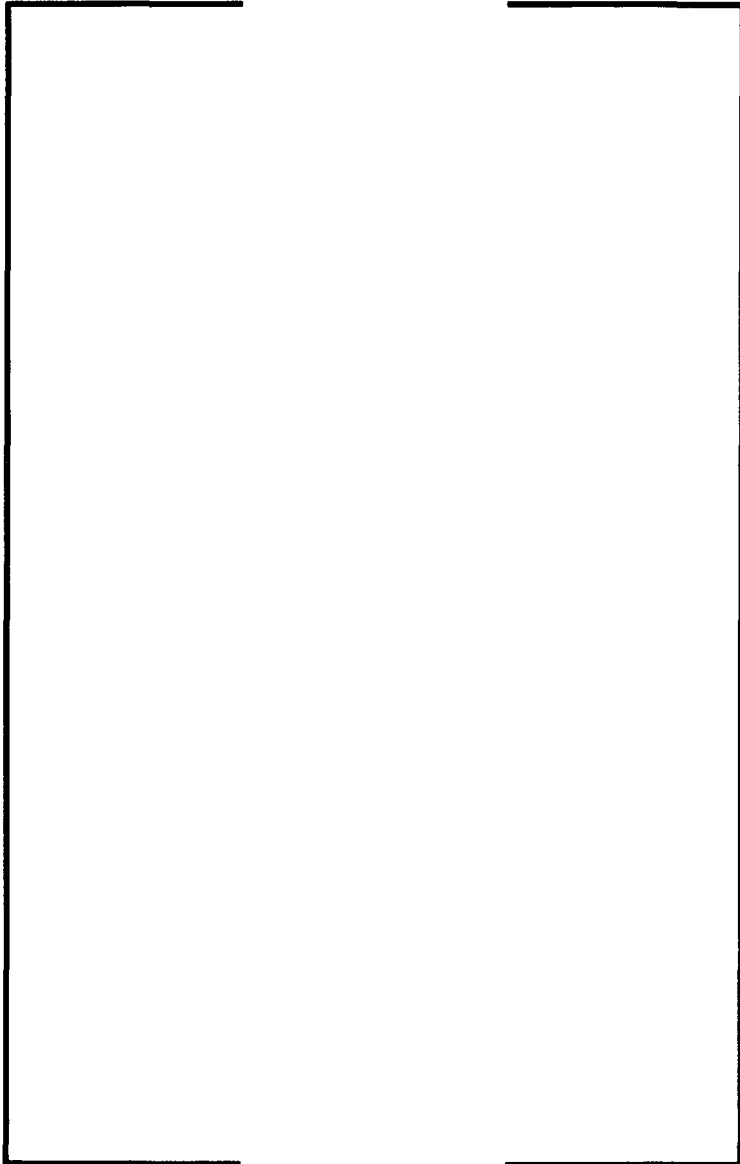


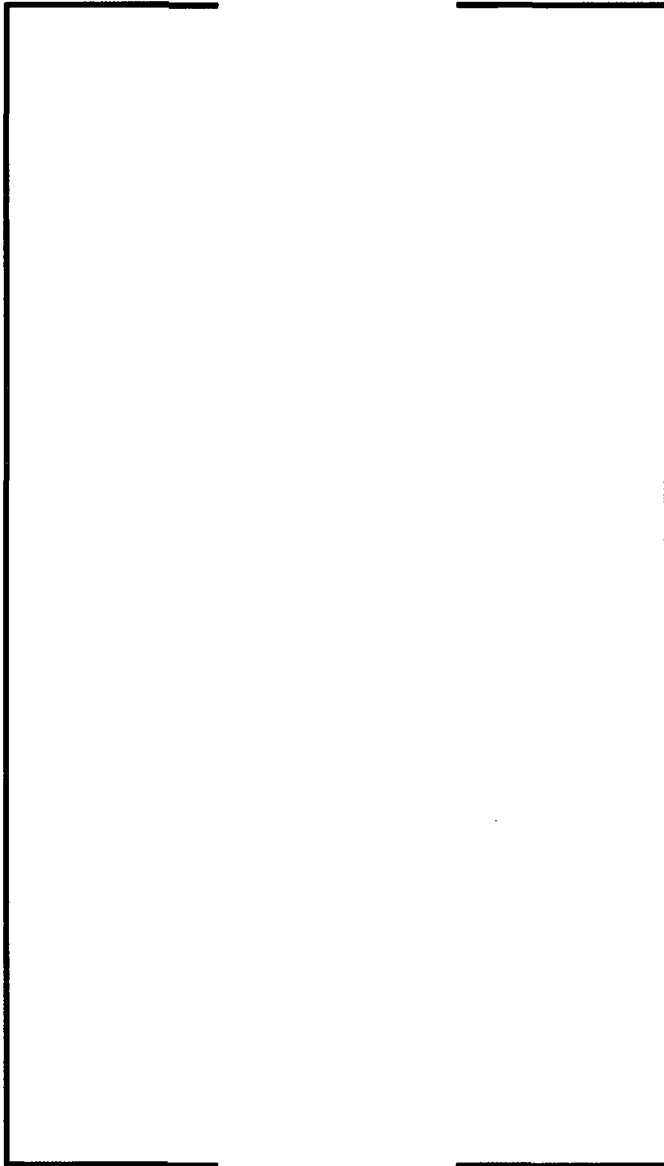


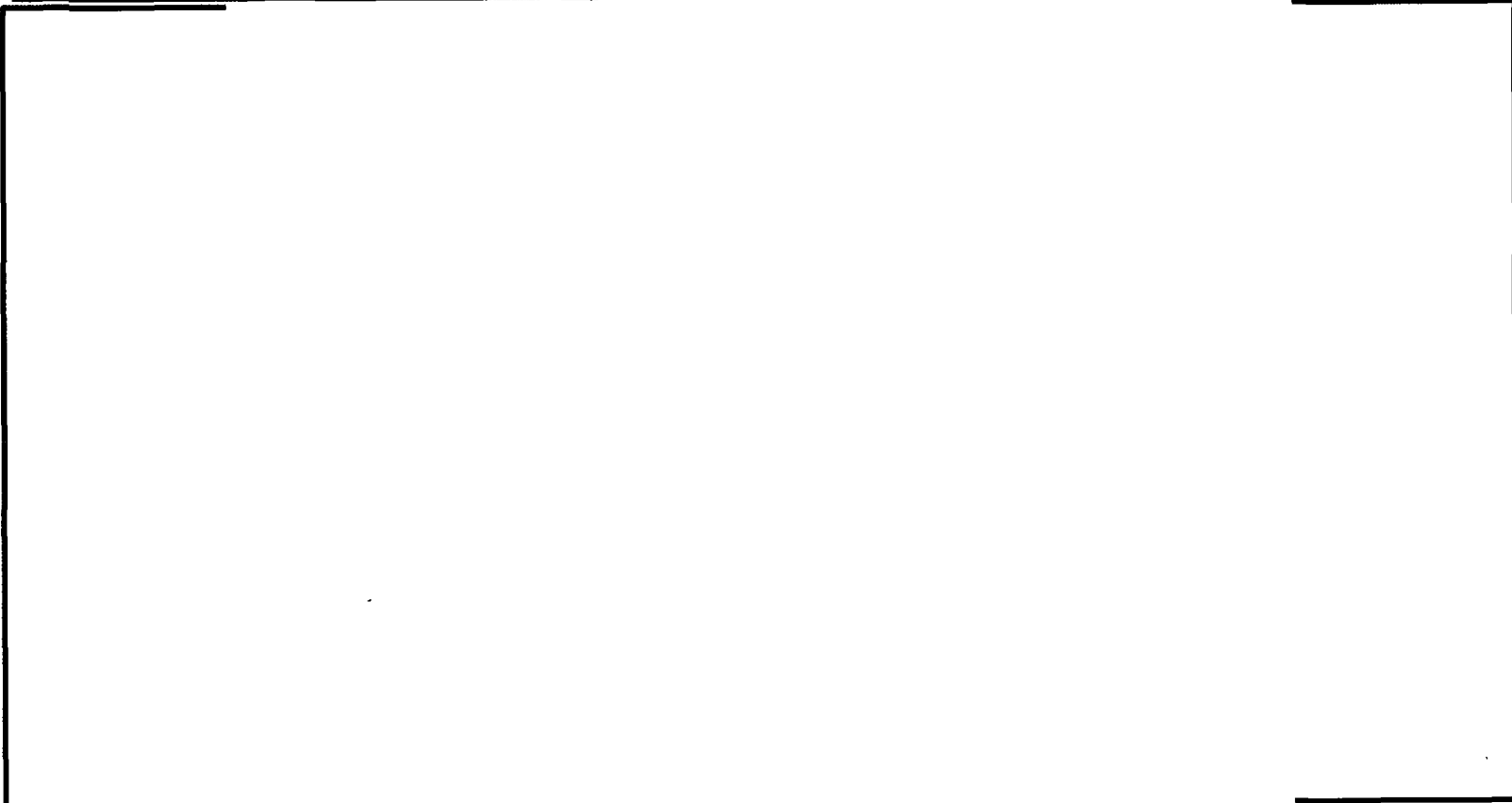


Record of iterations
The axial and crossflow errors variation during the outer iterations are given.







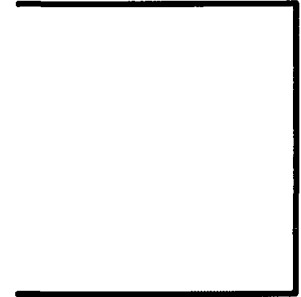
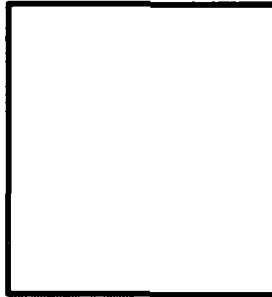


Mass balance and energy balance
- **Inlet and outlet mass flow and the total mass flow error [kg/s]**
- **Inlet and outlet flow energy and energy error [kW]**

| | |
|--|--|
| | |
|--|--|

Channel exit conditions

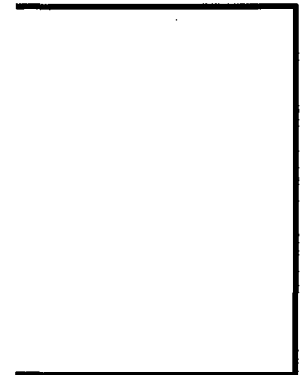
- channel number [-]
- enthalpy [kJ/kg]
- temperature [°C]
- density [kg/dm³]
- equilibrium quality [-]
- void fraction [-]
- flow [kg/s]
- mass flux [kg/(s m²)]

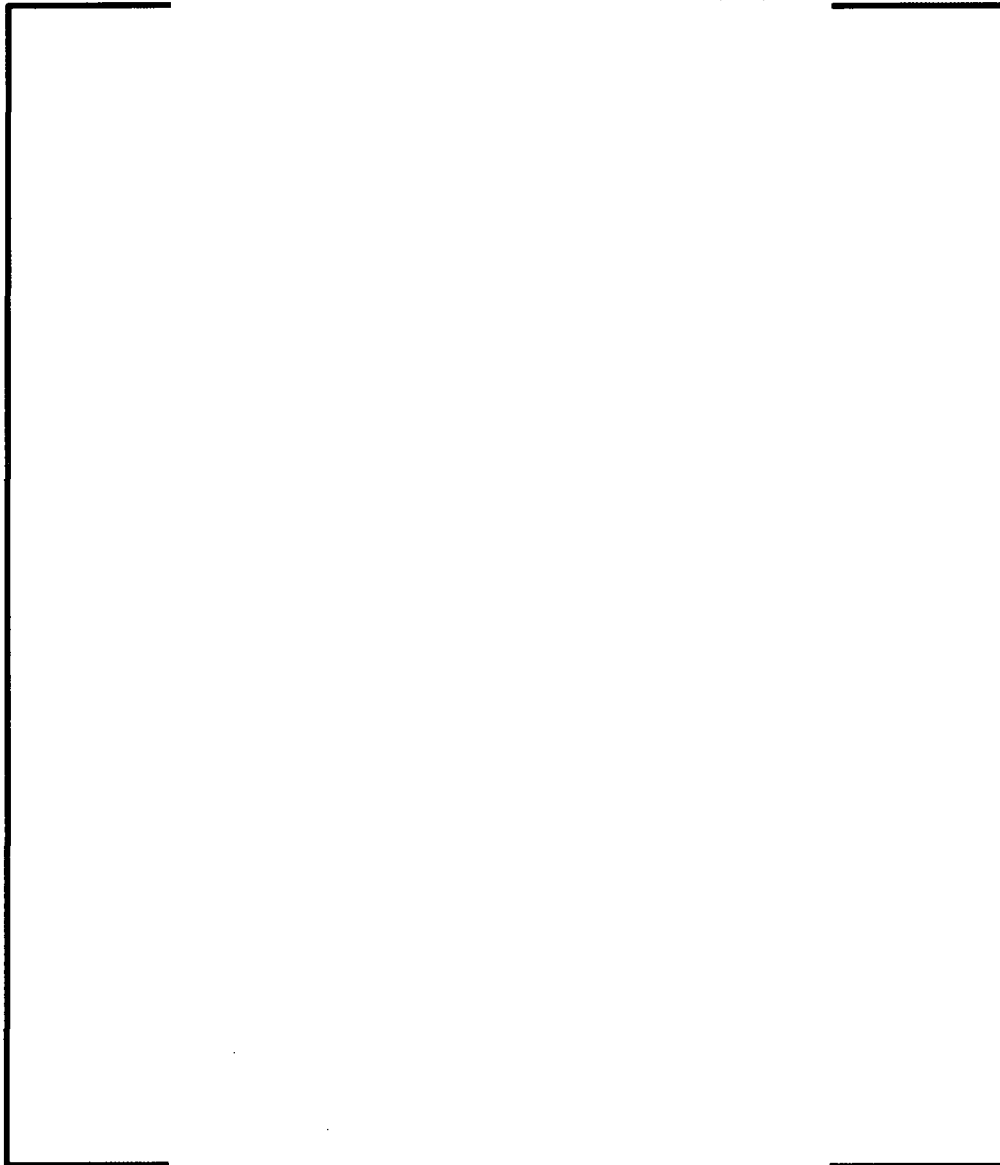


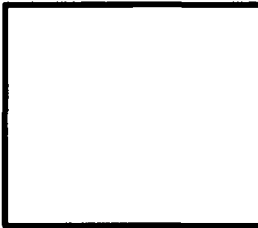
Bundle averaged results

This information is always printed for steady state calculations. In case of transient calculation the bundle averaged results are printed for the transient time steps if selected by input. The axial nodes at which the results are printed can be also specified by the user. The results printed at the selected axial locations are:

- axial distance [cm]
- pressure loss [bar]
- enthalpy [kJ/kg]
- temperature [°C]
- density [kg/dm³]
- equilibrium quality [-]
- void fraction [-]
- flow [kg/s]
- mass flux [kg/(s m²)]



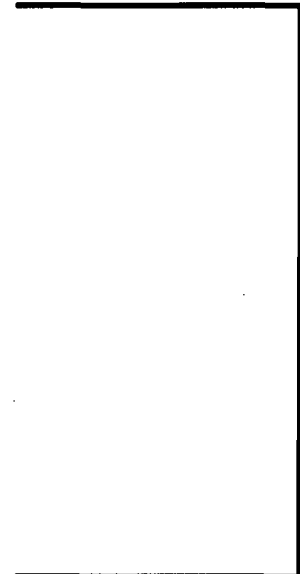




Channel results (as requested by user)

These results are always printed. The user may specify via input the channels and axial nodes for which the information is printed. The following results are printed for each selected channel:

- axial distance [cm]
- pressure loss [bar]
- enthalpy [kJ/kg]
- temperature [°C]
- density [kg/dm³]
- equilibrium quality [-]
- void fraction [-]
- flow [kg/s]
- mass flux [kg/(s m²)]
- minimum departure of nucleate boiling ratio (MDNBR) [-]
- rod number belonging to the channel and corresponding to MDNBR [-]
- Tong factor corresponding to MDNBR [-]
- CHF correlation number
- CHF correlation name
- CHF correlation type (typically DNBR)





*Cross flow results (as requested by user)
These results are printed only if requested by the user. The axial nodes for which the information is printed may be selected via input.*



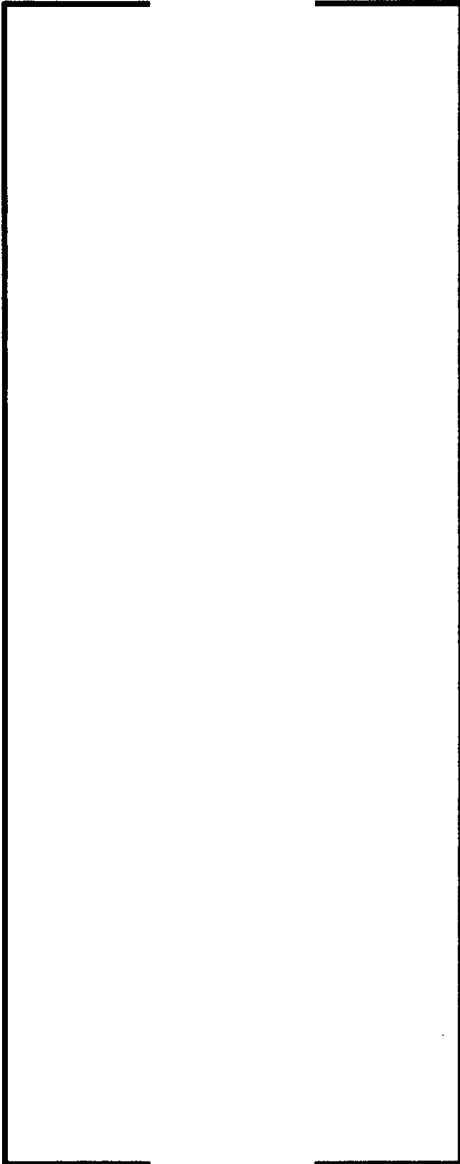


Rod results (as requested by user)

These results are printed only if requested by the user. The rod numbers and axial nodes for which the information is printed may be selected via input. For each selected rod the selected CHF correlation number and type is written first. Afterwards the following results are printed:

- axial distance [cm]
- heat flux [kW/m²]
- DNBR [-] – minimum DNBR over the adjacent channels to the rod
- Tong factor corresponding to the DNBR value [-]
- channel number belonging to the rod and corresponding to DNBR [-]







Critical heat flux (CHF) summary (case1/time =0.0 s)

The CHF summary for all channels includes:

- axial distance at which the MDNBR is reached for each channel [cm]
- heat flux corresponding to the MDNBR reached for the channel [kW/m²]
- MDNBR – minimum DNBR over all axial nodes for the channel [-]
- rod number belonging to the channel and corresponding to the MDNBR [-]
- channel number [-]
- CHF correlation number corresponding to the MDNBR [-]
- CHF correlation name corresponding to the MDNBR [-]

